

Studies on non-digestible carbohydrates in the human intestine

Focus on kinetics of fermentation
and degradation



Mara P. H. van Trijp

Propositions

1. Dietary fiber fermentation in the healthy human intestine will remain a 'black box' unless *in vivo* sampling tools and procedures are improved.
(*this thesis*)
2. Carbohydrate degradation models are of limited value without brush-border enzymes and luminal microbiota in the small intestine compartment.
(*this thesis*)
3. Small-scale feasibility studies in research designs are needed to reduce the costs of investigation and improve data quality and scientific integrity.
4. Dietary interventions targeting fermentation can impact planetary health.
5. Personalizing interventions will improve intervention effectiveness and subject engagement.
6. Interactions with animals deserve a more prominent role in care plans for patients and the elderly.
7. Creativity is a way to cope with a crisis effectively.

Propositions belonging to the thesis entitled

Studies on non-digestible carbohydrates in the human intestine. Focus on kinetics of fermentation and degradation.

Mara P.H. van Trijp
Wageningen, 11 February 2022

Studies on non-digestible carbohydrates in the human intestine

Focus on kinetics of fermentation and degradation

Mara P.H. van Trijp

Thesis committee

Promotor

Prof. Dr A.H. Kersten
Professor of Nutrition, Metabolism, and Genomics
Division of Human Nutrition and Health
Wageningen University & Research

Co-promotors

Dr G.J.E.J. Hooiveld
Assistant professor, Division of Human Nutrition and Health
Wageningen University & Research

Dr L.A. Afman
Associate Professor, Division of Human Nutrition and Health
Wageningen University & Research

Other members

Prof. Dr H. Smidt, Wageningen University & Research
Dr E. Capuano, Wageningen University & Research
Prof. Dr K. Verbeke, Katholieke Universiteit Leuven, Belgium
Prof. Dr D.M.A.E. Jonkers, Maastricht University

This research was conducted under the auspices of the Graduate School VLAG (Advanced studies in Food Technology, Agrobiotechnology, Nutrition and Health Sciences).

Studies on non-digestible carbohydrates in the human intestine

Focus on kinetics of fermentation and degradation

Mara P.H. van Trijp

Thesis

submitted in fulfilment of the requirements for the degree of doctor
at Wageningen University
by the authority of the Rector Magnificus,
Prof. Dr A.P.J. Mol,
in the presence of the
Thesis Committee appointed by the Academic Board
to be defended in public
on Friday 11 February 2022
at 1.30 p.m. in the Aula.

Mara P.H. van Trijp

Studies on non-digestible carbohydrates in the human intestine. Focus on kinetics of fermentation and degradation, 314 pages.

PhD thesis, Wageningen University, Wageningen, the Netherlands (2022)
With references, with summary in English and Dutch

ISBN: 978-94-6447-043-7

DOI: <https://doi.org/10.18174/558735>

Table of contents

Chapter 1	General introduction.	7
Chapter 2	Using naso- and oro-intestinal catheters in physiological research for intestinal delivery and sampling in vivo: practical and technical aspects to be considered.	43
Chapter 3	A toolbox for the comprehensive analysis of small volume human intestinal samples that can be used with gastrointestinal sampling capsules.	85
Chapter 4	Fermentation kinetics of selected dietary fibers by human small intestinal microbiota depend on the type of fiber and subject.	119
Chapter 5	Intra-intestinal degradation kinetics of non-digestible carbohydrates and the fate of short-chain fatty acids in human subjects.	153
Chapter 6	Detailed analysis of the digestibility of prebiotic fructo- and galacto-oligosaccharides in the human small intestine.	193
Chapter 7	A 12 week whole grain or refined wheat intervention had minor effects on the gut microbiota and their predicted functionality, but correlated with liver health in overweight and obese adults.	225
Chapter 8	General discussion.	261
	Summary	287
	Dutch summary Nederlandse samenvatting	295
	Acknowledgements Dankwoord	303
	About the author	309



General introduction

Poor diet is an important risk factor for ill health (1). Western diets typically include a too low intake of whole grains, vegetables, and fruits and an increased intake of saturated fats and sugars. Consumption of such diets often results in, amongst others, intakes of dietary fiber below the recommended levels (2). It also contributes to obesity development and related health disturbances. The World Health Organization (WHO) states that the worldwide prevalence of obesity nearly tripled after 1975 (3). In 2016, 39% of the adults were overweight (BMI 25-29.9 kg/m²), and 13% of these adults were obese (BMI ≥ 30 kg/m²) (3). In the Netherlands, 36% of the adults were overweight and 14% were obese in 2020 (4). Obesity is often associated with metabolic disturbances (5), which increase the risk of numerous chronic diseases, such as cardiovascular diseases and type 2 diabetes (5, 6). Obesity, therefore, is a serious public health concern and also poses a high economic burden (7, 8). There is a strong interest in improving health through the consumption of dietary fibers. An increased fiber intake has been associated with numerous health benefits, such as lower body weight (9, 10), a lower risk of for instance type 2 diabetes (11, 12), and certain gastrointestinal (GI) diseases (11) including colon cancer (13). One suggested underlying mechanism for the health effects is its fermentation by the intestinal microbiota resulting in the production of fermentation products. The fermentation products are an important energy source for the intestinal cells, and their uptake by the host has been associated with improvements in metabolic health markers in the blood (14, 15). Little is known about what exactly happens to dietary fibers at what stage during their passage through the human GI-tract. Novel methodology is therefore warranted to have a better understanding of dietary fibers (fermentation) in the human intestine.

Dietary fibers

Defining dietary fibers and prebiotics

Dietary fibers are present as natural constituents of food plant sources such as fruits, vegetables, and cereals. Around the world, there are multiple operative definitions for dietary fibers (16). The CODEX Alimentarius Commission, who sets international guidance standards for food, provided the following definition:

“Dietary fiber means carbohydrate polymers with ten or more monomeric units¹, which are not hydrolyzed by the endogenous enzymes in the small intestine of humans and belong to the following categories:

- 1. Edible carbohydrate polymers naturally occurring in the food as consumed;*
- 2. Carbohydrate polymers, obtained from food raw material by physical, enzymatic, or chemical means²;*

3. Synthetic carbohydrate polymers²;

¹International authorities are allowed to decide whether compounds with a degree of polymerization of 3–9 are allowed. ²Isolated or synthetic fibers must show a proven physiological benefit to health as demonstrated by generally accepted scientific evidence to competent authorities.” (17, 18)

Dietary fibers can also include prebiotic oligo- and polysaccharides. Prebiotic carbohydrates need to fulfill the following criteria, as demonstrated in man or animals: “Resists gastric acidity, hydrolysis by mammalian enzymes and gastrointestinal absorption; is fermented by the intestinal microbiota; and stimulates selectively the growth and/or activity of intestinal bacteria associated with health and wellbeing.” (19) More recently, in 2017, prebiotics were defined as “a substrate that is selectively utilized by the host microorganisms conferring a health benefit”, to expand the concept “to possibly also include non-carbohydrate substances, diverse categories other than food, and applications to body sites other than the gastrointestinal tract” (20).

Subcategories of dietary fibers

Dietary carbohydrates are highly diverse. They can be classified into sub-categories based on their chemical structures and (physical) properties. The properties include the character of individual monomeric units, the number of units (degree of polymerization; DP), and the type of linkages in between the units (21). There are three main groups of carbohydrates, namely sugars (DP1-2), oligosaccharides (DP3-9), and polysaccharides (DP≥10) (22) (**Figure 1**). A distinction is made between digestible carbohydrates, namely the mono- and disaccharides, maltodextrin and digestible starch, and the non-digestible carbohydrates (NDC). The latter include fermentable and non-fermentable oligo- and polysaccharides, coming from a variety of sources such as fruits, vegetables, nuts, legumes, cereals, and trees/woody plants (21, 23-26). Examples of non-digestible oligosaccharides are galacto-oligosaccharides (GOS) and fructo-oligosaccharides (FOS). Non-digestible polysaccharides are sub-divided into resistant starches, and non-starch polysaccharides (i.e., hemi-cellulose, pectin, inulin, gums, mucilage, and cellulose). The dietary fibers that will be discussed in this thesis are described in more detail below.

Inulin and fructo-oligosaccharides

Chicory fructans comprise inulin (DP≥10) and oligofructose (DP 2-10). Both inulin and oligofructose are often called fructo-oligosaccharides (FOS). Both are soluble, non-viscous, and fermentable (24) prebiotics. Inulin and FOS consist of a linear series of β-(2,1) linked fructose units, attached to a terminal fructose by a β-(2,1) bond (Fn series), or to a terminal alpha-D-glucose by an α-(2,1) bond (GFn series) (**Figure 2A**). Inulin is extracted and purified mainly from chicory roots (28). Chicory inulin can have

a DP up to 60. Inulin can be enzymatically processed into FOS, which has a similar chemical structure but a lower number of units, namely a DP up to 10 (29, 30). FOS can also be prepared synthetically from sucrose or fructose and is usually called short-chain FOS (28, 31). Fructans can be found in a variety of foods, such as whole grains (e.g. barley and rye), vegetables such as garlic, artichoke, chicory, onions, and fruits such as bananas (28, 32).

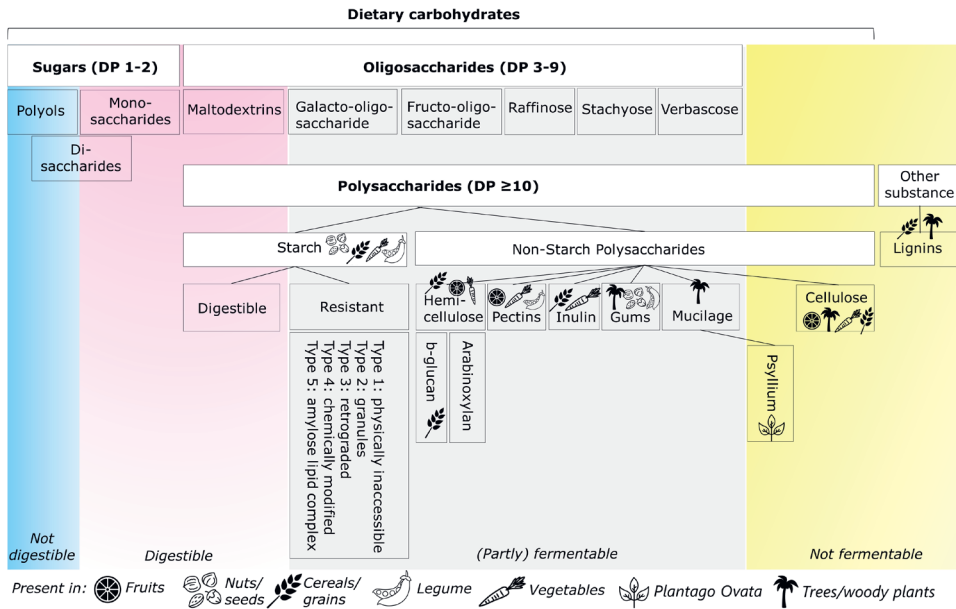


Figure 1. An overview of dietary carbohydrates and lignin, a complex polymer, and their categorisation.

Information about the classification is adapted from (21, 23-26). The lay-out of the figure is inspired by (27).

Galacto-oligosaccharides

Galacto-oligosaccharides (GOS) are also soluble and fermentable (24) prebiotics (33). GOS consist of complex mixtures of different galactose chains varying in DP (DP 2 to 8), and linkages, namely β -(1,2), β -(1,3), β -(1,4), or β -(1,6), attached to a terminal galactose or glucose unit, or isomers with a (1-1) linkage (**Figure 2B**) (34, 35). GOS can be produced by hydrolysis and transgalactosylation of lactose by β -galactosidases (34). They are used in infant milk formula and infant foods or incorporated into foods as prebiotic. GOS are naturally present in human milk (36), as well as in the generative part of plants such as beans or legumes such as lentils and chickpeas (37).

Pectins

Pectins are high molecular weight complex polysaccharides. They are thought to have stimulatory effects on specific microbial species in the colon, and to be supportive of the immune system in the intestine via a direct interaction (38). The pectin backbone consists of α -(1,4) linked galacturonic acids. The structure contains three major groups, namely homogalacturonan, rhamnogalacturonan II, and rhamnogalacturonan I (**Figure 2C**) (39), with varying degrees of acetyl- and methyl-esterification (39). Commercially available pectins are often extracted from citrus fruits (oranges, lemon, grapefruit) and apples. Pectin is naturally present in almost all plants as a compound of the cell wall and middle lamella (40).

Isomalto/malto-polysaccharides

Isomalto/malto-polysaccharides (IMMP) is a novel synthesized fiber derived from starch via enzymatic modification (41). IMMP resisted hydrolysis by small intestine (SI) host enzymes (i.e., amylglucosidase and α -amylase), and selectively increased bacteria *in vitro* that are associated with host benefits (42). Therefore, it is thought IMMP has the potential to become a novel prebiotic. IMMP is synthesized using 4,6- α -glucanotransferase, which transfers a non-reducing glucose moiety of an α -(1,4)-glucan chain to the non-reducing end of another α -(1,4)-glucan chain (41). This consequently results in a fiber with α -(1,6)-glycosidic linkages (**Figure 2D**). Depending on the source of the starting starch substrate, IMMPs with up to 92% of α -(1,6)-glycosidic linkages till DP35 are formed during synthesis.

Whole grain wheat fibers

Whole grains (WG) are a rich source of dietary fibers and an important staple food in many Western countries. In WG wheat specifically, cellulose, hemi-cellulose (e.g. arabinoxylan and β -glucan), fructan, and lignin were found (43, 44). Arabinoxylan was the dominating fiber (43, 44). Cellulose, present in plant cell walls, is long unbranched homopolymeric chains composed of β -(1,4)-glycosidic linked glucose units (45). β -Glucans are linear chains of glucopyranosyl monomers linked by single β -(1,3) linkages and consecutive β -(1,4) linkages, with linear cellotetraosyl and cellotriosyl blocks (46). Furthermore, arabinoxylan (**Figure 2E**), present in the grain cell walls, has a β -(1,4) linked xylose backbone with α -L-arabinofuranosyl substituents (47) via α -(1,2) or α -(1,3) linkages (48), with or without an esterified ferulic acid moiety. For arabinoxylans in WG wheat, around ~21% of the xylose backbone is monosubstituted, 13% is disubstituted, and 66% is unsubstituted (48). Ferulate can bind to lignin, which are phenolic polymers consisting of the monomers p-coumaryl alcohol, coniferyl alcohol, and sinapyl alcohol (49). Lignins are officially no dietary carbohydrates but are included in the dietary fiber definition, because they are closely associated with fibers in the plant cell wall.

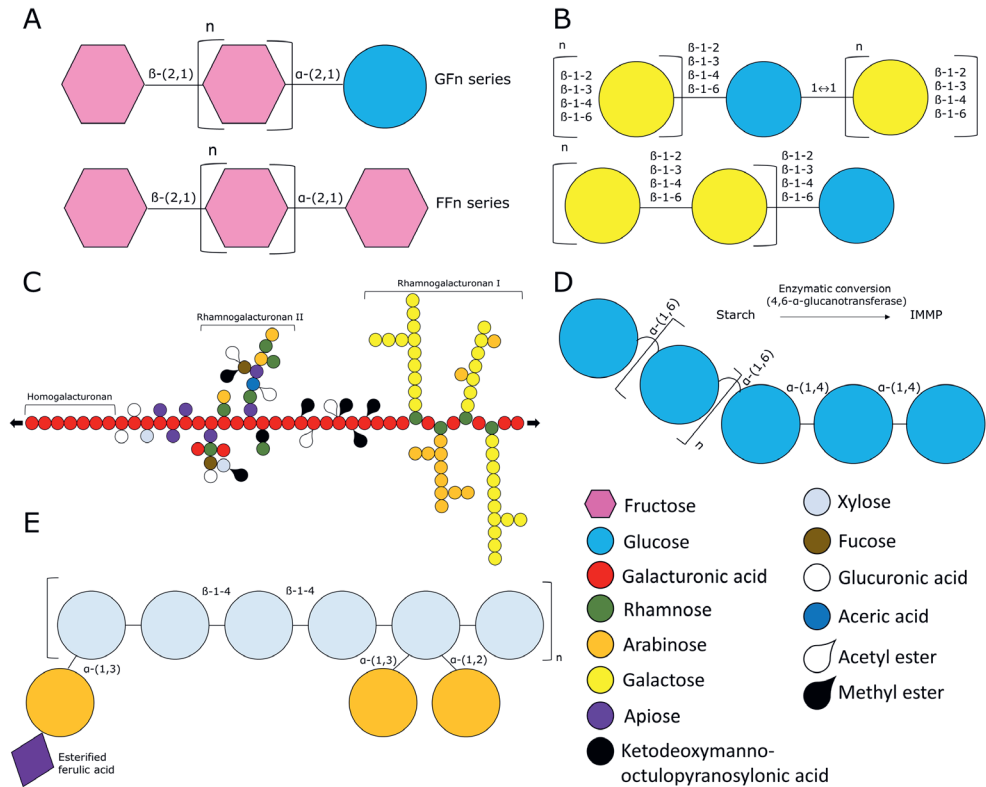


Figure 2. A schematic overview of the main structural features of a selected set of dietary fibers.

(A) fructans (28), (B) galacto-oligosaccharides (35, 50), (C) pectin (39), (D) isomalto/malto-polysaccharides (41), and (E) arabinoxylan (47, 48).

Dietary fiber intakes in relation to health

Fiber intake was negatively associated with all-cause mortality, with a risk reduction of 10% per 10 g/d increase in intake (51). Moreover, a dose-response relationship was found between the total fiber intake and total mortality, the incidence of coronary heart disease, type 2 diabetes, and colorectal cancer ((52), n=4635 adults). The greatest benefits were observed in individuals consuming 25–29 g/d fibers or more (52). The dietary fiber recommendations vary globally. For instance, the EFSA recommends an intake of 25 g/d in adults, because of the evidence of health benefits including normal laxation (53). In the Netherlands, the advice is to consume 30-40 g/d fibers through a diet rich in vegetables, fruit, and whole grains (54). Nonetheless, the average intakes often fall below the recommended levels, and vary widely around the globe (**Figure 3**) (2). In regions with predominantly plant-based diets, with plenty of vegetables, fruits, and whole grains products, higher fiber intakes were reported. In the Netherlands, the mean

intakes of fiber are 23 g/d for males and 18 g/d for females (55). People suffering from certain disorders, such as diabetes type 2 and constipated people, potentially benefit from supplementation of extra fibers to the diet to fill this ‘fiber gap’. The potential mechanisms of action are discussed below.

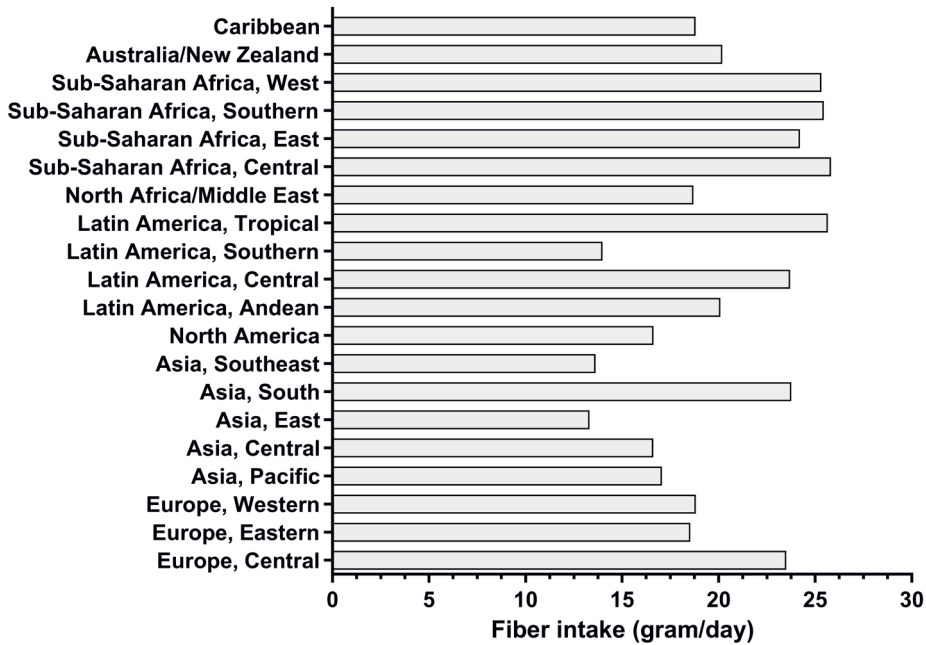


Figure 3. Dietary intakes of fibers around the globe.

Data is from 2010 and provided in mean intake/d. Total dietary fiber from all dietary sources, primarily fruits, vegetables, grains, legumes, pulses are included, while supplements are excluded. Source of the data: Global Nutrition and Policy Consortium/Global Dietary Database (2).

Potential mechanisms underlying the health effects of dietary fiber

Several mechanisms are suggested to underlie the health benefits of dietary fibers. These include, but are not limited to, increased satiety (23), improved insulin sensitivity and glycemia, lowered blood pressure, lowered low-density lipoprotein (LDL) cholesterol levels (56), enhanced immune function (12), and favorable postprandial glucose and insulin responses (57). Already decades ago, it was noted that fibers were important for intestinal functioning and intestinal health (58). A clear definition for ‘intestinal health’ is still lacking. It generally entails effective digestion and absorption of food, a normal and stable intestinal microbiota, an effective immune status which includes barrier function and normal mucus production, and a status of well-being in the absence of GI

illnesses (59). Fibers have three main functional characteristics in the GI-tract, namely viscosity, bulking, and fermentability (**Figure 4**). Fibers can increase the fecal mass and the intestinal transit time via several mechanisms (60, 61), resulting in a laxative effect. Minimally fermentable fibers contribute to bulking, and viscous fibers also have a water-holding and gel-forming capacity (62), that consequently impact fecal consistency (63). This consistency is correlated with feces water content (64). Examples of bulking fibers are cellulose and lignin, and examples of viscous fibers are certain types of hemicelluloses, gums, and pectins (62). Fermentable fibers can increase fecal bulk via increased (microbial) biomass and fermentation by-products. This fermentation process can result in microbiota changes, production of short-chain fatty acids (SCFAs), increased osmotic load, or bloating or flatulence due to gas production. It has been hypothesized that SCFAs are a link between fiber fermentation and host health improvements (65).

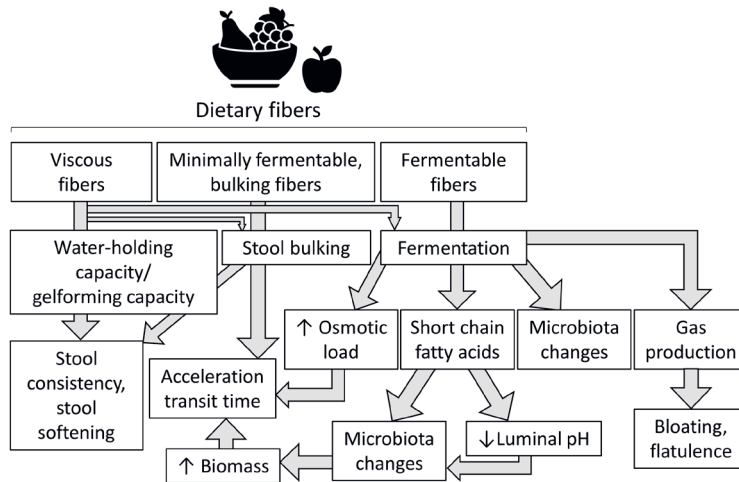


Figure 4. Mechanisms of how dietary fibers can affect GI function.

The figure is reproduced and adapted from (58) with permission. Information is obtained from (58, 60, 62-64).

Effects of fructo- and galacto-oligosaccharides on metabolic and gut health

GOS and chicory FOS, both soluble and fermentable prebiotics, can selectively stimulate the growth and/or activity of specific intestinal bacteria linked to health benefits (19, 66). They are added to infant formula to mimic the health effects of endogenous oligosaccharides in human milk (67). Furthermore, they are also added to food products to improve the nutrition value (fiber content) of the food and/or for health purposes for adults. In **Table 1**, a non-exclusive overview of systematic reviews and/or intervention trials is provided that investigated the effects of FOS, inulin, or

GOS supplementation on metabolic and gut health in adults. Comparisons were made with isocaloric digestible maltodextrin (68-73), monomers (74, 75), or cellulose (76). Consumption of fructans can decrease fasting glucose, homeostatic model assessment of insulin resistance (HOMA-IR), HbA1c (77, 78), or LDL cholesterol (79), although the effects on glucose homeostasis were not always consistent (77-80). Supplementation of a combination of FOS and inulin (range 10-16 g/d) also resulted in increased fecal *Bifidobacterium* in the majority of studies (69, 71, 81-83). No effects on fecal SCFAs were found (71, 76, 83, 84). Studies do show an increased frequency of defecation and improved fecal consistency (85-87). Moreover, there is a European authorized health claim for inulin for increasing stool frequency (88). For GOS, one study (73) reported a decrease in the plasma inflammation marker C-reactive protein (CRP), and in plasma insulin, total cholesterol, and triglycerides in overweight and obese subjects after 12-weeks 5.5 g/d supplementation. After 2 weeks GOS supplementation also the plasma endotoxin lipopolysaccharide (LPS) was found to be decreased (75). In most studies (Table 1) no significant effects on metabolic health outcomes were found when GOS was compared to the control. Most interventions with GOS increased fecal *Bifidobacterium*, which was often not accompanied by improved gut health markers. Overall, the longer-term intervention effects of FOS, inulin, and GOS on metabolic and gut health are not consistent across studies. Some of them point towards improved metabolic or gut health including changes in the fecal microbiota composition.

Intestinal microbiota and health

One factor thought to mediate the health benefits of fibers is the micro-organisms residing in the GI-tract. The human GI-tract comprises the stomach, the SI (duodenum, jejunum, ileum), and the large intestine (ascending colon, transverse colon, descending colon, sigmoid colon, rectum) (**Figure 5**). The micro-organisms in the GI-tract include mostly bacteria, but also viruses, fungi, and archaea. They are collectively called the microbiota. The genes the microbiota encode are known as the microbiome. Different sequencing and bioinformatics strategies are available to measure and characterize the microbiota. To study which bacteria are present, the DNA-based method 16S rRNA gene amplicon sequencing is routinely used, which classifies bacteria up to the genus level (93). Another DNA-based method is deep shotgun metagenomic sequencing, which provides information about the microbiota composition up to the strain level, and additionally identifies the genetic potential of the community (93). To study what the microbiota community is doing, RNA-based methods such as metatranscriptomics provide information about the actively expressed genes (93).

Table 1. The effects of FOS or GOS on outcomes related to metabolic or gut health.

Systematic reviews that reported the effects of FOS and inulin were selected. A selection of human intervention placebo-controlled trials that assessed the effects of GOS or chicory FOS/inulin on outcomes related to metabolic or gut health. A PubMed search was performed in July 2020, and randomized clinical trials in healthy adults and elderly published after the year 2010 were selected.

Study	Study design	Main conclusions related to metabolic health (compared to control)	Main conclusions related to gut health (compared to control)
(77)	Systematic review 6 RCTs, n=661 adults.	↓ Fasting glucose, HOMA-IR, HbA1c.	N.D.
(78)	Systematic review 33 RCTs, n=1346 adults (prediabetic and diabetic population).	↓ Fasting glucose, insulin, HOMA-IR, HbA1c.	N.D.
(79)	Systematic review 20 RCTs, n=607 adults.	↓ LDL cholesterol. ↔ Fasting glucose, insulin, HDL cholesterol.	N.D.
(80)	Systematic review 25 RCTs, type 2 diabetic or obese adults.	↔ BMI. ↔ Blood glucose, insulin, HOMA-IR, HbA1c.	N.D.
(82)	Systematic review 14 RCTs (FOS/inulin) in adults.	N.D.	↑ Fecal <i>Bifidobacterium</i> .
(83)	Systematic review 7 RCTs, adults.	N.D.	↑ Fecal <i>Bifidobacterium</i> (most consistent), <i>Anaerostipes</i> , <i>Faecalibacterium</i> , and <i>Lactobacillus</i> (concordant). ↔ Fecal SCFAs.
(87)	Systematic review 5 RCTs, n=252 adults with constipation.	N.D.	↑ Fecal frequency, consistency. ↓ Transit time, fecal hardness. ↔ Pain, bloating.
(89)	Systematic review 47 RCTs, adults and patients.	N.D.	↑ Feces frequency (FOS), wet weight, consistency. ↔ Feces frequency (inulin). ↔ Fecal SCFAs. ↓ Fecal microbiota diversity.
(76)	N=12 overweight and obese adults. Double-blind, cross-over RCT. 20 g/d chicory inulin for 6 weeks, or 20 g/d cellulose, 4 week wash-out in between.	↑ Insulin sensitivity. ↓ Fasting insulin.	

(84)	N=50 healthy adults. Double-blind, cross-over RCT. 3 or 7 g/d chicory root inulin-type fructans for 4 weeks, or control, with 4 week wash-out in between.	Not measured.	<ul style="list-style-type: none"> ↑ Fecal <i>Bifidobacterium</i>. ↔ Fecal SCFAs. ↔ GI symptoms, and fecal consistency.
(85)	N=22 adults with low stool frequency. Double-blind, cross-over RCT. 10 g/d chicory inulin for 5 weeks, or control maltodextrin with 2 week wash-out in between.	Not measured.	<ul style="list-style-type: none"> ↑ Feces frequency. ↑ Improved fecal consistency. ↔ GI symptoms. ↔ Microbiota composition.
(86)	N=44 adults with constipation. Double-blind, cross-over RCT. 12 g/d chicory inulin for 4 weeks, or maltodextrin, with 2 week wash-out in between.	Not measured.	<ul style="list-style-type: none"> ↑ Feces frequency. ↑ Improved fecal consistency. ↔ GI symptoms.
(69)	N=30 obese women. Parallel, double-blind RCT. 16 g/d chicory inulin+FOS (1:1) for 12 weeks, or maltodextrin.	↔ BMI and waist/hip ratio.	<ul style="list-style-type: none"> ↑ Fecal <i>Bifidobacterium</i> and <i>Faecalibacterium prausnitzii</i>.
(71)	N=35 healthy subjects with a habitual high fiber (HDF) or low dietary fiber (LDF) intake. Cross-over, double-blind, RCT. 16 g/d chicory FOS and inulin (1:1) for 3 weeks, or maltodextrin, with 3 week wash-out in between.	↔ Appetite ratings.	<ul style="list-style-type: none"> ↑ Fecal <i>Bifidobacterium</i> in both HDF and LDF; <i>Faecalibacterium</i> in HDE ↓ Fecal <i>Coprococcus</i>, <i>Dorea</i>, <i>Ruminococcus</i> in HDF group. ↔ Fecal SCFAs. ↑ Flatulence.
Galacto-oligosaccharides			
(90)	N=44 obese and overweight men and women. Double-blind, parallel RCT. 15 g/d GOS for 12 weeks or isocaloric placebo.	<ul style="list-style-type: none"> ↔ Peripheral and adipose tissue insulin sensitivity, body composition, and energy and substrate metabolism. ↔ Plasma inflammation markers. 	<ul style="list-style-type: none"> ↑ Fecal <i>Bifidobacterium</i>. ↔ Fecal microbiota diversity. ↔ Fecal or fasting plasma SCFAs. ↔ Plasma gut-derived hormones/incretins.
(74)	N= 18 healthy adults. Cross-over RCT. 0.0 g, 2.5 g, 5.0 g, and 10.0 g/d GOS for 3 weeks, or control (syrup and sugar).	Not measured.	<ul style="list-style-type: none"> ↑ Flatulence. ↑ Fecal <i>Bifidobacterium</i>. ↔ Bowel movement, consistency, discomfort, abdominal pain, or bloating.
(75)	N=88 overweight adults. Parallel RCT. 6, 12, or 18 g/d α-GOS for 2 weeks, or control (glucose).	<ul style="list-style-type: none"> ↑ Satiety during a test meal. ↓ Energy intake. ↓ Plasma LPS. 	<ul style="list-style-type: none"> ↑ Fecal <i>Bifidobacterium</i>. ↔ Bloating, and fecal consistency.
(91)	N=29 men with type 2 diabetes. Parallel RCT. 5.5 g/d GOS for 12 weeks, or maltodextrin.	<ul style="list-style-type: none"> ↔ Glucose tolerance. ↔ Inflammation markers. 	<ul style="list-style-type: none"> ↔ Fecal microbiota. ↔ Intestinal permeability.

(73)	<p>N=45 overweight or obese adults with metabolic syndrome risk factors. Cross-over RCT. 5.5 g/d b-GOS for 12 weeks, or maltodextrin, with 4 weeks wash-out in between.</p>	<p>↓ Plasma CRP ↓ Plasma insulin, total cholesterol, triglycerides.</p>	<p>↑ Fecal <i>Bifidobacterium</i>, and fecal IgA. ↓ Fecal calprotectin.</p>
(72)	<p>N=40 elderly. Cross-over RCT. 5.5 g/d b-GOS for 10 weeks, or maltodextrin, with 4 weeks wash-out in between.</p>	<p>Not measured.</p>	<p>↑ Fecal <i>Bacteroides</i> and <i>Bifidobacterium</i>. ↔ Bowel function, fecal sIgA and calprotectin.</p>
(92)	<p>N=37 adults. Cross-over RCT. 8 g/d GOS for 3 weeks, or placebo, with 3 weeks wash-out in between.</p>	<p>Not measured.</p>	<p>↑ Fecal <i>Bifidobacterium</i>. ↔ Fecal consistency, bloating, abdominal discomfort, or flatulence.</p>

Significant findings compared to control are reported in the table. ↔ no effects, ↑ increased, ↓ decreased. Abbreviations: AUC, area under the curve; BCFA, branched-chain fatty acids; CRP, C-reactive protein; FOS, fructo-oligosaccharides; GOS, galacto-oligosaccharides; HDL, high-density lipoprotein; HOMA-IR, Homeostatic Model Assessment for Insulin Resistance; LDL, low-density lipoprotein; LPS, lipopolysaccharide; RCT, randomized controlled trial; SCFA, short-chain fatty acids.

The intestinal microbiota plays an important role in health and disease. They have protective functions (*e.g.* pathogen displacement), structural functions (*e.g.* enhancing the gut barrier), and metabolic functions (*e.g.* vitamin synthesis, degrading indigestible nutrients) (94). A decreased microbiota diversity or a shift in their composition or activity is known as microbial dysbiosis. A dysbiosis in feces has been linked to many diseases (95). A dysbiosis of the SI microbiota is also proposed to play a role in disease pathogenesis (96). The associations are reported mostly in cross-sectional studies, which do not provide information about the causal effect of microbiota changes on disease. The causal effects of the microbiota on the host metabolic phenotype have been supported by numerous animal studies. For instance, they applied microbiota transplantation (97, 98) or compared conventionally raised mice versus germ-free mice (99). Also in humans, fecal transplantation studies highlighted the causal role of the microbiota in metabolic and intestinal diseases. For instance, when feces from lean donors were transplanted to metabolic syndrome patients their insulin sensitivity temporarily improved (100). This indicates that health-markers can directly be influenced via changes in the gut microbiota.

The small and large intestinal microbiota

The microbial density increases along GI-tract, ranging from 10^{3-4} bacteria cells/gram content in the stomach to $10^{11-10^{12}}$ bacteria cells/gram content in the transverse and distal colon (101) (Figure 5). Besides the bacterial load, also the diversity and composition vary throughout the GI-tract (102, 103). This can be explained by the distinct environment in the different GI regions, such as the presence of digestive secretions, gas composition, the availability of (macro)nutrients, and the transit times. The SI is a more harsh environment for microbiota with a relatively short exposure to (macro)nutrients and the presence of more digestive secretions such as bile acids (96). Compared to the large intestine microbiota, the SI microbiota is expected to be more dynamic and to respond rapidly to changing luminal conditions (96).

Feces is typically used as a proxy for the large intestine microbiota. In the colonic mucosa and feces of healthy subjects, around 700 bacteria were detected (104). The main phyla are Firmicutes, Bacteroidetes, Proteobacteria, and Actinobacteria, but also Verrucomicrobia, Fusobacteria, and Tenericutes were detected (105). Commonly found fecal bacteria at the genus level are *Bifidobacterium*, *Faecalibacterium*, *Clostridium*, *Bacteroides*, *Eubacterium*, *Escherichia/Klebsiella*, *Enterococcus*, and *Streptococcus* (94, 106). In contrast to the large intestine microbiota, the human SI microbiota is less well characterized, mainly due to the complexity and invasiveness of sample collection. In the human distal SI (ileum) *Streptococcus*, *Lactobacillus*, *Staphylococcus*, *Escherichia*, *Bacteroides*, *Clostridium* (clusters IV and XIVa), and *Veillonella* were consistently detected (107-110). It has been previously shown that these bacteria were also encountered in ileostomy effluent (110-112). This effluent can be collected non-invasively from ileostomy patients without a colon, which

has been removed as a result of the disease. The colonic microbiota is more equipped to degrade complex fibers, while the SI microbiota is expected to rapidly metabolize simple carbohydrates for community maintenance (110).

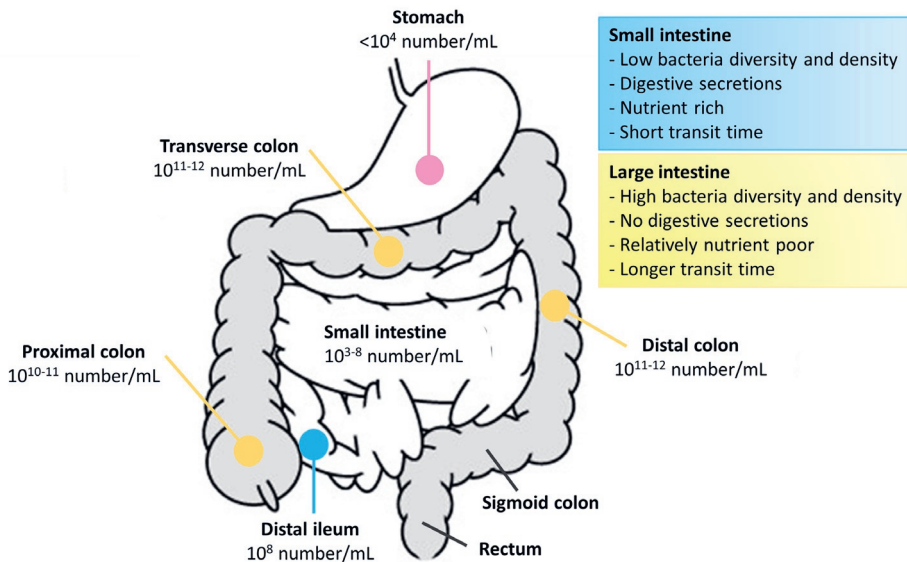


Figure 5. A schematic representation of the different regions of the GI-tract, and the number of bacteria cells/mL residing in that region.

Factors that shape microbial communities, and distinguishing characteristics of the small and large intestine are included. The figure is, with permission, adapted from (96, 113). The bacteria numbers were previously reported by (101).

Diet as a modulator of the intestinal microbiota?

A plethora of factors play a role in shaping the intestinal microbiota. Examples are the geographical location, host genetics, age, the mode of delivery, the use of medication, and the habitual diet (114, 115). In a large cohort study that included 503 clinical and (dietary) questionnaire-based covariates, it was shown that all these factors explained only 7.7% of the fecal microbiota variation between individuals ($n=3948$, (115)). This highlights the complexity and variability of the microbiota between people. The medication intake had the largest explanatory power on the microbiome, followed by blood parameters, bowel characteristics (*e.g.* stool consistency), and then dietary information (*e.g.* fruit intake and bread preference) (115). Long-term dietary intake and patterns (116-118), such as a strict vegan or vegetarian diet or an omnivorous diet (119), were strongly associated with the fecal microbiota composition. Also, the intake of specific food products and the quality and type of dietary patterns were linked to the fecal microbiota composition (118). Cross-sectional studies showed that changing the microbiota via the habitual diet can take months to years (120, 121). Drastic short-term dietary changes, however, altered the human fecal microbiota already in a week

(122). The effect of controlled dietary interventions on the microbiota is often less well studied (123). Because the composition of the intestinal microbiota in the small and large intestine plays an important role in health, modulating the microbiota through changes in diet can be a strategy to improve health status. Increasing the dietary fiber intake via supplementation can be an effective strategy to modulate the fecal microbiota composition (124). Examples of fibers that influence the fecal microbiota are resistant starch, inulin, FOS, GOS, and arabinoxylan (82, 125). Fiber-rich products such as whole grains are also expected to modulate the microbiota (125). One underexplored topic is the effect of diet, including fibers, on the SI microbiota, while this may also have the potential to influence host health (126, 127).

Digesting the indigestibles: dietary fiber fermentation

An important route by which the microbiota interacts with the host is via the production of metabolites from nutrients that escape digestion. Some metabolites reach the circulation where they can influence organ functioning (128). The microbiota is therefore sometimes called the (neglected) endocrine organ. The type of microbial metabolites that are produced depends on the availability of the nutrients, including diet- or host-derived proteins, polyphenolics, fat and host-derived bile acids, and dietary fiber (129). Microbial metabolites can be both health-promoting and toxic (129). In the scope of this thesis, we will focus on complex dietary carbohydrates as substrates for bacteria. The process of carbohydrate (and protein) breakdown by strictly or facultatively anaerobic intestinal bacteria under anaerobic conditions is known as fermentation (130, 131). The extent and rate of fermentation are influenced by host factors as well as the amount and characteristics of the available dietary fibers. Examples are solubility, sugar composition, degree of polymerization, and molecular conformation (132, 133). The microbiota enzymatically breaks down complex carbohydrates by a huge diversity of carbohydrate-active enzymes (CAZymes). While the intestinal microbiome contains an estimated 15.882 different CAZymes genes (134), the human genome encodes only 17 glycoside hydrolases for carbohydrate digestion (135). The human carbohydrases involved in carbohydrate digestion are summarized in **Table 2**. Recently, it is debated to what extent host digestive enzymes, located on the intestinal brush-border, are also capable to degrade certain NDCs (136). This hypothesis is based on *in vitro* carbohydrate digestion models, while little is known about to what extent human host enzymes digest such NDCs.

Table 2. Host (human) enzymes that are involved in the digestion of dietary carbohydrates.
The table is adapted from (136) with permission.

Enzyme	Digestion site	Main substrate, glycosidic linkage specificity
Salivary α -amylase, secreted	Mouth	Starch; linear malto-oligosaccharides (n>6) Glc α (1 \rightarrow 4)Glc
Pancreatic α -amylase, secreted	Small intestine	Starch; linear malto-oligosaccharides (n>6) Glc α (1 \rightarrow 4)Glc
Sucrase-isomaltase, mucosal*	Small intestine brush-border	Sucrose, isomaltose, maltose, maltotriose, α -dextrins Glc α (1 \leftrightarrow 2) β Fru, Glc α (1 \rightarrow 4)Glc, Glc α (1 \rightarrow 6)Glc
Maltase-glucoamylase, mucosal	Small intestine brush-border	Linear and branched malto-oligosaccharides (n=2-9) Glc α (1 \rightarrow 4)Glc, Glc α (1 \rightarrow 6)Glc
Lactase-phlorizin hydrolase, mucosal	Small intestine brush-border	Lactose, cellobiose, cellotriose, cellulose Glc α (1 \rightarrow 4)Gal, Glc α (1 \rightarrow 4)Glc
Trehalase, mucosal	Small intestine brush-border	Trehalose Glc α (1 \leftrightarrow 1) α Glc

* Mucosal enzymes are located on the brush-border membrane of the small intestine.

Degradation of galacto- and fructo-oligosaccharides

Degradation of GOS requires β -galactosidases (137). GOS is selectively utilized by several bacteria via intra- and extra-cellular β -galactosidases, involving both intracellular and extracellular hydrolysis (*e.g.* cell membrane-bound enzymes) (138). Degradation of inulin and FOS requires endo- and exo-inulinases. Endo-inulinases split molecules by breaking internal β -(2,1) fructofuranosidic linkages in inulin to produce FOS of different chain lengths, whereas exo-inulinases split off fructose units at the terminal non-reducing end (139). FOS is utilized via extracellular hydrolysis by cell wall-bound β -fructofuranosidases, followed by the uptake of fructose, sucrose, and glucose by one or more transporters, or transported intact into the cell (*e.g.* via ABC transporters) and consequently hydrolyzed by cytoplasmic β -fructofuranosidases (137).

Production of fermentation products

Major fermentation end products are SCFAs, gases (CO₂, H₂S, CH₄, and H₂), ammonia, and energy (131). Intermediate fermentation products are for instance H₂, lactate, formate, succinate, and ethanol (140). The main produced SCFAs are acetate, propionate, and butyrate, which are estimated to account for 85-95% of the total SCFA in the colon (131). Other organic acids, such as lactate and succinate, are present in lower concentrations (141). There are several known pathways for SCFA production (**Figure 6**) (14, 142-145). Important enzymes involved in propionate formation are propionate CoA transferase, methylmalonyl-CoA decarboxylase, propionyl-CoA:succinate CoA transferase, and for butyrate formation butyrate kinase and butyryl-CoA:acetate CoA-transferase (145). During active fermentation, bacteria produce hydrogen (146), which can be further metabolized by hydrogen-utilizing micro-organisms by sulfate-reducing

bacteria, methanogenic organisms, acetogenic bacteria, amino acid fermenting bacteria, and dissimilatory nitrate-reducing bacteria (146). For instance, acetogenic bacteria convert H_2 and CO_2 into acetate, and methanogenic archaea such as *Methanobrevibacter smithii* or certain *Clostridium* and *Bacteroides* bacteria species produce CH_4 from CO_2 and H_2 (147). Gas is eliminated both through the lungs via exhaled breath and expelled as flatus.

Substrate cross-feeding is the utilization of carbohydrate breakdown products after the initial degradation of complex carbohydrates from a given micro-organism by other organisms (148). Metabolic cross-feeding is the utilization of (fermentation) products from a given micro-organism by others (149). An important cross-feeding reaction is the conversion from acetate to butyrate (150-153), but also conversions of butyrate into acetate or propionate, and propionate into butyrate were reported (150). Bacterial cross-feeding interactions manipulate the availability of substrates in the intestine. Studying these interactions is crucial in determining the final balance of intestinal metabolite production.

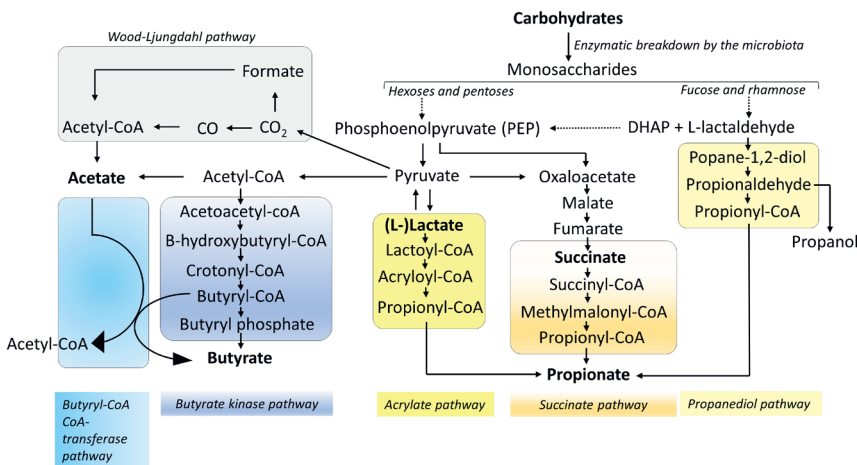


Figure 6. A schematic overview of the fermentation pathways leading to the production of acetate, propionate, and butyrate.

Dotted arrows indicate several intermediates. Hexoses are for instance glucose and fructose, and pentoses are for instance xylose and arabinose. The figure and information are adapted from information in references (14, 142-144).

Short-chain fatty acids and health

It has been hypothesized that SCFAs from a link between fiber fermentation and host health improvements (154). SCFAs are an energy source for the enterocytes, can function as signaling molecules, and may play a role in intestinal disorders (14, 143,

155). There is an increased interest in studying the fate of SCFAs and their appearance in the systemic circulation (65, 143, 156), as they can bind to receptors on different (metabolic) organs (157). In humans, the SCFAs circulating in blood correlated with insulin sensitivity and other metabolic markers of the host (158), while this correlation was absent for fecal SCFA concentrations. This suggests that the SCFA uptake and availability likely provide a more direct link to metabolic health than fecal SCFAs.

Concentrations of short-chain fatty acids in the human body

SCFAs are absorbed by enterocytes via facilitated diffusion, via transporters, or exchange with bicarbonate (150) (**Figure 7**). SCFAs are oxidized to CO_2 , producing energy for the enterocytes (159). SCFAs that are not metabolized by the enterocytes enter the portal circulation as free acids (160). In the liver, they are further metabolized, and the remaining SCFAs end up in the systemic circulation.

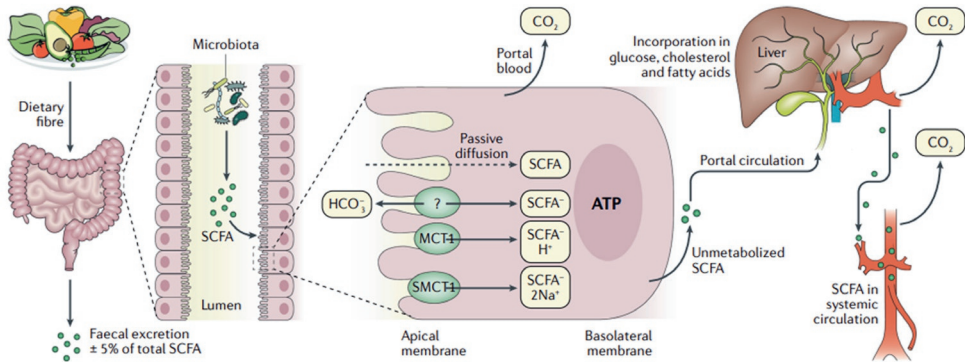


Figure 7. The metabolism of short-chain fatty acids.

The figure was reproduced with permission from (159). MCT1, monocarboxylate transporter 1; SMCT1, sodium-dependent monocarboxylate transporter 1.

Measurements of SCFA concentrations in the mesenteric veins, the portal vein, and the hepatic vein of people indicate that the gut is the main SCFA releasing organ (**Table 3**). The liver takes up most of the propionate and butyrate. The liver uses SCFAs as an energy source and as substrates for metabolite synthesis. Previously a splanchnic extraction (gut and liver) of butyrate of almost 100% was reported (161), followed by propionate, whereas more acetate was released from this area. The estimated splanchnic extraction in healthy individuals of colonic-administered acetate, propionate, or butyrate was 64%, 91%, or 98%, respectively (153). Fasting plasma concentrations of acetate in the peripheral veins were maximally $200 \mu\text{mol/L}$ (Table 3). In contrast, propionate and butyrate concentrations in the peripheral circulation were much lower ($<10 \mu\text{mol/L}$). This does not necessarily exclude an impact of butyrate in tissues other than the

intestine or liver, since butyrate supplementation has been shown to influence adipose, cardiac, and skeletal muscle metabolic processes (162-164). Acetate concentrations were reduced between arterial and venous blood, showing the utilization by peripheral tissues (165-167), such as the adipose tissue and muscle (168). Consumption of fermentable substrates such as lactulose (165, 169) and pectin (165) increased postprandial acetate in the peripheral circulation. Gut-derived acetate mixes with endogenous acetate released by tissues and organs (168, 170). Recently it has been shown that differences in macronutrient composition, with matching amounts of fibers, also affected serum SCFA concentrations (171).

Direct examination of SCFAs inside the intestine and portal blood healthy subjects is invasive and/or not possible. As a result of the extensive metabolism of SCFAs in the intestine and liver, often estimations of their concentrations are reported. In sudden death victims, the ratios of acetate, propionate, and butyrate were approximately 60:20:20 in the colon, 81:12:7 in the hepatic vein, and 91:5:4 in the peripheral blood (172). Other researchers (173) estimated that the colonic production of SCFAs upon 15 gram inulin in healthy subjects was 137 ± 75 mmol for acetate, 11 ± 9 mmol for propionate, and 20 ± 17 mmol for butyrate. In healthy subjects, most of the ^{13}C label from colonic-administered ^{13}C -SCFAs was recovered as $^{13}\text{CO}_2$ in breath, while the excretion of SCFAs via urine was very low (153). It has been estimated that only 5-10% of the SCFAs are excreted in the feces (174). Overall, SCFA measurements in the peripheral circulation will underestimate SCFA production by the intestinal microbiota, because of metabolism in the intestine and liver. Information about carbohydrate fermentation and SCFA production and absorption inside the human intestine is currently unknown.

Short-chain fatty acids as signaling molecules and their role in metabolism

Numerous tissues, including enteroendocrine cells and liver tissue, express receptors for SCFAs (157). An important set of targets for SCFAs are G-protein-coupled receptors (GPRs), including GPR43/FFAR2, GPR41/FFAR3, and GPR109A (175). These receptors can be activated by SCFAs as reviewed previously (14, 143, 157, 159, 176, 177), with resulting distinct downstream effects. For instance, SCFAs are thought to influence hormone secretion of GLP-1 and peptide YY (PYY) from enteroendocrine cells, both known to play a role in satiety (177). Another example is that SCFAs phosphorylate and activate pAMPK in the liver, which enhances fatty acid oxidation (143), and decreases fatty acid synthesis and gluconeogenesis (143). In the adipose tissue, SCFAs might activate GPR43 to reduce fatty acid and glucose uptake, which potentially improves systemic insulin sensitivity and reduces adiposity (177). SCFAs have been also suggested to play a role in fatty acid-, glucose- and cholesterol metabolism (150). The use of stable ^{13}C isotopes is an elegant tool to study organ and/or systemic metabolism. Information about intestinal fluxes of SCFAs and their metabolic fate can be obtained via the delivery

of isotopic labeling (^{13}C) of SCFA inside the intestine (178, 179). In two studies in mice (150) and humans (153), the label from gut-derived ^{13}C -SCFA was incorporated into different biological relevant molecules, such as fatty acids and amino acids (150). Known biochemical pathways showed that acetate enters the tricarboxylic acid (TCA) cycle as acetyl-CoA, where it is converted finally to oxaloacetate. Acetyl-CoA can also be used as a substrate for the synthesis of long-chain fatty acids, cholesterol, or ketone bodies (150, 180). Propionate can be converted into succinate and enters the TCA cycle as succinyl-CoA, and supports gluconeogenesis via oxaloacetate (150). Butyrate is supposed to be taken up by the mitochondria where it undergoes β -oxidation to form in a series of steps acetyl-CoA, which subsequently enters the TCA cycle (181).

Studying the kinetics of fermentation in the human intestine

Novel methodology is needed to have a better understanding of dietary fiber (fermentation) in the human intestine with consequent effects on the luminal environment, to understand the potential mechanisms underlying their health effects.

Human studies

Most commonly, the effects of dietary fiber fermentation on intestinal bacteria and bacterial metabolites are studied through analysis of feces (82). Feces is easy to collect, but it is a static measurement and does not provide direct information on dynamic kinetic microbial processes occurring during and at the site of fermentation. Metabolite concentrations in feces namely represent the balance between production, utilization, and absorption (174). Furthermore, the fecal microbiota may differ from the intestinal lumen microbiota (103, 182). For this reason, additional methods are needed to sample more locally to better understand the effects of dietary compounds, including fibers, inside the intestine. Hence, medical procedures and tools are required such as colonoscopies and intestinal catheters. Also, the application of less-invasive sampling capsules is appearing in the literature (183, 184). Indirect postprandial measurements, as an indication for microbial fermentation, include monitoring breath hydrogen and methane levels (185-188), or tracing the appearance of labeled (189) or non-labeled (190) blood metabolites, such as SCFAs, to estimate the fiber fermentation kinetics. Important to note is that these measurements are not a direct reflection of what is happening at the site of fermentation. As yet, information about fiber fermentation and SCFA production and absorption inside the human intestine, and the consequent effect on the luminal microbiota is still mostly unknown.

Fermentation models

Before *in vivo* digestion and fermentation studies, *in vitro* models can be used to mimic

this process. Such studies take place outside the body, intending to mimic a process in the GI-tract in a cost-efficient way. One major advantage is that these models are not restricted by ethical considerations. *In vitro* fermentation models, inoculated with human intestinal bacteria, can be used to study fiber degradation kinetics (187, 191). During such experiments, the human intestinal microbiota is cultured for a defined period. Numerous model designs are available that vary in complexity, as recently reviewed (192). Designs range from relatively simple batch fermentation models to multistage continuous flow models (113). Initial screenings of the interplay between fibers and the intestinal microbiota are often first evaluated in batch fermentations (193). This provides relevant information about breakdown kinetics, metabolite production, and the effects on the microbiota. Batch fermentation models are closed systems, such as bottles or reactors inoculated with the intestinal microbiota, often feces, in culturing medium maintained under anaerobic conditions at 37°C. The advantages of batch cultures are the easy set-up, inexpensiveness, and high throughput. The operational time is restricted to several hours due to substrate depletion and accumulation of (toxic) products. Multistage continuous fermentation models mimic various regions in the GI-tract via connected vessels that each have their own specified, specific parameters (113, 194). Examples are the SHIME system (195) and the TIM-2 system (196). The latter system also mimics for example peristaltic movements and entails an absorption mimicking dialysis system (196). A general limitation of *in vitro* models is the lack of feedback mechanisms of the host.

Table 3. SCFA concentrations in blood or in the GI-tract of human subjects.

Condition	Acetate: site and concentrations	Propionate: site and concentrations	Butyrate: site and concentrations	Population	Study				
Fasting	Intestine:	Intestine:	Intestine:	Sudden death victims, maximum of four hours after death (n=6, 16–89 years).	(172)				
	- Jejunum 0.6±0.6 mmol/kg	- Jejunum N.D.	- Jejunum N.D.						
	- Ileum 7.9±4.1 mmol/kg	- Ileum 1.5±1.0 mmol/kg	- Ileum 2.3±1.3 mmol/kg						
	- Ascending colon 63.4±6.8 mmol/kg	- Ascending colon 26.7±4.0 mmol/kg	- Ascending colon 24.5±4.2 mmol/kg						
	- Transverse colon 57.9±5.4 mmol/kg	- Transverse colon 23.1±2.8 mmol/kg	- Transverse colon 24.4±2.2 mmol/kg						
	- Descending colon 43.5±11.1 mmol/kg	- Descending colon 14.2±3.1 mmol/kg	- Descending colon 14.7±2.9 mmol/kg						
	- Sigmoid/rectum 50.1±16.2 mmol/kg	- Sigmoid/rectum 19.5±6.7 mmol/kg	- Sigmoid/rectum 17.9 ±5.6 mmol/kg						
	Blood:	Blood:	Blood:						
	- Portal vein 258±40.1 μmol/L	- Portal vein 88±27.8 μmol/L	- Portal vein 29±7.9 μmol/L						
	- Hepatic vein 115±28.2 μmol/L	- Hepatic vein 21±9.8 μmol/L	- Hepatic vein 12±4.4 μmol/L						
- Peripheral vein 70±18.6 μmol/L	- Peripheral vein 5±1.8 μmol/L	- Peripheral vein 4±1.7 μmol/L							
Fasting	- Superior mesenteric vein 50.4±11.3 μmol/L	- Superior mesenteric vein 19.5±3.5 μmol/L	- Superior mesenteric vein 22.7±7.4 μmol/L	Healthy/Overweight upper abdominal surgery patients (n=20 subjects, 54–75 years, BMI 18.7-29.3).	(197)				
	- Inferior mesenteric vein 102.7±27.2 μmol/L	- Inferior mesenteric vein 64.8±13.4 μmol/L	- Inferior mesenteric vein 62.9±13.4 μmol/L						
	- Portal vein 41.4±7.8 μmol/L	- Portal vein 24.5±6.1 μmol/L	- Portal vein 21.1±4.4 μmol/L						
	- Hepatic vein 23.6±4.8 μmol/L	- Hepatic vein 2.8±0.8 μmol/L	- Hepatic vein 2.6±0.8 μmol/L						
	- Radial artery 21.8±7.6 μmol/L	- Radial artery 1.0±0.2 μmol/L	- Radial artery 0.8±0.2 μmol/L						
	- Portal vein 262.8±31.2 μmol/L	- Portal vein 30.3±5.6 μmol/L	- Portal vein 30.1±4.8 μmol/L			Abdominal surgery patients with normal liver function (n=22, 30-78 years).	(161)		
	- Hepatic vein 219.5±22.8 μmol/L	- Hepatic vein 6.9±1.2 μmol/L	- Hepatic vein 12±2.6 μmol/L						
	- Artery 172.9±19.1 μmol/L	- Artery 3.6±0.4 μmol/L	- Artery 7.5±1.2 μmol/L						
	- Portal vein 177.5±21.5 μmol/L	- Portal vein 15.6±2.4 μmol/L	- Portal vein 19.5±4.3 μmol/L					Patients with liver cirrhosis (n=12, 38-73 years).	(198)
	- Hepatic vein 157.3±21.5 μmol/L	- Hepatic vein 5.6±1.3 μmol/L	- Hepatic vein 4.8±1.0 μmol/L						
- Artery 124.5±12.5 μmol/L	- Artery 8.2±0.9 μmol/L	- Artery 10.1±1.8 μmol/L							
- Portal vein 114.0±59.8 μmol/L	- Portal vein 32.0±13.5 μmol/L	- Portal vein 9.4±17.0 μmol/L	Subjects during gall bladder surgery (n=5).	(199)					
- Basilic vein (arm) 34.9±17.2 μmol/L	- Basilic vein (arm) 1.9±31.6 μmol/L	- Basilic vein (arm) 1.0±50.0 μmol/L							

Fasting	Antecubital vein: range 0-450 µmol/L Serum: acetate 2230 ng/mL (range 1200-4060 ng/mL)	Antecubital vein: range 0-12 µmol/L Serum: propionate 195 ng/mL (range 159-239 ng/mL)	Antecubital vein: range 0-8 µmol/L Serum: butyrate 85 ng/mL (range 70-99 ng/mL)	Adults (n=160, 20-70 years). Healthy subjects (n=163, 47-60 years).	(158) (171)
Fasting	- Artery 72±7 µmol/L - Vein 51±5 µmol/L (range 2-99 µmol/L)	Not measured.	Not measured.	Normal subjects (n=27).	(166)
Fasted compared to after consumption of non-digestible carbohydrates					
Fasting	- Peripheral vein 44±4.4 µmol/L (healthy) - Antecubital vein 48.0±4.2 pmol/L (healthy) and 21.3±0.8 pmol/L (ileostomy)	Not measured.	Not measured.	Ileostomy subjects (n=10, 56-80 years), healthy controls (n=21, 19-73 years and n=8 19-21 years).	(169)
Lactulose	- Peripheral vein: 10 gram: 114.4±16.2 µmol/L (healthy)				
Fasting	- Peripheral artery 125.6±13.4 µmol/L - Peripheral vein <2 µmol/L - Peripheral artery <2 µmol/L	- Peripheral vein <2 µmol/L - Peripheral artery <2 µmol/L	- Peripheral vein <2 µmol/L - Peripheral artery <2 µmol/L	Healthy subjects (n=14, 19-41 years).	(165)
Lactulose	- Peripheral vein: 5 gram: 98.6±23.1 µmol/L* 10 gram: 127.3±18.2 µmol/L* 20 gram: 181.3±23.9 µmol/L*	Not measured.	Not measured.		
Pectin	- Peripheral vein: 20 gram: 95.8±11.7 µmol/L*	Not measured.	Not measured.		
Inulin	15 gram, after 12 hour: - Antecubital vein: 55±30 mmol (cumulative amount) - Colonic production*: 137±75 mmol (cumulative amount)	15 gram, after 12 hour: - Antecubital vein: 1.1±0.9 mmol (cumulative amount) - Colonic production*: 11±9 mmol (cumulative amount)	15 gram, after 12 hour: - Antecubital vein: 1.0±0.9 mmol (cumulative amount) - Colonic production*: 20±17 mmol (cumulative amount)	Healthy subjects (n=12, 18-65 years)	(173)

Mean ± SEM are presented if not stated otherwise. N.D. not detected. * are the peak concentrations detected over time. **Colonic production was estimated by the dilution of the constant intravenous infusion of ¹³C-labeled SCFA by unlabeled (¹²C) SCFA produced upon inulin in blood samples. SCFAs, short-chain fatty acids.

Thesis outline and aims

The work described in this thesis aims to study the kinetics of fermentation and degradation of non-digestible carbohydrates, mainly in the human small intestine, and consequent effects on the microbiota and bacterial metabolites. To achieve this aim, we applied several models to study digestion and fermentation (**Figure 8**). We used *in vitro* batch models, as well as intervention trials in human subjects with the use of naso-intestinal catheters and stable isotopes. We investigated the acute short- and longer-term effects of varying NDC types and concentrations on the intestinal environment, including the microbiota and metabolites, in relation to metabolism.

More specifically, the objective of **chapter 2** and **chapter 3** was to describe two methodologies of studying the human intestinal lumen. **Chapter 2** provides a systematic review of practical and technical aspects of using intestinal catheters in human subjects for delivery and sampling from the jejunum, ileum, and colon. **Chapter 3** describes a new toolbox that can be used with human intestinal sampling capsules, for stabilizing and analyzing the fermentation of GOS, FOS, and inulin by the human ileostomy or fecal microbiota. Furthermore, we studied *in vitro* (**chapter 4**), and in healthy men (**chapter 5**) the breakdown of selected dietary fibers and production of metabolites by the SI microbiota. To this end, we performed batch fermentations with the human ileostomy microbiota and chicory FOS/inulin, GOS, lemon pectin, and IMMP (**chapter 4**), and two clinical feasibility trials to study acute fermentation kinetics of a FOS:GOS mix in the human intestine using intestinal catheters (**chapter 5**). We also aimed to investigate the effect of a 7-day FOS:GOS supplementation compared to maltodextrin on the same acute fermentation kinetics. Moreover, the fate of intestinal-delivered SCFA as substrates for glucose and lipid metabolism was assessed using a stable labeled isotope approach (**chapter 5**). In **chapter 6**, we investigated in detail the digestibility of all compounds present in the FOS:GOS mixture in the small intestine of healthy men, using advanced chemical analyses. Moreover, we investigated the effects of a 12-week intervention with WG wheat or refined wheat products, with a 10 g/d fiber difference, on the composition and functions of the fecal bacteria in relation to changes in liver health parameters (**chapter 7**). Finally, in **chapter 8** the outcomes of **chapters 2 to 7** are discussed.

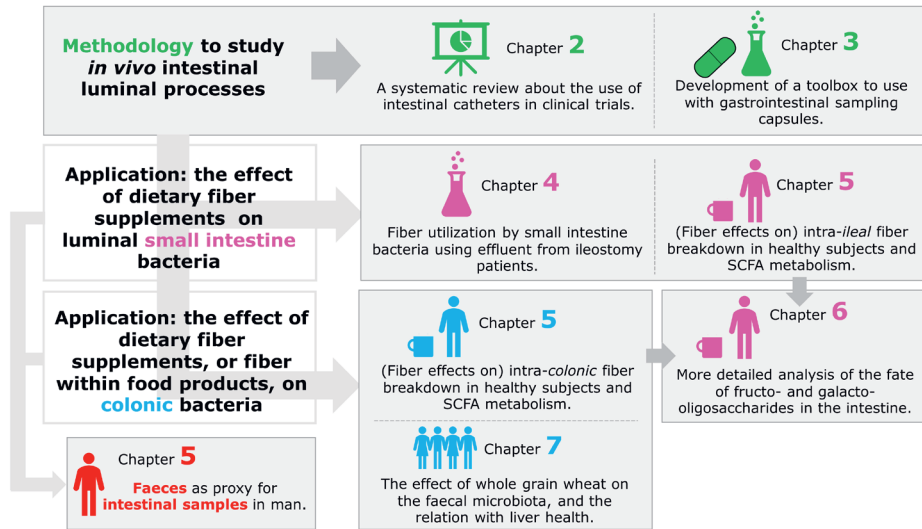


Figure 8. Graphical outline of the thesis.

The research presented in chapters 2 and 3 focuses on methods (development) to study the intestinal lumen of human subjects. Research in chapters 4 focuses on the impact of dietary fibers on the small intestine microbiota. Research in chapter 5 focuses on the impact of dietary fibers (FOS:GOS) on the small and large intestine microbiota and the metabolic fate of short-chain fatty acids. Faeces is used as proxy for intestinal measurements. In chapter 6 the digestibility of all compounds in the FOS and GOS mixtures in the intestine were analysed in detail. Chapter 7 focuses on the effect of whole grain wheat products on the faecal microbiota. Results presented in chapter 3 and 4 originate solely from *in vitro* data.

References

1. The lancet. Life, death, and disability in 2016. *Lancet*. 2017;390(10100):1083.
2. Global nutrition and policy consortium. Dietary intake of major foods by region. 2017 [cited 17 July 2020]. Available from: <https://www.globaldietarydatabase.org/>.
3. Obesity and overweight. World Health Organization. 2020. [updated 1 April 2020; cited 17 July 2020]. Available from: <https://www.who.int/en/news-room/fact-sheets/detail/obesity-and-overweight>.
4. Gezond gewicht. Rijksinstituut voor volksgezondheid en milieu (RIVM). 2020. [cited 17 July 2020]. <https://www.rivm.nl/leefstijlmonitor/gezond-gewicht>.
5. Sherling DH, Perumareddi P, Hennekens CH. Metabolic syndrome. *J Cardiovasc Pharmacol Ther*. 2017;22(4):365-7.
6. Mozumdar A, Liguori G. Persistent increase of prevalence of metabolic syndrome among U.S. Adults: Nhanes iii to Nhanes 1999-2006. *Diabetes Care*. 2011;34(1):216-9.
7. O'Connell JM, Manson SM. Understanding the economic costs of diabetes and prediabetes and what we may learn about reducing the health and economic burden of these conditions. *Diabetes Care*. 2019;42(9):1609-11.
8. Leal J, Luengo-Fernández R, Gray A, Petersen S, Rayner M. Economic burden of cardiovascular diseases in the enlarged european union. *Eur Heart J*. 2006;27(13):1610-9.
9. Miller WC, Niederpruem MG, Wallace JP, Lindeman AK. Dietary fat, sugar, and fiber predict body fat content. *J Am Diet Assoc*. 1994;94(6):612-5.
10. Appleby PN, Thorogood M, Mann JI, Key TJ. Low body mass index in non-meat eaters: The possible roles of animal fat, dietary fibre and alcohol. *Int J Obes Relat Metab Disord*. 1998;22(5):454-60.
11. Kendall CWC, Esfahani A, Jenkins DJA. The link between dietary fibre and human health. *Food Hydrocolloids*. 2010;24(1):42-8.
12. Anderson JW, Baird P, Davis RH, Jr, Ferreri S, Knudtson M, Koraym A, et al. Health benefits of dietary fiber. *Nutr Rev*. 2009;67(4):188-205.
13. Bingham SA, Day NE, Luben R, Ferrari P, Slimani N, Norat T, et al. Dietary fibre in food and protection against colorectal cancer in the european prospective investigation into cancer and nutrition (epic): An observational study. *The Lancet*. 2003;361(9368):1496-501.
14. Koh A, De Vadder F, Kovatcheva-Datchary P, Bäckhed F. From dietary fiber to host physiology: Short-chain fatty acids as key bacterial metabolites. *Cell*. 2016;165(6):1332-45.
15. den Besten G, Havinga R, Bleeker A, Rao S, Gerding A, van Eunen K, et al. The short-chain fatty acid uptake fluxes by mice on a guar gum supplemented diet associate with amelioration of major biomarkers of the metabolic syndrome. *PLoS One*. 2014;9(9):e107392-e.
16. Jones JM. Codex-aligned dietary fiber definitions help to bridge the 'fiber gap'. *Nutr J*. 2014;13(1):34.
17. Alimentarius C. Guidelines on nutrition labelling cac/gl 2-1985 as last amended 2010. Joint FAO/WHO Food Standards Programme, Secretariat of the Codex Alimentarius Commission, FAO, Rome. 2010.
18. Zielinski G, DeVries JW, Craig SA, Bridges AR. Dietary fiber methods in codex alimentarius: Current status and ongoing discussions. *Cereal Food World*. 2013;58:148-53.
19. Gibson GR, Roberfroid MB. Dietary modulation of the human colonic microbiota: Introducing the concept of prebiotics. *J Nutr*. 1995;125(6):1401-12.
20. Gibson GR, Hutkins R, Sanders ME, Prescott SL, Reimer RA, Salminen SJ, et al. Expert consensus document: The international scientific association for probiotics and prebiotics (ISAPP) consensus statement on the definition and scope of prebiotics. *Nat Rev Gastroenterol Hepatol*. 2017;14(8):491-502.
21. Cummings JH, Stephen AM. Carbohydrate terminology and classification. *Eur J Clin Nutr*. 2007;61 Suppl 1:S5-18.

22. Iub-iupac joint commission on biochemical nomenclature (JCBN): Abbreviated terminology of oligosaccharide chains. Recommendations 1980. *J Biol Chem.* 1982;257(7):3347-51.
23. Slavin J, Green H. Dietary fibre and satiety. *Nutr Bull.* 2007;32(s1):32-42.
24. O'Grady J, O'Connor EM, Shanahan F. Review article: Dietary fibre in the era of microbiome science. *Aliment Pharmacol Ther.* 2019;49(5):506-15.
25. Dhingra D, Michael M, Rajput H, Patil RT. Dietary fibre in foods: A review. *J Food Sci Technol.* 2012;49(3):255-66.
26. Zartl B, Silberbauer K, Loeppert R, Viernstein H, Praznik W, Mueller M. Fermentation of non-digestible raffinose family oligosaccharides and galactomannans by probiotics. *Food Funct.* 2018;9(3):1638-46.
27. Rosch C. In vitro fermentation and immunomodulating characteristics of dietary fibres, chapter 1.: Wageningen University; 2016.
28. Shoaib M, Shehzad A, Omar M, Rakha A, Raza H, Sharif HR, et al. Inulin: Properties, health benefits and food applications. *Carbohydr Polym.* 2016;147:444-54.
29. Roberfroid MB, Delzenne NM. Dietary fructans. *Annu Rev Nutr.* 1998;18(1):117-43.
30. Flamm G, Glinsmann W, Kritchevsky D, Prosky L, Roberfroid M. Inulin and oligofructose as dietary fiber: A review of the evidence. *Crit Rev Food Sci Nutr.* 2001;41(5):353-62.
31. Cooper PD, Rajapaksha KH, Barclay TG, Ginic-Markovic M, Gerson AR, Petrovsky N. Inulin crystal initiation via a glucose-fructose cross-link of adjacent polymer chains: Atomic force microscopy and static molecular modelling. *Carbohydr Polym.* 2015;117:964-72.
32. Varney J, Barrett J, Scarlata K, Catsos P, Gibson PR, Muir JG. Foodmaps: Food composition, defining cutoff values and international application. *J Gastroenterol Hepatol.* 2017;32 Suppl 1:53-61.
33. Glibowski P, Skrzypczak K. Chapter 6 - prebiotic and synbiotic foods. In: Holban AM, Grumezescu AM, editors. *Microbial production of food ingredients and additives*: Academic Press; 2017. p. 155-88.
34. Torres DPM, Gonçalves MdPF, Teixeira JA, Rodrigues LR. Galacto-oligosaccharides: Production, properties, applications, and significance as prebiotics. *Compr Rev Food Sci Food Saf.* 2010;9(5):438-54.
35. Logtenberg MJ, Donners KMH, Vink JCM, van Leeuwen SS, de Waard P, de Vos P, et al. Touching the high complexity of prebiotic vivinal galacto-oligosaccharides using porous graphitic carbon ultra-high-performance liquid chromatography coupled to mass spectrometry. *J Agric Food Chem.* 2020.
36. Miller JB, Bull S, Miller J, McVeagh P. The oligosaccharide composition of human milk: Temporal and individual variations in monosaccharide components. *J Pediatr Gastroenterol Nutr.* 1994;19(4):371-6.
37. Brummer Y, Kaviani M, Tosh SM. Structural and functional characteristics of dietary fibre in beans, lentils, peas and chickpeas. *Food Res Int.* 2015;67:117-25.
38. Lim BO, Yamada K, Nonaka M, Kuramoto Y, Hung P, Sugano M. Dietary fibers modulate indices of intestinal immune function in rats. *J Nutr.* 1997;127(5):663-7.
39. Danielle Biscaro Pedrolli ACM, Eleni Gomes, Eleonora Cano Carmona. Pectin and pectinases: Production, characterization and industrial application of microbial pectinolytic enzymes. *Open Biotechnol J.* 2009;3:9-18.
40. Lara-Espinoza C, Carvajal-Millán E, Balandrán-Quintana R, López-Franco Y, Rascón-Chu A. Pectin and pectin-based composite materials: Beyond food texture. *Molecules (Basel, Switzerland).* 2018;23(4):942.
41. Leemhuis H, Dobruchowska JM, Ebbelaar M, Faber F, Buwalda PL, van der Maarel MJ, et al. Isomalto/malto-polysaccharide, a novel soluble dietary fiber made via enzymatic conversion of starch. *J Agric Food Chem.* 2014;62(49):12034-44.
42. Gu F, Borewicz K, Richter B, van der Zaal PH, Smidt H, Buwalda PL, et al. In vitro fermentation behavior of isomalto/malto-polysaccharides using human fecal inoculum indicates prebiotic potential. *Mol Nutr Food Res.* 2018;62(12):1800232.

43. Frølich W, Aman P, Tetens I. Whole grain foods and health - a Scandinavian perspective. *Food Nutr Res.* 2013;57:10.3402/fnr.v57i0.18503.
44. Montané D, Farriol X, Salvadó J, Jollez P, Chornet E. Fractionation of wheat straw by steam-explosion pretreatment and alkali delignification. Cellulose pulp and byproducts from hemicellulose and lignin. *J Wood Chem Technol.* 1998;18(2):171-91.
45. Cosgrove DJ. Growth of the plant cell wall. *Nat Rev Mol Cell Biol.* 2005;6(11):850-61.
46. Tosh SM, Brummer Y, Wood PJ, Wang Q, Weisz J. Evaluation of structure in the formation of gels by structurally diverse (1→3)(1→4)-β-d-glucans from four cereal and one lichen species. *Carbohydr Polym.* 2004;57(3):249-59.
47. Cassie Anderson SS. What are the characteristics of arabinoxylan gels? *Food Sci Nutr.* 2018;9(7):818-33.
48. Kiszonas AM, Fuerst EP, Morris CF. Wheat arabinoxylan structure provides insight into function. *Cereal Chem.* 2013;90(4):387-95.
49. Dimmel D. Lignin and lignans. *Advances in chemistry.* Chapter 1.: CRC Press, Boca Raton, FL, USA 2010.
50. Sela DA, Mills DA. Nursing our microbiota: Molecular linkages between bifidobacteria and milk oligosaccharides. *Trends Microbiol.* 2010;18(7):298-307.
51. Yang Y, Zhao L-G, Wu Q-J, Ma X, Xiang Y-B. Association between dietary fiber and lower risk of all-cause mortality: A meta-analysis of cohort studies. *Am J Epidemiol.* 2015;181(2):83-91.
52. Reynolds A, Mann J, Cummings J, Winter N, Mete E, Te Morenga L. Carbohydrate quality and human health: A series of systematic reviews and meta-analyses. *The Lancet.* 2019;393(10170):434-45.
53. Authority EEFS. Scientific opinion on dietary reference values for carbohydrates and dietary fibre. Efsa panel on dietetic products, nutrition, and allergies (nda). *Efsa Journal.* 2010;8(3):1462.
54. Voedingscentrum. Voedingsvezels: Voedingscentrum Nederland. [cited 17-07-2020]. Available from: <https://www.voedingscentrum.nl/encyclopedie/vezels.aspx>.
55. Rossum CTMv, Buurma-Rethans EJM, Dinnissen CS, Beukers MH, Brants HAM, Dekkers ALM, et al. The diet of the dutch: Results of the Dutch national food consumption. Survey 2012-2016. 2020.
56. Kirby RW, Anderson JW, Sieling B, Rees ED, Chen WJ, Miller RE, et al. Oat-bran intake selectively lowers serum low-density lipoprotein cholesterol concentrations of hypercholesterolemic men. *Am J Clin Nutr.* 1981;34(5):824-9.
57. Lightowler H, Thondre S, Holz A, Theis S. Replacement of glycaemic carbohydrates by inulin-type fructans from chicory (oligofructose, inulin) reduces the postprandial blood glucose and insulin response to foods: Report of two double-blind, randomized, controlled trials. *Eur J Nutr.* 2018;57(3):1259-68.
58. Eswaran S, Muir J, Chey WD. Fiber and functional gastrointestinal disorders. *Am J Gastroenterol.* 2013;108(5):718-27.
59. Bischoff SC. 'Gut health': A new objective in medicine? *BMC Med.* 2011;9(1):24.
60. Tomlin J, Read NW. Laxative properties of indigestible plastic particles. *BMJ (Clinical research ed).* 1988;297(6657):1175-6.
61. Lewis SJ, Heaton KW. Roughage revisited: The effect on intestinal function of inert plastic particles of different sizes and shape. *Dig Dis Sci.* 1999;44(4):744-8.
62. So D, Gibson PR, Muir JG, Yao CK. Dietary fibres and ibs: Translating functional characteristics to clinical value in the era of personalised medicine. *Gut.* 2021;70(12):2383-94.
63. Stephen AM, Cummings JH. Mechanism of action of dietary fibre in the human colon. *Nature.* 1980;284(5753):283-4.
64. McRorie J, Pepple S, Rudolph C. Effects of fiber laxatives and calcium docusate on regional water content and viscosity of digesta in the large intestine of the pig. *Dig Dis Sci.* 1998;43(4):738-45.
65. Tan J, McKenzie C, Potamitis M, Thorburn AN, Mackay CR, Macia L. The role of short-chain fatty acids in health and disease. *Adv Immunol.* 2014;121:91-119.

66. Watson D, O'Connell Motherway M, Schoterman MH, van Neerven RJ, Nauta A, van Sinderen D. Selective carbohydrate utilization by lactobacilli and bifidobacteria. *J Appl Microbiol.* 2013;114(4):1132-46.
67. Verkhnyatskaya S, Ferrari M, de Vos P, Walvoort MTC. Shaping the infant microbiome with non-digestible carbohydrates. *Front Microbiol.* 2019;10:343.
68. Scheid MM, Genaro PS, Moreno YM, Pastore GM. Freeze-dried powdered yacon: Effects of fos on serum glucose, lipids and intestinal transit in the elderly. *Eur J Nutr.* 2014;53(7):1457-64.
69. Dewulf EM, Cani PD, Claus SP, Fuentes S, Puylaert PG, Neyrinck AM, et al. Insight into the prebiotic concept: Lessons from an exploratory, double blind intervention study with inulin-type fructans in obese women. *Gut.* 2013;62(8):1112-21.
70. Dehghan P, Pourghassem Gargari B, Asghari Jafar-abadi M. Oligofructose-enriched inulin improves some inflammatory markers and metabolic endotoxemia in women with type 2 diabetes mellitus: A randomized controlled clinical trial. *Nutrition.* 2014;30(4):418-23.
71. Healey G, Murphy R, Butts C, Brough L, Whelan K, Coad J. Habitual dietary fibre intake influences gut microbiota response to an inulin-type fructan prebiotic: A randomised, double-blind, placebo-controlled, cross-over, human intervention study. *Br J Nutr.* 2018;119(2):176-89.
72. Vulevic J, Juric A, Walton GE, Claus SP, Tzortzis G, Toward RE, et al. Influence of galacto-oligosaccharide mixture (b-gos) on gut microbiota, immune parameters and metabonomics in elderly persons. *Br J Nutr.* 2015;114(4):586-95.
73. Vulevic J, Juric A, Tzortzis G, Gibson GR. A mixture of trans-galactooligosaccharides reduces markers of metabolic syndrome and modulates the fecal microbiota and immune function of overweight adults. *J Nutr.* 2013;143(3):324-31.
74. Davis LMG, Martínez I, Walter J, Goin C, Hutkins RW. Barcoded pyrosequencing reveals that consumption of galactooligosaccharides results in a highly specific bifidogenic response in humans. *PLoS One.* 2011;6(9):e25200.
75. Morel FB, Dai Q, Ni J, Thomas D, Parnet P, Faça-Berthon P. A-galacto-oligosaccharides dose-dependently reduce appetite and decrease inflammation in overweight adults. *J Nutr.* 2015;145(9):2052-9.
76. Chambers ES, Byrne CS, Morrison DJ, Murphy KG, Preston T, Tedford C, et al. Dietary supplementation with inulin-propionate ester or inulin improves insulin sensitivity in adults with overweight and obesity with distinct effects on the gut microbiota, plasma metabolome and systemic inflammatory responses: A randomised cross-over trial. *Gut.* 2019;68(8):1430-8.
77. Zhang W, Tang Y, Huang J, Yang Y, Yang Q, Hu H. Efficacy of inulin supplementation in improving insulin control, hba1c and homa-ir in patients with type 2 diabetes: A systematic review and meta-analysis of randomized controlled trials. *J Clin Biochem Nutr.* 2020;66(3):176-83.
78. Wang L, Yang H, Huang H, Zhang C, Zuo HX, Xu P, et al. Inulin-type fructans supplementation improves glycemic control for the prediabetes and type 2 diabetes populations: Results from a grade-assessed systematic review and dose-response meta-analysis of 33 randomized controlled trials. *J Transl Med.* 2019;17(1):410.
79. Liu F, Prabhakar M, Ju J, Long H, Zhou HW. Effect of inulin-type fructans on blood lipid profile and glucose level: A systematic review and meta-analysis of randomized controlled trials. *Eur J Clin Nutr.* 2017;71(1):9-20.
80. Rao M, Gao C, Xu L, Jiang L, Zhu J, Chen G, et al. Effect of inulin-type carbohydrates on insulin resistance in patients with type 2 diabetes and obesity: A systematic review and meta-analysis. *J Diabetes Res.* 2019;2019:5101423.
81. Hiel S, Bindels LB, Pachikian BD, Kalala G, Broers V, Zamariola G, et al. Effects of a diet based on inulin-rich vegetables on gut health and nutritional behavior in healthy humans. *Am J Clin Nutr.* 2019;109(6):1683-95.
82. Swanson KS, de Vos WM, Martens EC, Gilbert JA, Menon RS, Soto-Vaca A, et al. Effect of fructans, prebiotics and fibres on the human gut microbiome assessed by 16s rRNA-based approaches: A review. *Benef Microbes.* 2020;11(2):101-29.

83. Le Bastard Q, Chapelet G, Javaudin F, Lepelletier D, Batard E, Montassier E. The effects of inulin on gut microbial composition: A systematic review of evidence from human studies. *Eur J Clin Microbiol Infect Dis*. 2020;39(3):403-13.
84. Reimer RA, Soto-Vaca A, Nicolucci AC, Mayengbam S, Park H, Madsen KL, et al. Effect of chicory inulin-type fructan-containing snack bars on the human gut microbiota in low dietary fiber consumers in a randomized crossover trial. *Am J Clin Nutr*. 2020;111(6):1286-96.
85. Watson AW, Houghton D, Avery PJ, Stewart C, Vaughan EE, Meyer PD, et al. Changes in stool frequency following chicory inulin consumption, and effects on stool consistency, quality of life and composition of gut microbiota. *Food Hydrocoll*. 2019;96:688-98.
86. Micka A, Siepelmeyer A, Holz A, Theis S, Schön C. Effect of consumption of chicory inulin on bowel function in healthy subjects with constipation: A randomized, double-blind, placebo-controlled trial. *Int J Food Sci Nutr*. 2017;68(1):82-9.
87. Collado Yurrita L, San Mauro Martín I, Ciudad-Cabañas MJ, Calle-Purón ME, Hernández Cabria M. Effectiveness of inulin intake on indicators of chronic constipation; a meta-analysis of controlled randomized clinical trials. *Nutr Hosp*. 2014;30(2):244-52.
88. EFSA Panel on Dietetic Products NA. Scientific opinion on the substantiation of a health claim related to “native chicory inulin” and maintenance of normal defecation by increasing stool frequency pursuant to article 13.5 of regulation (ec) no 1924/2006. *EFSA Journal*. 2015;13(1):3951.
89. De Vries J, Le Bourgot C, Calame W, Respondek F. Effects of β -fructans fiber on bowel function: A systematic review and meta-analysis. *Nutrients*. 2019;11(1):91.
90. Canfora EE, van der Beek CM, Hermes GDA, Goossens GH, Jocken JWE, Holst JJ, et al. Supplementation of diet with galacto-oligosaccharides increases bifidobacteria, but not insulin sensitivity, in obese prediabetic individuals. *Gastroenterology*. 2017;153(1):87-97.e3.
91. Pedersen C, Gallagher E, Horton F, Ellis RJ, Ijaz UZ, Wu H, et al. Host–microbiome interactions in human type 2 diabetes following prebiotic fibre (galacto-oligosaccharide) intake. *Br J Nutr*. 2016;116(11):1869-77.
92. Walton GE, van den Heuvel EGHM, Kusters MHW, Rastall RA, Tuohy KM, Gibson GR. A randomised crossover study investigating the effects of galacto-oligosaccharides on the faecal microbiota in men and women over 50 years of age. *Br J Nutr*. 2012;107(10):1466-75.
93. Bikel S, Valdez-Lara A, Cornejo-Granados F, Rico K, Canizales-Quinteros S, Soberón X, et al. Combining metagenomics, metatranscriptomics and viromics to explore novel microbial interactions: Towards a systems-level understanding of human microbiome. *Comput Struct Biotechnol J*. 2015;13:390-401.
94. O’Hara AM, Shanahan F. The gut flora as a forgotten organ. *EMBO reports*. 2006;7(7):688-93.
95. Spor A, Koren O, Ley R. Unravelling the effects of the environment and host genotype on the gut microbiome. *Nat Rev Microbiol*. 2011;9(4):279-90.
96. Kastl AJ, Terry NA, Wu GD, Albenberg LG. The structure and function of the human small intestinal microbiota: Current understanding and future directions. *Cell Mol Gastroenterol Hepatol*. 2020;9(1):33-45.
97. Turnbaugh PJ, Ley RE, Mahowald MA, Magrini V, Mardis ER, Gordon JI. An obesity-associated gut microbiome with increased capacity for energy harvest. *Nature*. 2006;444(7122):1027-31.
98. Ridaura VK, Faith JJ, Rey FE, Cheng J, Duncan AE, Kau AL, et al. Gut microbiota from twins discordant for obesity modulate metabolism in mice. *Science*. 2013;341(6150):1241214.
99. Rabot S, Membrez M, Bruneau A, Gérard P, Harach T, Moser M, et al. Germ-free c57bl/6j mice are resistant to high-fat-diet-induced insulin resistance and have altered cholesterol metabolism. *FASEB J*. 2010;24(12):4948-59.
100. Vrieze A, Van Nood E, Holleman F, Salojärvi J, Kootte RS, Bartelsman JFWM, et al. Transfer of intestinal microbiota from lean donors increases insulin sensitivity in individuals with metabolic syndrome. *Gastroenterology*. 2012;143(4):913-6.e7.
101. Sender R, Fuchs S, Milo R. Revised estimates for the number of human and bacteria cells in the body. *PLoS Biol*. 2016;14(8):e1002533-e.

102. Sekirov I, Russell SL, Antunes LCM, Finlay BB. Gut microbiota in health and disease. *Physiol Rev.* 2010;90(3):859-904.
103. Stearns JC, Lynch MDJ, Senadheera DB, Tenenbaum HC, Goldberg MB, Cvitkovitch DG, et al. Bacterial biogeography of the human digestive tract. *Sci Rep.* 2011;1(1):170.
104. Eckburg PB, Bik EM, Bernstein CN, Purdom E, Dethlefsen L, Sargent M, et al. Diversity of the human intestinal microbial flora. *Science.* 2005;308(5728):1635-8.
105. Huttenhower C, Gevers D, Knight R, Abubucker S, Badger JH, Chinwalla AT, et al. Structure, function and diversity of the healthy human microbiome. *Nature.* 2012;486(7402):207-14.
106. Segata N, Haake SK, Mannon P, Lemon KP, Waldron L, Gevers D, et al. Composition of the adult digestive tract bacterial microbiome based on seven mouth surfaces, tonsils, throat and stool samples. *Genome Biol.* 2012;13(6):R42.
107. Wang M, Ahrné S, Jeppsson B, Molin G. Comparison of bacterial diversity along the human intestinal tract by direct cloning and sequencing of 16S rRNA genes. *FEMS Microbiol Ecol.* 2005;54(2):219-31.
108. Hayashi H, Takahashi R, Nishi T, Sakamoto M, Benno Y. Molecular analysis of jejunal, ileal, caecal and recto-sigmoidal human colonic microbiota using 16s rRNA gene libraries and terminal restriction fragment length polymorphism. *J Med Microbiol.* 2005;54(Pt 11):1093-101.
109. Thadepalli H, Lou SMA, Bach VT, Matsui TK, Mandal AK. Microflora of the human small intestine. *Am J Surg.* 1979;138(6):845-50.
110. Zoetendal EG, Raes J, van den Bogert B, Arumugam M, Booijink CCGM, Troost FJ, et al. The human small intestinal microbiota is driven by rapid uptake and conversion of simple carbohydrates. *ISME J.* 2012;6(7):1415-26.
111. Booijink CCGM, El-Aidy S, Rajilić-Stojanović M, Heilig HGHJ, Troost FJ, Smidt H, et al. High temporal and inter-individual variation detected in the human ileal microbiota. *Environ Microbiol.* 2010;12(12):3213-27.
112. van den Bogert B, Erkus O, Boekhorst J, de Goffau M, Smid EJ, Zoetendal EG, et al. Diversity of human small intestinal streptococcus and veillonella populations. *FEMS Microbiol Ecol.* 2013;85(2):376-88.
113. Payne AN, Zihler A, Chassard C, Lacroix C. Advances and perspectives in in vitro human gut fermentation modeling. *Trends Biotechnol.* 2012;30(1):17-25.
114. Clarke G, Sandhu KV, Griffin BT, Dinan TG, Cryan JF, Hyland NP. Gut reactions: Breaking down xenobiotic-microbiome interactions. *Pharmacol Rev.* 2019;71(2):198-224.
115. Falony G, Joossens M, Vieira-Silva S, Wang J, Darzi Y, Faust K, et al. Population-level analysis of gut microbiome variation. *Science.* 2016;352(6285):560-4.
116. De Filippo C, Cavalieri D, Di Paola M, Ramazzotti M, Poullet JB, Massart S, et al. Impact of diet in shaping gut microbiota revealed by a comparative study in children from Europe and rural Africa. *PNAS.* 2010;107(33):14691-6.
117. Wu GD, Chen J, Hoffmann C, Bittinger K, Chen Y-Y, Keilbaugh SA, et al. Linking long-term dietary patterns with gut microbial enterotypes. *Science.* 2011;334(6052):105-8.
118. Asnicar F, Berry SE, Valdes AM, Nguyen LH, Piccinno G, Drew DA, et al. Microbiome connections with host metabolism and habitual diet from 1,098 deeply phenotyped individuals. *Nat Med.* 2021;27(2):321-32.
119. Zimmer J, Lange B, Frick JS, Sauer H, Zimmermann K, Schwiertz A, et al. A vegan or vegetarian diet substantially alters the human colonic faecal microbiota. *Eur J Clin Nutr.* 2012;66(1):53-60.
120. Vangay P, Johnson AJ, Ward TL, Al-Ghalith GA, Shields-Cutler RR, Hillmann BM, et al. US immigration westernizes the human gut microbiome. *Cell.* 2018;175(4):962-72. e10.
121. Claesson MJ, Jeffery IB, Conde S, Power SE, O'connor EM, Cusack S, et al. Gut microbiota composition correlates with diet and health in the elderly. *Nature.* 2012;488(7410):178-84.
122. David LA, Maurice CF, Carmody RN, Gootenberg DB, Button JE, Wolfe BE, et al. Diet rapidly and reproducibly alters the human gut microbiome. *Nature.* 2014;505(7484):559-63.

123. Zoetendal EG, de Vos WM. Effect of diet on the intestinal microbiota and its activity. *Curr Opin Gastroenterol.* 2014;30(2).
124. Scott KP, Duncan SH, Flint HJ. Dietary fibre and the gut microbiota. *Nutr Bull.* 2008;33(3):201-11.
125. Graf D, Di Cagno R, Fåk F, Flint HJ, Nyman M, Saarela M, et al. Contribution of diet to the composition of the human gut microbiota. *Microb Ecol Health Dis.* 2015;26(1):26164.
126. El Aidy S, van den Bogert B, Kleerebezem M. The small intestine microbiota, nutritional modulation and relevance for health. *Curr Opin Biotechnol.* 2015;32:14-20.
127. Kleerebezem M. Microbial metabolic gatekeeping in the jejunum. *Nat Microbiol.* 2018;3(6):650-1.
128. Clarke G, Stilling RM, Kennedy PJ, Stanton C, Cryan JF, Dinan TG. Minireview: Gut microbiota: The neglected endocrine organ. *Molecular endocrinology (Baltimore, Md).* 2014;28(8):1221-38.
129. Krautkramer KA, Fan J, Bäckhed F. Gut microbial metabolites as multi-kingdom intermediates. *Nat Rev Microbiol.* 2021;19(2):77-94.
130. Müller V. Bacterial fermentation. e LS. 2001.
131. Cummings J, Macfarlane G. The control and consequences of bacterial fermentation in the human colon. *J Appl Bacteriol.* 1991;70(6):443-59.
132. Montagne L, Pluske JR, Hampson DJ. A review of interactions between dietary fibre and the intestinal mucosa, and their consequences on digestive health in young non-ruminant animals. *Anim Feed Sci Technol.* 2003;108(1):95-117.
133. Jonathan MC, van den Borne JJGC, van Wiechen P, Souza da Silva C, Schols HA, Gruppen H. In vitro fermentation of 12 dietary fibres by faecal inoculum from pigs and humans. *Food Chem.* 2012;133(3):889-97.
134. Kaoutari AE, Armougom F, Gordon JI, Raoult D, Henrissat B. The abundance and variety of carbohydrate-active enzymes in the human gut microbiota. *Nat Rev Microbiol.* 2013;11(7):497-504.
135. Cantarel BL, Lombard V, Henrissat B. Complex carbohydrate utilization by the healthy human microbiome. *PLoS One.* 2012;7(6):e28742.
136. Ferreira-Lazarte A, Moreno FJ, Villamiel M. Bringing the digestibility of prebiotics into focus: Update of carbohydrate digestion models. *Crit Rev Food Sci Nutr.* 2020:1-12.
137. Goh YJ, Klaenhammer TR. Genetic mechanisms of prebiotic oligosaccharide metabolism in probiotic microbes. *Annu Rev Food Sci Technol.* 2015;6(1):137-56.
138. Amaretti A, Bernardi T, Tamburini E, Zannoni S, Lomma M, Matteuzzi D, et al. Kinetics and metabolism of *Bifidobacterium adolescentis* mb 239 growing on glucose, galactose, lactose, and galactooligosaccharides. *Appl Environ Microbiol.* 2007;73(11):3637.
139. Singh RS, Chauhan K, Kennedy JF. A panorama of bacterial inulinases: Production, purification, characterization and industrial applications. *Int J Biol Macromol.* 2017;96:312-22.
140. Macfarlane G, Gibson G, Cummings J. Comparison of fermentation reactions in different regions of the human colon. *J Appl Bacteriol.* 1992;72(1):57-64.
141. Cummings JH, Englyst HN. Fermentation in the human large intestine and the available substrates. *Am J Clin Nutr.* 1987;45(5):1243-55.
142. Louis P, Scott KP, Duncan SH, Flint HJ. Understanding the effects of diet on bacterial metabolism in the large intestine. *J Appl Microbiol.* 2007;102(5):1197-208.
143. den Besten G, van Eunen K, Groen AK, Venema K, Reijngoud DJ, Bakker BM. The role of short-chain fatty acids in the interplay between diet, gut microbiota, and host energy metabolism. *J Lipid Res.* 2013;54(9):2325-40.
144. Miller TL, Wolin MJ. Pathways of acetate, propionate, and butyrate formation by the human fecal microbial flora. *Appl Environ Microbiol.* 1996;62(5):1589-92.
145. Xiao S, Jiang S, Qian D, Duan J. Modulation of microbially derived short-chain fatty acids on intestinal homeostasis, metabolism, and neuropsychiatric disorder. *Appl Microbiol Biotechnol.* 2020;104(2):589-601.

146. Macfarlane GT, Macfarlane S. Human colonic microbiota: Ecology, physiology and metabolic potential of intestinal bacteria. *Scand J Gastroenterol Suppl.* 1997;222:3-9.
147. de Lacy Costello B, Ledochowski M, Ratzliffe NM. The importance of methane breath testing: A review. *J Breath Res.* 2013;7(2):024001.
148. Rossi M, Corradini C, Amaretti A, Nicolini M, Pompei A, Zanoni S, et al. Fermentation of fructooligosaccharides and inulin by bifidobacteria: A comparative study of pure and fecal cultures. *Appl Environ Microbiol.* 2005;71(10):6150-8.
149. Flint HJ, Duncan SH, Scott KP, Louis P. Interactions and competition within the microbial community of the human colon: Links between diet and health. *Environ Microbiol.* 2007;9(5):1101-11.
150. Besten Gd, Lange K, Havinga R, Dijk THv, Gerding A, Eunen Kv, et al. Gut-derived short-chain fatty acids are vividly assimilated into host carbohydrates and lipids. *Am J Physiol Gastrointest Liver Physiol.* 2013;305(12):G900-G10.
151. Samuel BS, Gordon JI. A humanized gnotobiotic mouse model of host–archaeal–bacterial mutualism. *PNAS.* 2006;103(26):10011-6.
152. Duncan SH, Holtrop G, Lobley GE, Calder AG, Stewart CS, Flint HJ. Contribution of acetate to butyrate formation by human faecal bacteria. *Br J Nutr.* 2004;91(6):915-23.
153. Boets E, Gomand SV, Deroover L, Preston T, Vermeulen K, De Preter V, et al. Systemic availability and metabolism of colonic-derived short-chain fatty acids in healthy subjects: A stable isotope study. *J Physiol.* 2017;595(2):541-55.
154. Blaak EE, Canfora EE, Theis S, Frost G, Groen AK, Mithieux G, et al. Short chain fatty acids in human gut and metabolic health. *Benef Microbes.* 2020;11(5):411-55.
155. Bose S, Ramesh V, Locasale JW. Acetate metabolism in physiology, cancer, and beyond. *Trends Cell Biol.* 2019;29(9):695-703.
156. Macfarlane GT, Macfarlane S. Bacteria, colonic fermentation, and gastrointestinal health. *J AOAC Int.* 2012;95(1):50-60.
157. Canfora EE, Jocken JW, Blaak EE. Short-chain fatty acids in control of body weight and insulin sensitivity. *Nat Rev Endocrinol.* 2015;11(10):577-91.
158. Müller M, Hernández MAG, Goossens GH, Reijnders D, Holst JJ, Jocken JWE, et al. Circulating but not faecal short-chain fatty acids are related to insulin sensitivity, lipolysis and glp-1 concentrations in humans. *Sci Rep.* 2019;9(1):12515.
159. Dalile B, Van Oudenhove L, Vervliet B, Verbeke K. The role of short-chain fatty acids in microbiota-gut-brain communication. *Nat Rev Gastroenterol Hepatol.* 2019;16(8):461-78.
160. Schönfeld P, Wojtczak L. Short- and medium-chain fatty acids in energy metabolism: The cellular perspective. *J Lipid Res.* 2016;57(6):943-54.
161. Bloemen JG, Venema K, van de Poll MC, Olde Damink SW, Buurman WA, Dejong CH. Short chain fatty acids exchange across the gut and liver in humans measured at surgery. *Clin Nutr.* 2009;28(6):657-61.
162. Khan S, Jena G. Sodium butyrate reduces insulin-resistance, fat accumulation and dyslipidemia in type-2 diabetic rat: A comparative study with metformin. *Chem Biol Interact.* 2016;254:124-34.
163. Hong J, Jia Y, Pan S, Jia L, Li H, Han Z, et al. Butyrate alleviates high fat diet-induced obesity through activation of adiponectin-mediated pathway and stimulation of mitochondrial function in the skeletal muscle of mice. *Oncotarget.* 2016;7(35):56071-82.
164. Henagan TM, Stefanska B, Fang Z, Navard AM, Ye J, Lenard NR, et al. Sodium butyrate epigenetically modulates high-fat diet-induced skeletal muscle mitochondrial adaptation, obesity and insulin resistance through nucleosome positioning. *Br J Pharmacol.* 2015;172(11):2782-98.
165. Pomare EW, Branch WJ, Cummings JH. Carbohydrate fermentation in the human colon and its relation to acetate concentrations in venous blood. *The Journal of clinical investigation.* 1985;75(5):1448-54.
166. Tollinger CD, Vreman HJ, Weiner MW. Measurement of acetate in human blood by gas chromatography: Effects of sample preparation, feeding, and various diseases. *Clin Chem.* 1979;25(10):1787-90.

167. Richards RH, Dowling JA, Vreman HJ, Feldman C, Weiner MW. Acetate levels in human plasma. *Proc Clin Dial Transplant Forum.* 1976;6:73-9.
168. Knowles SE, Jarrett IG, Filsell OH, Ballard FJ. Production and utilization of acetate in mammals. *Biochem J.* 1974;142(2):401-11.
169. Scheppach W, Pomare EW, Elia M, Cummings JH. The contribution of the large intestine to blood acetate in man. *Clin Sci.* 1991;80(2):177-82.
170. Ballard FJ. Supply and utilization of acetate in mammals. *Am J Clin Nutr.* 1972;25(8):773-9.
171. Mueller NT, Zhang M, Juraschek SP, Miller ER, 3rd, Appel LJ. Effects of high-fiber diets enriched with carbohydrate, protein, or unsaturated fat on circulating short chain fatty acids: Results from the omniheart randomized trial. *Am J Clin Nutr.* 2020;111(3):545-54.
172. Cummings JH, Pomare EW, Branch WJ, Naylor CP, Macfarlane GT. Short chain fatty acids in human large intestine, portal, hepatic and venous blood. *Gut.* 1987;28(10):1221-7.
173. Boets E, Deroover L, Houben E, Vermeulen K, Gomand SV, Delcour JA, et al. Quantification of in vivo colonic short chain fatty acid production from inulin. *Nutrients.* 2015;7(11):8916-29.
174. Wong JM, de Souza R, Kendall CW, Emam A, Jenkins DJ. Colonic health: Fermentation and short chain fatty acids. *J Clin Gastroenterol.* 2006;40(3):235-43.
175. Kimura I, Ichimura A, Ohue-Kitano R, Igarashi M. Free fatty acid receptors in health and disease. *Physiol Rev.* 2020;100(1):171-210.
176. McNabney SM, Henagan TM. Short chain fatty acids in the colon and peripheral tissues: A focus on butyrate, colon cancer, obesity and insulin resistance. *Nutrients.* 2017;9(12):1348.
177. Janssen AWF, Kersten S. The role of the gut microbiota in metabolic health. *FASEB J.* 2015;29(8):3111-23.
178. Schmitt MG, Jr., Soergel KH, Wood CM, Steff JJ. Absorption of short-chain fatty acids from the human ileum. *Am J Dig Dis.* 1977;22(4):340-7.
179. Jouet P, Moussata D, Duboc H, Boschetti G, Attar A, Gorbachev C, et al. Effect of short-chain fatty acids and acidification on the phasic and tonic motor activity of the human colon. *Neurogastroenterol Motil.* 2013;25(12):943-9.
180. Weinman EO, Strisower EH, Chaikoff IL. Conversion of fatty acids to carbohydrate; application of isotopes to this problem and role of the krebs cycle as a synthetic pathway. *Physiol Rev.* 1957;37(2):252-72.
181. De Preter V, Arijis I, Windey K, Vanhove W, Vermeire S, Schuit F, et al. Impaired butyrate oxidation in ulcerative colitis is due to decreased butyrate uptake and a defect in the oxidation pathway. *Inflamm Bowel Dis.* 2012;18(6):1127-36.
182. Vasapolli R, Schütte K, Schulz C, Vital M, Schomburg D, Pieper DH, et al. Analysis of transcriptionally active bacteria throughout the gastrointestinal tract of healthy individuals. *Gastroenterology.* 2019;157(4):1081-92.e3.
183. Tang Q, Jin G, Wang G, Liu T, Liu X, Wang B, et al. Current sampling methods for gut microbiota: A call for more precise devices. *Front Cell Infect Microbiol.* 2020;10:151.
184. Rezaei Nejad H, Oliveira BCM, Sadeqi A, Dehkharghani A, Kondova I, Langermans JAM, et al. Ingestible osmotic pill for in vivo sampling of gut microbiomes. *Adv Intell Syst* 2019;1(5):1900053.
185. Lund EK, Johnson IT. Fermentable carbohydrate reaching the colon after ingestion of oats in humans. *J Nutr.* 1991;121(3):311-7.
186. Boll EV, Ekstrom LM, Courtin CM, Delcour JA, Nilsson AC, Bjorck IM, et al. Effects of wheat bran extract rich in arabinoxylan oligosaccharides and resistant starch on overnight glucose tolerance and markers of gut fermentation in healthy young adults. *Eur J Nutr.* 2016;55(4):1661-70.
187. Ibrugger S, Vigsnaes LK, Blennow A, Skuffic D, Raben A, Lauritzen L, et al. Second meal effect on appetite and fermentation of wholegrain rye foods. *Appetite.* 2014;80:248-56.
188. Fernandes J, Vogt J, Wolever TM. Inulin increases short-term markers for colonic fermentation similarly in healthy and hyperinsulinaemic humans. *Eur J Clin Nutr.* 2011;65(12):1279-86.

189. Deroover L, Verspreet J, Luypaerts A, Vandermeulen G, Courtin CM, Verbeke K. Wheat bran does not affect postprandial plasma short-chain fatty acids from (13)C-inulin fermentation in healthy subjects. *Nutrients*. 2017;9(1).
190. Rahat-Rozenbloom S, Fernandes J, Cheng J, Wolever TMS. Acute increases in serum colonic short-chain fatty acids elicited by inulin do not increase GLP-1 or PYY responses but may reduce ghrelin in lean and overweight humans. *Eur J Clin Nutr*. 2017;71(8):953-8.
191. Aguirre M, Bussolo de Souza C, Venema K. The gut microbiota from lean and obese subjects contribute differently to the fermentation of arabinogalactan and inulin. *PLoS One*. 2016;11(7):e0159236.
192. Nissen L, Casciano F, Gianotti A. Intestinal fermentation in vitro models to study food-induced gut microbiota shift: An updated review. *FEMS Microbiol Lett*. 2020;367(12).
193. Pompei A, Cordisco L, Raimondi S, Amaretti A, Pagnoni UM, Matteuzzi D, et al. In vitro comparison of the prebiotic effects of two inulin-type fructans. *Anaerobe*. 2008;14(5):280-6.
194. Venema K, van den Abbeele P. Experimental models of the gut microbiome. *Best Pract Res Clin Gastroenterol*. 2013;27(1):115-26.
195. Van den Abbeele P, Grootaert C, Marzorati M, Possemiers S, Verstraete W, Gérard P, et al. Microbial community development in a dynamic gut model is reproducible, colon region specific, and selective for bacteroidetes and clostridium cluster ix. *Appl Environ Microbiol*. 2010;76(15):5237-46.
196. Venema K. The tno in vitro model of the colon (tim-2). In: Verhoeckx K, Cotter P, López-Expósito I, Kleiveland C, Lea T, Mackie A, et al., editors. *The impact of food bioactives on health: In vitro and ex vivo models*. Cham: Springer International Publishing; 2015. p. 293-304.
197. Neis EP, van Eijk HM, Lenaerts K, Olde Damink SW, Blaak EE, Dejong CH, et al. Distal versus proximal intestinal short-chain fatty acid release in man. *Gut*. 2019;68(4):764-5.
198. Bloemen JG, Olde Damink SW, Venema K, Buurman WA, Jalan R, Dejong CH. Short chain fatty acids exchange: Is the cirrhotic, dysfunctional liver still able to clear them? *Clin Nutr*. 2010;29(3):365-9.
199. Dankert J, Zijlstra JB, Wolthers BG. Volatile fatty acids in human peripheral and portal blood: Quantitative determination by vacuum distillation and gas chromatography. *Clin Chim Acta*. 1981;110(2):301-7.



Using naso- and oro-intestinal catheters in physiological research for intestinal delivery and sampling *in vivo*: practical and technical aspects to be considered

Mara P.H. van Trijp¹, Ellen Wilms², Melany Ríos-Morales³, Ad A.M. Masclee², Robert Jan Brummer⁴, Ben J.M. Witteman^{1,5}, Freddy J. Troost^{2,6}, Guido J.E.J. Hooiveld¹

¹ Division of Human Nutrition and Health, Wageningen University, the Netherlands

² Division Gastroenterology-Hepatology, Department of Internal Medicine; NUTRIM School of Nutrition and Translational Research in Metabolism, Maastricht University, the Netherlands

³ Laboratory of Pediatrics, University of Groningen, University Medical Center Groningen, the Netherlands

⁴ Nutrition-Gut-Brain Interactions Research Centre, School of Medical Sciences, Faculty of Medicine and Health, Örebro University, Sweden

⁵ Hospital Gelderse Vallei, Department of Gastroenterology and Hepatology, Ede, the Netherlands

⁶ Food Innovation and Health, Centre for Healthy Eating and Food Innovation, Maastricht University, the Netherlands

Abstract

Intestinal catheters are used for decades in human nutrition, physiology, pharmacokinetics, and gut microbiome research, facilitating the delivery of compounds directly into the intestinal lumen or the aspiration of intestinal fluids in human subjects. Such research provides insights about (local) dynamic metabolic and other intestinal luminal processes, but working with catheters might pose challenges to biomedical researchers and clinicians. Here, we provide an overview of practical and technical aspects of applying naso- and oro-intestinal catheters for delivery of compounds and sampling luminal fluids from the jejunum, ileum and colon *in vivo*. The recent literature was extensively reviewed, and we have included experiences and insights gained through our clinical trials. 60 studies were included that involved a total of 720 healthy subjects and 42 patients. Most of the studies investigated multiple intestinal regions (24 studies), followed by only the jejunum (21 studies), ileum (13 studies), or colon (2 studies), of which the ileum and colon used to be relatively inaccessible regions *in vivo*. Custom-made state-of-the-art catheters are available with numerous options for the design, such as multiple lumina, side holes, and inflatable balloons for catheter progression or isolation of intestinal segments. These allow for multiple controlled sampling and compound delivery options in different intestinal regions. Intestinal catheters were often used for delivery (23 studies), sampling (10 studies), or both (27 studies). Sampling speed decreased with increasing distance from the sampling syringe to the specific intestinal segment (i.e., speed highest in duodenum, lowest in ileum/colon). No serious adverse events were reported in the literature, and a dropout rate of around 10% was found for these types of studies. This review is highly relevant for researchers who are active in various research areas and want to expand their research with the use of intestinal catheters in humans *in vivo*.

Keywords

Intestinal catheter; small intestine; ileum; colon; aspiration; delivery; human; trials

Introduction

Intestinal catheters have been used for decades in physiology, nutrition, microbiology, and pharmacokinetics research. Studies involving catheters have helped to shed light on the functioning of the human gastrointestinal (GI) tract. Researchers have learned about for example digestion and absorption of (macro)nutrients, secretion, and flow rate (1-3) as well as intestinal physiology (4-6), luminal and adherent microbiome composition (7), and metabolite production (8) *in vivo*. *In vitro* GI-tract models, animal models, or measurements in fecal samples are not directly representative of intraluminal (patho-) physiological processes or bacteria in the human GI-tract *in vivo* (9). These models lack essential aspects of host interaction and do not capture the variation in response between human subjects. Intestinal catheters can be used to aspirate intestinal fluids to examine intestinal luminal processes or to deliver compounds inside the intestinal lumen (10, 11). The latter provides valuable information about dynamic metabolic effects after targeted intestinal delivery of a test compound (12), and allows researchers to study changes in systemic metabolisms relevant to health and disease.

As opposed to feeding tubes used to deliver enteral nutrition inside the stomach or the proximal small intestine of patients, working with intestinal catheters that need to be placed in the more distal small intestine or proximal colon pose more challenges to biomedical researchers and clinicians. In-depth information about working with intestinal catheters, including positioning catheters, aspirating intestinal fluids, and standardizing delivery and sampling, as well as a summary of state-of-the-art intestinal catheter designs, is currently lacking in the literature. The objective of this review is to provide an overview of the practical and technical aspects of applying naso- and oro-intestinal catheters to human subjects for delivery of compounds and sampling luminal fluids from the jejunum, ileum, and colon *in vivo*. For this review, not only did we examine the available literature from experts in this field but we also included insights from our clinical trials with intestinal catheters: thus, this review extends beyond the boundaries of a conventional systematic review. This information will be helpful for researchers in setting up and performing trials.

Search strategy and inclusion criteria

A search strategy was developed for PubMed. Combinations of three grouped search terms were used to find papers that described clinical trials using intestinal catheters in human subjects (**Supplementary Table 1**). Papers written in English and published after 1960 were included. Detailed information about the search strategy can be found in Supplementary Table 1. The search terms were adapted accordingly for a search in

the Web of Science. Both searches (PubMed and Web of Science) were conducted in March 2020. This resulted in 6338 papers. After removing 971 duplicates, 5367 papers were screened based on titles and abstracts (**Figure 1**). Inclusion criteria were: (I) full-text clinical trials with human subjects; (II) original research articles; and (III) the use of an intestinal catheter where the tip of the catheter was placed in the jejunum, ileum, or colon. Exclusion criteria were: (I) studies where the catheter was not placed to answer study questions (observational study); (II) studies with catheters that were inserted via rectum/anus; (III) studies that used manometry catheters or focused on motility and motor complex functions; (IV) studies where catheters were not used to deliver compounds to the intestine or to sample intestinal fluids; (V) studies with gastric- or duodenal catheters; and (VI) studies that did not conform to the inclusion criteria. After excluding 5060 irrelevant papers, 293 papers remained, which were split into two groups: papers published before and after 2000. The list of papers published before the year 2000 is provided in the **Online Supplementary Information**. The full texts of the 81 papers published after 2000 were examined for state-of-the-art methodology. Finally, 58 papers were included.

Insights from our own selected clinical trials

We also included in-depth information from several of our own (un)published clinical trials. We included (non-published) insights from the CRIB study about applying catheters for simultaneous aspiration of duodenal, jejunal, and ileal content (ClinicalTrials.gov, NCT02018900, (13)). Insights obtained during the FiberKinetics study were also described, where a catheter was used for delivery and aspiration in the distal ileum (ClinicalTrials.gov, NCT04013607, unpublished study). Also included were observations from the ileal brake study (14), where nutrients were introduced via the ileum, and an iron oxidation study (15) in which a 40-cm segment of the proximal small intestine was perfused and fluid samples collected. All studies were approved by an Institutional Review Board (METC Wageningen University or Maastricht University, the Netherlands). All subjects gave written informed consent.

The use of intestinal catheters in research

General overview of the included studies

We included 58 studies as well as 2 unpublished studies from our research groups reviewing methods for the use of intestinal catheters. These studies are summarized in **Supplementary Table 2**.

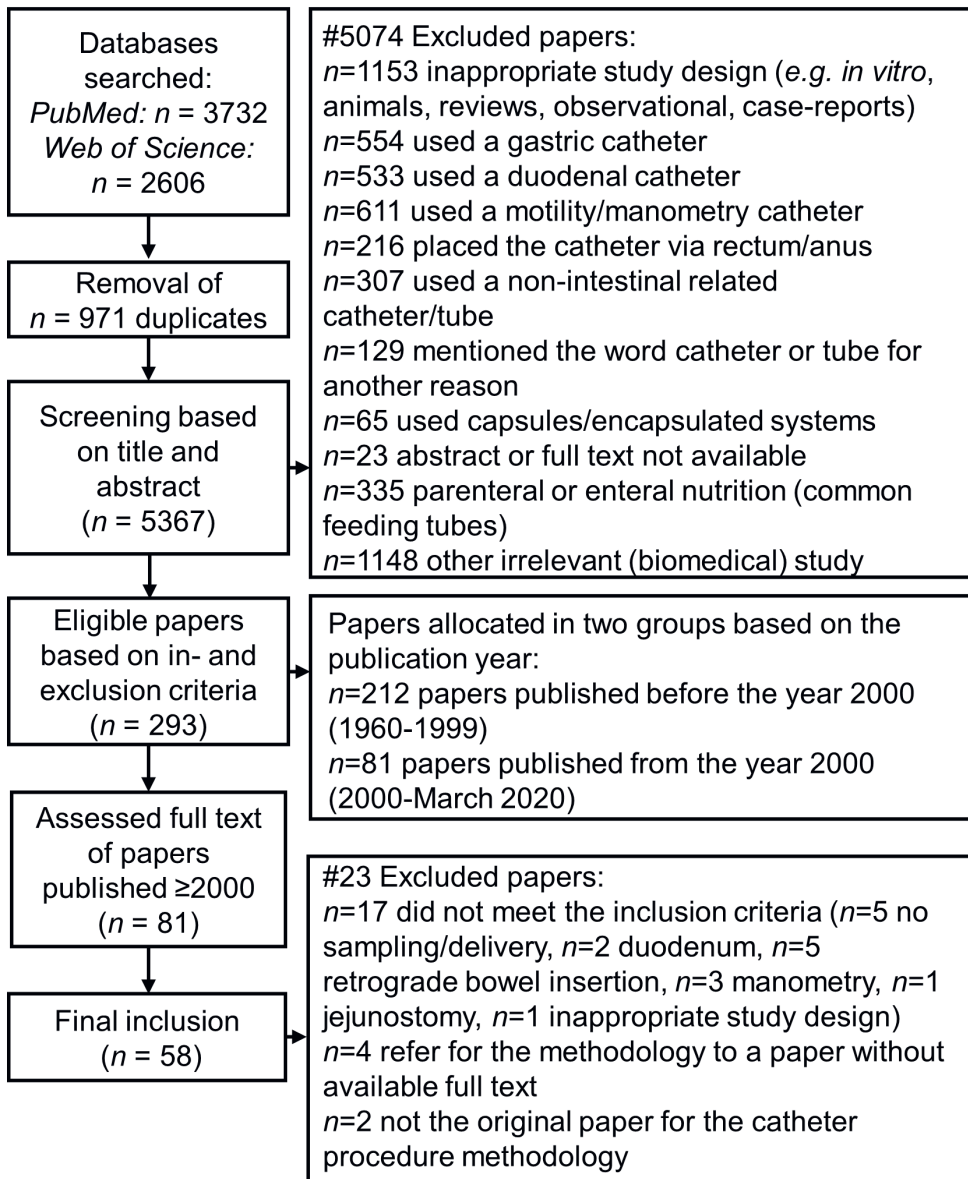


Figure 1. Flowchart of the literature search.

Articles were included that used an intestinal catheter where the tip was in the jejunum, ileum, or colon for research purposes in human subjects. Searches were performed up to 16 March 2020.

Most studies focused on nutrition and (intestinal) physiology research (34 studies), followed by pharmacological research (20 studies), microbiome research (3 studies), and another category (3 studies) (**Figure 2**). Most of these studies investigated multiple intestinal regions (24 studies), followed by only the jejunum (21 studies), ileum (13 studies), or colon (2 studies). 56 studies included healthy subjects, 1 study included both healthy subjects and patients, and 3 studies included patients. Studies involved a total of 720 healthy subjects and 42 patients (with type 2 diabetes (16), slow transit constipation (17), ulcerative colitis (18), or cystinosis (19)). The mean number of subjects per trial was 12 ± 6 (range, 5-27 subjects). In most studies, the subjects were intubated once (39 studies) and in the other 21 studies, subjects were intubated ≥ 2 times (maximum 10 times (20)) in a cross-over fashion with a wash-out period in between. In general, catheters placed in the distal regions of the GI-tract (ileum, colon) required a longer intubation period. The mean number of days per intubation was 2.1 ± 1.3 (range, 1-5 days).

Recruitment and inclusion

It is important to note that in more-invasive studies, recruitment and inclusion are generally more challenging compared with non-invasive studies. This should be considered when setting the study inclusion and exclusion criteria, although it is of paramount importance to include sample sizes that have enough statistical power. For the CRIB study, 49 people responded to our recruitment efforts over a period of 6 months (13). For the FiberKinetics study, 20 people replied within one month after the recruitment started (21).

Considerations in the catheter design

A summary of state-of-the-art intestinal catheter designs in the included studies is provided in Supplementary Table 2.

Catheter length and outer diameter

The total catheter length differed depending on the targeted intestinal regions. Jejunal catheters had a mean length of 286.3 ± 120.4 cm (range, 150-500 cm), ileal catheters 307.4 ± 34.6 cm (range, 270-400 cm), and colonic catheters 466.7 ± 23.6 cm (range, 450-500 cm). To keep track of the length of the catheter inserted into the GI-tract, it is useful to have centimeter markings along the full length of the tube (**Figure 3A, B, D**). The intestinal catheters placed via the nose had a mean outer diameter of 2.9 ± 1.2 mm (range, 0.6-4.2 mm), whereas the intestinal catheters placed via the mouth had a bigger outer diameter, namely 4.7 ± 0.9 mm (range, 2.5-6.3 mm). Generally, catheters with a bigger outer diameter are easier to place, owing to their increased stiffness, and intestinal delivery and/or sampling becomes easier. The diameter of the aspiration channel should be large enough to sample intestinal content at the site of interest.

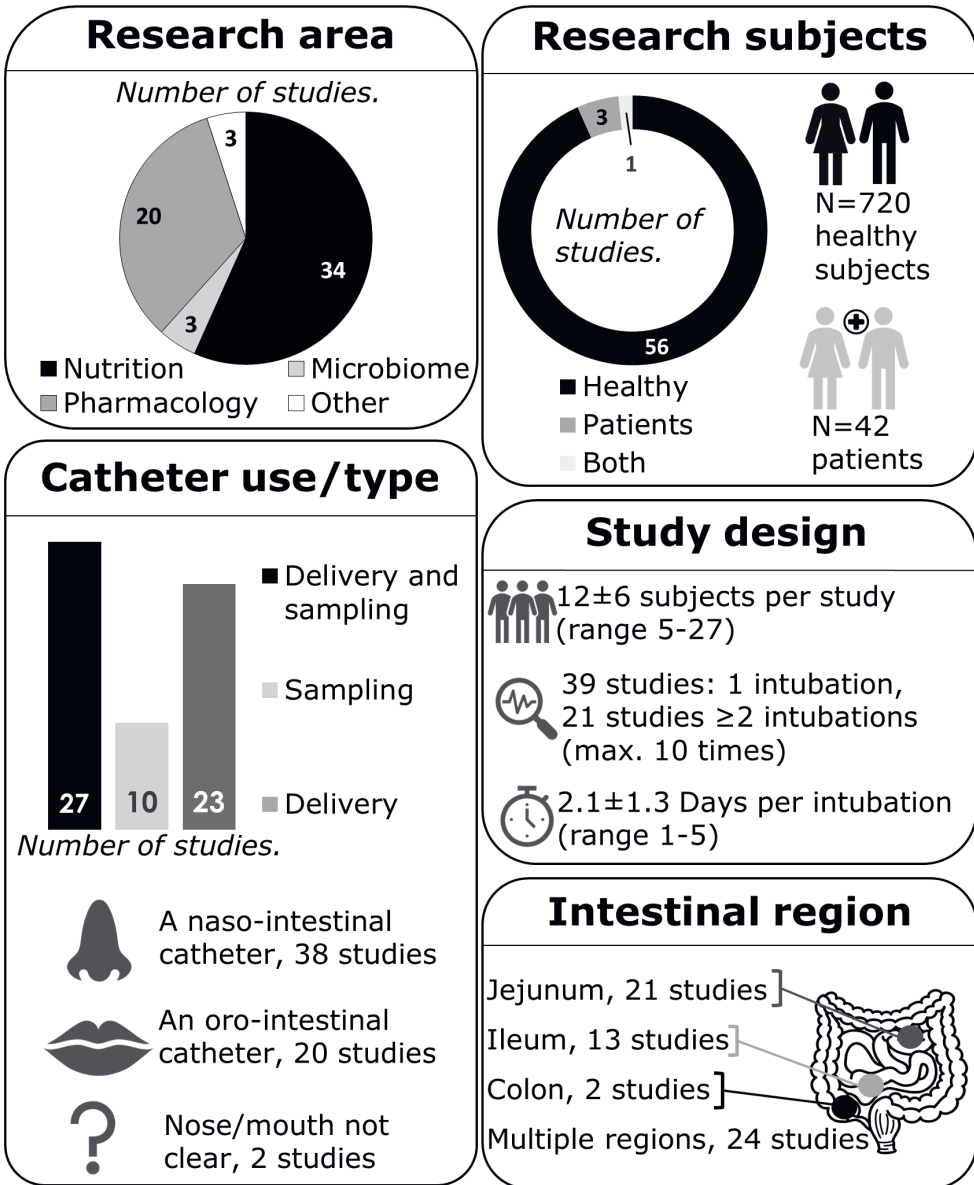


Figure 2. An overview of the general characteristics of the 60 studies included that used an oro- or naso-intestinal catheter.
The catheter was placed in the jejunum, ileum or colon in human subjects.

The sample homogeneity and viscosity differ between sampling locations (*e.g.*, the small intestine compared with the proximal colon), and the condition of the study participant (fasted, or consumption of liquid or solid foods) (22). The proximal colon contains more thick, less homogeneous material so sampling from this region can be improved by using a catheter with a larger diameter. However, a bigger outer diameter might be less comfortable for participants. In the only study reporting on outer diameter in relation to tolerability, nasally placed tubes with outer diameters of both 2.1 and 3.8 mm did not result in increased postprandial supine gastroesophageal reflux in 8 healthy subjects (23). In our experience, intestinal catheters with an outer diameter of maximally 3.5 mm and made from soft materials, such as silicone, were generally well tolerated by subjects (10, 13, 14, 24), whereas oral intubations were less well tolerated and not used for prolonged measurements. Tolerability is a combination of the burden caused by tube insertion and the burden and duration of the transfer of the tube to the target location. The latter is often less comfortable for tubes inserted via the mouth as compared to the nose. A trade-off between practical considerations and participant (dis)comfort must be made when designing and using intestinal catheters.

Catheter material

Intestinal catheters are often made from polyurethane, silicone, or polyvinyl chloride. Polyurethane and silicone tubes, also called fine-bore tubes, are softer and more flexible than polyvinyl chloride tubes. Therefore, they are more comfortable for the subject and easier to place along the curves of the small intestine. On the other hand, higher flexibility increases the risk of curling and coiling inside the GI-tract upon introducing the catheter, mainly in the stomach. This hampers the positioning of the catheter post-pylorus. In the included studies, the materials used were silicone (10 studies), silicone rubber (12 studies), polyvinyl chloride (14 studies), polyethylene (3 studies), or not mentioned (21 studies). The use of stiffener or guidewire (see section 4.3.2.1) results in a more rigid catheter, which can especially be of added value to silicone catheters due to their high flexibility. Fine-bore tubes can better withstand GI-circumstances (25) such as gastric acid, bile acid, and other GI secretions. Thus, re-usable fine-bore tubes, silicone or polyurethane, will likely last longer than polyvinyl chloride tubes.

Multi-lumen catheters with side holes

In some studies, several different catheters were synchronously introduced, with each separate catheter tip located in another intestinal region ((26-29), published prior to 2007). Introducing several catheters at once increases the burden during positioning and the subsequent experiment because the outer diameter of the combined catheters is substantially larger than that of only a single catheter.

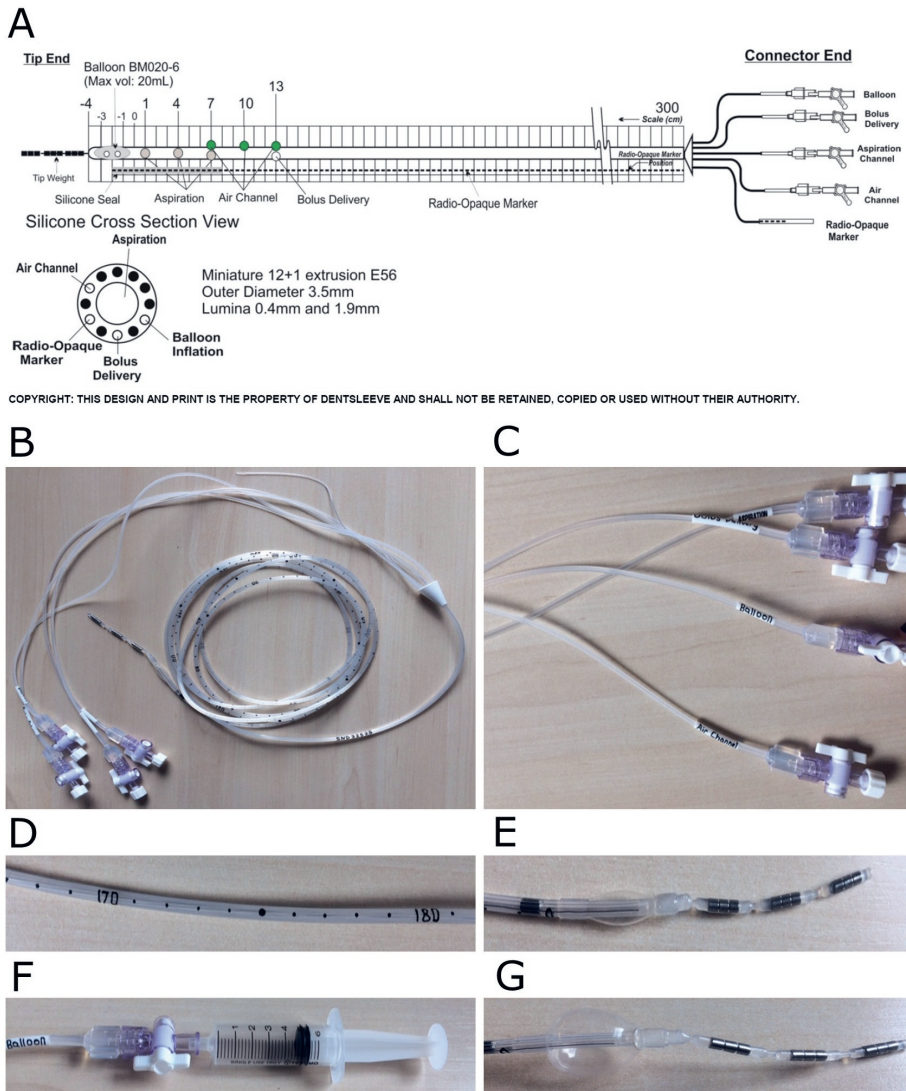


Figure 3. An example of a naso-ileal catheter design that can be used for intestinal aspiration and delivery in human subjects.

(A) The schematic design including the cross-sectional view of the different lumina (reproduced with permission from Mui Scientific, Ontario, Canada). Photos show the (B) naso-intestinal catheter with 300 cm tubing, excluding the connector end; (C) multiple lumina, closed with a stopcock and lid; (D) the centimeter indications on the tubing; (E) the deflated balloon and the three tip weights; (F) the inflation of the balloon via the balloon channel using a syringe; and (G) the balloon that is inflated with 5 mL air (maximum capacity 20 mL).

In one study, the same tube was used for the collection of intestinal content from various intestinal regions (30), which may have led to contamination of luminal contents from one intestinal region to the other. Nowadays, these issues are resolved using multi-lumen catheters (in 41 studies, ranging from 2 to 23 lumina per catheter). Multi-lumen means that multiple so-called “lumen” or “channels” with various dimensions are combined in one tube construction (Figure 3A, cross-section view). The numerous lumina are labeled according to their proposed function and separately protrude at the connector end (Figure 3B, C). The different lumina within one catheter can serve different purposes such as simultaneous sampling/delivery, sometimes from various intestinal regions (*e.g.*, duodenum and ileum) or inflating or deflating balloons. The diameter of a specific lumen can be adapted according to the use (aspiration versus delivery) or intestinal region (proximal versus distal). Often, one lumen is used for balloon inflation/deflation, as further explained below, and another lumen is used to transport radio-opaque material. A lumen for air inflation may be included in the design to prevent the catheter from adhering to the intestinal wall due to the creation of a local vacuum during fluid sampling, which may cause intestinal sampling issues. When lumina are not in use, they can be closed at the connector end with a stopcock and/or lid (Figure 3C). Side holes can be positioned in one or more lumina to enable targeted exposure of specific intestinal segments. In Figure 3A, three side holes in the catheter aspiration channel used to obtain aspirates of a ~7 cm intestinal segment can be seen. Multiple side holes in one lumen reduce the risk of obtaining no sample due to a potential blockage of one side hole or the catheter sticking to the intestinal wall.

The use of inflatable balloons and weighted tips

Most of the catheters were equipped with an inflatable balloon (35 studies) or bag (3 studies). These inflatable accessories, or a capsule (30 mm x 10 mm, (31-33)), attached to the distal tip are often used to enhance catheter progression making it move distally with peristaltic contractions. The bags and balloons can be inflated via a specific inflation channel (Figure 3E-G) with water, saline, or air. These balloons have a maximum inflation capacity of 5 mL (19), 10 mL (13, 14, 16, 34-36), or 20 mL (21). Since water or saline is heavier than the same volume of air, this might beneficially impact progression of the catheter when the person is positioned in such a way that gravity can exert its normal downward pulling action. However, whether the balloon or bag can be filled with liquid depends on the material and cleaning/sterilization protocols of re-usable catheters. For example, our silicone catheters and the encased balloon had to be completely free of water before sterilization. Therefore, the balloon was filled with air. In one study, a rubber balloon was first filled with 1.5 mL of mercury and, after reaching the duodenum, the mercury was replaced by 15 mL of air to facilitate further progression into the small intestine (15). Other studies used a rubber bag with 30 gram of mercury (37), an inflatable mercury bag (38), a lead weight (30), or a finger cot with

2 mL of mercury (39) at the tip. Although using mercury has the advantage of increasing the weight of the balloon and, therefore, speeding up progression, it is a highly toxic compound that is dangerous if it leaks from the balloon. Nowadays, to avoid the use of heavy metals, (tungsten) weights/pellets are often encased at the distal tip to promote movement from the stomach to the duodenum.

Catheter design for perfusion experiments

Another reason that inflatable balloons were incorporated into catheter design was to isolate a closed segment of the intestine or to isolate proximal and distal segments from each other (40-43). Such catheters can be used for intestinal perfusion experiments, i.e. infusion and sampling within one test segment (44, 45). Perfusion experiments using occluding balloons allow researchers to investigate for instance the net absorption/transport or secretion of water or solutes in this segment of the intestine. The occluding balloons were placed at a variable distance apart from each other (1, 46, 47) to create independent segments of 10 cm (48) or 20 cm (49-52). Balloons were inflated with a relatively high quantity of air (~30-45 mL (43, 51, 52) to maintain a constant pressure of ~25 mm Hg) as compared to balloons used for progression. Air was added until pressure sensations (i.e., without inducing discomfort) were experienced by the subjects (43), to achieve total occlusion of the intestinal segment and to prevent progression of the catheter by peristalsis. To achieve this inflation, balloons were bigger, namely 5-10 cm long (42, 43, 49-52). After inflation, pressure was continuously monitored to ensure sustained inflation (43). Non-absorbable markers, such as phenol red (phenolsulfonphthalein), can be used to check for leakages from the intestinal segment. The occluding balloon proximal to the study segment prevents endogenous secretions, with an unknown quantity of salts and water, from contaminating the test segment (44). Semi-open perfusion systems/segments can also be used by inflating the distal balloon with 26-30 mL air (48, 53, 54). Another option is to use an open perfusion system without balloons, with an infusion port located a few centimeters proximally from the sampling port(s), to determine absorption or secretion between the infusion site and the aspiration site(s). This method aims not to influence the flow rate at the sampling point, but to calculate the real liquid flow rate using a marker. Non-absorbable markers, for instance, polyethylene glycol (PEG), have to be added to infusions in known concentrations to correct for the dilution.

Placement, progression, and removal of the catheter

Catheter insertion

Intestinal catheters were positioned via the nose in 38 studies, or via the mouth in 20 studies (Figure 2). Endoscopic insertion via the nose was tolerated significantly better in comparison to conventional oral gastroscopy in 181 consecutive outpatients (55). Before placement, the tube is lubricated with a medical-grade lubrication gel, sometimes

also containing a local anesthetic, to reduce friction. Moreover, local anesthesia, if preferred by the subject, can be applied to the nasal mucosa (*e.g.*, lidocaine 10% spray/Xylocain® (10)) or the upper throat/pharynx (*e.g.*, using lidocaine spray (51, 53, 54)) to reduce potential pain and discomfort during insertion. Previously, topical pharyngeal anesthesia given before endoscopy was effective in reducing discomfort in 201 patients undergoing the procedure for the first time (56). In one study, a topical anesthetic, namely 1 mL 4% lidocaine, was administered to prevent a gag reflex (20). Moreover, in a randomized controlled trial in 100 patients, infusion of 100 mL of NaCl 0.9% with 10 mg metoclopramide 15 minutes before the procedure significantly reduced overall discomfort, nausea, and vomiting (57). However, the use of medication other than lubrication gel before the start of a study should be thoroughly thought out, because it could potentially affect the study outcomes. The possible impact of medication on the outcomes is higher when experimental tests take place shortly after the intubation procedure. After lubrication and local anesthesia, the tube was inserted via the nose or oral cavity and pushed through the esophagus to the stomach. During this procedure, the subject was asked to drink sips of water, to ensure closure of the esophagus by the epiglottis.

Transpyloric migration

Different strategies for transpyloric migration were described in the studies. One strategy was to inflate the balloon inside the stomach (with ~3 mL saline (58) or 1.5 mL mercury (15)), facilitating progression of the catheter tip towards the pylorus by peristalsis. To stimulate peristalsis, participants were offered snacks (58) or were placed in a supine position on their right side with their upper body lifted 45° and their feet raised (15). By positioning the subject on the right side, the pyloric sphincter was in the lowest part of the stomach. Gravity forced the mercury balloon to migrate towards the pyloric sphincter, facilitating catheter progression into the small intestine. In two other studies, the subjects were also intubated while in the supine position (16, 59). In several studies, the tube was allowed to pass into the duodenum without inflating the balloon inside the stomach (31-35, 42, 43, 60, 61), and three of these studies used a tube with a capsule attached at the tip to stimulate progression (31-33). In 30 healthy subjects, 87% of the inflated ballooned tubes passed the pyloric sphincter with the aid of normal peristaltic movements after 6 hours, compared to 67% of the non-inflated ballooned tubes (62). Thus, balloon inflation in the stomach improves spontaneous transpyloric migration. Theoretically, the inter-digestive migrating motor complex, responsible for letting particles larger than a few millimeters pass the pylorus, only occurs in the fasting state (63). This could imply that post-pyloric placement after overnight fasting is good timing. In practice, however, we experienced that simultaneous feeding could stimulate transpyloric migration of the catheter. An intravenous dose of erythromycin, a prokinetic, significantly increased successful post-pyloric tube placement in randomized controlled

trials (64). Another strategy was to guide manual catheter progression from the stomach into the proximal small intestine under (freeze-frame) intermittent fluoroscopic control (1, 10, 13, 14, 20, 21, 24, 26-29, 59) or static X-rays (65).

The use of a guidewire, stiffener, and/or endoscope

Stiffeners allow for more control while manually introducing a catheter into the GI-tract, facilitating the progression from the stomach to the duodenum/jejunum. In four studies, guidewires (66) (coated with polytetrafluoroethylene (47) or Teflon (48, 53)) were used to facilitate passage into the small intestine, sometimes monitored by fluoroscopy. Guidewires were mostly used to insert shorter tubes (i.e., duodenum, and jejunum tubes) 150-200 cm long. In one study, one channel within a silicone catheter was filled with a guide-wire stiffener to facilitate passage (58). Wilms et al. (13) used an assembly stiffener of 0.3 mm in the center lumen within a silicone catheter. This resulted in a catheter with increased rigidity, which was still flexible enough to pass easily along the curves of the small intestine. In one study, a guidewire was first inserted 60 cm distally from the pylorus with the aid of an endoscope. The endoscope was then retracted, leaving the guidewire in place. Upon removal of the endoscope, the guidewire could be retracted back into the stomach (67). After retracting the endoscope, the correct positioning of the guidewire needs to be confirmed using radiography. Only in one other study was the use of an endoscope mentioned (17). The catheter was subsequently introduced over this guidewire into the proximal small intestine, all under fluoroscopic guidance (68). After the catheter was correctly positioned, the guidewire was removed. One advantage of this procedure was the rapid placement in the proximal small intestine, i.e., a median of 18 minutes (range, 12-45 minutes) in 22 patients (69), due to easy detection of the pylorus.

Other ways to monitor gastric and post-pyloric placement

Smithard et al. (70) described the use of electromagnetic access systems for tube placement. The average time of post-pyloric placement using these devices was 16 minutes, whereas blind placement took 42 minutes on average (70). pH measurement of the aspirate could be used to determine the position of the tube since the pH in the stomach is pH 3 to 4. To move the catheter from the stomach into the duodenum, six studies used the antral and duodenal transmucosal potential difference gradient (TMPD) for continuous monitoring of the catheter position (antral TMPD < -20 mV, duodenal TMPD > -15 mV, difference > 15 mV). To establish this gradient, isotonic sodium chloride was perfused via the catheter infusion channels at the gastroduodenal junction (16, 49-52, 60). The disadvantage of this method is the requirement of manometry equipment for monitoring to ensure correct placement (60).

Progression towards the distal intestine

To assist with tube passage through the GI-tract, inflatable accessories such as balloons or bags at the catheter tip can be inflated with water (7 mL (20)), saline (~3 mL (58)), or air (5 mL (10, 13), ~6 mL (71), 8 mL (21, 66), 10 mL (60, 72), 15 mL (15)). In many studies, the balloon was inflated once it passed the pyloric valve (15, 21, 49-52, 60, 73-76) or after passing the ligament of Treitz (19, 34-36, 66, 77). In five studies, the participants were instructed to inflate and deflate the balloon every other hour and inflate the balloon upon waking up to advance further passage of the tube (10, 13, 14, 24, 77) to ensure the inflated balloon did not block the passage of food or GI excretions. In some studies, the catheter progressed with gravity/peristalsis, and no balloon inflation was mentioned (30-32, 59, 78). Keeping the balloon continuously inflated directly after reaching the duodenum until it reaches the region of interest will result in optimal progression, but the risk of full intestinal occlusion for a longer period should be avoided. Occlusion may result in symptoms such as abdominal pain, nausea, and vomiting (79). A 2.1-cm balloon inflated with 5 mL of air is equivalent to a spherical volume of 4.8 mL (equation: $V=(4/3)\pi r^3$). The balloon is also soft and malleable so it is unlikely that (full) occlusion will occur when it is kept inflated. Moreover, the small intestine is known to dilate (80) after administration of a (food) bolus (81), and even allows passage of solid objects. In our studies, the balloon gradually deflated spontaneously over time (after >30 minutes) *ex vivo*. In the FiberKinetics study, progression was not successful in n=2 subjects, as the balloon was not continuously inflated during manual insertion (10 cm/hour) to promote further progression (21). This resulted in a coiled tube inside the stomach. On the subsequent test days, the subjects had to empty and re-fill the balloon every hour to ensure sustained inflation, since apparently this was crucial for successful catheter positioning in our study. When applying re-usable catheters, the balloon should be checked for leakages *ex vivo* before each intubation.

Along with inflating and deflating the balloon, the subjects needed to further insert the catheter into the nose or mouth to advance the tube. In our studies, the tube was manually inserted at a rate of 10 cm/hour starting after the tube passed the ligament of Treitz (21), or at a rate of 5-10 cm/hour starting ~2 hours after placement (13). In the study of Zarate et al. (66), the tube was inserted at a rate of ~10 cm/30 min, after the tip passed the ligament of Treitz. Pulling at the nares might be caused by coiling of the tube within the stomach/small intestine (58). However, pulling at the nares is usually a sign of spontaneous catheter progression inside the intestine. When an excessive length of the tube is quickly inserted into the stomach, there is a risk of tube knot formation (82). Therefore, very fast insertion of catheters should be prevented by adhering to a maximum rate per hour, such as 10 cm/hour.

Practical procedures to stimulate catheter progression

To stimulate progression, participants can be offered drinks (*e.g.*, tea/coffee) or food (13, 34, 36) and be encouraged to walk around/move periodically (13, 20) during the day of intubation. Due to the upright posture, progression will also benefit due to gravity (13, 20). In one study, when the tip did not reach the desired location within the scheduled time, an intravenous injection of metoclopramide (Primperan; 10 mg in 2 mL) was given to increase GI-motility (33). Other examples of (intravenous) drugs to stimulate GI-motility are domperidone (83, 84) and erythromycin (85). Erythromycin is a motilin agonist and initiates the inter-digestive migrating contractions (86), the effects were previously mostly seen on gastric contractions (87, 88). The use of pro-motility drugs may influence the test procedures.

Hospitalization or home-based stay?

Some study participants were hospitalized during the full intubation period when progression took more than one day (53, 71, 75, 89). Subjects could also be instructed to assist the passage of the catheter at home from the time the catheter had to progress via natural peristalsis of the GI-tract (36, 90). This was the case in our own studies. With the catheter inserted, participants could perform daily activities such as eating, drinking, showering, moving, and sleeping. Though, in the latter case, it is crucial to provide the participants with clear instructions on the actions that are expected from them, such as carefully sticking to a maximum insertion rate. In one study the participants were allowed to go home after ~140 cm tube was inserted (66), and had to insert the catheter further at home to a depth of 180 cm. The researcher and medically responsible person should be available for questions or unexpected circumstances. Nevertheless, we advise to regularly check progression the first hours after intubation at the research center with fluoroscopy or pH measurement to ensure the catheter is progressing as expected, until at least with the tip is placed beyond the ligament of Treitz, before participants leave the research facility. Ideally, the ligament of Treitz may be used as a cut-off, because previously drop-outs were caused due to the inability of the tube to pass this specific small intestinal curve (section 4.5).

Progression time

Placement of the tube into the stomach takes between 10 and 15 minutes (21, 58). Transpyloric migration of the tip can take ~10 minutes (66), although we experienced that manual transpyloric tube placement using fluoroscopy took between 10 and 45 minutes (21). Automatic post-pyloric migration with a 1.5 mL mercury-inflated balloon took 1-2 hours after catheter ingestion (15). Moreover, jejunal catheters were positioned mostly on the same day as the experimental tests took place (1, 33, 52, 53, 61), and positioning the tube in the (proximal) jejunum took ~1 hour (1, 53), 2.2±0.2 hours (52), or 1-3 hours (61).

Ileum and colon intubations, however, require more time due to a longer progression period. In (terminal) ileum intubation studies, the subjects always visited the research facilities the day prior to the experimental tests for catheter insertion, allowing the catheter to progress over time (a full 24-hour period). The next day, the subjects returned between 7.30 and 10.00 A.M. (10, 13, 14, 21, 39, 58, 73, 75, 76) to check the position of the tip and, when appropriate placed, start the experiments. Depending on the insertion procedures, within 24 hours the catheter tip could be located ~100-120 cm distal to the ligament of Treitz (CRIB study), or 240-250 cm from the nose (13, 21). In some other studies, an intubation 120 cm distal from Treitz (34), or ≥ 175 cm from the nose (35, 36) took less than 24 hours (34-36, 66). In the study of Borg et al. (16), the terminal ileum was intubated within 5 hours. To reach the terminal ileum, a progression period of 20 hours (including overnight) might be too short in some subjects. Colonic intubations may take slightly more time compared to ileum intubations, but in most studies, the subjects were also intubated in ~24 hours (33, 78, 90). In one study, the catheter progressed from the jejunum to the proximal colon within 18 hours, or from the mouth to cecum within 20-48 hours (72). In the study of Dohil et al. (19), the ballooned tube entered the proximal small intestine after 3 days and the cecum after 5 or 7 days in all subjects, whereas in another study, the tube reached the cecum after only 6 to 10 hours using a balloon filled with 30 gram mercury (37).

After reaching the correct intestinal segment

After reaching the correct GI-segment, the tube can be held in place by fixing it to the face and deflating the balloon (37, 60, 72). In one study, a residual volume of 3 mL was kept inside the balloon to avoid retraction (66). Marteau et al. (37) flushed the sampling lumen with nitrogen in the ileum and colon, likely to ensure that no residual oxygen present in the sampling lumen disturbed the anaerobic environment in the colon. Moreover, after correct positioning the catheter, subjects remained in a semi-recumbent position (37, 38, 73-75), or a semi-reclining position (72) to avoid further progression of the tube. Since the tube can still progress further (47) over time, especially in studies that take several days, the position of the tube should be verified before important measurements are carried out.

Removal, and cleaning (of re-usable catheters)

Before removal of the catheter, the inflatable bag or balloon must be completely deflated. After deflation, the catheter can be removed by pulling it out gently, either by the subjects (15) or by medical staff. In two studies, the tube was cut off near the nose and allowed to leave the body naturally in the feces (31, 32). When colonic catheters are removed via the nose or mouth, the colonic bacteria could potentially contaminate the small intestine (91). Moreover, spasming of the ileo-cecal valve caused by retracting the colonic catheter may cause severe discomfort or pain. In this case, the use of spasmolytic

intravenous glucagon or hyoscine butylbromide (buscopan) is recommended. We used custom-made, multi-use catheters which could be sterilized up to 50 times (13, 21). For cleaning, the tube can be flushed with alkaline enzymatic detergent used for cleaning medical devices (MediClean Forte, Dr. Weigert, Hamburg, Germany) (21), or enzymatic presoak detergents and disinfectants (20). The tube was then manually flushed with water using a syringe and completely dried before sterilization. It is advised to check with the manufacturer the compatibility between cleaning reagents and the material, and with the central sterilization department in the hospital about standard cleaning procedures.

Determination of the catheter location

Radiography

There are multiple methods to determine the catheter location during placement, progression and final positioning (during test days). Most studies made use of imaging techniques using radiation (46 out of 60 studies), such as plain abdominal X-ray static pictures or fluoroscopy. Freeze-frame fluoroscopy, intermittent periods of fluoroscopy instead of continuous real-time monitoring, is often applied to minimize radiation exposure during insertion of the catheter and when verifying the location (66). Radio-opaque markers integrated into the catheter design enable visualization by fluoroscopy or static X-rays. Radio-opaque material can be added close to infusion ports or (all) side holes (10) to select the appropriate infusion channel from multi-lumen catheters for an intestinal segment (24). Radio-opaque material can also be added to the tip of the tube (19, 92), as a capsule at the distal end (31), or every 10 cm to measure the length in cm distal to Treitz. Tungsten weights at the tip can also be visualized with radiation. Another approach is to fill one lumen inside the catheter with radio-opaque material to visualize the complete tube length (21, 58, 65, 73, 76). The marker along the catheter can assist with tube placement using fluoroscopy, since visualizing the marker distribution throughout the intestine shows whether the catheter tip passes the pyloric sphincter and the ligament of Treitz (**Figure 4A**) or whether the catheter is coiled or looped in the stomach or small intestine (58, 77).

Radiography in combination with contrast liquid

Only after infusion of contrast fluid via de most distal catheter lumen can X-ray and fluoroscopy examination determine the catheter position more precisely with respect to intestinal anatomical structures such as the ileocecal valve (19, 36, 71, 77). Studies used diluted barium sulphate (71), meglumine-ioxitalamate (Telebrix® GASTRO, Guerbet, France, 50 mL in total, diluted 1:2 with water, (21)), or Gastrografin (Bayer, Berkshire, UK, 20 mL, (66)) as contrast fluid. Contrast can be delivered directly via a catheter lumen into the intestine, facilitating the visualization of a small segment of the intestine within a few minutes (30–60 cm, (77)).

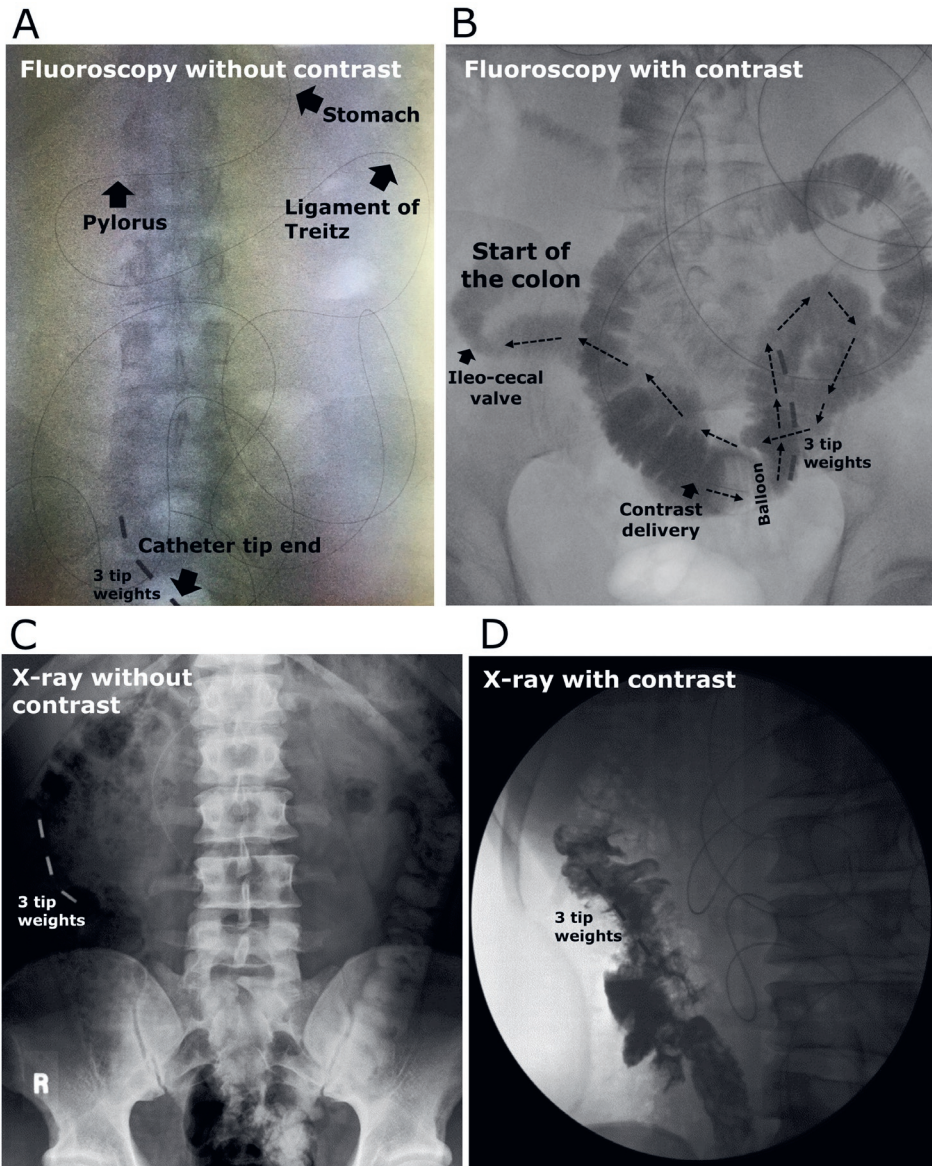


Figure 4. Examples of visualization of the catheter tip location using fluoroscopy or X-rays with/without the delivery of contrast liquid in human subjects.

(A, B) Fluoroscopy pictures (A) without, or (B) in combination with the delivery of a contrast liquid, where the contrast liquid appears in black and will follow the direction of the arrows towards the colon; (C, D) Abdominal X-ray pictures (C) without, or (D) in combination with the delivery of a contrast liquid. Panels C and D were reproduced with permission from Dohil et al. (19). The black line in the pictures is the radio-opaque marker, and three small metal (or radio-opaque) weights/markers are located at the tip of the catheter.

Contrast liquid allows researchers to discriminate between the small- and large intestine (Figure 4A, C versus Figure 4B, D) and determine the catheter tip position (in centimeter distance) in relation to the ileocecal valve (19, 21). If the side holes allow, contrast can be delivered distally from the inflated balloon to prevent backflow into the more proximal intestine. When contrast can only be delivered via side holes located proximal to the balloon, it is best to deflate the balloon for optimal visualization of the more distal intestine. Knowing the exact position of the catheter can be important for delivery or aspiration at the right location, as well as standardization and interpretation of the research outcomes. Gastrografin and meglumine-ioxitalamate are both water-soluble, hyperosmolar contrast media and, therefore, draw water into the lumen, which may impact study outcomes such as the microbiome composition. Thus, delivering contrast media after completing experimental tests may be better for accurate test results. Gastrografin might cause diarrhea (93), whereas barium sulfate is not hyperosmolar and almost insoluble in water. Radiography allows accurate verification of the catheter location but it exposes participants to radiation.

In the FiberKinetics study, the total radiation effective dose was calculated to be 0.014 ± 0.018 mSv in five subjects (range, 0.001 to 0.05 mSv) based on machine settings and exposure time. The procedure included intubation of the small intestine under free-frame fluoroscopy and verification of the location on the next day at two moments. The dose area product in the study of Klaassen et al. ((10), radiation data not published in this reference) was for the available data of five subjects on average $500 \text{ mGy}\cdot\text{cm}^2$ (range, $55\text{--}1442 \text{ mGy}\cdot\text{cm}^2$). This gives a calculated effective dose of 0.06 mSv, for intubation of the small intestine under free-frame fluoroscopy. Only two trials published information about the radiation exposure (20, 66). Zarate et al. (66) found an effective dose of 0.3 mSv for maximum 12 freeze frames of fluoroscopy during 1 intubation. Seekatz et al. (20) limited the radiation exposure time to maximally 1.5 minutes but the effective dose was not mentioned (10 intubations). Overall, the radiation effective dose for fluoroscopy can be considered low, when compared to *e.g.* the an annual average natural radiation dose of 2.2 mSv in the UK (94). A conventional abdominal static X-ray made with a so-called 'bucky' system results in maximally 0.4 mSv radiation per imaging moment (95) and will therefore result in a higher radiation exposure as compared to fluoroscopy, but results in better quality images (Figure 4A,B versus Figure 4C, D). Overall, the total radiation exposure for fluoroscopy in general is low and dependent of the exposure time and may consequently differ depending on the experience of the medical personnel and anatomical differences of the small intestine, such as curviness, which may postpone adequate placement. Machine settings, such as the field of view, play a relatively minor role compared to the exposure time. One should be aware that the investigator may also be exposed to a low dose of radiation during procedures with radiography, dependent on the equipment used as well as the use of protective gear. Importantly, pregnant women

and the unborn child should be protected from radiation exposure. We advise that all female subjects perform a pregnancy test at the day(s) of radiation exposure, and a positive test results in exclusion or drop-out.

Other methods to monitor catheter location

Another method to estimate the location of the catheter tip is the use of centimeter marks or color marks (32, 33) along the tube, indicating the distance from nose to catheter tip (the total tube length). This, often in combination with fluoroscopy or X-ray, indicates the tube location (30, 34, 92). A summary of distances (cm) for the different assumed intestinal regions used by previous studies is provided in **Table 1**. The tip near the pylorus was estimated at ~70 cm distance from the nose (58). However, distances can vary between individuals. Body height was not significantly correlated to small intestine length so tube distance could not be predicted based on height (96, 97). The length of the small intestine was negatively correlated with age, and was found to be longer in males as compared to females (96).

The antral and duodenal transmucosal potential difference gradient can be used for continuous monitoring on the catheter position (16, 49-52, 60). Moreover, measurement of pH is also often used as an indirect measure to check tube positioning throughout the experiments. pH can be easily determined in aspirates from various locations using pH strips (10). Intraluminal pH was also measured continuously via pH electrodes that were fitted in the catheter close to the injection port (68), at the tube tip (15), or two pH probes near the tip and one 35 cm proximal to the tip (72). Another option is real-time confirmation of transpyloric migration using electromagnetic guidance (70). This eliminates or reduces the need of radiography, and thus exposure to radiation and dependence on the hospital radiology department. One example is the Cortrak feeding tube™ (Viasys Healthcare, UK) for which the placement and real-time location information is provided via a Cortrak Enteral Access System™. This tube has been used in research to sample inside the stomach and duodenum (99). The maximum length of the Cortrak tube is 140 cm (outer diameter max. 4 mm) with an electromagnetic transmitting tip and, therefore, it cannot be used in studies targeting the ileum or colon. If needed, radio-opaque markers can be integrated into the tube design for precise visualization with contrast liquid and fluoroscopy or X-ray.

Adverse events and drop-outs

There are several tube-related adverse events (AEs) that can occur during the phase of tube placement or maintenance. In the studies with healthy individuals, the residence time of the catheter *in situ* was a maximum of 5 days (Supplementary Table 2). Related AEs included nasopharyngeal discomfort such as a sore throat, thirst, dysphagia (25), rhinorrhea (100), nasal bleeding, nausea or throwing up (100).

Table 1. Indications of centimeter insertion of the catheter for the assumed intestinal regions.

Information was found in research papers that described clinical trials applying intestinal catheters in human subjects¹.

Intestinal region	Distance from the nose or mouth (cm)	Distance from the pylorus (cm)	Distance from the ligament of Treitz (cm)
Duodenum	86 ± 5 cm (78)	5 cm (24)	-
		5-10 cm (26)	
		12 cm (42)	
		13 cm (16)	
		~15 cm (58, 60)	
Jejunum	100 cm: proximal jejunum (33)	20 cm (50)	~30 cm (2)
	167 cm (89)	40-50 cm (24)	
		50 cm: first segment (98)	
		50 cm: proximal jejunum (43)	
		70 cm (42)	
		~100 cm (26)	
Ileum	160-180 cm (13)	≥120 cm (14, 24, 77),	≥120 cm (34)
	≥175-195 cm (35, 36)	≥170 cm (58)	
	180 cm (66)	190 cm (16)	
	186 ± 21 cm: terminal ileum (78)		
	214 cm: terminal ileum (89)		
	240-250 cm: terminal ileum (21)		
	260 ± 20 cm: terminal ileum (33)		
	300 cm (59)		
Colon	Ascending colon: 330 cm (33)	-	-

¹The centimeter distances were often used in combination with fluoroscopy/X-ray to confirm the location.

Sinusitis and laryngitis were also tube-related complications (101) but normally occurred during long-term maintenance in patients (>2 weeks). Therefore, they are expected to be not relevant in short-term trials. Nasopharyngeal discomfort could be partly prevented by using smaller diameter and/or softer tubes (25). There is a risk of tube misplacement and dislocation (e.g., endobronchial placement) which is often caused by the lack of a gag, swallowing and cough reflex, or by altered consciousness in patients because they cannot indicate what they feel (25). The lack of these reflexes is generally not a problem in healthy subjects. A proper swallowing reflex contributed significantly to the overall tolerance of catheter placement, as shown in patients who had undergone gastroscopy (102). In general, the presence of an intestinal tube *in situ* can slow down swallowing in healthy subjects (103). Gastrointestinal perforation during forceful tube insertion or the reinsertion of the guidewire with the tube *in situ* has been described (25), but in

the included articles (n=762 subjects in total) no cases of perforation were mentioned, likely because the catheter or guidewire tips were soft and rounded. Gastro-esophageal reflux with aspiration is a potential AE, which can occur during catheter placement or after insertion, because the tube slightly relaxes the lower esophageal sphincter. The risk during placement can be minimized if participants have fasted (*e.g.*, minimum of 6 hours with no solid foods, and minimum of 2 hours with no liquid foods before catheter placement). Overall, in the studies, which included a total of 762 subjects, nothing was mentioned about serious AEs such as reflux with aspiration or perforation. Some studies specifically mentioned that the study procedures were (well) tolerated without AEs (16, 19, 43, 60, 92). Five other studies described AEs which were (possibly) related to the procedure, including dizziness (n=1) (31), nausea/vomiting (n=3) (21, 31), nasal irritation (n=2) (21, 52), distension discomfort from a balloon inflated with 45±9 mL air (n=2) (52), and local throat irritation (n=14) (72).

A summary of the dropouts in the included studies are shown in **Table 2**. In total, 52 subjects dropped out due to the use of the intestinal catheter, especially due to discomfort induced by the catheter (24 subjects), problems with catheter positioning (18 subjects), or sampling difficulties (6 subjects). Moreover, 11 subjects dropped out because of other reasons not related to the catheter or no reason was mentioned. Overall, a dropout rate of around ~10% is expected for these types of studies.

Intestinal catheters as tool for intestinal delivery and sampling

Intestinal catheters are often used for delivery (23 studies), sampling (10 studies), or both delivery and sampling (27 studies).

Delivery of compounds inside the intestine

To study local dynamic metabolic changes as well as absorption and digestion processes, a variety of tools are available for delivery, namely calibrated volumetric pumps (1), infusion pumps (32, 33, 58, 65), peristaltic pumps (68), calibrated (syringe) pumps (48, 61), and motor-driven syringes (49, 50, 52) for the delivery at a constant rate, or 'normal' syringes (31) for one bolus delivery. Some of these devices were equipped with a luer-lock fit between the catheter and the syringe (32, 33) or device. Such a fit ensures a leak-free connection and should be considered when designing a catheter (luer-lock at the connector end). Before delivery, compounds were dissolved in water (19) or saline solution (0.9% NaCl, (72, 90)). Infusion is often performed at a constant rate, expressed in mL/min, kcal/min or kJ/min when delivering nutrients (**Table 3**). In the included studies, solutions were delivered within a set period of time (15 min (52), 60 min (24, 36, 61), 90 min (14, 41, 54), 195 min (15)), or for the full duration of the experimental tests (73). Constant infusion rates can be used to reach steady-state conditions (15).

Table 2. A summary of the number of dropouts and reasons for dropping out, as reported in the 60 research papers that described clinical trials applying intestinal catheters in human subjects¹.

Number of dropouts	Reason for dropping out	Reference
Discomfort (n=24)		
10	Due to discomfort induced by the catheter/inability to tolerate the catheter, reasons not mentioned.	(10, 13, 14, 24, 72)
2	Due to nausea and vomiting.	(21, 42)
9	Due to various difficulties with the tolerance of the tube (failure of the tube to fit through the nose, pain, vomiting, non-migration through the pylorus, excessive pulling of the tube at the nares).	(39, 58)
3	Due to discomfort during catheter positioning (e.g., nausea, vomiting).	(34-36)
Catheter positioning (n=18)		
5	Due to difficulties when positioning the catheter, or incorrect positioning of the catheter.	(10, 46, 73)
4	Due to failure to position the tip of the catheter beyond the ligament of Treitz.	(34-36)
7	The tube did not progress below the upper small intestine.	(19, 21, 74)
2	The tube did not reach below the mid-ileum.	(19)
Sampling difficulties (n=6)		
1	The aspirated sample volume (jejunum) was not sufficient to allow proper evaluation.	(46)
5	Experiments did not last for the full period or intestinal samples were not be obtained, reasons not mentioned.	(47)
Other (n=11)		
9	Other reasons or reasons not mentioned (e.g., not properly following the instructions, vasovagal reaction on blood withdrawal).	(2, 10, 20, 31, 46, 92, 98)
2	Due to the discomfort of the study procedure, reasons not mentioned.	(42)

¹From the 60 studies, involving 720 healthy subjects and 42 patients, 56 studies included healthy subjects, 1 study included both healthy subjects and patients, and 3 studies included patients.

Moreover, compounds were also administered as a single dose bolus injection which was completed within 5 minutes, regardless of the bolus viscosity, and the length and diameter of the tube (Table 3). If preferred, the delivery time can be reduced by concentrating the compounds as much as possible. However, it must be noted that hypertonic solutions can influence peristalsis, and can increase intestinal secretions (104) which in turn dilute the infused compound. Increasing the temperature of solutions to 37°C before infusion (61) could make participants more comfortable than using cold infusions, and warm infusions and are less likely to cause GI disturbances (105).

After delivery, the tube was flushed with water (10-50 mL (46, 59, 92)), saline (range 1-50 mL (17, 18, 32, 33, 72, 90)), or another dissolvent (3 mL (31)) to ensure that all compounds were delivered inside the intestine. The catheter should be flushed with

at least the volume of water or saline to rinse the dead space of the tube (calculated according to the equation of cylindrical volume $V=\pi r^2h$, where r =radius and h =height). The dead space can be minimized by reducing the tube length and lumen diameter. Another important point is the use of a control infusion in randomized controlled trials. In two studies, multiple intestinal regions were infused in a randomized, cross-over fashion. At the time the treatment, solution was delivered to one intestinal site and in the other site(s), saline (34, 60) or water (24) was infused, and vice versa. This was done to ensure the blinding of the subjects with regards to the timing and the nature of the infusion.

Sampling of intestinal content

Additionally, intestinal catheters can be applied to aspirate intestinal fluids. Adhesion of analytes of interest to the material could be checked for in *ex vivo* studies. Syringes were often used as a sampling tool by connecting a syringe to the proximal end of the sampling lumen in the intestinal catheter (13, 20, 21, 27, 30, 38) via manual suction (38, 74). To ensure efficient aspiration, in two studies, the catheter drainage channels were connected to a vacuum pump (46, 53), which facilitated sampling from the duodenum and jejunum. In other studies, aspirates were obtained using the catheter lever properties (40 cm segment of the proximal small intestine (68)), gravity (jejunum (1)), or simply by siphoning/slight aspiration through the opening of the tube (ileum (39)). Zilberstein et al. (30) and Wilms et al. (13) used a 20 mL syringe to take samples from the duodenum, jejunum, and ileum. In contrast, in one of our other studies, gentle aspiration using 5 mL syringes was more efficient for aspiration from the ileum (21). In our experience, applying gentle and regular manual suction (37, 61) worked most optimally, although continuous suction (28, 38) was also applied. Stopcocks attached to the syringe and the aspiration channel can be used for opening and closing before and after sampling to prevent air (i.e., oxygen) from going into the anaerobic environment of the cecum (37). Importantly, catheter patency inside the GI-tract, i.e. not being vacuumed against the intestinal wall, should be ensured (27) to avoid damage to the intestinal epithelium. Perfusates can be checked for signs of damage, such as blood contamination (52). Overall, sampling rates are dependent on the diameter and total length of the aspiration channel, the tube stiffness, the pressure applied, and the intestinal region sampled (i.e., viscosity of intestinal fluid).

Intestinal sample volumes

The relatively large sample volumes obtained from the duodenum and jejunum indicate that sample collection from the duodenum and jejunum entailed few challenges (Table 3). Flow rates of intestinal contents into fasted test segments were previously estimated to be around 2.2 mL/min in the jejunum, and 0.7 mL/min in the ileum in various studies. Flow rates of intestinal contents after a meal were estimated to be 10 mL/min

in the proximal jejunum (45). Matsson et al. (46) mentioned that in one subject (from the n=8 in total), the aspirated sample volume from the duodenum and jejunum was not sufficient (<3 mL after 1 h sampling time). Jejunal samples were collected at 10-15 min intervals (15, 48, 50-52, 54), over periods of 1.5 hours (54) to 6 hours (52, 78), and the volumes of the jejunum aspirates ranged from 0 to >10 mL (Table 3). The short sampling intervals of sample collection indicate rapid sampling. In contrast, samples from the ileum were collected in aliquots at longer intervals of 30 min (28, 29, 75), 1 hour (38, 106), 2 hours (74), or until enough sample was obtained (37) over a total maximum period of 8 hours (28, 29, 74, 76, 78, 106). When samples are collected at multiple time points, the remaining intestinal fluid in the aspiration channel after sampling can be re-injected into the intestine to minimize contamination caused by sample remainders present in the dead space volume (27). Gaudichon et al. (106) indicated that sample collection in the fasted state (volume not mentioned) from the ileum took 30 minutes. In another study (28), one subject was excluded from the study due to practical problems concerning sampling of ileal content (lumen diameter 1.5 mm). For the sampling of colonic content in one study, >5 mL (5 to 50 mL) was aspirated ((37), catheter diameter 3.5 mm). After collection, samples needed to be put on (dry) ice to stop enzyme and/or bacterial activity.

Intestinal sampling rates

In our study ((13) unpublished data) duodenum, jejunum, and ileum samples were aspirated using a multi-lumen ileal catheter at several time points. The diameters of the duodenum and jejunum aspiration channels were 0.65 mm, and the diameter of the ileum aspiration channel was 0.9 mm. In a representative selection of three subjects, we found that duodenum samples were aspirated at a rate of 0.45 (0.61 [IQR]) mL/min, jejunum samples at 0.37 (0.36 [IQR]) mL/min, and ileum samples at 0.30 (0.17 [IQR]) mL/min. Another study reported a sampling rate of 0.5 mL/min for the proximal and distal jejunum (61). In conclusion, sampling speed decreases with increasing distance from the sampling syringe to the specific intestinal segment (i.e., speed highest in duodenum, lowest in ileum), despite the highest diameter of the ileum aspiration channel. In the FiberKinetics study (21), 2-3 mL distal ileum samples were aspirated per time point using a naso-ileal catheter (300 cm long, 1.9 mm diameter aspiration channel) over a span of 340 minutes. Due to sampling difficulties, it was not possible to aspirate a sample in the fasted state. The ileum samples were aspirated at a rate of 0.35 (0.05 [IQR]) mL/min, after consumption of a drink with water-soluble dietary fibers. In most studies, comprehensive information regarding sampling volumes, rates and difficulties was lacking (Supplementary Table 2).

Table 3. An overview of the constant rates and single bolus injections that were used for delivery of compounds in the intestine, and the sample volumes that could be obtained from the duodenum and jejunum.

Information was described in 60 clinical trials applying intestinal catheters in human subjects¹.

Intestinal delivery				Intestinal sampling	
Constant rates		Single bolus injection		Sample volume (mL)	
mL/min	mL/hour	kcal/min or kJ/min	Volume (mL) and timing (minutes)	Duodenum	Jejunum
0.67 mL/min (35)	50 mL/h (65)	0.6 kcal/min (35, 77)	2 mL (32, 33) in 2-3 min	~1 mL (20)	~1 mL (20)
1 mL/min (34, 36, 39, 73, 75-78, 89, 106)	220 mL/h (2)	0.9 kcal/min (34, 36)	10 mL (19) in 1-2 min	1 mL (mucus) (30)	1 mL (mucus) (30)
2 mL/min (10, 14, 41, 48, 54)		1 kcal/min (60)	10 mL (72, 92)	0-10 mL (27)	4 mL per time point (98)
2.5 mL/min (41, 51)		1.35 kcal/min (77)	10 mL (21) in 5 min	5-10 mL (65)	>4 mL pooled sample over 30 min (75)
3 mL/min (24, 31)		2 kcal/min (40)	15 mL (59)		5 mL aliquots (1)
3.15 mL/min (42)		2.5 kJ/min (35)	40 mL (16, 90)		0-10 mL (27)
5 mL/min (1)					5-10 mL: 60 cm distal to duodenum (65)
10 mL/min (15, 61, 68)					>10 mL (26)

¹From the 60 studies included; 50 studies used an intestinal catheter for the delivery of compounds (sometimes in combination with sampling).

Practical procedures to improve sampling rates

Marteau et al. provided a standard meal to subjects before sampling from the colon (37), because colonic sampling after an overnight fast was not always possible (107). In one of our studies (21), it was also not possible to obtain a sample after an overnight fast, but after consumption of a fiber-rich drink, a sample was collected. This suggests that providing subjects with a drink including dissolved macronutrients improves sampling. Feeding increases the flow rates of intestinal contents in the jejunum, ileum, and terminal ileum in human subjects (108). Additionally, in the case of unsuccessful sampling, nitrogen gas (5-10 mL) can be flushed through the lumen to ensure catheter patency, followed by gentle suction until a sample is collected (37). For colonic sampling specifically, insertion of nitrogen gas is preferred over ambient air, to not disturb the anaerobic environment of the colon. Marteau et al. (37) obtained a colonic sample (5-50 mL) 2 h after a meal in 64% of the experiments, and 2.5-3 h after a meal in the other 36% (aspiration channel 3.5 mm). Another option to improve sampling speed is the delivery of water or saline, preferably with a dilution marker, via the catheter channel directly in the sampling location. However, this should be considered and carried out carefully because the intestinal fluid, and, therefore, the analytes of interest, may become too diluted for analyses. Troost et al. (15) measured a dilution of ~100-fold in the intestinal samples. The dilution factor can be measured with the addition of inert recovery markers, such as PEG-4000 or phenol red, and corrected if needed. Repeated flushing with 10 mL of physiological salt without the addition of compounds through a port of the naso-ileal catheter shifted the relative microbiota composition (109). Alternating the position of the subjects, such as sitting, lying, or walking, could also improve sampling rates. One study mentioned that sampling took place while the subjects were in a semi-recumbent position (76).

Discussion

We reviewed practical and technical aspects of using naso- and oro-intestinal catheters in human studies for delivering compounds and sampling luminal fluids from the jejunum, ileum, and colon *in vivo*. An extensive review of the available literature was provided to include the experiences of experts in this field. We also included insights obtained during the execution of our own clinical trials. A limited number of studies used colonic catheters as compared to small intestinal catheters. Unfortunately, the catheter design and any related study procedures were often only briefly described. To aid future researchers, we recommend describing all procedures related to the use of the intestinal catheter in detail. This will facilitate comparisons between clinical trials and improve the reproducibility of results, allowing other researchers to benefit from the information when designing and performing new studies.

Naso- and oro-intestinal catheters

Intestinal catheters have been useful tools in studying *in vivo* processes of the GI-tract, greatly advancing the existing knowledge in the fields of physiology, gut microbiota, nutrition, and pharmacology. These human studies are superior to *in vitro* and *ex vivo* models of the GI-tract due to the presence of all complex and relevant physiological processes. Nowadays, tubes can be custom-made, with multiple options for the catheter design (*e.g.*, the number of lumen), which can be used to sample and deliver to very specific sites in the intestinal region of interest. The more advanced catheters are often re-usable, reducing costs when using this medical device to study *in vivo* processes. As seen during early investigations (110), the possibility of including inflatable accessories at the distal tip of the catheter facilitates (rapid) intubation of the distal small intestine and proximal colon. This allows researchers to study these relatively inaccessible regions in people. Applying naso- and oro- intestinal catheters for the study of distal regions of the GI-tract is a time-consuming procedure, which can be considered a disadvantage. The practical tools outlined in this paper can be helpful to improve intestinal sampling from the ileum and colon. Although the use of these tools can cause discomfort in participants, resulting in a potentially more challenging recruitment procedure, we are not aware of serious AEs reported in the literature and the dropout rate seems to be acceptable (~10%). Most study participants had no direct benefit from the procedure or the study results. Offering a disproportionate financial reimbursement for participating in the study is ethically doubtful, therefore, reimbursement should mainly compensate for the invested time and body measurements. An overview of the main recommendations related to the catheter design, catheter placement, determination of catheter location, and intestinal delivery or sampling is provided in **Table 4**.

Research gaps

Many papers used only the centimeter indication on the sampling tube to locate the catheter in the ileum for delivery and/or sampling. However, the length of the small intestine/ileum can vary substantially between subjects. This makes it difficult to determine beforehand how far the catheter needs to be inserted to reach the distal ileum or proximal colon in a study subject. Currently, there is no best practice for placing the catheter in exactly the same location in the intestine in all subjects in the same trial, which could be of importance when interpreting the study outcomes. Secondly, having an intestinal tube with a latex balloon *in situ* increased gastric emptying time and decreased small bowel residence (111), and a small inflated balloon influenced motor patterns (112). Therefore, it cannot be excluded that intestinal intubations affect GI-tract functioning and the luminal environment, which can be of potential concern. Having a control group with the tube *in situ* in the study design is important when testing interventions. More research is needed to determine the time period between intestinal intubation and the return to a normal luminal environment. In microbiome studies,

potential contamination from the upper GI-tract regions should be considered when using this tool for sample collection from the ileum or colon, although the transit of bacteria can also be considered a physiological aspect. How important the disruption is and how long the bacteria from non-sampling sites (potentially) remain in the sampling site is currently unknown. As the total bacteria load in the ileum or colon is higher when compared to more proximal GI-tract regions (113), the impact is likely minor.

Alternatives for intestinal delivery and sampling in humans

Alternatives for delivery and sampling in the terminal ileum and colon are colonoscopies and rectal/anal catheters (intra-colonic tubing) (114, 115). To reach the terminal ileum and proximal colon, laxatives are administered to prepare the bowel for a colonoscopy. During this step, the luminal environment may become disturbed, resulting in changes in the microbiota load, diversity, and composition (116-118). Alternatively, enemas were used to clean the distal colon (30-40 cm), leaving the proximal colonic content undisturbed. Reaching these segments can be challenging for the endoscopist, although catheters are normally positioned within ~45 minutes. The procedure can be invasive for subjects, especially when sampling or infusing at multiple time points. In this case, rectally placed catheters can be attached to the colonic mucosa to secure the position with an endoclip fixation technique (114). Reaching and studying the distal colon is easier as compared to the more proximal colon, since the length of the endoscope/catheter to be introduced is shorter and no laxatives or sedative agents are needed. Endoscopies can be used to obtain epithelial tissue in different anatomical regions of the GI-tract, whereas oro- and naso-intestinal catheters only allow sampling of intestinal lumen content or mucus. Compared to the intestinal lumen content, epithelial tissue provides more information about the host. Non-endoscopic biopsy techniques are available or currently in development, such as (wireless) biopsy capsules (119, 120). Intestinal luminal content and tissue samples can be collected from sudden death victims (121) or during surgery, which is mainly limited to patients (122). These kinds of samples cannot easily be combined with an intervention. Non-invasive human studies have been performed in patients with an ostomy bag attached to the small intestine or colon. This allowed researchers to collect samples from the ostomy bag and test for absorption and digestion during oro-ileal transit (123). It is not clear whether these patients are representative of the healthy population, but microbiota encountered in ileostomy effluent resembled microbiota in the proximal small intestine in healthy subjects (124).

For intestinal delivery, also capsules coated with a pH-dependent film have been used (125, 126). Since the delivery is gradual and depends on local pH levels, it is impossible to guarantee a continuous delivery rate (mL/min) to reach steady-state conditions and researchers have no control over the complete volume that is delivered.

Table 4. A non-exclusive overview of the main recommendations when working with intestinal catheters.

Phase	Recommendations
Catheter design (details in section 4.2)	<ul style="list-style-type: none"> ▪ Best tolerated: outer diameter of ≤ 3.5 mm, soft material (<i>e.g.</i>, silicone), intubation via the nose.
	<ul style="list-style-type: none"> ▪ Dependent on intestinal region of interest, and aim of use, decide on: <ol style="list-style-type: none"> 1) Total length of the tube; 2) Number and diameter of lumen (delivery versus sampling); 3) Number of side holes → multiple side holes reduce the risk of obtaining no sample; 4) For distal jejunum/ileum and colon: include inflatable balloon or bags.
	<ul style="list-style-type: none"> ▪ Include radio-opaque markers for visualization.
	<ul style="list-style-type: none"> ▪ Stiffeners reduce the risk of tube coiling.
Catheter placement (details in section 4.3)	<ul style="list-style-type: none"> ▪ Use medical lubrication gel.
	<ul style="list-style-type: none"> ▪ Pro-motility drugs/other medication can be used but may influence study outcomes.
	<ul style="list-style-type: none"> ▪ The use of a guidewire/endoscope can assist placement of shorter tubes (often maximally 150-200 cm).
	<ul style="list-style-type: none"> ▪ Specific body position of the participant, such as lying on the right side, can assist correct placement.
	<ul style="list-style-type: none"> ▪ Stick to a maximum insertion rate to prevent tube coiling.
	<ul style="list-style-type: none"> ▪ Inflate the balloon/bag to stimulate catheter progression.
	<ul style="list-style-type: none"> ▪ Check the progression regularly (<i>via e.g.</i>, radiography or pH).
Catheter location determination (details in section 4.4)	<ul style="list-style-type: none"> ▪ Stimulate progression by offering drinks/food and encourage participant to move/walk periodically.
	<ul style="list-style-type: none"> ▪ Fluoroscopy and X-ray enable visualization of radio-opaque markers → fluoroscopy provides lower radiation dosage.
	<ul style="list-style-type: none"> ▪ Examination with radiography and contrast liquid enables catheter position assessment with respect to intestinal anatomical structures (<i>e.g.</i>, ileocecal valve).
Intestinal delivery (details in section 4.6)	<ul style="list-style-type: none"> ▪ The use of centimeter distance of tube insertion, the pH of aspirate, or an enteral access system are not specific.
	<ul style="list-style-type: none"> ▪ Use of pumps and motor-driven syringes to deliver at a constant rate.
	<ul style="list-style-type: none"> ▪ Ensure a leak-free connection by luer-lock equipment.
	<ul style="list-style-type: none"> ▪ Avoid delivery of a hypertonic solution.
	<ul style="list-style-type: none"> ▪ Infusion of a pre-warmed solution (body temperature) is more comfortable for the participant.
Intestinal sampling (details in section 4.6)	<ul style="list-style-type: none"> ▪ Use inert non-absorbable recovery markers to correct for dilution.
	<ul style="list-style-type: none"> ▪ Correct for the dead space volume of the tube.
	<ul style="list-style-type: none"> ▪ Choose the number of time points and intervals of sample collection wisely.
	<ul style="list-style-type: none"> ▪ Apply gentle and regular manual suction during sampling.
	<ul style="list-style-type: none"> ▪ Ensure catheter patency when there are sampling difficulties → inject ambient air (small intestine) or nitrogen gas (colon).
	<ul style="list-style-type: none"> ▪ Correct for the dead volume of the tube → <i>e.g.</i>, discard dead space volume.
	<ul style="list-style-type: none"> ▪ Providing drinks/food, and alternating positioning of subjects (short walks etc.).

The recommendations are a combination of expert experiences as obtained from the papers included in this literature review, as well as insights obtained during the execution of our own clinical trials.

Alternatively, more advanced capsules with *in vivo* real-time monitoring possibilities can be used for targeted intestinal delivery (127). Nowadays, efforts are being put into the development of novel gastrointestinal sampling capsules (128-130), which are described in the review of Tang et al. (129). For future studies, there are multiple possibilities for intestinal delivery and sampling *in vivo* to consider, all of them with specific advantages and disadvantages.

Concluding remarks

This extensive review is relevant for researchers active in various research areas during the set-up and execution of experiments using intestinal catheters in human subjects. We provided an overview with technical and practical, expert-based information on the use of intestinal catheters. Catheters are often used for intestinal delivery and fluid sampling to obtain direct data on the human intestinal (patho-)physiology. Custom-made state-of-the-art catheters are available with numerous options for the design, and the development of new catheters is ongoing. Hence, researchers can control sampling and delivery sites in the intestinal region of interest. The use of intestinal catheters enabled intubations of the distal small intestine and proximal colon, allowing the study of relatively inaccessible regions in humans. Although working with catheters might pose challenges to the researcher, clinician, and study participants, most can be overcome. These challenges do not outweigh the numerous advantages of its use. The dropout rate and overall burden to healthy subjects caused by related study procedures seem to be acceptable.

Acknowledgments

We would like to acknowledge Tim Klaassen (Division of Gastroenterology and Hepatology, Maastricht University Medical Center, the Netherlands) for the information about radiation data measured in his study and for sharing his expertise about naso-ileal catheters, and Bart Vermolen (medical physicist, Hospital Gelderse Vallei, the Netherlands) for calculations of the exposure radiation dosage. Furthermore, we thank Maaïke Witjes-Kroon (Hospital Gelderse Vallei, the Netherlands) for the medical assistance during the FiberKinetics study and the discussions about intestinal catheters. We thank prof. dr. Dirk-Jan Reijngoud (University Medical Center Groningen, the Netherlands) for the critical review of the manuscript. Members from the Wageningen University Library are acknowledged for their support during the conceptualization of the search terms and search strategy. The FiberKinetics study was funded by the public-private partnership 'CarboKinetics' coordinated by the Carbohydrate Competence

Center (CCC, www.cccresearch.nl). CarboKinetics is financed by participating industrial partners Agrifirm Innovation Center B.V., Nutrition Sciences N.V., Cooperatie Avebe U.A., DSM Food Specialties B.V., VanDrie Holding N.V. and Sensus B.V., and allowances of The Netherlands Organization for Scientific Research (NWO). The funders had no role in data collection and analysis, or preparation of the manuscript.

References

1. Nagy K, Ramos L, Courtet-Compondu MC, Braga-Lagache S, Redeuil K, Lobo B, et al. Double-balloon jejunal perfusion to compare absorption of vitamin e and vitamin e acetate in healthy volunteers under maldigestion conditions. *Eur J Clin Nutr.* 2013;67(2):202-6.
2. Luttkhold J, van Norren K, Buijs N, Ankersmit M, Heijboer AC, Gootjes J, et al. Jejunal casein feeding is followed by more rapid protein digestion and amino acid absorption when compared with gastric feeding in healthy young men. *J Nutr.* 2015;145(9):2033-8.
3. Strocchi A, Levitt MD. Measurement of starch absorption in humans. *Can J Physiol Pharmacol.* 1991;69(1):108-10.
4. Flourie B, Vidon N, Florent CH, Bernier JJ. Effect of pectin on jejunal glucose absorption and unstirred layer thickness in normal man. *Gut.* 1984;25(9):936-41.
5. Hecketsweiler P, Vidon N, Emonts P, Bernier JJ. Absorption of elemental and complex nutritional solutions during a continuous jejunal perfusion in man. *Digestion.* 1979;19(3):213-7.
6. Silk DB, Perrett D, Webb JP, Clark ML. Absorption of two tripeptides by the human small intestine: A study using a perfusion technique. *Clin Sci Mol Med.* 1974;46(3):393-402.
7. Singh RK, Chang H-W, Yan D, Lee KM, Ucmak D, Wong K, et al. Influence of diet on the gut microbiome and implications for human health. *J Transl Med.* 2017;15(1):73.
8. Chalet C, Rubbens J, Tack J, Duchateau GS, Augustijns P. Intestinal disposition of quercetin and its phase-II metabolites after oral administration in healthy volunteers. *J Pharm Pharmacol.* 2018;70(8):1002-8.
9. Vasapolli R, Schütte K, Schulz C, Vital M, Schomburg D, Pieper DH, et al. Analysis of transcriptionally active bacteria throughout the gastrointestinal tract of healthy individuals. *Gastroenterology.* 2019;157(4):1081-92.e3.
10. Klaassen T, Alleleyn AME, van Avesaat M, Troost FJ, Keszthelyi D, Masclee AAM. Intraintestinal delivery of tastants using a naso-duodenal-ileal catheter does not influence food intake or satiety. *Nutrients.* 2019;11(2).
11. Ripken D, van Avesaat M, Troost FJ, Masclee AA, Witkamp RF, Hendriks HF. Intraileal casein infusion increases plasma concentrations of amino acids in humans: A randomized cross over trial. *Clin Nutr.* 2017;36(1):143-9.
12. Reisz JA, D'Alessandro A. Measurement of metabolic fluxes using stable isotope tracers in whole animals and human patients. *Curr Opin Clin Nutr Metab Care.* 2017;20(5):366-74.
13. Wilms E, Gerritsen J, Smidt H, Besseling-van der Vaart I, Rijkers GT, Garcia Fuentes AR, et al. Effects of supplementation of the synbiotic ecologic(r) 825/fos p6 on intestinal barrier function in healthy humans: A randomized controlled trial. *PLoS One.* 2016;11(12):e0167775.
14. van Avesaat M, Troost FJ, Ripken D, Hendriks HF, Masclee AA. Ileal brake activation: Macronutrient-specific effects on eating behavior? *Int J Obes (Lond).* 2015;39(2):235-43.
15. Troost FJ, Saris WH, Haenen GR, Bast A, Brummer RJ. New method to study oxidative damage and antioxidants in the human small bowel: Effects of iron application. *Am J Physiol Gastrointest Liver Physiol.* 2003;285(2):G354-9.
16. Borg MJ, Bound M, Grivell J, Sun Z, Jones KL, Horowitz M, et al. Comparative effects of proximal and distal small intestinal administration of metformin on plasma glucose and glucagon-like peptide-1, and gastric emptying after oral glucose, in type 2 diabetes. *Diabetes Obes Metab.* 2019;21(3):640-7.
17. Ge XL, Tian HL, Ding C, Gu LL, Wei Y, Gong JF, et al. Fecal microbiota transplantation in combination with soluble dietary fiber for treatment of slow transit constipation: A pilot study. *Arch Med Res.* 2016;47(3):236-42.
18. Angelberger S, Reinisch W, Makrithatis A, Lichtenberger C, Dejaco C, Papay P, et al. Temporal bacterial community dynamics vary among ulcerative colitis patients after fecal microbiota transplantation. *Am J Gastroenterol.* 2013;108(10):1620-30.

19. Dohil R, Fidler M, Barshop BA, Gangoiti J, Deutsch R, Martin M, et al. Understanding intestinal cysteamine bitartrate absorption. *J Pediatr*. 2006;148(6):764-9.
20. Seekatz AM, Schnizlein MK, Koenigsnecht MJ, Baker JR, Hasler WL, Bleske BE, et al. Spatial and temporal analysis of the stomach and small-intestinal microbiota in fasted healthy humans. *mSphere*. 2019;4(2).
21. van Trijp M, Ríos-Morales M, Afman L, Witteman B, Reijngoud D, Bakker B, et al. The study of fiber fermentation, and short chain fatty acid kinetics and utilization inside the gut and systemic circulation. The fiberkinetics study: Unpublished work. *ClinicalTrials.gov*: U.S. National Library of Medicine; 2019 [Available from: <https://www.clinicaltrials.gov/ct2/show/NCT04013607>].
22. Schönfeld J, Evans DF, Wingate DL. Effect of viscous fiber (guar) on postprandial motor activity in human small bowel. *Dig Dis Sci*. 1997;42(8):1613-7.
23. Kuo B, Castell DO. The effect of nasogastric intubation on gastroesophageal reflux: A comparison of different tube sizes. *Am J Gastroenterol*. 1995;90(10):1804-7.
24. van Avesaat M, Ripken D, Hendriks HF, Masclee AA, Troost FJ. Small intestinal protein infusion in humans: Evidence for a location-specific gradient in intestinal feedback on food intake and gi peptide release. *Int J Obes (Lond)*. 2017;41(2):217-24.
25. Braegger C, Decsi T, Dias JA, Hartman C, Kolacek S, Koletzko B, et al. Practical approach to paediatric enteral nutrition: A comment by the espghan committee on nutrition. *J Pediatr Gastroenterol Nutr*. 2010;51(1):110-22.
26. Perez de la Cruz Moreno M, Oth M, Deferme S, Lammert F, Tack J, Dressman J, et al. Characterization of fasted-state human intestinal fluids collected from duodenum and jejunum. *J Pharm Pharmacol*. 2006;58(8):1079-89.
27. Brouwers J, Ingels F, Tack J, Augustijns P. Determination of intraluminal theophylline concentrations after oral intake of an immediate- and a slow-release dosage form. *J Pharm Pharmacol*. 2005;57(8):987-96.
28. Mariotti F, Pueyo ME, Tome D, Berot S, Benamouzig R, Mahe S. The influence of the albumin fraction on the bioavailability and postprandial utilization of pea protein given selectively to humans. *J Nutr*. 2001;131(6):1706-13.
29. Mariotti F, Mahe S, Luengo C, Benamouzig R, Tome D. Postprandial modulation of dietary and whole-body nitrogen utilization by carbohydrates in humans. *Am J Clin Nutr*. 2000;72(4):954-62.
30. Zilberstein B, Quintanilha AG, Santos MAA, Pajeccki D, Moura EG, Alves PRA, et al. Digestive tract microbiota in healthy volunteers. *Clinics*. 2007;62(1):47-54.
31. Dahlgren D, Roos C, Lundqvist A, Abrahamsson B, Tannergren C, Hellstrom PM, et al. Regional intestinal permeability of three model drugs in human. *Mol Pharm*. 2016;13(9):3013-21.
32. Seidegard J, Nyberg L, Borga O. Differentiating mucosal and hepatic metabolism of budesonide by local pretreatment with increasing doses of ketoconazole in the proximal jejunum. *Eur J Pharm Sci*. 2012;46(5):530-6.
33. Seidegard J, Nyberg L, Borga O. Presystemic elimination of budesonide in man when administered locally at different levels in the gut, with and without local inhibition by ketoconazole. *Eur J Pharm Sci*. 2008;35(4):264-70.
34. Maljaars PW, van der Wal RJ, Wiersma T, Peters HP, Haddeman E, Masclee AA. The effect of lipid droplet size on satiety and peptide secretion is intestinal site-specific. *Clin Nutr*. 2012;31(4):535-42.
35. Maljaars PW, Peters HP, Kodde A, Geraedts M, Troost FJ, Haddeman E, et al. Length and site of the small intestine exposed to fat influences hunger and food intake. *Br J Nutr*. 2011;106(10):1609-15.
36. Maljaars J, Romeyn EA, Haddeman E, Peters HP, Masclee AA. Effect of fat saturation on satiety, hormone release, and food intake. *Am J Clin Nutr*. 2009;89(4):1019-24.
37. Marteau P, Pochart P, Dore J, Bera-Maillet C, Bernalier A, Corthier G. Comparative study of bacterial groups within the human cecal and fecal microbiota. *Appl Environ Microbiol*. 2001;67(10):4939-42.
38. Vesa T, Pochart P, Marteau P. Pharmacokinetics of *Lactobacillus plantarum* ncbm 8826, *Lactobacillus fermentum* kld, and *Lactococcus lactis* mg 1363 in the human gastrointestinal tract. *Aliment Pharmacol Ther*. 2000;14(6):823-8.

39. Oberli M, Marsset-Baglieri A, Airinei G, Sante-Lhoutellier V, Khodorova N, Remond D, et al. High true ileal digestibility but not postprandial utilization of nitrogen from bovine meat protein in humans is moderately decreased by high-temperature, long-duration cooking. *J Nutr.* 2015;145(10):2221-8.
40. Wu T, Thazhath SS, Marathe CS, Bound MJ, Jones KL, Horowitz M, et al. Comparative effect of intraduodenal and intrajejunal glucose infusion on the gut-incretin axis response in healthy males. *Nutr Diabetes.* 2015;5:e156.
41. Takamatsu N, Kim ON, Welage LS, Idkaidek NM, Hayashi Y, Barnett J, et al. Human jejunal permeability of two polar drugs: Cimetidine and ranitidine. *Pharm Res.* 2001;18(6):742-4.
42. Rigda RS, Trahair LG, Little TJ, Wu T, Standfield S, Feinle-Bisset C, et al. Regional specificity of the gut-incretin response to small intestinal glucose infusion in healthy older subjects. *Peptides.* 2016;86:126-32.
43. Wu TZ, Bound MJ, Standfield SD, Jones KL, Horowitz M, Rayner CK. Effects of taurocholic acid on glycemic, glucagon-like peptide-1, and insulin responses to small intestinal glucose infusion in healthy humans. *J Clin Endocrinol Metab.* 2013;98(4):E718-E22.
44. Cooper H, Levitan R, Fordtran JS, Ingelfinger FJ. A method for studying absorption of water and solute from the human small intestine. *Gastroenterology.* 1966;50(1):1-7.
45. Modigliani R, Rambaud JC, Bernier JJ. The method of intraluminal perfusion of the human small intestine. I. Principle and technique. *Digestion.* 1973;9(2):176-92.
46. Matsson EM, Eriksson UG, Palm JE, Artursson P, Karlgren M, Lazorova L, et al. Combined in vitro-in vivo approach to assess the hepatobiliary disposition of a novel oral thrombin inhibitor. *Mol Pharm.* 2013;10(11):4252-62.
47. Knutson L, Koenders DJ, Fridblom H, Viberg A, Sein A, Lennernas H. Gastrointestinal metabolism of a vegetable-oil emulsion in healthy subjects. *Am J Clin Nutr.* 2010;92(3):515-24.
48. Lennernas H, Knutson L, Knutson T, Hussain A, Lesko L, Salmonson T, et al. The effect of amiloride on the in vivo effective permeability of amoxicillin in human jejunum: Experience from a regional perfusion technique. *Eur J Pharm Sci.* 2002;15(3):271-7.
49. Glaeser H, Drescher S, Hofmann U, Heinkele G, Somogyi AA, Eichelbaum M, et al. Impact of concentration and rate of intraluminal drug delivery on absorption and gut wall metabolism of verapamil in humans. *Clin Pharmacol Ther.* 2004;76(3):230-8.
50. Drescher S, Glaeser H, Murdter T, Hitzl M, Eichelbaum M, Fromm MF. P-glycoprotein-mediated intestinal and biliary digoxin transport in humans. *Clin Pharmacol Ther.* 2003;73(3):223-31.
51. Glaeser H, Drescher S, van der Kuip H, Behrens C, Geick A, Burk O, et al. Shed human enterocytes as a tool for the study of expression and function of intestinal drug-metabolizing enzymes and transporters. *Clin Pharmacol Ther.* 2002;71(3):131-40.
52. von Richter O, Greiner B, Fromm MF, Fraser R, Omari T, Barclay ML, et al. Determination of in vivo absorption, metabolism, and transport of drugs by the human intestinal wall and liver with a novel perfusion technique. *Clin Pharmacol Ther.* 2001;70(3):217-27.
53. Bergman E, Forsell P, Persson EM, Knutson L, Dickinson P, Smith R, et al. Pharmacokinetics of gefitinib in humans: The influence of gastrointestinal factors. *Int J Pharm.* 2007;341(1-2):134-42.
54. Persson EM, Nilsson RG, Hansson GI, Lofgren LJ, Liback F, Knutson L, et al. A clinical single-pass perfusion investigation of the dynamic in vivo secretory response to a dietary meal in human proximal small intestine. *Pharm Res.* 2006;23(4):742-51.
55. Campo R, Montserrat A, Brullet E. Transnasal gastroscopy compared to conventional gastroscopy: A randomized study of feasibility, safety, and tolerance. *Endoscopy.* 1998;30(5):448-52.
56. Soma Y, Saito H, Kishibe T, Takahashi T, Tanaka H, Munakata A. Evaluation of topical pharyngeal anesthesia for upper endoscopy including factors associated with patient tolerance. *Gastrointest Endosc.* 2001;53(1):14-8.
57. Wood C. New strategy to ease the discomfort of insertion of nasogastric tubes. *Int J Clin Pract.* 2005;59(12):1373-4.

58. Poppitt SD, Shin HS, McGill AT, Budgett SC, Lo K, Pahl M, et al. Duodenal and ileal glucose infusions differentially alter gastrointestinal peptides, appetite response, and food intake: A tube feeding study. *Am J Clin Nutr.* 2017;106(3):725-35.
59. Drewe J, Narjes H, Heinzl G, Brickl RS, Rohr A, Beglinger C. Absorption of lefradafiban from different sites of the gastrointestinal tract. *Br J Clin Pharmacol.* 2000;50(1):69-72.
60. Chaikomin R, Wu KL, Doran S, Meyer JH, Jones KL, Feinle-Bisset C, et al. Effects of mid-jejunal compared to duodenal glucose infusion on peptide hormone release and appetite in healthy men. *Regul Pept.* 2008;150(1-3):38-42.
61. Coeffier M, Hecketsweiler B, Hecketsweiler P, Dechelotte P. Effect of glutamine on water and sodium absorption in human jejunum at baseline and during pge1-induced secretion. *J Appl Physiol* (1985). 2005;98(6):2163-8.
62. Cohen LD, Alexander DJ, Catto J, Mannion R. Spontaneous transpyloric migration of a ballooned nasojejunal tube: A randomized controlled trial. *JPEN J Parenter Enteral Nutr.* 2000;24(4):240-3.
63. Deloose E, Janssen P, Depoortere I, Tack J. The migrating motor complex: Control mechanisms and its role in health and disease. *Nature Reviews Gastroenterology & Hepatology.* 2012;9(5):271-85.
64. Jiang Q-J, Jiang C-F, Chen Q-T, Shi J, Shi B. Erythromycin for promoting the postpyloric placement of feeding tubes: A systematic review and meta-analysis. *Gastroenterol Res Pract.* 2018;2018:1671483.
65. Nissinen M, Gylling H, Vuoristo M, Miettinen TA. Micellar distribution of cholesterol and phytosterols after duodenal plant stanol ester infusion. *Am J Physiol Gastrointest Liver Physiol.* 2002;282(6):G1009-15.
66. Zarate N, Mohammed SD, O'Shaughnessy E, Newell M, Yazaki E, Williams NS, et al. Accurate localization of a fall in pH within the ileocecal region: Validation using a dual-scintigraphic technique. *Am J Physiol Gastrointest Liver Physiol.* 2010;299(6):G1276-G86.
67. Rafferty GP, Tham TC. Endoscopic placement of enteral feeding tubes. *World J Gastrointest Endosc.* 2010;2(5):155-64.
68. Troost FJ, Brummer RJ, Haenen GR, Bast A, van Haaften RI, Evelo CT, et al. Gene expression in human small intestinal mucosa in vivo is mediated by iron-induced oxidative stress. *Physiol Genomics.* 2006;25(2):242-9.
69. Mahadeva S, Malik A, Hilmi I, Qua C-S, Wong C-H, Goh K-L. Transnasal endoscopic placement of nasoenteric feeding tubes: Outcomes and limitations in non-critically ill patients. *Nutr Clin Pract.* 2008;23(2):176-81.
70. Smithard D, Barrett NA, Hargroves D, Elliot S. Electromagnetic sensor-guided enteral access systems: A literature review. *Dysphagia.* 2015;30(3):275-85.
71. Byrne CS, Blunt D, Burn J, Chambers E, Dagbasi A, Franco Becker G, et al. A study protocol for a randomised crossover study evaluating the effect of diets differing in carbohydrate quality on ileal content and appetite regulation in healthy humans. *F1000Res.* 2019;8:258.
72. Gervasio JM, Brown RO, Lima J, Tabbaa MG, Abell T, Werkman R, et al. Sequential group trial to determine gastrointestinal site of absorption and systemic exposure of azathioprine. *Dig Dis Sci.* 2000;45(8):1601-7.
73. Miner-Williams W, Deglaire A, Benamouzig R, Fuller MF, Tome D, Moughan PJ. Endogenous proteins in the ileal digesta of adult humans given casein-, enzyme-hydrolyzed casein- or crystalline amino-acid-based diets in an acute feeding study. *Eur J Clin Nutr.* 2014;68(3):363-9.
74. Rochet V, Rigottier-Gois L, Levenez F, Cadiou J, Marteau P, Bresson JL, et al. Modulation of lactobacillus casei in ileal and fecal samples from healthy volunteers after consumption of a fermented milk containing lactobacillus casei dn-114 001rif. *Can J Microbiol.* 2008;54(8):660-7.
75. Deglaire A, Moughan PJ, Airinei G, Benamouzig R, Tome D. Intact and hydrolyzed casein lead to similar ileal endogenous protein and amino acid flows in adult humans. *Am J Clin Nutr.* 2020;111(1):90-7.

76. Miner-Williams W, Deglaire A, Benamouzig R, Fuller MF, Tome D, Moughan PJ. Endogenous proteins in terminal ileal digesta of adult subjects fed a casein-based diet. *Am J Clin Nutr.* 2012;96(3):508-15.
77. Maljaars PW, Symersky T, Kee BC, Haddeman E, Peters HP, Masclee AA. Effect of ileal fat perfusion on satiety and hormone release in healthy volunteers. *Int J Obes (Lond).* 2008;32(11):1633-9.
78. Bos C, Juillet B, Fouillet H, Turlan L, Dare S, Luengo C, et al. Postprandial metabolic utilization of wheat protein in humans. *Am J Clin Nutr.* 2005;81(1):87-94.
79. Gore RM, Silvers RI, Thakrar KH, Wenzke DR, Mehta UK, Newmark GM, et al. Bowel obstruction. *Radiol Clin North Am.* 2015;53(6):1225-40.
80. Jacobs SL, Rozenblit A, Ricci Z, Roberts J, Milikow D, Chernyak V, et al. Small bowel faeces sign in patients without small bowel obstruction. *Clin Radiol.* 2007;62(4):353-7.
81. Shi H, Liu C, Ding HY, Li CW. Magnesium sulfate as an oral contrast medium in magnetic resonance imaging of the small intestine. *Eur J Radiol.* 2012;81(3):e370-e5.
82. Matsushita M, Mori S, Tahashi Y, Wakamatsu T, Okazaki K. Excessive length of a tube in the stomach: A risk factor for a tangled or knotted tube. *Gastrointest Endosc.* 2011;74(1):237-8.
83. Barone JA. Domperidone: A peripherally acting dopamine2-receptor antagonist. *Ann Pharmacother.* 1999;33(4):429-40.
84. Baeyens R, van de Velde E, De Schepper A, Wollaert F, Reyntjens A. Effects of intravenous and oral domperidone on the motor function of the stomach and small intestine. *Postgrad Med J.* 1979;55 Suppl 1:19-23.
85. Tack J, Janssens J, Vantrappen G, Peeters T, Annese V, Depoortere I, et al. Effect of erythromycin on gastric motility in controls and in diabetic gastroparesis. *Gastroenterology.* 1992;103(1):72-9.
86. Kawamura O, Sekiguchi T, Itoh Z, Omura S. Effect of erythromycin derivative em5231 on human interdigestive gastrointestinal tract. *Dig Dis Sci.* 1993;38(6):1026-31.
87. Lee AL, Kim C-B. The effect of erythromycin on gastrointestinal motility in subtotal gastrectomized patients. *J Korean Surg Soc.* 2012;82(3):149-55.
88. Deloosse E, Vos R, Corsetti M, Depoortere I, Tack J. Endogenous motilin, but not ghrelin plasma levels fluctuate in accordance with gastric phase iii activity of the migrating motor complex in man. *Neurogastroenterol Motil.* 2015;27(1):63-71.
89. Bos C, Airinei G, Mariotti F, Benamouzig R, Berot S, Evrard J, et al. The poor digestibility of rapeseed protein is balanced by its very high metabolic utilization in humans. *J Nutr.* 2007;137(3):594-600.
90. Geboes KP, De Preter V, Luybaerts A, Bammens B, Evenepoel P, Ghooys Y, et al. Validation of lactose[15n,15n]ureide as a tool to study colonic nitrogen metabolism. *Am J Physiol Gastrointest Liver Physiol.* 2005;288(5):G994-9.
91. Kastl AJ, Jr., Terry NA, Wu GD, Albenberg LG. The structure and function of the human small intestinal microbiota: Current understanding and future directions. *Cell Mol Gastroenterol Hepatol.* 2020;9(1):33-45.
92. Lee L, Hossain M, Wang Y, Sedek G. Absorption of rivastigmine from different regions of the gastrointestinal tract in humans. *J Clin Pharmacol.* 2004;44(6):599-604.
93. Slater A, Betts M, D'Costa H. Laxative-free ct colonography. *Br J Radiol.* 2012;85(1016):e410-e5.
94. Hughes JS, Watson SJ, Jones AL, Oatway WB. Review of the radiation exposure of the uk population. *J Radiol Prot.* 2005;25(4):493-6.
95. Röntgenonderzoek: Hand/bucky onderzoeken. Ministerie van Volksgezondheid Welzijn en Sport, the Netherlands, editor.: Rijksinstituut voor Volksgezondheid en Milieu (RIVM); 2011.
96. Hounnou G, Destrioux C, Desmé J, Bertrand P, Velut S. Anatomical study of the length of the human intestine. *Surg Radiol Anat.* 2002;24(5):290-4.
97. Minko E, Pagano A, Caceres N, Adar T, Márquez S. Human intestinal tract length and relationship with body height (916.4). *The FASEB Journal.* 2014;28(S1):916.4.
98. Hens B, Corsetti M, Brouwers J, Augustijns P. Gastrointestinal and systemic monitoring of posaconazole in humans after fasted and fed state administration of a solid dispersion. *J Pharm Sci.* 2016;105(9):2904-12.

99. König J, Holster S, Bruins MJ, Brummer RJ. Randomized clinical trial: Effective gluten degradation by aspergillus niger-derived enzyme in a complex meal setting. *Sci Rep*. 2017;7(1):13100.
100. Long C, Yu Y, Cui B, Jagessar SAR, Zhang J, Ji G, et al. A novel quick transendoscopic enteral tubing in mid-gut: Technique and training with video. *BMC Gastroenterol*. 2018;18(1):37.
101. Prabhakaran S, Doraiswamy VA, Nagaraja V, Cipolla J, Ofurum U, Evans DC, et al. Nasoenteric tube complications. *Scand J Surg*. 2012;101(3):147-55.
102. Walmsley RS, Montgomery SM. Factors affecting patient tolerance of upper gastrointestinal endoscopy. *J Clin Gastroenterol*. 1998;26(4):253-5.
103. Huggins PS, Tuomi SK, Young C. Effects of nasogastric tubes on the young, normal swallowing mechanism. *Dysphagia*. 1999;14(3):157-61.
104. Abbott WO, Karr WG, Miller TG. Intubation studies of the human small intestine: Vii. Factors concerned in absorption of glucose from the jejunum and ileum. *Am J Dig Dis*. 1937;4(11):742-52.
105. Kagawa-Busby KS, Heitkemper MM, Hansen BC, Hanson RL, Vanderburg VV. Effects of diet temperature on tolerance of enteral feedings. *Nurs Res*. 1980;29(5):276-80.
106. Gaudichon C, Bos C, Morens C, Petzke KJ, Mariotti F, Everwand J, et al. Ileal losses of nitrogen and amino acids in humans and their importance to the assessment of amino acid requirements. *Gastroenterology*. 2002;123(1):50-9.
107. Marteau P, Flourié B, Cherbut C, Corrèze JL, Pellier P, Seylaz J, et al. Digestibility and bulking effect of ispaghula husks in healthy humans. *Gut*. 1994;35(12):1747-52.
108. Kerlin P, Zinsmeister A, Phillips S. Relationship of motility to flow of contents in the human small intestine. *Gastroenterology*. 1982;82(4):701-6.
109. van den Bogert B. Community and genomic analysis of the human small intestine microbiota. Chapter 7, general discussion. 2013.
110. Ingelfinger FJ, Abbott WO. Intubation studies of the human small intestine. *Am J Dig Dis*. 1940;7(11):468-74.
111. Read NW, Al Janabi MN, Bates TE, Barber DC. Effect of gastrointestinal intubation on the passage of a solid meal through the stomach and small intestine in humans. *Gastroenterology*. 1983;84(6):1568-72.
112. Kerlin P, Tucker R, Phillips SF. Rapid intubation of the ileo-colonic region of man. *Aust N Z J Med*. 1983;13(6):591-3.
113. Sender R, Fuchs S, Milo R. Revised estimates for the number of human and bacteria cells in the body. *PLoS Biol*. 2016;14(8):e1002533-e.
114. van der Beek CM, Canfora EE, Lenaerts K, Troost FJ, Damink S, Holst JJ, et al. Distal, not proximal, colonic acetate infusions promote fat oxidation and improve metabolic markers in overweight/obese men. *Clin Sci (Lond)*. 2016;130(22):2073-82.
115. Wolever TM, Brighenti F, Royall D, Jenkins AL, Jenkins DJ. Effect of rectal infusion of short chain fatty acids in human subjects. *Am J Gastroenterol*. 1989;84(9):1027-33.
116. Bucher P, Gervaz P, Egger J-F, Soravia C, Morel P. Morphologic alterations associated with mechanical bowel preparation before elective colorectal surgery: A randomized trial. *Dis Colon Rectum*. 2006;49(1):109-12.
117. Shobar RM, Velinini S, Keshavarzian A, Swanson G, DeMeo MT, Melson JE, et al. The effects of bowel preparation on microbiota-related metrics differ in health and in inflammatory bowel disease and for the mucosal and luminal microbiota compartments. *Clinical and translational gastroenterology*. 2016;7(2):e143.
118. Jalanka J, Salonen A, Salojärvi J, Ritari J, Immonen O, Marciani L, et al. Effects of bowel cleansing on the intestinal microbiota. *Gut*. 2015;64(10):1562-8.
119. Crosby WH, Kugler HW. Intraluminal biopsy of the small intestine; the intestinal biopsy capsule. *Am J Dig Dis*. 1957;2(5):236-41.
120. Otuya DO, Verma Y, Farrokhi H, Higgins L, Rosenberg M, Damman C, et al. Non-endoscopic biopsy techniques: A review. *Expert Rev Gastroenterol Hepatol*. 2018;12(2):109-17.

121. Cummings JH, Pomare EW, Branch WJ, Naylor CB, Macfarlane GT. Short chain fatty acids in human large intestine, portal, hepatic and venous blood. *Gut*. 1987;28(10):1221-7.
122. Vander Noot MR, 3rd, Eloubeidi MA, Chen VK, Eltoun I, Jhala D, Jhala N, et al. Diagnosis of gastrointestinal tract lesions by endoscopic ultrasound-guided fine-needle aspiration biopsy. *Cancer*. 2004;102(3):157-63.
123. Edwards CH, Grundy MM, Grassby T, Vasilopoulou D, Frost GS, Butterworth PJ, et al. Manipulation of starch bioaccessibility in wheat endosperm to regulate starch digestion, postprandial glycemia, insulinemia, and gut hormone responses: A randomized controlled trial in healthy ileostomy participants. *Am J Clin Nutr*. 2015;102(4):791-800.
124. Zoetendal EG, Raes J, van den Bogert B, Arumugam M, Booijink CCGM, Troost FJ, et al. The human small intestinal microbiota is driven by rapid uptake and conversion of simple carbohydrates. *The ISME Journal*. 2012;6(7):1415-26.
125. Boets E, Gomand SV, Deroover L, Preston T, Vermeulen K, De Preter V, et al. Systemic availability and metabolism of colonic-derived short-chain fatty acids in healthy subjects: A stable isotope study. *J Physiol*. 2017;595(2):541-55.
126. Weerts Z, Keszthelyi D, Vork L, Aendekerk NCP, Frijlink HW, Brouwers J, et al. A novel ileocolonic release peppermint oil capsule for treatment of irritable bowel syndrome: A phase i study in healthy volunteers. *Adv Ther*. 2018;35(11):1965-78.
127. Munoz F, Alici G, Li W. A review of drug delivery systems for capsule endoscopy. *Adv Drug Del Rev*. 2014;71:77-85.
128. Jianguo Cui, Xiaolin Zheng, Wensheng Hou, YinPing Zhuang, Xitian Pi, Yang J. The study of a remote-controlled gastrointestinal drug delivery and sampling system. *Telemedicine and e-Health*. 2008;14(7):715-9.
129. Tang Q, Jin G, Wang G, Liu T, Liu X, Wang B, et al. Current sampling methods for gut microbiota: A call for more precise devices. *Front Cell Infect Microbiol*. 2020;10(151).
130. Nejad HR, Oliveira BC, Sadeqi A, Dehkharghani A, Kondova I, Langermans JA, et al. Ingestible osmotic pill for in-vivo sampling of gut microbiome. *BioRxiv*. 2019:690982.

Supplementary Information

Supplementary Table 1. Search strategy adopted for a search using PubMed to find papers that describe clinical trials applying intestinal catheters in human subjects.

Key concept, SC	Search terms	Hits PubMed
Intestine (SC1)	(intestine OR intestines OR intestinal OR gastrointestinal OR cecum OR caecum OR colon OR ascending colon OR descending colon OR sigmoid colon OR transverse colon OR colon OR duodenum OR duodenal OR ileum OR ileal OR jejunum OR jejunal)	1085143
Intestinal catheter (SC2)	(catheter OR catheters OR tube OR tubes OR intubation OR intubations OR intubated OR feeding tube OR tube feeding OR feeding, tube OR Gastrointestinal Intubation OR Gastrointestinal Intubations OR Intubations, Gastrointestinal OR nasoduodenal OR naso-duodenal OR nasojejunal OR naso-jejunal OR nasoileal OR naso-ileal OR nasointestinal OR naso-intestinal OR naso-intestinal tube OR intra-intestinal OR inraintestinal OR intra-duodenal OR intraduodenal OR intrajejunal OR intrajejunal OR intra-ileal OR intraileal OR intraluminal OR intraluminal OR intra-colonic OR intracolonic)	478254
SC1 AND SC2		46032
Human (SC3)	(human OR humans OR homo sapiens OR healthy volunteers [MeSH] OR healthy volunteer OR healthy participants OR healthy participant OR healthy subjects OR healthy subject OR human volunteers OR human volunteer OR normal volunteers OR normal volunteer OR volunteer OR volunteers OR participant OR participants OR subject OR subjects OR men OR women OR woman OR patients OR patient OR client OR clients)	20196326
SC1 AND SC2 AND SC3		36165
Added to SC1 AND SC2 AND SC3 (related to SC2 about catheters):		
	NOT (indwelling catheters [MeSH] OR Catheter, Indwelling OR Indwelling Catheter OR Indwelling Catheters OR In-Dwelling Catheters OR Catheter, In-Dwelling OR Catheters, In-Dwelling OR In Dwelling Catheters OR In-Dwelling Catheter OR Implantable Catheters)	35159
	NOT (urinary catheters [MeSH] OR Catheter, Urinary OR Catheters, Urinary OR Urinary Catheter OR Ureteral Catheters OR Catheter, Ureteral OR Catheters, Ureteral OR Ureteral Catheter OR Urethral Catheters OR Catheter, Urethral OR Catheters, Urethral OR Urethral Catheter)	34286
	NOT (vascular access devices [MeSH] OR Port Catheters OR Catheter, Port OR Catheters, Port OR Port Catheter OR Vascular Catheters OR Catheter, Vascular OR Catheters, Vascular OR Vascular Catheter OR central venous catheter OR central catheter)	33112
	NOT (catheter obstruction [MeSH] OR Catheter Obstructions OR Obstruction, Catheter OR Obstructions, Catheter)	32669
	NOT (pigtail OR pig-tail)	32623

Added SC1 AND SC2 AND SC3 (related to SC2 about tubes and intubation)		
NOT (Neural Tubes OR Tube, Neural OR Tubes, Neural OR tube formation[All fields] OR tube-lined[All fields] OR tube voltage[All fields])		31935
NOT (Intratracheal Intubation OR Intratracheal Intubations OR Intubations, Intratracheal OR Intubation, Endotracheal OR Endotracheal Intubation OR Endotracheal Intubations OR Intubations, Endotracheal)		31006
NOT (fallopian tube OR Disease, Fallopian Tube OR Diseases, Fallopian Tube OR Fallopian Tube Disease)		30267
Added to SC1 and SC2 and SC3 (related to SC3 about human subjects)		
NOT (child OR children OR infant OR infants OR neonate OR neonates OR newborn OR newborns OR postmortem OR cadaver OR corpse OR corpses)		24655
NOT (mouse OR mice OR mus musculus OR murine OR rat OR rats OR hamster OR hamsters OR pig OR pigs OR piglet OR piglets OR swine OR veterinary OR dog OR dogs)		22822
Additions to the search terms		
NOT (parenteral nutrition [MeSH] OR enterostomy OR enterostomies OR gastrostomy OR Gastrostomies OR Duodenostomy OR duodenostomies OR jejunostomy OR jejunostomies OR peg-j OR peg tube)		18874
NOT (colonoscopy [MeSH] OR colonoscopies OR colonoscope OR Colonography, Computed Tomographic [MeSH] OR colonography OR scintigraphy OR sigmoidoscopy [MeSH])		17409
Additions to refine the type of publication, language and publication year		
NOT (review[Publication Type] OR literature review OR systematic review OR case reports[Publication Type] OR case report OR case reports OR case study OR Meta-Analysis[Publication Type] OR Observational Study[Publication Type])		11962
NOT (retrospective OR prospective)		9946
AND (English[Language])		7387
AND ("1960"[Date - Publication] : "3000"[Date - Publication])		7195
Additions to further refine the search		
NOT (surgery)		4166
NOT (intensive care OR emergency department OR Care, Critical Intensive Care OR Care, Intensive OR Surgical Intensive Care OR Care, Surgical Intensive OR Intensive Care, Surgical OR palliative care OR Palliative Treatment OR hospitalized OR hospitalized patient)		3799
NOT (Brachytherapy OR gastrectomy OR Electrocolonography OR angiography)		3732

Abbreviations: MeSH, medical subject headings; SC, search combination.

Supplementary Table 2. An overview of the information on oro- and naso-intestinal catheters' methods, retrieved from the included papers (n=58), and from unpublished studies of our research groups (n=2).

Due to the extensive size of the table, the reader is referred the supporting information of the online version of the publication: van Trijp MPH et al. Using naso- and oro-intestinal catheters in physiological research for intestinal delivery and sampling in vivo: practical and technical aspects to be considered. Am J Clin Nutr. 2021;114(3):843-861. <https://doi.org/10.1093/ajcn/nqab149>.



A toolbox for the comprehensive analysis of small volume human intestinal samples that can be used with gastrointestinal sampling capsules

Melany Rios-Morales^{*1}, Mara P.H. van Trijp^{*2}, Christiane Rösch³, Ran An⁴, Theo Boer⁵, Albert Gerding^{1,5}, Naomi de Ruiter⁵, Martijn Koehorst^{1,5}, M. Rebecca Heiner-Fokkema⁵, Henk A. Schols³, Dirk-Jan Reijngoud¹, Guido J.E.J. Hooiveld^{#2}, Barbara M. Bakker^{#1}

* Shared first authors, #shared senior authors.

¹ Laboratory of Pediatrics, University of Groningen, University Medical Center Groningen, Groningen, the Netherlands

² Nutrition, Metabolism and Genomics Group, Division of Human Nutrition and Health, Wageningen University, the Netherlands

³ Laboratory of Food Chemistry, Wageningen University, the Netherlands

⁴ Laboratory of Microbiology, Wageningen University, the Netherlands

⁵ Department of Laboratory Medicine, University of Groningen, University Medical Center Groningen, the Netherlands.

Abstract

Detailed knowledge on the fate of dietary components inside the human intestinal tract is lacking. Access to this inner world of digestion is now possible through novel human gastrointestinal sampling capsules. Due to the novelty of such devices, no methodology has been published to stabilise and analyse the resulting samples. A complicating factor is that excretion of such capsules in faeces may take days, while degradation of the dietary components continues. Therefore a stabilising reagent should be pre-loaded in the capsule to ensure the measurement of a representative sample. Considering the small volume of recovered samples, analytical methods must be optimized to collect as much data as possible from little material. We present a complete workflow for stabilising and analysing the fermentation status of dietary fibres in such samples, including microbiota, fibre degradation, and short chain fatty acids. The final quenching reagent was designed based on safety and effectiveness to inhibit fructo- and galacto-oligosaccharides degradation and short chain fatty acids production by human ileostomy microbiota, and subsequently validated in faecal samples. The final composition of the stock quenching reagent is 175 mM Tris, 525 mM NaCl, 35 mM EDTA, 12% SDS, and 8 M urea at pH 8.5.

Keywords

Gastrointestinal sampling capsules; human microbiome; dietary fibres; bacteria metabolites

Introduction

Consumption of dietary fibres has been linked to many health benefits (1, 2). Many fibres are fermented by gut microbiota, resulting in the production of short chain fatty acids (SCFA) and other metabolites (3). Diet, and especially fibres, affect the gut microbiota composition and metabolism. Distinctive microbiota profiles have been associated with healthy and diseased states (4), including metabolic and intestinal disorders. One of the mechanisms of how microbiota affect host health is via the production of the SCFAs acetate, propionate, and butyrate (5, 6). In mice, the SCFA uptake into the host has been associated with the improvement of different metabolic markers such as insulin sensitivity (7). In humans, most of our knowledge about microbial fermentation in the human gut derives from analysing stool samples. Such samples are not necessarily representative of the content of the intestinal lumen, since the gut environment changes throughout the complete length of the gut (8, 9). To study the gut-host interaction, we mostly rely on animal models, due to difficult access to the intestinal lumen in humans. Conventional methods of exploring and collecting human lumen samples remain invasive and include intestinal catheters or colonoscopies (10).

Recently non-invasive access to this inner world of gut microbiota and fermentation products has become possible with the development of novel human gastrointestinal capsules, some of which allow sampling of the luminal content (11-17). Such devices allow a deeper understanding of diet-microbiota-host interactions. Nevertheless, due to the novelty of these devices, no associated analytical methodologies have been published. The current challenges are the small sampling volumes of around maximum 200 μ L (14), and the time delay between sampling and harvesting at body temperature, since excretion of the capsule from the body can take up to days (12). Therefore, at the moment of actuation, the sample needs to be stabilised to block further metabolism so that a representative sample is obtained. In order to do so, a suitable quenching reagent needs to be loaded in the capsule prior to swallowing. Because of the small sample volumes, as much information as possible should be obtained from a single sample. This can be done by combining multiple analytical methods.

Here we present a toolbox comprising a complete workflow for analysing quenched intestinal samples from gastrointestinal sampling capsules. We developed a quenching reagent, which efficiently blocked microbial activity, i.e. fibre degradation, production of SCFA, and stabilised microbial DNA for 48 h at 37°C. Bacterial fibre fermentation in the human intestine was mimicked by *in vitro* batch fermentations with different dietary fibres. Moreover, an efficient extraction procedure and workflow were developed to combine different analytical assays in the same small sample. Importantly, the safety of the quenching reagent for human use was taken into account. As a result, we obtained

a toolbox of procedures to analyse a small representative intestinal sample obtained from gastrointestinal sampling capsules.

Materials and methods

Materials

Fibres used for small intestine (SI) samples were chicory inulin (degree of polymerization (DP) of 3-60; Frutafit HD, Sensus, Roosendaal, The Netherlands), chicory root-derived fructose-oligosaccharides (FOS, DP2-9; Frutalose OFP, Sensus), and galacto-oligosaccharides (GOS) composed of approximately 69% GOS and 28% mono- and disaccharides (Vivinal GOS, FrieslandCampina, Wageningen, The Netherlands). For faecal samples, fibres used were FOS (DP2-9) (Frutalose OFP, Sensus) and GOS (Vivinal GOS, FrieslandCampina). The commercial enzymes glycoside hydrolase enzyme β -galactosidase (EC 3.2.1.23) (18) isolated from *Aspergillus oryzae* (Lactase DS-K, Amano Enzyme Inc., Japan), and endo-inulinase (EC3.2.1.7) isolated from *Aspergillus niger* (19) (Novozym 960, Novozymes A/S, Denmark) were used. SCFA were used as sodium salts (sodium acetate, sodium propionate, and sodium butyrate), and were all obtained from Sigma Aldrich (Missouri, USA). All other chemicals used were at least of (bio)chemical grade.

Ethics approval and consent to participate

The Medical Ethical Reviewing Committee of Wageningen University has evaluated this study and concluded that research in which subjects are not physically involved and anonymously donate faeces, does not require ethical approval from a recognized medical ethics committee. The subjects gave oral consent for the use of their faeces or ileostomy effluent in the *in vitro* experiments. All specimens were used and coded anonymously.

Conditioning of human small intestine samples

Ileostomy effluents from five male and female Caucasian volunteers were collected from the distal ileum, as previously described (20). The subjects had not been treated with antibiotics, pre- or probiotics for at least 3 months directly before effluent donation. The ileostomy effluent was collected after a 14 h fasting period in the morning, and kept at -20°C to minimize bacterial activity until further use within 9 h. Effluents were diluted to a 20% (w/v) slurry in standard ileal efflux medium (SIEM) (21) at pH 7.0. The SIEM was adapted as described elsewhere (22). In short, Tween 80 was left out, fewer carbohydrates were added (0.24 mg/mL), and 0.8 mg/mL MgSO_4 was added (20). The diluted ileostomy effluents were sieved (1.6 mm sieve) to get rid of large food particles, and afterwards directly used for preselection of the ileostomy effluent in SIEM for 15 h under anoxic conditions (81% N_2 , 15% CO_2 , and 4% H_2 , at 37°C , shaking at 100 rpm)

(23). This preselected sample was incubated in SIEM containing the selected dietary fibres for conditioning. This resulted in a final 10% slurry (w/v) of the SI sample and 10 g/L dietary fibres, namely inulin and FOS in a 1:1 w/w ratio or GOS. Conditioning incubation took also place under anoxic conditions at 37°C, shaking at 100 rpm for 5 h. Subsequently, the content of the fermentation bottles was transferred to sterile tubes, frozen in liquid nitrogen, and stored at -80°C till further experiments.

Conditioning of human faecal samples

Faecal samples from four healthy female and male adults were diluted in SIEM with fibres at pH 6.0. For each faecal sample, an 8% faecal slurry (w/v) and 10 g/L dietary fibres was obtained. Conditioning incubation took place under anoxic conditions at 37°C, shaking at 100 rpm for 30 minutes to avoid complete fibre degradation. Afterwards, the content of the fermentation bottles was transferred to sterile tubes, frozen in liquid nitrogen, and stored at -80°C till further experiments.

Composition of the quenching reagent

The final composition of the stock quenching reagent after optimisation contained 175 mM Tris, 525 mM NaCl, 35 mM EDTA, 12% SDS, and 8 M urea at pH 8.5. The quenching reagent solution was heated at 37°C until clear. The quenching reagent was freshly prepared on the day of experiments. In the fermentation samples the quenching reagent was used in a 1:5 v/v ratio, resulting in a final concentration of the components in the mixture of 35 mM Tris, 105 mM NaCl, 7 mM EDTA, 2.4% SDS, and 1.6 M urea.

Estimation of interference and efficacy of the quenching reagent

To test the interference of the quenching reagent, and its individual components urea, NaCl, and SDS, with the analytical methods, the quenching reagent or its components were separately added to standard mixtures of fibres and SCFA. For fibres, 50 µL quenching reagent was added to 200 µL of standard mixtures of 5 mg/mL fibres in water. The mixture of quenching reagent with fibres was diluted in water to a final concentration of 200 µg/mL fibres in the sample before oligosaccharide analysis. For SCFA analysis, 100 µL of quenching reagent or urea, NaCl, and SDS diluted in water (1:5 v/v ratio), were added to a mixture of SCFA with concentrations between 0-20 mM. For precipitation of the SDS, different volumes (32, 65, 130 µL) of 4 M KCl were added on ice to the mixture and centrifuged before organic solvent extraction was performed.

To test the efficacy of the quenching reagent, incubations were started using conditioned fermentation samples. In an Eppendorf tube, either 50 µL of PBS as control or 50 µL of quenching reagent was added to 200 µL of conditioned fermentation samples. The tube was flushed with nitrogen gas to create an anoxic environment. The mixtures were

incubated for 48 h at 37°C with shaking at 400 rpm. The incubations were stopped by freezing at -80°C (Supplementary Figure 1). Reference samples at time 0 h were frozen at -80°C directly for comparison.

Analysis of short chain fatty acids

Samples (100 μ L) were thawed and the following additions were made in the order of 400 μ L of PBS, 100 μ L of 0.5 mg/mL 2-ethylbutyric acid solution (internal standard, the same stock of internal standard was used for calibration curves and samples within the same run), and 20 μ L of 20% 5-sulfosalicylic acid (24). SDS in the quenched samples was precipitated by adding 32 μ L of 4 M KCl and keeping the samples on ice (molar concentration ratio of 17:1 of KCl over SDS in the final sample). Next, the samples were homogenized by bead beating for 30 sec at 5000 rpm with 4-5 zirconium beads of 2.3 mm (Precellys 24, Bertin Technologies, Montigny Le Bretonneux, France) at 4°C. Afterwards, the samples were centrifuged (20 min, 15 000 \times g, 4°C) and the supernatant was transferred to a glass vial. To the supernatant, a spatula tip of solid NaCl and 2 mL diethylether were added. Tubes were vortexed for 10 min at 4°C and centrifuged (10 min, 1200 \times g, 4°C). To 500 μ L of the organic layer, 50 μ L of N-tert-butyltrimethylsilyl-N-methyltrifluoroacetamide (MTBSTFA) was added for overnight SCFA derivatization in a glass vial. The remaining aqueous phase was stored at -80°C for the oligosaccharide analysis. SCFA concentrations were measured using an Agilent 5975C series gas chromatography/mass spectrometry (GC-MS) (Agilent Technologies, Santa Clara, USA). The GC was equipped with a ZB-1 column (Phenomenex, Torrance, USA). Mass spectrometry analysis was performed by positive electron ionization. Ions monitored were m/z 117 for acetate, m/z 131 for propionate, m/z 145 for butyrate, and m/z 173 for 2-ethylbutyric acid (24).

Analysis of the oligosaccharide composition

The obtained aqueous phase after SCFA extraction was centrifuged 10 min at RT at 15 000 \times g. 200 μ L were used directly for analysis of mono-, di-, and oligosaccharide profiles of GOS, FOS, and inulin by HPAEC-PAD (Dionex Corporation, Sunnyvale, CA, USA). The system, columns, elution gradient, and flow rate were used as described elsewhere (25).

Determination of the 16S rRNA gene copy number and microbiota composition

100 μ L of the fermentation sample was used for DNA extraction. Cell lysis was achieved by a repeated bead beating (26), in combination with ASL Stool lysis buffer (Qiagen, Hilden, Germany). The obtained lysate (supernatant) was stored at -20°C, and used for DNA extraction. First, 200 μ L AL buffer (Qiagen) was added to 250 μ L lysate. Afterwards, DNA was extracted and purified using the QIAamp DNA Mini Kit (Qiagen). The total bacterial 16S rRNA gene copy number in the pellet versus the supernatant was quantified

by amplifying a conserved region of the 16S rRNA gene in a CFX384 Real-Time PCR detection system (Bio-Rad Laboratories, Hercules, USA). gDNA was diluted to 5 ng/ μ L. The primers and PCR cycling conditions were described elsewhere (27). Microbiota composition was determined via sequencing of the variable V4 region of the 16S rRNA gene. Triplicate PCR reactions were performed in 35 μ L, containing 7 μ L 5x Phusion Green HF buffer, 0.7 μ L 10 mM dNTPs (Promega, Madison, USA), 0.4 μ L Phusion hot start II DNA polymerase (2 U/ μ L), 25.5 μ L nuclease-free water, 0.7 μ L of extracted template DNA (20 ng/ μ L) and 0.7 μ L of each of the barcoded primers 515F (28) and 806R (29) (10 μ M) (30). Cycling conditions were as follows: 98°C 30 sec, 25 cycles of 98°C 10 sec, 50°C 10 sec, 72°C 10 sec, and 72°C for 7 minutes. Pooled PCR products were checked on a 1.3% agarose gel, and purified using magnetic beads (MagBio Genomics Inc., Gaithersburg, USA). PCR product concentrations were measured using Qubit dsDNA BR buffer and dye (Invitrogen, California, USA), on a DS-11 FX fluorometer (DeNovix, Wilmington, USA). Afterwards, a library containing an equimolar mix (200 ng each) of purified PCR products was prepared. The resultant library was concentrated by using magnetic beads and sequenced on the Illumina HiSeq2500 platform (Eurofins GATC Biotech, Konstanz, Germany). Raw sequencing data were processed using NG-Tax analysis pipeline version 1.0 with default settings (31, 32). Reads were selected with perfect matching primer sequences and de-multiplexed by selecting read pairs with perfectly matching valid barcodes. Amplicon sequence variants (ASV) were picked as follows: sequences were ordered by abundance per sample and reads were considered valid when their cumulative abundance was $\geq 0.1\%$. Taxonomy was assigned using the SILVA database (version 128), with a confidence of $>80\%$ for genus level classification.

Statistical analysis

Statistical analysis and microbiota composition analysis were performed using R version 3.5.1. Microbiota composition at time points 0 and 48 h were correlated using the relative abundances at the genus level with Pearson correlations. The same individuals were present in both the control and quenching reagent groups (related groups). Distribution was checked with the Shapiro-Wilk Normality Test. Statistical analysis on % fibre remainders at the 48 h time point in the faecal samples was performed using independent t-tests for non-normal distribution. P-values of < 0.05 were considered statistically significant.

Results

Quenching reagent development

Incubations with commercial carbohydrate degrading enzymes and fibres

When gastrointestinal sampling capsules are used to study microbial metabolism of fibres in the gut *in vivo*, there is a considerable time delay between sampling and

retrieving the capsule after defecation. Therefore, microbial metabolism should be stopped immediately after sampling, while at the same time the quenching solution should not decompose the fibre. The presence of a quenching solution inside sampling devices becomes essential. After several unsuccessful attempts to develop a quenching fluid based on their potential to inhibit fibre degrading enzymes (Supplementary table 1), a commonly used bacterial lysis buffer was adopted as quenching reagent (NaCl, EDTA, Tris, SDS, pH 8.5) (33), to which urea was added as general protein denaturant (34). This quenching reagent was first tested for its effectiveness to inhibit the degradation of GOS and chicory FOS/inulin by commercially available β -galactosidase and endo-inulinase, respectively (Supplementary table 2, Supplementary Figure 2). This enhanced bacterial lysis buffer almost abolished GOS and FOS/inulin degradation as is clear from the comparison of the DP profiles after incubation with those of the initial substrates (Supplementary table 2, Supplementary Figure 2). Furthermore, the effect of the metal ions in water, Ag^+ , Cu^{2+} , Zn^{2+} , and $\text{Ag}^+/\text{Cu}^{2+}$ were tested because of their known inhibitory effect in enzymatic fibre degradation (35, 36). Ag^+ inhibited GOS breakdown but did not completely inhibit FOS/inulin breakdown by their corresponding enzymes (Supplementary table 1). Subsequent addition of Ag^+ to the quenching reagent effectively inhibited GOS degradation completely (Supplementary Figure 2A-B), whereas the addition of proteinase K to the quenching reagent did not have added value for inhibiting fibre degradation.

Next, the effectiveness of the quenching reagent set at different pH values was evaluated compared to degradation in water (Supplementary Figure 2C-D), to see whether a pH outside the optimal enzyme pH activity range (4.0 - 9.0 (37-40)) improved quenching. At pH 6.5 the enzymatic FOS/inulin breakdown was completely inhibited, while GOS breakdown was only partially inhibited. At pH 9.5 both GOS and FOS/inulin breakdown were completely inhibited. When compared to the degradation of both type of fibres in quenching reagent at the normal pH 8.5, inhibition of degradation at pH 9.5 was very similar to that at pH 8.5 (Supplementary Figure 2A versus 2C, and Fig. 2B with 2D). Therefore, taking into account the pH sensitivity of DNA (41), the pH of the quenching reagent was set at 8.5 (42). Combining all the preliminary results we continued testing with the quenching reagent containing 50 mM NaCl, 10 mM EDTA, 1.5% SDS, 8 M urea, 50 mM Tris at pH 8.5 with or without 20 mM Ag^+ .

Evaluation of fibre breakdown quenching in human small intestine fermentation samples

For experiments in humans, gastrointestinal sampling capsules have to be preloaded with a quenching reagent. To mimic the *in vivo* situation, the effectiveness of the quenching reagent to inhibit fibre breakdown was studied *in vitro* using ileostomy samples, representative for small intestine samples, at various dilution ratios of the quenching

reagent. Chicory FOS/inulin or GOS were incubated with ileostomy samples for 24 h at volume ratios of quenching fluid over ileostomy samples of 1:2, 1:3 and 1:4 (v/v) with or without 20 mM Ag^+ (Figure 1A). At all ratios tested, fibre degradation was almost completely inhibited, irrespective of the presence of Ag^+ . Therefore, Ag^+ was further omitted from the quenching reagent. The components in the quenching reagent were concentrated to achieve effective quenching also in other volume ratios. Therefore, we continued testing with the stock solution of quenching reagent containing 175 mM Tris, 525 mM NaCl, 35 mM EDTA, 12% SDS, and 8 M urea, with pH 8.5. Degradation was minimal over 48 h incubation of both GOS and FOS/inulin in the presence of this quenching reagent (Figure 1B-C) at a ratio of quenching reagent of 1:5 v/v in ileostomy samples from five different subjects ($97.9\% \pm 7.9\%$ GOS; $99.0\% \pm 4.8\%$ FOS/inulin) compared to PBS control ($30.3\% \pm 14\%$ GOS; $51.2\% \pm 21\%$ FOS/inulin). Overall, the quenching reagent at pH 8.5 effectively blocked GOS and FOS/inulin degradation in ileostomy samples at a ratio of 1:5 v/v.

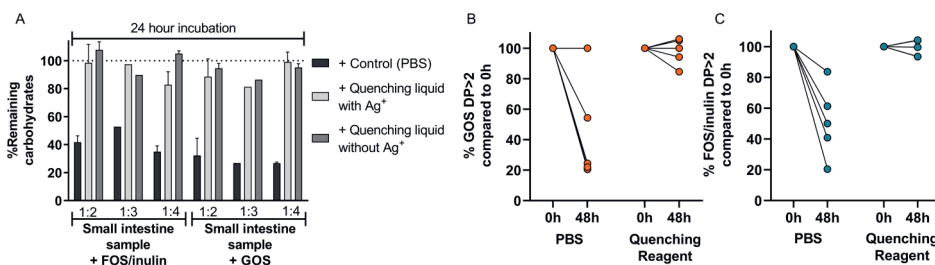


Figure 1. Quenching reagent effectiveness in human small intestine fermentation samples. (A) The quenching reagent stock solution (pH 8.5, 50 mM Tris, 150 mM NaCl, 10 mM EDTA, 1.5% SDS, 8 M urea) with/without Ag^+ was tested on chicory FOS/inulin and GOS breakdown by one human small intestine sample in a 24 h incubation. The tested ratios of quenching reagent:fermentation sample were 1:2, 1:3, 1:4 v/v. Fermentation samples were centrifuged and the supernatant was diluted in water, so the maximum fibre concentration became 0.5 mg/mL, and analyzed by HPAEC-PAD. (B-C) The percentage of GOS DP>2 (B) or FOS/inulin DP>2 (C) after 48 h *in vitro* fermentation by five human small intestine samples in the presence of quenching reagent (pH 8.5, 175 mM Tris, 525 mM NaCl, 35 mM EDTA, 12% SDS, and 8 M urea) or control, 1:5 v/v. Each line represents one individual. Breakdown was expressed as % remaining carbohydrates after incubation versus the initial carbohydrates present at 0 h. GOS; galacto-oligosaccharides, FOS; fructo-oligosaccharides.

Interference of the quenching reagent and its components in analytical protocols

Next, the interference of the quenching reagent and its components in the analytical techniques were evaluated.

Interference of the quenching reagent in SCFA analysis

After we optimized the analysis of SCFA for intestinal and faecal samples (24) (Supplementary Figure 3), we tested whether the quenching reagent affected the extraction and the performance of the SCFA analysis (Figure 2A-B). SCFA standard solutions were analysed in the presence or absence of the quenching reagent or its separate components by GC-MS. The quenching reagent led to an underestimation of SCFA concentrations, and SDS was found to be the interfering component (Figure 2A and Supplementary Figure 4A, C). Therefore, SDS was precipitated on ice by the addition of various amounts of KCl prior to SCFA extraction (Figure 2B and Supplementary Figure 4B, D). At a molar concentration ratio of 17:1 of KCl over SDS (1M of KCl over 0.06 M of SDS in the mixture) SCFA were fully recovered as compared to the analysis in water. Precipitation of SDS by the addition of KCl on ice was effective in preventing SDS from interfering in the analysis of SCFA.

Interference of the quenching reagent in oligosaccharide analysis

The effect of SDS and its precipitation was also studied on the analysis of fibre by HPAEC-PAD. Standard mixtures of GOS and FOS in water were prepared without quenching reagent, with quenching reagent, and with quenching reagent with SDS removed using KCl precipitation and analysed. The quenching reagent per se did not affect the analysis of fibre standards (Figure 2C, E). The combined addition of the quenching reagent and KCl influenced the retention time of the mono- di- and oligomers (Figure 2D, F), but did not affect the signal response for the various compounds in the FOS and GOS mixtures nor the total peak area (Supplementary table 3). Elution from the column shifted to more early retention times, probably caused by chloride ions (anions) from KCl. For correct peak identification, the quenching solution and KCl were also added to oligosaccharide standards from hereon.

Interference of the quenching reagent on the recovery of bacterial DNA

Commonly the pellet obtained from samples with microbial content by centrifugation is used for bacterial DNA extraction. However, since the quenching reagent is a lysing reagent, we investigated if the bacterial DNA was fully recovered in the pellet. To this end, two faecal samples were incubated for 48 h in the presence of quenching reagent or PBS. Afterwards, the pellet was separated from the supernatant by centrifugation (15 min, 4°C, 18 000 x g). Subsequently, DNA was extracted from the pellet and from the supernatant. For both faecal samples, in the presence of quenching reagent a substantial part of the 16S rRNA bacterial copy number was found in the supernatant at 0 h and 48 h, compared to 0-1% in the PBS controls (Figure 2G). Therefore, an aliquot of the intact homogenized sample must be used for DNA extraction, rather than only the pellet of the sample.

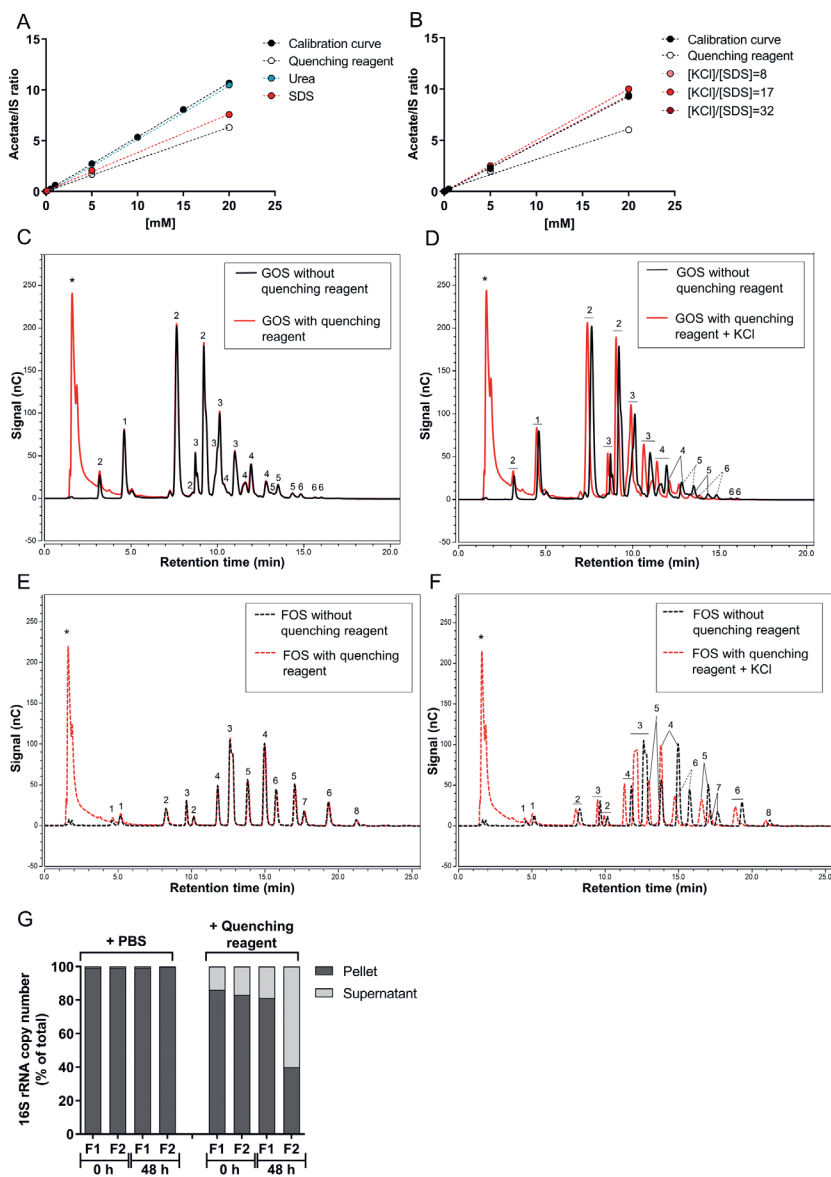


Figure 2. Quenching reagent interference in analysis of SCFA, oligosaccharides, and bacterial 16S rRNA copy number.

(A) The acetate concentration calibration curves made in PBS in the presence of quenching reagent or its major components. (B) Calibration curve of acetate after precipitation of SDS with KCl in different KCl/SDS molar ratios. The HPAEC chromatograms of GOS (C, D) and FOS (E, F) prepared in water. The black lines represent the mixture of fibre in water. The red lines represent the fibre in water in the presence of quenching reagent (C, E) or in the presence of quenching reagent after precipitation of SDS with KCl (D, F). The numbers in the chromatograms represent the degree of polymerization, 1 = monomers, 2 = dimers, ≥ 3 = oligomers, and * are components present in the quenching reagent. (G) The % 16S rRNA bacteria copy number in the supernatant or in the pellet versus the total number from two faecal fermentation samples in the presence of quenching reagent or PBS at 0 and 48 h. The total represents the 16S rRNA copy number in pellet plus supernatant.

Validation of quenching reagent efficiency in *in vitro* fermentations with human faecal microbiota

Now that we developed a quenching reagent and a protocol to analyse fibre degradation, SCFA concentrations, and bacteria numbers in quenched samples, the protocol was evaluated in faecal samples. Such samples are expected to be a more challenging matrix with respect to fibre fermentation. To this end, four human faecal samples were inoculated in *in vitro* batch fermentations of GOS and chicory FOS.

Quenching of oligosaccharides degradation and SCFA appearances in faecal samples

After 48 h fermentation, less than 18% GOS and less than 21% chicory FOS were left in PBS control incubations without the quenching reagent (Figure 3A, E). Addition of the quenching reagent at a ratio of 1:5 v/v preserved on average 80.0% \pm 6.0% of the GOS, and on average 89.5% \pm 11.1% of chicory FOS during 48 h incubations, significantly more than in PBS controls ($P < 0.05$). During 48 h incubation in the presence of the quenching reagent, SCFA production and interconversion were completely blocked as can be concluded from the constant SCFA concentrations compared to 0 h (Figure 3B-D, F-H). In the absence of the quenching reagent, the SCFA concentrations, mainly acetate, increased substantially over 48 h.

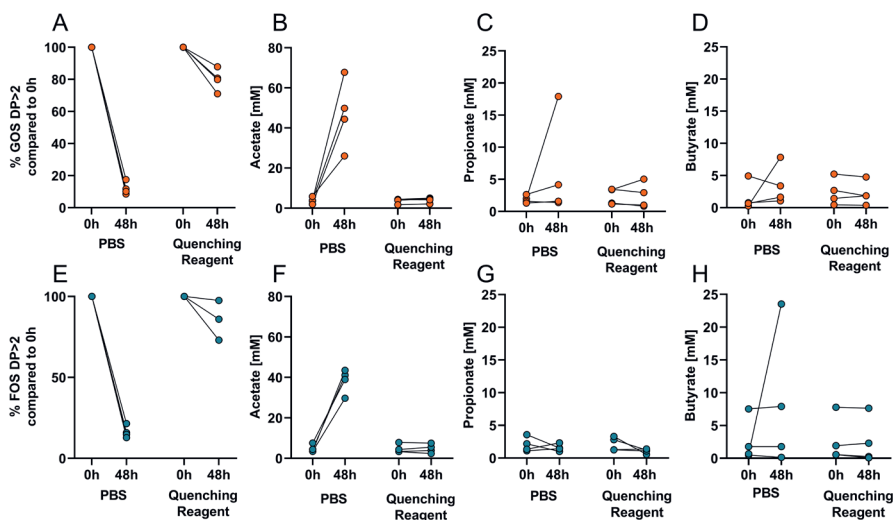


Figure 3. Quenching reagent effectiveness in faecal samples.

The percentage of GOS DP>2 (A) or FOS DP>2 (E), and concentrations of SCFA in fermentations of GOS DP>2 (B-D), or FOS DP>2 (F-H) from four human faecal samples after 48 h of *in vitro* incubation versus the start of the incubation (0 h). Each line represents one individual. Fibres breakdown was expressed as % remaining carbohydrates after incubation versus the initial carbohydrates present at 0 h. FOS; fructo-oligosaccharides, GOS; galacto-oligosaccharides.

Quenching of bacterial 16S rRNA copy number and microbiota composition in faecal samples

The 16S rRNA bacterial copy number is used as an indication for the total number of bacteria. In the PBS incubations, the total 16S rRNA bacterial copy number increased substantially over 48 h, except for one faecal sample, demonstrating bacterial proliferation over time (Figure 4A), likely due to the presence of undigested material in the faecal sample. In one faecal fermentation the 16S rRNA copy number decreased, which may be due to *e.g.* substrate depletion and accumulation of (toxic) products. Nevertheless, in all samples where the quenching reagent was added at a ratio of 1:5 v/v, the total 16S rRNA copy number did not change, indicating effectively blocking biomass changes (Figure 4A). The microbiota composition was determined in two faecal samples for GOS and chicory FOS fermentation at 0 and 48 h (Figure 4B). In the PBS conditions the microbiota composition changed between 0 and 48 h, as indicated by the low correlation coefficients of the relative microbiota composition, namely <0.15 and <0.69. When quenching reagent was added at a ratio of 1:5 v/v, the 48 h microbiota mimicked the microbiota present at the start, as indicated by the correlation coefficients of the relative microbiota composition between 0 and 48 h, which were >0.92 and >0.74. In conclusion, the addition of the quenching reagent did not only preserve the bacterial 16S rRNA copy number, but also the microbial composition.

Development of a toolbox to measure fibre fermentation in very small gastrointestinal samples

Volumes of gastrointestinal samples, obtained from gastrointestinal sampling devices, are maximally 200 μ L (14). To obtain as much information as possible, we developed a workflow in which analyses were combined to allow the most efficient workup of the samples. In the final workflow (Figure 5A), prior to extraction of SCFA and oligosaccharides, an aliquot of the intact homogenized sample was taken for microbiota analysis. For fibre and SCFA analysis, the analytical protocols were optimized to avoid splitting the sample before extraction.

With extraction of SCFA with organic solvents after acidification of the sample using HCl (24), the hydrophilic GOS and chicory FOS were expected to remain in the aqueous layer (Figure 5A). Therefore, the recovery of GOS and chicory FOS from the aqueous phase after SCFA extraction was compared to that from the intact sample (Figure 5B-E). We observed that in the aqueous layer the oligosaccharides in GOS and FOS were lost (Figure 5B, D), and were mostly hydrolysed into monomeric units. The SCFA extraction procedure caused hydrolysis of GOS and chicory FOS, expectedly due to samples acidification by addition of HCl prior to SCFA extraction. When HCl was omitted from the sample treatment, acid hydrolysis of GOS and chicory FOS was prevented, and the fibres were completely recovered in the aqueous phase (Figure 5C,

E). The extraction procedure only caused a slight shift in retention time.

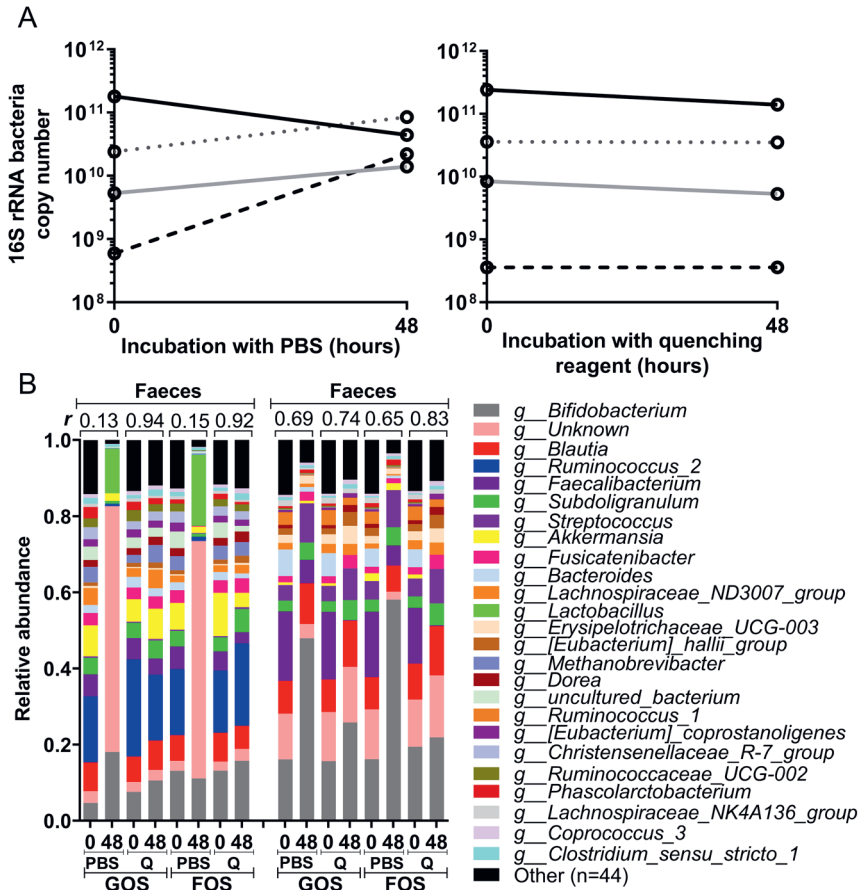


Figure 4. Quenching of the 16S rRNA bacteria copy numbers and microbiota composition in human faecal samples.

(A) The total bacteria 16S rRNA copy numbers in the faecal fermentation samples, mixed and diluted in SIEM medium with fibres, in the presence of PBS or quenching reagent at 0 and 48 h. The same colour represents faeces from the same individual. (B) The relative microbiota composition at 0 h and 48 h after addition of PBS or quenching reagent 'Q' in conditions with added GOS or chicory FOS for two faecal donors. The top 25 genera are shown. Correlation coefficients were calculated on the relative abundances at genus level, and shown in the graph as correlation number. Q; quenching reagent, FOS; fructo-oligosaccharides, GOS; galacto-oligosaccharides.

We then tested if omission of HCl would affect the extraction of SCFA. Without HCl addition, but still in the presence of sulfosalicylic acid, the pH in the aqueous layer was 1.7, well below the pKa of the SCFA. Consequently, the SCFA concentrations measured in standard curves (Figure 5F-H) and in faeces (Figure 5I) were very similar. Apparently, under these conditions, recovery of SCFA did not depend on the addition

of HCl. In conclusion, the SCFA extraction without HCl allows the measurements of SCFA and also soluble fibres without splitting the sample. The final combined protocol to investigate all primary outcomes is shown in Figure 6.

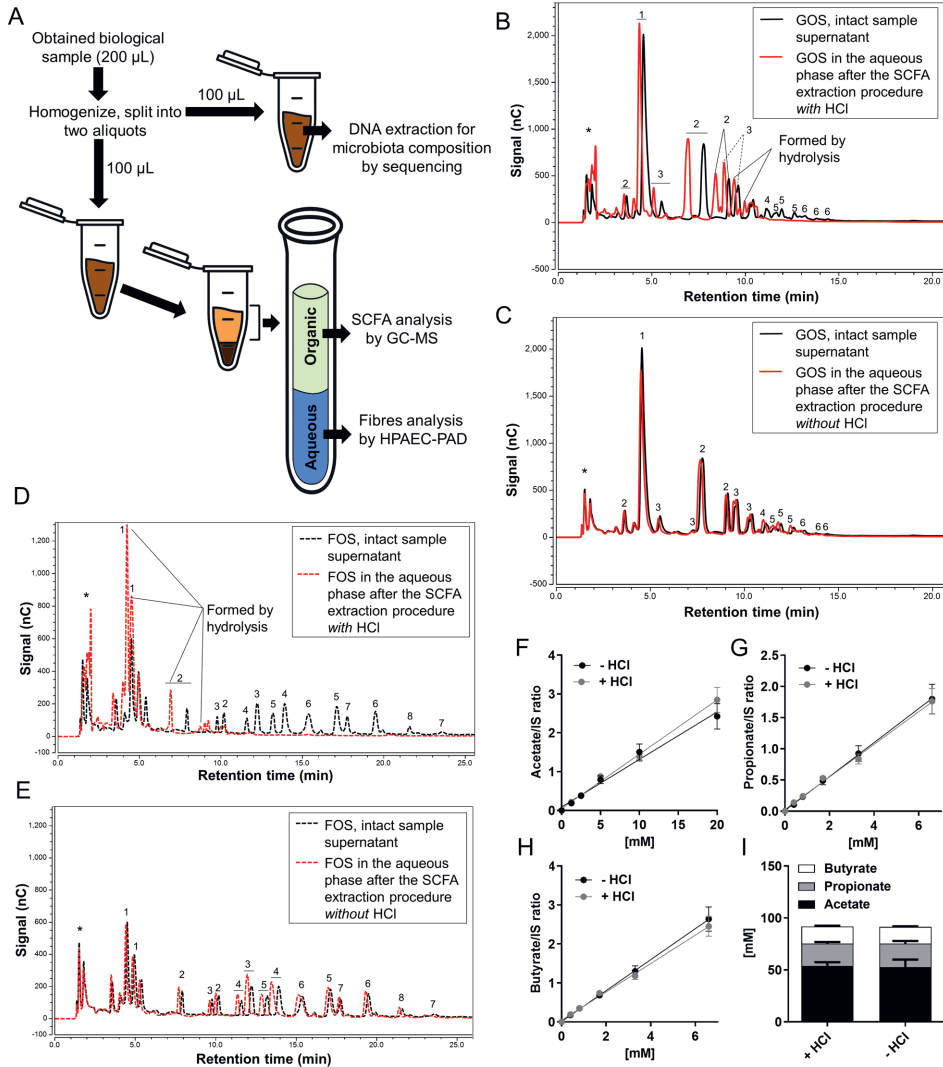


Figure 5. Combined protocol of fibres and SCFA analysis.

(A) A schematic workflow for the combined analysis of 200 µL gastrointestinal sample. HPAEC chromatograms of GOS faecal fermentation samples (B, C) and chicory FOS faecal fermentation samples (D, E). The black lines represent fibres present in the intact sample supernatant, and the red lines represent fibres present in the aqueous phase after the SCFA extraction procedure with HCl (B, D) or without HCl (C, E). The numbers in the chromatograms represent the degree of polymerization, 1 = monomers, 2 = dimers, ≥ 3 = oligomers, and * are components present in the quenching reagent and in the medium. The calibration curves of concentrations of acetate (F), propionate (G), and butyrate (H) with and without the addition of HCl in the extraction protocol,

and SCFA concentrations (I) in the same faecal sample with and without the addition of HCl (mean \pm SEM, $n=3-5$). GC-MS; gas chromatography-mass spectrometry, HPAEC-PAD; high performance anion exchange chromatography with pulsed amperometric detection.

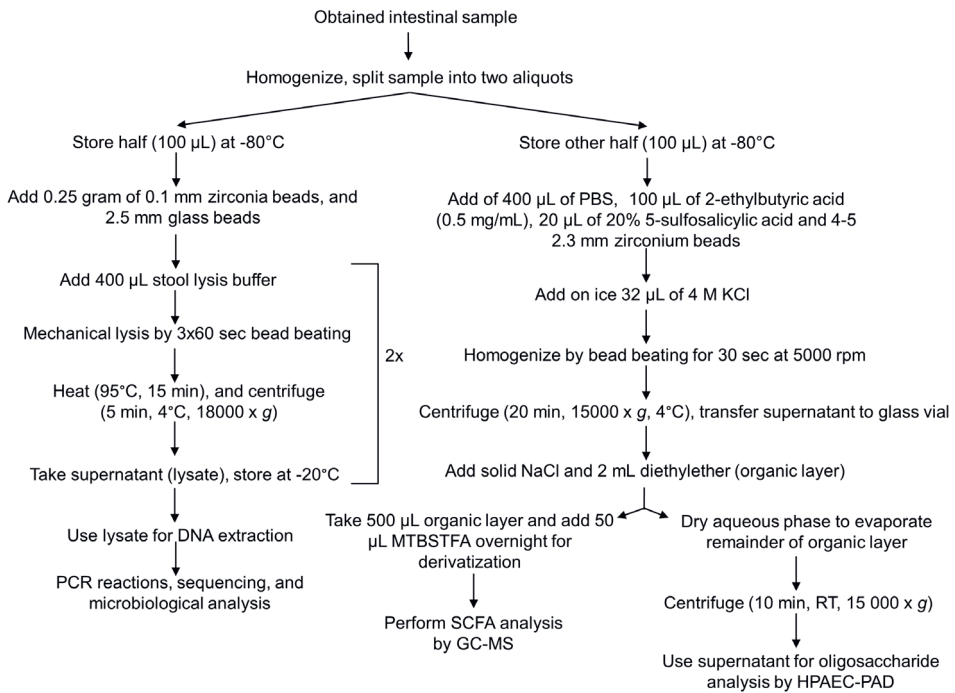


Figure 6. A schematic overview of the complete protocol to measure oligosaccharides, SCFA, and microbiota composition.

GC-MS; gas chromatography-mass spectrometry, HPAEC-PAD; high performance anion exchange chromatography with pulsed amperometric detection, SCFA; short chain fatty acids.

Discussion

In humans, the consumption of dietary fibres has been linked to beneficial health effects (1, 2). Detailed knowledge on the fate of fibres inside the human intestinal tract is however still very limited, due to the lack of convenient non-invasive methods. New gastrointestinal sampling capsules are being developed, which sample luminal content at a specific location in the intestinal lumen (11, 14, 15). The application of these novel devices poses several methodological challenges, because of their retrieval time delay and their small volume. In this study, we addressed these challenges and developed a toolbox for stabilising the sample by a quenching reagent and analysing the fermentation status of dietary fibres in such samples, i.e. the extent of fibre degradation, the microbiota composition, and the main fermentation products.

The developed quenching reagent

One main challenge is to obtain a representative sample due to the considerable time delay between sampling and retrieving the intestinal sample. For that purpose, we developed a quenching reagent and tested its effectiveness to inhibit fibre breakdown *in vitro* in human ileostomy and faecal samples. The quenching reagent was based on a bacterial lysis buffer with addition of several components to denature enzymes. This reagent can be preloaded in gastrointestinal capsules to block further fermentation of fibres in the obtained sample. The components in the quenching reagent (NaCl, EDTA, Tris, SDS, urea, at pH 8.5) were present for specific reasons. NaCl was needed to establish ionic strength outside the cells, EDTA is a chelating agent that complexes enzyme metal-cofactors and thereby blocks DNAses, and Tris is a buffering agent to maintain the pH around 8.5 for DNA stability. The anionic detergent SDS was added for disruption of bacterial cell membrane structures (43) and to inhibit nuclease activity, thereby preventing DNA degradation. Urea (8 M) was added as a general protein denaturant (34). The quenching reagent showed efficient quenching of dietary fibre fermentation *in vitro* for up to 48 h.

Importantly, the developed methodology was evaluated in faecal samples from different donors. Blocking fibre breakdown could be donor and consequently microbiota dependent due to differences in microbial capacity of degrading non-digestible carbohydrates. Faecal samples are a more challenging matrix than small intestine samples, and better represent the large intestine where most of the fermentation occurs. As is clear from this study, the quenching reagent stopped degradation effectively in all faecal samples, irrespective of the fibre tested or microbial composition present. The concentrations of SCFA measured in the samples in this study before the start of fermentation were lower than typically measured in faeces (44), because the faecal samples had been diluted in SIEM with dietary fibres to prepare the faecal slurry.

The microbiota composition can differ between *in vitro* fermentation samples and the *in vivo* situation in humans, since *in vitro* only the viable fraction will persist. It is noteworthy that different faecal donors and fibre mixes produced strikingly different SCFA patterns. Considering these different breakdown patterns by different compositions of microbiota, we developed an effective quenching reagent for all individuals. Since it contains general enzyme inhibitors and components for cell lysing, we expect that all microbial activity is stopped when added, preserving the sample for a broader range of metabolites. Furthermore, we showed that our quenching reagent was effective over a period of 48 h, which we expect to be the maximum intestinal transit time *in vivo* for most people. Previously, the human whole gut transit time was shown to be 30.6 ± 7.7 h (12). In this way, we ensure that the sample obtained is a representative sample of the sampling location.

Toxicological report of components in quenching reagent

Gastrointestinal sampling capsules have a reservoir opening towards the gastrointestinal lumen. Although leaking of quenching reagent into the human intestinal lumen is very unlikely, the quenching reagent should be safe for human oral intake. A safety risk assessment focussed on the oral acute toxicity of the components in the quenching reagent was performed. For this assessment, it was assumed that the lumen would be exposed to the total volume of 50 μL quenching reagent present in the capsule reservoir. An overview of the quenching reagent component concentrations and the toxicology information is given in Table 1.

Table 1. Toxicology information about the components in the quenching reagent.

Chemical name	CAS registration number	Concentration	Amount mg / 50 μL	Toxicology information
Trisaminomethane, thrometamine (Tris)	77-86-1	175 mM	1.1	Oral (non-human) NOAEL = 4000 mg/kg
Sodium chloride (NaCl)	7647-14-5	530 mM	1.5	GRAS component
Ethylenediaminetetraacetic acid (EDTA)	60-00-4	35 mM	0.7	EFSA, no safety concern (humans) = 1.9 mg/kg/day
Sodium dodecylsulfate, sodium laurylsulfate (SDS)	151-21-3	12 %	6	Oral (non-human) NOAEL = 100 mg/kg/day
Urea	57-13-6	8 M	24	GRAS component

The concentrations of all components and amounts of the components present in 50 μL of the quenching reagent, the CAS registration numbers, and information about toxicology is presented. CAS, chemical abstracts service; GRAS, generally recognized as safe; NOAEL, no observed adverse effect level; EFSA, European Food Safety Authority.

Trisaminomethane (Tris) is also known as pharmaceutical registered under the name THAM, and is a biological buffer agent that regulates acid–base regulation (45, 46). The no observed adverse effect level (NOAEL) for repeated oral intake of Tris is 4000 mg/kg body weight (47). Therefore, a single dose of 1.1 mg Tris in the quenching agent is not considered as being harmful. SDS is on the Food and Drug Administration (FDA) list of multipurpose additives allowed to be directly and indirectly added to food (48). Adult consumers may be exposed to up to 0.030 mg SDS/kg body weight/day, and the NOAEL was established for repeated dose toxicity being 100 mg SDS/kg body weight/day. The amount of 6 mg SDS in our quenching reagent is therefore not considered to be harmful for adults. The other components sodium chloride (NaCl), urea, and (disodium) EDTA are generally recognized as safe food substances by the FDA (49, 50). Therefore, the presence of small amounts in this quenching reagent are not of concern.

In conclusion, based on literature research none of the quenching reagent components that are present in 50 μL will lead to acute toxicity effects in humans, and can therefore be considered as safe.

The toolbox for combined analysis of small samples

Another challenge of the technology for intestinal sampling, is the small volume of sample that can be obtained. Therefore, to retrieve as much information as possible from a single small sample, analytical protocols were optimized for the measurement of fibres, microbiota composition, and SCFA in a small sample in the presence of the quenching reagent. We started from the assumption that the expected maximal volume to be retrieved from a sampling capsule will be around 200 μL (14). In the final protocol after homogenization, the sample was therefore divided in two aliquots of 100 μL , one for SCFA and fibres, and the other for microbiota analysis. For complete recovery of bacterial DNA from the sample, the sample needed to be divided into two aliquots first, since the quenching reagent partially lysed the cells, leading to the presence of bacterial DNA in the supernatant. This prevented recovery of bacterial DNA from the pellet only, and therefore a separate aliquot of the intact sample had to be used. For SCFA analysis, precipitation of SDS using KCl was found to be crucial to measure correct SCFA amounts in a sample in the presence of the quenching reagent. Perturbations of the analysis of fibres were minimal. Only retention times shifted due to the high salt content. Analysis of the fibre standard in the presence of salts corrected for this problem sufficiently. When using our protocol to measure SCFA using GC with HCl acidification of the samples, the fibres of interest were hydrolysed to their respective mono- and disaccharides. Therefore, HCl was omitted while maintaining 5-sulfosalicylic acid for protein precipitation. Apparently, the pH of the sample decreased enough to recover the SCFAs and avoid oligosaccharide hydrolysis. The optimizations of the combined analytical protocols enabled us to use only 100 μL to measure both SCFA and fibres. This combined protocol is also applicable and relevant for other research fields, where researchers have to deal, for other reasons, with small sample volumes. We also identified the main sources of disturbance to be tested in other analytical assays, in order to expand the toolbox to study other interesting microbial processes.

Conclusions

We developed and validated a toolbox that can be used to obtain and analyse a representative sample of intestinal content using novel gastrointestinal sampling capsules. The quenching reagent presented, can completely block fibres fermentation and SCFA production for up to 48 h. Furthermore, a mixed protocol was developed to measure fibres, bacterial DNA, and SCFA from a small sample in the presence of the quenching

reagent. This work is the basis for a more extensive analytical approach to also study other gut microbial processes. Considering the small volumes of samples expected to be obtained and the cost of novel gastrointestinal sampling capsules, the developed toolbox will be a major advantage in this rapidly developing research field.

Acknowledgements

We greatly thank the volunteers in this study for donation of ileostomy effluent or faeces. We thank FrieslandCampina and Sensus B.V. for providing us the fibres and all the consortium partners involved for the critical feedback during the development of the project. This research was performed in the public-private partnership 'CarboKinetics' coordinated by the Carbohydrate Competence Center (CCC, www.cccresearch.nl). CarboKinetics is financed by participating industrial partners Agrifirm Innovation Center B.V., Cooperatie AVEBE U.A., DSM Food Specialties B.V., FrieslandCampina Nederland B.V., Nutrition Sciences N.V., VanDrie Holding N.V. and Sensus B.V., and allowances of The Netherlands Organisation for Scientific Research (NWO). The funders had no role in data collection and analysis, or preparation of the manuscript.

References

1. Anderson JW, Baird P, Davis Jr RH, Ferreri S, Knudtson M, Koraym A, et al. Health benefits of dietary fiber. *Nutr Rev*. 2009;67(4):188-205.
2. Slavin J. Fiber and prebiotics: Mechanisms and health benefits. *Nutrients*. 2013;5(4):1417-35.
3. den Besten G, van Eunen K, Groen AK, Venema K, Reijngoud D-J, Bakker BM. The role of short-chain fatty acids in the interplay between diet, gut microbiota, and host energy metabolism. *J Lipid Res*. 2013;54(9):2325-40.
4. Round JL, Mazmanian SK. The gut microbiota shapes intestinal immune responses during health and disease. *Nat Rev Immunol*. 2009;9:313.
5. Koh A, De Vadder F, Kovatcheva-Datchary P, Bäckhed F. From dietary fiber to host physiology: Short-chain fatty acids as key bacterial metabolites. *Cell*. 2016;165(6):1332-45.
6. Nicholson JK, Holmes E, Kinross J, Burcelin R, Gibson G, Jia W, et al. Host-gut microbiota metabolic interactions. *Science*. 2012;336(6086):1262.
7. den Besten G, Havinga R, Bleeker A, Rao S, Gerding A, van Eunen K, et al. The short-chain fatty acid uptake fluxes by mice on a guar gum supplemented diet associate with amelioration of major biomarkers of the metabolic syndrome. *PLoS One*. 2014;9(9):e107392-e.
8. Stearns JC, Lynch MD, Senadheera DB, Tenenbaum HC, Goldberg MB, Cvitkovitch DG, et al. Bacterial biogeography of the human digestive tract. *Sci Rep*. 2011;1:170.
9. Vasopoli R, Schütte K, Schulz C, Vital M, Schomburg D, Pieper DH, et al. Analysis of transcriptionally active bacteria throughout the gastrointestinal tract of healthy individuals. *Gastroenterology*. 2019;157(4):1081-92.e3.
10. Kastl AJ, Terry NA, Wu GD, Albenberg LG. The structure and function of the human small intestinal microbiota: Current understanding and future directions. *Cell Mol Gastroenterol Hepatol*. 2020;9(1):33-45.
11. Amoako-Tuffour Y, Jones ML, Shalabi N, Labbe A, Vengallatore S, Prakash S. Ingestible gastrointestinal sampling devices: State-of-the-art and future directions. *Crit Rev Biomed Eng*. 2014;42(1):1-15.
12. Koziolok M, Grimm M, Becker D, Iordanov V, Zou H, Shimizu J, et al. Investigation of pH and temperature profiles in the GI tract of fasted human subjects using the intellicap® system. *J Pharm Sci*. 2015;104(9):2855-63.
13. van der Schaar PJ, Dijkman JF, Broekhuizen-de Gast H, Shimizu J, van Lelyveld N, Zou H, et al. A novel ingestible electronic drug delivery and monitoring device. *Gastrointest Endosc*. 2013;78(3):520-8.
14. Rezaei Nejad H, Oliveira BCM, Sadeqi A, Dehkharghani A, Kondova I, Langermans JAM, et al. Ingestible osmotic pill for in vivo sampling of gut microbiomes. *Adv Intell Syst*. 2019;1(5):1900053.
15. Ge Jin GW, Xiang Liu, Hailong Cao, Bangmao Wang. Intestine microbiome aspiration (imba) capsule: A new autonomous and minimally-invasive device for whole gut microbiome sampling and mapping. Available from: [https://www.gastrojournal.org/article/S0016-5085\(19\)37309-3/pdf](https://www.gastrojournal.org/article/S0016-5085(19)37309-3/pdf).
16. Tang Q, Jin G, Wang G, Liu T, Liu X, Wang B, et al. Current sampling methods for gut microbiota: A call for more precise devices. *Front Cell Infect Microbiol*. 2020;10(151).
17. Boets E, Gomand SV, Deroover L, Preston T, Vermeulen K, De Preter V, et al. Systemic availability and metabolism of colonic-derived short-chain fatty acids in healthy subjects: A stable isotope study. *J Physiol*. 2017;595(2):541-55.
18. Tavares TM, FX. Whey and whey powders | fermentation of whey. In: Caballero B, Finglas P, Toldra F, editors. *Encyclopedia of food sciences and nutrition* (second edition). Oxford: Academic Press; 2003. p. 6157-63.
19. Sirisansaneeyakul S, Worawuthiyanan N, Vanichsriratana W, Srinophakun P, Chisti Y. Production of fructose from inulin using mixed inulinases from *Aspergillus niger* and *Candida guilliermondii*. *World J Microbiol Biotechnol*. 2007;23(4):543-52.

20. van Trijp MPH, Rösch C, An R, Keshtkar S, Logtenberg MJ, Hermes GDA, et al. Fermentation kinetics of selected dietary fibers by human small intestinal microbiota depend on the type of fiber and subject. *Mol Nutr Food Res*. 2020;64(20):2000455.
21. Gibson GR, Cummings JH, Macfarlane GT. Use of a three-stage continuous culture system to study the effect of mucin on dissimilatory sulfate reduction and methanogenesis by mixed populations of human gut bacteria. *Appl Environ Microbiol*. 1988;54(11):2750-5.
22. Ramasamy US, Venema K, Schols HA, Gruppen H. Effect of soluble and insoluble fibers within the in vitro fermentation of chicory root pulp by human gut bacteria. *J Agric Food Chem*. 2014;62(28):6794-802.
23. Aguirre M, Eck A, Koenen ME, Savelkoul PHM, Budding AE, Venema K. Evaluation of an optimal preparation of human standardized fecal inocula for in vitro fermentation studies. *J Microbiol Methods*. 2015;117:78-84.
24. Besten Gd, Lange K, Havinga R, Dijk THv, Gerding A, Eunen Kv, et al. Gut-derived short-chain fatty acids are vividly assimilated into host carbohydrates and lipids. *Am J Physiol Gastrointest Liver Physiol*. 2013;305(12):G900-G10.
25. Jonathan MC, van den Borne JJGC, van Wiechen P, Souza da Silva C, Schols HA, Gruppen H. In vitro fermentation of 12 dietary fibres by faecal inoculum from pigs and humans. *Food Chem*. 2012;133(3):889-97.
26. Salonen A, Nikkilä J, Jalanka-Tuovinen J, Immonen O, Rajilić-Stojanović M, Kekkonen RA, et al. Comparative analysis of fecal DNA extraction methods with phylogenetic microarray: Effective recovery of bacterial and archaeal DNA using mechanical cell lysis. *J Microbiol Methods*. 2010;81(2):127-34.
27. Janssen AWF, Dijk W, Boekhorst J, Kuipers F, Groen AK, Lukovac S, et al. Angptl4 promotes bile acid absorption during taurocholic acid supplementation via a mechanism dependent on the gut microbiota. *BBA Mol Cell Biol L*. 2017;1862(10, Part A):1056-67.
28. Parada AE, Needham DM, Fuhrman JA. Every base matters: Assessing small subunit rRNA primers for marine microbiomes with mock communities, time series and global field samples. *Environ Microbiol*. 2016;18(5):1403-14.
29. Apprill A, McNally S, Parsons R, Weber L. Minor revision to v4 region ssu rRNA 806r gene primer greatly increases detection of sar11 bacterioplankton. *Aquat Microb Ecol*. 2015;75(2):129-37.
30. Walters W, Hyde ER, Berg-Lyons D, Ackermann G, Humphrey G, Parada A, et al. Improved bacterial 16S rRNA gene (v4 and v4-5) and fungal internal transcribed spacer marker gene primers for microbial community surveys. *mSystems*. 2016;1(1):e00009-15.
31. Poncheewin W, Hermes GDA, van Dam JCJ, Koehorst JJ, Smidt H, Schaap PJ. Ng-tax 2.0: A semantic framework for high-throughput amplicon analysis. *Front Genet*. 2020;10(1366).
32. Ramiro-Garcia J, Hermes G, Giatsis C, Sipkema D, Zoetendal E, Schaap P, et al. Ng-tax, a highly accurate and validated pipeline for analysis of 16S rRNA amplicons from complex biomes [version 2; referees: 1 approved, 1 approved with reservations, 1 not approved]. *F1000Research*. 2018;5(1791).
33. Wilson K. Preparation of genomic DNA from bacteria. *Curr Protoc Mol Biol*. 2001;56(1):2.4.1-2.4.5.
34. Bannion BJ, Daggett V. The molecular basis for the chemical denaturation of proteins by urea. *Proc Natl Acad Sci*. 2003;100(9):5142.
35. Chi Z, Chi Z, Zhang T, Liu G, Yue L. Inulinase-expressing microorganisms and applications of inulinases. *Appl Microbiol Biotechnol*. 2009;82(2):211-20.
36. Dey PM. Inhibition, transgalactosylation and mechanism of action of sweet almond α -galactosidase. *Enzymology*. 1969;191(3):644-52.
37. Pandey A, Soccol CR, Selvakumar P, Soccol VT, Krieger N, Fontana JD. Recent developments in microbial inulinases. *Appl Biochem Biotechnol*. 1999;81(1):35-52.
38. Tanaka Y, Kagamiishi A, Kiuchi A, Horiuchi T. Purification and properties of β -galactosidase from *Aspergillus oryzae*. *J Biochem*. 1975;77(1):241-7.

39. Hsu CA, Yu RC, Chou CC. Production of β -galactosidase by bifidobacteria as influenced by various culture conditions. *Int J Food Microbiol.* 2005;104(2):197-206.
40. Husain Q. B galactosidases and their potential applications: A review. *Crit Rev Biotechnol.* 2010;30(1):41-62.
41. Sowers LC, Shaw BR, Veigl ML, David Sedwick W. DNA base modification: Ionized base pairs and mutagenesis. *Mutat Res.* 1987;177(2):201-18.
42. Christian Birkner HvdE, Monika Soukupova inventor; Roche Diagnostics Operations Inc assignee. Reagents for lysis of bacterial cells. U.S.2009-09-02.
43. Harrison STL. Bacterial cell disruption: A key unit operation in the recovery of intracellular products. *Biotechnol Adv.* 1991;9(2):217-40.
44. Primec M, Mičetić-Turk D, Langerholc T. Analysis of short-chain fatty acids in human feces: A scoping review. *Anal Biochem.* 2017;526:9-21.
45. Kallet RH, Jasmer RM, Luce JM, Lin LH, Markes JD. The treatment of acidosis in acute lung injury with tris-hydroxymethyl aminomethane (tham). *Am J Respir Crit Care Med.* 2000;161(4):1149-53.
46. Marfo K, Garala M, Kvetan V, Gasperino J. Use of tris-hydroxymethyl aminomethane in severe lactic acidosis due to highly active antiretroviral therapy: A case report. *J Clin Pharm Ther.* 2009;34(1):119-23.
47. Becker L, Bergfeld W, Belsito D, Hill R, Klaassen C, Liebler D, et al. Safety assessment of tromethamine, aminomethyl propanediol, and aminoethyl propanediol as used in cosmetics. *Int J Toxicol.* 2018;Vol. 37(Supplement 1) 5S-18S.
48. Chapter 1 food and drug administration department of health and human services, subchapter b - food for human consumption (continued). Sect. Sec. 172.822 Sodium lauryl sulfate. (Revised as of April 1, 2018).
49. Select committee on gras substances (SCOGS) opinion: Sodium chloride. GRAS Substances (SCOGS) Database: FDA U.S. Food & Drug administration; 1979. Contract No.: ID Code: 7647-14-5, SCOGS-Report Number: 102*.
50. Select committee on gras substances (SCOGS) opinion: Urea. GRAS Substances (SCOGS) Database: FDA U.S. Food & Drug administration; 1978. Contract No.: ID Code: 57-13-6, SCOGS-Report Number: 103*.

Supplementary Methods

Quenching reagent development

During quenching reagent development, the inhibiting potential of selected quenching components based on literature research was tested on fibre substrates incubated with commercially available fibre degrading enzymes (Supplementary table 1). Standard mixtures of GOS (2.5 mg/mL), and chicory FOS/inulin (2.5 mg/mL) were prepared in MES buffer (25 mM, pH 5.8). For the incubations, 100 μ L of GOS was incubated with 15 μ L of 10 mg/mL β -galactosidase (EC 3.2.1.23) (1) isolated from *Aspergillus oryzae* (Lactase DS-K, Amano Enzyme Inc., Japan), with either 100 μ L water or potential quenching reagent components. Furthermore, 100 μ L of FOS/inulin was incubated with 2 μ L endo-inulinase (EC 3.2.1.7) isolated from *Aspergillus niger* (2) (Novozym 960, Novozymes A/S, Denmark), with either 100 μ L water or potential quenching reagent components. Incubations took place for 16 hours at 37°C.

Supplementary Results

Quenching reagent development

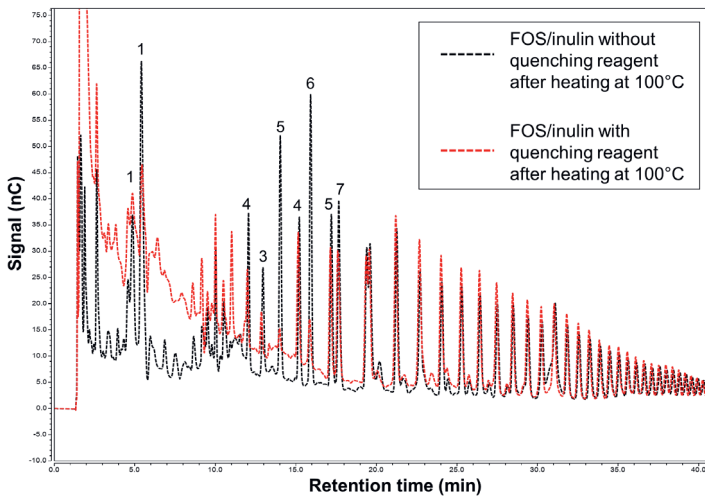
Known metal ion inhibitors of β -galactosidase and inulinases (Supplementary table 1) were tested (3-5). Ag^+ and the combination $\text{Ag}^+/\text{Cu}^{2+}$ inhibited β -galactosidase, since 90% GOS 1<DP>7 or 96% GOS 1<DP>7 was left after incubation, respectively. Cu^{2+} did not inhibit GOS breakdown. Ag^+ , Cu^{2+} , and Zn^{2+} only partially inhibited exo- and endo-inulinases, compared to the water incubations. A protein denaturing formulation (PDF) was tested as a more general enzyme inhibitor (6) (Supplementary table 1). PDF did not inhibit β -galactosidases (4% GOS 1<DP>7) compared to control (0.5% GOS 1<DP>7), nor inulinases (15.8% FOS/inulin 11<DP>20) compared to control (0% FOS/inulin 11<DP>20). The components in the PDF interfered with HPAEC-PAD analysis. Moreover, a RNA conserving reagent (7) was tested (Supplementary table 1), but it did not inhibit inulinases (346% DP=1 formed) compared to control (318% DP=1 formed). Overall, both the PDF and the RNA conserving reagent were not tested in more detail.

Considerations after sample retrieval

When samples were retrieved at the end of the incubations, reactions in the presence of quenching reagent should be stopped by freezing at -80°C, and not by heat inactivation, unlike what is sometimes described in the literature (8). When fermentation samples were heat inactivated in the presence of quenching reagent, FOS DP<7 disappeared from the sample (Supplementary Figure 1). This likely happened due to a reaction between saccharides and urea during heating.

Analytical methods validation of SCFA

The measurement of SCFA in human faecal samples by GC-MS was validated. After collection, faeces were stored at 4°C, homogenized using a paint shaker and afterwards stored at -80°C. For SCFA analysis, there are two pre-analytical steps: extraction and derivatisation. Standard curves and samples should always be prepared using the same PBS volume, due to a putative partitioning effect between the aqueous and organic solvent phase ratio. Bead beating of faeces led to a more effective extraction of SCFAs, eliminating any matrix effect, since after the standard addition of known SCFA concentrations to the same faecal sample, the slope of the standard curve remained the same (Supplementary Figure 3A-D). Afterwards, SCFAs were extracted into the diethyl-ether layer and derivatised by silylation (9), resulting in tert-butyldimethylsilyl (TBS/TBDMS) derivatives. These are highly volatile, less polar, and more thermostable (9). During the entire pre-analytical process, the bead beating and all centrifugation and vortex steps were performed at 4°C. Ten aliquots of the same faeces were prepared at the same time, and SCFA were measured in the same GC-MS sequence. The intra-assay variation of acetate, propionate, and butyrate of coefficient of variation (CV) was <10% (Supplementary Figure 3E). The ten aliquots of the same faeces sample were measured at 10 different times with an inter-assay variation of acetate, propionate, and butyrate CV <15%, without carry-over or changes in GC-MS injection repeatability (Supplementary Figure 3E). For 100 mg faeces, the final validated protocol is described in the Methodology.



Supplementary Figure 1. The effect of heating on one small intestine chicory FOS/inulin fermentation sample with and without quenching reagent.

The black chromatogram represents FOS/inulin without added quenching reagent after heating at 100°C, the red chromatogram represents FOS/inulin present in the same sample with added quenching reagent after heating at 100°C. The numbers in the chromatogram represent the degree of polymerization, 1 = monomers, 2 = dimers, ≥ 3 = oligomers. FOS; fructo-oligosaccharides.

Supplementary Table 1. The quenching components that were tested for quenching chicory FOS/inulin and GOS in the presence of inulinases or galactosidase, respectively.

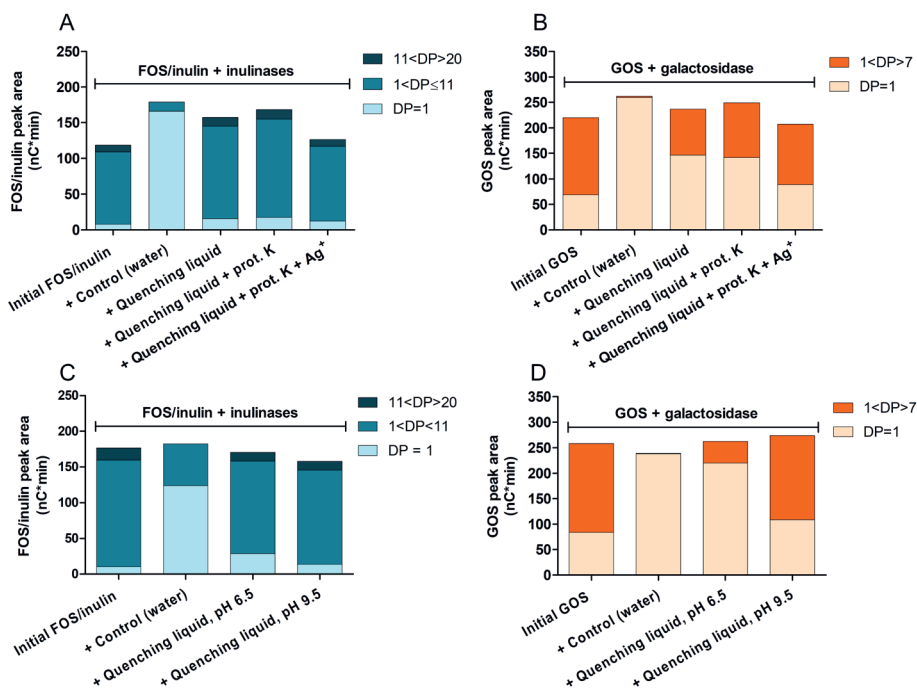
Quenching components	Concentrations of components in stock solution	Remaining chicory FOS/inulin (area %)			Remaining GOS (area %)	
		DP=1	1<DP≤11	11<DP>20	DP=1	1<DP>7
Metal ions						
Control	Water	943.6	7.29	0	357.0	0.516
Ag ⁺	5 mM	50.9	44.3	36.6	187.2	90.76
Cu ²⁺	10 mM	161.5	46.3	23.3	347.6	13.34
Zn ²⁺	10 mM	161.9	114.0	31.95	N.A.	N.A.
Cu ²⁺ , Ag ⁺	5 mM each	393.5	27.16	26.0	154.9	96.24
RNA conserving reagent						
Control	Water	318.3	109.6	5.36	N.A.	N.A.
RNA conserving reagent	Sodium citrate (25 mM) EDTA (10 mM) Ammonium sulphate (50 gram/100 mL)	346.4	100.8	73.15	N.A.	N.A.
Protein denaturing formulation						
Control	Water	943.6	7.29	0	357.0	0.516
Protein denaturing formulation (PDF)	Ethanol (40% v/v) Lithium chloride (3.5 M) Sodium citrate (50 mM)	162.0	58.3	15.8	414.4	3.97

The values represent the area under the peaks after incubation compared to the area under the peaks before incubation (area %). Fibres profiles were obtained with HPAEC-PAD as described in Materials and Methods. Peak area was quantified per component up to the maximum degree of polymerization (DP) measured by HPAEC-PAD which is dependent on the structure of the fibre. N.A. is not analyzed. DP; degree of polymerization, FOS; fructo-oligosaccharides, GOS; galacto-oligosaccharides.

Supplementary Table 2. The bacterial lysis buffer combinations that were tested for quenching chicory FOS/inulin and GOS in the presence of inulinases or galactosidase, respectively.

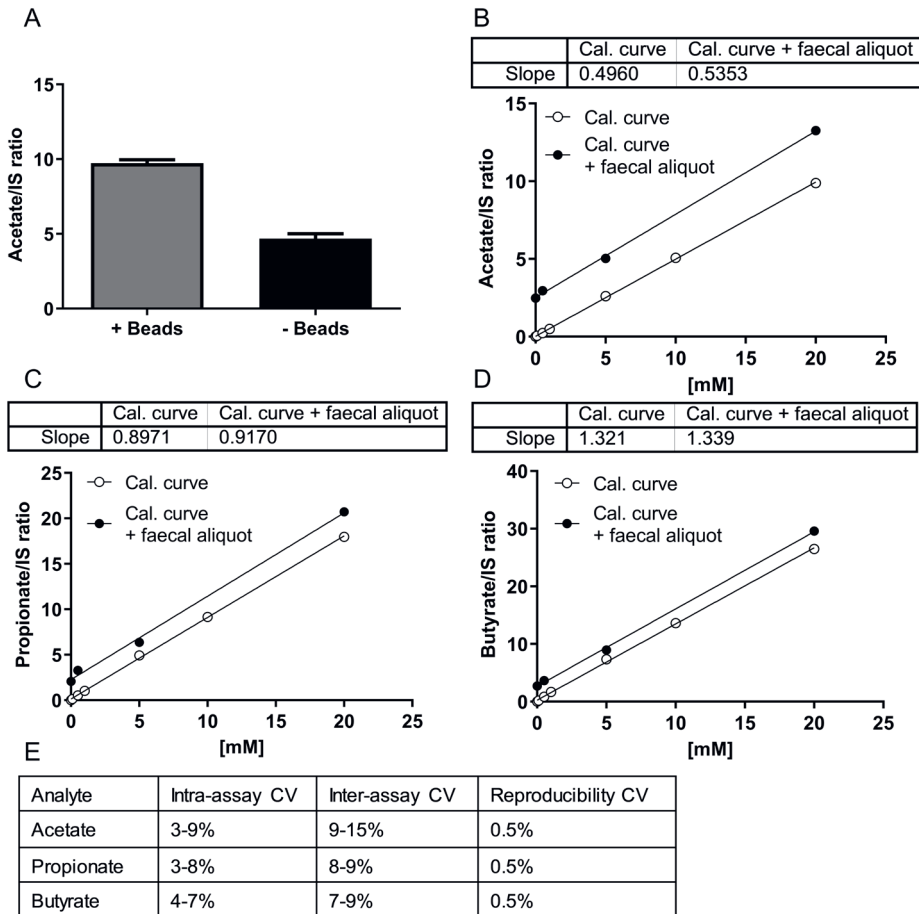
Quenching combinations	Concentrations of components in stock solution	pH	Remaining chicory FOS/inulin (area %)			Remaining GOS (area %)	
			DP=1	1<DP≤11	11<DP>20	DP=1	1<DP>7
Bacterial lysis buffer combinations							
Control	Water	-	1233	39	0.3	284	0.4
Bacterial lysis buffer with Urea	Tris (50 mM)	6.5	286	86	71	262	24
	NaCl (150 mM)	8.5	201	127	131	146	60
	EDTA (10 mM)	9.5	136	88	72	129	95
	SDS (1.5%) Urea (8 M)						
Bacterial lysis buffer with Urea, proteinase K	Tris (50 mM)	8.5	221	135	140	141	71
	NaCl (150 mM)						
	EDTA (10 mM)						
	SDS (1.5%)						
	Urea (8 M)						
	Proteinase K (300 µg/mL)						
Bacterial lysis buffer with Urea, proteinase K, Ag ⁺	Tris (50 mM)	8.5	154	106	100	89	78
	NaCl (150 mM)						
	EDTA (10 mM)						
	SDS (1.5%)						
	Urea (8 M)						
	Proteinase K (300 µg/mL) Ag ⁺ (20 mM)						

The values represent the area under the peaks after incubation compared to the area under the peaks before incubation (area %). Fibres profiles were obtained with HPAEC-PAD as described in Materials and Methods. Peak area was quantified per component up to the maximum DP measured by HPAEC-PAD which is dependent on the structure of the fibre. DP; degree of polymerization, FOS; fructo-oligosaccharides, GOS; galacto-oligosaccharides.



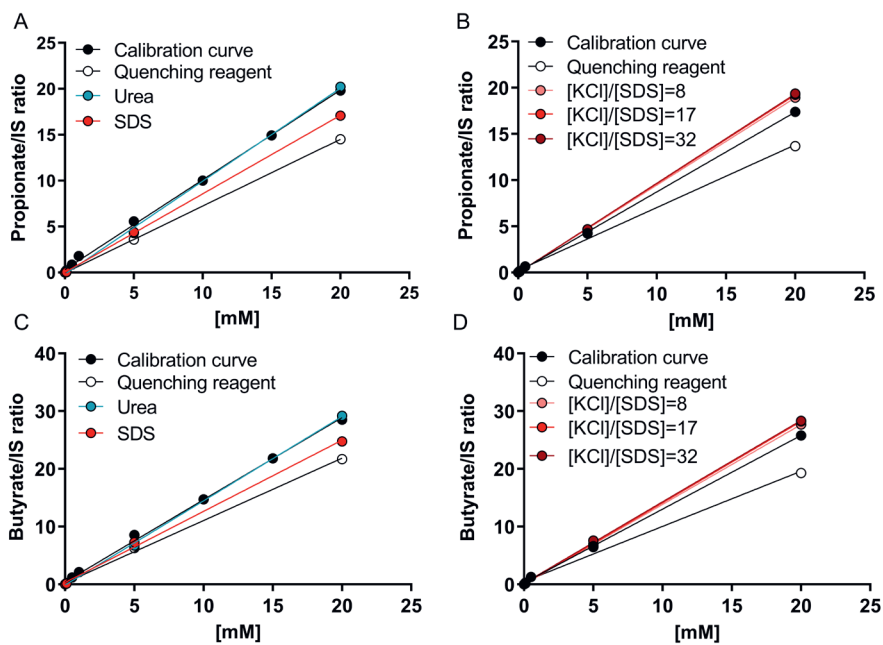
Supplementary Figure 2. Quenching reagent development: the effectiveness of blocking breakdown of chicory FOS/inulin and GOS.

The inhibitory capacity of the quenching stock solution (pH 8.5, 50 mM Tris, 150 mM NaCl, 10 mM EDTA, 1.5% SDS, 8 M urea) on degradation of FOS/inulin (A, C) and GOS (B, D) by commercially available inulinases or galactosidase with additions of proteinase K (300 µg/mL) or additions of proteinase K and Ag⁺ (20 mM) (A, B), also tested at different pH values (C, D). The area under the peaks of the HPAEC-PAD chromatograms of mono- di and oligosaccharides after 16 h incubation is presented (the maximum DP is dependent on the structure of the fibre). The peak area is given in nanocoulomb (nC)*retention time in minutes. No error bars are shown. DP; degree of polymerization, FOS; fructo-oligosaccharides, GOS; galacto-oligosaccharides, prot. K; proteinase K.



Supplementary Figure 3. SCFA protocol validation using human faecal samples.

(A) Acetate/internal standard ratio after extraction with and without bead beating homogenization. (B,C,D) Standard addition of acetate, propionate, and butyrate respectively after performing the protocol as described in Materials and Methods including the bead beating homogenization. (E) Intra-assay, inter-assay and reproducibility coefficients of variation % of acetate, propionate, and butyrate. CV, coefficient of variation.



Supplementary Figure 4. Quenching reagent interference in SCFAs analysis by GC-MS.

(A, C) Calibration curves of propionate and butyrate made in PBS with known concentrations in the presence of the quenching reagent or its main components urea and SDS. (B, D) Calibration curves of propionate and butyrate with SDS precipitation by KCl in different KCl/SDS molar ratios.

Supplementary Table 3. The peak areas and total peak area of the chromatograms from FOS and GOS standards in water with or without quenching reagent and with and without the addition of KCl.

Sample	Peak area (nC*min)	Peak 1 (DP2)	Peak 2 (DP3)	Peak 3 (DP2)	Peak 4 (DP4)	Peak 5 (DP3)	Peak 6 (DP5)	Peak 7 (DP4)	Peak 8 (DP6)	Peak 9 (DP5)	Peak 10 (DP7)	Peak 11 (DP6)	Peak 12 (DP8)	Total peak area (nC*min)	% total peak area of fibres mixtures in water
FOS															
in water	5.2	3.9	1.9	8.3	33.3	11.3	22.5	9.3	10.9	3.8	6.9	1.7		119.1	-
in water with quenching reagent	5.1	3.7	1.9	8.1	32.2	10.9	21.8	9.0	10.6	3.8	6.8	1.7		115.6	97.1
in water with quenching reagent and with KCl	5.2	3.7	1.9	8.1	31.9	10.6	21.1	10.7	10.1	4.6	6.7	1.7		116.4	97.7
GOS															
in water	14.9	2.4	1.6	44.8	8.6	36.6	31.5	13.2	6.0	7.8	4.8	4.4	1.7	186.0	-
in water with quenching reagent	15.2	0.9	1.3	45.1	9.8	36.8	31.4	13.1	5.8	7.8	4.7	4.3	1.6	182.6	98.2
in water with quenching reagent and with KCl	14.3	1.8	1.3	45.5	8.7	36.9	31.3	13.2	5.7	8.5	4.8	4.5	1.7	183.8	98.8

The peaks and the total peak area of FOS and GOS between retention time 6-23 or 3.7-17 minutes were quantified, respectively. The area is given in nanoCoulomb multiplied by the retention time in minutes (nC × min). The peak area was subsequently expressed as % of the peak area of fibre in water (without quenching reagent and without KCl). DP; degree of polymerization, FOS, fructo-oligosaccharides; GOS, galacto-oligosaccharides.

References Supplementary Information

1. Tavares TM, FX. Whey and whey powders | Fermentation of Whey. In: Caballero B, Finglas P, Toldra F, editors. *Encyclopedia of Food Sciences and Nutrition (Second Edition)*. Oxford: Academic Press; 2003. p. 6157-63.
2. Sirisansaneeyakul S, Worawuthiyanan N, Vanichsriratana W, Srinophakun P, Chisti Y. Production of fructose from inulin using mixed inulinases from *Aspergillus niger* and *Candida guilliermondii*. *World J Microbiol Biotechnol*. 2007;23(4):543-52.
3. Uchiyama T, Miyazaki K, Yaoi K. Characterization of a novel β -glucosidase from a compost microbial metagenome with strong transglycosylation activity. *J Biol Chem*. 2013;jbc. M113. 471342.
4. Dey PM. Inhibition, transgalactosylation and mechanism of action of sweet almond α -galactosidase. *Enzymology*. 1969;191(3):644-52.
5. Chi Z, Chi Z, Zhang T, Liu G, Yue L. Inulinase-expressing microorganisms and applications of inulinases. *Appl Microbiol Biotechnol*. 2009;82(2):211-20.
6. Paulsen KE, inventor; Qiagen North American Holdings Inc assignee. Formulations and methods for denaturing proteins. U.S. 2003-12-16.
7. Lader ES, inventor; Applied Biosystems LLC assignee. Methods and reagents for preserving RNA in cell and tissue samples. U.S. 2001-03-20.
8. Ahern T, Klibanov A. The mechanisms of irreversible enzyme inactivation at 100C. *Science*. 1985;228(4705):1280-4.
9. Primec M, Mićetić-Turk D, Langerholc T. Analysis of short-chain fatty acids in human feces: A scoping review. *Anal Biochem*. 2017;526:9-21.



Fermentation kinetics of selected dietary fibers by human small intestinal microbiota depend on the type of fiber and subject

Mara P.H. van Trijp¹, Christiane Rösch², Ran An³, Shohreh Keshtkar¹, Madelon J. Logtenberg², Gerben D.A. Hermes³, Erwin G. Zoetendal³, Henk A. Schols², Guido J.E.J. Hooiveld¹

¹ Nutrition, Metabolism and Genomics Group, Division of Human Nutrition and Health, Wageningen University, the Netherlands

² Laboratory of Food Chemistry, Wageningen University, the Netherlands

³ Laboratory of Microbiology, Wageningen University, the Netherlands

Abstract

Scope

An underexplored topic is the investigation of the health effects of dietary fibers via modulation of the human small intestine (SI) microbiota. A few previous studies hint at fermentation of some dietary fibers in the distal SI of humans and pigs. We investigated the potential of human SI microbiota to degrade dietary fibers and produce metabolites *in vitro*.

Methods and results

Fructans, galacto-oligosaccharides, lemon pectins, and isomalto/malto-polysaccharides were subjected to *in vitro* batch fermentations inoculated with ileostomy effluent from five subjects. Fiber degradation products, formation of bacterial metabolites, and microbiota composition were determined over time. Galacto- and fructo-oligosaccharides were rapidly utilized by the SI microbiota of all subjects. At 5 h of fermentation, 31-82% of galacto-oligosaccharides and 29-89% fructo-oligosaccharides (degree of polymerization DP4-8) were utilized. Breakdown of fructo-oligosaccharides/inulin DP \geq 10, lemon pectin, and iso-malto/maltopolysaccharides only started after 7 h incubation. Degradation of different fibers resulted in the production of mainly acetate, and changed the microbiota composition over time.

Conclusion

Human SI microbiota have hydrolytic potential for prebiotic galacto- and fructo-oligosaccharides. In contrast, the higher molecular weight fibers inulin, lemon pectin, and iso-malto/maltopolysaccharides showed a slow fermentation rate. Fiber degradation kinetics and microbiota responses were subject dependent, therefore personalized nutritional fiber-based strategies are required.

Keywords

Fiber; *in vitro* fermentation; microbiota; prebiotics; small intestine

Introduction

Currently, there is a strong interest in optimizing human health through the consumption of dietary fibers, due to their direct and indirect health benefits (1-3). Dietary fibers are present as natural constituents of leguminous seeds, fruits, vegetables, and cereals. Per definition, they resist hydrolysis by host digestive enzymes in the small intestine (SI) (4), and some fibers can be fermented by the human intestine microbiota (5). During fermentation, there is formation of for example glycosidic degradation products, and fermentation end products like short-chain fatty acids (SCFA) (6). SCFAs have been suggested to play a key role in the treatment of metabolic syndrome (7, 8). Soluble galacto-oligosaccharides (GOS), fructans including long-chain inulin and short-chain fructo-oligosaccharides (FOS), more complex fibers such as pectins, and a novel fiber type isomalto/malto-polysaccharides (IMMP), are known to stimulate the growth of a number of microbial species in the intestinal tract such as *Bifidobacterium* species (9, 10). Part of the health benefits of fibers is thought to be mediated by changing the gut microbiota composition and/or activity. Although the bacterial load is highest in the large intestine, also considerable numbers of bacteria are present in the distal SI of humans, namely 10^{7-8} bacteria numbers/gram of content compared to 10^{11} bacteria numbers/gram in colonic content (11).

An emerging field of research focuses on the interaction between the diet and the SI microbiota. The SI microbiota is likely very responsive to dietary perturbations, such as dietary lipids (12-14). Some dietary fibers, including pectins, have the potential to directly activate the immune system in the SI, as was shown before *in vitro* (15). One underexplored field is their possible indirect effects via modulations of SI microbiota. The microbiota can affect host metabolism and health through for instance immune responses and excretion of signaling molecules that affect glucose homeostasis (14, 16). Previous studies hinted at fermentation of some dietary fibers in the distal SI of humans and pigs (17-20), suggesting the potential health impact of fibers via influencing the microbiota residing in the upper intestinal tract. Ileostomy effluent was previously found to resemble the microbiota in the jejunum and ileum of healthy subjects, and can therefore be used as a model to study human SI microbiota (21).

Since there is limited knowledge on the capability of human SI microbiota to metabolize dietary fibers, we investigated in an explorative way the potential of individual human SI microbiota to break down dietary fibers and produce metabolites of health interest. We performed *in vitro* batch fermentations with human ileostomy microbiota with FOS/inulin, GOS, and the complex high molecular weight fibers lemon pectin, and IMMP.

Material and methods

Fiber substrates

The following prebiotic oligo- and polysaccharides were used: inulin (DP2-60) mixed with FOS (DP2-10) in a 1:1 w/w ratio (Frutafit® TEX! and Frutalose® OFP; Sensus, Roosendaal, the Netherlands), GOS (Vivinal, FrieslandCampina, Wageningen, the Netherlands) composed of approximately 69% GOS, with a DP composition (on weight percentage oligosaccharide) as follows: 31% DP2 (other than lactose), 38% DP3, 18% DP4, 8% DP5, and 5% DP6 or higher, 28% mono- and disaccharides and 3% moisture. Furthermore, lemon pectin with a degree of methyl esterification of 67 (DM67) (CP Kelco, Copenhagen, Denmark), and IMMMP with 92% α -1,6-linked glycosidic linkages produced from potato starch by the enzyme 4,6- α -glucanotransferase, with an average DP of 50 (22) (AVEBE, Veendam, the Netherlands) were used.

Subject characteristics

Ileostomy effluent was collected from five subjects with an ileostomy bag attached to the distal ileum. Subjects were otherwise healthy and did not use anti-, pre- or probiotics for at least 3 months before effluent donation. Subjects gave informed consent. The five individuals were denoted as I1, I2, I3, I4, and I5. Participants filled in food diaries to determine the total daily fiber intake in the habitual diet during the two consecutive days before effluent collection. The diaries were analyzed based upon the NEVO table 2016 according to AOAC985.29 (Prosky) (23) and AOAC991.43 (Lee) (24) methods by research dietitians. The ileostomy effluent was collected in the morning after 14 hours of fasting, and kept at -20°C to minimize bacterial activity until use on the same day (within 9 hours after sampling).

Small intestinal inoculum preparations

Ileostomy effluent was diluted in standard ileal efflux medium (SIEM) in a 1:5 (v/v) ratio. SIEM was modified from (25) with adaptations as described elsewhere (26). Tween 80 was excluded to avoid interference with apparatus for oligosaccharide measurement, with less carbohydrates (a mixture of pectins, xylan, arabinogalactan, amylopectin, and starch, in total 0.24 g/L), and with MgSO₄ (0.8 g/L). All medium compounds were obtained from Tritium Microbiology (Veldhoven, The Netherlands). The pH of the medium was set at 7 using a 1 M 2-(N-morpholino)ethanesulfonic acid (MES) buffer, based on pH measurements in the ileum of ileostomates and healthy adults (21, 27). The diluted inocula were filtered using a sieve with 1.6 mm holes to remove large food particles. After sieving, the ileostomy effluent in SIEM was subjected to a preselection step of 15 hours under anoxic conditions (37°C, shaking at 100 rpm) (28, 29) for removal of leftover carbohydrates in the inoculum.

***In vitro* batch fermentation**

The fermentation bottles were filled under anoxic conditions (81% N₂, 15% CO₂, and 4% H₂) with preselected SI inoculum, and SIEM containing the fibers of interest, in a volume ratio 1:1. At the start of fermentation, the mixture consisted of 10% of the original SI sample in SIEM and 10 g/L added dietary fibers. The SI inoculum without added fiber was included as control to monitor the background fermentation. Fibers without SI inoculum were included to check for contamination. FOS/inulin, and GOS were tested with all five subjects I1-I5. Additionally, in an explorative way, two high molecular weight fibers were included. Lemon pectin was tested with two subjects (I1-I2), and in subsequent fermentation experiments, which was based on the date of ileostomy effluent donation, and consequently the date of the experiment, IMMP was tested with three other subjects (I3-I5). Fermentations of different fibers using fresh effluent from one subject were always performed on the same date. Duplicated fermentation bottles were closed by a rubber cap and metal ring in an anaerobic chamber. Incubation took place in duplicate at 37°C with continuously shaking at 100 rpm. Since slow or no fiber fermentation by SI microbiota was expected, samples were taken at 0 h, and after 5, 7, 9, and 24 h of incubation using a 2.5 mL syringe with a 0.8 mm x 50 mm needle. Aliquots were directly frozen in liquid nitrogen and stored at -80°C until analysis.

Molecular weight distribution of polysaccharides and oligosaccharide profiling

The molecular weight distribution of lemon pectin was analyzed by high performance size exclusion chromatography (HPSEC, Ultimate 3000 HPLC, Dionex, Sunnyvale, CA, USA) with refractive index (RI, Showa Denko, Tokyo, Japan) detection. Samples were centrifuged (10 min, RT, 15000 x g), and supernatant was diluted with demineralized water to a maximum concentration of 5 mg/mL fiber before analysis. The analysis was performed as described elsewhere (30). Samples (10 µL) were eluted with NaNO₃ (0.2 M, flow rate 0.6 mL/min, at 55°C). Mono- di- and oligosaccharides profiles of GOS, FOS/inulin, and IMMP were analyzed by high performance anion exchange chromatography (HPAEC, Dionex) with pulsed amperometric detection (PAD, ICS5000 ED, Dionex). Samples were centrifuged (10 min, RT, 15000 x g), and supernatant was diluted with water to a fiber concentration of 0.5 mg/mL before analysis. The analysis was performed as described elsewhere (31). Peak areas between different fermentation time points were calculated and expressed as the percentage present of the initial fiber.

Production of microbial fermentation products

Acetate, propionate, and butyrate were analyzed by gas chromatography (GC TRACE 1300, Thermo Scientific) with a flame ionisation detector (FID, Interscience, Breda, the Netherlands), equipped with a capillary column (25 m x 0.53 mm x 1.00 µm, Agilent CP-FFAPCB for free fatty acids, Varian-Chrompack). Before analysis of SCFAs, the

fermentation samples were centrifuged (10 min, RT, 15000 x g). 100 μ L supernatant was mixed with 50 μ L solution containing HCl (0.3 M), oxalic acid (0.09 M), and internal standard 2-ethyl butyric acid (0.45 mg/mL). Samples were vortexed, incubated 30 min at room temperature, and centrifuged (5 min, RT, 15000 x g). The GC oven program was as follows: 100°C for 0.5 min, raised to 180°C (8°C/min) hold for 1 minute, raised to 200°C (20°C/min) and hold for 5 min. The split flow was 40 mL/min. Helium was used as carrier gas. Data were analyzed with Thermo Xcalibur software version 2.2. Formate, lactate, and succinate were analyzed using HPLC UltiMate 3000 system with a Shodex RI-101 detector (Dionex, Sunnyvale, CA, USA). The fermentation samples were centrifuged before use (10 min, RT, 15000 x g). The supernatant was diluted four times with demineralized water. The methods, column, guard column, and software were used as described elsewhere (32).

Microbiota profiling

Bacterial DNA was extracted from 300 μ L fermentation sample, or 0.25 g ileostomy effluent. Cell lysis was achieved by a repeated bead beating method, in combination with ASL Stool lysis buffer (Qiagen, Hilden, Germany) as described previously (33). The obtained lysate was used for DNA extraction and purification using the QIAamp DNA Mini Kit (Qiagen). 20 ng/ μ L extracted DNA was used in triplicate PCR reactions, containing 7 μ L 5x Phusion Green HF buffer, 0.7 μ L 10 mM dNTPs (Promega), 0.4 μ L Phusion hot start II DNA polymerase (2U/ μ L), 25.5 μ L nuclease-free water, 0.7 μ L of template DNA (20 ng/ μ L) and 0.7 μ L of each of the barcoded primers F784-R1064 (10 μ M) (34, 35). Cycling conditions were as follows: 98°C 30 sec, 25 cycles of 98°C 10 sec, 42°C 10 sec, 72°C 10 sec, and 72°C for 7 minutes. Pooled PCR products were checked for correct size on a 1.3% agarose gel, and subsequently purified using magnetic beads (MagBio Genomics Inc., Gaithersburg, USA), and quantified using Qubit dsDNA BR buffer and dye (Invitrogen, California, USA) on a Qubit 2.0 Fluorometer. Afterwards, a library containing an equimolar mix of 200 ng of each purified PCR product was prepared. To test for the reproducibility of the sequencing two synthetic samples of known composition were sequenced (35). In total, 136 fermentation samples, theoretical mock controls, and negative controls (DNA isolated from nuclease-free water, and a negative control from the fermentation experiment) were prepared. Technical replicates of the same DNA sample, but different PCR barcode were also included. Microbiota composition was determined via sequencing of the 16S rRNA gene using the variable region V5-V6 on the Illumina HiSeq2500 platform (Eurofins GATC Biotech, Konstanz, Germany). Raw sequencing data were processed and amplicon sequence variants (ASV) were picked with NG-Tax version 1.0 using default settings (35, 36). Libraries were quality checked by selecting reads with perfect matching primer sequences and de-multiplexed by selecting read pairs with perfectly matching valid barcodes. ASVs, which are individual sequence variants, were picked as follows: sequences were ordered

by abundance per sample, and reads were considered valid when their cumulative abundance was $\geq 0.1\%$. Taxonomy was assigned with the SILVA database (version 128), with a confidence of $>80\%$ for genus level classification.

Microbiota composition analysis

R version 3.5.1. was used for all analyses (37). Before analysis, contaminants were removed based on their abundance in the negative extraction control, and being flagged previously in literature as laboratory reagent contaminants (38), namely *Nesterenkonia*, *Ralstonia*, *Epulopiscium*, *Trichococcus*, and *Caldalkalibacillus*. These bacteria were only present in low abundance in biological samples with a low input DNA concentration. Counts were transformed to relative abundance. Quality control was performed by calculating pairwise Pearson correlations were calculated between the known composition of the control and sequenced positive mock controls, and within technical and biological replicates using genus level relative abundance. Pearson correlations were also calculated for pairwise combinations of microbiota composition using genus level relative abundance in ileostomy effluents from the different subjects. Alpha-diversity, the within-sample diversity, was calculated using inverse Simpson diversity index using the microbiome package (39). Beta-diversity, the between-sample diversity, was used to determine overall microbiota differences between groups and was calculated by Bray-Curtis dissimilarity on the relative bacterial abundances. To visualize the microbiota variation, a principal coordinate analysis (PCoA) was performed using Bray-Curtis as implemented in the phyloseq package (40). Permutational multivariate analysis of variance (PERMANOVA) as implemented in the vegan package (41) with post-hoc testing was used to determine differences in overall community composition between subjects, fibers, and time points. Sample-wise distances were calculated within individual for fiber samples versus background control samples at each time point using Bray-Curtis. The heatmap was generated using pheatmap (42), scaled per row, and hierarchically clustered using the Ward.D2 algorithm. Fermentation samples were clustered using Bray-Curtis dissimilarity.

Bacterial 16S rRNA gene copy number quantification

The total bacterial abundance was determined by amplifying a conserved region of the 16S rRNA gene (in between the V8 and V9 region) with quantitative PCR. The PCR reaction mixture contained SensiMix (Bioline, GC biotech, Alphen aan den Rijn, Netherlands), the primers 1369F and 1492R (100 μM), and 2 μL of 5 ng/ μL gDNA. Apparatus, primers, and PCR cycling conditions were used as described elsewhere (43).

Statistical analysis

Statistical analysis of SCFAs was performed on PQN-transformed data (44). Linear mixed models were used to assess the effects of fiber and time on the SCFA

concentrations, using the lme4 package (45). Fiber type, time, and their interactions were included as fixed effects, subjects as a random effect with time added as a random slope. A P -value <0.05 was considered significant.

Results

Subject characteristics, dietary intake, and ileostomy effluent

The five ileostomy subjects included 2 males and 3 females with a mean age of 53.2 ± 21.2 years (range 30-75 years) and a mean BMI of 21.1 ± 4.8 kg/m². The mean time of ileostomy wearing was 6.4 ± 5.0 years (range 1-14 years). They were not using medication or medication unrelated to intestinal disease, namely blood pressure lowering drugs (I2) and anti-histamine (I4), except for anti-constipation drugs used by I1. The reason for the ileostomy was ulcerative colitis ($n=3$), colon cancer ($n=1$), or a damaged colonic epithelial layer ($n=1$). The two consecutive days before ileostomy effluent donation, I1, I2, and I5 consumed on average 28 ± 0.6 , 20 ± 3.4 , and 21 ± 2.7 gram dietary fibers/day, whereas I3 and I4 consumed 16 ± 1.6 , and 13 ± 1.8 gram dietary fibers/day, respectively (**Table S1**).

The microbiota dataset was of sufficient quality (**Figure S1**). The average number of reads per sample was 182736 ± 78324 . In total 884 unique ASV were identified in the microbiota dataset, within 89 unique genera. To check for the effect of sequencing depth on diversity, we correlated an alpha diversity metric with the number of reads and found no correlation (**Figure S1 A**). The correlations of the theoretical composition with the sequenced results were >0.81 for the mock controls, between biological duplicates 0.972 ± 0.04 , and between technical duplicates >0.98 between and within library (**Figure S1 B**). The microbiota profiles in the ileostomy effluents used in this study showed high variation ($R=0.37\pm 0.22$) among subjects and included bacterial taxa that were previously also found in the human SI (**Figure S2**). All ileostomy effluents contained members of genera *Streptococcus* and *Clostridium cluster I*, and the family Peptostreptococcaceae and Enterobacteriaceae. In addition, also genera such as *E. eligens*, *Veillonella*, *Lactobacillus*, *Enterococcus*, *Haemophilus*, *Bifidobacterium*, *Terrisporobacter*, *Klebsiella*, *Turicibacter*, and *Escherichia-Shigella*, were detected.

Breakdown kinetics of GOS

Degradation of GOS, a well-known soluble prebiotic, by SI microbiota was studied (**Figure 1 A**). GOS DP >2 were quickly utilized by the microbiota of all SI samples (**Figure 1A**). After 5 h of incubation, the breakdown of GOS varied from 31% - 84%. The amount of GOS further decreased over time from 5 to 9 h. In all incubations, small amounts of GOS were remaining after 24 h (8% - 24%). In the control fermentations without added fibers, no GOS was detected. Overall, GOS was degraded by the SI microbiota of all individuals, with differences in kinetics mainly observed before 7 h of incubation.

Breakdown kinetics of FOS/inulin

Degradation of FOS/inulin, also well-known soluble prebiotics, by SI microbiota was studied (Figure 1 B-E). The DP cut-off values of degradation of oligomers in the FOS/inulin mixture were based on breakdown kinetics of all SI samples, from fast (DP3, Figure 1 B) to slower (DP4-8, Figure 1 C and DP9, Figure 1 D) and slowest or no breakdown at all (DP10-20, Figure 1 E). Oligomers present in FOS/inulin (DP3, DP4-8) were utilized quickly by SI samples of all subjects (Figure 1 B, C). The utilization of DP3 at 5 h varied from 100% (I4, I5) to 82% (I2), and the utilization of DP4-8 at 5 h varied from 29% (I2) to 88% (I4). The breakdown of FOS/inulin DP10-20 breakdown was negligible before 7 h (Figure 1 D). I1 and I4 displayed no capacity to break down FOS/inulin DP10-20, whereas breakdown of DP10-20 was observed in I2, I3, and I5, typically after 7-9 h when the DP4-8 fraction was mostly utilized. In the control fermentations without added fibers, no FOS/inulin was detected. Taken together, fermentation kinetics of FOS/inulin was dependent on the chain size of present molecules, and FOS/inulin DP3 and DP4-8 degradation by SI microbiota were fast.

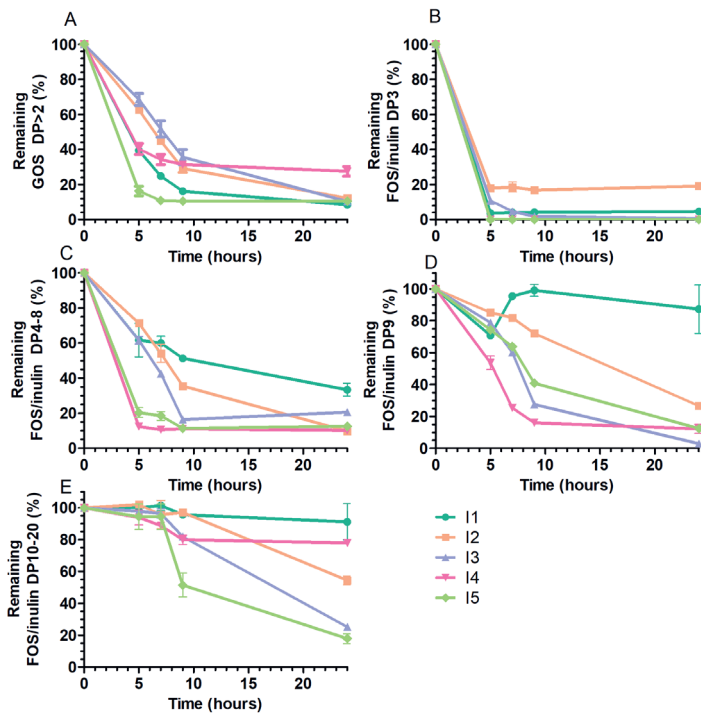


Figure 1. Degradation kinetics of GOS and FOS/inulin by human SI microbiota. Degradation of GOS DP>2 (A), FOS/inulin DP3 (B), FOS/inulin DP4-8 (C), FOS/inulin DP9 (D), and FOS/inulin DP10-20 (E) during fermentation at 0, 5, 7, 9, and 24 h. The lines represent the five subjects (I1-I5). Degradation is expressed as the percentage remaining from the initially present oligomers in the substrate. Data is presented as mean \pm SD, n=2 technical replicates per subject. Abbreviations: DP, degree of polymerization; FOS, fructo-oligosaccharides; GOS, galacto-oligosaccharides; I, ileostomy inoculum; SI, small intestine.

Breakdown kinetics of lemon pectin

A high molecular weight fiber was studied, namely water-soluble lemon pectin. Changes in lemon pectin abundance during fermentation were only studied using I1 and I2 (**Figure 2**). The molecular weight (MW) distributions of the lemon pectin (13-500 kDa) revealed that pectin was very slowly degraded by the SI microbiota, since no degradation of pectin by I1 (**Figure 2 A**) and I2 (**Figure 2 B**) was observed until 9 h. Between 9 and 24 h, the lemon pectin 13-500 kDa was completely utilized in both I1 and I2. Since lemon pectin was very slowly degraded by I1 and I2, another fiber was therefore selected for use in subsequent experiments with I3, I4, and I5 to investigate whether this was also the case for another type of high complexity fiber with a different backbone and linkages, namely IMMP.

Breakdown kinetics of IMMP

IMMP fermentation (**Figure 3**) was studied using I3 (**Figure 3 A**), I4 (**Figure 3 B**), and I5 (**Figure 3 C**). During IMMP fermentation, negligible amounts of isomaltoligosaccharides (IMO), previously found to have α -1,6-glycosidic linkages (9), appeared at 24 h by I3 (**Figure 3 A**). No IMMP breakdown was observed by I4 over 24 h time (**Figure 3 B**). In contrast, IMMP was degraded by I5 between 7 and 24 h, shown by the IMO with DP11-23 that became apparent at 7 and 9 h (**Figure 3 C**). At 24 h the unseparated polysaccharide fraction and the IMO were completely utilized. Overall, IMMP was not degraded by I3 and I4, and slowly degraded by I5.

Formation of microbial fermentation products

The main microbial metabolites acetate, propionate, butyrate and lactate, formate, succinate were measured as an indicator of fiber fermentation (**Figure 4**). Independent of the type of fiber, the activity of SI microbiota was reflected mostly by increased acetate concentrations over time (P -values <0.05). FOS/inulin and GOS increased propionate concentrations at 5, 7, and 9 h compared to control (P -values <0.05) when taken the five subjects together (**Figure 4 A-E**). FOS/inulin and GOS also significantly increased lactate formation at 5, 7, and 9, or at 7 and 9 h, respectively, compared to control. Lactate concentrations were increased mostly in FOS/inulin and GOS fermentation samples of I4 (**Figure 4 D**) and I5 (**Figure 4 E**). The increased metabolite concentrations during GOS and FOS/inulin fermentation before 9 h were reflected by decreased pH values compared to controls (**Figure S3**).

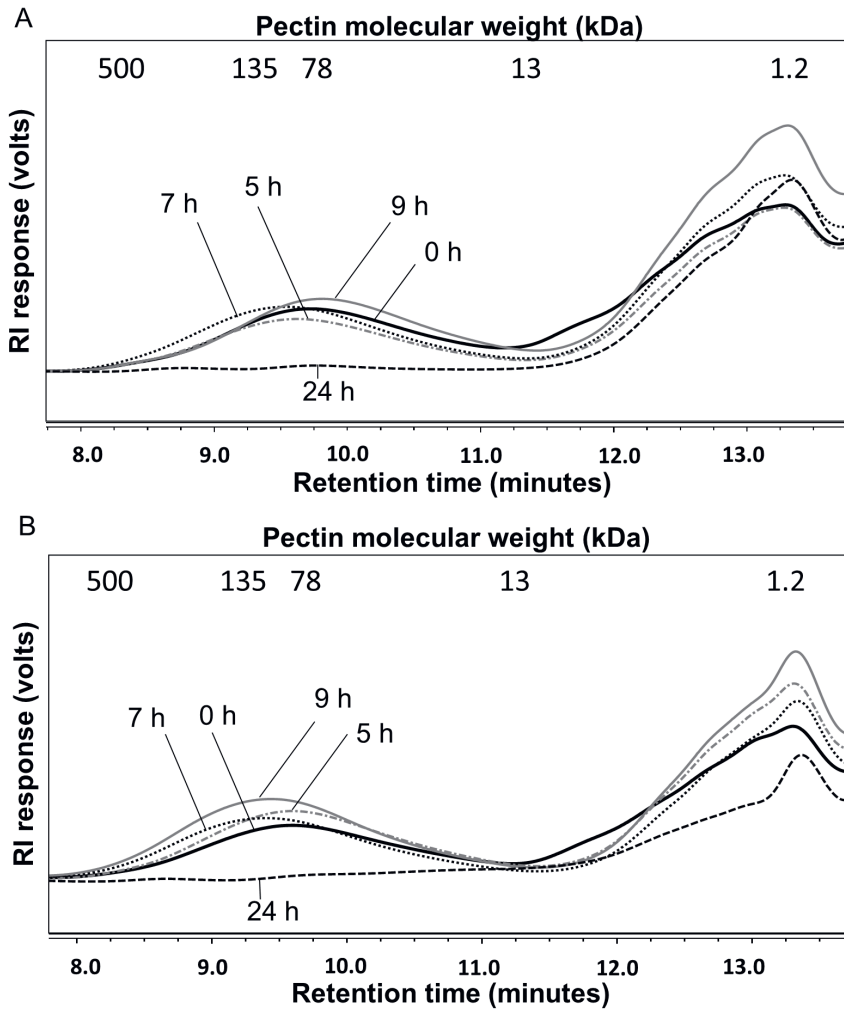


Figure 2. Degradation kinetics of lemon pectin by human SI microbiota.

Degradation of lemon pectin by two subjects I1 (A) and I2 (B) during fermentation at 0, 5, 7, 9, and 24 h. The indicated molecular weight in kDa was based on pullulan standards. The lemon pectin has a molecular weight distribution between 15-500 kDa. The lower molecular weight components of 1.2-13 kDa originate from the ileostomy effluent and SIEM medium. Technical replicates are not shown. Abbreviations: RI, refractive index; SI, small intestine.

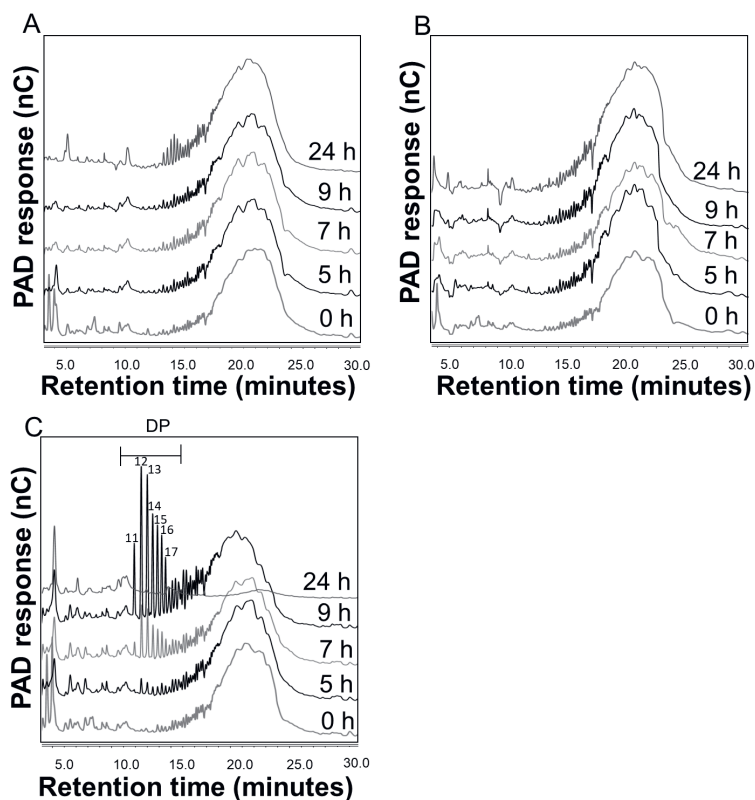


Figure 3. Degradation kinetics of IMMP by human SI microbiota.

Degradation of IMMP *in vitro* by three subjects I3 (A), I4 (B), and I5 (C) during fermentation at 0, 5, 7, 9 and 24 h. Different DPs of IMMP are annotated. Larger carbohydrates elute later from the column, and appear more to the right side of the HPAEC-PAD chromatogram. Technical replicates are not shown. Abbreviations: DP, degree of polymerization; HPAEC, high performance anion exchange chromatography; IMMP, isomaltotopolysaccharides; PAD, pulsed amperometric detection; SI, small intestine.

Lemon pectin (Figure 4 A, B) and IMMP (Figure 4 C-E) did not significantly increase fermentation products compared to control before 9 h (P -values >0.05). This was in line with slow fiber breakdown, which started only after 9 h, or not at all (Figure 2, Figure 3). The total metabolite concentrations in the controls without added fiber also increased, mainly between 9 and 24 h. Therefore at 24 h, no statistical comparisons between control and fiber were made. Overall, FOS/inulin and GOS, but not IMMP and pectin, significantly increased the concentrations of some SCFA before 9 h compared to control without added fibers.

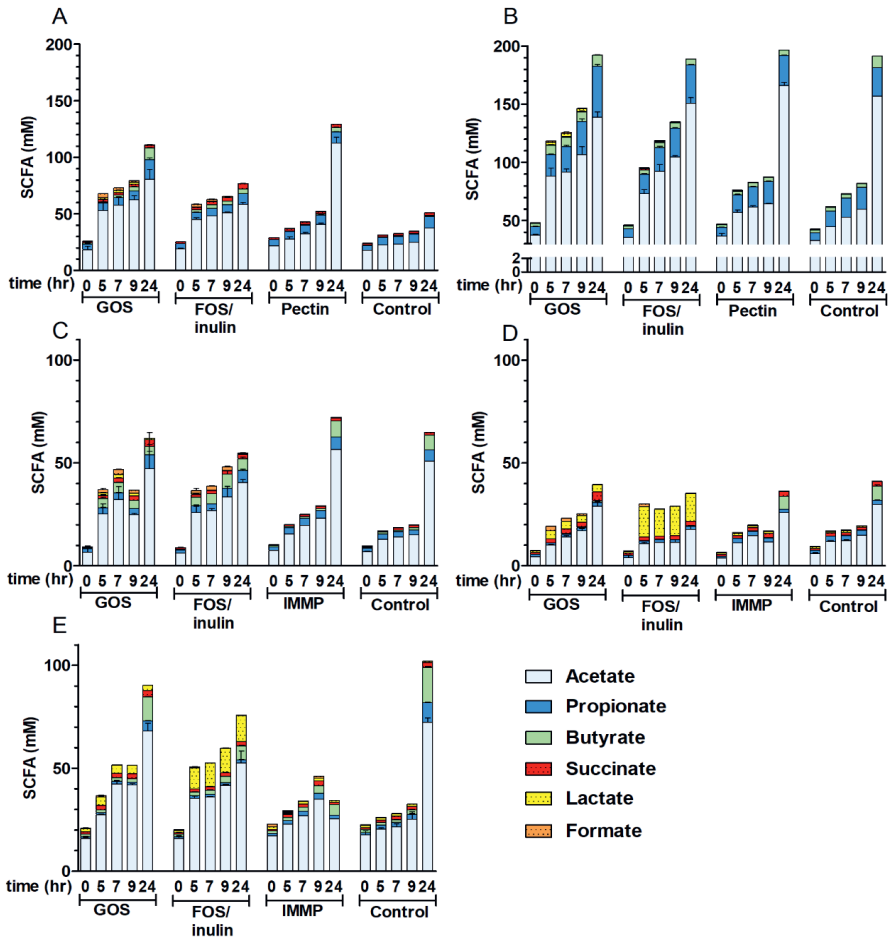


Figure 4. Production of microbial fermentation products by human SI microbiota. SCFA concentrations during fermentation of different fibers at 0, 5, 7, 9, and 24 h by five subjects I1 (A), I2 (B), I3 (C), I4 (D), and I5 (E). Values are means \pm SDs, $n=2$ technical replicates per subject. Abbreviations: FOS, fructo-oligosaccharides; GOS, galacto-oligosaccharides; I, ileostomy inoculum; IMMP, isomalto-maltopolysaccharides.

Microbiota diversity during fermentation of fibers

Subsequently, the impact of fibers on the microbiota composition was studied. Visualization of beta-diversity in microbiota composition during fiber fermentations revealed main clusters based on individuals (Figure 5, PERMANOVA P-value=0.001). Subjects explained 70% of the variation in the dataset (R^2 subject=0.70). The bacterial communities in the fermentation samples from different subjects were all different from each other (PERMANOVA P-values<0.05). The results in the PCoA plot are represented

in a heatmap, visualizing the bacteria causing differences between the fermentation samples (**Figure S4**). 9% of the microbiota variation was explained by fiber type (PERMANOVA P-value=0.002, R^2 fibers = 0.090) and 2% by the fermentation time point (PERMANOVA P-value=0.06, R^2 time = 0.023).

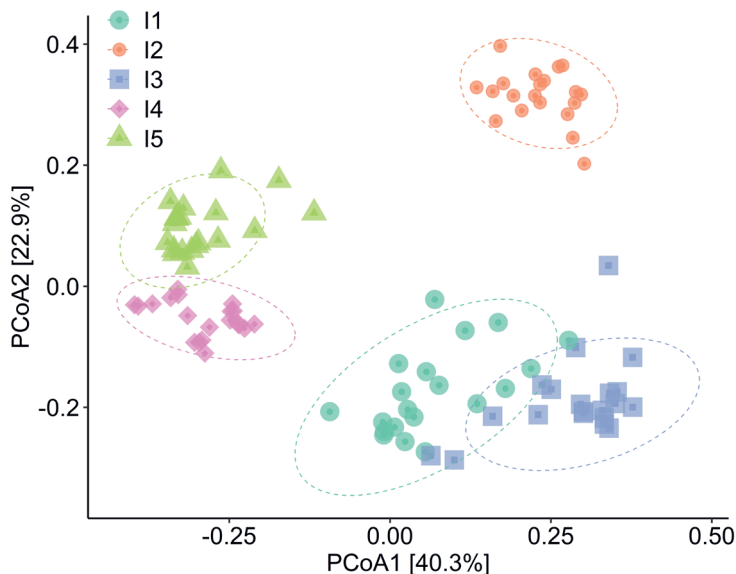


Figure 5. Overall microbiota differences (beta-diversity) in the in vitro fermentation samples.

PCoA plots to visualize microbiota variation between five different subjects (I1-I5), where 95 percent confidence ellipses are shown. Abbreviations: PCoA, principal coordinates analysis.

Microbiota alpha-diversity increased over time by FOS/inulin in I2 and I3 and by GOS in I2 compared to control (**Figure S5**). Pectin did not increase alpha-diversity compared to control, and IMMP increased diversity after 7 h in I5 compared to control. Microbiota dissimilarity between fermentation reactions with fibers compared to control without fiber (**Figure S6**) revealed that GOS and FOS/inulin over time caused a more dissimilar microbiota composition in I1 (Figure S6 A), I3 (Figure S6 C), and I5 (Figure S6 D). FOS/inulin, but not GOS, caused a dissimilar microbiota in I2 (Figure S6 B) compared to their controls. Pectin did not change the microbiota in I1 compared to control (Figure S6 A), but in I2 the microbiota dissimilarity increased after 9 h compared to control (Figure S6 B). IMMP did not change the microbiota profile in I3 and I4, but it was changed after 7 h in I5, compared to the controls (Figure S6 C-E).

Microbiota composition during fiber fermentation

To investigate microbiota changes over time, the relative microbiota composition after addition of GOS and FOS/inulin (**Figure 6**), and lemon pectin and IMMP (**Figure S7**) was plotted. Preselection of ileostomy effluent in medium caused a relative increase of *Escherichia-Shigella* and *Klebsiella* (Enterobacteriaceae) at the start of the fermentation (Figure 6), compared to microbiota composition in the ileostomy effluent (Figure S2). GOS increased the abundance of *Clostridium cluster 1* in I1 and I3 between 0 and 9 h (Figure 6 A) compared to the changes in the microbiota in their controls (**Figure S8**). Even though GOS was degraded by I2 and I4, the relative microbiota composition did not change over time. GOS increased *Bifidobacterium* (from 16% to 28%) between 0 and 5 h in I5, and when GOS was utilized, *Fusobacterium* abundance (from 0.34% to 31%) increased between 9 and 24 h.

FOS/inulin increased abundance of *Clostridium cluster_1* and decreased *Escherichia-shigella* upon fermentation by I1 (Figure 6 B), and increased *Bifidobacterium*, *Veillonella*, and *Erysipelatoclostridium* over time in I2, compared to their controls. FOS/inulin did not selectively influence the microbiota profile for I3. *Streptococcus* increased between 0 and 5 h in both I4 and I5, together with increased *Bifidobacterium* in I5. Lemon pectin did not change the microbiota profile for I1 (Figure S7 A), but increased abundance of *Cellulosilyticum* in I2 between 9 and 24 h compared to their controls. IMMP breakdown increased *Bacteroides* and *Bifidobacterium* after 7 h (Figure S7 B) in I5 compared to control.

Changes in total bacterial number

Indications of the total bacteria were generated by quantification of total bacterial 16S rRNA gene copy numbers in the fermentation samples over time (**Figure S9**). Compared to control, GOS and FOS/inulin increased the total 16S rRNA gene copy numbers on average 1.74 ± 0.68 times and 2.50 ± 1.04 times at 9 h, respectively. Pectin and IMMP increased the copy numbers on average 1.38 ± 0.52 and 1.46 ± 0.63 times compared to control at 9 h, respectively.

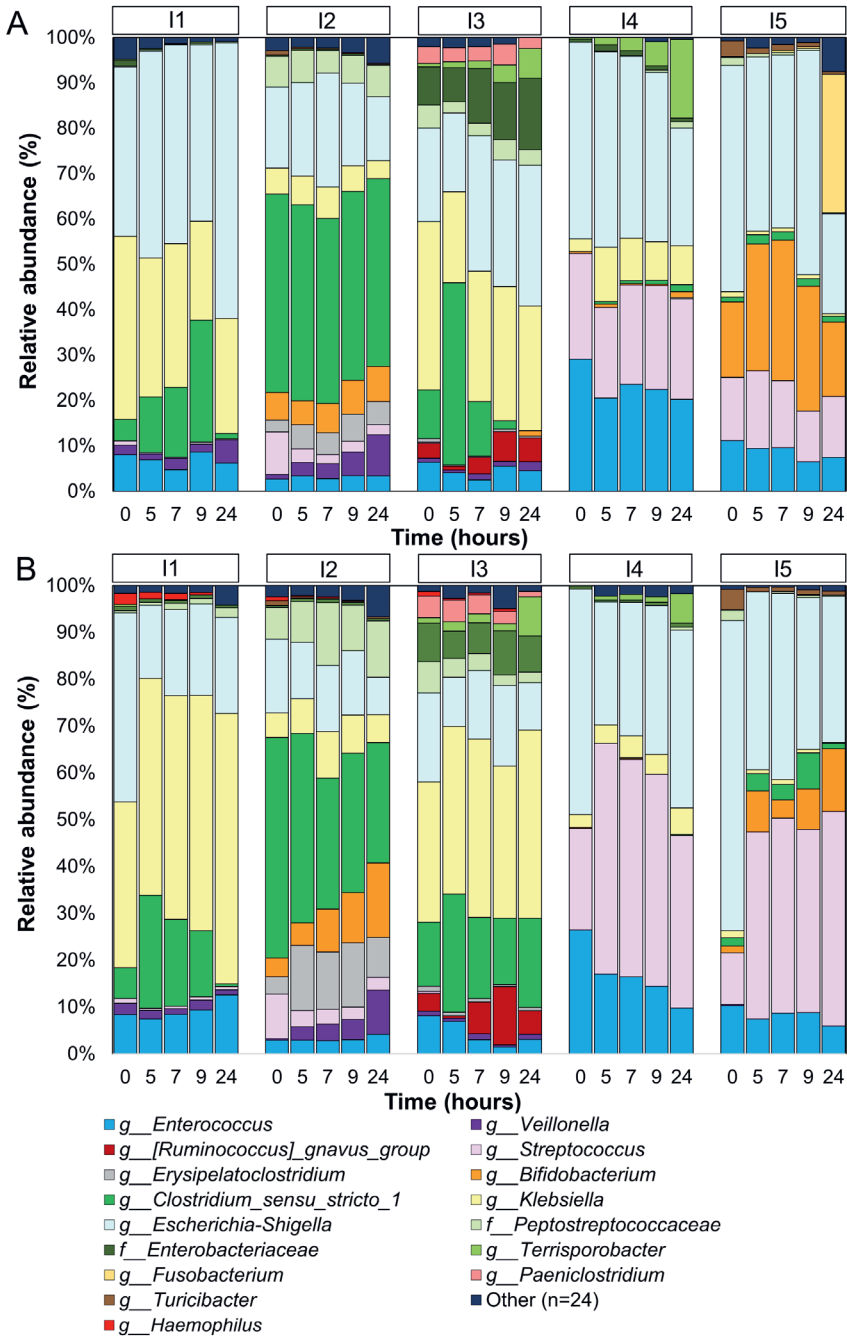


Figure 6. Human SI microbiota composition during GOS and FOS/inulin fermentation. Microbiota relative abundance of the top 15 genera (or highest known taxonomy) at 0, 5, 7, 9, and 24 h during *in vitro* fermentation of GOS (A) and FOS/inulin (B) by microbiota from the five subjects (I1-I5). Abbreviations: FOS, fructo-oligosaccharides; GOS, galacto-oligosaccharides; I, ileostomy inoculum.

Discussion

We investigated the potential of human SI microbiota to degrade dietary fibers *in vitro*, using ileostomy effluent samples. We showed a capacity of SI microbiota from five subjects to degrade GOS and FOS/inulin (DP3-9), which started already before 5 h of incubation. Higher concentrations of metabolites were produced upon GOS and FOS/inulin fermentation compared to controls, which confirmed fiber fermentability. Although inclusion of only five subjects can be considered a weakness, in many *in vitro* fermentation studies fecal samples of different subjects are pooled. This ignores the individual variation. By using five individual SI samples in this study, we were able to show that despite different subject characteristics the SI microbiota from all individuals degraded GOS and FOS. In two studies that used metagenomics data, it was hypothesized that SI microbes depend on the capacity of rapid import and fermentation of available carbohydrates (21) and that human ileal mucosa bacteria are capable of breaking down GOS and FOS via expression of exo- and endo-acting glycosidehydrolases (17) although ileum mucosa bacteria are not directly comparable to luminal microbiota. We found that FOS/inulin with a lower DP was hydrolyzed before longer-chain FOS/inulin (DP10-20), a preference also found for the colonic microbiota (46). Chain length preference is likely caused by expression of different microbial enzymes needed for optimal degradation of FOS (exo-inulinases) and inulin (both exo- and endo-inulinases), and carbohydrate transporters (47) for their transportation (48). In a human ileostomy intervention study, it has been shown that lower molecular weight oligomers present in Jerusalem artichoke inulin (DP2-60) were partly fermented (13%) in the SI, this breakdown was related to DP but unrelated to the transit time (49).

The applied batch fermentation approach has some limitations, hampering the translation of the *in vitro* fermentation kinetics to the *in vivo* situation. First, the relative microbiota composition at the start of the fermentations differed from the microbiota composition in the ileostomy effluents. This compositional shift was likely caused by the preselection step in culture medium, which was applied to remove the remaining carbohydrates from the ileostomy effluent. The proteins and amino acids in this medium might have shifted the composition towards an increased abundance of protein-fermenters such as Enterobacteriaceae, resulting in differences in microbial functionality (50). We have confirmed previous findings (21) by detection of facultative and strict anaerobes in ileostomy effluent, but others also detected aerobic bacteria in the SI (51). The preparation procedure can impact bacteria cultivability and microbiota composition (29). By choosing anaerobic culturing methods, the SI microbiota composition possibly shifted towards a more anaerobic microbiota *in vitro*. This could influence the fermentation kinetics and increase SCFA production. However, bacteria known to be prebiotic utilizers, such as *Bifidobacterium*, *Lactobacillus*, and *Streptococcus*

(10) were already present in the initial microbiota composition of the ileostomy effluents, suggesting their growth can also be stimulated by prebiotics inside the SI. Moreover, concentrations of acetate, lactate, butyrate, and occasionally formate were found previously in ileostomy effluent, confirming the presence of SI bacteria with fermentative capacity (21). In sudden death victims, only 13 ± 6 mM total SCFAs were measured in the terminal ileum, in contrast to 131 ± 9 mM in the proximal colon (52). The higher SCFA concentrations and production in this study might be explained by the (pre-)incubation that increased the bacteria numbers. Furthermore, the bacteria numbers were estimated to be greater in ileostomy effluent than in the ileum of healthy subjects (53). Mainly acetate was produced by SI the microbiota upon fiber degradation in this study. In line with this finding, in pigs fed a human-type diet, the acetate production was higher during ileal fermentation compared to hindgut fermentation, whereas less butyrate was synthesized (20). Also considerable concentrations of acetate, but low concentrations of butyrate were detected in ileal contents of pigs (54). The lower butyrate production by SI microbiota compared to colonic microbiota can be explained by a colon metagenome that was more enriched with the butyrate fermentation pathway compared to the SI microbiota metagenome (21).

The presence of metabolites in the SI could have health implications, either locally in the intestine, such as anti-inflammatory effects (55), although mainly described for butyrate, or metabolic health effects via uptake in the systemic circulation (7) since SCFA can also be absorbed in the human SI (56). On the other hand, fermentation in the SI might lead to bloating due to the production of gasses in combination with the smaller diameter of the SI compared to the colon (57). Priming and activation of SI bacteria by dietary fibers could potentially result in better and faster growth when these activated bacteria enter the ascending colon with a more favorable environment (i.e., lower pH, anaerobic gases). This could lead to more efficient breakdown of fibers in the ascending colon. Overall, our results indicate that GOS and FOS/inulin could have effects in the SI via the residing microbiota, because breakdown started before 5 h of fermentation. Although the time points used in this model cannot be directly translated to the SI transit time, by the selection of more extreme, longer incubation times allowed us to investigate whether SI microbiota have functionality to degrade dietary fibers. Therefore, to study the potential effects of GOS and FOS inside the SI, human trials are needed that capture the short transit time of the SI (median 4.1 h, IQR 3.5–5.9 h) (27) and the luminal microbiota of healthy subjects.

Lemon pectin was found to be slowly fermented after 9 hour by SI microbiota of two subjects when compared to the fast GOS and FOS degradation within these subjects. An efficient *in vitro* utilization of pectin by human colonic microbiota was reported before (58). IMMP was found to be slowly fermented by the SI microbiota of subject

I5, associated with an increased abundance of *Bacteroides* between 7 and 24 h, whereas the other two subjects did not have the capacity to degrade IMMP. *In vitro* fermentation with pooled fecal inoculum showed the breakdown of IMMP between 12 and 24 h (9), so also for the fecal microbiota, IMMP is a slowly degradable fiber. Fiber fermentation kinetics varied depending on molecular weight, and sugar and linkage composition, as shown before (58). Different enzymes are required for their degradation. For instance, FOS and inulin can be classified as low-specificity fibers, because many bacteria are able to access and degrade them (59). In contrast, pectin degradation requires multiple enzymes for degradation. *Bacteroides thetaiotaomicron* is known to use the complex pectic polysaccharides (60), but also for instance *Eubacterium* spp., *Clostridium* spp., and *Bifidobacterium* spp. are pectin-degraders (61). *Bifidobacterium* and *Clostridium_sensu_stricto_1* were detected in the microbiota of subjects I1 and I2, and *Bacteroides* spp. were detected previously in the human ileum (62). Breakdown of lemon pectin was related to increased abundance of *Cellulosilyticum* in I2 after 9 h. *Cellulosilyticum* spp. are known to produce pectinases (63), but at the start of fermentation, this bacteria was not yet detected. The slow fermentation rate of lemon pectin and also IMMP can be explained by the growth of total bacteria, but more likely by growth of specific bacterial groups that produced carbohydrate degrading enzymes required for degradation. Previously it was shown that the human ileum mucosal bacteria encompasses enzymatic potential for degradation of complex fibers, namely plant cell wall polysaccharides carboxymethylcellulose and xylans (64). Of note, the luminal ileum microbiota was not studied, and this information was based on metagenomics data, which does not capture information about fiber utilization. Overall, considering the SI transit time *in vivo*, utilization of lemon pectin and IMMP by the SI microbiota is unlikely. We showed that the metabolism of dietary fibers by SI microbiota is dependent on the molecular structure of the fiber.

The ileostomy effluent samples used in this study contained similar SI bacteria as found before in healthy subjects, for example, *Veillonella*, *Streptococcus*, *Lactobacillus*, *Clostridium cluster_I*, and *Enterococcus* (21, 65-67). As shown before (65), the SI microbiota profile was highly personal. Fiber fermentation triggered microbiota changes *in vitro*, which were dependent on the initial microbiota composition of the subject. All subjects were able to degrade GOS and FOS/inulin (DP3-8) despite the different microbiota profiles, which is not surprising since different bacteria can have similar functions (68). Lactate, known to be an intermediate for the production of acetate, propionate, or butyrate (69) was mainly produced by I4 and I5 upon FOS/inulin and GOS. This could link to the presence of lactate-producing *Streptococcus* in these subjects (70). In contrast, fiber breakdown was not always associated with specific microbiota changes as observed by a stable microbiota dissimilarity over time, indicative of no microbiota differences compared to the control. The differences in microbiota composition between subjects at

baseline could explain why some subjects degrade a fiber. The personalized microbiota responses to the same fiber substrate were previously confirmed by others for the colonic microbiota in response to food (71). Ultimately, having a personalized nutrition focus with respect to various dietary fibers in future studies may be of interest.

Concluding remarks

The applied *in vitro* batch fermentation enabled us to elucidate SI microbiota functionality with respect to dietary fiber breakdown. Fermentation and degradation kinetics were dependent on the type and size of the fiber. Degradation of prebiotics GOS and FOS by the SI microbiota from all ileostomy subjects was demonstrated. In contrast, the higher molecular weight fibers FOS/inulin DP \geq 10, lemon pectin, and IMMP showed a slow fermentation rate, exceeding *in vivo* SI transit time. Acetate was the predominant produced metabolite by the SI microbiota. Microbiota responses *in vitro*, and consequently metabolite profiles, were dependent on the initial microbiota composition of the individuals, supporting the importance of a personalized nutrition approach that could be relevant for dietary fibers.

Acknowledgements

We greatly thank the volunteers in this study for ileostomy effluent donation. We thank FrieslandCampina, Sensus B.V., AVEBE for providing us the fibers. We thank all the consortium partners involved for the critical feedback during the development of this project. This research was performed in the public-private partnership ‘CarboKinetics’ coordinated by the Carbohydrate Competence Center (CCC, www.cccresearch.nl). CarboKinetics is financed by participating industrial partners Agrifirm Innovation Center B.V., Cooperatie AVEBE U.A., DSM Food Specialties B.V., FrieslandCampina Nederland B.V., Nutrition Sciences N.V., VanDrie Holding N.V. and Sensus B.V., and allowances of The Netherlands Organisation for Scientific Research (NWO). The funders had no role in data collection and analysis, or preparation of the manuscript.

References

1. Kendall CW, Esfahani A, Jenkins DJ. The link between dietary fibre and human health. *Food Hydrocoll.* 2010;24(1):42-8.
2. Anderson JW, Baird P, Davis RH, Ferreri S, Knudtson M, Koraym A, et al. Health benefits of dietary fiber. *Nutr Rev.* 2009;67(4):188-205.
3. Veronese N, Solmi M, Caruso MG, Giannelli G, Osella AR, Evangelou E, et al. Dietary fiber and health outcomes: An umbrella review of systematic reviews and meta-analyses. *Am J Clin Nutr.* 2018;107(3):436-44.
4. FAO. Secretariat of the codex alimentarius commission: Codex alimentarius (codex) guidelines on nutrition labeling cac/gl 2-1985 as last amended 2010.
5. Flint HJ, Scott KP, Duncan SH, Louis P, Forano E. Microbial degradation of complex carbohydrates in the gut. *Gut microbes.* 2012;3(4):289-306.
6. Cummings J, Macfarlane G. The control and consequences of bacterial fermentation in the human colon. *J Appl Bacteriol.* 1991;70(6):443-59.
7. den Besten G, Havinga R, Bleeker A, Rao S, Gerding A, van Eunen K, et al. The short-chain fatty acid uptake fluxes by mice on a guar gum supplemented diet associate with amelioration of major biomarkers of the metabolic syndrome. *PLoS One.* 2014;9(9):e107392.
8. Nicholson JK, Holmes E, Kinross J, Burcelin R, Gibson G, Jia W, et al. Host-gut microbiota metabolic interactions. *Science.* 2012;336(6086):1262.
9. Gu F, Borewicz K, Richter B, van der Zaal PH, Smidt H, Buwalda PL, et al. In vitro fermentation behavior of isomalto/malto-polysaccharides using human fecal inoculum indicates prebiotic potential. *Mol Nutr Food Res.* 2018;62(12):1800232.
10. Gibson GR, Probert HM, Loo JV, Rastall RA, Roberfroid MB. Dietary modulation of the human colonic microbiota: Updating the concept of prebiotics. *Nutr Res Rev.* 2004;17(2):259-75.
11. Sender R, Fuchs S, Milo R. Revised estimates for the number of human and bacteria cells in the body. *PLoS Biol.* 2016;14(8):e1002533.
12. Kleerebezem M. Microbial metabolic gatekeeping in the jejunum. *Nature Microbiology.* 2018;3(6):650-1.
13. Martinez-Guryn K, Hubert N, Frazier K, Urluss S, Musch MW, Ojeda P, et al. Small intestine microbiota regulate host digestive and absorptive adaptive responses to dietary lipids. *Cell Host Microbe.* 2018;23(4):458-69.e5.
14. El Aidy S, van den Bogert B, Kleerebezem M. The small intestine microbiota, nutritional modulation and relevance for health. *Curr Opin Biotechnol.* 2015;32:14-20.
15. Vogt LM, Sahasrabudhe NM, Ramasamy U, Meyer D, Pullens G, Faas MM, et al. The impact of lemon pectin characteristics on tlr activation and t84 intestinal epithelial cell barrier function. *J Funct Foods.* 2016;22:398-407.
16. Tolhurst G, Heffron H, Lam YS, Parker HE, Habib AM, Diakogiannaki E, et al. Short-chain fatty acids stimulate glucagon-like peptide-1 secretion via the g-protein-coupled receptor ffar2. *Diabetes.* 2012;61(2):364-71.
17. Cecchini DA, Laville E, Laguerre S, Robe P, Leclerc M, Doré J, et al. Functional metagenomics reveals novel pathways of prebiotic breakdown by human gut bacteria. *PLoS One.* 2013;8(9):e72766.
18. Montoya CA, de Haas ES, Moughan PJ. Development of an in vivo and in vitro ileal fermentation method in a growing pig model. *J Nutr.* 2018;148(2):298-305.
19. Tian L, Bruggeman G, van den Berg M, Borewicz K, Scheurink AJW, Bruininx E, et al. Effects of pectin on fermentation characteristics, carbohydrate utilization, and microbial community composition in the gastrointestinal tract of weaning pigs. *Mol Nutr Food Res.* 2017;61(1):1600186.
20. Hoogeveen AME, Moughan PJ, de Haas ES, Blatchford P, McNabb WC, Montoya CA. Ileal and hindgut fermentation in the growing pig fed a human-type diet. *Br J Nutr.* 2020:1-27.

21. Zoetendal EG, Raes J, Van Den Bogert B, Arumugam M, Booijsink CC, Troost FJ, et al. The human small intestinal microbiota is driven by rapid uptake and conversion of simple carbohydrates. *The ISME journal*. 2012;6(7):1415.
22. Leemhuis H, Dobruchowska JM, Ebbelaar M, Faber F, Buwalda PL, van der Maarel MJEC, et al. Isomalto/malto-polysaccharide, a novel soluble dietary fiber made via enzymatic conversion of starch. *J Agric Food Chem*. 2014;62(49):12034-44.
23. Deutsch MJ. AOAC official method 985.29, total dietary fiber in foods, enzymatic-gravimetric method. *Official methods of analysis of AOAC international*. 1995.
24. AOAC, Total. 16th ed. AOAC international, AOAC method 991.43, total, insoluble and soluble dietary fiber in food—enzymatic-gravimetric method, MES-Tris buffer. 1995.
25. Gibson GR, Cummings JH, Macfarlane GT. Use of a three-stage continuous culture system to study the effect of mucin on dissimilatory sulfate reduction and methanogenesis by mixed populations of human gut bacteria. *Appl Environ Microbiol*. 1988;54(11):2750-5.
26. Ladirat SE, Schols HA, Nauta A, Schoterman MHC, Keijser BJF, Montijn RC, et al. High-throughput analysis of the impact of antibiotics on the human intestinal microbiota composition. *J Microbiol Methods*. 2013;92(3):387-97.
27. Koziolok M, Grimm M, Becker D, Iordanov V, Zou H, Shimizu J, et al. Investigation of pH and temperature profiles in the GI tract of fasted human subjects using the intellicap® system. *J Pharm Sci*. 2015;104(9):2855-63.
28. Aguirre M, Eck A, Koenen ME, Savelkoul PHM, Budding AE, Venema K. Evaluation of an optimal preparation of human standardized fecal inocula for in vitro fermentation studies. *J Microbiol Methods*. 2015;117:78-84.
29. Rajilic-Stojanovic M, Maathuis A, Heilig HG, Venema K, de Vos WM, Smidt H. Evaluating the microbial diversity of an in vitro model of the human large intestine by phylogenetic microarray analysis. *Microbiology*. 2010;156(Pt 11):3270-81.
30. Rosch C, Taverne N, Venema K, Gruppen H, Wells JM, Schols HA. Effects of in vitro fermentation of barley beta-glucan and sugar beet pectin using human fecal inocula on cytokine expression by dendritic cells. *Mol Nutr Food Res*. 2017;61(1).
31. Cardarelli H, Martinez R, Albrecht S, Schols H, Franco B, Saad S, et al. In vitro fermentation of prebiotic carbohydrates by intestinal microbiota in the presence of *Lactobacillus amylovorus* DSM 16998. *Beneficial microbes*. 2016;7(1):119-33.
32. Ladirat SE, Schuren FHJ, Schoterman MHC, Nauta A, Gruppen H, Schols HA. Impact of galacto-oligosaccharides on the gut microbiota composition and metabolic activity upon antibiotic treatment during in vitro fermentation. *FEMS Microbiol Ecol*. 2014;87(1):41-51.
33. Salonen A, Nikkilä J, Jalanka-Tuovinen J, Immonen O, Rajilic-Stojanovic M, Kekkonen RA, et al. Comparative analysis of fecal DNA extraction methods with phylogenetic microarray: Effective recovery of bacterial and archaeal DNA using mechanical cell lysis. *J Microbiol Methods*. 2010;81(2):127-34.
34. Cole JR, O'Sullivan O, O'Toole PW, Wang Q, Ross RB, Greene-Diniz R, et al. Comparison of two next-generation sequencing technologies for resolving highly complex microbiota composition using tandem variable 16S rRNA gene regions. *Nucleic Acids Res*. 2010;38(22):e200-e.
35. Ramiro-Garcia J, Hermes G, Giatsis C, Sipkema D, Zoetendal E, Schaap P, et al. Ng-tax, a highly accurate and validated pipeline for analysis of 16S rRNA amplicons from complex biomes [version 1; referees: 2 approved with reservations, 1 not approved]. *F1000Research*. 2016;5(1791).
36. Poncheewin W, Hermes GDA, van Dam JCJ, Koehorst JJ, Smidt H, Schaap PJ. Ng-tax 2.0: A semantic framework for high-throughput amplicon analysis. *Front Genet*. 2019;10:1366.
37. Team RC. R: A language and environment for statistical computing. R foundation for statistical computing, Vienna, Austria. 2018.
38. Salter SJ, Cox MJ, Turek EM, Calus ST, Cookson WO, Moffatt ME, et al. Reagent and laboratory contamination can critically impact sequence-based microbiome analyses. *BMC Biology*. 2014;12(1):87.

39. Leo Lahti. Tools for microbiome analysis in R. Microbiome package version 1.5.25. Bioconductor 2017.
40. McMurdie PJ, Holmes S. Phyloseq: An R package for reproducible interactive analysis and graphics of microbiome census data. PLOS ONE. 2013;8(4):e61217.
41. Jari Oksanen FGB, Michael Friendly, Roeland Kindt, Pierre Legendre, Dan McGlenn, Peter R. Minchin, R. B. O'Hara, Gavin L. Simpson, Peter Solymos, M. Henry H. Stevens, Eduard Szoecs and Helenev Wagner. Vegan: Community ecology package. R package version 2.5-3. 2018.
42. Kolde R. Pheatmap: Pretty heatmaps. R package version 1.0.10. 2018.
43. Janssen AWF, Dijk W, Boekhorst J, Kuipers F, Groen AK, Lukovac S, et al. Angptl4 promotes bile acid absorption during taurocholic acid supplementation via a mechanism dependent on the gut microbiota. Biochim Biophys Acta Mol Cell Biol Lipids. 2017;1862(10, Part A):1056-67.
44. Di Guida R, Engel J, Allwood JW, Weber RJM, Jones MR, Sommer U, et al. Non-targeted uhplc-ms metabolomic data processing methods: A comparative investigation of normalisation, missing value imputation, transformation and scaling. Metabolomics. 2016;12(5):93.
45. Bates D, Maechler M, Bolker B, Walker S, Christensen RHB, Singmann H, et al. Package 'lme4'. Convergence. 2015;12(1).
46. Stewart ML, Timm DA, Slavin JL. Fructooligosaccharides exhibit more rapid fermentation than long-chain inulin in an *in vitro* fermentation system. Nutr Res. 2008;28(5):329-34.
47. Gänzle M, Follador R. Metabolism of oligosaccharides and starch in lactobacilli: A review. Front Microbiol. 2012;3(340).
48. Apolinário AC, de Lima Damasceno BPG, de Macêdo Beltrão NE, Pessoa A, Converti A, da Silva JA. Inulin-type fructans: A review on different aspects of biochemical and pharmaceutical technology. Carbohydr Polym. 2014;101:368-78.
49. Bach Knudsen KE, Hessov I. Recovery of inulin from jerusalem artichoke (*helianthus tuberosus* l.) in the small intestine of man. Br J Nutr. 1995;74(1):101-13.
50. Richardson AJ, McKain N, Wallace RJ. Ammonia production by human faecal bacteria, and the enumeration, isolation and characterization of bacteria capable of growth on peptides and amino acids. BMC Microbiol. 2013;13(1):6.
51. Kalantar-Zadeh K, Berean KJ, Ha N, Chrimes AF, Xu K, Grando D, et al. A human pilot trial of ingestible electronic capsules capable of sensing different gases in the gut. Nature Electronics. 2018;1(1):79.
52. Cummings JH, Pomare EW, Branch WJ, Naylor CP, Macfarlane GT. Short chain fatty acids in human large intestine, portal, hepatic and venous blood. Gut. 1987;28(10):1221-7.
53. Gorbach SL, Nahas L, Weinstein L, Levitan R, Patterson JF. Studies of intestinal microflora. Iv. The microflora of ileostomy effluent: A unique microbial ecology. Gastroenterology. 1967;53(6):874-80.
54. Haenen D, Zhang J, Souza da Silva C, Bosch G, van der Meer IM, van Arkel J, et al. A diet high in resistant starch modulates microbiota composition, scfa concentrations, and gene expression in pig intestine. J Nutr. 2013;143(3):274-83.
55. Vinolo MAR, Rodrigues HG, Nachbar RT, Curi R. Regulation of inflammation by short chain fatty acids. Nutrients. 2011;3(10):858-76.
56. Schmitt MG, Jr., Soergel KH, Wood CM, Steff JJ. Absorption of short-chain fatty acids from the human ileum. Am J Dig Dis. 1977;22(4):340-7.
57. Helander HF, Fändriks L. Surface area of the digestive tract - revisited. Scand J Gastroenterol. 2014;49(6):681-9.
58. Jonathan MC, van den Borne JJGC, van Wiechen P, Souza da Silva C, Schols HA, Gruppen H. *In vitro* fermentation of 12 dietary fibres by faecal inoculum from pigs and humans. Food Chemistry. 2012;133(3):889-97.
59. Cantu-Jungles TM, Hamaker BR. New view on dietary fiber selection for predictable shifts in gut microbiota. mBio. 2020;11(1):e02179-19.

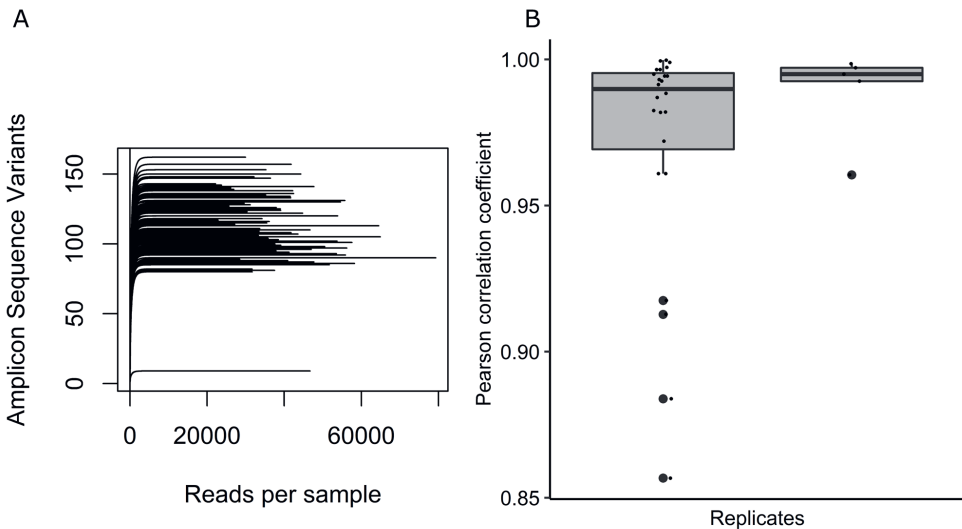
60. Ndeh D, Rogowski A, Cartmell A, Luis AS, Baslé A, Gray J, et al. Complex pectin metabolism by gut bacteria reveals novel catalytic functions. *Nature*. 2017;544(7648):65-70.
61. Dongowski G, Lorenz A, Anger H. Degradation of pectins with different degrees of esterification by bacteroides thetaiotaomicron isolated from human gut flora. *Appl Environ Microbiol*. 2000;66(4):1321-7.
62. Villmones HC, Haug ES, Ulvestad E, Grude N, Stenstad T, Halland A, et al. Species level description of the human ileal bacterial microbiota. *Sci Rep*. 2018;8(1):4736.
63. Cai S, Shao N, Dong X. *Cellulosilyticum*. In *bergey's manual of systematics of archaea and bacteria*. 2016.
64. Patrascu O, Béguet-Crespel F, Marinelli L, Le Chatelier E, Abraham A-L, Leclerc M, et al. A fibrolytic potential in the human ileum mucosal microbiota revealed by functional metagenomic. *Sci Rep*. 2017;7:40248-.
65. Booijink CC, El-Aidy S, Rajilic-Stojanovic M, Heilig HG, Troost FJ, Smidt H, et al. High temporal and inter-individual variation detected in the human ileal microbiota. *Environ Microbiol*. 2010;12(12):3213-27.
66. Hayashi H, Takahashi R, Nishi T, Sakamoto M, Benno Y. Molecular analysis of jejunal, ileal, caecal and recto-sigmoidal human colonic microbiota using 16s rrna gene libraries and terminal restriction fragment length polymorphism. *J Med Microbiol*. 2005;54(11):1093-101.
67. Zmora N, Zilberman-Schapira G, Suez J, Mor U, Dori-Bachash M, Bashiardes S, et al. Personalized gut mucosal colonization resistance to empiric probiotics is associated with unique host and microbiome features. *Cell*. 2018;174(6):1388-405.e21.
68. Kaoutari AE, Armougom F, Gordon JI, Raoult D, Henrissat B. The abundance and variety of carbohydrate-active enzymes in the human gut microbiota. *Nat Rev Microbiol*. 2013;11:497.
69. Muñoz-Tamayo R, Laroche B, Walter É, Doré J, Duncan SH, Flint HJ, et al. Kinetic modelling of lactate utilization and butyrate production by key human colonic bacterial species. *FEMS Microbiol Ecol*. 2011;76(3):615-24.
70. Van den Bogert B, Boekhorst J, Herrmann R, Smid EJ, Zoetendal EG, Kleerebezem M. Comparative genomics analysis of streptococcus isolates from the human small intestine reveals their adaptation to a highly dynamic ecosystem. *PLoS One*. 2014;8(12):e83418.
71. Johnson AJ, Vangay P, Al-Ghalith GA, Hillmann BM, Ward TL, Shields-Cutler RR, et al. Daily sampling reveals personalized diet-microbiome associations in humans. *Cell Host Microbe*. 2019;25(6):789-802.e5.

Supplementary Information

Table S1. Information about the dietary intake of the five subjects on the two days consecutive to ileostomy effluent donation.

Subject	Day	Energy (kcal)	Total protein (energy%)	Total fat (energy%)	Total carbohydrates (energy%)	Total dietary fibers (energy%)	Total carbohydrates ^{a)} (gram)	Total dietary fibers ^{b)} (gram)	Total alcohol (gram)
I1	1	1611	22.9	32.0	41.9	3.3	166.5	27.9	0.0
	2	1502	18.4	20.3	51.0	3.7	189.3	29.0	14.8
I2	1	2062	14.8	34.1	48.2	1.5	245.6	16.2	0.0
	2	2199	18.2	26.7	51.7	2.0	281.4	22.9	0.0
I3	1	1468	15.7	28.5	53.0	2.3	192.0	17.5	0.0
	2	898	13.3	28.2	55.1	3.0	122.6	14.4	0.0
I4	1	3275	14.3	37.4	44.9	0.8	363.0	14.6	12.5
	2	2057	9.9	34.3	54.9	1.0	279.9	11.1	0.0
I5	1	2619	20.0	42.9	32.7	1.3	210.9	18.1	10.0
	2	2292	16.8	39.8	41.0	2.0	231.4	23.5	0.0

The five ileostomy subjects are numbered from I1 to I5. 24-hour food diaries kept the two days consecutive to ileostomy sample donation. ^{a)}Total carbohydrates without dietary fibers. ^{b)}Included in dietary fibers are high molecular weight dietary fiber (e.g. cellulose, resistant starch, cereal β -glucan, guar gum and certain xylans), insoluble dietary fiber in water (e.g. cellulose, resistant starch and certain xylans), dietary fiber soluble in water and precipitated by 78% ethanol (e.g. cereal β -glucan, guar gum and certain xylans). Excluded are low molecular weight dietary fiber (e.g. FOS, GOS, a portion of Polydextrose®, inulin and resistant maltodextrins) and non-resistant starch.

**Figure S1. Quality characteristics of the amplicon sequencing data.**

The rarefaction curve of all samples (A), and the correlation coefficients of biological and technical replicates pairs (B). Boxplots show the distribution of the data via quartiles.

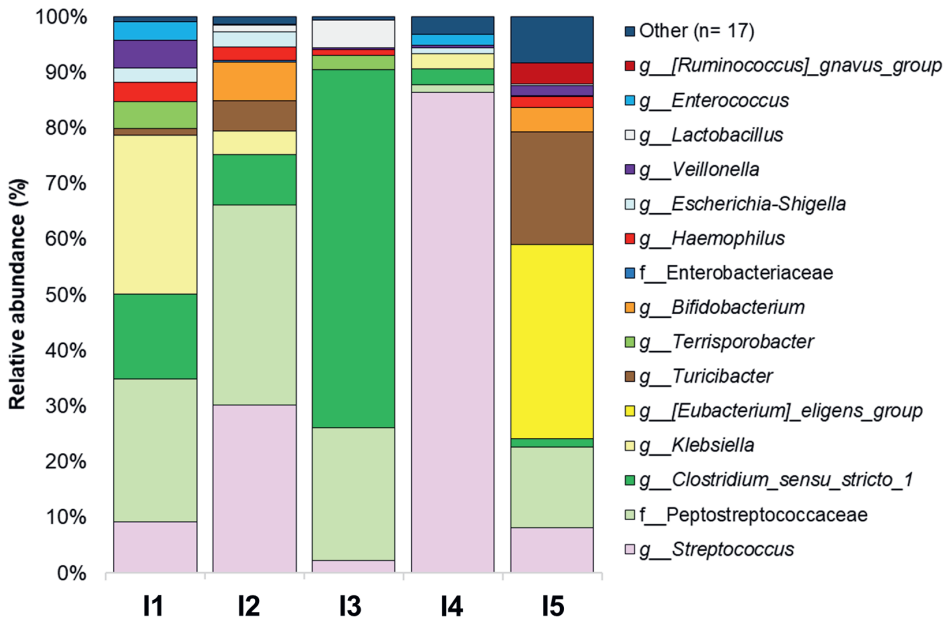


Figure S2. The microbiota composition in the ileostomy effluent obtained from five subjects (I1-I5).

The relative abundances of the 15 most abundant genera are shown. If genera were not classified or the genus was an uncultured bacteria, only the family level is depicted in the graph. Abbreviations: I, ileostomy inoculum.

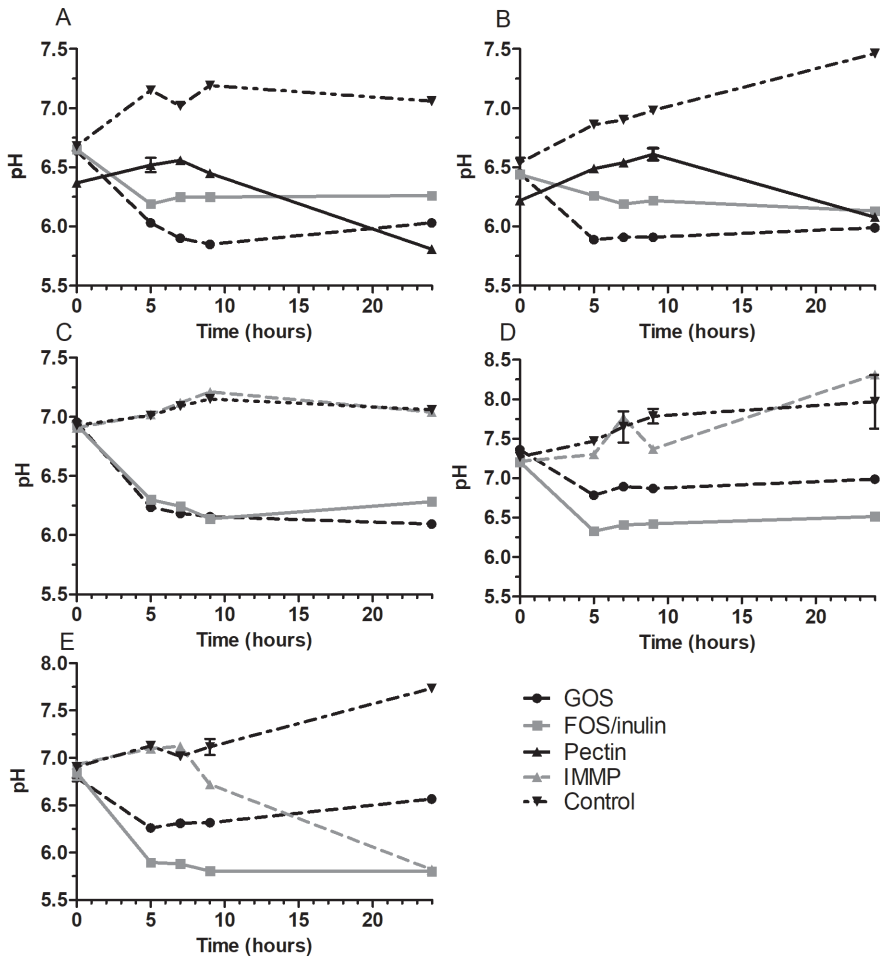


Figure S3. The pH values in the *in vitro* fermentation samples over time.

The changes in pH by five subjects I1 (A), I2 (B), I3 (C), I4 (D), and I5 (E) for the different dietary fibers at 0, 5, 7, 9, and 24 h and the control without added fiber during fermentation. Values are means of replicates \pm SD. Abbreviations: FOS, fructo-oligosaccharides; GOS, galacto-oligosaccharides; I, ileostomy inoculum; IMMP, isomalto-maltopolysaccharides.

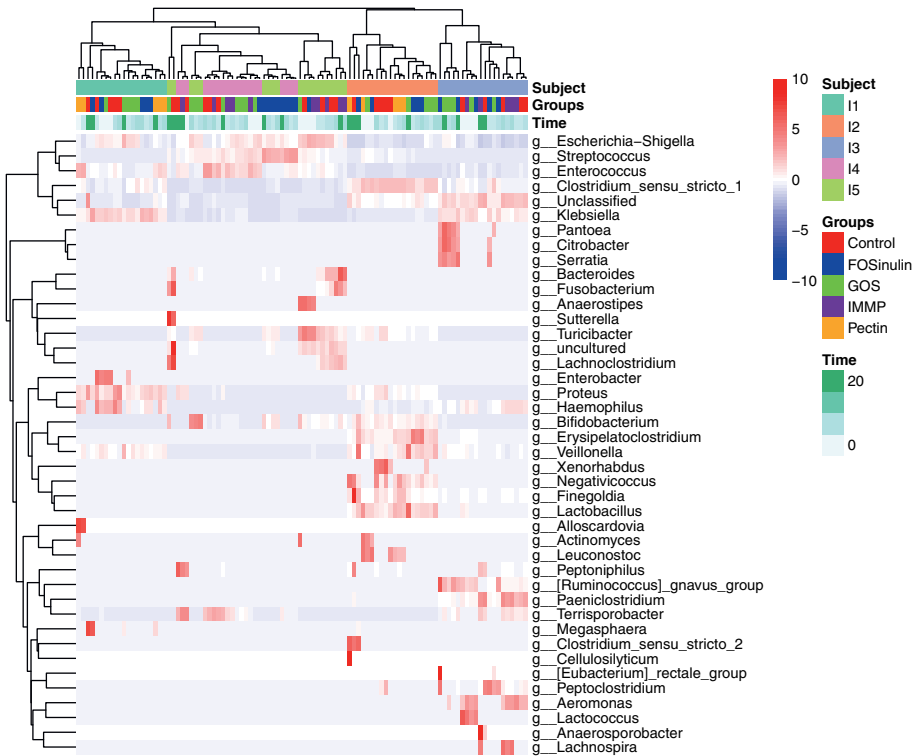


Figure S4. A heatmap of all in vitro fermentation samples, to visualize taxa causing differences between the subjects and fibers.

Each column represents a sample, each row a unique genus. On top of the heatmap, diverse colors depict the five subjects, fibers, and time points. Fermentation samples were clustered on Bray-Curtis microbial dissimilarity, and genera were hierarchically clustered using the Ward.D2 algorithm. Colors in the heatmap were given by taxa scaling, with the mean relative abundance set at 0, and taxa relative abundances above the mean in red, taxa relative abundances below the mean in blue. White means the taxa was not detected in the sample. Abbreviations: FOS, fructo-oligosaccharides; GOS, galacto-oligosaccharides; IMMP, isomalto/malto-polysaccharide; I, ileostomy inoculum.

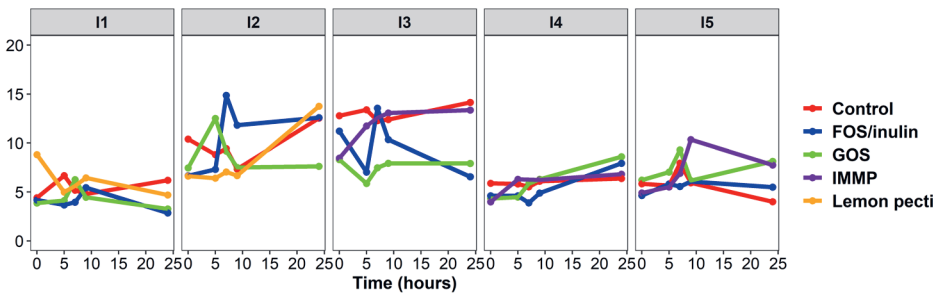


Figure S5. Alpha-diversity in the in vitro fermentation samples using SI microbiota from five subjects (I1-I5).

The lines depict the alpha-diversity using inverse simpson during fermentation with different fibers, or control without added fiber at 0, 5, 7, 9, and 24 h. Abbreviations: FOS, fructo-oligosaccharides; GOS, galacto-oligosaccharides; I, ileostomy inoculum; IMMP, isomalto/malto-polysaccharides.

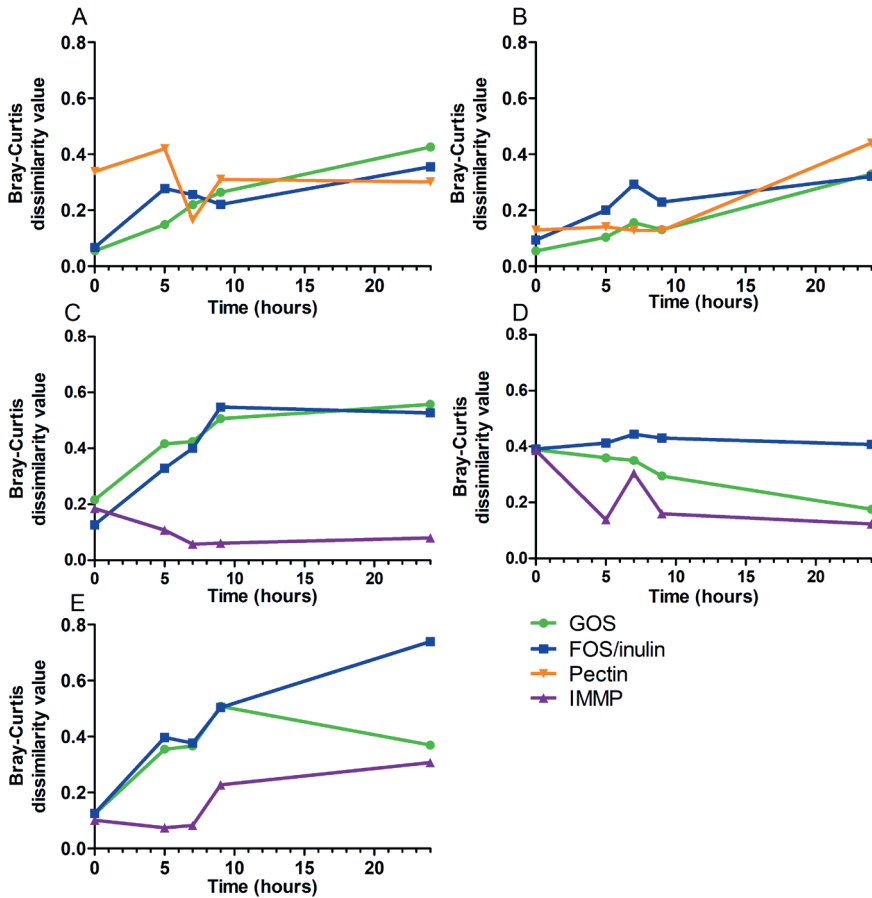


Figure S6. Microbiota dissimilarity of the fermentation samples with added fiber compared to control.

The Bray-Curtis dissimilarity values were calculated for the fibers compared to control without added fiber at 0, 5, 7, 9, and 24 h during *in vitro* fermentation, within each of the five subjects: I1 (A), I2 (B), I3 (C), I4 (D), and I5 (E). Abbreviations: FOS, fructo-oligosaccharides; GOS, galacto-oligosaccharides; IMMP, isomalto/malto-polysaccharide.

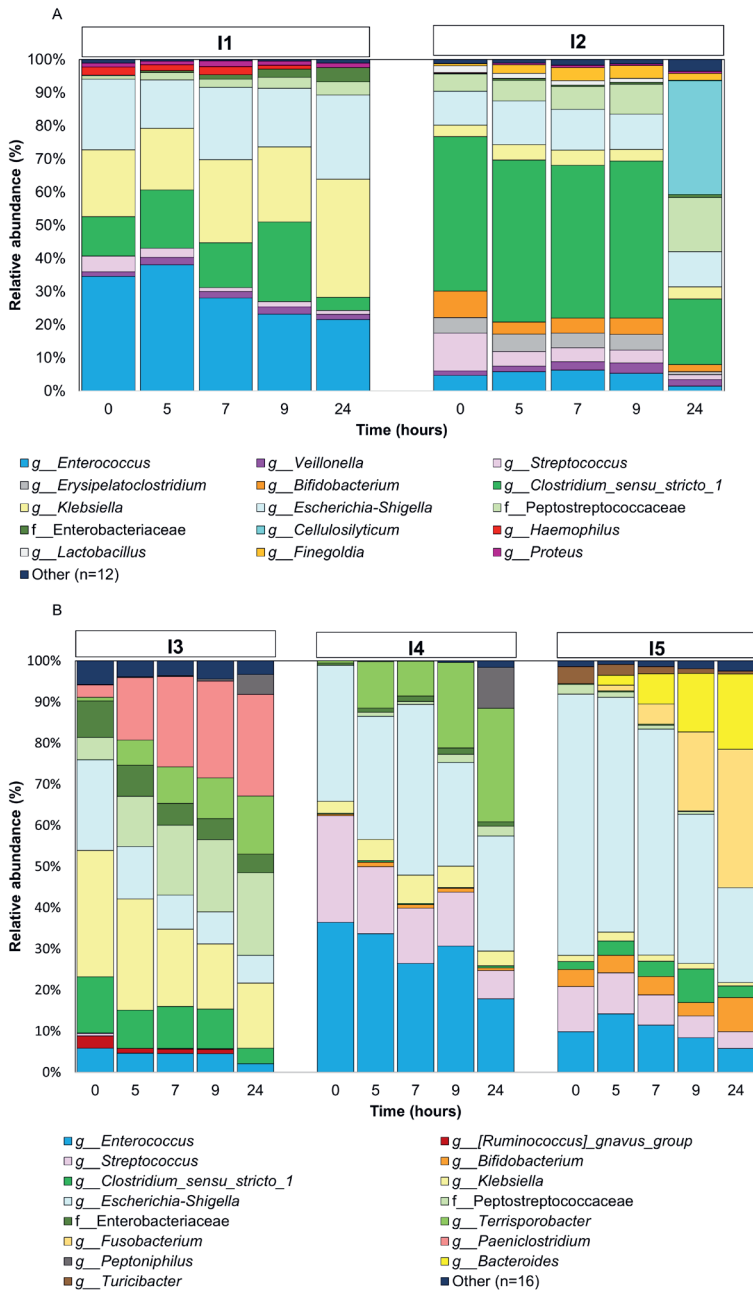


Figure S7. Human SI microbiota composition during pectin and IMMP fermentation. Microbiota relative abundance differences of the top 15 genera (or highest known taxonomy) at 0, 5, 7, 9, and 24 h during *in vitro* fermentation of lemon pectin (A) by microbiota from two subjects I1, I2, and during IMMP (B) fermentation by microbiota from three subjects I3, I4, and I5. Abbreviations: I, ileostomy inoculum. IMMP, isomalto/malto-polysaccharide.

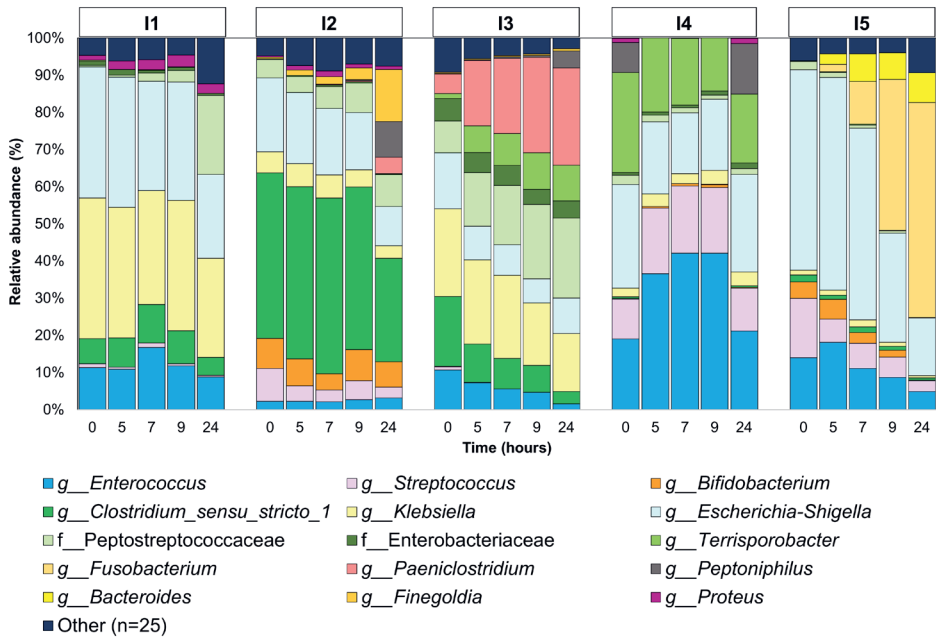


Figure S8. Human SI microbiota composition during background fermentation.

Microbiota relative abundance of the top 15 genera (or highest known taxonomy) at 0, 5, 7, 9, and 24 h during *in vitro* fermentation without added fiber by microbiota from the five subjects I1-I5 (A). Abbreviations: I, ileostomy inoculum.

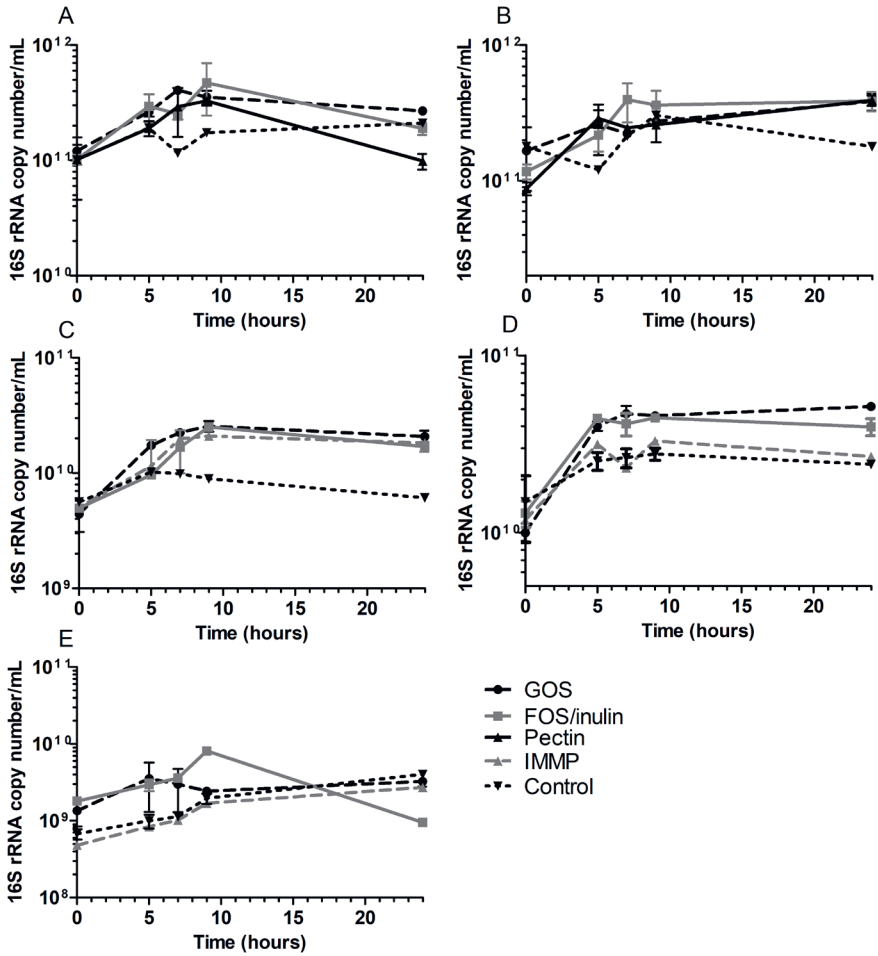


Figure S9. 16S rRNA gene copy numbers over time during *in vitro* fermentations.

The total 16S rRNA copy numbers during *in vitro* fermentation of different fibers or control without added fiber at 0, 5, 7, 9, and 24 h for the five subjects I1 (A), I2 (B), I3 (C), I4 (D), and I5 (E). Values are means \pm SDs. Abbreviations: FOS, fructo-oligosaccharides; GOS, galacto-oligosaccharides; IMMP, isomaltomaltopolysaccharides; rRNA, ribosomal RNA.



Intra-intestinal degradation kinetics of non-digestible carbohydrates and the fate of short-chain fatty acids in human subjects

Mara P.H. van Trijp^{1*}, Melany Rios-Morales^{2*}, Ben Witteman^{1,3}, Fentaw Abegaz^{2,4}, Albert Gerding^{2,5}, Ran An⁶, Martijn Koehorst^{2,5}, Bernard Evers², Katja C.V van Dongen⁷, Erwin G. Zoetendal⁶, Henk Schols⁸, Lydia A. Afman¹, Dirk-Jan Reijngoud², Barbara M. Bakker^{2#}, Guido J.E.J. Hooiveld^{1#}

*Shared first authors, #shared last authors.

¹ Division of Human Nutrition and Health, Wageningen University, Wageningen, The Netherlands.

² Laboratory of Pediatrics, Center for Liver, Digestive and Metabolic Diseases, University of Groningen, University Medical Center Groningen, Groningen, The Netherlands.

³ Hospital Gelderse Vallei, Department of Gastroenterology and Hepatology, Ede, The Netherlands.

⁴ Statistics and Probability Unit, University of Groningen, Groningen, The Netherlands.

⁵ Department of Laboratory Medicine, University of Groningen, University Medical Center Groningen, Groningen, The Netherlands.

⁶ Laboratory of Microbiology, Wageningen University, Wageningen, The Netherlands.

⁷ Division of Toxicology, Wageningen University, Wageningen, The Netherlands.

⁸ Laboratory of Food Chemistry, Wageningen University, Wageningen, The Netherlands.

In preparation.

Abstract

Consumption of non-digestible carbohydrates (NDC), such as chicory FOS or GOS, is linked to many health benefits. Intestinal microbiota can use FOS and GOS as substrates to produce short-chain fatty acids (SCFA), mainly acetate, propionate and butyrate. Uptake rates of SCFA were previously correlated with amelioration of metabolic syndrome markers such as glucose and insulin levels. However, detailed knowledge of NDC fermentation within the human intestine is lacking. Our aim was to determine acute fermentation kinetics of a FOS:GOS mix in the human intestine, including effects on the microbiota, using a naso-intestinal catheter for infusion and sampling, without (study 1) and with (study 2) preceding NDC supplementation. Moreover, we studied the fate of intestinal-delivered SCFA as substrates for glucose and lipid metabolism by the host by measuring label incorporation in blood metabolites.

In study 1, five healthy males were included to test acute NDC kinetics. In study 2, ten healthy males were included to also assess the effect of 15 g/day FOS:GOS (n=5) or isocaloric maltodextrin (n=5) supplementation for 7 days on the acute NDC kinetics. Subjects were 18-60yrs with a BMI 18.5-30 kg/m². A naso-intestinal catheter was positioned in the distal ileum or colon. At the start of the test day, all subjects consumed a NDC bolus with 5 gram FOS and 5 gram GOS. After 120 minutes, isotopically ¹³C-labeled acetate, propionate and butyrate were delivered directly in the intestinal lumen. Before and postprandially after NDC consumption, intestinal content, blood, and breath samples were collected.

No changes were found in ratios of the FOS:GOS in the distal ileum over time when compared to these ratios in the original bolus. After isotope delivery, intraluminal SCFA enrichment patterns did not change significantly, and no bacterial SCFA cross-feeding was detected during the time the isotopes remained in the sampling location. Breath hydrogen significantly increased after NDC consumption (0 min: 5.3±6.0 ppm, peak at 185 min: 39.6±28.1 ppm) suggesting fermentation. The relative composition of microbiota changed rapidly during the test day. ¹³C from all ¹³C-SCFA were incorporated into glucose, with propionate contributing to the net glucose synthesis (up to 2% of ¹³C-glucose). Acetate and butyrate were substrates for citrate production with butyrate as the main contributor. No label incorporation was found in amino acids. Propionate was also converted to propionyl-carnitine. No label incorporation was detected in fatty acids.

In the human distal ileum no fermentation of the selected NDCs, nor SCFA production or bacterial cross-feeding was observed. Nevertheless, the FOS:GOS mix was most likely fermented more distal in the intestine, in the colon, as indicated by increased proxies for microbial fermentation. SCFA were vividly taken up and metabolized by the host.

Introduction

The incidence of obesity and diabetes has rapidly increased, making them worldwide public health problems (1). Consumption of non-digestible carbohydrates (NDC, 25-50 gram/day) is associated with numerous health benefits, including decreased risk of diabetes and obesity (2). Many NDCs can be fermented by the intestinal microbiota, and some NDCs, such as fructo- and galacto-oligosaccharides (FOS and GOS) have been shown to selectively increase specific groups of bacteria such as *Bifidobacterium* (3). During NDC fermentation, short chain fatty acids (SCFA) are produced, mainly acetate, propionate, and butyrate (4). Furthermore, metabolic cross-feeding by bacteria in which fermentation products from certain microbes are subsequently used by other microbes, plays a key role in maintaining the microbial ecosystem and is crucial to determine the final SCFA profile in the intestine (5). It has been hypothesized that SCFA are an important link between fiber fermentation and host health improvements (6, 7). In order to avoid invasive sampling, feces are mostly used when studying NDC degradation, SCFA production, and intestinal microbiota in humans. However, feces are expected to only be a surrogate representative of the microbiota residing in the lumen (8, 9). Moreover, colonic SCFA are readily absorbed, with likely only 5-10% being excreted in the feces (10). Additionally, NDC degradation and SCFA production is often studied in *in vitro* gut models that can reproduce physicochemical parameters of the human gut, however, SCFA absorption in this model does not directly mimic luminal dynamics (11, 12). Furthermore, *in vitro* models are mostly inoculated with human feces, results of which cannot be directly translated to the *in vivo* situation in humans. Another indirect method to measure carbohydrate fermentation in healthy subjects is by isotopic labeling of the substrate of interest, such as ^{13}C -inulin (13), followed by tracking postprandial ^{13}C -metabolites in plasma as an indication of carbohydrate degradation, or the use of hydrogen and methane concentrations in the breath as an indicator of microbial fermentation (14-17). Still, this does not provide us with direct information about carbohydrate fermentation and SCFA production inside the human intestinal lumen, nor on the direct impact of NDC on the luminal microbiota.

In mice fed with diets supplemented with different amounts of fermentable fiber (guar gum), only the *in vivo* uptake fluxes of SCFA, and not their cecal concentrations, correlated linearly with the improvements on metabolic syndrome markers (18). To better understand the health benefits of fiber fermentation, accurate estimation of SCFA production, uptake and their metabolic fate in the host is essential. Assessing such kinetics of fermentation *in vivo* in humans comes with major challenges. Boets et al. pioneered such studies, by measuring SCFA appearance in blood derived from inulin ingestion after a continuous ^{13}C -SCFA intravenous infusion (19), or by directly delivering the labeled SCFA in the proximal colon using capsules with a pH-responsive coating and measuring

the label appearance in blood (20). However, no samples were obtained from the actual luminal fermentation site. The measurement of feces, blood, and breath necessitates assumptions for the calculation of intestinal fluxes that are debatable, since there is an unknown degree of first-pass SCFA metabolism before reaching peripheral blood circulation. Moreover, SCFA can have a local effect for instance working as signaling molecules to promote the release of satiety-inducing hormones such as glucagon-like peptide 1 (GLP-1) and peptide YY (PYY) (21). They are also metabolized locally by colonocytes in the gut, or after absorption into the portal circulation by the liver (22). In humans and mice, SCFA can be used as precursors for glucose and lipids by the host (20, 23). Nonetheless, the mechanisms by which SCFAs can regulate host metabolism and to which extent they could be beneficial in humans needs to be further studied. Here, we present the results of two clinical feasibility trials in healthy men. The aim of the first trial was to study acute NDC fermentation kinetics in the (small) intestine in humans using a novel approach based on intestinal catheters for in situ sampling and administration of ¹³C labeled SCFA. The same methodology was implemented in the second trial, where we aimed to investigate the effect of a 7-day NDC supplementation versus maltodextrin on the acute NDC fermentation kinetics. Moreover, the use of stable isotopes allowed us to assess the fate of intestinal-delivered SCFA as substrates in systemic glucose and lipid metabolism. Our studies provide valuable information about the feasibility of this new approach to study NDC fermentation inside the human intestine and the fate of fermentation products.

Material and methods

Study subjects

In both trials, healthy male subjects with an age between 18-60 years, a BMI between 18.5-30 kg/m², and regular bowel movements (defecation on average once a day) were included. The main exclusion criteria were having a history of medical or surgical events, the use of any prescribed or non-prescribed medication during the three weeks prior to study start, smoking, use of pro- pre- or antibiotics within 3 months before the study start, having infrequent bowel movements (less than three times per week), and the abuse of alcohol (more than 21 consumptions per week). All subjects filled in a food frequency questionnaire during screening for determination of their habitual fiber intake. All subjects gave written informed consent. The studies were approved by the Medical Ethics Committee of Wageningen University, and registered at ClinicalTrials.gov, identifiers: NCT04013607 (study 1) and NCT04499183 (study 2).

Study designs and intervention products

Study 1: to test a novel approach to study acute fermentation kinetics

Study 1 consisted of two days in total. On day one, subjects were intubated with a naso-intestinal catheter (**Supplementary Figure 1**, Mui Scientific, Ontario, Canada) that progressed during the day towards the distal small intestine (for protocol see **Supplementary Methods**). In the evening a standardized meal was consumed (540 gram in total, 131 kcal/100 g, 8.6 g fat/100 g, 7.8 g carbohydrates/100 g, 4.8 g protein/100 g). On day two, after an overnight fast, the experimental test day took place.

Study 2: to study the effects of an NDC intervention on acute fermentation kinetics

Study 2 was designed as a randomized, double-blind, placebo-controlled, parallel-group study. Randomization was performed to assign participants to the placebo or the NDC intervention arm. First, pairs were matched based on a similar BMI and age. An independent person randomly allocated within one couple one person to NDC and the other to placebo using a computerized procedure. All study participants and investigators were blinded to intervention allocations until all analyses were completed. Participants in the NDC group received a mixture of 7.5 g/day of chicory FOS (synonym oligofructose, Frutalose® OFP; Sensus, Roosendaal, the Netherlands) and 7.5 g/day GOS (Vivinal GOS, FrieslandCampina, Wageningen, the Netherlands) for seven days. Participants in the placebo group received isocaloric maltodextrin (13.2 g/day, Paselli MD 12, Avebe, Veendam, the Netherlands) for seven days. The NDCs were packed in closed, non-transparent jars. Subjects were asked to ingest the supplements twice daily (7.5 g mixed FOS/GOS per dose), with breakfast in the morning and with dinner in the evening. The empty and remaining jars were returned to assess compliance. Subjects were instructed to maintain their habitual diet during the study. On day seven, a fecal sample was collected immediately after defecation at home using a “FecesCatcher” (https://www.fecesvanger.nl/en_GB/), stored at -20°C for maximally 24 hours, and afterwards stored at -80°C . Next, identical to study 1, subjects were equipped with a naso-intestinal catheter in the Hospital. In the evening, a standardized meal was consumed (380 gram in total, 137 kcal/100 g, 4.7 g fat/100 g, 17.4 g carbohydrates/100 g, 6.9 g protein/100 g). On day eight, after an overnight fast, the experimental test day took place.

Design and placement of the naso-intestinal catheter

A naso-intestinal catheter was used as an intestinal sampling and delivery tool (24). On day one (study 1) or day seven (study 2) between 07.30-09.30 h, subjects were intubated with a custom-made intestinal catheter (**Supplementary Methods**) positioned as distally as possible in the intestine. Details of the placement procedure are described in the **Supplementary Methods**.

The experimental test day to study acute fermentation kinetics

After an overnight fast, subjects returned to the hospital for the test day. Before the experiment started, the location of the catheter was verified with fluoroscopy. When the position of the catheter was estimated to be in the distal ileum or proximal colon, the experimental procedures started. After taking baseline samples of breath, blood, and intestinal content (the latter when possible), the subjects consumed a NDC bolus (assumed $t=0$ min). The NDC bolus consisted of 5 gram chicory FOS (Fruitalose® OFP; Sensus), 5 gram GOS (Vivinal GOS, FrieslandCampina), and 5 gram of non-digestible marker polyethylene glycol 4000 (PEG 4000 gram/mol) (Dulcosoft, Sanofi-Aventis, Germany) in 200 mL tap water. GOS contained ≤ 10 bacteria colony-forming units (CFU)/gram mixture, and FOS contained ≤ 100 CFU/gram mixture. Subjects were not allowed to eat or drink during measurements, except for (tap) water. In the period the study took place, tap water in the hospital contained on average < 1 CFU/mL, and maximally 5 CFU/mL (Vitens Laboratory, Leeuwarden, the Netherlands). The NDC bolus contained maximally 1550 CFU, and the intra-intestinal infusion contained ≤ 15 CFU (measured as 16S rRNA gene copies). After NDC bolus consumption, ^{13}C -labeled SCFA were directly delivered into the intestinal lumen via the catheter delivery channel, at 145 minutes in study 1 and 125 minutes in study 2 respectively. The ^{13}C -SCFA infusion consisted of 0.96 M Na-[1- $^{13}\text{C}_1$]-acetate, 0.40 M Na-[1,2,3- $^{13}\text{C}_3$]-propionate, and 0.09 M Na-[1,2,3,4- $^{13}\text{C}_4$]-butyrate, all with an isotopic purity over 99% (IsoLife B.V., Wageningen, the Netherlands), in 10 mL ultrapure water (Merck Millipore, United States). After delivery, 100 mg non-digestible absorption marker TiO_2 as E-171 (BrandNewCake, Baktotaal, Goor, the Netherlands) in 10 mL (study 1) or 5 mL (study 2) of ultrapure water was delivered. Both ^{13}C -SCFA and TiO_2 solutions were delivered via the delivery channel of the naso-intestinal catheter. During the test day, blood, breath, and intestinal content were collected at multiple time points. The time points and frequency of sampling differed slightly between study 1 and study 2, as study 1 had 100 minutes longer test day (**Figure 1**). At the end of the test day, the exact location of the catheter was determined using 50 mL contrast liquid (Telebrix GASTRO, Guerbet, Aulnay-sous-bois, France, diluted 1:1 with water) and fluoroscopy. In study 2 subjects were asked to indicate the intensity of (dis)comfort caused by the study procedures by marking a 100-mm-long horizontal line, visual analog scales (VAS), that is labeled with 'no pain/discomfort' at the 0 mm end and 'a lot of pain/discomfort' at the 100 mm end.

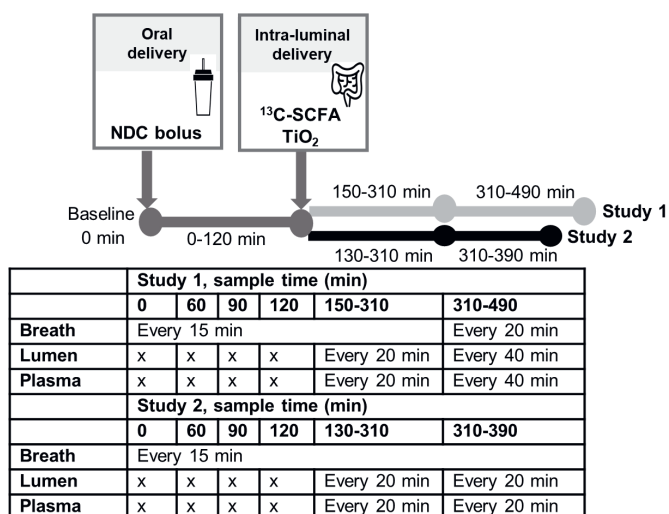


Figure 1. Schematic overview of the experimental test day.

Breath samples, intestinal luminal content, and blood were collected over time. Differences in the timeline between study 1 and study 2 are indicated in light grey and black, respectively. FOS, fructo-oligosaccharides; GOS, galacto-oligosaccharides; NDC, non-digestible carbohydrates; TiO_2 , titanium dioxide; SCFA, short-chain fatty acids.

Sample collection

Breath samples were collected in collection bags (QuinTron instrument company, Milwaukee, United States) that were closed with a stopcock. Luminal samples were collected in 5 mL tubes, homogenized, and divided into aliquots which were put on dry ice immediately, and at the end of the test day stored at -80°C . The time to take ~ 2.0 mL luminal sample through the aspiration channel was monitored per time point during the complete experimental test day. Blood samples (4.5 mL per time point) were collected from an indwelling venous cannula (IVC) in the left arm vena in lithium heparin tubes for SCFA and metabolite (^{13}C enrichment) analysis (25). In study 2, additionally, 4 mL blood per time point was collected in tubes coated with potassium EDTA and aprotinin, pre-filled with 44 μL DPP IV Inhibitor (Merck Millipore), and kept on ice, for analysis of gut hormones. All blood tubes were put on ice immediately after blood withdrawal, inverted 10 times, and centrifuged (10 min, $1200\times g$, 4°C). The plasma was collected and divided into aliquots. All aliquots of luminal and plasma samples were kept on dry ice during the experimental test day, and afterwards stored at -80°C .

Analysis of breath samples

H_2 and CH_4 parts per million (ppm) in the exhaled breath were analyzed in a BreathTracker DP (QuinTron), according to the manufacturer's instructions. The BreathTracker was calibrated with calibration gas with known composition (149 ppm

H₂, 74 ppm CH₄, 6.1% CO₂, QuinTron). To measure ¹³CO₂ enrichment in breath, samples were transferred (flushed in excess) from the collection bags to a 12 mL glass tubes with lid, and measured in a GC (Agilent Technologies, 7890A GC system), coupled to an IRMS (Thermo Scientific, Delta5Advantage) with helium as a carrier gas, as described (26). CO₂ was separated from nitrogen and oxygen on a Chrompack PLOT fused silica 25mx0.25 mm ID, coated with Poraplot Q (DF= 8 μm). Water was removed after column separation by Nafion tubing. The isotopologue spectra were recorded at m/z:44 and m/z:45 for ¹²CO₂ and ¹³CO₂, respectively and corrected for ¹⁷O.

Analysis of luminal content

Analysis of NDC in the luminal content

Luminal samples were analyzed for mono-, di-, and oligosaccharide profiles by high performance anion exchange chromatography (HPAEC) with pulsed amperometric detection (PAD), as described (27). 100 μL luminal content was centrifuged (10 min, 4°C, 15 000xg), and the supernatant was diluted (10-300 times). Identification of FOS and GOS isomers was based on commercial standards, and the elution profiles of the luminal content were compared with the elution profiles of FOS, Vivinal GOS, and its DP fractions, and to GOS and FOS profiles obtained in previous research (28, 29). Data were analyzed with Chromeleon 7.2 SR4 software.

Microbiota composition, predicted functionality and 16S rRNA gene copy numbers in the luminal content

50-250 μL of intestinal sample or 150 mg feces was used for the analysis of the microbiota composition, as described in (27), with minor changes. The obtained lysate (around 500 μL) from luminal samples after cell lysis was divided into two aliquots and used separately for DNA isolation, DNA of both aliquots was collected in the same elution tube within 30 μL nuclease-free water. The PCR amplification, purification, quantification, and pooling are described elsewhere (27). Microbiota composition was determined via sequencing of the variable V4 region of the 16S rRNA gene using Illumina HiSeq2500. Raw sequencing data were processed using NG-Tax 2.0 pipeline with default settings (30, 31). Taxonomy was assigned using the SILVA database (version 132). Microbial functions were predicted based on the 16S rRNA gene sequences using the phylogenetic investigation of communities by reconstruction of unobserved states algorithm (version PICRUSt2) with default settings but the minimum alignment was set to 60% (32). The total 16S rRNA gene copy numbers were determined by digital droplet PCR (ddPCR), using universal 16S rRNA gene primers (33) (**Supplementary Methods**).

Analysis of SCFA concentration and ¹³C enrichment in the luminal content

SCFA concentration and ¹³C-enrichment in luminal sample were analyzed as described

previously (27). Briefly, luminal samples were thawed and 100 μL were diluted in PBS and spiked with 100 μL of (0.5 mg/mL) 2-ethyl butyric acid as internal standard. After adding 20 μL of 20% 5-sulfosalicylic acid and 10 μL of HCl, samples were homogenized, extracted, and derivatized as previously described (27). Mass spectrometry analysis was performed by electron ionization. The mass isotopologue spectra of ($[M-57]^+$) fragment of the t-BDMS derivatives of acetate (m/z 117-1119, m_0 - m_2), propionate (m/z 131-134, m_0 - m_3) and butyrate (m/z 173-149, m_0 - m_4) were monitored.

Measurement of non-absorbable markers in the luminal content

Titanium dioxide (TiO_2) in the intestinal content was analyzed in 100 μL sample. The samples were dissolved in 1000 μL water, transferred to a digestion tube, and digested with 1 mL HF and 7 mL HNO_3 in a total volume of 50 mL water. These digested samples were analyzed by HR-ICPMS, according to (34). The limit of quantification was 0.05 mg Ti/kg of wet sample. PEG-4000 was quantified by ELISA using “rat5M-PABM-A anti-PEG” as coating, and “6.3-PABG-B biotin anti-PEG” as detection antibodies, respectively (IBMS Academia Sinica, Taiwan), according to manufacturer’s instructions.

Analysis of plasma samples

Short chain fatty acid quantification in plasma

To quantify SCFA concentrations in plasma, the samples were derivatized with 3-nitrophenylhydrazine hydrochloride (3NPH-HCl) and subsequently measured by LC-MS/MS as previously described (35). A short description is added in **Supplementary Methods**.

^{13}C enrichment and concentration of various metabolites in plasma

Glucose ^{13}C enrichment was measured by GC/MS using a penta-acetate derivative according to Van Dijk et al. (36). Free carnitine and acyl-carnitines were measured according to Derks et al. (37). All methods are described in **Supplementary Methods**. Organic and amino acids concentrations and ^{13}C enrichments and fatty acids ^{13}C enrichments were measured in the plasma samples obtained from both studies, as described in **Supplementary Methods**.

GLP-1 and PYY concentrations in plasma

Total GLP-1 and total PYY concentrations were measured in 50 μL of undiluted plasma, using the multiplex sandwich immunoassay system from MesoScale Discovery (Gaithersburg, MD) according to manufacturer’s instructions. The intra-assay CV of the total GLP-1 assay was 8.4%, the intra-assay CV of the total PYY assay was 9.1%.

Corrections and calculations

Normalization of the mass isotopologues distributions measured by GC-MS

All data measured by GC-MS was first corrected for the natural abundance of ^{13}C by multiple linear regression according to Lee et al. (38) as described in **Supplementary Methods** to obtain the excess fractional distribution of mass isotopologues.

Acetate, propionate, and butyrate contribution to glucose

The individual contributions of ^{13}C of acetate, propionate, and butyrate to the glucose enrichment, were calculated using known biochemical pathways, the stoichiometry of labeled glucose molecules per molecule of SCFA, and the amount delivered in the intestine, as described in **Supplementary Methods**.

Statistical analysis

Differences in baseline characteristics between groups were evaluated with the Kruskal Wallis test. Differences in the fecal microbiota composition between groups were evaluated with the non-parametric Mann-Whitney U test, followed by a false discovery rate correction for multiple comparisons. Per parameter, normality was tested by histograms, Q-Q-plots, and the Shapiro-Wilk test of normality. If not normally distributed, the variable was log transformed (base 10) to improve normality. A one-way repeated measures ANOVA, or mixed models when there were numerous missing values, was applied to check for changes over time during the experimental test day. For the microbiota analyses, the 16S rRNA gene counts were normalized to relative abundance. Bray–Curtis dissimilarity was calculated within each subject for the microbiota in the luminal content at each time point compared to the first sample that was collected on the test day. The alpha-diversity was calculated based on the amplicon sequence variants, using several diversity indices. Principle coordinate analysis based on weighted UniFrac was used to evaluate the overall microbiota variation at the amplicon sequence variant level (beta-diversity). To investigate changes in microbiota alpha-diversity indices or selected arcsin-square root transformed bacteria proportions over time, mixed models were used. In case of significant overall time effects, pairwise post-hoc comparisons were made. Statistical significance was accepted as $P < 0.05$. Statistical and microbiota analyses were performed in R version 4.0.3.

Results

Study logistics and subject characteristics

Two out of five subjects fully completed study 1 (no intervention), and six out of ten subjects (n=4 NDC group, n=2 placebo group) fully completed study 2 (**Supplementary**

Figure 2). Five subjects dropped out due to failure of proper catheter placement in the distal ileum or colon and two subjects dropped out due to adverse events during the study. More details on the individual studies, including study flow charts and drop-outs, can be found in the **Supplementary Results**. The baseline characteristics between studies and groups were similar (**Table 1**).

Table 1. Baseline characteristics and habitual daily intake of (macro)nutrients in healthy male subjects¹.

	Study 1: no intervention (n = 2)	Study 2: NDC group (n = 4)	Study 2: placebo group (n = 2)	P-value
Age, y	39.5 ± 18.5	26.0 ± 8.2	39.0 ± 28.3	0.939
BMI, kg/m ²	25.3 ± 0.8	22.0 ± 0.7	24.2 ± 5.4	0.363
Total kcal/day	2648.6 ± 79.1	2436.1 ± 235.3	3092.1 ± 616.5	0.205
Total carbohydrates, g/day ²	294.1 ± 35.4	239.8 ± 31.2	285.2 ± 50.0	0.205
Mono- and disaccharides, g/day	94.9 ± 19.1	83.7 ± 48.5	112.9 ± 25.9	0.472
Polysaccharides, g/day	199.2 ± 16.3	155.9 ± 17.5	172.2 ± 24.1	0.210
Fiber, g/day ³	36.5 ± 9.6	23.9 ± 2.2	32.4 ± 0.9	0.069
Total protein, g/day	101.9 ± 0.3	92.8 ± 19.1	112.7 ± 13.3	0.248
Total fat, g/day	99.2 ± 11.8	104.5 ± 20.4	141.0 ± 41.1	0.248
Alcohol, g/day	12.2 ± 2.1	15.8 ± 4.3	21.7 ± 0.7	0.097

¹Values are presented as group means ± SD. ²Total carbohydrates does not include dietary fiber, ³Included are high molecular weight fibers (e.g. cellulose, resistant starch, cereal β-glucan, guar gum, and certain xylans), insoluble fibers in water (e.g. cellulose, resistant starch, and certain xylans), fibers soluble in water and precipitated by 78% ethanol (e.g. cereal β-glucan, guar gum, and certain xylans). Excluded are low molecular weight fibers (e.g. fructan, GOS, polydextrose, and resistant maltodextrins), and non-resistant starch.

Although we aimed to sample from a uniform location in all subjects, namely the proximal colon as main NDC fermentation site, in practice this was not feasible due to placement difficulties and clogging of tube when sampling. The intestinal regions that were studied included the distal ileum (n=6), proximal colon (n=1), and transverse colon (n=1) (**Table 2**). Luminal sampling was only possible after NDC consumption, but was in some individuals still not possible at every time point.

As shown in Table 2, all measurements in the distal ileum were performed in subjects in study 1 without intervention (n=2) or in those who consumed NDC supplements for 7 days (n=4) in study 2, while the measurements in the colon were performed in subjects that consumed placebo supplements for 7 days (n=2) in study 2. The microbiota composition was distinct between sampling sites (i.e., distal ileum versus colon and feces), while no clusters, i.e. a more comparable intestinal microbiota, were revealed based on the dietary intervention groups (**Figure 2**). Also, the fecal microbiota and SCFA were not different between intervention groups (**Supplementary Table 1**). Since the main outcome, acute

NDC fermentation *in vivo*, strongly depends on the luminal microbiota composition at the sampling location, we decided to combine the data per sampling site.

Table 2. Intestinal regions studied in the participants.

Subject	Study and intervention	Catheter distance from the nose	Catheter tip location	Estimated distance from the ileo-cecal valve ¹	Number of collected aspirates	Sampling duration (minutes) ²
S1	1, None	240 cm	Distal ileum	15 cm	14	4.4 (3.6)
S2	1, None	230 cm	Distal ileum	25 cm	6	15.0 (6.0)
S3	2, Placebo	270 cm	Proximal colon	10 cm	5	8.0 (5.5)
S4	2, Placebo	300 cm	Transverse/ descending colon	-	4 [#]	5.0 (1.3) [#]
S5	2, NDC	270 cm	Distal ileum	<25 cm	9	3.0 (0.9)
S6	2, NDC	290 cm	Distal ileum	10 cm	5	5.0 (6.0)
S7	2, NDC	240 cm	Distal ileum	<50 cm	13	2.0 (3.5)
S8	2, NDC	275 cm	Distal ileum	10 cm	13	5.0 (2.0)

¹As calculated from the fluoroscopy pictures that were taken after the delivery of contrast liquid inside the intestine,

²the time required to take a 2-2.5 mL sample, in minutes as median and inter-quartile range [#]samples could only be collected after infusion of saline solution in the aspiration channel to dilute the aspirate.

Intra-intestinal non-digestible carbohydrates fermentation over time

To assess acute fermentation kinetics in the intestine, we investigated intestinal NDC degradation and NDC-induced SCFA production and interconversions over time. The constituents present in the NDC bolus (DP1-DP8) were detected in the distal ileum of all subjects starting 60-120 minutes after consumption (**Figure 3**). No changes in ratios of NDCs DP \geq 3 were found in the distal ileum over time when compared to those ingested via the NDC bolus. Only after 210-250 minutes, monosaccharides (DP1) were increased relative to first time points in the ileum of two subjects (Figure 3A, F), but the total amount of the NDCs was very low at these time points (Figure 3, black lines). The changes over time of total NDC peak area in the intestine followed that of the non-absorbable marker PEG-4000 (**Supplementary Figure 3**), suggesting removal from the sampling site via intestinal peristalsis rather than fermentation.

Luminal SCFA concentrations and ¹³C-SCFA enrichment were measured to determine bacterial SCFA production and interconversion induced by NDC fermentation (**Figure 4**). It is important to note that we only present the isotope data (Figure 4A-F) where samples after isotope delivery could be obtained, which was in 4 subjects where samples were collected in the distal ileum. First, we examined SCFA interconversion by measuring all different label patterns of acetate, propionate and butyrate.

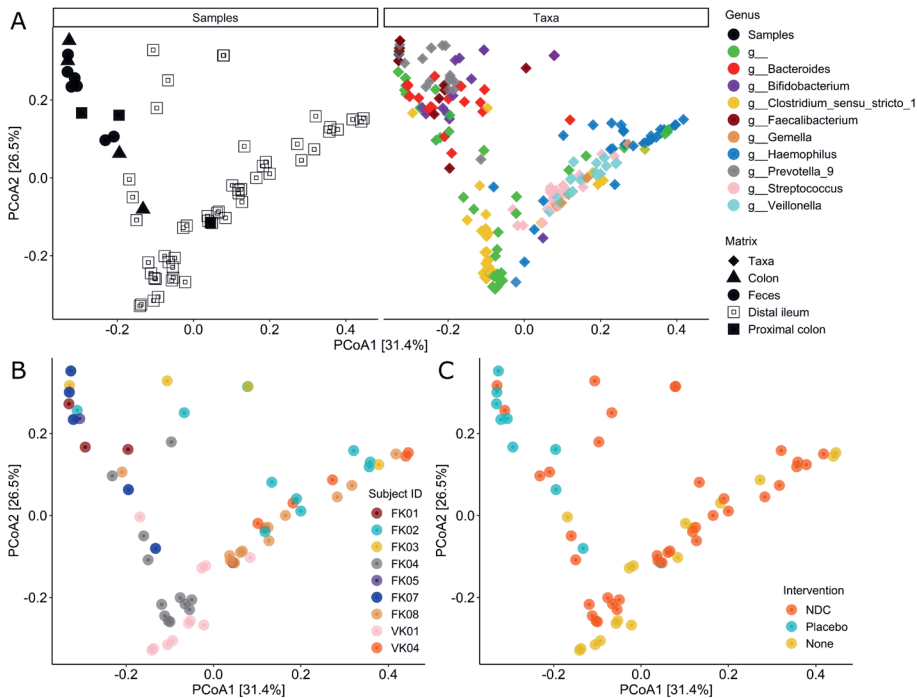


Figure 2. The overall microbiota variation between the samples in the dataset.

Principle coordinate analysis plots based on weighted UniFrac (beta-diversity) of (A) samples from the different matrixes (distal ileum, proximal colon, transverse colon, and faeces) in the left facet, and in the right facet the contributions of the top 10 bacteria genera shown on the same graphical space, (B) visualization of the microbiota variation between subjects, (C) visualization of the microbiota variation between the intervention groups. All luminal samples are shown, including multiple time points per subject.

Besides the mass isotopologues to be expected from the delivered SCFA (acetate M^{+1} , propionate M^{+3} , and butyrate M^{+4}) no other label patterns were found, suggesting no interconversion of SCFA by ileum microbiota (Figure 4A-F). The delivery of labeled SCFA resulted in a steep increase and subsequent decrease of the luminal concentration of ^{13}C -SCFA, indicating its appearance by infusion and its disappearance from the sampling location in the distal ileum (Figure 4A-C). The luminal kinetics of all three SCFA were similar, and their ratios in the luminal samples remained similar to those delivered (Figure 4A-C). The increase in ^{13}C -SCFA concentration was accompanied by an almost instantaneous increase of ^{13}C -SCFA enrichment of the delivered isotopologues (i.e., ^{13}C relative to total) reaching a plateau at nearly 100% of ^{13}C enrichment (Figure 4D-F). Moreover, the ^{13}C enrichment only decreased when its concentration approached pre-delivery level (Figure 4A-C) and there was no increase of SCFA from NDC fermentation (Figure 4G-I). This was in line with the lack of NDC degradation in the distal ileum. During the test day, from two subjects samples were obtained from the proximal colon and

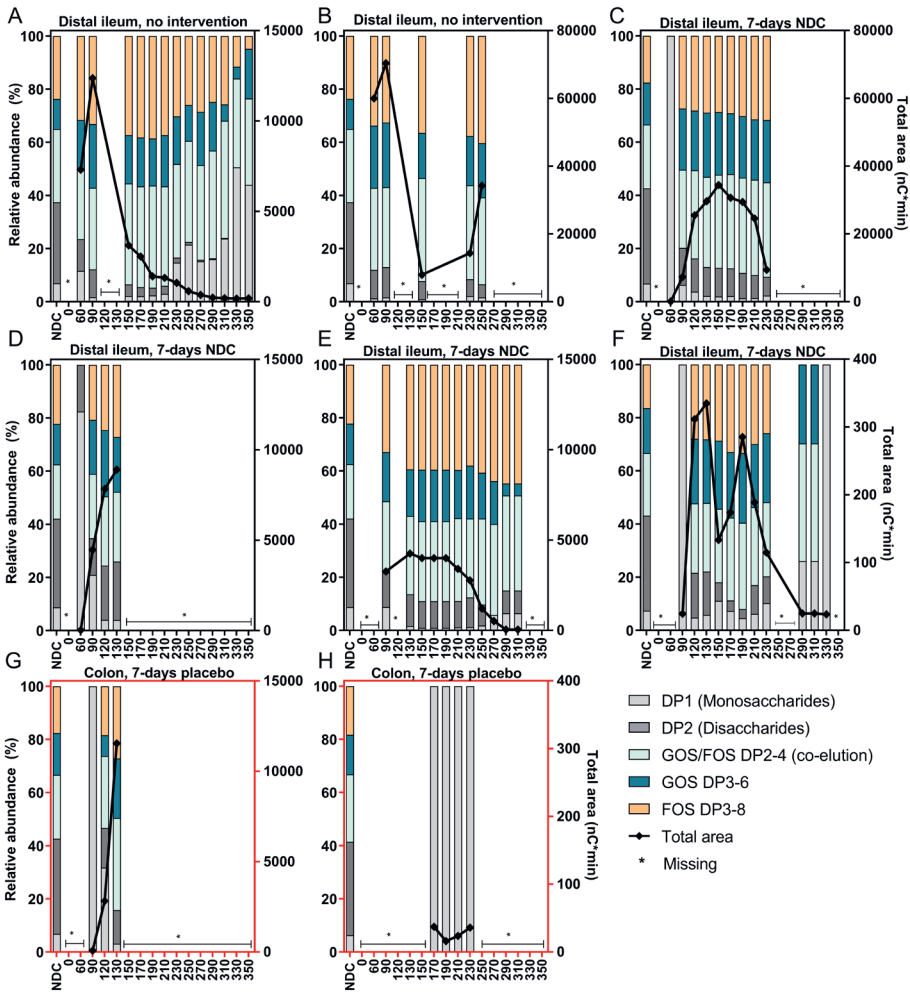


Figure 3. Non-digestible carbohydrates in the distal ileum (A-F) or colon (G, H) of eight healthy male subjects over time.

The relative abundances of each constituent of the NDC bolus are shown on the left y-axis. The black line represents the total area of all NDC constituents, indicated on the right y-axis. * For this time point, a sample could not be obtained due to sampling difficulties. DP, degree of polymerization; FOS, fructo-oligosaccharides; GOS, galacto-oligosaccharides.

the distal colon, but only prior to ^{13}C -SCFA delivery. In the proximal colon, non-labeled SCFA concentrations increased up to 30 mM acetate, 6 mM propionate, 6 mM butyrate after 120 minutes of NDC bolus consumption (Figure 4G-I). In the transverse colon, SCFA concentrations did not increase, likely due to dilution of the sample after saline delivery through the aspiration channel to decrease sampling clogging. Overall, NDC degradation and SCFA production by the distal ileum bacteria was minimal, and there was no bacterial SCFA cross-feeding during the time the isotopes remained in the sampling location.

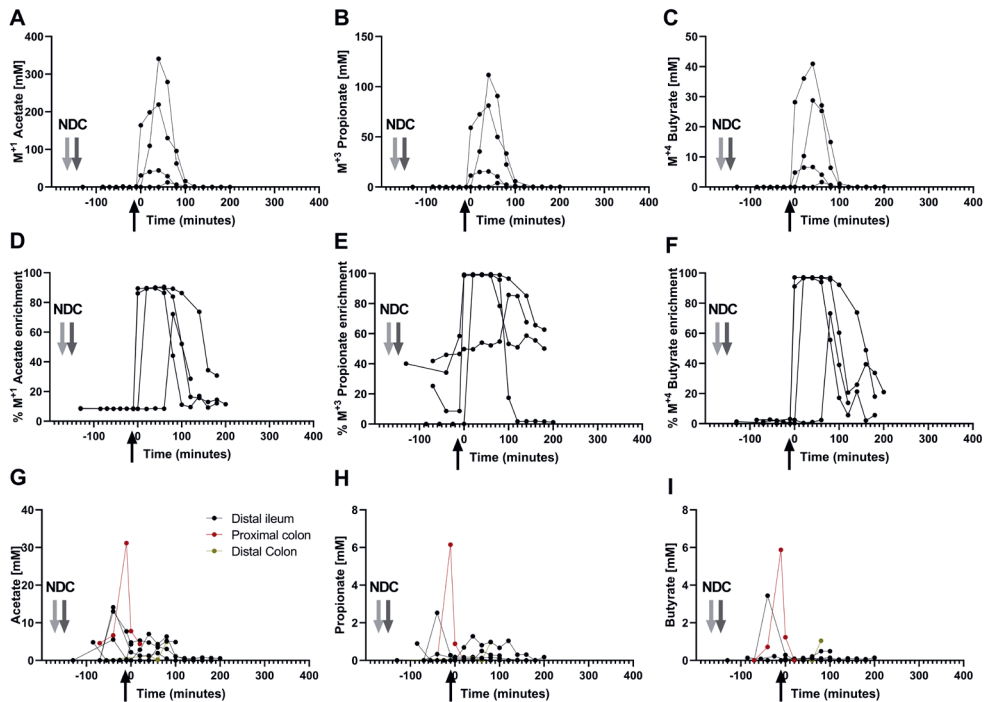


Figure 4. Luminal SCFA enrichments and concentrations in the intestinal samples of healthy male subjects.

^{13}C -SCFA concentrations (A-C) and enrichments (D-F) over time from the 4 subjects from whom luminal samples could be collected before and after isotope delivery (all these 4 subjects had the catheter tip located in the distal ileum). Non-labeled SCFA concentrations (G-I) from all subjects over time. The lines represent the individual subjects separately. The black arrow indicates the start of luminal isotope infusion (10 mL containing 10 mmol $[1\text{-}^{13}\text{C}]$ -acetate, 4 mmol $[1,2,3\text{-}^{13}\text{C}_3]$ -propionate and 1 mmol $[1,2,3,4\text{-}^{13}\text{C}_4]$ -butyrate) through the catheter. This is considered to be time 0 for all subjects to match both studies. The grey arrows indicate the drinking of the non-digestible carbohydrates (NDC) bolus in both studies (-150 min for study 1, light grey arrow; and -120 min for study 2, dark grey arrow).

Microbial dynamics in the intestine over time

Although no fermentation at the small intestinal sampling location was detected by our experimental setup, we studied whether the consumption of NDCs affected the intestinal microbiota during the test day. All samples passed the quality control for microbiota analyses (**Supplementary Figure 4**). On the individual level, the relative microbiota composition in the intestinal samples changed rapidly over time, as indicated by the Bray-Curtis dissimilarity values that increased during the day when compared to the first collected sample (**Figure 5**, red line). Even though the relative microbiota composition changed, the total bacteria numbers, signified by analyses of 16S rRNA gene copy numbers, did not increase over time. Selected and detected bacteria known to be stimulated by the provided FOS or GOS, namely *Bifidobacterium*, *Lactobacillus*, *Streptococcus*, and *Bacteroides*, did not significantly increase over time (**Supplementary Figure 5**).

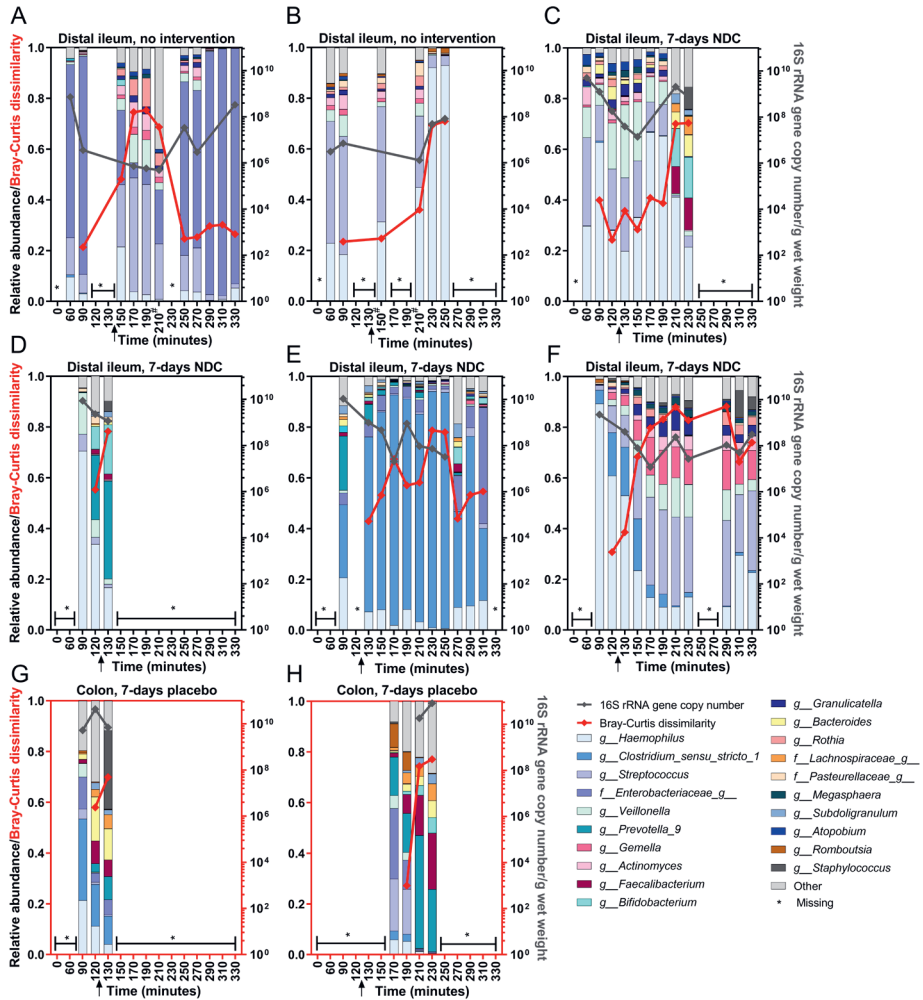


Figure 5. The microbiota, the microbiota dissimilarity, and total 16S rRNA gene copy number in distal ileum (A-F) or colon (G, H) of healthy male subjects over time after consumption of the NDC bolus.

The top 20 bacteria on genus level are shown. The arrow shows the moment of intra-intestinal infusion (¹³C-SCFA/TiO₂) close to the sampling location. The right y-axis indicates the total 16S rRNA gene copy number which is depicted by the grey line (missing values were due to low availability of DNA). The Bray-Curtis dissimilarity values are visualized by the red line on the left y-axis, which show the dissimilarity of the microbiota at each time point compared to the microbiota in the first collected sample. Bray-Curtis dissimilarity values range between 0 and 1, when closer to 1 means the two samples do not share any bacteria. *For this time point, a sample could not be obtained due to sampling difficulties. #Samples contained less than 10.000 sequencing reads.

To evaluate whether the lack of fermentation in the distal ileum was the result of the lack of fermentation capacity of the ileum microbiota, we compared the microbial pathways related to fermentation between the ileum and the feces (**Table 3**), since it has been

shown previously that fecal microbiota more efficiently ferments FOS and GOS *in vitro*. The specific microbial pathways were derived from the total predicted genomes, predicted based on the 16S rRNA gene sequencing outcomes. Indeed, three microbial fermentation pathways were about twofold lower in relative abundance in the ileum compared to the colon and/or feces ($p < 0.05$).

Table 3. The relative abundances (%) of selected microbial fermentation pathways in the predicted microbial genome of luminal content or feces of healthy male subjects¹.

Microbial pathway	Pathway number	Relative abundance distal ileum ($n = 6$ subjects, 52 samples)	Relative abundance colonic content ($n = 2$ subjects, 7 samples)	Relative abundance feces ($n = 7$ subjects)	P-value ²
Pyruvate fermentation to acetate and lactate II	PWY-5100	0.790±0.302	0.761±0.082	0.771±0.035	0.857
Pyruvate fermentation to propanoate I / succinate-propionate fermentation pathway	P108-PWY	0.134±0.102	0.269±0.089	0.248±0.132	0.002 ^a
Acetyl-CoA fermentation to butanoate III/butyrate II	PWY-5676	0.082±0.063	0.175±0.060	0.164±0.087	0.000 ^a
Pyruvate fermentation to butanoate/butyrate	CENTFERM-PWY	0.071±0.063	0.153±0.060	0.081±0.057	0.014 ^b
Succinate fermentation to butanoate/butyrate	PWY-5677	0.015±0.015	0.010±0.009	0.009±0.008	0.690
Bifidobacterium shunt / glucose fermentation to lactate	P124-PWY	0.111±0.084	0.082±0.033	0.243±0.176	0.086

¹Data are presented as mean relative abundance (%) ± SD. ²The relative abundances in the ileum were compared to those in the feces or colon using an independent samples Kruskal-Wallis test. Because of the high variability in microbiota composition during the day, all samples collected *in vivo* are treated as an independent observation. ^aIleum samples were significantly different from both colon and feces samples, ^bileum samples were significantly different from colon samples.

Systemic biomarkers for fiber fermentation: breath gases and blood SCFA

To determine if fermentation occurred beyond the sampling site, systemically available markers for NDC fermentation, namely H₂ and CH₄ in breath, and SCFA in blood were evaluated after NDC consumption. Breath hydrogen was significantly increased between 50 and 245 minutes after consumption of FOS and GOS when compared to baseline (**Figure 6A**), with a peak mean concentration (± SD) of 39.6±28.1 ppm at 185 minutes. The start of fermentation, as indicated by increased breath hydrogen, was highly variable between subjects (35-170 minutes), while breath CH₄ did not significantly increase over

time after NDC consumption. The measurement of SCFA in the blood (Figure 6B) over time showed that acetate increased over time ($p=0.003$, baseline: $56\pm 39\ \mu\text{M}$, 330 min: $120\pm 51\ \mu\text{M}$), while propionate and butyrate did not significantly change compared to baseline (baseline: $1.96\pm 1.28\ \mu\text{M}$ and $5.03\pm 1.20\ \mu\text{M}$, respectively). Since we did not measure fermentation in the distal ileum *in vivo*, these increased markers likely point to fermentation of FOS and GOS in the colon.

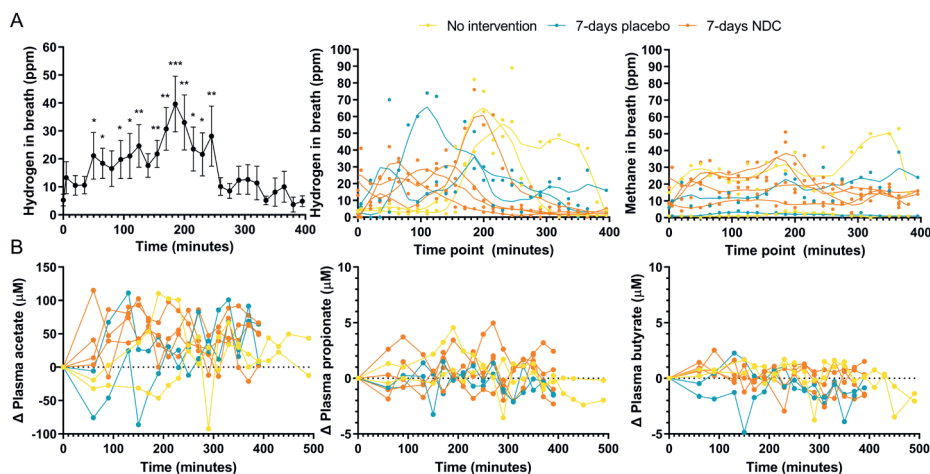


Figure 6. Biomarkers of NDC fermentation.

(A) Breath concentrations of methane and hydrogen and (B) the changes of SCFA in the blood of healthy male subjects after consumption of the NDC bolus with 10 grams FOS and GOS. Data is represented as mean \pm SD, $n = 8$ subjects in study 1 and study 2 or as the individual responses. LOWESS (Locally Weighted Scatterplot Smoothing) curves plot was applied to the breath hydrogen and methane to show the general trends over time, with 10 data points in the smoothing window. Significance is shown as * = $P < 0.05$, ** = $P < 0.01$, *** = $P < 0.001$ compared to baseline. NDC, non-digestible carbohydrates.

The role of SCFA in host metabolism

SCFA can function locally in their production site as signaling molecules by promoting the release of satiety hormones. Before and over time after consumption of the NDC bolus, the total PYY concentrations ($p=0.92$) and the total GLP-1 ($p=0.37$) concentrations did not significantly change over time (**Supplementary Figure 6**). To study SCFA metabolism in the human body, we measured the label incorporation from the delivered ^{13}C -SCFA into plasma glucose, organic acids, amino acids, acyl-carnitines, and fatty acids and for whole body metabolism, into breath CO_2 . Label incorporation in plasma glucose rapidly appeared after isotope infusion with $M^{+2} > M^{+1} > M^{+3}$ (**Supplementary Figure 7A**). The different isotopologue distributions were first calculated back to the SCFA source (**Supplementary Methods**). All three SCFA transferred ^{13}C to glucose, with butyrate being the most efficient with on average 6.1% of

glucose labeled (Figure 7A-C). Glucose concentrations remained constant over time for most of the subjects (Supplementary Figure 7B). As a proxy of fatty-acid synthesis, the different enrichments patterns in the different acyl-carnitines were measured in plasma. The only enrichment found was M^{+3} in propionyl-carnitine. M^{+3} propionyl-carnitine reaching 15-20% of propionyl-carnitine labeled (Figure 7D). The most likely source of M^{+3} propionyl-carnitine enrichment is $[1,2,3-^{13}C_3]$ -propionate that can be bound to carnitine and released into the circulation. The organic acids measurement showed an increase in citrate enrichment, mostly as M^{+1} and M^{+2} coming from acetate and butyrate, respectively (Supplementary Figure 7C). After normalizing by source and delivered amounts, butyrate was the most efficient contributor to citrate enrichment (Figure 7E-

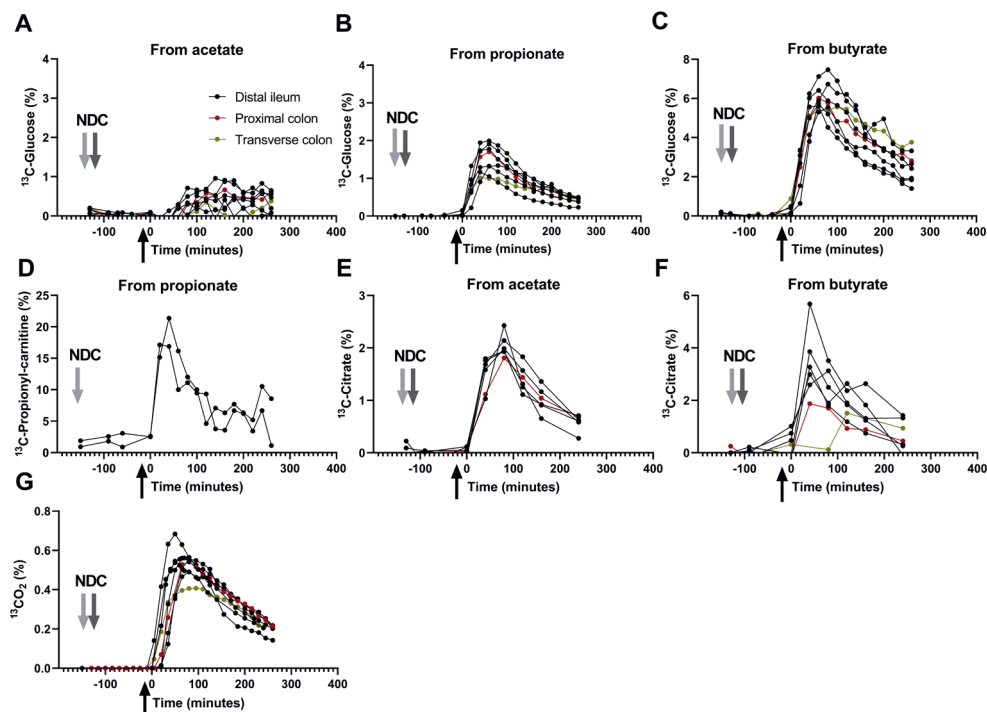


Figure 7. Assimilation of ^{13}C -SCFA into glucose and acyl-carnitines in blood and its oxidation to $^{13}CO_2$ in breath.

(A-C) Glucose enrichment from labeled acetate, propionate, and butyrate delivered in the distal ileum, proximal colon or distal colon. (D) ^{13}C -propionyl-carnitine (M^{+3}) enrichment from labeled propionate delivered in the distal ileum, proximal colon, or distal colon, and (E) ^{13}C incorporation into CO_2 , over time from all three ^{13}C -SCFA delivered in the distal ileum, proximal colon, or distal colon. The black arrow indicates luminal isotope infusion through the catheter. This is considered to be time 0 for all subjects to match both studies. The grey arrows indicate the consumption of the non-digestible carbohydrates (NDC) bolus in both studies (-150 min for study 1, light grey arrow, and -120 min for study 2, dark grey arrow). Data is represented as individual subjects, $n=6$ subjects for distal ileum, $n=1$ for proximal colon, and $n=1$ for distal colon. Acyl-carnitines (D) show the individual patterns of only $n=2$ subjects in study 1, the $n=6$ subjects in study 2 are to be analysed.

F), contributing on average 3.5% to labeled citrate. We did not find any enrichment in plasma amino acids and fatty acids. To estimate whole-body SCFA metabolism, ^{13}C label incorporation into CO_2 generated from ^{13}C -substrates was measured in exhaled breath after isotope infusion. CO_2 immediately incorporated the label (Figure 7E) and $^{13}\text{C}\text{-CO}_2$ slowly decreased over time (Figure 7D). This ^{13}CO enrichment curve initially represents the direct oxidation of all three luminal SCFA (since the specific source SCFA cannot be identified in this case) and at the later time points the oxidation of the secondary metabolites derived from the luminal SCFA as substrates, such as glucose. Together, these observations show that delivered SCFA were extensively taken up and metabolized by the host.

Discussion

We used for the first time the novel approach of naso-intestinal catheters in two independent trials, in an effort to monitor carbohydrate fermentation, SCFA production and absorption inside the human intestinal lumen, as well as the direct impact of FOS:GOS on the luminal microbiota. Moreover, the fate of SCFA as substrates for host metabolism was assessed using a stable isotope approach. Biomarkers of fermentation, namely breath hydrogen and plasma SCFAs increased upon consumption of FOS:GOS, indicating fermentation, but no changes in luminal NDC breakdown profiles were found. Moreover, SCFA production was minimal and there was no interconversion of SCFA in the distal ileum. The relative microbiota abundances in the intestine changed dynamically during the test day. SCFA were rapidly metabolized by the host as shown by $^{13}\text{CO}_2$ enrichment, and incorporation of ^{13}C in various host metabolites. Independently of SCFA delivery location through the intestine, assimilation of SCFA was entirely comparable among all subjects, suggesting complete absorption by the host.

Evaluation of the study methodology

Due to the high number of drop-outs due to catheter placement in the NDC intervention group in study 2, we were not able to detect study an effect of the 7-day FOS:GOS intervention on the acute fermentation kinetics. In most subjects, the catheter was placed in the distal ileum, and as expected (8, 39), the distal ileum microbiota composition and predicted functionality were distinct from those in the colon. Standardization of the sampling site in the intestine amongst subjects is therefore crucial for interpretation and comparison of the study outcomes between people, but standardizing the catheter position was challenging. We expect that a longer progression period in combination with regular checks using fluoroscopy and contrast liquid will improve positioning and standardizing of the catheter location in the proximal colon. We only used contrast liquid at the end of the test day, because it could affect some of the outcome measurements.

Sampling in the fasted state (both ileum and colon) and in the colon through the 1.9 mm-aspiration channel in the catheter was not feasible. The intestinal contents were obtained from a localized area of the intestine (aspiration holes within 10 cm catheter), providing local information on NDC fermentation and SCFA kinetics. To estimate the volume of the sampling location, we relied on the measurements of the dilution of the delivered TiO_2 . However, this non-absorbable marker was sensitive to the luminal matrix, precipitating and forming a colloidal, nonuniform intestinal liquid. Overall, the use of the naso-intestinal catheter had disadvantages, but at the moment it is one of the few available sampling tools to study the intestinal lumen in humans. Nevertheless, we have provided novel data about the kinetics of NDCs and the fate of SCFAs in humans as well as technical challenges to be considered when conducting *in vivo* studies in the human intestine.

Luminal NDC breakdown, SCFA production and inter-conversion

Chicory FOS and GOS are prebiotics, and both are well fermentable by fecal bacteria *in vitro* (40). Moreover, small intestinal bacteria from ileostomy subjects *in vitro* before 5 hours of incubation, namely 29-89% hydrolysis of FOS, 31-82% hydrolysis of GOS [66]. Moreover, human ileum mucosa bacteria have hydrolytic activities towards FOS and GOS *in vitro* [67]. To the best of our knowledge, however, we are the first to study the behavior of a mixture of both in humans. The carbohydrate profiles of the higher DP constituents in the distal ileum or proximal colon over time were comparable to those in the NDC bolus. This indicates no or only minor breakdown of NDCs in the ileum, in agreement with two earlier trials using FOS in ileostomy or healthy subjects (41, 42). For GOS, no other *in vivo* studies were performed previously. We used an isotope approach to estimate SCFA production. We observed that the enrichment of the ^{13}C -SCFA fraction remained close to 100%, which suggested that there was negligible production of unlabeled SCFA from fermentation of FOS and GOS over time inside the distal ileum. This result was in line with the absence of NDC breakdown in the location. While others reported high concentrations of SCFA in ileostomy effluent (41, 43), we measured maximally 8 mmol/L SCFAs in the ileum, which was in line with previous data on sudden death humans victims that measured only 13 ± 6 mmol/kg SCFAs in the terminal ileum, but 10-fold higher concentrations in the colon (44). In both mice (23) and humans (20) interconversion of SCFA in the cecum was mainly from acetate to butyrate. In humans, this was previously studied indirectly by measuring labeled-SCFA in blood after intestinal delivery of other individual SCFA (20). If SCFA would have been interconverted by bacterial cross-feeding, we should have seen other SCFA isotopologues than we had administered. However, no changes in SCFA isotopologues were observed, indicating that no bacterial interconversion took place in the ileum. We hypothesize that the SCFAs are rapidly absorbed or moved distally from the ileum, leaving hardly a possibility for interconversion.

Although previous longer-term intervention studies suggested a role for FOS (45), GOS (46, 47) or propionate (21) in increasing plasma gut hormones GLP-1 and PYY, we did not find significant postprandial effects on these hormones during the test day. Overall, we showed that all subjects increased H_2 in breath and non-labeled plasma acetate upon NDC consumption, but we did not find NDC fermentation or SCFA production and interconversion in the distal ileum. Therefore, the breath hydrogen increase shown here indicated most likely colonic NDC fermentation. We hypothesize that the short microbial exposure to NDC in this location due to the rapid transit time in the small intestine (48) does not allow for this fermentation process to take place. This can be considered an advantage, since the colon is prepared for microbial fermentation of NDC to SCFAs and gasses, because of the larger diameter and its capacity for distension with gas, in contrast to the small intestine where fermentation may lead to discomfort (49).

Dynamic changes in microbiota composition

In a review (50) it was suggested that the small intestine microbiota rapidly responds to changes in the luminal environment, also demonstrated in ileostomy effluent microbiota that fluctuated from the morning to the afternoon on the same day (43, 51). In our study, dynamic changes of the relative microbiota composition *in vivo* were found during the day. Characterizing the luminal microbiota over several hours *in vivo* was until now relatively unexplored. Two other clinical trials (using intestinal catheters) also show rapid fluctuations in the duodenum (52) or duodenal, jejunal, and proximal ileal microbiota (39) on the same day after ingestion of medication or a synbiotic, respectively. FOS and GOS are known to influence the fecal microbiota, as shown in human intervention trials where supplements were consumed for a longer period (i.e., weeks) (3), or in *in vitro* models where bacteria were in contact with the substrates for up to 24-48 hours (40, 53). We are the first to measure several bacteria known to be stimulated by NDCs (3) *in vivo* during the day, namely *Bifidobacterium*, *Lactobacillus*, *Bacteroides* and *Streptococcus*, that did not significantly fluctuate over time. The lack of significance could be the result of the short contact period between microbiota and NDCs due to the rapid transit time. Since there was no fermentation at the sampling location, nor increased FOS or GOS bacterial targets or total bacteria numbers, we hypothesize that other factors, unrelated to the studied NDCs, play a role in explaining the changes in relative microbiota composition during the day.

The effects of the non-absorbable markers PEG-4000 (54, 55) and TiO_2 (56-61) on the microbiota is expected to be minor. Possibly at some time points we sampled more mucus, resulting in a higher fraction of mucus-related bacteria such as *Haemophilus*. Flushing infusions, as we also did during the ^{13}C -SCFA delivery, through the catheter close to the sampling site could have impacted the relative microbiota profiles as shown previously while flushing saline through an ileal catheter (62). On the other hand, the

transit of bacteria in the small intestine throughout one day can also be considered as a physiological aspect. Others have shown that bacteria can also grow and survive in the small intestine (41), quickly utilizing small dietary compounds such as sugars (43), but the rapid bacteria fluctuations in this study are unlikely caused by bacteria doubling, given the known doubling times of minimally ~25 min, but often one hour or longer (*Bifidobacterium* and *Lactobacillus*) (63-65). Moreover, the total bacteria numbers did not increase. It is therefore more likely that most of the dynamic changes are caused by the bacterial transit throughout the GI-tract via constantly swallowing (viable or non-viable) oral and stomach bacteria (66, 67). Using 16S rRNA gene sequencing we cannot distinguish between the viable and non-viable bacteria. We hypothesize that fast transit of intestinal content rather than the studied NDCs, play a role in explaining the changes in relative microbiota composition during the day. A reference group that did not consume NDCs was not included in our acute feeding study, making it difficult to conclude about the effects of potential bacteria passage as a consequence of transit time versus the effect of the NDC bolus on the microbiota *in vivo*. The link between rapid fluctuations in small intestine and effects on digestive processes remains to be uncovered and our findings demonstrate the relevance of sampling over time to track acute responses of the microbial community towards interventions.

Host metabolism of luminal SCFA

To understand the mechanism by which SCFA regulate host metabolism, we studied their fate by monitoring the incorporation of ^{13}C -label from the delivered SCFA into different metabolites from carbohydrates (glucose, organic acids), amino acids and lipids (fatty acids, acyl-carnitines) metabolism. After isotope delivery, the label from ^{13}C -SCFA was readily incorporated into $^{13}\text{CO}_2$ in breath, and blood metabolites. Previously it has been estimated in humans that almost 95% of the produced SCFAs were rapidly absorbed (68). The delivered TiO_2 was also intended to be used as a marker to differentiate between the decrease of the infused isotopes by excretion or absorption. Even though absorption is different through the complete length of the intestine (69), in our study, independent of the delivery location, absorption happened rapidly likely at the delivery site (distal ileum, proximal colon, or distal colon). We conclude this from the fast appearance of label in other metabolites after ^{13}C -SCFA delivery and the very similar profiles of incorporation among subjects, irrespective of the delivery location. ^{13}C label from all three SCFA were incorporated into glucose. Gluconeogenesis starts at the conversion of oxaloacetate in the TCA cycle into phospho-*enol*-pyruvate. Acetate and butyrate enter the TCA cycle as acetyl-CoA. Both acetate and butyrate transfer the label into glucose via oxaloacetate but do not contribute to net carbons (70) since two carbon atoms are lost as CO_2 during the conversion of acetyl-CoA to succinate, precursor of oxaloacetate. Our results showed that the most efficient label transfer to glucose comes from butyrate, which is in line with previous results in mice (18). Moreover,

label incorporation from acetate to glucose suggests that acetate follows a different metabolic pathway than butyrate, even though both enter the TCA cycle as acetyl-CoA. Acetate can be activated in the cytosol and further metabolized before entering the mitochondria to be oxidized in the TCA cycle (71), whereas butyrate directly enters the mitochondria to be oxidized to two acetyl-CoA in a single round of β -oxidation that can immediately enter the TCA cycle (72). Acetate had the lowest contribution to glucose enrichment, which may be due to the high dilution by endogenous acetate production. For instance, in mice, ^{13}C -acetate is diluted in blood nine times compared to cecum (23). Propionate is the only SCFA that contributes to net glucose synthesis and is a known contributor to gluconeogenesis in ruminants entering the TCA cycle as succinyl-CoA (73). Boets et al. (20) also described propionate as the main contributor to glucose synthesis. Glucose enrichment from propionate could have taken place in the liver or, as recently described in rats, from intestinal gluconeogenesis (74). Glucose from intestinal gluconeogenesis can signal through the peri-portal afferent neural system to the brain promoting metabolic benefits in energy homeostasis, such as decreased body weight and better glucose control, including a decreased hepatic glucose production (74). This could explain the link between fermentable NDCs and health improvement. Nevertheless, in healthy volunteers it is not feasible to collect portal blood to differentiate between intestinal and hepatic propionate metabolism.

Organic acids enrichments analysis showed label incorporation from acetate and butyrate only in citrate. No label incorporation was detected from propionate into any of the organic acids. Butyrate, in line with the results on glucose enrichment, was the main contributor to citrate enrichment, since the label from butyrate is transferred to citrate as a fully labeled acetate in the TCA cycle. Untargeted amino acids analysis showed no incorporation of label, suggesting that the delivered amount of ^{13}C -SCFA was either too low or not involved in their metabolism under fasting conditions. Moreover, we did not find incorporation of label in the most abundant plasma fatty acids, namely palmitic acid (C16:0), palmitoleic acid (C16:1), stearic acid (C18:0) and oleic acid (C18:1). It has been reported that 15% of the colonic-delivered acetate ended up in palmitic acid under standardized feeding conditions in humans (20), which corresponded to minimal newly synthesized fatty acids. Our even lower incorporation in fatty acids compared to Boets et al. (20) could be due to the fasted state of the volunteers during the test day, since it is known that fasting stimulates fatty-acid oxidation rather than synthesis. Our studies, in combination with previous findings (20, 75-77), show that it is unlikely that acetate produced by microbes from fermentable fiber will lead to increased blood cholesterol and fatty acid levels. In the present study, we measured carnitines as an estimate for fatty acid oxidation. The only acyl-carnitine enrichment in blood was M^{+3} propionyl-carnitine, coming from fully labeled propionate. We did not detect M^{+2} acetyl-carnitine or M^{+4} butyryl-carnitine, which can be explained by rapid

mitochondrial conversion of butyrate into acetyl-CoA that can enter the TCA cycle as described above. The rapid increase of the percentage of labeled CO₂ in breath comes from the metabolism of all three SCFA at the same time and can be explained by a direct oxidation of SCFA and a subsequent oxidation of secondary metabolites, such as glucose. This rapid label incorporation could have been potentiated by the fasted state of the volunteers. In conclusion, SCFA are rapidly absorbed and metabolized by the host, independent of intestinal delivery location.

Concluding remarks

We aimed to study acute fermentation kinetics GOS and chicory FOS in the (small) intestine in humans using a naso-intestinal catheter. We are the first to show that no NDC breakdown, and subsequent SCFA production or bacterial cross-feeding occurred in the distal ileum of healthy humans. Dynamic changes in the relative microbiota composition during the day were observed. SCFA were rapidly taken up and metabolized by the host independent of the location delivery, which could explain the lack of detecting bacterial SCFA conversions. Future studies should focus on colonic NDC fermentation for a better understanding of how NDC can influence host health to improve dietary intervention.

Acknowledgements

We greatly thank the volunteers that participated in this study. We thank Maaïke Witjes-Kroon (Hospital Gelderse Vallei, the Netherlands) for the excellent medical assistance during the studies. Claire van der Aa, Ying-Bei Lin, Lisanne Vintcent, Jasmijn Mencke, Tamar Ravestein and Christoff Odendaal are greatly acknowledged for their outstanding practical support during the human trials. Moreover, Roos Versteegen and Tamar Ravenstein are acknowledged for their help with the ddPCR analyses. We thank FrieslandCampina, Sensus B.V., and Cooperatie AVEBE U.A. for providing the supplements, and all the consortium partners involved for the critical feedback during the development of the project. This research was performed in the public-private partnership 'CarboKinetics' coordinated by the Carbohydrate Competence Center (CCC, www.cccresearch.nl). CarboKinetics is financed by participating industrial partners Agrifirm Innovation Center B.V., Cooperatie AVEBE U.A., DSM Food Specialties B.V., FrieslandCampina Nederland B.V., Nutrition Sciences N.V., VanDrie Holding N.V. and Sensus B.V., and allowances of The Netherlands Organisation for Scientific Research (NWO). The funders had no role in data collection and analysis, or preparation of the manuscript. Bernard Evers was funded by University Medical Centre

Groningen and a Dutch Cancer Society grant awarded to Mathilde Jalving (KWF 10913/2017-1). Fentaw Abegraz was funded by the Netherlands Organization for Scientific Research and DSM Nutritional products in the framework of the Complexity programme (grant 645.001.001/ 3501).

References

1. Zhu T, Goodarzi MO. Metabolites linking the gut microbiome with risk for type 2 diabetes. *Curr Nutr Rep.* 2020.
2. Anderson JW, Randles KM, Kendall CW, Jenkins DJ. Carbohydrate and fiber recommendations for individuals with diabetes: A quantitative assessment and meta-analysis of the evidence. *J Am Coll Nutr.* 2004;23(1):5-17.
3. Swanson KS, de Vos WM, Martens EC, Gilbert JA, Menon RS, Soto-Vaca A, et al. Effect of fructans, prebiotics and fibres on the human gut microbiome assessed by 16S rRNA-based approaches: A review. *Benef Microbes.* 2020;11(2):101-29.
4. Flint HJ, Scott KP, Duncan SH, Louis P, Forano E. Microbial degradation of complex carbohydrates in the gut. *Gut Microbes.* 2012;3(4):289-306.
5. Flint HJ, Duncan SH, Scott KP, Louis P. Interactions and competition within the microbial community of the human colon: Links between diet and health. *Environ Microbiol.* 2007;9(5):1101-11.
6. den Besten G, van Eunen K, Groen AK, Venema K, Reijngoud DJ, Bakker BM. The role of short-chain fatty acids in the interplay between diet, gut microbiota, and host energy metabolism. *J Lipid Res.* 2013;54(9):2325-40.
7. Tan J, McKenzie C, Potamitis M, Thorburn AN, Mackay CR, Macia L. The role of short-chain fatty acids in health and disease. *Adv Immunol.* 2014;121:91-119.
8. Vasapolli R, Schütte K, Schulz C, Vital M, Schomburg D, Pieper DH, et al. Analysis of transcriptionally active bacteria throughout the gastrointestinal tract of healthy individuals. *Gastroenterology.* 2019;157(4):1081-92.e3.
9. Zmora N, Zilberman-Schapira G, Suez J, Mor U, Dori-Bachash M, Bashiardes S, et al. Personalized gut mucosal colonization resistance to empiric probiotics is associated with unique host and microbiome features. *Cell.* 2018;174(6):1388-405.e21.
10. Wong JM, de Souza R, Kendall CW, Emam A, Jenkins DJ. Colonic health: Fermentation and short chain fatty acids. *J Clin Gastroenterol.* 2006;40(3):235-43.
11. Minekus M, Smeets-Peters M, Bernalier A, Marol-Bonin S, Havenaar R, Marteau P, et al. A computer-controlled system to simulate conditions of the large intestine with peristaltic mixing, water absorption and absorption of fermentation products. *Appl Microbiol Biotechnol.* 1999;53(1):108-14.
12. Blaak E, Canfora E, Theis S, Frost G, Groen A, Mithieux G, et al. Short chain fatty acids in human gut and metabolic health. *Beneficial microbes.* 2020;11(5):411-55.
13. Deroover L, Verspreet J, Luybaerts A, Vandermeulen G, Courtin CM, Verbeke K. Wheat bran does not affect postprandial plasma short-chain fatty acids from (13)C-inulin fermentation in healthy subjects. *Nutrients.* 2017;9(1).
14. Lund EK, Johnson IT. Fermentable carbohydrate reaching the colon after ingestion of oats in humans. *J Nutr.* 1991;121(3):311-7.
15. Boll EV, Ekstrom LM, Courtin CM, Delcour JA, Nilsson AC, Bjorck IM, et al. Effects of wheat bran extract rich in arabinoxylan oligosaccharides and resistant starch on overnight glucose tolerance and markers of gut fermentation in healthy young adults. *Eur J Nutr.* 2016;55(4):1661-70.
16. Ibrugger S, Vignas LK, Blennow A, Skuffic D, Raben A, Lauritzen L, et al. Second meal effect on appetite and fermentation of wholegrain rye foods. *Appetite.* 2014;80:248-56.
17. Fernandes J, Vogt J, Wolever TM. Inulin increases short-term markers for colonic fermentation similarly in healthy and hyperinsulinaemic humans. *Eur J Clin Nutr.* 2011;65(12):1279-86.
18. den Besten G, Havinga R, Bleeker A, Rao S, Gerding A, van Eunen K, et al. The short-chain fatty acid uptake fluxes by mice on a guar gum supplemented diet associate with amelioration of major biomarkers of the metabolic syndrome. *PLoS One.* 2014;9(9):e107392-e.

19. Boets E, Deroover L, Houben E, Vermeulen K, Gomand SV, Delcour JA, et al. Quantification of in vivo colonic short chain fatty acid production from inulin. *Nutrients*. 2015;7(11):8916-29.
20. Boets E, Gomand SV, Deroover L, Preston T, Vermeulen K, De Preter V, et al. Systemic availability and metabolism of colonic-derived short-chain fatty acids in healthy subjects: A stable isotope study. *J Physiol*. 2017;595(2):541-55.
21. Chambers ES, Viardot A, Psichas A, Morrison DJ, Murphy KG, Zac-Varghese SE, et al. Effects of targeted delivery of propionate to the human colon on appetite regulation, body weight maintenance and adiposity in overweight adults. *Gut*. 2015;64(11):1744-54.
22. Canfora EE, Jocken JW, Blaak EE. Short-chain fatty acids in control of body weight and insulin sensitivity. *Nat Rev Endocrinol*. 2015;11(10):577-91.
23. den Besten G, Lange K, Havinga R, van Dijk TH, Gerding A, van Eunen K, et al. Gut-derived short-chain fatty acids are vividly assimilated into host carbohydrates and lipids. *Am J Physiol Gastrointest Liver Physiol*. 2013;305(12):G900-10.
24. van Trijp M, Wilms E, Ríos-Morales M, Masclee AA, Brummer RJ, Witteman BJ, et al. Using naso- and oro-intestinal catheters in physiological research for intestinal delivery and sampling in vivo: Practical and technical aspects to be considered. *Am J Clin Nutr*. 2021.
25. Deroover L BE, Tie Y, Vandermeulen G, Verbeke K. Quantification of plasma or serum short-chain fatty acids: Choosing the correct blood tube. 2017.
26. Patel SK, Pratap CB, Jain AK, Gulati AK, Nath G. Diagnosis of helicobacter pylori: What should be the gold standard? *World J Gastroenterol*. 2014;20(36):12847.
27. Rios-Morales M, van Trijp MPH, Rösch C, An R, Boer T, Gerding A, et al. A toolbox for the comprehensive analysis of small volume human intestinal samples that can be used with gastrointestinal sampling capsules. *Sci Rep*. 2021;11(1):8133.
28. van Leeuwen SS, Kuipers BJH, Dijkhuizen L, Kamerling JP. Comparative structural characterization of 7 commercial galacto-oligosaccharide (GOS) products. *Carbohydr Res*. 2016;425:48-58.
29. Akbari P, Fink-Gremmels J, Willems RHAM, Difilippo E, Schols HA, Schoterman MHC, et al. Characterizing microbiota-independent effects of oligosaccharides on intestinal epithelial cells: Insight into the role of structure and size. *Eur J Nutr*. 2017;56(5):1919-30.
30. Poncheewin W, Hermes GDA, van Dam JCJ, Koehorst JJ, Smidt H, Schaap PJ. Ng-tax 2.0: A semantic framework for high-throughput amplicon analysis. *Front Genet*. 2019;10:1366.
31. Ramiro-Garcia J, Hermes G, Giatsis C, Sipkema D, Zoetendal E, Schaap P, et al. Ng-tax, a highly accurate and validated pipeline for analysis of 16s rrna amplicons from complex biomes [version 2; peer review: 2 approved, 1 approved with reservations, 1 not approved]. *F1000Research*. 2018;5(1791).
32. Langille MGI, Zaneveld J, Caporaso JG, McDonald D, Knights D, Reyes JA, et al. Predictive functional profiling of microbial communities using 16s rrna marker gene sequences. *Nat Biotechnol*. 2013;31(9):814-21.
33. Ramseier CA, Kinney JS, Herr AE, Braun T, Sugai JV, Shelburne CA, et al. Identification of pathogen and host-response markers correlated with periodontal disease. *J Periodontol*. 2009;80(3):436-46.
34. Peters RJB, van Bommel G, Herrera-Rivera Z, Helsper HPGF, Marvin HJP, Weigel S, et al. Characterization of titanium dioxide nanoparticles in food products: Analytical methods to define nanoparticles. *J Agric Food Chem*. 2014;62(27):6285-93.
35. van Dongen KCW, van der Zande M, Bruyneel B, Vervoort JMM, Rietjens IMCM, Belzer C, et al. An in vitro model for microbial fructoselysine degradation shows substantial interindividual differences in metabolic capacities of human fecal slurries. *Toxicol In Vitro*. 2021;72:105078.
36. van Dijk TH, Boer TS, Havinga R, Stellaard F, Kuipers F, Reijngoud DJ. Quantification of hepatic carbohydrate metabolism in conscious mice using serial blood and urine spots. *Anal Biochem*. 2003;322(1):1-13.
37. Derks TG, Boer TS, van Assen A, Bos T, Ruiter J, Waterham HR, et al. Neonatal screening for medium-chain acyl-coa dehydrogenase (mcad) deficiency in the Netherlands: The importance of enzyme analysis to ascertain true mcad deficiency. *J Inherit Metab Dis*. 2008;31(1):88-96.

38. Lee W-NP, Byerley LO, Bergner EA, Edmond J. Mass isotopomer analysis: Theoretical and practical considerations. *Biol Mass Spectrom.* 1991;20(8):451-8.
39. An R. Modulating the human intestinal microbiome in healthy adults and elderly through dietary supplements: Wageningen University; 2020.
40. Fehlbaum S, Prudence K, Kieboom J, Heerikhuisen M, van den Broek T, Schuren FHJ, et al. In vitro fermentation of selected prebiotics and their effects on the composition and activity of the adult gut microbiota. *Int J Mol Sci.* 2018;19(10).
41. Knudsen BKE, Hessov I. Recovery of inulin from jerusalem artichoke (*helianthus tuberosus* l.) in the small intestine of man. *Br J Nutr.* 1995;74(1):101-13.
42. Molis C, Flourié B, Ouarne F, Gailing MF, Lartigue S, Guibert A, et al. Digestion, excretion, and energy value of fructooligosaccharides in healthy humans. *Am J Clin Nutr.* 1996;64(3):324-8.
43. Zoetendal EG, Raes J, van den Bogert B, Arumugam M, Booiijink CCGM, Troost FJ, et al. The human small intestinal microbiota is driven by rapid uptake and conversion of simple carbohydrates. *The ISME J.* 2012;6(7):1415-26.
44. Cummings JH, Pomare EW, Branch WJ, Naylor CP, Macfarlane GT. Short chain fatty acids in human large intestine, portal, hepatic and venous blood. *Gut.* 1987;28(10):1221-7.
45. Piche T, des Varannes SB, Sacher-Huvelin S, Holst JJ, Cuber JC, Galmiche JP. Colonic fermentation influences lower esophageal sphincter function in gastroesophageal reflux disease. *Gastroenterology.* 2003;124(4):894-902.
46. Hong KB, Kim JH, Kwon HK, Han SH, Park Y, Suh HJ. Evaluation of prebiotic effects of high-purity galactooligosaccharides in vitro and in vivo. *Food Technol Biotechnol.* 2016;54(2):156-63.
47. Savignac HM, Corona G, Mills H, Chen L, Spencer JP, Tzortzis G, et al. Prebiotic feeding elevates central brain derived neurotrophic factor, n-methyl-d-aspartate receptor subunits and d-serine. *Neurochem Int.* 2013;63(8):756-64.
48. Koziolok M, Grimm M, Becker D, Iordanov V, Zou H, Shimizu J, et al. Investigation of pH and temperature profiles in the GI tract of fasted human subjects using the Intellicap® system. *J Pharm Sci.* 2015;104(9):2855-63.
49. Helander HF, Fändriks L. Surface area of the digestive tract - revisited. *Scand J Gastroenterol.* 2014;49(6):681-9.
50. El Aidy S, van den Bogert B, Kleerebezem M. The small intestine microbiota, nutritional modulation and relevance for health. *Curr Opin Biotechnol.* 2015;32:14-20.
51. Booiijink CC, El-Aidy S, Rajilić-Stojanović M, Heilig HG, Troost FJ, Smidt H, et al. High temporal and inter-individual variation detected in the human ileal microbiota. *Environ Microbiol.* 2010;12(12):3213-27.
52. Seekatz AM, Schnizlein MK, Koenigsnecht MJ, Baker JR, Hasler WL, Bleske BE, et al. Spatial and temporal analysis of the stomach and small-intestinal microbiota in fasted healthy humans. *mSphere.* 2019;4(2):e00126-19.
53. van Trijp MPH, Rösch C, An R, Keshtkar S, Logtenberg MJ, Hermes GDA, et al. Fermentation kinetics of selected dietary fibers by human small intestinal microbiota depend on the type of fiber and subject. *Mol Nutr Food Res.* 2020;64:2000455.
54. Bouhnik Y, Neut C, Raskine L, Michel C, Riottot M, Andrieux C, et al. Prospective, randomized, parallel-group trial to evaluate the effects of lactulose and polyethylene glycol-4000 on colonic flora in chronic idiopathic constipation. *Aliment Pharmacol Ther.* 2004;19(8):889-99.
55. Mangin I, Bouhnik Y, Suau A, Rochet V, Raskine L, Crenn P, et al. Molecular analysis of intestinal microbiota composition to evaluate the effect of peg and lactulose laxatives in humans. *Microb Ecol Health Dis.* 2002;14(1):54-62.
56. Kerr BJ, Weber TE, Ziemer CJ. Dietary marker effects on fecal microbial ecology, fecal vfa, nutrient digestibility coefficients, and growth performance in finishing pigs. *J Anim Sci.* 2015;93(5):2183-90.
57. Chen H, Zhao R, Wang B, Cai C, Zheng L, Wang H, et al. The effects of orally administered ag, TiO₂ and SiO₂ nanoparticles on gut microbiota composition and colitis induction in mice. *NanoImpact.* 2017;8:80-8.

58. Pinget G, Tan J, Janac B, Kaakoush NO, Angelatos AS, O'Sullivan J, et al. Corrigendum: Impact of the food additive titanium dioxide (e171) on gut microbiota-host interaction. *Front Nutr.* 2019;6(100).
59. Chen Z, Han S, Zhou D, Zhou S, Jia G. Effects of oral exposure to titanium dioxide nanoparticles on gut microbiota and gut-associated metabolism in vivo. *Nanoscale.* 2019;11(46):22398-412.
60. Dufefoi W, Moniz K, Allen-Vercoe E, Ropers MH, Walker VK. Impact of food grade and nano-tio(2) particles on a human intestinal community. *Food Chem Toxicol.* 2017;106:242-9.
61. Radziwill-Bienkowska JM, Talbot P, Kamphuis JBJ, Robert V, Cartier C, Fourquaux I, et al. Toxicity of food-grade tio(2) to commensal intestinal and transient food-borne bacteria: New insights using nano-sims and synchrotron uv fluorescence imaging. *Front Microbiol.* 2018;9:794.
62. van den Bogert B. Community and genomic analysis of the human small intestine microbiota. Chapter 7, general discussion.2013.
63. Roostalu J, Jöers A, Luidalepp H, Kaldalu N, Tenson T. Cell division in escherichia colicultures monitored at single cell resolution. *BMC Microbiol.* 2008;8(1):68.
64. Alsharafani M, Schnell S, Ratering S, Krawinkel M. Improving the growth and stability following of lyophilized bifidobacterium breve m4a and bifidobacterium longum subsp. Longum fa1 in skimmed milk media: Universitätsbibliothek; 2016.
65. Weaver JC, Williams GB, Klivanov A, Demain AL. Gel microdroplets: Rapid detection and enumeration of individual microorganisms by their metabolic activity. *Biotechnology.* 1988;6(9):1084-9.
66. Takeshita T, Kageyama S, Furuta M, Tsuboi H, Takeuchi K, Shibata Y, et al. Bacterial diversity in saliva and oral health-related conditions: The hisayama study. *Sci Rep.* 2016;6(1):22164.
67. Nardone G, Compare D. The human gastric microbiota: Is it time to rethink the pathogenesis of stomach diseases? *United European Gastroenterol J.* 2015;3(3):255-60.
68. Ruppin H, Bar-Meir S, Soergel KH, Wood CM, Schmitt MG. Absorption of short-chain fatty acids by the colon. *Gastroenterology.* 1980;78(6):1500-7.
69. Schmitt MG, Jr., Soergel KH, Wood CM, Steff JJ. Absorption of short-chain fatty acids from the human ileum. *Am J Dig Dis.* 1977;22(4):340-7.
70. Weinman EO, Srisower EH, Chaikoff IL. Conversion of fatty acids to carbohydrate: Application of isotopes to this problem and role of the krebs cycle as a synthetic pathway. *Physiol Rev.* 1957;37(2):252-72.
71. Bose S, Ramesh V, Locasale JW. Acetate metabolism in physiology, cancer, and beyond. *Trends Cell Biol.* 2019;29(9):695-703.
72. Astbury SM, Corfe BM. Uptake and metabolism of the short-chain fatty acid butyrate, a critical review of the literature. *Curr Drug Metab.* 2012;13(6):815-21.
73. Bergman EN. Energy contributions of volatile fatty acids from the gastrointestinal tract in various species. *Physiol Rev.* 1990;70(2):567-90.
74. De Vadder F, Kovatcheva-Datchary P, Goncalves D, Vinera J, Zitoun C, Duchamp A, et al. Microbiota-generated metabolites promote metabolic benefits via gut-brain neural circuits. *Cell.* 2014;156(1):84-96.
75. McBurney MI, Thompson LU. In vitro fermentabilities of purified fiber supplements. *J Food Sci.* 1989;54(2):347-50.
76. McBurney MI, Thompson LU, Cuff DJ, Jenkins DJ. Comparison of ileal effluents, dietary fibers, and whole foods in predicting the physiological importance of colonic fermentation. *Am J Gastroenterol.* 1988;83(5):536-40.
77. Cummings JH, Macfarlane GT. Colonic microflora: Nutrition and health. *Nutrition.* 1997;13(5):476-8.

Supplementary Methods

Catheter design and placement

A custom-made 300 cm long, silicone multi-channel naso-intestinal catheter with an outer diameter of 3.5 mm, a 0.4 mm delivery channel, and a 1.9 mm aspiration channel was used. The aspiration channel contained three side holes with 3-cm interspacing between each side hole (at position 1, 4, 7 cm). An inflatable balloon and three small weights were located at the tip end, and a radio-opaque marker was present for visualization by fluoroscopy. After manual placement past the ligament of Treitz using fluoroscopy, the balloon was kept inflated with 5 cc air and inserted by the subjects themselves with a maximum of 10 cm/hour. Freeze-frame fluoroscopy was applied during intubation of the duodenum, and afterwards for verification of the location at three moments. In study 2 only, the subjects were requested to set a wake-up call the morning of the experimental test day (day 8) to reconvene with the catheter progression protocol.

Droplet generation for total 16S rRNA gene copy number measurement

All materials for this analysis were ordered from Bio-Rad Laboratories, CA, USA. DNA was diluted to 0.005 ng/ μ L. Per 1 μ L diluted DNA, 19 μ L mastermix was added (7 μ L MQ water, 10 μ L QX200 EvaGreen ddPCR Supermix, 1 μ L universal 16S rRNA gene forward and reverse primers (1)) in cartridges. The 20 μ L sample with mix was pipetted perpendicular into cartridges for QX200 Droplet Generator and placed in cartridge holders. Wells without sample were filled with 1 μ L water and 19 μ L mastermix. 70 μ L Droplet Generation Oil for EvaGreen was also added in the cartridge, covered with Droplet Generator DG8 Gaskets, and droplets were generated (QX100 Droplet Generator). Next, 40 μ L of the generated droplets was transferred into a ddPCR 96-well plate, and sealed with Pierceable Foil Heat Seal in the PX1 PCR plate sealer at 170°C for 5 seconds. PCR amplification took place at 95.0°C for 10 min, 40 times 95.0°C for 30 sec and 58°C for 1 min, followed by 4°C for 5 min, and 90.0°C for 4 min. Data was generated using the QX200 Droplet Reader, and analyzed using QuantaSoft software (Version 1.7.4.0917).

Short chain fatty acid quantification in plasma

Plasma samples were diluted 1:3 with 100% acetonitrile (ACN) on room temperature and mixed by hand, and centrifuged for 20 min at 14000xg at 21°C. The samples were derivatized with 3-nitrophenylhydrazine hydrochloride (3NPH-HCl). 50 μ L of the supernatants were mixed with 50 μ L 200 mM 3NPH-HCl in 50% (v/v) aqueous ACN and 50 μ L 120 mM N-(3-dimethylaminopropyl)-N'-ethylcarbodiimide in 6% (v/v) pyridine in 50% (v/v) aqueous ACN solution in low binding Eppendorf tubes. After mixing, the tubes were incubated in an Eppendorf thermomixer at 40°C for 30

min, afterwards placed on ice for at least 1 min and further diluted with 100 μL milli-Q water. 90 μL of the derivatized sample was transferred to a UPLC vial containing a 10 μL internal standard mix containing 125 μM acetate- ^{13}C -3NPH, 100 μM propionate- ^{13}C -3NPH and 100 μM butyrate- ^{13}C -3NPH. Samples were measured by LC-MS/MS using a Shimadzu LCMS-8050 triple quadrupole mass spectrometer (Kyoto, Japan). SCFA concentrations were quantified using an external calibration curve constructed under the same conditions as the plasma samples. All plasma samples were derivatized and measured.

Glucose enrichment and concentration in plasma

In short, to 50 μL of plasma 500 μL ice-cold ethanol was added and samples were kept on ice for 45 min. Subsequently, samples were centrifuged (10 min, RT, 20,000 $\times g$), and 200 μL supernatant was transferred to a Teflon-capped reaction tube and dried at 60°C under a stream of nitrogen. After cooling to room temperature, 100 μL pyridine and 200 μL acetic anhydride were added to the samples, incubated for 30 minutes at 60°C, and subsequently dried at 60°C under a stream of nitrogen. Finally, the residues were dissolved in 200 μL ethylacetate and transferred into GC injection vials with insert. Ions monitored were m/z 408-414 (m_0 - m_6). Total glucose concentrations were measured in 10 μL plasma by using a blood glucose meter (Accu Check Performa) and test strips (Roche, Indiana, USA).

Measurement of free carnitine and acylcarnitines concentrations and enrichments in plasma

Briefly, for carnitine analysis the samples were prepared for concentration and ^{13}C enrichments. For concentration: 100 μL of cold acetonitrile was added to 10 μL of plasma sample, shortly vortexed and then 100 μL of internal standard ([8,8,8- $^2\text{H}_3$]-octanoyl-L-carnitine and [10,10,10- $^2\text{H}_3$]-decanoyl-L-carnitine) was also added to the mix. For enrichments: 100 μL of cold acetonitrile was added to 10 μL of plasma sample, shortly vortexed, and then 100 μL of 80% methanol in milli-Q water was added to the mix. After, samples from both sets were vortexed again and centrifuged (RT, max speed 20,000 g) for 10 min. Finally, 150 μL from each sample were transferred to a GC injection vial with insert for analysis.=

Organic and amino acids concentrations and ^{13}C enrichments in plasma

Organic and amino acids were analyzed according to Evers et al. (2). To 100 μL of plasma in a glass tube 900 μL of milli-Q water was added. Next, on ice, 2 mL ice-cold chloroform was added, the tubes were closed and vortexed for 30 min at 4°C. After, samples were centrifuged at 1250 $\times g$ for 10 min. The upper aqueous phase was transferred to a clean glass tube and dried at 37°C under a stream of nitrogen. The sample was derivatized by the addition of 40 μL methoxyamine-HCl in pyridine (2%

v/v), incubated for 90 min at 37°C, cooled down at RT, centrifuged for 1 min at 1250xg at RT, after which 60 µL of MBTSTFA + 1% TBDMCS was added, incubated at 55°C for 60 min and cooled down at RT. Finally, all tubes were centrifuged for 10 min at 1250xg RT, and the derivatized sample was transferred into a glass vial with an insert with a screw-cap for GC-MS analysis.

Fatty acids ¹³C enrichments in plasma

To 50 µL of plasma, C17 internal standard (50 mg C17:0 in 100 mL methanol) were added. Fatty acids were hydrolyzed in 2 mL of methanol-HCl (5:1 vol/vol) for 4 hours at 90°C in a closed glass tubes. Fatty acids were later extracted in 2 mL hexane, vortex, centrifuged (5 min at 800xg) and evaporated while heating at 45°C. The methylated fatty acids were re-dissolved in 200 µL hexane and pipette into a new GC-vial with insert to be analyzed (3).

Corrections and calculations

Normalization of the mass isotopologues distributions measured by GC-MS

All data measured by GC-MS (m0-m+6) was first corrected for the natural abundance of ¹³C by multiple linear regression according to Lee et al. (4) to obtain the excess fractional distribution of mass isotopologues (M⁰-M⁺⁶).

Acetate, propionate, and butyrate contribution to glucose

The individual contributions of acetate, propionate, and butyrate to the labeling of glucose were calculated by taking into consideration known biochemical pathways, the stoichiometry to molecules of glucose per each SCFA, and the amount delivered. ¹³C carbons in [1,2,3-¹³C₃]-propionate will be scrambled when converted to fumarate resulting in [1,2,3-¹³C₃]-oxaloacetate and [2,3,4-¹³C₃]-oxaloacetate, respectively. The conversion of these oxaloacetate isotopologues into phosphoenolpyruvate (PEP) by the PEP carboxykinase (PEPCK) will result in [1,2,3-¹³C₃]-PEP and [2,3-¹³C₂]-PEP, respectively, and equal contribution of M⁺³ and M⁺² glucose to the isotopologue distribution, respectively. The breakdown of [1,2,3,4-¹³C₄]-butyrate to two [1,2-¹³C₂]-acetyl-CoA could lead to equal contribution of M⁺¹ and M⁺² to glucose due to scrambling at fumarate in the TCA cycle. Moreover, 1 molecule of butyrate gives rise to 2 molecules of acetate labeling 2 molecules of glucose. [1-¹³C₁]-acetate is converted to [1-¹³C₁]-acetyl-CoA equally contributing to M⁺⁰ and M⁺¹ glucose to the isotopologue distribution due to scrambling at fumarate in the TCA cycle. Multiple linear regression was performed with the measured and corrected isotopologue distribution of glucose and the expected labeling of glucose by the SCFA.

Supplementary Results

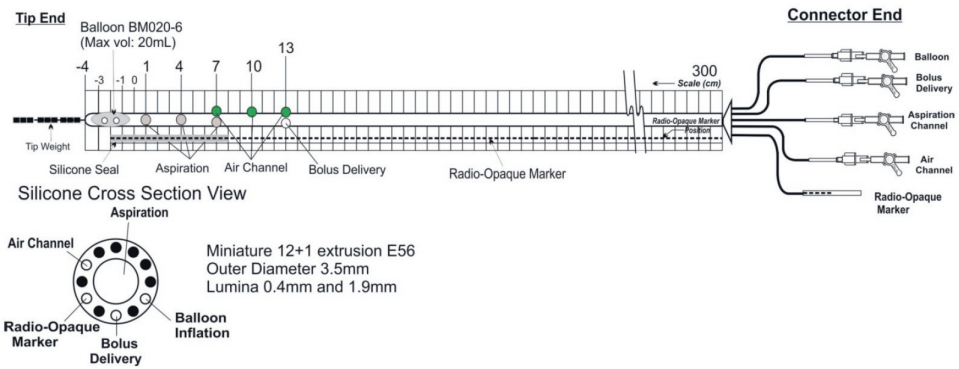
Study logistics and drop-outs

In study 1 during the first test session, two subjects were excluded due to failure of catheter placement in the ileum/colon (the catheter coiled up in the stomach). This resulted in adaptations in the catheter progression protocol, namely the balloon was kept inflated continuously and the insertion speed was reduced to a maximum (10 cm/hour). After these adaptations, the progression of the catheter occurred as expected, but one subject had to stop due to vomiting. Thus, from the five subjects, only two subjects fully completed study 1. In study 2, 10 subjects were included in the study and randomly allocated to the NDC (n=5) or placebo (n=5) group. One subject dropped out during the supplementation period due to the emergence of AEs, namely diarrhea. Three subjects were excluded due to failure of post-pyloric catheter placement. The remaining six subjects completed study 2, and compliance was $101\pm 4.9\%$ for the different intervention products, based on percentages of product packages returned. The percentage is higher than 100, because one subject incidentally also consumed the extra supplement that was provided. The total radiation effective dose that subjects were exposed to while verifying the catheter positioning using fluoroscopy was a calculated mean of 0.06 (range 0.005-0.22) mSv, which can be considered very low. The dose varied upon the exposure time to fluoroscopy, mainly depending on the time the placement procedure took.

Evaluation of (dis)comfort

The study procedures caused expected discomfort and AEs. Only in study 2, the participants were asked to fill in a questionnaire with visual analog scales about the study procedures, labeled with 'no pain/discomfort' (0 mm end) and 'a lot of pain/discomfort' (100 mm end). Nine subjects that had the catheter inserted graded throat pain with 33 ± 22 mm, nasal pain with 38 ± 23 mm, and nausea with 28 ± 37 mm. Catheter placement was graded with 45 ± 24 mm, catheter progression with 29 ± 24 mm (n=7), and catheter removal with 51 ± 33 mm. 67% of the participants indicated that they would undergo the same procedure again for clinical research, but only 33% of the participants indicated that they would undergo this procedure twice within two months.

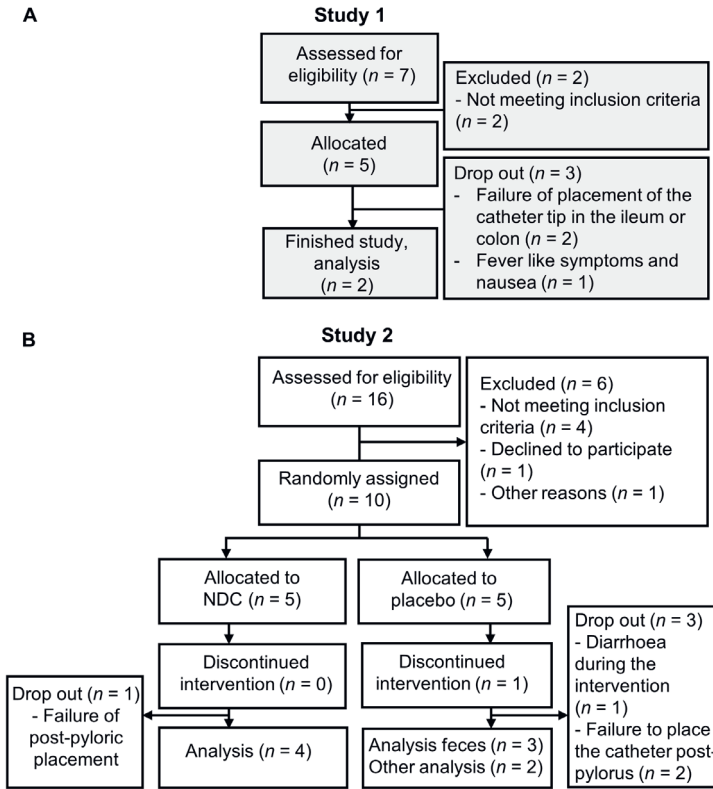
Supplementary Figures and Tables



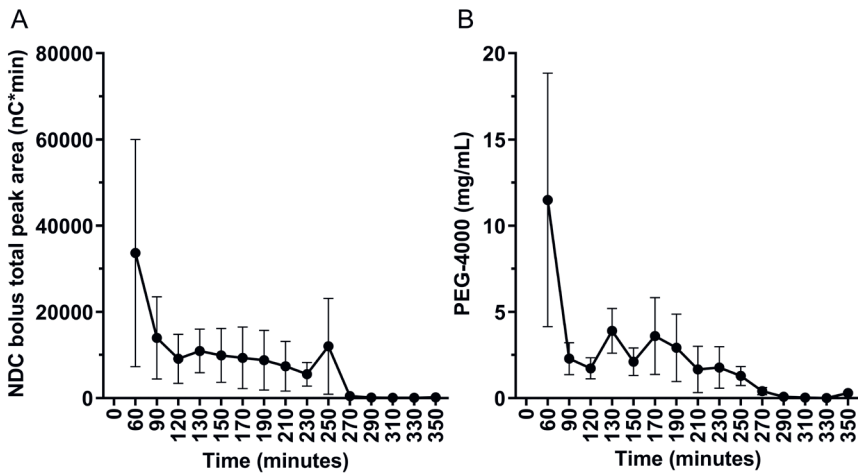
COPYRIGHT: THIS DESIGN AND PRINT IS THE PROPERTY OF DENTSLEEVE AND SHALL NOT BE RETAINED, COPIED OR USED WITHOUT THEIR AUTHORITY.

Supplementary Figure 1. Design of the naso-intestinal catheter.

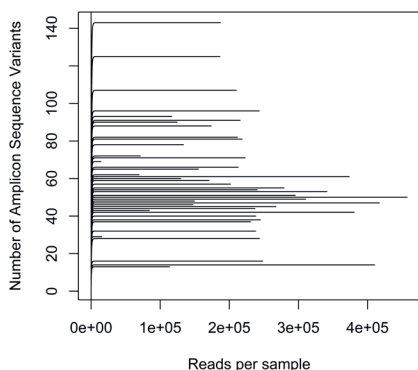
In the cross-section view, the different lumina are shown. The radio-opaque marker is used for visualization by fluoroscopy.



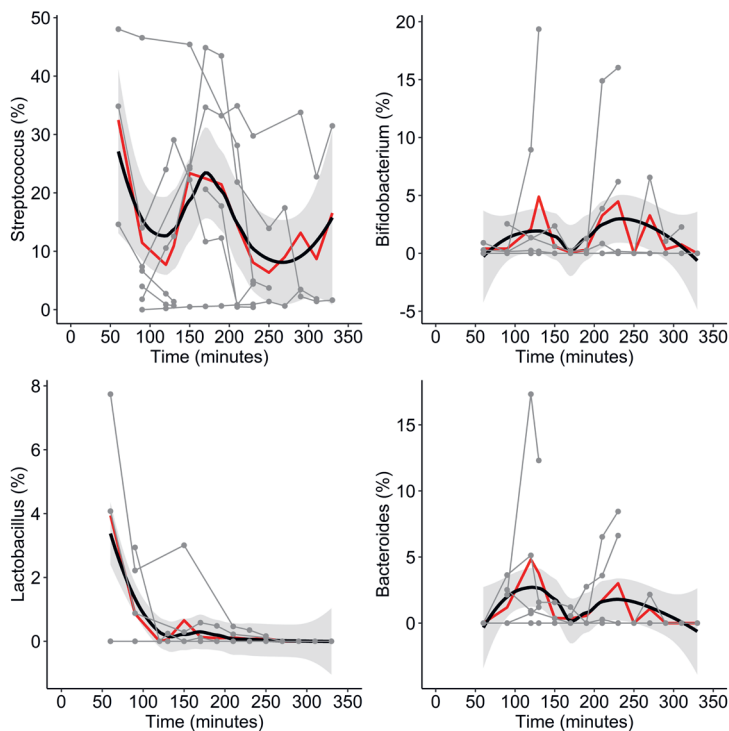
Supplementary Figure 2. Flow chart of study 1 and study 2.



Supplementary Figure 3. The presence of NDC constituents (A) or the non-absorbable marker PEG-4000 (B) in the ileum or proximal colon of healthy male subjects over time. Data is shown as mean \pm SD, n=7 subjects. The data of the transverse colon, is not included in this figure.

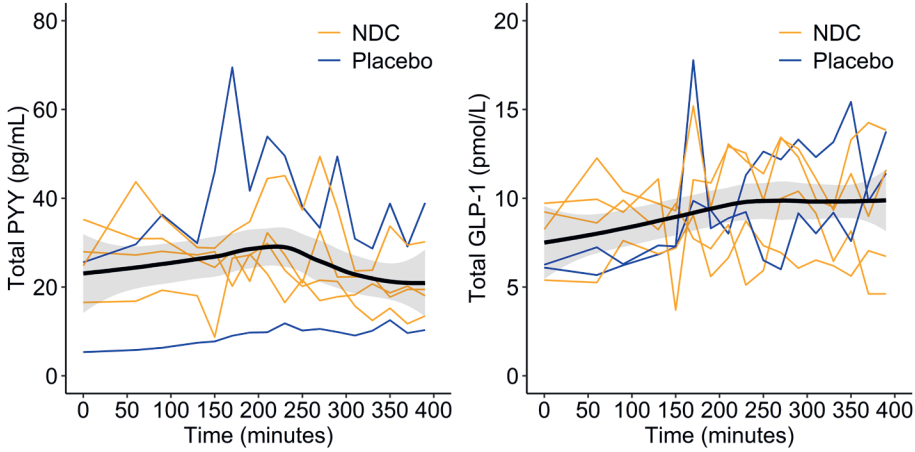


Supplementary Figure 4. The rarefaction curves of all intestinal and fecal samples. When the curve reaches a plateau, this means the sequencing depth (reads per sample) was high enough to measure all amplicon sequence variants (bacteria) present in the sample. Control samples (water, TiO_2 and MOCKs) are excluded from this figure.



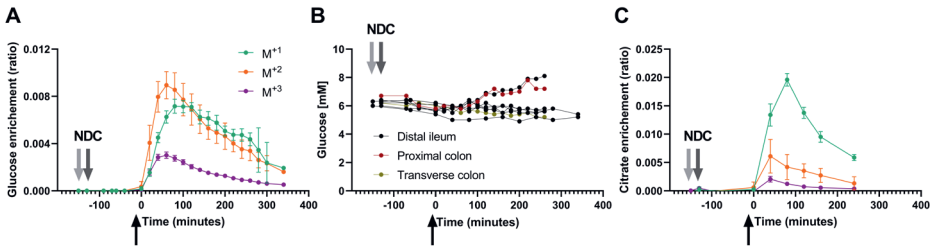
Supplementary Figure 5. The relative abundances of the selected bacteria *Streptococcus*, *Bifidobacterium*, *Lactobacillus*, and *Bacteroides* over time inside the ileum or colon of healthy male subjects.

The grey dots and lines represent the individual patterns. The red line represents the mean relative abundance, and the black line represents the locally estimated scatterplot smoothing curve. All samples that could be obtained from $n=8$ subjects were included in the graphs.



Supplementary Figure 6. Concentrations of total PYY and total GLP-1 in plasma of healthy male subjects before and after consumption of the NDC bolus with 10 grams FOS and GOS.

The lines represent the individual patterns. The black line represents the locally estimated scatterplot smoothing curve ($n=6$ subjects in study 2). PYY, peptide YY; GLP-1, glucagon-like peptide 1; NDC, non-digestible carbohydrates.



Supplementary Figure 7. The glucose and citrate enrichment ratios per labeled pattern (M^0 - M^{+5} , M^{+6} not detected) from SCFA delivered in the intestine, and the total plasma glucose concentration over time.

(A) Glucose enrichments per label pattern detected and (B) blood glucose concentrations. (C) Citrate glucose enrichments per label pattern detected. The black arrow indicates the start of luminal isotope infusion (10 mL containing 10 mmol [1-¹³C]-acetate, 4 mmol [1,2,3-¹³C₃]-propionate and 1 mmol [1,2,3,4-¹³C₄]-butyrate) through the catheter. This is considered to be time 0 for all subjects to match both studies. The grey arrows indicate the drinking of the non-digestible carbohydrates (NDC) bolus in both studies (-150 min for study 1, light grey arrow, and -120 min for study 2, dark grey arrow). Data is represented as mean (A, C) and $n=8$ individual subjects (B).

Supplementary Table 1. The differential fecal bacteria (P-values<0.05) and short-chain fatty acids in feces of healthy male subjects after 7-days supplementation.

The NDC group received 15 g/day FOS:GOS for 7 days, and the placebo group received isocaloric maltodextrin.

	NDC group (n = 4)	Placebo group (n = 3)		
Bacteria on genus level	Relative abundance (%)	Relative abundance (%)	P-value	FDR P-value
<i>g_Holdemanella</i>	0 ± 0	1.98 ± 3.66	0.0319	N.S.
<i>g_Coprococcus_3</i>	0.112 ± 0.135	0.337 ± 0.332	0.0497	N.S.
<i>g_Ruminococcaceae_NK4A214_group</i>	0.0841 ± 0.112	0.483 ± 0.591	0.0497	N.S.
Short-chain fatty acid	Concentration (mM)	Concentration (mM)	P-value	
Acetate	120.6 ± 78.3	96.0 ± 67.8	0.289	-
Propionate	36.8 ± 20.2	30.9 ± 18.0	0.289	-
Butyrate	29.6 ± 21.2	23.8 ± 17.3	0.157	-

References Supplementary Information

1. Ramseier CA, Kinney JS, Herr AE, Braun T, Sugai JV, Shelburne CA, et al. Identification of pathogen and host-response markers correlated with periodontal disease. *J Periodontol.* 2009;80(3):436-46.
2. Evers B, Gerding A, Boer T, Heiner-Fokkema MR, Jalving M, Wahl SA, et al. Simultaneous Quantification of the Concentration and Carbon Isotopologue Distribution of Polar Metabolites in a Single Analysis by Gas Chromatography and Mass Spectrometry. *Anal Chem.* 2021;93(23):8248-8256.
3. Muskiet FAJ, van Doormaal JJ, Martini IA, Wolthers BG, van der Slik W. Capillary gas chromatographic profiling of total long-chain fatty acids cholesterol in biological materials. *J Chromatogr B Biomed Appl.* 1983;278:231-44.
4. Lee W-NP, Byerley LO, Bergner EA, Edmond J. Mass isotopomer analysis: Theoretical and practical considerations. *Biol Mass Spectrom.* 1991;20(8):451-8.



Detailed analysis of the digestibility of prebiotic fructo- and galacto-oligosaccharides in the human small intestine

Mara van Trijp¹, Melany Rios-Morales², Madelon Logtenberg³, Shohreh Keshtkar¹, Lydia Afman¹, Ben Witteman^{1,4}, Barbara Bakker², Dirk-Jan Reijngoud², Henk Schols³, Guido Hooiveld¹

¹ Division of Human Nutrition and Health, Wageningen University, the Netherlands

² Laboratory of Pediatrics, Center for Liver, Digestive and Metabolic Diseases, University of Groningen, University Medical Center Groningen, Groningen, the Netherlands

³ Laboratory of Food Chemistry, Wageningen University, the Netherlands

⁴ Hospital Gelderse Vallei, Department of Gastroenterology and Hepatology, Ede, the Netherlands

In preparation.

Abstract

Background

The non-digestible carbohydrates (NDC), galacto-oligosaccharides (GOS) and fructo-oligosaccharides (FOS; synonym oligofructose), are food ingredients applied to improve human health. The knowledge about the digestibility of FOS and GOS throughout the small intestine of people is, however, scarce. We investigated the breakdown kinetics of FOS and GOS mixtures inside the intestine of healthy men.

Methods

Data was used of seven healthy Dutch male subjects (18-60 years, BMI 18.5-30 kg/m²) obtained through two clinical trials. Subjects were intubated with a catheter in the distal ileum or proximal colon. They consumed an NDC bolus with 5 gram chicory derived FOS (degree of polymerization DP₂₋₁₀), 5 gram GOS (DP₂₋₆), and 5 gram non-absorbable marker PEG-4000. Postprandially, intestinal content was frequently collected over a period until 350 minutes. Mono-, di, and oligosaccharide profiles and PEG-4000 were analyzed in the intestinal content.

Results and Conclusion

The mean estimated recoveries of FOS and GOS were 96±25% and 76±28%, respectively. The relative abundances of FOS DP_{≥2} and GOS DP_{≥3} compounds in the distal small intestine or proximal colon were similar to the consumed NDC bolus dose. GOS dimers, the DP₂ fraction, had a lower relative and absolute abundance in the distal ileum and proximal colon compared to the NDC bolus. The mean estimated recoveries were 22.8±11.1% for β-D-Gal-(1↔1)-α-D-Glc+β-D-Gal-(1↔1)-β-D-Glc, and 19.3±19.1% for β-D-Gal-(1→2)-D-Glc+β-D-Gal-(1→3)-D-Glc, while the recoveries for β-D-Gal-(1→6)-D-Gal and β-D-Gal-(1→4)-D-Gal were 43.7±24.6% and 68.0±38.5%, respectively. Lactose, present in the GOS mixture, was still present at the end of the small intestine or the proximal colon of all participants (recovery range, 27.9-47.5%). Altogether, our findings show that FOS of DP_{≥2} and GOS of DP_{≥3} were not digested in the small intestine *in vivo* in healthy adults, while most of the prebiotic GOS DP₂ fraction was hydrolyzed in the small intestine in a structure-dependent fashion. We provide direct evidence on the resistances of GOS (DP₂ fraction) with distinct β-linkages in the human intestine. This is opening the future development of new tailored GOS prebiotics that completely resist digestion in the small intestine.

Keywords

Digestion; oligosaccharides; small intestine; ileum; prebiotics; lactose; human

Background

Non-digestible carbohydrates (NDCs) are valuable food ingredients applied for their health benefits (1). Galacto-oligosaccharides (GOS) and fructo-oligosaccharides (FOS) are examples of soluble NDCs that serve as fermentable substrates for the gut microbiota, and their degree of polymerization (DP) fractions ≥ 3 are also classified as dietary fibers (2, 3). Moreover, they are also prebiotics, which are defined as is 'a substrate that is selectively utilized by the host microorganisms conferring a health benefit' (4). Both FOS and GOS are naturally present in various foods. However, they are also industrially produced as ingredients to add to foods or supplements to improve the nutritional value of the food and/or for human health purposes (2). For instance, FOS and GOS are added to infant formula to mimic the health effects of endogenous oligosaccharides in human milk (5). They are also added to food products to increase the fiber content for adults (6). Both FOS and GOS are known to selectively stimulate beneficial gut bacteria (7).

Fructans, including inulin and oligofructose, are naturally found in a variety of foods such as whole grains, vegetables (*e.g.* garlic, artichoke, chicory root, onions), and fruits (*e.g.* bananas) (8-10). FOS (DP 2-10) is produced via partial enzymatic hydrolysis of inulin that is extracted mainly from chicory roots (11). Alternatively, FOS (DP2-5) may be prepared from sucrose or fructose (9). FOS consist of a linear series of β -(2,1) linked fructose units, attached to a terminal fructose by a β -(2,1) bond (Fn series), or to a terminal alpha-D-glucose by an α -(2,1) bond (GFn series) at the non-reducing end, with a DP up to 10 (9, 12). Inulinases degrade FOS and can be classified into endo- and exo-inulinases. Endo-inulinases (2,1- β -D-fructan fructanohydrolase) split internal β -(2,1) fructofuranosyl linkages, whereas exo-inulinases (β -D-fructohydrolase) split off fructose units at the terminal non-reducing end (13). Several micro-organisms residing in the human gut possess these enzymes (13), whereas host enzyme sucrase-isomaltase in the small intestine can split sucrose (α -D-Glc-(1 \rightarrow 2)- β -D-Fru) (14) but not β -(2,1) linked fructose units.

GOS is naturally present in human milk (15), as well as in the generative part of plants such as beans or legumes (*e.g.* lentils, chickpeas) (16). They can also be produced via hydrolysis and transgalactosylation of lactose by β -galactosidases (17). The production results in a mixture of galactose chains varying in DP (2 to 8), and linkages (17), namely β -(1,2), β -(1,3), β -(1,4), or β -(1,6), attached to a terminal galactose or glucose unit (17-19), or isomers with a (1 \leftrightarrow 1) linkage (18). The effects of GOS on the microbiota composition, intestinal immunity, and intestinal barrier function are dependent on monomer composition, DP, or linkage type (20-22). This highlights the importance of structure-dependent health effects. Degradation of GOS in the intestinal tract requires

glycoside hydrolases, specifically β -galactosidases (23, 24). Specific micro-organisms residing in the gut, such as bifidobacteria, contain β -galactosidases with different activities (25). One type of β -galactosidase, lactase, hydrolyzes lactose into galactose and glucose. Lactase is the only β -galactosidase that is also encoded by humans and is found attached to the intestinal brush border membrane (26, 27). Its levels are decreased by early childhood and further decline during aging. The decline however varies among ethnic backgrounds, as for instance Northern European adults have persistent lactase activity, potentially caused by a mutation (28).

Despite the large interest in FOS and GOS due to their potential health benefits, the information about their digestibility in the human small intestine is limited. Developing and applying carbohydrates that are non-digestible in foods is of interest because they have low caloric value (obesity prevention), give a low or extended glycemic response, and can function as substrates for the colonic microbiota. There is a generally accepted view that NDCs pass through the small intestine without substantial modifications (29). However, some animal studies hint towards some NDC fermentation in the small intestine (30, 31), and *in vitro* FOS and GOS can be fermented by ileostomy bacteria (32). Breakdown of FOS by human intestinal bacteria *in vitro* was shown to occur in a size-dependent fashion (32). Moreover, FOS (33, 34) and 4'-galactosyllactose (GOS DP3) (35) are resistant to digestion by the rat digestive enzymes of the GI-tract *in vitro* (33-35), but GOS with specific linkages (*e.g.* β -(1,4)) was slightly digested *in vitro* by rat (34, 36) or pig digestive enzymes (37). Several studies investigated the resistance of FOS (38) or inulin (39, 40) to digestion and absorption in the human small intestine. Chicory inulin and oligofructose were recovered in the ileostomy effluent of patients, 88% and 89% respectively, suggesting minor losses due to hydrolysis or bacterial degradation during small intestinal passage (40). In another study in ileostomy patients, artichoke inulin was not fully recovered from the small intestine (39). Similarly, using intestinal aspiration in healthy volunteers, a minor fraction of chicory FOS was not recovered from the small intestine (38). However, a detailed analysis of the fate of individual FOS DP fractions was not provided. So far, no clinical trials studying GOS digestion in humans have been conducted. Consequently, there is a need for studies to investigate *in vivo* digestibility, as well as potential acid hydrolysis of FOS and GOS through the stomach and small intestine of healthy subjects with analysis of their final DP to verify their intact arrival in the colon. Intestinal catheters proved to be valuable tools to study digestion in the human intestine (41).

In the current publication, we assessed the digestibility of FOS and GOS, including the digestible carbohydrates (*i.e.*, mono- and dimers) in these mixtures, in the distal small intestine or proximal colon of healthy men. We used data from two previously performed feasibility trials (chapter 5), where intestinal samples were collected over

time after consumption of a drink with FOS and GOS. We provide direct evidence in humans on the resistances of prebiotic compounds with distinct linkages, monomer compositions, and sizes, opening the future development of new tailored (potential) prebiotics.

Material and methods

Study subjects

We used data from two previously performed human clinical trials (chapter 5). In both studies, Dutch subjects with an age between 18-60 years and a BMI between 18.5-30 kg/m² were included. The main exclusion criteria were having a history of medical or surgical events, the use of any prescribed or non-prescribed medication during the three weeks prior to study start, smoking, use of pro- pre- or antibiotics within 3 months before the study start, having infrequent bowel movements (less than three times per week), and more than 21 alcoholic consumptions per week. They were not lactose intolerant. Both studies were approved by the Medical Ethics Committee of Wageningen University, and registered at ClinicalTrials.gov, identifiers: NCT04013607 (study 1) and NCT04499183 (study 2). All subjects gave written informed consent. All subjects filled in a food frequency questionnaire to determine their habitual dietary intake. The six subjects with measurements in the distal ileum are referred to as distal ileum 1-6, one subject with measurements in the proximal colon is referred to as proximal colon 1. Two subjects finalized study 1 (distal ileum 1-2), and six subjects finalized study 2 (distal ileum 3-6 and proximal colon 1). The data of both studies are jointly analyzed and presented in the current study.

Study design

All details about the study designs and study logistics are described previously (chapter 5). In short, study 1 was an acute feeding test day. Study 2 was a 7-day parallel intervention with either 15 g/d NDCs or isocaloric maltodextrin, followed by the same acute feeding test day. The 7-day intervention study was found not to affect the luminal microbiota and was therefore not further researched in this publication. One day before the acute feeding test day, subjects were intubated with a 300 cm long naso-intestinal catheter with a 1.9 mm aspiration channel (Mui Scientific, Ontario, Canada) that progressed towards the distal small intestine or proximal colon using an inflatable balloon. The next morning, after an overnight fast, subjects visited the hospital again for the test day. Subjects consumed a liquid bolus with NDCs. Afterwards, subjects were not allowed to eat or drink, except water. 120 minutes after NDC bolus consumption, an intra-intestinal infusion was delivered with a total volume of 20 mL. This part of the study is described in chapter 5 and will not be discussed here. Using the catheter aspiration

channel, we aimed to collect luminal samples at baseline, 60, 90, 120, every 20 minutes between 130-310 minutes (study 1) or between 130-390 minutes (study 2), and every 40 minutes between 310-490 minutes (study 1 only). Intestinal luminal content was collected using 5 cc syringes in 5 mL tubes, thoroughly mixed, and divided into aliquots which were put on dry ice immediately, and stored at -80°C.

The NDC bolus

The NDC bolus (**Figure 1**) consisted of 5.4 gram chicory FOS (Frutalose® OFP; Sensus, the Netherlands: 7% mono- and dimers and 93% oligosaccharides) and 7.1 gram GOS (Vivinal DOMO GOS, FrieslandCampina, the Netherlands: 30% mono- and dimers, of which ~20% lactose, and 70% oligosaccharides) to reach a 1:1 ratio of FOS and GOS oligosaccharides (5 gram each) in the final bolus in 200 mL tap water. Additionally, 5 gram of non-digestible marker polyethylene glycol 4000 (PEG-4000, Dulcosoft, Sanofi-Aventis, Germany) was dissolved in the bolus. Frutalose® OFP contains 93% oligosaccharides with a $DP \leq 10$, and 7% fructose, glucose, and sucrose. Vivinal GOS contains 70% oligosaccharides with a $DP \leq 6$ and 30% glucose, galactose, and lactose, of which around 20% lactose. In total, the NDC bolus contained a mean amount (\pm SD) of 0.36 ± 0.00 g glucose+galactose, 0.26 ± 0.22 g fructose, 1.7 ± 0.46 g lactose, and 0.41 ± 0.09 g sucrose. The water-soluble PEG-4000 is not absorbed or metabolized in the GI-tract (42) and was therefore used to correct for removal of FOS and GOS from the sampling location by transit time rather than digestion.

Measurement of the carbohydrates in intestinal contents

Luminal samples were analyzed for their mono-, di-, and oligosaccharide profiles by high performance anion exchange chromatography (HPAEC) with pulsed amperometric detection (PAD). The HPAEC-PAD system, columns, and elution conditions were used as described elsewhere (43). Hundred μ L luminal content was centrifuged (10 min, 4°C, 15 000xg). The supernatants of most of the samples from subjects distal ileum1 were 10x diluted, distal ileum2 50x diluted, distal ileum3 10x diluted, distal ileum4 300x diluted, distal ileum5 200x diluted, distal ileum6 200x diluted, and from the proximal colon1 100x diluted. The dilution factor was based on a pre-measurement. A range of dilutions of the NDC bolus (50-200 μ g/mL) was included in the run, to cover the linear range of each compound in the bolus. Identification of individual FOS and GOS isomers was partly based on commercial standards. For identification of FOS and GOS isomers for which commercial standards were not available, the elution profiles of the luminal content were compared with the elution profiles of Frutalose® FOS (50-200 μ g/mL), Vivinal GOS (50-200 μ g/mL), Vivinal GOS DP fractions (DP2, DP3, DP4, and DP5), and FOS and GOS profiles characterized in previous research (19, 22). The standards of the constituent DPs of GOS were obtained previously by size-exclusion chromatographic fractionation of Vivinal GOS (18). We relied on the tentative identification of GOS

(DP2) compounds described in previous studies (19, 44). Quantification of glucose, galactose, fructose, sucrose, lactose, 1-kestose, 4-galactosyllactose, 6-galactosyllactose was possible by including these as standards (Sigma-Aldrich) in the range of 4-20 µg/mL. The data were analyzed with Chromeleon 7.2 SR4 software. The area of each peak was quantified, and peak areas were normalized to the total NDC area of that specific sample to calculate the relative abundance. The total peak area of compounds from FOS and GOS mixtures that co-eluted in one peak were included in both the analysis of FOS and GOS. The percentage recovery of the NDC compounds in the intestine compared to the NDC bolus was estimated using the following formula: [(NDC compound in the intestine/PEG in the intestine)/(NDC compound in the bolus/PEG in the bolus)]*100%.

Measurement of the non-absorbable marker in intestinal contents

Concentrations of PEG-4000 were quantified using an anti-PEG sandwich ELISA assay. In short, plates (Nunc MaxiSorp) were coated with 50 µL per well with 5 µg/mL rat5M-PABM-A anti-PEG antibody (IBMS Academia Sinica, Taiwan) in coating buffer (5.3 g/L Na₂CO₃, 4.2 g/L NaHCO₃, pH 8.0) overnight (4°C, shaking at 50 rpm). Plates were washed five times with 1x phosphate-buffered saline (PBS) and blocked with 200 µL 1% BSA/1x PBS per well for two hours at room temperature. Tween was not added to the washing buffer, because the structure is similar to PEG-4000, and therefore interferes with the assay. PEG-4000 standards (0.1-10000 µg/mL) and samples were diluted in buffer (1% BSA/1x PBS). After another washing step, 50 µL standards or 50 µL intestinal content (500 or 1000 times diluted) was added for one hour at room temperature, while shaking at 50 rpm. To assess matrix effects, known PEG-4000 concentrations were spiked in small intestinal content without PEG that was diluted 10, 100, or 1000x in dilution buffer. Afterwards the plates were washed, and 50 µL per well 6.3-PABG-B biotin anti-PEG detection antibody (IBMS Academia Sinica, Taiwan) was added in a concentration of 5 µg/mL in dilution buffer for 1 hour at room temperature. After plate washing, 50 µL per well of 0.5 µg/mL streptavidin conjugated to horseradish peroxidase (Jackson ImmunoResearch Europe Ltd, UK) in dilution buffer was added for 45 minutes at room temperature. The plate was washed again, and 100 µL freshly prepared 0.5 mg/mL AzBTS-(NH₄)₂ (Sigma-Aldrich) in 100 mM phosphate-citrate buffer was added per well. Directly before use, 0.2 µL/mL 30% H₂O₂ was added to the AzBTS-(NH₄)₂ substrate solution. After 8 minutes of incubation in the dark, absorbance was read at 414 nm.

Presence of predicted microbial genes related to FOS and GOS breakdown

Microbiota composition in the luminal content was determined via sequencing of the variable V4 region of the 16S rRNA gene using Illumina HiSeq2500, as described previously (chapter 5). The predicted functionality of bacteria in the intestinal lumen was

compared to the predicted functionality of fecal bacteria. A fecal sample was collected on the day before the test day. The abundances of microbial genes were predicted based on the 16S rRNA gene sequences using the phylogenetic investigation of communities by reconstruction of unobserved states algorithm (version PICRUSt2) with default settings, but the minimum alignment was set to 60% (45). The mean (\pm SD) nearest sequenced taxon index, which is the average branch length that separates each amplicon sequence variant (ASV) from a reference bacterial genome, weighted by the abundance of that ASV in the sample, was 0.17 ± 0.16 . Within the sample, the abundance of the selected microbial gene was divided by the abundance of the total microbial genes to calculate the relative abundance. Relative abundance in the ileal samples was compared to the relative abundances in feces using the non-parametric Kruskal-Wallis test.

Results

Subject characteristics

In total, eight healthy male subjects finalized both clinical trials. One subject was excluded from the analyses, because the catheter tip was located in the transverse colon. The baseline characteristics of the other seven subjects are jointly summarized in **Table 1**. In six subjects, the catheter was located in the distal ileum, at a mean estimated distance of 21 ± 16 cm (range 10-50 cm) from the ileo-cecal valve. In one subject, the catheter was located in the proximal colon. Due to sampling difficulties, particularly in the proximal colon, not at every time point an intestinal sample was collected.

Table 1. Baseline characteristics and habitual daily intake of (macro)nutrients in healthy male subjects¹.

	<i>n</i> = 7 subjects
Age, years	34.6 ± 17.4
BMI, kg/m ²	23.8 ± 2.5
Total kcal/d	2528.3 ± 207.3
Total carbohydrates ² , g/d	256.8 ± 39.6
Mono- and disaccharides, g/d	88.5 ± 36.5
Polysaccharides ³ , g/d	168.2 ± 26.3
Fiber ⁴ , g/d	28.8 ± 8.5

¹Values are presented as means \pm SD, *n*=7 subjects. ²Dietary fiber is not included in the total carbohydrates.

³Polysaccharides include digestible carbohydrates and low molecular weight fibers. ⁴Fibers include high molecular weight fibers, insoluble fibers in water, fibers soluble in water and precipitated by 78% ethanol, not low molecular weight fibers (e.g. fructan, GOS).

Characterization of the NDC bolus

The HPAEC-PAD chromatograms of the NDC bolus, and the original FOS and GOS

supplements are visualized separately (**Figure 1**). Some peaks represent compounds coming from both the FOS supplement and the GOS supplement, so-called co-elution, namely glucose+galactose (peak #3), GOS DP3+FOS DP2 (peak #13), GOS DP4+FOS DP4 (peak #15), and GOS DP4+DP5+FOS DP3 (peak #17). Most compounds were distinguished to come from either the GOS mixture or from the chicory-derived FOS. An overview of all characterized compounds is presented in **Table 2**. Except for the monomers, lactose, and sucrose, the quantification was limited to the relative abundance of each component in the total NDC bolus due to the lack of commercial standards.

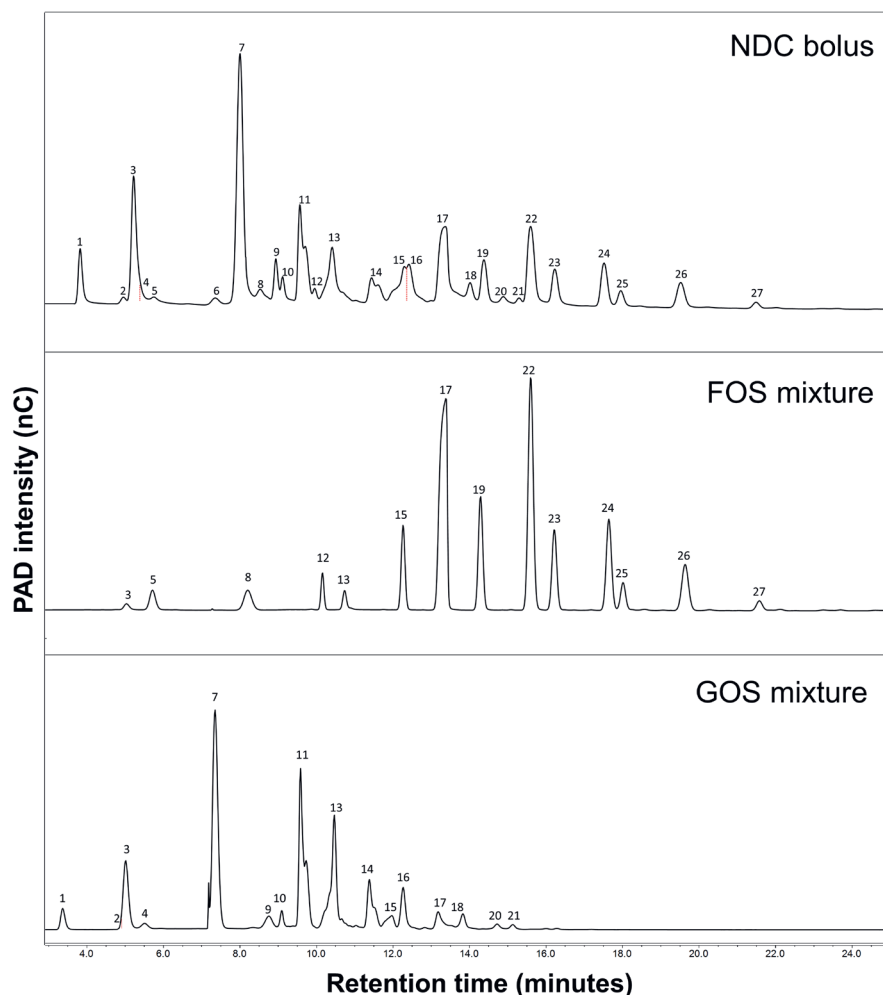


Figure 1. HPAEC-PAD elution patterns of the NDC bolus, the FOS mixture, and the GOS mixture.

The peaks are numbered 1-27, the corresponding compounds are described in Table 2. FOS, fructo-oligosaccharides; GOS, galacto-oligosaccharides; NDC, non-digestible carbohydrates; PAD, pulsed amperometric detection.

Table 2. Compounds present in the NDC bolus¹.

The peak area is expressed as relative abundance compared to the total area of all compounds in the NDC bolus, as analyzed by HPAEC-PAD. The NDC bolus elution pattern is shown in Figure 1. The sum of all percentages is 100% within sample.

Peak in chromatogram	Identification of peak	Structures of FOS compounds	Structures of GOS compounds ³	% of total NDC bolus
1	GOS DP2	-	β -D-Gal-(1 \leftrightarrow 1)- α -D-Glc β -D-Gal-(1 \leftrightarrow 1)- β -D-Glc	2.18 \pm 0.62
2	GOS DP3	-	No information available	0.30 \pm 0.18
3 ²	Glucose + galactose DP1	β -D-Glcp (glucose)	β -D-Glcp (glucose) β -D-Galp (galactose)	6.39 \pm 0.97
4	GOS DP2	-	β -D-Galp-(1 \rightarrow 6)-D-Galp	0.98 \pm 0.37
5 ²	Fructose DP1	β -D-Fru	-	0.85 \pm 0.20
6	GOS DP3	-	No information available	0.51 \pm 0.30
7 ²	Lactose DP2	-	β -D-Galp-(1 \rightarrow 6)-D-Glcp (<i>allo</i> -lactose) β -D-Galp-(1 \rightarrow 4)-D-Glcp (lactose)	17.66 \pm 1.40
8 ²	Sucrose DP2	β -D-Fru(2 \rightarrow 1)- α -D-Glc	-	1.74 \pm 0.35
9	GOS DP3	-	β -D-Galp-(1 \rightarrow 4)- β -D-Galp-(1 \rightarrow 6)-D-Glcp β -D-Galp-(1 \rightarrow 6)- β -D-Galp-(1 \rightarrow 4)-D-Glcp (6 galactosyllactose)	1.93 \pm 0.38
10	GOS DP2+ GOS DP4	-	β -D-Galp-(1 \rightarrow 4)-D-Galp	1.32 \pm 0.39
11	GOS DP2	-	No information available about DP4. β -D-Galp-(1 \rightarrow 2)-D-Glcp β -D-Galp-(1 \rightarrow 3)-D-Glcp	11.56 \pm 2.40
12	FOS DP3	GF2; β -D-Fru(2 \rightarrow 1)- β -D-Fru(2 \rightarrow 1)- α -DGlc (1-kestose)	-	1.23 \pm 0.32
13	GOS DP3 + FOS DP2	F2; β -D-Fru(2 \rightarrow 1)- β -D-Fru (inulobiose)	β -D-Galp-(1 \rightarrow 2)- β -D-Galp-(1 \rightarrow 4)-D-Glcp β -D-Galp-(1 \rightarrow 2)- β -D-Galp-(1 \rightarrow 6)-D-Glcp β -D-Galp-(1 \rightarrow 3)- β -D-Galp-(1 \rightarrow 6)-D-Glcp β -D-Galp-(1 \rightarrow 4)- β -D-Galp-(1 \rightarrow 4)-D-Glcp (4 galactosyllactose)	10.15 \pm 1.81
14	GOS DP3+DP4	-	β -D-Galp-(1 \rightarrow 4)- β -D-Galp-(1 \rightarrow 2)-D-Glcp β -D-Galp-(1 \rightarrow 4)- β -D-Galp-(1 \rightarrow 3)-D-Glcp β -D-Galp-(1 \rightarrow 4)- β -D-Galp-(1 \rightarrow 2)- β -D-Galp-(1 \rightarrow 4)-D-Glcp β -D-Galp-(1 \rightarrow 2)- β -D-Galp-(1 \rightarrow 4)-D-Glcp	4.70 \pm 0.72

15	GOS DP4 + FOS DP4	GF3: β -D-Fru(2 \rightarrow 1)- β -D-Fru(2 \rightarrow 1)- β -D-Fru(2 \rightarrow 1)- α -DGlc (nyctose) D-Fru(2 \rightarrow 1)- α -DGlc (nyctose)	β -D-Galp(1 \rightarrow 4)- β -D-Galp(1 \rightarrow 2)- $[\beta$ -D-Galp(1 \rightarrow 6)-]D-Glcp β -D-Galp(1 \rightarrow 2)- $[\beta$ -D-Galp(1 \rightarrow 4)- β -D-Galp(1 \rightarrow 6)-]D-Glcp β -D-Galp(1 \rightarrow 4)- β -D-Galp(1 \rightarrow 4)- β -D-Galp(1 \rightarrow 6)-D-Glcp β -D-Galp(1 \rightarrow 4)- β -D-Galp(1 \rightarrow 4)- β -D-Galp(1 \rightarrow 4)-D-Glcp	4.34 \pm 0.41
16	GOS DP4	-	β -D-Galp(1 \rightarrow 4)- β -D-Galp(1 \rightarrow 4)- β -D-Galp(1 \rightarrow 4)-D-Glcp	3.12 \pm 0.56
17	GOS DP4+DP5 + FOS DP3	F3: β -D-Fru(2 \rightarrow 1)- β -D-Fru(2 \rightarrow 1)- β -D-Fru (inulotriose) D-Fru (inulotriose)	β -D-Galp(1 \rightarrow 4)- β -D-Galp(1 \rightarrow 2)-D-Glcp β -D-Galp(1 \rightarrow 4)- β -D-Galp(1 \rightarrow 4)- β -D-Galp(1 \rightarrow 3)-D-Glcp β -D-Galp(1 \rightarrow 2)- $[\beta$ -D-Galp(1 \rightarrow 4)- β -D-Galp(1 \rightarrow 4)- β -D-Galp(1 \rightarrow 6)-] D-Glcp β -D-Galp(1 \rightarrow 4)- β -D-Galp(1 \rightarrow 2)- $[\beta$ -D-Galp(1 \rightarrow 6)-] D-Glcp β -D-Galp(1 \rightarrow 4)- β -D-Galp(1 \rightarrow 2)- $[\beta$ -D-Galp(1 \rightarrow 4)- β -D-Galp(1 \rightarrow 6)-] D-Glcp β -D-Galp(1 \rightarrow 2)- $[\beta$ -D-Galp(1 \rightarrow 4)- β -D-Galp(1 \rightarrow 4)- β -D-Galp(1 \rightarrow 6)-] D-Glcp β -D-Galp(1 \rightarrow 4)- β -D-Galp(1 \rightarrow 4)- β -D-Galp(1 \rightarrow 2)- $[\beta$ -D-Galp(1 \rightarrow 6)-] D-Glcp β -D-Galp(1 \rightarrow 4)- β -D-Galp(1 \rightarrow 4)- β -D-Galp(1 \rightarrow 2)- $[\beta$ -D-Galp(1 \rightarrow 6)-] D-Glcp β -D-Galp(1 \rightarrow 4)- β -D-Galp(1 \rightarrow 2)- $[\beta$ -D-Galp(1 \rightarrow 4)- β -D-Galp(1 \rightarrow 6)-] D-Glcp	9.64 \pm 1.76
18	GOS DP4+DP5	-	β -D-Galp(1 \rightarrow 4)- β -D-Galp(1 \rightarrow 4)- β -D-Galp(1 \rightarrow 4)-D-Glcp	1.63 \pm 0.32
19	FOS DP5	GF4: β -D-Fru(2 \rightarrow 1)- β -D-Fru(2 \rightarrow 1)- β -D-Fru(2 \rightarrow 1)- β -D-Fru(2 \rightarrow 1)- α -DGlc (1- β -fructofuranosyl nyctose)	-	3.19 \pm 0.54
20	GOS DP5	-	β -D-Galp(1 \rightarrow 4)- β -D-Galp(1 \rightarrow 4)- β -D-Galp(1 \rightarrow 4)-D-Glcp β -D-Galp(1 \rightarrow 4)- β -D-Galp(1 \rightarrow 4)- β -D-Galp(1 \rightarrow 4)-D-Glcp β -D-Galp(1 \rightarrow 4)- β -D-Galp(1 \rightarrow 4)- β -D-Galp(1 \rightarrow 4)-D-Glcp	0.84 \pm 0.23
21	GOS DP6	-	β -D-Galp(1 \rightarrow 4)- β -D-Galp(1 \rightarrow 4)- β -D-Galp(1 \rightarrow 4)- β -D-Galp(1 \rightarrow 4)-D-Glcp	0.51 \pm 0.10
22	FOS DP4	F4: β -D-Fru(2 \rightarrow 1)- β -D-Fru(2 \rightarrow 1)- β -D-Fru(2 \rightarrow 1)- β -D-Fru (inulotetraose)	-	6.32 \pm 1.55
23	FOS DP6	GF5: β -D-Fru(2 \rightarrow 1)- β -D-Fru(2 \rightarrow 1)- β -D-Fru(2 \rightarrow 1)- β -D-Fru(2 \rightarrow 1)- β -D-Fru(2 \rightarrow 1)- α -DGlc	-	2.16 \pm 0.50
24	FOS DP5	F5: β -D-Fru(2 \rightarrow 1)- β -D-Fru(2 \rightarrow 1)- β -D-Fru(2 \rightarrow 1)- β -D-Fru(2 \rightarrow 1)- β -D-Fru (inulopentaose)	-	3.10 \pm 0.46

25	FOS DP7	GF6: β-D-Fru(2→1)-β-D-Fru(2→1)-β-D-Fru(2→1)-β-D-Fru(2→1)-β-D-Fru(2→1)-β-D-Fru(2→1)-α-DGlc Fru(2→1)-β-D-Fru(2→1)-β-D-Fru(2→1)-β-D-Fru(2→1)-β-D-Fru(2→1)-β-D-Fru(2→1)-β-D-Fru(2→1)-β-D-Fru(2→1)-β-D-Fru(2→1)-β-D-Fru(2→1)-β-D-Fru(2→1)-α-DGlc (inulo-hexaose) GF7: β-D-Fru(2→1)-β-D-Fru(2→1)-β-D-Fru(2→1)-β-D-Fru(2→1)-β-D-Fru(2→1)-β-D-Fru(2→1)-β-D-Fru(2→1)-β-D-Fru(2→1)-α-DGlc	- -	1.10 ± 0.18 2.08 ± 0.30
26	FOS DP6 + EOS DP8		-	
27	FOS DP7	F7: β-D-Fru(2→1)-β-D-Fru(2→1)-β-D-Fru(2→1)-β-D-Fru(2→1)-β-D-Fru(2→1)-β-D-Fru(2→1)-β-D-Fru(2→1)-β-D-Fru(2→1)-β-D-Fru(2→1)-β-D-Fru(2→1)-β-D-Fru(2→1)-α-DGlc (inulo-eptaose)	-	0.46 ± 0.05

¹Data is represented as mean ± SD, n=5 NDC boluses used during different test days during two clinical trials. ²Compound was quantified using commercial standards.
³Tentative peak identification of a GOS compound based on previous characterization by van Leeuwen et al. (19), Coulter et al. (44), and adopted from Führen et al. (46).
DP; degree of polymerization; F, fructose series attached to a fructose moiety; FOS, fructo-oligosaccharides; Fru, fructose; GF, fructose series attached to a glucose moiety; Gal, galactose; Glc, glucose; GOS, galacto-oligosaccharides; NDC, non-digestible carbohydrates.

The fate of FOS and GOS in the intestine over time

FOS and GOS appeared in the distal ileum or proximal colon within 60-120 minutes after consumption (**Figure 2**). The appearance and disappearance of the non-digestible fraction of FOS and GOS were similar (**Figure 2 A, B**), namely decreasing from 60 to 270 minutes after bolus consumption, with traces remaining from 270-350 minutes. Within person (**Figure 2 C-I**), the concentration of the NDC bolus compounds over time generally had the same pattern as the concentrations of PEG-4000 over time in the intestine. Overall, the similar behavior of FOS and GOS compared to PEG-4000 implies the removal of FOS and GOS from the aspiration site due to transit through the small intestine.

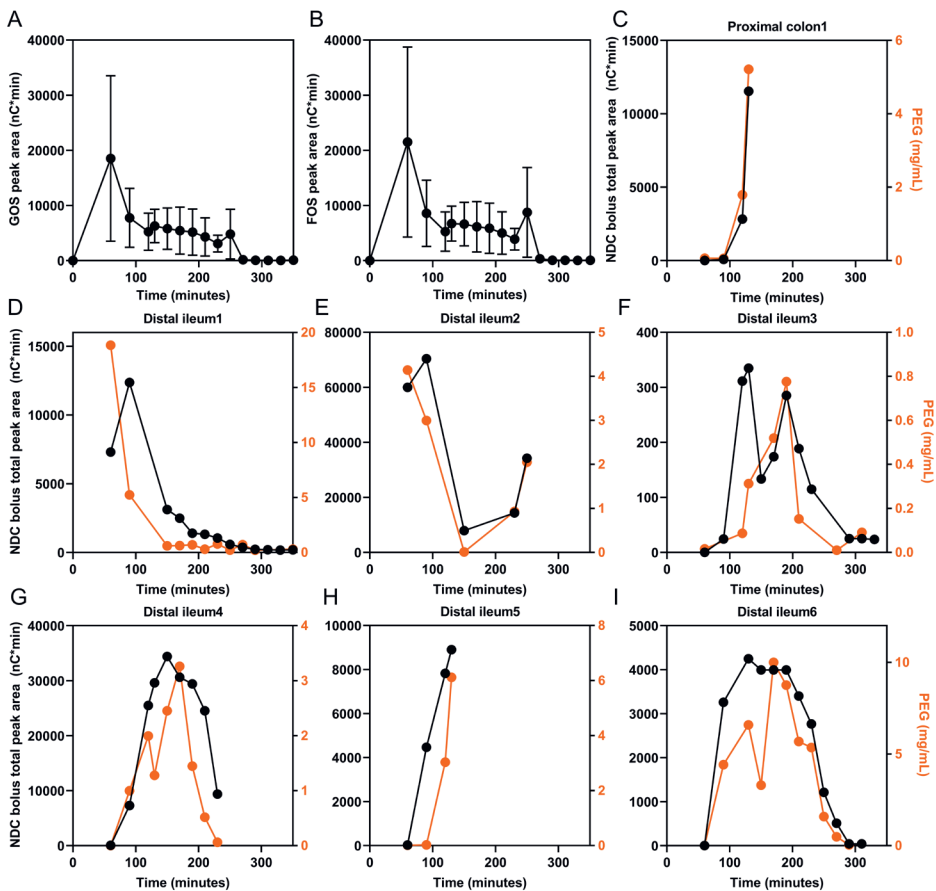


Figure 2. The fate of the NDC bolus compounds in distal ileum or proximal colon of healthy male subjects.

The amount of GOS mixture (A), or the FOS mixture (B) is shown as mean \pm SD, $n=7$ subjects. Compounds from FOS and GOS mixtures that co-eluted (peak #13, peak #15, and peak #17) are included in both the FOS and GOS peak area. The total peak area of all NDC bolus compounds, and the concentrations of PEG-4000

over time in every subject (C-I). The NDC bolus peak area is shown by the black line (left y-axis), and the PEG-4000 concentrations are shown by the orange line (right y-axis). The starting time point of appearance differs per individual, dependent on when the first sample could be obtained. The digestible carbohydrates of the mixtures, glucose+galactose, fructose, sucrose, and lactose, are excluded from this figure. FOS, fructo-oligosaccharides; GOS, galacto-oligosaccharides; NDC, non-digestible carbohydrates; PEG, polyethylene glycol.

FOS in the intestine over time

The digestibility of individual compounds in the prebiotic fraction of the FOS mixture in the small intestine was evaluated (**Figure 3**). The mean estimated recovery of this FOS fraction was $96\pm 25\%$ ($n=7$ subjects). Over time, the relative abundances of the FOS compounds in the intestine indeed remained constant and were the same as those in the NDC bolus. Only after 270 minutes, relatively decreased higher DP fractions and increased GOS DP3+FOS DP2 (F2) (peak #13) was found in three subjects (**Figure 3A, F, H**). However, the absolute amounts of peak #13 decreased (**Supplementary Figure 2**) in a similar manner as PEG-4000. This makes it unlikely that GOS DP3+FOS DP2 was formed upon degradation of compounds with $DP\geq 3$. After hydrolysis of constituents in FOS, mainly fructose, and to a lower extent glucose, would remain, but traces of fructose and sucrose were detected only at the first time points of sampling, in maximum of two or four subjects, respectively (**Supplementary Table 1**). This indicates no hydrolysis of FOS or most likely fast fructose absorption in the small intestine. Minor shifts in the abundances of FOS compounds $DP\geq 2$ were found over time in the distal ileum compared to those ingested, which indicates FOS was mostly resistant to digestion in the small intestine.

GOS in the intestine over time

We evaluated the digestibility of individual compounds in the GOS mixture in the small intestine (**Figure 4**). The digestible carbohydrates in this mixture, glucose, galactose, and lactose, are excluded from this figure to visualize changes in the prebiotic fraction (GOS DP2-6). The mean estimated recovery of GOS was $76\pm 28\%$ ($n=7$ subjects), which indicates that some digestion occurred in the small intestine. When comparing the relative abundance profiles of in the intestine compared to the bolus, clearly GOS DP3-6 did not change before 250 minutes, while the relative abundance of the prebiotic GOS dimers (DP2 fraction, peaks #1, #4, #10, #11) decreased in the small intestine of all subjects. Traces of glucose+galactose, as well as lactose, were detected in the distal ileum or proximal colon of all subjects over time (**Supplementary Table 1**). In the ileum of four subjects, negligible concentrations of glucose+galactose were measured already before the arrival of other NDC bolus constituents. Overall, a lowered abundance of the prebiotic GOS DP2 fraction was found in the distal ileum and proximal colon, while abundances of GOS DP3-6 did not change.

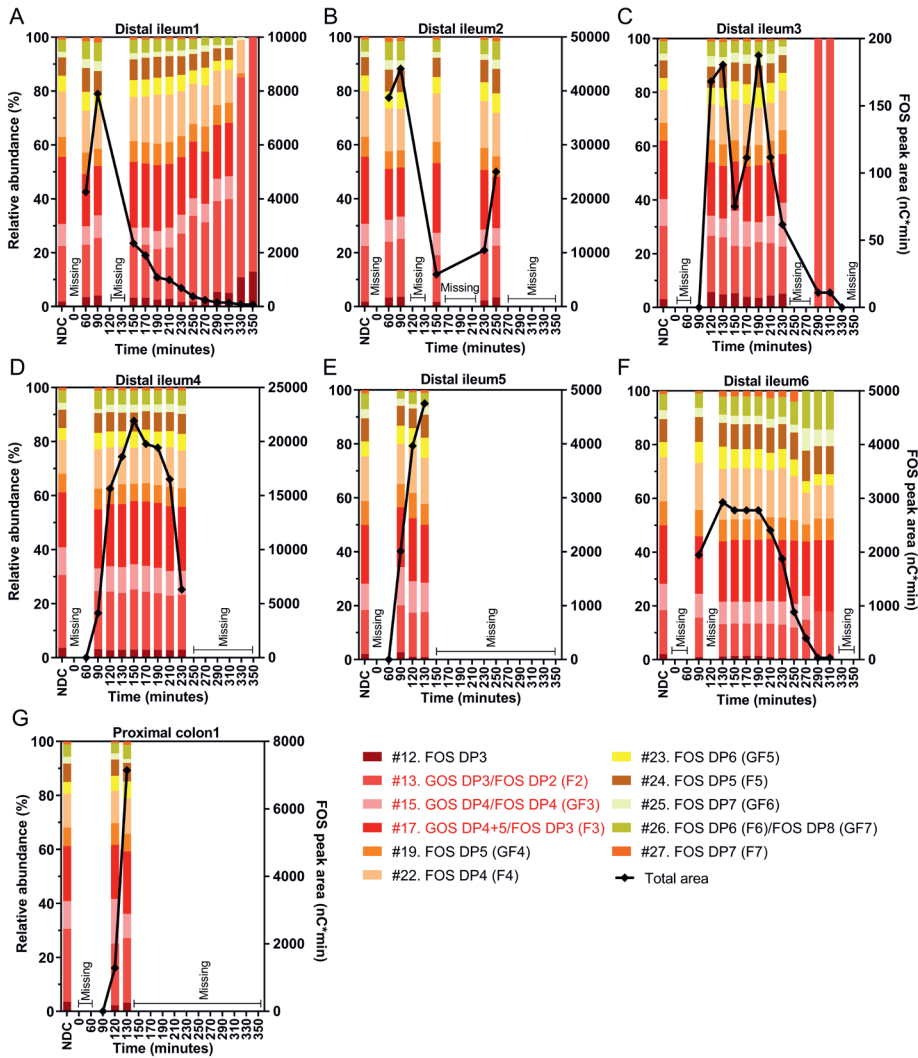


Figure 3. The profile of the compounds originating from the chicory-derived FOS mixture in the distal ileum or proximal colon of healthy male subjects over time after NDC consumption.

The relative abundances are shown on the left y-axis, and the diamond shapes connected by the black line show the area of compounds from the FOS mixture, as measured by HPAEC-PAD (right y-axis). Compounds FOS DP2 (F2, peak #13), FOS DP4 (GF3, peak #15), and FOS DP3 (F3, peak #17) co-eluted with a compound from the GOS mixture, indicated in red in the legends. The digestible carbohydrates, glucose+galactose, fructose, and sucrose, are excluded from this figure. The numbers in the legends correspond with peaks in the chromatograms in Figure 1. Missing samples were the result of sampling difficulties. DP, degree of polymerization; F, fructose series attached to a fructose moiety; FOS, fructo-oligosaccharides; GF, fructose series attached to a glucose moiety; GOS; galacto-oligosaccharides.

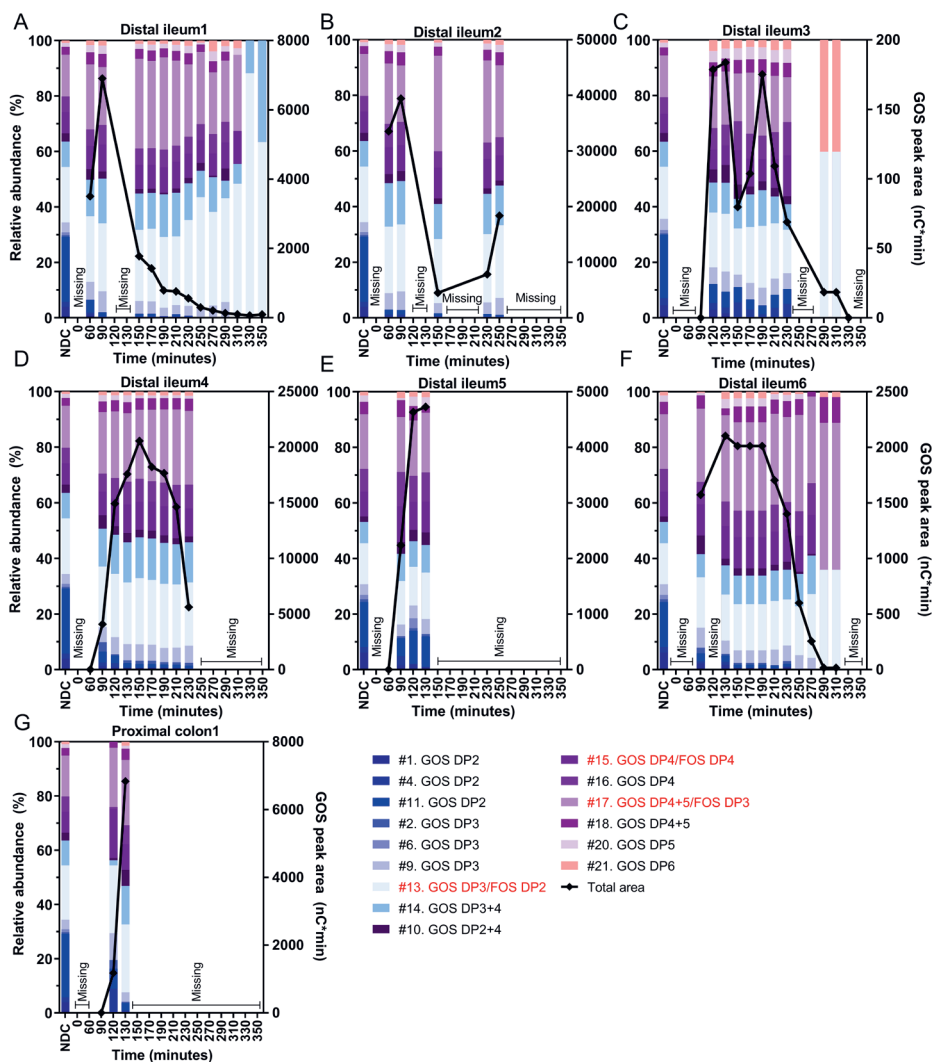


Figure 4. The profile of the compounds originating from the GOS mixture in the distal ileum or proximal colon of healthy male subjects over time after NDC consumption.

The relative abundances are shown on the left y-axis, and the diamond shapes connected by the black line show the area of compounds from the GOS mixture, as measured by HPAEC-PAD (right y-axis). Compounds GOS DP3 (peak #13), GOS DP4 (peak #15), and GOS DP4 (peak #17) co-eluted with a compound from the FOS mixture, indicated in red in the legends. The digestible carbohydrates, namely glucose+galactose and lactose, are excluded from this figure. The numbers in the legends correspond with peaks in the chromatograms in Figure 1. Missing samples were the result of sampling difficulties. DP, degree of polymerization; F, fructose series attached to a fructose moiety; FOS, fructo-oligosaccharides; GF, fructose series attached to a glucose moiety; GOS, galacto-oligosaccharides.

GOS DP2 compounds in the intestine over time

Since especially the GOS DP2 fraction decreased during transit in the small intestine, we have plotted the kinetics of all GOS dimers separately (Figure 5, $n=7$ subjects). The mean relative abundance of the total GOS DP2 fraction in the distal ileum after NDC consumption was lower compared to those in the NDC bolus (Figure 5A). Especially the relative abundances of β -D-Gal-(1 \leftrightarrow 1)- α -D-Glc+ β -D-Gal-(1 \leftrightarrow 1)- β -D-Glc (Figure 5B) and β -D-Gal-(1 \rightarrow 2)-D-Glc+ β -D-Gal-(1 \rightarrow 3)-D-Glc (Figure 5E) were decreased. Also, the absolute amounts of these dimers in the intestine were reduced (Supplementary Figure 1). The mean estimated recoveries (i.e., arrival) in the distal ileum or proximal colon at time points 60-130 minutes after consumption were $22.8\pm 11.1\%$ for β -D-Gal-(1 \leftrightarrow 1)- α -D-Glc+ β -D-Gal-(1 \leftrightarrow 1)- β -D-Glc and $19.3\pm 19.1\%$ for β -D-Gal-(1 \rightarrow 2)-D-Glc+ β -D-Gal-(1 \rightarrow 3)-D-Glc (Supplementary Table 2). In contrast, β -D-Gal-(1 \rightarrow 6)-D-Gal (Figure 5C) and β -D-Gal-(1 \rightarrow 4)-D-Gal+GOS DP4 (Figure 5D) had higher recoveries, namely $43.7\pm 24.6\%$ and $68.0\pm 38.5\%$, respectively (Supplementary Table 2). Overall, the digestibility of the GOS DP2 fraction was dependent on the type of linkage between the monomers, with β (1 \rightarrow 6) and β (1 \rightarrow 4) linked dimers being more resistant to digestion in the small intestine than β (1 \leftrightarrow 1) and β (1 \rightarrow 2)+ β (1 \rightarrow 3) linked dimers.

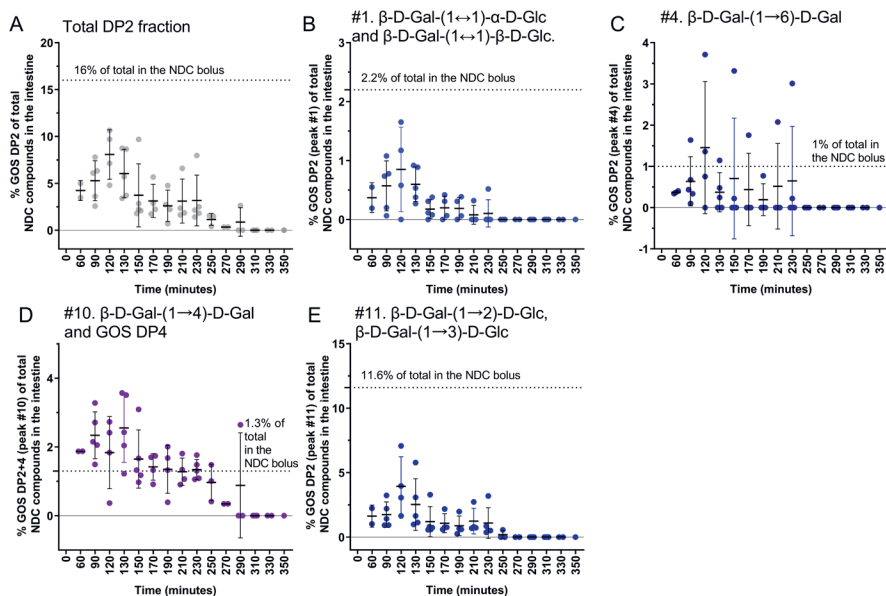


Figure 5. Relative abundances of the GOS dimers in the distal ileum or proximal colon of healthy male subjects over time.

(A) The total GOS DP2 fraction, (B) GOS DP2 peak #1, (C) GOS DP2 peak #4, (D) GOS DP2+4 (peak#10), and (E) GOS DP2 (peak #11) as a percentage of all NDC compounds detected in the intestine over time. The means \pm SDs are shown, $n=7$ subjects. The dots show the individual values. The dotted line indicates the GOS DP2 mean relative abundance (%) in the NDC bolus ($n=$ NDC boluses). Lactose is excluded from the DP2 fraction. DP, degree of polymerization; Gal, galactose; Glc, glucose; GOS, galacto-oligosaccharides.

Lactose in the intestine over time

Lactose can be digested in the small intestine by the brush-border enzyme lactase. **Figure 6** illustrates the lactose concentrations in the distal ileum or proximal colon of all subjects over time. The initial mean estimated lactose recovery in the intestine was $42.1 \pm 0.3\%$ at 60 minutes, $40.1 \pm 4.5\%$ at 90 minutes, $40.0 \pm 7.0\%$ at 120 minutes, and $36.3 \pm 7.9\%$ at 130 minutes (**Supplementary Table 2**). The decrease in lactose over time (**Figure 6**, blue line) followed the decrease of PEG-4000 (**Figure 6**, grey line). This shows the removal of lactose from the aspiration site by peristalsis and not digestion. The NDC bolus contained a mean amount (\pm SD) of 1.7 ± 0.46 g lactose (8.5 mg/mL). Even though we included lactose tolerant subjects, a fraction of lactose likely coming from the 1.7 g lactose in the NDC bolus was recovered at the end of the small intestine or in the proximal colon.

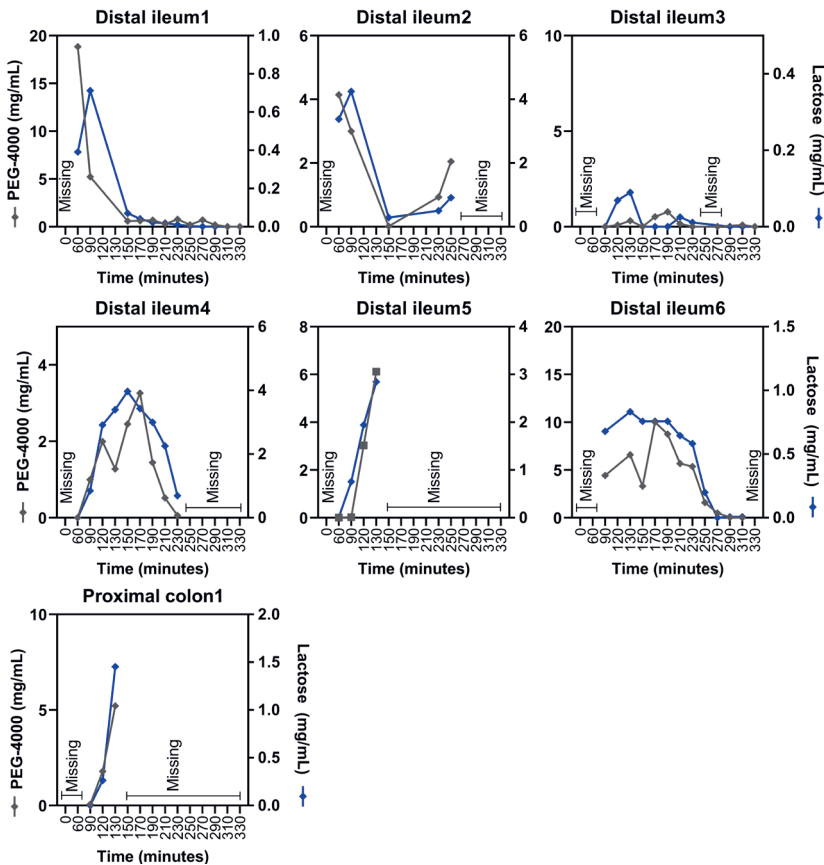


Figure 6. Presence of lactose over time in the distal ileum or proximal colon of healthy male subjects over time.

The PEG-4000 concentration is shown by the grey line on the left y-axis, and the lactose concentration is shown by the blue line (right y-axis). Lactose originated from the GOS mixture. Missing = no intestinal sample could be collected at this time point. PEG, polyethylene glycol.

The presence of predicted FOS or GOS degrading enzymes in the intestinal samples

Finally, we aimed to address the potential role of the small intestinal microbiota in the hydrolysis of the GOS dimers. Hence, selected microbial genes were derived from the total predicted genome, which was predicted based on the microbiota composition (16S rRNA gene sequencing data). We compared the relative abundance of microbial β -galactosidase in the ileal samples and feces (**Table 3**). Feces is used as comparison, because it has been shown that human fecal bacteria efficiently break down FOS and GOS *in vitro*, and hence we expected a higher predicted abundance. The predicted β -galactosidase relative abundance was significantly lower in ileum microbiota ($0.245 \pm 0.109\%$) compared to fecal microbiota ($0.506 \pm 0.108\%$). Fructan β -fructosidase, involved in FOS breakdown, also had a significantly lower relative abundance in the ileum versus fecal microbiota, while sucrase had a significantly higher relative abundance compared to fecal microbiota.

Table 3. The abundance¹ of selected microbial genes involved in the breakdown of FOS and GOS of luminal content and feces of healthy male subjects.

Microbial gene	EC number	KO number	Relative abundance distal ileum, % (n = 6 subjects, 52 samples)	Relative abundance feces, % (n = 7 subjects)	P-value ²
GOS breakdown					
β -galactosidase/ β -D-galactohydrolase	EC 3.2.1.23	K01190/ K12111/ K12308/ K12309	0.245 ± 0.109	0.506 ± 0.108	0.000 ^a
FOS breakdown					
Fructan β -fructosidase/ β -D-fructohydrolase [*]	EC 3.2.1.80	K03332	0.016 ± 0.018	0.042 ± 0.025	0.001 ^a
Sucrase/ β -fructofuranosidase ^{**}	EC 3.2.1.26	K01193	0.236 ± 0.146	0.097 ± 0.030	0.000 ^a

¹Data are presented as mean relative abundance (%) of the total genes present in the predicted microbial genome of the sample \pm SD. ²The abundances of the selected genes relative to the total genes in the ileum and feces were compared using a non-parametric independent samples test. Because of the high variability in microbiota composition during the day (chapter 5), all samples collected in the intestine are treated as an independent observation. ^{*}Hydrolysis of terminal, non-reducing (2 \rightarrow 1) β -D-fructofuranose residues in fructans and sucrose. ^{**}The substrate includes sucrose. Endo-inulinase (EC 3.2.1.7) was not detected in the dataset. EC, Enzyme Commission number; FOS, fructo-oligosaccharides; GOS, galacto-oligosaccharides; KO, KEGG Ortholog.

Discussion

We investigated the digestibility of all constituents of FOS and GOS in the human small intestine in detail, including the digestible mono- and dimers. The relative abundances

of FOS compounds in the distal ileum or proximal colon of all subjects were comparable to those ingested, whereas a reduction in GOS dimers was observed. The digestible dimer lactose present in the GOS mixture was still partly present at the end of the small intestine or the proximal colon of most participants.

FOS are not digested in the distal small intestine

It has been shown in a previous study that only the GF3 fraction of FOS was slightly subjected to digestion in an *in vitro* static digestion model (2 hours incubation, 4-6% hydrolysis) (47). In another previous *in vitro* study, using rat small intestine extract, 15% hydrolysis of FOS after 120 minutes of digestion was reported (34). Based on these findings, we expected minor digestion of FOS in the human small intestine. Indeed, 96% of FOS was recovered in the distal small intestine or upon arrival in the proximal colon. In healthy and ileostomy subjects slightly lower recoveries from the small intestine were reported for FOS (89±9%, (38)) or inulin (87±4%, (39)), respectively. These recoveries were calculated based on the total ileostomy effluent excretion (39) or after infusing known PEG-4000 concentrations at a constant rate proximal to the aspiration site to estimate the total ileal output, and consequently the total output of FOS (38). The profiles of both FOS F2-F7 fractions (Fn series) and FOS GF2-GF7 fractions (GFn series) in the human small intestine were comparable to the ratios in the NDC bolus. The stable profiles in our study, in line with previous findings for FOS GF2, GF3, and GF4 (38), clearly indicate a negligible breakdown of FOS. When digestive enzymes or microbiota degrade fructans, a specificity towards lower DP compounds can be expected (32, 34, 48, 49). In contrast to the GOS dimer digestion, we did not find digestion of FOS dimers (F2). This shows the resistance of β -(2,1) linked fructose units towards digestion. This confirms that not only DP and linkages between monomers determine resistance towards digestion, but also the monomer composition. Overall, FOS is minimally or not digested by host enzymes or hydrolyzed (33, 34, 50), nor absorbed (38), nor fermented by bacteria in the human small intestine.

Linkage- and size-dependent GOS DP2 digestion in the human small intestine, without digestion of DP≥3

To the best of our knowledge, we are the first to study the digestibility of GOS in the small intestine of human subjects. Several studies using *in vitro* static carbohydrate digestion models showed that GOS was hydrolyzed by small intestine brush-border enzymes from pigs or rats within two hours, namely 34% (34) and 33% (36) using rat enzymes, or 23-50% (dependent on the type of linkage) using pig enzymes (37). Based on these findings and the mean human intestinal transit time, some digestion by the brush-border enzymes was expected (36). Indeed, the assumed prebiotic and non-digestible GOS DP2 fraction was digested in a glycosidic-linkage dependent fashion, in line with previous findings in rats (51). GOS β (1↔1) and β (1→2)+ β (1→3) linked

dimers showed higher digestion of 77% and 81%, respectively, than GOS $\beta(1\rightarrow4)$ and $\beta(1\rightarrow6)$ linked dimers (32% and 56%, respectively). This linkage-specific breakdown can be clarified by the binding site of carbohydrases that better accommodates certain glycosidic linkages (52).

As previously shown, the small intestine bacteria can also ferment GOS (32, 53) with 31-82% degraded before 5 hours (32), but we did not detect fermentation end-products upon FOS:GOS consumption in the ileum (chapter 5). Differentiating between digestion by host lactase, which is a type of galactosidase, or degradation by microbial galactosidases is not possible, since lactase may be released into the intestinal lumen (54-56). Another explanation for the decreased GOS dimers could be the passage of intact di- or oligosaccharides across the intestinal wall as shown before (57-60), but we did not analyze the appearance of GOS in the blood or urine. In contrast to a study in rats (51), we showed that in the human intestine the relative abundances of GOS DP3-6 did not change compared to the abundances ingested via the bolus. This discrepancy may be explained by the small differences in hydrolyzing activity of disaccharidases between animals and humans (61). Overall, we show linkage-dependent GOS dimer digestion, while GOS DP \geq 3 is not digested in the small intestine of healthy subjects.

Glucose and galactose presence in the distal small intestine

Glucose and/or galactose were detected in the distal ileum or proximal colon of all subjects over time. Glucose and galactose could have originated from the consumed NDC bolus, although absorption takes place in the (proximal) jejunum at rates between 0.15 and 0.3 g/min (62-64). The NDC bolus only contained 0.36 g glucose+galactose, which was expected to be absorbed within minutes. Their presence could also have resulted from GOS DP2 breakdown (i.e., consisting of glucose and galactose monomers). A more likely explanation is interference in the analysis due to host compounds, for instance, mucus saccharides, in the intestinal aspirates with the same elution time as glucose+galactose. This hypothesis is corroborated by the finding that in four subjects, low concentrations of glucose+galactose were measured already before the arrival of other NDC constituents. However, four mucus sugars, galactosamine, glucosamine, N-acetylglucosamine, N-acetylgalactosamine, did not interfere with glucose+galactose detection. We may have sampled other (unknown) mucus or host digestive compounds while aspirating from the intestinal catheter.

Lactose presence in the distal small intestine of healthy Dutch adults

Surprisingly, some lactose was still recovered at the end of the small intestine or in the proximal colon of all participants. Since we did not observe breakdown of GOS DP \geq 3, the lactose fraction is expected to originate from the NDC bolus. Lactose is degraded by host lactase, highly abundant in the proximal jejunum and gradually

declining towards the ileum (65, 66). Therefore, we did not expect to detect lactose in the distal ileum or proximal colon. There was an initial loss of lactose after passage through the small intestine (52.5-72.1%), while 27.9-47.5% from the 1.7 g ingested lactose was still present. Afterwards, lactose removal is expected due to peristalsis rather than digestion in the distal ileum, because the removal of lactose was constant to the decrease of PEG-4000. The amount of lactose in the NDC bolus was much lower than the dose, 12-18 g, usually reported giving problems in lactose-intolerant persons (28), which were excluded in this study. All participants indicated to consume dairy products, for instance, milk or yogurt, without complaints such as bloating or flatulence (data not shown). There was no relation between age and lactose recovery and most subjects were below the age of 25. The supplements, including lactose, were dissolved in only water, which may have resulted in a rapid GI transit. It is known that when ingested via food, the intestinal content will have different physical characteristics, flow behavior (mixing), transit time (67) with consequent effects on nutrient digestion. Our test conditions may have limited the diffusion of lactose from the lumen to the mucosal epithelium (68). There is no literature stating that intestinal catheters cause nutrient malabsorption or influence digestive processes, although intubations may have decreased the small intestine residence of foods (69) or changed intestinal motor patterns (70). Overall, a portion of the ingested lactose, present in GOS, was detected at the end of the ileum or in the proximal colon of healthy Dutch subjects.

Measurement of compounds in the NDC bolus

We provided FOS and GOS together in one drink. By using HPAEC-based characterization we were able to distinguish most compounds coming from either FOS or GOS, but not all due to co-elution. Moreover, due to the co-elution of GOS isomers and oligomers with a different DP, not all individual GOS compounds in the complex GOS mixture could be annotated (71). Future research could benefit from applying a characterization method based on UHPLC-MS using a porous graphitic carbon column to further zoom in to individual GOS components (18). The used non-absorbable marker in this study, soluble PEG-4000, showed comparable flow behavior as FOS and GOS in the GI-tract, even though the molecular weight of PEG-4000 (~4000 g/mol) is higher than the molecular weights of FOS and GOS (*e.g.* FOS DP5: 828.7 g/mol). In human trials, PEG-4000 is commonly used and quantified in intestinal contents using a turbidimetric method as proposed by Hyden et al. already decades ago (72). As the turbidity of intestinal samples differed over time and is expected to be influenced by other factors besides only PEG, we used a more direct measurement to quantify PEG-4000. We detected PEG-4000 using high performance size-exclusion chromatography, but the presence of FOS and GOS interfered with quantification. In the end, we successfully applied a sandwich ELISA assay using a detection antibody that binds directly to the PEG-4000 backbone with a low detection limit (0.1 µg/mL) and

without interference from FOS, GOS, or fecal water without PEG.

Conclusions and implications

In this study, we confirmed that in the human small intestine, FOS/oligofructose chains of $DP \geq 2$ from chicory roots are not digested, absorbed, or fermented by bacteria in the small intestine. Similarly, GOS chains of $DP \geq 3$ were not digested in the small intestine of healthy adults. Nowadays there is increased interest in structure-function relationships of NDCs, since depending on the structure they can exert direct immunostimulatory effects through toll-like receptors or directly in immune cells (49, 73, 74), which are present mainly in the small intestine. Hence, GOS $DP \geq 3$ and FOS ≥ 2 structures can exert direct effects in this GI-tract region. GOS dimers were partially digested and/or absorbed in the small intestine in a linkage-specific fashion, showing the key role of the glycosidic linkage in GOS dimer digestion. Individual compounds with different linkages and DP have been shown to differ in bioactivity for fermentability in the colon with consequent health impact (22). One may speculate that studying the effects of GOS dimers derived from lactose on colonic processes is less relevant, since these may not all reach the colon as an available substrate *in vivo*. GOS mixtures can be structurally distinct, dependent on the source of enzymes used for the production (19). We tested GOS produced from lactose, thus our results may not apply directly to for instance GOS produced from lactulose. We provide direct evidence on the resistances of GOS (DP2) with distinct β -linkages in humans opening the future development of new tailored (potential) prebiotics, to increase the small intestine indigestibility of prebiotics.

Acknowledgements

We thank all participants in the study. Furthermore, we thank all medical personnel and master students for their practical work during the study. We thank FrieslandCampina, Sensus B.V., and Cooperatie AVEBE U.A. for providing the supplements, and all the consortium partners involved for the critical feedback during the development of the project. This research was performed in the public-private partnership 'CarboKinetics' coordinated by the Carbohydrate Competence Center (CCC, www.cccresearch.nl). CarboKinetics is financed by participating industrial partners Agrifirm Innovation Center B.V., Cooperatie AVEBE U.A., DSM Food Specialties B.V., FrieslandCampina Nederland B.V., Nutrition Sciences N.V., VanDrie Holding N.V. and Sensus B.V., and allowances of The Netherlands Organisation for Scientific Research (NWO). The funders had no role in data collection and analysis, or preparation of the manuscript.

References

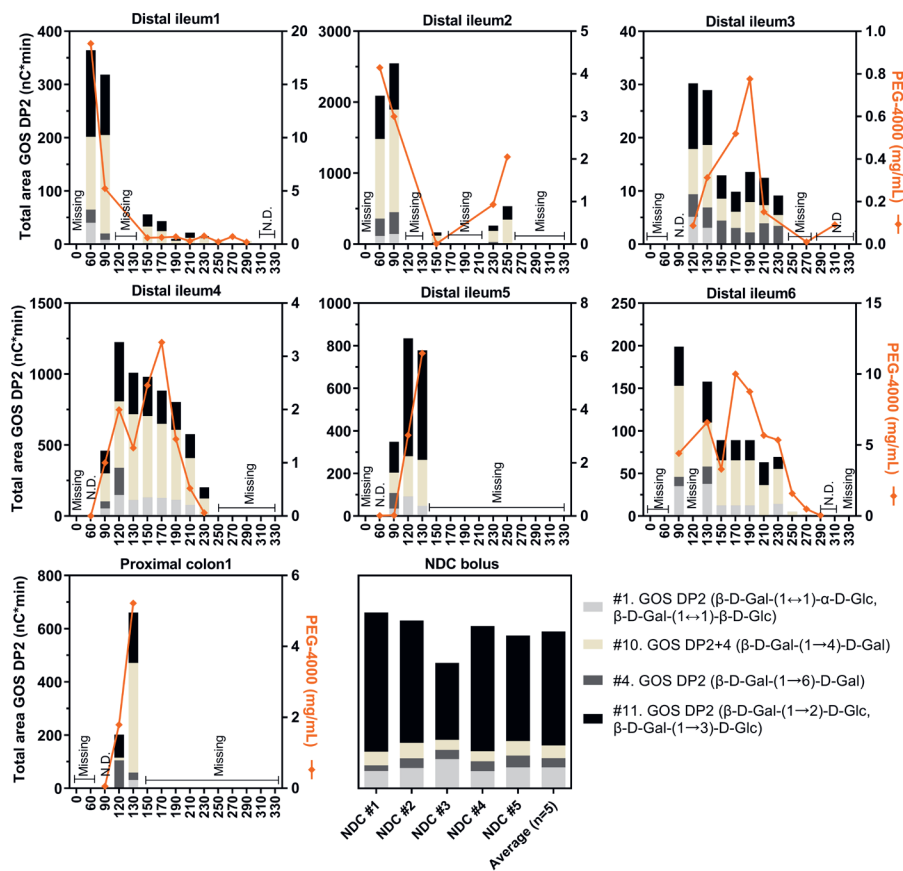
1. Slavin J. Fiber and prebiotics: Mechanisms and health benefits. *Nutrients*. 2013;5(4):1417-35.
2. Gibson GR, Roberfroid MB. Dietary modulation of the human colonic microbiota: Introducing the concept of prebiotics. *J Nutr*. 1995;125(6):1401-12.
3. O'Grady J, O'Connor EM, Shanahan F. Review article: Dietary fibre in the era of microbiome science. *Aliment Pharmacol Ther*. 2019;49(5):506-15.
4. Gibson GR, Hutkins R, Sanders ME, Prescott SL, Reimer RA, Salminen SJ, et al. Expert consensus document: The international scientific association for probiotics and prebiotics (isapp) consensus statement on the definition and scope of prebiotics. *Nat Rev Gastroenterol Hepatol*. 2017;14(8):491-502.
5. Verkhnyatskaya S, Ferrari M, de Vos P, Walvoort MTC. Shaping the infant microbiome with non-digestible carbohydrates. *Front Microbiol*. 2019;10(343).
6. de Luis DA, de la Fuente B, Izaola O, Aller R, Gutiérrez S, Morillo M. Double blind randomized clinical trial controlled by placebo with a fos enriched cookie on satiety and cardiovascular risk factors in obese patients. *Nutr Hosp*. 2013;28(1):78-85.
7. Watson D, O'Connell Motherway M, Schoterman MH, van Neerven RJ, Nauta A, van Sinderen D. Selective carbohydrate utilization by lactobacilli and bifidobacteria. *J Appl Microbiol*. 2013;114(4):1132-46.
8. Varney J, Barrett J, Scarlata K, Catsos P, Gibson PR, Muir JG. Fodmaps: Food composition, defining cutoff values and international application. *J Gastroenterol Hepatol*. 2017;32(S1):53-61.
9. Shoaib M, Shehzad A, Omar M, Rakha A, Raza H, Sharif HR, et al. Inulin: Properties, health benefits and food applications. *Carbohydr Polym*. 2016;147:444-54.
10. Moshfegh AJ, Friday JE, Goldman JP, Ahuja JKC. Presence of inulin and oligofructose in the diets of americans. *J Nutr*. 1999;129(7):1407S-11S.
11. Anderson-Dekkers I, Nouwens-Roest M, Peters B, Vaughan E. Chapter 17 - inulin. In: Phillips GO, Williams PA, editors. *Handbook of hydrocolloids (third edition)*: Woodhead Publishing; 2021. p. 537-62.
12. Flamm G, Glinemann W, Kritchevsky D, Prosky L, Roberfroid M. Inulin and oligofructose as dietary fiber: A review of the evidence. *Crit Rev Food Sci Nutr*. 2001;41(5):353-62.
13. Singh RS, Chauhan K, Kennedy JF. A panorama of bacterial inulinases: Production, purification, characterization and industrial applications. *Int J Biol Macromol*. 2017;96:312-22.
14. Conklin KA, Yamashiro KM, Gray GM. Human intestinal sucrase-isomaltase. Identification of free sucrase and isomaltase and cleavage of the hybrid into active distinct subunits. *J Biol Chem*. 1975;250(15):5735-41.
15. Newburg DS, Ko JS, Leone S, Nanthakumar NN. Human milk oligosaccharides and synthetic galactosyloligosaccharides contain 3', 4-, and 6'-galactosyllactose and attenuate inflammation in human t84, ncm-460, and h4 cells and intestinal tissue ex vivo. *J Nutr*. 2016;146(2):358-67.
16. Brummer Y, Kaviani M, Tosh SM. Structural and functional characteristics of dietary fibre in beans, lentils, peas and chickpeas. *Food Res Int*. 2015;67:117-25.
17. Torres DPM, Gonçalves MdPF, Teixeira JA, Rodrigues LR. Galacto-oligosaccharides: Production, properties, applications, and significance as prebiotics. *Compr Rev Food Sci Food Saf*. 2010;9(5):438-54.
18. Logtenberg MJ, Donners KMH, Vink JCM, van Leeuwen SS, de Waard P, de Vos P, et al. Touching the high complexity of prebiotic vivinal galacto-oligosaccharides using porous graphitic carbon ultra-high-performance liquid chromatography coupled to mass spectrometry. *J Agric Food Chem*. 2020;68(29):7800-8.
19. van Leeuwen SS, Kuipers BJH, Dijkhuizen L, Kamerling JP. Comparative structural characterization of 7 commercial galacto-oligosaccharide (gos) products. *Carbohydr Res*. 2016;425:48-58.

20. Rodriguez-Colinas B, Kolida S, Baran M, Ballesteros AO, Rastall RA, Plou FJ. Analysis of fermentation selectivity of purified galacto-oligosaccharides by in vitro human faecal fermentation. *Appl Microbiol Biotechnol.* 2013;97(13):5743-52.
21. Ladirat SE, Schols HA, Nauta A, Schoterman MHC, Schuren FHJ, Gruppen H. In vitro fermentation of galacto-oligosaccharides and its specific size-fractions using non-treated and amoxicillin-treated human inoculum. *Bioact Carbohydr Diet Fibre.* 2014;3(2):59-70.
22. Akbari P, Fink-Gremmels J, Willems R, Difilippo E, Schols HA, Schoterman MHC, et al. Characterizing microbiota-independent effects of oligosaccharides on intestinal epithelial cells: Insight into the role of structure and size : Structure-activity relationships of non-digestible oligosaccharides. *Eur J Nutr.* 2017;56(5):1919-30.
23. Goh YJ, Klaenhammer TR. Genetic mechanisms of prebiotic oligosaccharide metabolism in probiotic microbes. *Annu Rev Food Sci Technol.* 2015;6:137-56.
24. Van Laere KM, Abee T, Schols HA, Beldman G, Voragen AG. Characterization of a novel beta-galactosidase from *Bifidobacterium adolescentis* dsm 20083 active towards transgalactooligosaccharides. *Appl Environ Microbiol.* 2000;66(4):1379-84.
25. Hinz SWA, van den Broek LAM, Beldman G, Vincken J-P, Voragen AGJ. B-galactosidase from *bifidobacterium adolescentis* dsm20083 prefers $\beta(1,4)$ -galactosides over lactose. *Appl Microbiol Biotechnol.* 2004;66(3):276-84.
26. Van Beers EH, Büller HA, Grand RJ, Einerhand AWC, Dekker J. Intestinal brush border glycohydrolases: Structure, function, and development. *Crit Rev Biochem Mol Biol.* 1995;30(3):197-262.
27. Asp N-G, Dahlqvist A. Human small intestine β -galactosidases: Specific assay of three different enzymes. *Anal Biochem.* 1972;47(2):527-38.
28. Swagerty Jr DL, Walling A, Klein RM. Lactose intolerance. *Am Fam Physician.* 2002;65(9):1845.
29. Cummings JH. Fermentation in the human large intestine: Evidence and implications for health. *Lancet (USA).* 1983.
30. Montoya CA, de Haas ES, Moughan PJ. Development of an in vivo and in vitro ileal fermentation method in a growing pig model. *J Nutr.* 2018;148(2):298-305.
31. Tian L, Bruggeman G, van den Berg M, Borewicz K, Scheurink AJW, Bruininx E, et al. Effects of pectin on fermentation characteristics, carbohydrate utilization, and microbial community composition in the gastrointestinal tract of weaning pigs. *Mol Nutr Food Res.* 2017;61(1):1600186.
32. van Trijp MPH, Rösch C, An R, Keshtkar S, Logtenberg MJ, Hermes GDA, et al. Fermentation kinetics of selected dietary fibers by human small intestinal microbiota depend on the type of fiber and subject. *Mol Nutr Food Res.* 2020;64(20):2000455.
33. Oku T, Tokunaga T, Hosoya N. Nondigestibility of a new sweetener, "neosugar," in the rat. *J Nutr.* 1984;114(9):1574-81.
34. Ferreira-Lazarte A, Olano A, Villamiel M, Moreno FJ. Assessment of in vitro digestibility of dietary carbohydrates using rat small intestinal extract. *J Agric Food Chem.* 2017;65(36):8046-53.
35. Ohtsuka K, Tsuji K, Nakagawa Y, Ueda H, Ozawa O, Uchida T, et al. Availability of 4' galactosyllactose (o-beta-d-galactopyranosyl-(1->4)-o-beta-d-galactopyranosyl-(1->4)- d-glucopyranose) in rat. *J Nutr Sci Vitaminol (Tokyo).* 1990;36(3):265-76.
36. Ferreira-Lazarte A, Montilla A, Mulet-Cabero A-I, Rigby N, Olano A, Mackie A, et al. Study on the digestion of milk with prebiotic carbohydrates in a simulated gastrointestinal model. *J Funct Foods.* 2017;33:149-54.
37. Ferreira-Lazarte A, Gallego-Lobillo P, Moreno FJ, Villamiel M, Hernandez-Hernandez O. In vitro digestibility of galactooligosaccharides: Effect of the structural features on their intestinal degradation. *J Agric Food Chem.* 2019;67(16):4662-70.
38. Molis C, Flourié B, Ouarne F, Gailing MF, Lartigue S, Guibert A, et al. Digestion, excretion, and energy value of fructooligosaccharides in healthy humans. *Am J Clin Nutr.* 1996;64(3):324-8.
39. Knudsen BKE, Hessov I. Recovery of inulin from jerusalem artichoke (*helianthus tuberosus* l.) in the small intestine of man. *Br J Nutr.* 1995;74(1):101-13.

40. Ellegård L, Andersson H, Bosaeus I. Inulin and oligofructose do not influence the absorption of cholesterol, or the excretion of cholesterol, ca, mg, zn, fe, or bile acids but increases energy excretion in ileostomy subjects. *Eur J Clin Nutr.* 1997;51(1):1-5.
41. PH van Trijp M, Wilms E, Ríos-Morales M, Masclee AA, Brummer RJ, Witteman BJ, et al. Using naso- and oro-intestinal catheters in physiological research for intestinal delivery and sampling in vivo: Practical and technical aspects to be considered. *Am J Clin Nutr.* 2021.
42. MacRae JC. The use of intestinal markers to measure digestive function in ruminants. *Proc Nutr Soc.* 1974;33(2):147-54.
43. Jonathan MC, van den Borne JJGC, van Wiechen P, Souza da Silva C, Schols HA, Gruppen H. In vitro fermentation of 12 dietary fibres by faecal inoculum from pigs and humans. *Food Chem.* 2012;133(3):889-97.
44. Coulier L, Timmermans J, Bas R, Van Den Dool R, Haaksman I, Klarenbeek B, et al. In-depth characterization of prebiotic galacto-oligosaccharides by a combination of analytical techniques. *J Agric Food Chem.* 2009;57(18):8488-95.
45. Douglas GM, Maffei VJ, Zaneveld JR, Yurgel SN, Brown JR, Taylor CM, et al. Picrust2 for prediction of metagenome functions. *Nat Biotechnol.* 2020;38(6):685-8.
46. Jori Führen MS, Lucía Peralta-Marzal, Christiane Rösch, Henk A. Schols and Michiel Kleerebezem. Synbiotic matchmaking in lactobacillus plantarum for enhanced in situ delivery in the intestinal tract. Chapter 3. Phenotypic and genetic characterisation of differential galacto-oligosaccharide utilisation in *Lactobacillus plantarum*. Wageningen University; 2021.
47. Nobre C, Sousa SC, Silva SP, Pinheiro AC, Coelho E, Vicente AA, et al. In vitro digestibility and fermentability of fructo-oligosaccharides produced by *aspergillus ibericus*. *J Funct Foods.* 2018;46:278-87.
48. Chonan O, Shibahara Sone H, Takahashi R, Ikeda M, Kikuchi Hayakawa H, Ishikawa F, et al. Undigestibility of galactooligosaccharides. *J Jpn Soc Food Sci.* 2004; 51: 28–33.
49. Logtenberg MJ, Akkerman R, An R, Hermes GDA, de Haan BJ, Faas MM, et al. Fermentation of chicory fructo-oligosaccharides and native inulin by infant fecal microbiota attenuates pro-inflammatory responses in immature dendritic cells in an infant-age-dependent and fructan-specific way. *Mol Nutr Food Res.* 2020;64(13):2000068.
50. Nilsson U, Öste R, Jägerstad M, Birkhed D. Cereal fructans: In vitro and in vivo studies on availability in rats and humans. *The Journal of nutrition.* 1988;118(11):1325-30.
51. Hernández-Hernández O, Marín-Manzano MC, Rubio LA, Moreno FJ, Sanz ML, Clemente A. Monomer and linkage type of galacto-oligosaccharides affect their resistance to ileal digestion and prebiotic properties in rats. *J Nutr.* 2012;142(7):1232-9.
52. Lee B-H, Rose DR, Lin AH-M, Quezada-Calvillo R, Nichols BL, Hamaker BR. Contribution of the individual small intestinal α -glucosidases to digestion of unusual α -linked glycemic disaccharides. *J Agric Food Chem.* 2016;64(33):6487-94.
53. Cecchini DA, Laville E, Laguerre S, Robe P, Leclerc M, Doré J, et al. Functional metagenomics reveals novel pathways of prebiotic breakdown by human gut bacteria. *PLoS One.* 2013;8(9):e72766.
54. Yeh K-Y, Yeh M, Pan P-c, Holt PR. Posttranslational cleavage of rat intestinal lactase occurs at the luminal side of the brush border membrane. *Gastroenterology.* 1991;101(2):312-8.
55. Quak SH, Brown GA, Booth IW, McNeish AS. The nature of small bowel luminal fluid lactase. *Clin Chim Acta.* 1991;204(1):145-54.
56. Hooton D, Lentle R, Monro J, Wickham M, Simpson R. The secretion and action of brush border enzymes in the mammalian small intestine. *Rev Physiol Biochem Pharmacol.* 2015:59-118.
57. Menzies IS. Absorption of intact oligosaccharide in health and disease. Portland Press Ltd.; 1974.
58. Bjarnason I, Macpherson A, Hollander D. Intestinal permeability: An overview. *Gastroenterology.* 1995;108(5):1566-81.
59. Difilippo E, Bettonvil M, Willems R, Braber S, Fink-Gremmels J, Jeurink PV, et al. Oligosaccharides in urine, blood, and feces of piglets fed milk replacer containing galacto-oligosaccharides. *J Agric Food Chem.* 2015;63(50):10862-72.

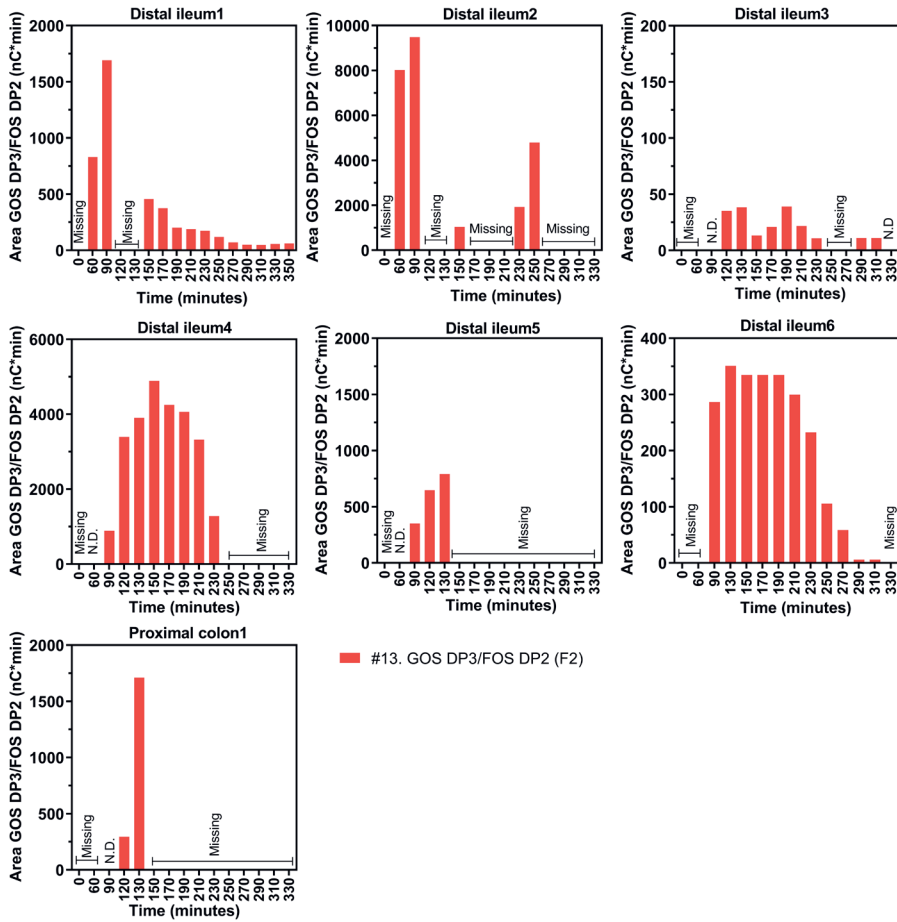
60. Goehring KC, Kennedy AD, Prieto PA, Buck RH. Direct evidence for the presence of human milk oligosaccharides in the circulation of breastfed infants. *PLoS One*. 2014;9(7):e101692.
61. Oku T, Tanabe K, Ogawa S, Sadamori N, Nakamura S. Similarity of hydrolyzing activity of human and rat small intestinal disaccharidases. *Clin Exp Gastroenterol*. 2011;4:155-61.
62. Beaugerie L, Flourié B, Pernet P, Achour L, Franchisseur C, Rambaud JC. Glucose does not facilitate the absorption of sorbitol perfused in situ in the human small intestine. *J Nutr*. 1997;127(2):341-4.
63. Gulliford MC, Bicknell EJ, Pover GG, Scarpello JH. Intestinal glucose and amino acid absorption in healthy volunteers and noninsulin-dependent diabetic subjects. *Am J Clin Nutr*. 1989;49(6):1247-51.
64. Jones BJ, Higgins BE, Silk DB. Glucose absorption from maltotriose and glucose oligomers in the human jejunum. *Clin Sci (Lond)*. 1987;72(4):409-14.
65. Antonowicz I, Lebenthal E. Developmental pattern of small intestinal enterokinase and disaccharidase activities in the human fetus. *Gastroenterology*. 1977;72(6):1299-303.
66. Forsgård RA. Lactose digestion in humans: Intestinal lactase appears to be constitutive whereas the colonic microbiome is adaptable. *Am J Clin Nutr*. 2019;110(2):273-9.
67. Lentle RG, Janssen PW. Physical characteristics of digesta and their influence on flow and mixing in the mammalian intestine: A review. *J Comp Physiol B*. 2008;178(6):673-90.
68. Grundy MML, Edwards CH, Mackie AR, Gidley MJ, Butterworth PJ, Ellis PR. Re-evaluation of the mechanisms of dietary fibre and implications for macronutrient bioaccessibility, digestion and postprandial metabolism. *Br J Nutr*. 2016;116(5):816-33.
69. Read NW, Al Janabi MN, Bates TE, Barber DC. Effect of gastrointestinal intubation on the passage of a solid meal through the stomach and small intestine in humans. *Gastroenterology*. 1983;84(6):1568-72.
70. Walton GE, van den Heuvel EG, Kosters MH, Rastall RA, Tuohy KM, Gibson GR. A randomised crossover study investigating the effects of galacto-oligosaccharides on the faecal microbiota in men and women over 50 years of age. *Br J Nutr*. 2012;107(10):1466-75.
71. Van Leeuwen SS, Kuipers BJ, Dijkhuizen L, Kamerling JP. 1h NMR analysis of the lactose/ β -galactosidase-derived galacto-oligosaccharide components of vivinal® GOS up to DP5. *Carbohydr Res*. 2014;400:59-73.
72. Hyden S. A turbidimetric method for the determination of higher polyethylene glycols in biological materials. *Kungliga Lantbrukshogskolans Annaler*. 1956;22:139-45.
73. Bermudez-Brito M, Faas MM, de Vos P. Modulation of dendritic-epithelial cell responses against *sphingomonas paucimobilis* by dietary fibers. *Sci Rep*. 2016;6(1):30277.
74. Bermudez-Brito M, Sahasrabudhe NM, Rösch C, Schols HA, Faas MM, de Vos P. The impact of dietary fibers on dendritic cell responses in vitro is dependent on the differential effects of the fibers on intestinal epithelial cells. *Mol Nutr Food Res*. 2015;59(4):698-710.

Supplementary Information



Supplementary Figure 1. The peak area of the GOS DP2 fractions in the GOS mixture and the PEG-4000 concentrations in the distal ileum or proximal colon of healthy man over time.

The GOS DP2 peak areas were analyzed by HPAEC-PAD (left y-axis), and the non-absorbable marker PEG-4000 concentrations are shown by the orange line (right y-axis). Missing samples were the result of sampling difficulties. N.D. = GOS DP2 was not detected in this sample. DP, degree of polymerization; GOS, galactooligosaccharides; PEG, polyethylene glycol.



Supplementary Figure 2. The presence of the GOS DP3 + FOS DP2 (F2) fraction over time in the distal ileum or colon of healthy man over time after NDC consumption.

This fraction was peak #13 in the chromatogram. N.D. = not detected in this sample. Missing samples were the result of sampling difficulties. DP, degree of polymerization; F, fructose series attached to a fructose moiety; FOS, fructo-oligosaccharides; GOS, galacto-oligosaccharides.

Supplementary Table 1. Concentrations of glucose+galactose, fructose, sucrose, and lactose in the distal ileum or colon of healthy man over time¹.

Time point (min)	Sample collected in number of subjects	Glucose+galactose ($\mu\text{g}/\text{mL}^2$), detected in number of subjects (n, %)	Fructose ($\mu\text{g}/\text{mL}$), detected in number of subjects	Sucrose ($\mu\text{g}/\text{mL}$), detected in number of subjects	Lactose (mg/mL), number of subjects
0	n = 0	-	-	-	-
60	n = 4	133 \pm 102 (n = 4/4, 100%)	55.1 (n = 1/4, 25%)	15.1 \pm 20.8 (n = 2/4, 50%)	0.94 \pm 1.6 (n = 3/4, 75%)
90	n = 7	355 \pm 408 (n = 7/7, 100%)	60.5 \pm 121 (n = 2/7, 29%)	49.5 \pm 101 (n = 3/7, 43%)	1.03 \pm 1.46 (n = 5/7, 71%)
120	n = 5	422 \pm 386 (n = 5/5, 100%)	228 \pm 395 (n = 2/5, 40%)	124 \pm 160 (n = 4/5, 80%)	1.20 \pm 1.20 (n = 5/5, 100%)
130	n = 4	342 \pm 243 (n = 4/4, 100%)	138 \pm 167 (n = 2/4, 50%)	209 \pm 171 (n = 4/4, 100%)	1.94 \pm 1.48 (n = 4/4, 100%)
150	n = 5	150 \pm 276 (n = 5/5, 100%)	0 (n=0/5, 0%)	103 \pm 224 (n = 4/5, 80%)	1.02 \pm 1.68 (n = 4/5, 80%)
170	n = 4	173 \pm 291 (n = 4/4, 100%)	0 (n=0/4, 0%)	405 (n = 1/4, 25%)	1.06 \pm 1.62 (n = 3/4, 75%)
190	n = 4	109 \pm 166 (n = 4/4, 100%)	0 (n=0/4, 0%)	88.8 \pm 170 (n = 2/4, 50%)	0.94 \pm 1.41 (n = 3/4, 75%)
210	n = 4	99.9 \pm 148 (n = 4/4, 100%)	0 (n=0/4, 0%)	70.2 \pm 135 (n = 2/4, 50%)	0.74 \pm 1.05 (n = 4/4, 100%)
230	n = 5	68.3 \pm 52.1 (n = 5/5, 100%)	294 (n = 1/5, 20%)	22.0 \pm 49.1 (n = 1/5, 20%)	0.36 \pm 0.33 (n = 5/5, 100%)
250	n = 3	72.9 \pm 70.1 (n = 3/3, 100%)	0 (n=0/3, 0%)	47.6 (n = 1/3, 33%)	0.37 \pm 0.48 (n = 3/3, 100%)
270	n = 2	27.1 \pm 16.0 (n = 2/2, 100%)	0 (n = 0/2, 0%)	0 (n = 0/2, 0%)	0.0007 \pm 0.001 (n = 1/2, 50%)
290	n = 3	7.90 \pm 3.77 (n = 3/3, 100%)	0 (n=0/3, 0%)	0 (n=0/3, 0%)	0.003 \pm 0.004 (n = 2/3, 67%)
310	n = 3	8.92 \pm 4.81 (n = 3/3, 100%)	0 (n=0/3, 0%)	0 (n=0/3, 0%)	0.003 \pm 0.004 (n = 2/3, 67%)
330	n = 2	14.1 \pm 14.6 (n = 2/2, 100%)	0 (n = 0/2, 0%)	0 (n = 0/2, 0%)	0 (n = 0/2, 0%)
350	n = 1	23.5 (n = 1/1, 100%)	0 (n = 0/1, 0%)	0 (n = 0/1, 0%)	0 (n = 0/1, 0%)
NDC bolus		Glucose+galactose² 1816 \pm 226 $\mu\text{g}/\text{mL}$ 363142 $\mu\text{g}/200$ mL (total in NDC bolus)	Fructose 1304 \pm 1087 $\mu\text{g}/\text{mL}$ 260800 $\mu\text{g}/200$ mL (total in NDC bolus)	Sucrose 2055 \pm 443 $\mu\text{g}/\text{mL}$ 441000 $\mu\text{g}/200$ mL (total in NDC bolus)	Lactose 8.48 \pm 2.05 mg/mL 1695 $\text{mg}/200$ mL (total in NDC bolus)

¹Data is represented as mean \pm SD, n=7 subjects. ²The concentrations of glucose+galactose were estimated from the glucose standard curve.

Supplementary Table 2. The recoveries of the GOS DP2 fractions and lactose in the distal ileum or proximal colon of healthy man¹.

Subject and age	Time point (min)	Recovery of peak 1 β-D-Gal-(1↔1)-α-D- Glc+ β-D-Gal-(1↔1)-β-D-Glc (%)	Recovery of peak 4 β-D-Gal-(1→6)-D-Gal (%)	Recovery of peak 10 β-D-Gal-(1→4)-D- Gal + GOS DP4 (%)	Recovery of peak 11 β-D-Gal-(1→2)-D- Glc+ β-D-Gal-(1→3)-D-Glc (%)	Recovery of lactose (%)
Distal ileum1,	60	33.7	64.0	>100	15.3	42.3
	>35y	3.7	17.6	>100	6.0	43.1
Distal ileum2,	60	11.1	72.0	>100	6.6	41.9
	<25y	12.0	79.4	>100	6.1	46.1
Distal ileum3,	120	44.9	59.8	99.5	20.4	34.9
	>35y	25.8	52.1	>100	16.4	43.7
Distal ileum4,	90	26.1	50.6	>100	11.8	36.1
	<25y	19.3	53.0	>100	11.9	33.3
Distal ileum5,	90	28.3	>100	>100	42.9	39.7
	<25y	34.9	0	>100	76.5	47.5
Distal ileum6,	90	28.7	26.9	>100	13.7	35.7
	<25y	19.6	31.7	79.4	9.1	27.9
P r o x i m a l colon1, >35y	120	13.6	>100	25.0	25.3	44.3
	130	16.9	17.6	>100	8.6	37.3
Mean	60	22.4±16.0	68.0±5.7	>100	11.0±6.2	42.1±0.3
	90	19.8±11.3	54.9±34.7	>100	16.1±15.4	40.1±4.5
	120	28.2±14.3	37.6±32.7	62.3±52.7	33.5±29.2	40.0±7.0
	130	20.8±4.6	33.8±17.3	89.7±14.6	11.4±4.4	36.3±7.9

¹The recoveries in the first two samples that could be collected within person during the test day are shown. DP; degree of polymerization, GOS; galacto-oligosaccharides.



Minor changes in the composition and function of the gut microbiota during a 12-week whole grain wheat or refined wheat intervention correlate with liver fat in overweight and obese adults

Mara P.H. van Trijp¹, Sophie Schutte¹, Diederik Esser¹, Suzan Wopereis², Femke P.M. Hoevenaars², Guido J.E.J. Hooiveld¹, Lydia A. Afman¹

¹ Nutrition, Metabolism and Genomics Group, Division of Human Nutrition and Health, Wageningen University, the Netherlands

² TNO, Netherlands Organization for Applied Scientific Research, Zeist, the Netherlands

Abstract

Background

Whole grain wheat (WGW) products are advocated as a healthy choice when compared to refined wheat (RW). One proposed mechanism for these health benefits may be via the microbiota, as WGW contains multiple fibers. WGW consumption has been proposed to ameliorate non-alcoholic fatty liver disease, in which microbiota may play a role. We investigated the effect of WGW versus RW intervention on the fecal microbiota composition and functionality, and correlated intervention-induced changes in bacteria with changes in liver health parameters in adults with overweight or obesity.

Methods

We used data of a 12-week double-blind, randomized controlled parallel trial to examine the effects of WGW (98 g/d) or RW (98 g/d) intervention on the fecal microbiota composition, predicted microbiota functionality, and stool consistency in 37 women and men (45-70y, BMI 25-35kg/m²). The changes in microbiota composition, measured using 16S rRNA gene sequencing, upon 12-week intervention were analyzed with non-parametric tests, and correlated to changes in liver fat and circulating concentrations of liver enzymes including ALT, AST, GGT, and SAA.

Results

The WGW intervention increased the relative abundances of *Ruminococcaceae_UCG-014* (baseline: 2.2±4.6%, Δ 0.51±4.2%), *Ruminiclostridium_9* (baseline: 0.065±0.11%, Δ 0.054±0.14%), and *Ruminococcaceae_NK4A214_group* (baseline: 0.37±0.56%, Δ 0.17±0.83%), and also the predicted pathway acetyl-CoA fermentation to butyrate II (baseline: 0.23±0.062%, Δ 0.035±0.059%) compared to RW intervention (p-values<0.05). A change in *Ruminococcaceae_NK4A214_group* was positively correlated to the change in liver fat, in both the WGW (ρ =0.54, p=0.026) and RW (ρ =0.67, p=0.024) group.

Conclusions

In middle-aged overweight and obese adults, a 12-week WGW intervention increased the relative abundance of a number of bacteria from the family Ruminococcaceae and increased predicted fermentation pathways when compared to RW intervention. Potential protective health effects of replacement of RW by WGW on metabolic organs, such as the liver, via modulation of the microbiota, deserve further investigation. This trial was registered at ClinicalTrials.gov as NCT02385149.

Keywords

fatty liver; human microbiota; overweight/obesity; refined wheat; whole grain wheat; fermentation

Introduction

The consumption of whole grains (WG) is associated with a lower risk of diseases such as diabetes type 2, cardiovascular diseases, obesity, and certain types of cancer in observational studies (1-3). In addition, consumption of WG rather than refined grain has been proposed to prevent non-alcoholic fatty liver disease (NAFLD) (4). The presence of numerous bioactive compounds makes whole grain, including whole grain wheat (WGW), nutritionally superior to refined wheat (RW) products (5). In refined products, both the bran and germ in the wheat kernel, which are rich sources of dietary fiber, polyphenols, B-complex vitamins, betaine, choline, and minerals, have been removed (5, 6). However, multiple previous WG interventions in human subjects have reported conflicting results in improvements in health parameters such as insulin sensitivity and cholesterol levels (7-10).

The potential health benefits of WGW have also been ascribed to fiber. WGW is a source of both fermentable and non-fermentable dietary fibers, such as (hemi)cellulose including arabinoxylan and β -glucan, lignin, and the oligosaccharides raffinose, stachyose, and fructan (11). Dietary fibers are not hydrolyzed or absorbed in the small intestine, and therefore can directly interact with the gut microbiota, resulting in the production of metabolites that are relevant to health (12, 13). Diet affects the microbiota, and consequently possibly dietary changes (*e.g.* via interventions) can modulate the intestinal microbiota composition and functionality (13). Cereal fibers and other components in WGW such as iron (14), have been shown to be able to modulate the gut microbiota composition *in vitro* and *in vivo* (15, 16). Moreover, multiple human trials demonstrated an increase in bacteria associated with host health benefits after WGW interventions, including an enhanced abundance of *Bifidobacterium* (17, 18) and *Lactobacillus* (17, 19). Two trials report an increase in butyrate-producing bacteria upon WGW or WG consumption (19, 20). However, other human trials did not find effects of WG on the microbiota composition (21-23). The effects of WGW and WG on both the composition and functions of the gut microbiota in humans are therefore not yet well understood. Some previous trials investigated only a selected subset of bacteria (17, 18, 24) and may have failed to capture the full effects of WGW and RW on the gut microbiota. It remains to be elucidated if the gut microbiota mediates the health benefits of WGW in humans.

The fermentable dietary fibers can be broken down by the gut microbiota (11, 25), producing short-chain fatty acids (SCFAs), mainly acetate, butyrate, and propionate. SCFAs can reach the liver and the peripheral circulation, where they can affect organ function and metabolism (26, 27). *In vitro* studies and animal experiments have shown that SCFAs increase fat oxidation in liver tissue (28, 29), suggesting a link between

microbial-produced SCFAs and liver fat. Modulation of the gut microbiota is thought to play a role in the development of NAFLD and non-alcoholic steatohepatitis (30-33). In the review of Ross et al. (4) the effect of WG on the microbiota was proposed as a potential mechanism in the prevention of NAFLD. The presence of perturbed metabolic health status, such as being middle-aged and being overweight or obese, is often a prerequisite for the development of NAFLD (4).

Recently, we performed the Graandioos study (7, 34), and observed that a 12-week RW intervention increased intrahepatic triglycerides (IHTG) and decreased microbiota diversity in middle-aged adults with overweight and obesity, whereas a WGW intervention prevented an increase in liver fat (7). We have previously reported the effect of WGW and RW on the abundances of a pre-selected subset of bacteria (7). In the current manuscript, we describe the effects of this randomized, controlled, double-blind, parallel trial with a 12-week WGW versus RW intervention on the complete fecal microbiota composition with additional analyses, as well as the effects of the interventions on predicted microbial functionality. Moreover, we investigated the relationship between intervention-induced changes in bacterial composition and changes in various liver health parameters, such as IHTG and liver enzymes, to examine the potential role of microbiota in the preventative effect of WGW in hepatic fat accumulation.

Material and methods

Subjects

50 middle-aged, Dutch men and postmenopausal women (45-70 years, BMI 25-35 kg/m²) with mildly elevated plasma total cholesterol (>5 mmol/L) participated. Subjects using cholesterol-lowering medication or subjects that used antibiotics <1 month prior to day 1 of the study were excluded (for details see (7)). Subjects had no history of medical/surgical events that may affect the study outcomes. During the screening visit, subjects filled in a food frequency questionnaire to determine their habitual dietary intake. Whole grain consumption was quantified by research dieticians using the NEVO table 2010. This trial was approved by the Medical Ethical Committee of Wageningen University and registered at ClinicalTrials.gov under NCT02385149. All participants gave written consent before participation.

Study design and procedures

This study was a randomized, controlled, double-blind, parallel trial (**Supplemental Figure 1**). Recruitment and study logistics are described in (7). Before the start of the intervention, a 4-week run-in period with uncolored RW products was included to reduce WGW intake variation at baseline. Afterwards, subjects were randomly assigned

to a 12-week intervention with either WGW products or colored RW products. Age, gender, BMI, and cholesterol levels were stratified among the intervention groups. The randomization was conducted using block randomization (Microsoft Excel) by a researcher who was not involved in the study. Participants were asked to continue their dietary pattern and dietary habits during the intervention period. They were not allowed to lose or gain weight during the intervention. Before and after the 12-week intervention, feces were collected. At test days, liver fat accumulation and metabolic health parameters were measured. Participants weekly recorded stool consistency using the Bristol Stool Chart, which describes 7 types of stools ranging from 1: hard/lumpy to 7: watery without solid pieces. The day prior to the test day, participants consumed a standardized low-fat evening meal, refrained from alcohol or strenuous exercise, and were not allowed to eat or drink anything except water after 20:00 h to ensure a fasting state.

Intervention products

Participants received either WGW or RW products to replace the habitual intake of grain products. Four slices of bread (in total 100 g/d), and one serving of ready-to-eat-cereals (33.4 g/d) were consumed daily. In total, this added up to 98 grams of RW or WGW flour per day. RW products were colored with roasted wheat malt and caramelized sugar to match the appearance of WGW products. On the macronutrient and energy level, the RW and WGW products were similar, except for fiber content. The WGW products contained 17.6 g fiber/100 g, and the RW products 7.2 g fiber/100 g. The nutritional composition (macronutrients, vitamins and minerals) of the intervention products is provided in **Supplemental Table 1**. During the run-in and intervention period, consumption of additional whole grain food products was not allowed, including products from other grain sources (i.e. brown rice), in both the WGW and RW groups. All participants received a list of WG products to avoid during the intervention. Subjects were allowed to complement their daily diet with additional refined grain products.

Clinical chemistry and intrahepatic triglyceride accumulation

Lipid content in the liver was quantified with proton magnetic resonance spectroscopy using a 3T whole body MRI scanner (7). Plasma alanine transaminase (ALT), aspartate transaminase (AST), gamma-glutamyltransferase (GGT), C-reactive protein (CRP), and serum amyloid (SAA) were included as liver health markers, which were analyzed as described previously (7). Beta-hydroxybutyrate was also included as a marker as it can be synthesized in the liver via the metabolism of butyrate. As a biomarker for WGW intake, plasma alkylresorcinol was analyzed as described previously (7).

Microbiota library preparations

Feces were collected at home within three days before the test day and were stored at

-20°C for a maximum of three days. Samples were transferred to -80°C. Fecal material was mechanically homogenized, and genomic DNA was isolated with the use of an AGOWA mag Mini kit (AGOWA, Berlin, Germany) according to the manufacturer's instructions. The V4 hypervariable region of the 16S rRNA gene was PCR amplified using F515/R806 primers. PCR products were purified, followed by paired-end sequencing on an Illumina MiSeq platform, as described previously (7). 22 technical replicate samples were included in the dataset, which were two aliquots taken from the same fecal sample at the same time from which all consecutive steps were performed separately to isolate DNA. Raw sequencing data were first de-multiplexed by trimming barcodes and primer sequences. Afterwards, the data was processed and amplicon sequence variants (ASV) were picked with NG-Tax using default settings (35, 36). Chimeras were detected and filtered when the forward and reverse read of that ASV was identical to two different ASVs, and the abundance of the matched ASVs were at least two times the abundance of that specific ASV. The SILVA reference database version 128 was used to assign taxonomy, with a confidence of >80% for genus level classification.

Microbiota composition analyses

R version 3.5.1. was used for all analyses (37). Raw counts were transformed to relative abundance. Technical replicates were compared by calculating pairwise Pearson correlation using the genus level relative abundance. Afterwards, bacteria abundance in technical replicates was averaged. Alpha-diversity was calculated using Faith's phylogenetic diversity based on branch length connecting taxa in those samples and the root node of the phylogenetic tree. Pairwise Weighted Unifrac (38) distance based principle coordinate analysis (PCoA) was used to visualize overall microbial community variation (39). Permutational multivariate analysis of variance (PERMANOVA) (40) was used to test for significant differences in overall community composition between groups.

Prediction of microbiota functionality and markers for short chain fatty acid production

Microbial functions were predicted based on the 16S rRNA gene sequences using the PICRUSt2 (Phylogenetic Investigation of Communities by Reconstruction of Unobserved States) algorithm (41). The default workflow was followed (41). In short, ASVs were used as input and aligned to reference sequences using HMMER software to identify homologous nucleotide sequences using hidden Markov models (42). The aligned amplicon sequence variants were placed into a reference tree using phylogenetic placement algorithms (EPA-NG) (43) and GAPP (44). Nearest-sequenced taxon index (NSTI) values for each ASV were calculated, which correspond to the branch length of the tree from the placed ASV to the nearest reference sequence. The NSTI values default cut-off is 2. For bacteria without available genome sequences, the sequenced relative

was used as a reference. The tree of ASVs and reference sequences were combined with information about gene family copy numbers per ASV, to predict the gene content per ASV after normalizing by 16S rRNA gene copy number using castor (45). The read depth per ASV was divided by the predicted 16S rRNA gene copy numbers to control for variation in 16S rRNA gene copy numbers across bacteria. Afterwards, the predicted gene content per ASV was combined with the ASV known abundances input to determine gene family abundance per sample. These predicted sample gene family profiles were used as input, together with a map of gene families to pathways, to infer pathway abundances using a minimal set of pathways (MinPath, (46)). Per sample, predicted pathways, EC numbers, and KEGG orthology (KO) metagenomes were reconstructed for the dataset. Finally, EC numbers are re-grouped to MetaCyc reactions to predict pathway abundances and coverages (47). For more information about the PICRUSt2 workflow, we refer to the PICRUSt website: <https://github.com/picrust/picrust2>. The compositional count data of predicted pathways and KEGG orthologs was transformed to relative abundance.

Markers for predicted short chain fatty acid production

KEGG orthologs were selected that could be used as markers for predicted SCFA production. As markers for acetate production, the enzymes acetate kinase (K00925) (48), phosphate acetyltransferase (K13788), and putative phosphotransacetylase (K15024) were selected. As markers for propionate production, methylmalonyl-CoA decarboxylase (K11264), propionaldehyde dehydrogenase (K13922), propionate CoA-transferase (K01026) (49), and propionyl-CoA synthetase (K01908) were selected. As markers for butyrate production, butyrate kinase (K00929) and butyryl-coA:acetate CoA-transferase (α subunit: K01034, β subunit: K01035) were selected (50, 51). For lactate production, L-lactate dehydrogenase (K00016) and D-lactate dehydrogenase (K03778) were selected (52).

Statistical analysis

The non-parametric Wilcoxon test was applied for paired comparisons of bacteria and predicted pathway relative abundances within-diet group over time, due to the non-normal distribution of the data. The unpaired Mann-Whitney U test was used to determine the differences between groups at baseline and the differential changes over time (Δ) between intervention groups. Differences in baseline characteristics and food frequency questionnaire data were assessed using independent t-tests, or Mann-Whitney U tests, depending on the variable distribution. Bristol Stool Chart scores were analyzed using linear mixed effects modeling with interventions, time, and the interaction as fixed effects and subject ID as a random effect (R package lme4). Correlations between (changes of) relative abundances of bacteria on genus level and (changes of) liver health parameters between paired samples were assessed by Spearman's rank correlation tests.

Analyses were performed without and with adjustment for multiple comparisons using false discovery rate (FDR). Non-adjusted p-values of <0.05 were considered significant, because modest changes were expected due to the explorative character of this study.

Results

Subject characteristics and stool consistency

Participants with missing fecal samples before or after the intervention (n=5) or use of antibiotics during the intervention (n=8) were removed from the analysis, resulting in 16 participants in the RW group, and 21 participants in the WGW group. No significant differences in baseline characteristics were found between groups, except for beta-hydroxybutyrate (p=0.043), which was higher in the RW group (**Table 1**).

Table 1. Baseline characteristics of middle-aged overweight and obese subjects in the RW or WGW group in a subset of the total study population¹.

Variables	RW group	WGW group	P-value
Gender, n males ² (%)	9 (60)	12 (60)	0.96
Age, y	60 ± 6.0	60 ± 5.4	0.97
Body weight, kg	84 ± 7.0	86 ± 9.4	0.36
BMI, kg/m ²	27 ± 2.2	28 ± 2.0	0.14
IHTG ³ , %	3.6 ± 2.5	5.5 ± 6.4	0.83
Total cholesterol, mmol/L	6.0 ± 0.76	6.2 ± 0.71	0.38
CRP ² , µg/mL	2.9 ± 3.1	4.8 ± 7.3	0.95
SAA ² , µg/mL	2.1 ± 1.9	7.2 ± 16	0.76
GGT, U/L	19 ± 13	21 ± 13	0.61
AST, U/L	19 ± 5.6	19 ± 4.7	0.60
ALT, U/L	31 ± 9.4	36 ± 12	0.18
Beta-hydroxybutyrate, mmol/L	0.30 ± 0.20	0.20 ± 0.20	0.043

¹Values are presented as group means ± SD, n=16 (RW) or n=21 (WGW), ²Presented as the number and percentage of males, ³Non-parametric distribution, evaluated with the Mann-Whitney U test. Abbreviations: ALT, alanine transaminase; AST, aspartate transaminase; BMI, body mass index; CRP, C-reactive protein; GGT, gamma-glutamyltransferase; IHTG, intrahepatic triglycerides; RW, refined wheat; SAA, serum amyloid A; WGW, whole grain wheat.

The mean habitual WG intake before the start of the intervention was 60.1±59.2 g/d in the RW group, and 54.4±38.0 g/d in the WGW group (p=0.73; **Supplemental Table 2**). No significant differences in the habitual intake of WG, total carbohydrates, or dietary fibers were found between groups. Habitual medication use did not change during intervention, and analgesic use during the whole study period did not exceed 15 days in total. The stool consistency showed a non-specific trend during the run-

in and intervention period (**Supplemental Figure 2**), without a significant effect of time ($p=0.58$) or intervention ($p=0.64$) on the consistency score. The main findings in this subset of the study population reflected those in the total study population (7), namely RW significantly increased IHTG compared to the WGW group ($p=0.033$), and WGW consumption decreased SAA ($p=0.042$) and increased beta-hydroxybutyrate (**Supplemental Table 3**).

Microbiota composition and predicted pathways at baseline

The microbiota composition and predicted pathway datasets were of high quality (**Supplemental Figure 3, Supplemental information**). In total, 1450 unique ASV were identified in the microbiota dataset within 181 unique genera, and 356 pathways were predicted to be active in the dataset. Substantial inter-individual variation in microbiota composition at the genus level was observed at baseline (**Supplemental Figure 4**), without clear differences between intervention groups for the average composition. Without correcting for multiple testing, 7 bacteria and 11 predicted pathways were significantly different between groups at baseline (**Figure 1, Supplemental Table 4**). After FDR correction, none of the bacteria or pathways were significantly different at baseline.

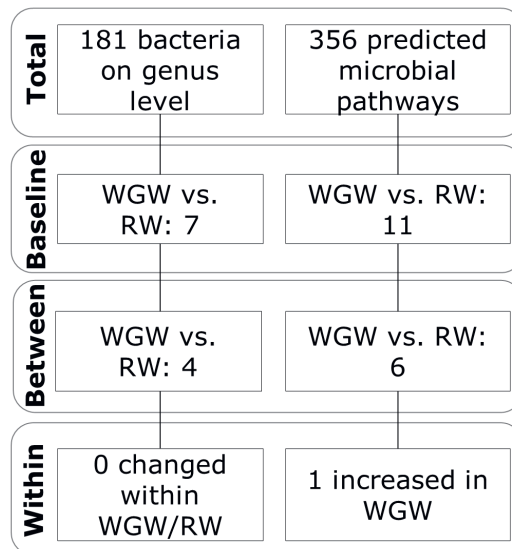


Figure 1. Significantly different fecal bacteria and bacteria pathways at baseline and upon 12 weeks of RW or WGW intervention in middle-aged overweight and obese adults.

The flow diagram shows the number of bacteria on genus level and the predicted pathways for which the change in relative abundance was significantly different among interventions. Abbreviations: RW, refined wheat; WGW, whole grain wheat.

The gut microbiota diversity

No significant clustering-effect was found between baseline and post-intervention within and between groups based on overall microbiota profiles (PERMANOVA $p = 0.63$, **Figure 2A**). However, the overall microbiota community of most individuals showed a shift over time.

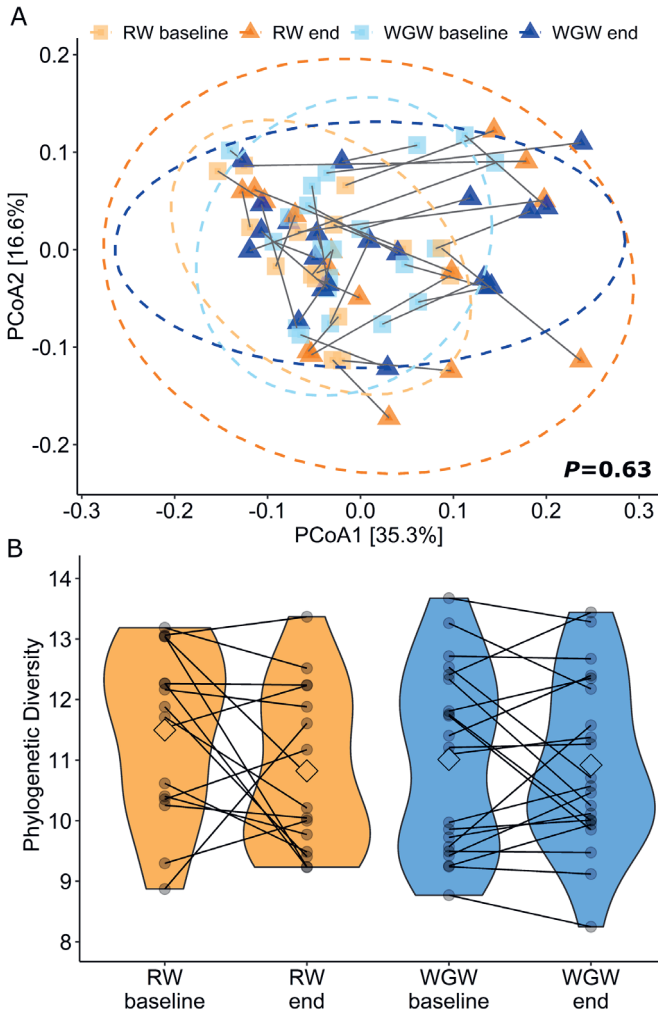


Figure 2. The effect of 12 weeks RW or WGW intervention on the fecal microbiota diversity in middle-aged overweight and obese adults.

(a) PCoA plot using Weighted UniFrac dissimilarity to visualize the overall microbiota community variation. Color and shape highlight the intervention groups before or after the intervention. The lines connect the within-person samples over time. 95% confidence intervals are plotted, and (b) Microbial diversity as assessed using Faith's Phylogenetic Diversity at baseline and after the 12 week intervention (end). Individual paired samples are connected by a line. The width of the colored shapes indicates the sample density, the squared shape inside indicates the group means. Abbreviations: PCoA, principle coordinate analysis; RW, refined wheat; WGW, whole grain wheat.

The change in microbial diversity (Phylogenetic Diversity, PD) (Figure 2B) was not significantly different between the RW and WGW intervention ($p=0.21$). Both RW and WGW intervention did not change microbial diversity (RW: baseline 11.5 ± 1.38 PD, $\Delta-0.67\pm 1.66$ PD, $p=0.19$; WGW: baseline 11.0 ± 1.50 PD, $\Delta-0.09\pm 1.10$ PD, $p=0.97$). On the group level, no differences were found in the overall microbiota community composition. Overall, the interventions did not change microbiota phylogenetic diversity (alpha-diversity) nor the overall community composition (beta-diversity).

The effect of RW and WGW intervention on the microbiota composition

Intervention effects on microbiota abundances were found on genus level between and within the WGW and the RW group (Table 2). Between groups, four bacteria were significantly different over time (Figure 3), namely *Ruminiclostridium_9* ($p=0.003$), *Ruminococcaceae_NK4A214_group* ($p=0.036$), *Lachnospiraceae_UCG-008* ($p=0.044$), and *Ruminococcaceae_UCG-014* ($p=0.033$), without significant differences within intervention groups. Not all of the aforementioned bacteria were present in all individuals; in Supplemental Table 5, the number of subjects in which the bacteria were detected is shown. Overall, WGW intervention increased three bacteria (within the Ruminococcaceae family) and decreased one bacterium (within the Lachnospiraceae family), whereas RW intervention mostly decreased these bacteria.

Correlations between the microbiota and liver health parameters

The relative abundances of all bacteria at baseline were then correlated to baseline IHTG. Significant positive correlations were found between IHTG and *Roseburia* (Figure 4, $\rho=0.38$, $p=0.025$), *Ruminococcus_2* ($\rho=0.39$, $p=0.021$), and *Faecalibacterium* ($\rho=0.39$, $p=0.020$). Significant negative correlations were found between IHTG and *Ruminococcaceae_UCG-010* ($\rho=-0.38$, $p=0.026$), *Ruminococcaceae_UCG-005* ($\rho=-0.40$, $p=0.018$), and *Akkermansia* ($\rho=-0.36$, $p=0.035$). After removal of two outliers (18% and 26% IHTG), the correlation between IHTG and *Ruminococcus_2* was still significant ($p=0.050$), whereas for the other bacteria there was a trend towards significance (p -values between 0.05 and 0.10). After FDR correction, none of these correlations were significant.

Table 2. Fecal bacteria abundances on genus level at baseline and change after 12 weeks of intervention that were found to be significantly different within and/or between the WGW and RW group in middle-aged overweight and obese adults¹.

Bacteria	RW group			WGW group			Within RW			Within WGW			Group comparison	
	Baseline relative abundance (%)	Δ Relative abundance after 12wk (%)	Baseline relative abundance (%)	Δ Relative abundance after 12wk (%)	P-value	FDR	P-value	FDR	P-value	FDR	P-value	FDR	P-value	FDR
<i>f_Ruminococcaceae; g_Ruminiclostridium_9</i>	0.20 ± 0.23	-0.081 ± 0.17	0.065 ± 0.11	0.054 ± 0.14	0.07	NS ²	0.07	NS	0.07	NS	0.003	NS	0.003	NS
<i>f_Ruminococcaceae; g_Ruminococcaceae_NK4A214_group</i>	0.64 ± 1.3	-0.15 ± 0.49	0.37 ± 0.56	0.17 ± 0.83	0.12	NS	0.11	NS	0.11	NS	0.036	NS	0.036	NS
<i>f_Lachnospiraceae; g_Lachnospiraceae_UCG-008</i>	0.00 ± 0.00	0.043 ± 0.10	0.10 ± 0.12	-0.023 ± 0.083	0.18	NS	0.19	NS	0.19	NS	0.044	NS	0.044	NS
<i>f_Ruminococcaceae; g_Ruminococcaceae_UCG-014</i>	1.6 ± 2.1	-0.31 ± 0.78	2.2 ± 4.6	0.51 ± 4.2	0.12	NS	0.13	NS	0.13	NS	0.033	NS	0.033	NS
<i>f_Lachnospiraceae; g_Dorea</i>	1.7 ± 1.1	-0.72 ± 0.91	1.6 ± 0.81	-0.018 ± 0.99	0.005	NS	0.61	NS	0.61	NS	0.055	NS	0.055	NS
<i>f_Tannerellaceae; g_Parabacteroides</i>	0.37 ± 0.30	0.60 ± 1.42	0.45 ± 0.41	0.35 ± 0.97	0.007	NS	0.18	NS	0.18	NS	0.32	NS	0.32	NS
<i>f_Lachnospiraceae; g_[Eubacterium]_ventriosum_group</i>	0.17 ± 0.23	-0.14 ± 0.24	0.14 ± 0.14	-0.050 ± 0.15	0.044	NS	0.71	NS	0.71	NS	0.18	NS	0.18	NS
<i>f_Peptostreptococcaceae; g_unknown</i>	1.2 ± 2.8	-0.64 ± 1.5	0.56 ± 0.71	-0.23 ± 0.69	0.024	NS	0.18	NS	0.18	NS	0.57	NS	0.57	NS
<i>f_Ruminococcaceae; g_Ruminococcus_2</i>	1.4 ± 1.3	-0.24 ± 1.5	2.1 ± 1.8	-1.1 ± 2.1	0.11	NS	0.024	NS	0.024	NS	0.44	NS	0.44	NS
<i>f_Ruminococcaceae; g_Subdoligranulum</i>	6.8 ± 4.7	-1.7 ± 4.6	6.1 ± 5.3	-1.8 ± 3.7	0.10	NS	0.024	NS	0.024	NS	0.89	NS	0.89	NS
<i>f_Burkholderiaceae; g_Sutterella</i>	0.27 ± 0.44	0.085 ± 0.45	0.35 ± 0.92	0.30 ± 0.49	0.31	NS	0.010	NS	0.010	NS	0.46	NS	0.46	NS
<i>f_Ruminococcaceae; g_Ruminococcaceae_UCG-005</i>	1.1 ± 1.1	0.38 ± 1.5	0.91 ± 1.1	0.21 ± 1.0	0.75	NS	0.042	NS	0.042	NS	0.47	NS	0.47	NS

¹Values are presented as group means ± SD, n=16 (RW) or n=21 (WGW). ²NS = P-value > 0.05. FDR, false discovery rate; RW, refined wheat; WGW, whole grain wheat.

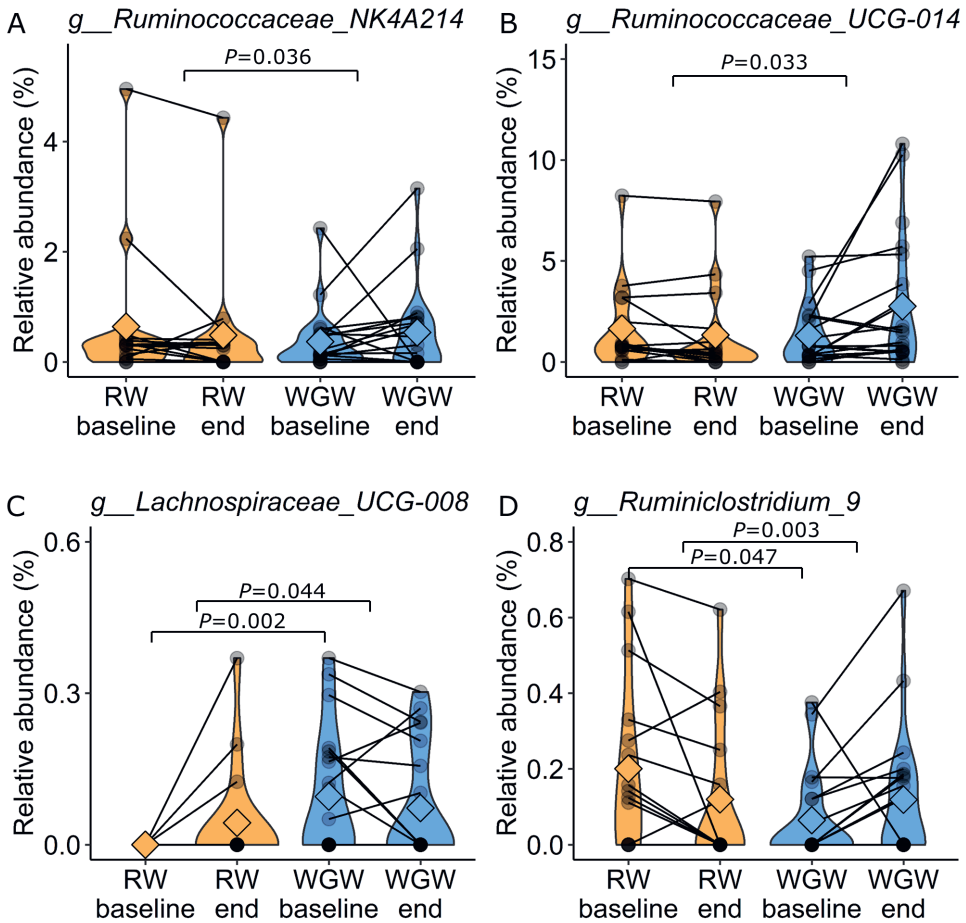


Figure 3. Fecal bacteria on genus level at baseline and after the 12 week of RW or WGW intervention (end) that were found to be significantly different between the groups in middle-aged overweight and obese adults.

The relative abundances of (a) *Ruminococcaceae_NK4A214_group*; (b) *Ruminococcaceae_UCG-014*; (c) *Lachnospiraceae_UCG-008*; and (d) *Ruminiclostridium_9* are shown. Data is presented as group mean (the squared shape), $n=16$ (RW) or $n=21$ (WGW), and the width of the colored shapes indicates the sample density. Individual paired samples are connected by a line. Abbreviations: RW, refined wheat; WGW, whole grain wheat.

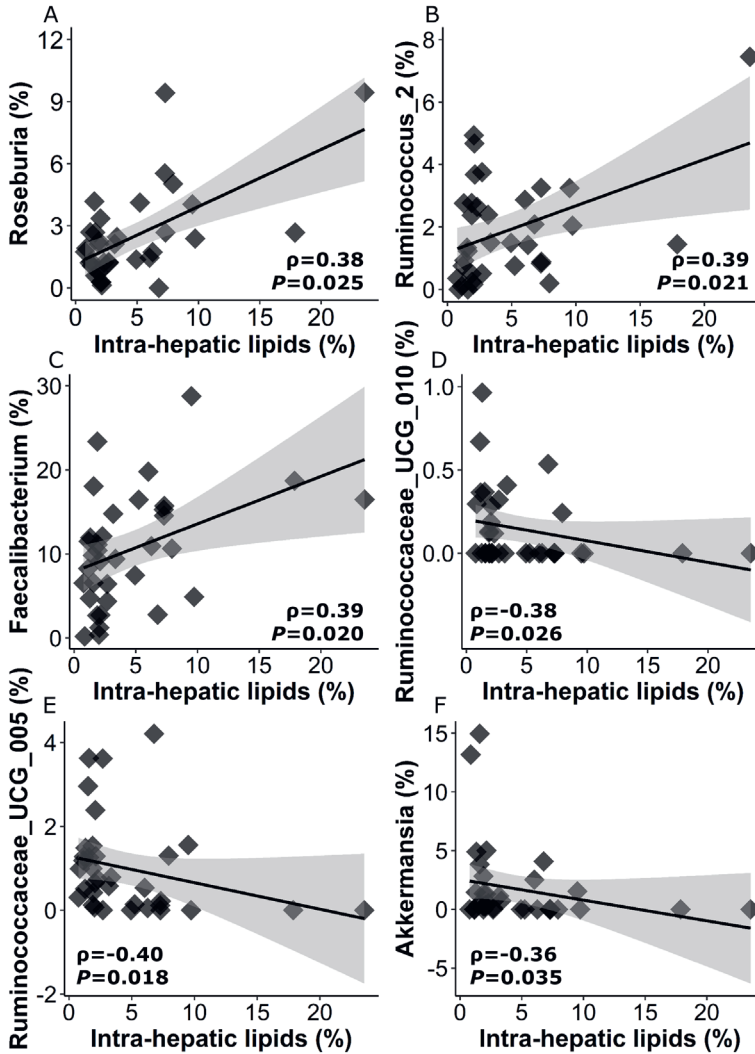


Figure 4. Fecal bacteria on genus level that were found to be significantly correlated with IHTG at baseline in middle-aged overweight and obese adults.

The relative abundances of (a) *Roseburia*; (b) *Ruminococcus_2*; (c) *Faecalibacterium*; (d) *Ruminococcaceae_UCG-010*; (e) *Ruminococcaceae_UCG-005*; and (f) *Akkermansia* are shown, fitted with a linear regression model with a 95% confidence level interval. Non-corrected p-values are shown. Data of n=35 participants is shown, who had both microbiota and IHTG data at baseline available. Abbreviations: IHTG, intrahepatic triglycerides.

Table 3. The significant correlations between changes in fecal bacteria abundances on genus level, and changes in liver health parameters upon 12 weeks of RW or WGW intervention in middle-aged overweight and obese adults¹.

Taxa (Δ 12 wk)	RW			WGW		
	Spearman rho	P-value	FDR P-value	Spearman rho	P-value	FDR P-value
IHTG (Δ 12 wk)						
<i>g_Ruminococcaceae_NK4A214_group</i>	0.67	0.024	NS ²	0.54	0.026	NS
ALT (Δ 12 wk)						
<i>g_Bacteroides</i>	0.30	NS	NS	-0.44	0.048	NS
<i>g_Bifidobacterium</i>	0.77	0.001	NS	-0.14	NS	NS
<i>g_Faecalibacterium</i>	-0.11	NS	NS	-0.46	0.037	NS
<i>g_Lachnospiraceae_NK4A136_group</i>	0.60	0.014	NS	-0.20	NS	NS
AST (Δ 12 wk)						
<i>g_[Eubacterium]_coprostanoligenes_group</i>	0.53	0.034	NS	0.065	NS	NS
<i>g_Butyricoccus</i>	0.51	0.045	NS	-0.22	NS	NS
<i>g_Lachnospiraceae_NK4A136_group</i>	0.51	0.045	NS	-0.48	0.027	NS
<i>g_Ruminococcus_2</i>	0.53	0.036	NS	0.35	NS	NS
<i>g_Ruminiclostridium_6</i>	0.10	NS	NS	0.46	0.036	NS
CRP (Δ 12 wk)						
<i>g_Butyricoccus</i>	-0.58	0.025	NS	-0.052	NS	NS
<i>g_Lachnospiraceae_NK4A136_group</i>	-0.68	0.007	NS	0.36	NS	NS
<i>g_Parabacteroides</i>	0.54	0.041	NS	0.25	NS	NS
<i>g_Uncultured</i>	-0.59	0.023	NS	-0.16	NS	NS
GGT (Δ 12 wk)						
<i>g_[Eubacterium]_coprostanoligenes_group</i>	-0.21	NS	NS	0.50	0.021	NS
<i>g_Erysipelotrichaceae_UCG-003</i>	0.55	0.028	NS	-0.071	NS	NS
Beta-hydroxybutyrate (Δ 12 wk)						
<i>g_Erysipelotrichaceae_UCG-003</i>	-0.027	NS	NS	0.67	0.002	NS
<i>g_Lachnospiraceae_ND3007_group</i>	-0.10	NS	NS	0.48	0.036	NS
<i>g_Ruminococcus_2</i>	0.13	NS	NS	0.46	0.049	NS
<i>g_Streptococcus</i>	0.61	0.011	NS	0.48	0.040	NS
SAA (Δ 12 wk)						
<i>g_Anaerostipes</i>	-0.23	NS	NS	0.52	0.018	NS
<i>g_Blautia</i>	-0.29	NS	NS	0.53	0.015	NS
<i>g_Butyricoccus</i>	-0.46	NS	NS	0.46	0.036	NS

¹Values represent the Spearman rho correlation coefficients, n=16 (RW) or n=21 (WGW). ²NS = P-value>0.05. ALT, alanine transaminase; AST, aspartate transaminase; CRP, C-reactive protein; FDR, false discovery rate; GGT, gamma-glutamyltransferase; b-HBA, beta-hydroxybutyrate; IHTG, intrahepatic triglycerides; RW, refined wheat; SAA, serum amyloid A; WGW, whole grain wheat.

Correlations between changes in liver health markers including IHTG, ALT, AST, GGT, SAA, CRP, and beta-hydroxybutyrate with changes in bacteria abundances upon 12 weeks of intervention were tested (**Supplemental Figure 5**). Change in IHTG was

positively correlated with change in *Ruminococcaceae_NK4A214_group* abundance in both the WGW ($\rho=0.54$, $p=0.026$) and RW ($\rho=0.67$, $p=0.024$) group (**Table 3**). Moreover, change in ALT was significantly correlated with changes of two bacteria in the RW and two in the WGW intervention. Change in AST was correlated with changes of three bacteria in the RW, one bacteria in the WGW, and one bacteria (*Lachnoclostridium*) in both groups. Changes in GGT or SAA were significantly correlated with changes in abundance of one bacteria in the RW and one in the WGW group, or three bacteria in the WGW group, respectively. Change in CRP was correlated with changes of three bacteria in the RW group. Furthermore, change in beta-hydroxybutyrate was positively correlated with three bacteria in the RW group and one bacteria (*Streptococcus*) in both groups. After FDR correction, none of these correlations were significant.

Changes in predicted microbial pathways

The intervention effects on predicted microbial pathways were investigated. Between the WGW and the RW interventions, six predicted pathways were significantly different over time (**Table 4**), namely hexitol degradation, pantothenate and coenzyme A biosynthesis, acetyl-CoA fermentation to butyrate II, pyruvate fermentation to acetone, aromatic biogenic amine degradation, and L-alanine biosynthesis. Subjects in both groups displayed a variation in response over time for the significantly different predicted pathways (**Figure 5**). Within the WGW group, acetyl-CoA fermentation to butyrate II was significantly increased ($p=0.017$). Within the RW group, a second pathway related to fermentation was predicted to be decreased, namely pyruvate fermentation to acetate and lactate II ($p=0.049$).

Since changes in predicted fermentation pathways were found, we examined the effect of the interventions on selected genes involved in SCFA production (**Supplemental Table 6**). No significant differences in changes of these predicted genes were observed over time between groups, but butyrate kinase was significantly increased within the WGW group ($p=0.038$), and phosphate acetyltransferase was significantly decreased within the RW group ($p=0.021$). Overall, WGW intervention showed a trend towards increased predicted fermentation pathways by the microbiota, whereas RW intervention showed opposite effects.

Table 4. Predicted fecal microbial pathway relative abundance at baseline and change after 12 weeks of intervention that were found to be significantly different within and/or between the WGW and RW group in middle-aged overweight and obese adults¹.

Pathway name	Pathway number	RW group				WGW group				Within RW				Within WGW				Group comparison	
		Baseline relative abundance (%)	Δ Relative abundance (%) after 12wk	Relative abundance (%) after 12wk	Δ Relative abundance (%) after 12wk	Baseline relative abundance (%)	Relative abundance (%) after 12wk	Δ Relative abundance (%) after 12wk	P-value	FDR	P-value	FDR	P-value	FDR	P-value	FDR	P-value	FDR	
superpathway of hexitol degradation	HEXITOLDEGSUPER.PWY	0.13 ± 0.049	-0.015 ± 0.056	0.13 ± 0.065	-0.00 ± 0.056	0.13 ± 0.065	0.70	NS ²	0.97	NS	0.97	NS	0.97	NS	0.97	NS	0.044	NS	
pantothenate and coenzyme A biosynthesis	PANTOSYN.PWY	0.58 ± 0.057	0.022 ± 0.039	0.55 ± 0.054	0.00 ± 0.034	0.11	NS	0.76	NS	0.76	NS	0.76	NS	0.76	NS	0.022	NS		
acetyl-CoA fermentation to butyrate	PWY.5676	0.26 ± 0.079	-0.026 ± 0.081	0.23 ± 0.062	0.035 ± 0.059	0.12	NS	0.017	NS	0.017	NS	0.017	NS	0.017	NS	0.031	NS		
pyruvate fermentation to acetone	PWY.6588	0.28 ± 0.12	-0.044 ± 0.12	0.20 ± 0.087	0.017 ± 0.068	0.32	NS	0.18	NS	0.18	NS	0.18	NS	0.18	NS	0.043	NS		
aromatic biogenic amine degradation	PWY.7431	0.010 ± 0.010	0.00 ± 0.010	0.010 ± 0.010	0.0059 ± 0.012	0.30	NS	0.56	NS	0.56	NS	0.56	NS	0.56	NS	0.047	NS		
L-alanine biosynthesis	PWY0.1061	0.36 ± 0.13	-0.067 ± 0.16	0.32 ± 0.10	-0.010 ± 0.12	0.30	NS	0.55	NS	0.55	NS	0.55	NS	0.55	NS	0.041	NS		
L-arginine degradation	AST.PWY	0.0048 ± 0.010	0.00 ± 0.011	0.010 ± 0.023	-0.00 ± 0.012	0.048	NS	0.23	NS	0.23	NS	0.23	NS	0.23	NS	0.15	NS		
L-lysine biosynthesis I	DAPLYSIESYN.PWY	0.77 ± 0.10	-0.065 ± 0.14	0.75 ± 0.079	-0.030 ± 0.079	0.041	NS	0.15	NS	0.15	NS	0.15	NS	0.15	NS	0.82	NS		
(Kdo)2-lipid A biosynthesis	KDO.NAGLIPASYN.PWY	0.024 ± 0.036	-0.010 ± 0.045	0.024 ± 0.045	0.010 ± 0.027	0.043	NS	0.28	NS	0.28	NS	0.28	NS	0.28	NS	0.50	NS		
pyruvate fermentation to acetate and lactate II	PWY.5100	0.94 ± 0.14	-0.049 ± 0.086	0.91 ± 0.084	-0.020 ± 0.071	0.049	NS	0.79	NS	0.79	NS	0.79	NS	0.79	NS	0.13	NS		
preQ0 biosynthesis	PWY.6703	0.32 ± 0.063	0.057 ± 0.077	0.31 ± 0.054	0.021 ± 0.044	0.046	NS	0.82	NS	0.82	NS	0.82	NS	0.82	NS	0.95	NS		
vitamin K2 biosynthesis	PWY.5845	0.023 ± 0.029	0.00 ± 0.038	0.025 ± 0.039	0.0022 ± 0.025	0.19	NS	0.037	NS	0.037	NS	0.037	NS	0.037	NS	0.52	NS		
superpathway of ubiquinol-8 biosynthesis	UBISYN.PWY	0.025 ± 0.023	0.00 ± 0.022	0.028 ± 0.028	0.0013 ± 0.021	0.61	NS	0.024	NS	0.024	NS	0.024	NS	0.024	NS	1.0	NS		

¹Values are presented as group means ± SD, n=16 (RW) or n=21 (WGW). ²NS = P-value > 0.05. FDR, false discovery rate; PWY, pathway; RW, refined wheat; WGW, whole grain wheat.

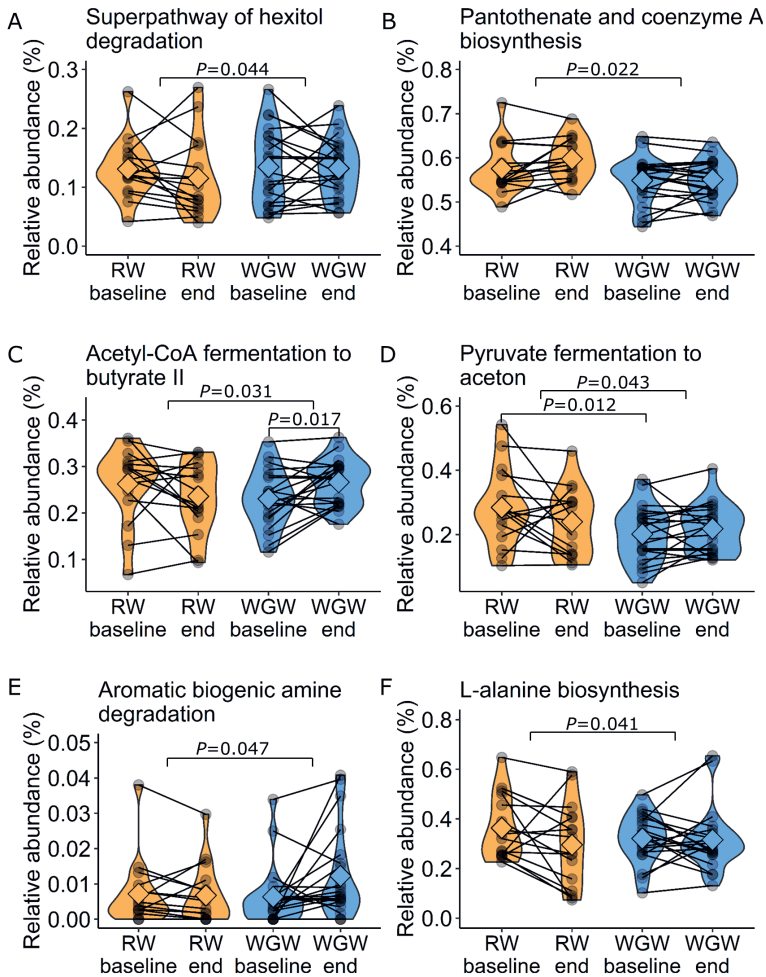


Figure 5. Predicted fecal microbial pathway relative abundance at baseline and after 12 weeks of RW or WGW intervention that were found to be significantly different between the groups in middle-aged overweight and obese adults.

The relative abundances of the predicted pathways (a) superpathway of hexitol degradation; (b) pantothenate and coenzyme A biosynthesis; (c) acetyl-CoA fermentation to butyrate II; (d) pyruvate fermentation to acetone; (e) aromatic biogenic amine degradation; and (f) L-alanine biosynthesis are shown. Data is presented as group mean (the squared shape), $n=16$ (RW) or $n=21$ (WGW), and the width of the colored shapes indicates the sample density. Individual paired samples are connected by a line. Abbreviations: RW, refined wheat; WGW, whole grain wheat.

Discussion

We investigated the effects of 12-week consumption of RW or WGW products on the gut microbiota composition and predicted microbiota functional pathways in men and women with overweight or obesity. We found significant differences between the WGW

and RW intervention on a number of bacteria from carbohydrate-degrading families and on predicted fermentation pathways, with a trend towards increased fermentation to butyrate within the WGW group, and a trend towards decreased fermentation within the RW group. Although WGW consumption is already quite high in the Netherlands, we provided an intervention with 98 g/d WGW that was higher than the mean habitual WG intake at baseline of participants in both the RW or WGW group of 60.1 or 54.4 WG g/d, respectively.

Even though the difference in fiber between the WGW and RW intervention was 10 g/d, we observed only subtle differences between intervention groups over time with respect to microbiota composition and functionality, and no effect on stool consistency. Microbial diversity within samples as calculated previously by the Shannon Index was decreased after RW intervention in Schutte et al. (7), but we did not find a significant difference in microbial diversity changes between groups in a subset of study participants with the Phylogenetic Diversity index, which takes into account phylogenetic relatedness between bacteria. Twelve weeks WGW intervention increased relative abundance of *Ruminiclostridium_9*, *Ruminococcaceae_NK4A214_group*, and *Ruminococcaceae_UCG-014*, and decreased *Lachnospiraceae_UCG-008*, whereas 12 weeks RW intervention decreased abundance, without significant effects within the groups. Ruminococcaceae genera have previously been shown to increase after a resistant starch or non-starch polysaccharide-diet high in wheat bran mainly comprised of hemi-cellulose (53, 54). Members within Ruminococcaceae can degrade cellulose and hemi-cellulose fibers (55-57), also present in WGW, whereas members within Lachnospiraceae are known to ferment a wide variety of fibers (55, 57). In line with our results, Vuholm et al. (58) found an increase in an unassigned genus of family Ruminococcaceae after 6 weeks WGW consumption, in healthy, overweight females.

We found the change in relative abundance of *Ruminococcaceae_NK4A214_group* and the intervention-induced change in liver fat correlated in both groups. Several studies showed that Ruminococcaceae was lower in the feces of NAFLD patients compared to controls (59-61). In this study, we found a positive correlation between a change in *Ruminococcaceae_NK4A214_group* and a change in liver fat in both intervention groups, although RW intervention increased liver fat and decreased abundance of *Ruminococcaceae_NK4A214_group* indicating that the changes relative to each other did not have a strong correlation. At baseline, however, we found a positive correlation between liver fat and *Ruminococcaceae_UCG-010*, and *Ruminococcaceae_UCG-005*. We could not identify any human trials on these specific bacteria in relation to liver fat. As in many previous dietary trials, the microbiota response to diet was subject-dependent. The microbiota at the start of intervention of one individual can determine the magnitude of response upon dietary changes (54). Korem et al. (62) found that

the gut microbiota composition was person-specific and generally resilient to bread interventions, but their intervention lasted only one week while our study encompassed a 12-week intervention. In contrast to previous findings (17, 18), WGW consumption did not increase *Bifidobacterium* and *Lactobacillus* in our study. This discrepancy may be partly explained by differences in the fermentable fiber composition and fractions in the intervention products. For instance, fructans can have prebiotic activity by inducing specific changes in the composition and/or activity of the microbiota such as *Bifidobacterium* and *Lactobacillus* (63). It has previously been described that the concentration of fructans differs in WGW (64).

Ruminococcaceae and Lachnospiraceae, together with Bacteroidetes, encompass ~85% of the total butyrate-producing potential of the gut microbiota (65). Changes in bacteria within Ruminococcaceae might point towards an effect on carbohydrate breakdown, which could fit the predicted changes in SCFA fermentation pathways in feces. WGW increased the relative abundance of fermentation to butyrate, whereas RW lowered the fermentation to butyrate as well as fermentation to acetone. The latter pathway can lead to formation of end-products such as acetone, butanol, ethanol, acetate, and butyrate. Moreover, a decreased fermentation to acetate and lactate was found within the RW group. Lactate-utilizing bacteria can use acetate and lactate for the production of butyrate (66), indicating that a lowered capacity to produce acetate and lactate potentially leads to reduced butyrate production. Despite the run-in period, the RW group showed a higher relative abundance for the predicted pyruvate fermentation to acetone pathway and for *Ruminiclostridium_9* compared to the WGW group at baseline. Both were decreased after RW and increased after WGW. Similarly, a higher abundance of *Lachnospiraceae_UCG-008* was observed in the RW group at baseline, which increased after RW and decreased after WGW. Therefore, the differential effects on this pathway and these bacteria between RW or WGW intervention may have been partly caused by regression to the mean. In this study, the effects on microbiota and predicted pathways lost statistical significance after correction for multiple comparisons, which shows that a 12-week WGW and RW intervention induced subtle changes in gut microbiota. This is not surprising considering the relatively modest modulation of diet, only altering wheat products.

In line with our finding that WGW increased two predicted fermentation pathways, Vanegas et al. (20) reported increased concentrations of acetate and total SCFAs in feces after 6 weeks of WG, predominantly wheat, intervention compared to refined grain in middle-aged adults. Moreover, Vuholm et al. (58) found that a 6-week RW intervention decreased stool butyrate concentrations when compared to a WGW intervention in adults with overweight. Additionally, a study in rats showed that a 6-week WGW intervention increased total SCFAs in colonic content and butyrate in

cecum content compared to RW intervention (67). Resistant starch and non-starch polysaccharide inside the whole-grain matrix were associated with increased production of metabolites (68). Overall, incorporating feasible doses of WGW in the diet favorably affects the gut microbiota phenotype as indicated by the increased predicted potential to produce butyrate. These findings may be explained by the decreased fiber content in the RW intervention products (12, 13), although only a fraction of the fiber in the WGW products is fermentable. The fermentability of fibers in WGW is relatively low, for instance when compared to fibers in WG rye (69, 70). Eriksen et al. (71) showed that WG rye resulted in increased *Bifidobacterium*, known to be stimulated by some fermentable fibers, in men with the metabolic syndrome, whereas WG wheat did not.

The reduced predicted potential to produce SCFAs after RW intervention can have implications for health. For instance, SCFAs can decrease intestinal inflammation, as demonstrated by human and animal *in vivo* studies (72). In addition to local health effects, SCFAs might also influence liver fat through stimulation of hepatic fat oxidation via activation of AMP-activated protein kinase (28, 29). As published previously, in this trial, the 12 week RW intervention significantly increased liver fat, while liver fat did not change in the WGW group (7). Therefore, we hypothesized that RW might increase liver fat content indirectly via decreased cereal fiber fermentation and SCFA production. We found that butyrate-producing (73) *Roseburia* positively correlated with liver fat at baseline. In line with our data, the study of Raman et al. (59) showed a significant over-representation of *Roseburia* in the microbiota of NAFLD patients. In contrast, *Roseburia* was decreased in non-obese NAFLD patients compared to healthy controls, and this depletion was linked to increased plasma ALT in 126 non-obese subjects (74). Several of our correlations of other bacteria with liver fat at baseline were in line with previous findings on bacterial composition in NAFLD patients compared to controls (75, 76). This was the case for *Ruminococcus_2* (75) and *Akkermansia* (76), but for *Faecalibacterium* opposite effects were observed (61). While a previous study showed that ALT and GGT were correlated with changes in specific fecal bacteria over time in a prospective, cross-sectional study (74), we could not confirm these findings in our correlation analysis. Although correlations do not provide information on causality, these outcomes might be of interest for future studies into the relationship between WGW, RW and liver health.

A limitation of our study is the analysis of microbiota functional metagenomes by PICRUSt based on the 16S rRNA gene sequencing data, instead of using more direct methods, such as metagenomics. Although the quality control indicated that closely related reference genomes were available for the bacteria present in this dataset, indicative for reliable pathway predictions, PICRUSt is subject to inherit biases. Another restraint of our study is that the SCFA concentrations in feces were not measured. Therefore, the

predicted pathway findings as well as the potential role of SCFAs for liver health could not be validated in this study. Another limitation of our study is the small sample size of 37 subjects. As the study was powered to detect changes in plasma cholesterol levels and participants had to be excluded due to missing fecal samples or antibiotic use, we might have missed the effects of either RW or WGW on the microbiota or predicted microbiota functionality. The strengths of our study include the long study duration of 16 weeks in total, and the good compliance to the diet based upon alkylresorcinol data (7). Therefore, our findings may show more long-term changes rather than acute effects. Comparisons with outcomes of existing literature about WGW, RW, and microbiota composition revealed few similarities with our trial (17-19, 24, 58). Some previous trials may have missed the subtle effects of WGW and RW on the microbiota since only a few selected bacteria were targeted in these studies via *e.g.* qPCR (17, 18, 24), while the fecal microbiota is a highly complex community with multiple species present. The use of 16S rRNA gene sequencing provided important insights into the effect of WGW and RW on microbiota as a whole, as well as effects on predicted microbial community functionality.

We demonstrated that a 12-week 98 g/d WGW intervention increased relative abundances of a number of bacteria that may be involved in carbohydrate degradation and SCFA production and predicted fermentation pathways, whereas a RW intervention decreased abundance of these bacteria or predicted fermentation capacity, pointing towards a less healthy gut microbiota phenotype. The difference in fiber intake during WGW intervention (17.6 g/d fiber) compared to RW intervention (7.2 g/d fiber) likely resulted in differences in predicted bacteria fermentation capacity. This may be one of the mechanisms underlying the significant increases of liver fat observed upon RW intervention. Potential health effects of replacement of RW by WGW via modulation of the microbiota, and consequent protective effects on metabolic organs such as the liver, deserve further investigation.

Acknowledgements

We thank the participants involved in the study. The MyNewGut project (financed by the European Commission in the 7th Framework Program FP7, grant agreement 613979) is acknowledged for sponsoring the microbiota analyses. This research was supported by the public-private partnership titled “Combining innovation with tradition: improving resilience with essential nutrients and whole wheat bread”, financed by Topsector Agri & Food (TKI-AF 12083) and TNO roadmap Nutrition & Health and co-funded by Cereal Partners Worldwide, the Dutch Bakery Center, and GoodMills Innovation GmbH. The funders had no role in the design of the study; in the collection, analyses, or interpretation of data; in the writing of the manuscript, or in the decision to publish the results.

References

1. de Munter JS, Hu FB, Spiegelman D, Franz M, van Dam RM. Whole grain, bran, and germ intake and risk of type 2 diabetes: A prospective cohort study and systematic review. *PLoS medicine*. 2007;4(8):e261.
2. Truswell A. Cereal grains and coronary heart disease. *Eur J Clin Nutr*. 2002;56(1):1.
3. Sahyoun NR, Jacques PF, Zhang XL, Juan W, McKeown NM. Whole-grain intake is inversely associated with the metabolic syndrome and mortality in older adults. *Am J Clin Nutr*. 2006;83(1):124-31.
4. Ross AB, Godin J-P, Minehira K, Kirwan JP. Increasing whole grain intake as part of prevention and treatment of nonalcoholic fatty liver disease. *Int J Endocrinol*. 2013;2013.
5. Bartłomiej S, Justyna R-K, Ewa N. Bioactive compounds in cereal grains—occurrence, structure, technological significance and nutritional benefits—a review. *Food Sci Technol Int*. 2012;18(6):559-68.
6. McKeivith B. Nutritional aspects of cereals. *Nutrition Bulletin*. 2004;29(2):111-42.
7. Schutte S, Esser D, Hoevenaars FP, Hooiveld GJ, Priebe MG, Vonk RJ, et al. A 12-wk whole-grain wheat intervention protects against hepatic fat: The graandioos study, a randomized trial in overweight subjects. *Am J Clin Nutr*. 2018;108(6):1264-74.
8. Kirwan JP, Malin SK, Scelsi AR, Kullman EL, Navaneethan SD, Pagadala MR, et al. A whole-grain diet reduces cardiovascular risk factors in overweight and obese adults: A randomized controlled trial. *J Nutr*. 2016;146(11):2244-51.
9. Tighe P, Duthie G, Vaughan N, Brittenden J, Simpson WG, Duthie S, et al. Effect of increased consumption of whole-grain foods on blood pressure and other cardiovascular risk markers in healthy middle-aged persons: A randomized controlled trial. *Am J Clin Nutr*. 2010;92(4):733-40.
10. Holländer PL, Ross AB, Kristensen M. Whole-grain and blood lipid changes in apparently healthy adults: A systematic review and meta-analysis of randomized controlled studies 1–3. *Am J Clin Nutr*. 2015;102(3):556-72.
11. Fardet A. New hypotheses for the health-protective mechanisms of whole-grain cereals: What is beyond fibre? *Nutr Res Rev*. 2010;23(1):65-134.
12. Makki K, Deehan EC, Walter J, Bäckhed F. The impact of dietary fiber on gut microbiota in host health and disease. *Cell Host Microbe*. 2018;23(6):705-15.
13. Holscher HD. Dietary fiber and prebiotics and the gastrointestinal microbiota. *Gut microbes*. 2017;8(2):172-84.
14. Kortman GA, Dutilh BE, Maathuis AJ, Engelke UF, Boekhorst J, Keegan KP, et al. Microbial metabolism shifts towards an adverse profile with supplementary iron in the tim-2 in vitro model of the human colon. *Front Microbiol*. 2016;6:1481.
15. Fehlbaum S, Prudence K, Kieboom J, Heerikhuisen M, van den Broek T, Schuren F, et al. In vitro fermentation of selected prebiotics and their effects on the composition and activity of the adult gut microbiota. *Int J Mol Sci*. 2018;19(10):3097.
16. Jefferson A, Adolphus K. The effects of intact cereal grain fibers, including wheat bran on the gut microbiota composition of healthy adults: A systematic review. *Front Nutr*. 2019;6(33).
17. Costabile A, Klinder A, Fava F, Napolitano A, Fogliano V, Leonard C, et al. Whole-grain wheat breakfast cereal has a prebiotic effect on the human gut microbiota: A double-blind, placebo-controlled, crossover study. *Br J Nutr*. 2008;99(1):110-20.
18. Christensen EG, Licht TR, Kristensen M, Bahl MI. Bifidogenic effect of whole-grain wheat during a 12-week energy-restricted dietary intervention in postmenopausal women. *Eur J Clin Nutr*. 2013;67(12):1316.
19. Vitaglione P, Mennella I, Ferracane R, Rivellese AA, Giacco R, Ercolini D, et al. Whole-grain wheat consumption reduces inflammation in a randomized controlled trial on overweight and obese subjects with unhealthy dietary and lifestyle behaviors: Role of polyphenols bound to cereal dietary fiber. *Am J Clin Nutr*. 2014;101(2):251-61.

20. Vanegas SM, Meydani M, Barnett JB, Goldin B, Kane A, Rasmussen H, et al. Substituting whole grains for refined grains in a 6-wk randomized trial has a modest effect on gut microbiota and immune and inflammatory markers of healthy adults. *Am J Clin Nutr.* 2017;105(3):635-50.
21. Lappi J, Salojärvi J, Kolehmainen M, Mykkänen H, Poutanen K, de Vos WM, et al. Intake of whole-grain and fiber-rich rye bread versus refined wheat bread does not differentiate intestinal microbiota composition in Finnish adults with metabolic syndrome. *J Nutr.* 2013;143(5):648-55.
22. Ampatzoglou A, Atwal KK, Maidens CM, Williams CL, Ross AB, Thielecke F, et al. Increased whole grain consumption does not affect blood biochemistry, body composition, or gut microbiology in healthy, low-habitual whole grain consumers. *J Nutr.* 2015;145(2):215-21.
23. Cooper DN, Kable ME, Marco ML, De Leon A, Rust B, Baker JE, et al. The effects of moderate whole grain consumption on fasting glucose and lipids, gastrointestinal symptoms, and microbiota. *Nutrients.* 2017;9(2):173.
24. Bird AR, Vuaran MS, King RA, Noakes M, Keogh J, Morell MK, et al. Wholegrain foods made from a novel high-amylose barley variety (himalaya 292) improve indices of bowel health in human subjects. *Br J Nutr.* 2008;99(5):1032-40.
25. Slavin J. Why whole grains are protective: Biological mechanisms. *Proc Nutr Soc.* 2003;62(1):129-34.
26. Boets E, Gomand SV, Deroover L, Preston T, Vermeulen K, Preter V, et al. Systemic availability and metabolism of colonic-derived short-chain fatty acids in healthy subjects: A stable isotope study. *J Physiol.* 2017;595(2):541-55.
27. Canfora EE, Jocken JW, Blaak EE. Short-chain fatty acids in control of body weight and insulin sensitivity. *Nat Rev Endocrinol.* 2015;11(10):577.
28. den Besten G, Bleeker A, Gerding A, van Eunen K, Havinga R, van Dijk TH, et al. Short-chain fatty acids protect against high-fat diet-induced obesity via a ppar γ -dependent switch from lipogenesis to fat oxidation. *Diabetes.* 2015;db141213.
29. Mollica MP, Raso GM, Cavaliere G, Trinchese G, De Filippo C, Aceto S, et al. Butyrate regulates liver mitochondrial function, efficiency, and dynamic, in insulin resistant obese mice. *Diabetes.* 2017;db160924.
30. Kobylak N, Abenavoli L, Mykhalchyshyn G, Kononenko L, Boccuto L, Kyriienko D, et al. A multi-strain probiotic reduces the fatty liver index, cytokines and aminotransferase levels in NAFLD patients: Evidence from a randomized clinical trial. *J Gastrointest Liver Dis.* 2018;27(1):41-9.
31. Malaguarnera M, Vacante M, Antic T, Giordano M, Chisari G, Acquaviva R, et al. *Bifidobacterium longum* with fructo-oligosaccharides in patients with non alcoholic steatohepatitis. *Dig Dis Sci.* 2012;57(2):545-53.
32. Manzhaliy E, Virchenko O, Falalyeyeva T, Beregova T, Stremmel W. Treatment efficacy of a probiotic preparation for non-alcoholic steatohepatitis: A pilot trial. *Journal of digestive diseases.* 2017;18(12):698-703.
33. Aller R, De Luis DA, Izaola O, Conde R, Gonzalez Sagrado M, Primo D, et al. Effect of a probiotic on liver aminotransferases in nonalcoholic fatty liver disease patients: A double blind randomized clinical trial. *Eur Rev Med Pharmacol Sci.* 2011;15(9):1090-5.
34. Hoevenaars FPM, Esser D, Schutte S, Priebe MG, Vonk RJ, van den Brink WJ, et al. Whole grain wheat consumption affects postprandial inflammatory response in a randomized controlled trial in overweight and obese adults with mild hypercholesterolemia in the graandios study. *J Nutr.* 2019;149(12):2133-44.
35. Ramiro-Garcia J, Hermes GD, Giatsis C, Sipkema D, Zoetendal EG, Schaap PJ, et al. Ng-tax, a highly accurate and validated pipeline for analysis of 16s rRNA amplicons from complex biomes. *F1000Research.* 2018;5.
36. Poncheewin W, Hermes GDA, van Dam JCJ, Koehorst JJ, Smidt H, Schaap PJ. Ng-tax 2.0: A semantic framework for high-throughput amplicon analysis. *Front Genet.* 2019;10:1366.
37. Team RC. R: A language and environment for statistical computing, R foundation for statistical computing, Vienna. Austria ISBN. 2007.

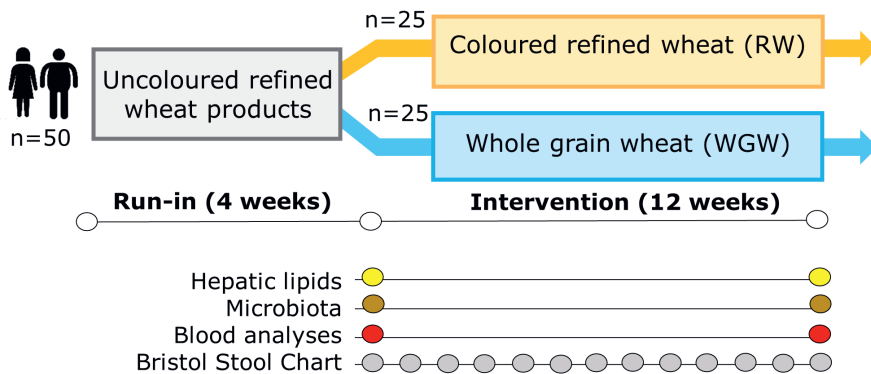
38. McMurdie PJ, Holmes S. Phyloseq: An r package for reproducible interactive analysis and graphics of microbiome census data. *PloS one*. 2013;8(4):e61217.
39. Weiss S, Xu ZZ, Peddada S, Amir A, Bittinger K, Gonzalez A, et al. Normalization and microbial differential abundance strategies depend upon data characteristics. *Microbiome*. 2017;5(1):27.
40. Oksanen J, Blanchet F, Friendly M, Kindt R, Legendre P, McGlinn D, et al. *Vegan: Community ecology package*. R package version 2.5-2. 2018.
41. Langille MGI, Zaneveld J, Caporaso JG, McDonald D, Knights D, Reyes JA, et al. Predictive functional profiling of microbial communities using 16s rrna marker gene sequences. *Nat Biotechnol*. 2013;31:814.
42. Institute CCHHM. Hmmer: Biosequence analysis using profile hidden markov models. Available from: <http://hmmer.org/>.
43. Barbera P, Kozlov AM, Czech L, Morel B, Darriba D, Flouri T, et al. Epa-ng: Massively parallel evolutionary placement of genetic sequences. *Syst Biol*. 2018;68(2):365-9.
44. Czech L, Barbera P, Stamatakis A. Genesis and gappa: Processing, analyzing and visualizing phylogenetic (placement) data. *bioRxiv*. 2019:647958.
45. Louca S, Doebeli M. Efficient comparative phylogenetics on large trees. *Bioinformatics*. 2017;34(6):1053-5.
46. Ye Y, Doak TG. A parsimony approach to biological pathway reconstruction/inference for genomes and metagenomes. *PLoS Comput Biol*. 2009;5(8):e1000465.
47. Caspi R, Altman T, Dreher K, Fulcher CA, Subhraveti P, Keseler IM, et al. The metacyc database of metabolic pathways and enzymes and the biocyc collection of pathway/genome databases. *Nucleic Acids Res*. 2011;40(D1):D742-D53.
48. Wolfe AJ. The acetate switch. *Microbiol Mol Biol Rev*. 2005;69(1):12-50.
49. Reichardt N, Duncan SH, Young P, Belenguer A, Leitch CM, Scott KP, et al. Phylogenetic distribution of three pathways for propionate production within the human gut microbiota. *ISME J*. 2014;8(6):1323.
50. Pryde SE, Duncan SH, Hold GL, Stewart CS, Flint HJ. The microbiology of butyrate formation in the human colon. *FEMS microbiology letters*. 2002;217(2):133-9.
51. Vital M, Howe AC, Tiedje JM. Revealing the bacterial butyrate synthesis pathways by analyzing (meta) genomic data. *MBio*. 2014;5(2):e00889-14.
52. Juturu V, Wu JC. Microbial production of lactic acid: The latest development. *Crit Rev Biotechnol*. 2016;36(6):967-77.
53. Salonen A, Lahti L, Salojärvi J, Holtrop G, Korpela K, Duncan SH, et al. Impact of diet and individual variation on intestinal microbiota composition and fermentation products in obese men. *ISME J*. 2014;8:2218.
54. Walker AW, Ince J, Duncan SH, Webster LM, Holtrop G, Ze X, et al. Dominant and diet-responsive groups of bacteria within the human colonic microbiota. *ISME J*. 2010;5:220.
55. Vos P, Garrity G, Jones D, Krieg NR, Ludwig W, Rainey FA, et al. *Bergey's manual of systematic bacteriology: Volume 3: The firmicutes*: Springer Science & Business Media; 2011.
56. Robert C, Bernalier-Donadille A. The cellulolytic microflora of the human colon: Evidence of microcrystalline cellulose-degrading bacteria in methane-excreting subjects. *FEMS Microbiol Ecol*. 2003;46(1):81-9.
57. Flint HJ, Scott KP, Duncan SH, Louis P, Forano E. Microbial degradation of complex carbohydrates in the gut. *Gut Microbes*. 2012;3(4):289-306.
58. Vuholm S, Nielsen DS, Iversen KN, Suhr J, Westermann P, Krych L, et al. Whole-grain rye and wheat affect some markers of gut health without altering the fecal microbiota in healthy overweight adults: A 6-week randomized trial. *J Nutr*. 2017;147(11):2067-75.
59. Raman M, Ahmed I, Gillevet PM, Probert CS, Ratcliffe NM, Smith S, et al. Fecal microbiome and volatile organic compound metabolome in obese humans with nonalcoholic fatty liver disease. *Clin Gastroenterol Hepatol*. 2013;11(7):868-75.e3.

60. Jiang W, Wu N, Wang X, Chi Y, Zhang Y, Qiu X, et al. Dysbiosis gut microbiota associated with inflammation and impaired mucosal immune function in intestine of humans with non-alcoholic fatty liver disease. *Sci Rep.* 2015;5(1):8096.
61. Iino C, Endo T, Mikami K, Hasegawa T, Kimura M, Sawada N, et al. Significant decrease in faecalibacterium among gut microbiota in nonalcoholic fatty liver disease: A large bmi- and sex-matched population study. *Hepato Int.* 2019;13(6):748-56.
62. Korem T, Zeevi D, Zmora N, Weissbrod O, Bar N, Lotan-Pompan M, et al. Bread affects clinical parameters and induces gut microbiome-associated personal glycemic responses. *Cell Metab.* 2017;25(6):1243-53. e5.
63. Vandeputte D, Falony G, Vieira-Silva S, Wang J, Sailer M, Theis S, et al. Prebiotic inulin-type fructans induce specific changes in the human gut microbiota. *Gut.* 2017;66(11):1968-74.
64. Markowiak P, Śliżewska K. Effects of probiotics, prebiotics, and synbiotics on human health. *Nutrients.* 2017;9(9):1021.
65. Vital M, Karch A, Pieper DH. Colonic butyrate-producing communities in humans: An overview using omics data. *mSystems.* 2017;2(6):e00130-17.
66. Muñoz-Tamayo R, Laroche B, Walter É, Doré J, Duncan SH, Flint HJ, et al. Kinetic modelling of lactate utilization and butyrate production by key human colonic bacterial species. *FEMS Microbiol Ecol.* 2011;76(3):615-24.
67. Han F, Wang Y, Han Y, Zhao J, Han F, Song G, et al. Effects of whole-grain rice and wheat on composition of gut microbiota and short-chain fatty acids in rats. *J Agric Food Chem.* 2018;66(25):6326-35.
68. Rose DJ. Impact of whole grains on the gut microbiota: The next frontier for oats? *Br J Nutr.* 2014;112(S2):S44-S9.
69. Andersson AA, Andersson R, Piironen V, Lampi A-M, Nyström L, Boros D, et al. Contents of dietary fibre components and their relation to associated bioactive components in whole grain wheat samples from the healthgrain diversity screen. *Food chemistry.* 2013;136(3-4):1243-8.
70. Andersson R, Fransson G, Tietjen M, Aman P. Content and molecular-weight distribution of dietary fiber components in whole-grain rye flour and bread. *J Agric Food Chem.* 2009;57(5):2004-8.
71. Eriksen AK, Brunius C, Mazidi M, Hellström PM, Risérus U, Iversen KN, et al. Effects of whole-grain wheat, rye, and lignan supplementation on cardiometabolic risk factors in men with metabolic syndrome: A randomized crossover trial. *Am J Clin Nutr.* 2020;111(4):864-76.
72. Bach Knudsen KE, Lærke HN, Hedemann MS, Nielsen TS, Ingerslev AK, Gundelund Nielsen DS, et al. Impact of diet-modulated butyrate production on intestinal barrier function and inflammation. *Nutrients.* 2018;10(10):1499.
73. Louis P, Flint HJ. Diversity, metabolism and microbial ecology of butyrate-producing bacteria from the human large intestine. *FEMS Microbiology Letters.* 2009;294(1):1-8.
74. Wang B, Jiang X, Cao M, Ge J, Bao Q, Tang L, et al. Altered fecal microbiota correlates with liver biochemistry in nonobese patients with non-alcoholic fatty liver disease. *Sci Rep.* 2016;6:32002-.
75. Del Chierico F, Nobili V, Vernocchi P, Russo A, De Stefanis C, Gnani D, et al. Gut microbiota profiling of pediatric nonalcoholic fatty liver disease and obese patients unveiled by an integrated meta-omics-based approach. *Hepatology.* 2017;65(2):451-64.
76. Nistal E, Sáenz de Miera LE, Ballesteros Pomar M, Sánchez-Campos S, García-Mediavilla MV, Álvarez-Cuenllas B, et al. An altered fecal microbiota profile in patients with non-alcoholic fatty liver disease (NAFLD) associated with obesity. *Rev Esp Enferm Dig.* 2019;111(4):275-82.

Supplementary Information

Technical information about the microbiota and predicted pathway datasets

The number of detected ASVs did not increase with higher sample reads (Supplemental Figure 3A). Correlation coefficients of the 23 technical duplicates were 0.97 ± 0.027 (Supplemental Figure 3B), and the mean number of reads per sample was 37399 ± 10216 . The microbiota functionality predictions were reliable, because the weighted NSTI for the samples in the dataset was 0.089 ± 0.048 (Supplemental Figure 3C), without differences between intervention groups (Supplemental Figure 3D). This suggests that closely related reference genomes were available for the ASVs in this dataset. Correlation coefficients of the predicted gene content in the 23 technical duplicate pairs were 0.99 ± 0.0013 (Supplemental Figure 3E).



Supplemental Figure 1. The study design of the randomized, controlled, double-blind parallel trial.

After 4 weeks run-in with RW products, subjects ($n=50$) were randomly assigned to the WGW ($n=25$) or RW ($n=25$) intervention group. Before and after the intervention hepatic lipids were measured, and feces and blood was collected. Subjects weekly recorded stool consistency using The Bristol Stool chart.

Supplemental Table 1. Nutritional composition of the RW and WGW intervention products¹.

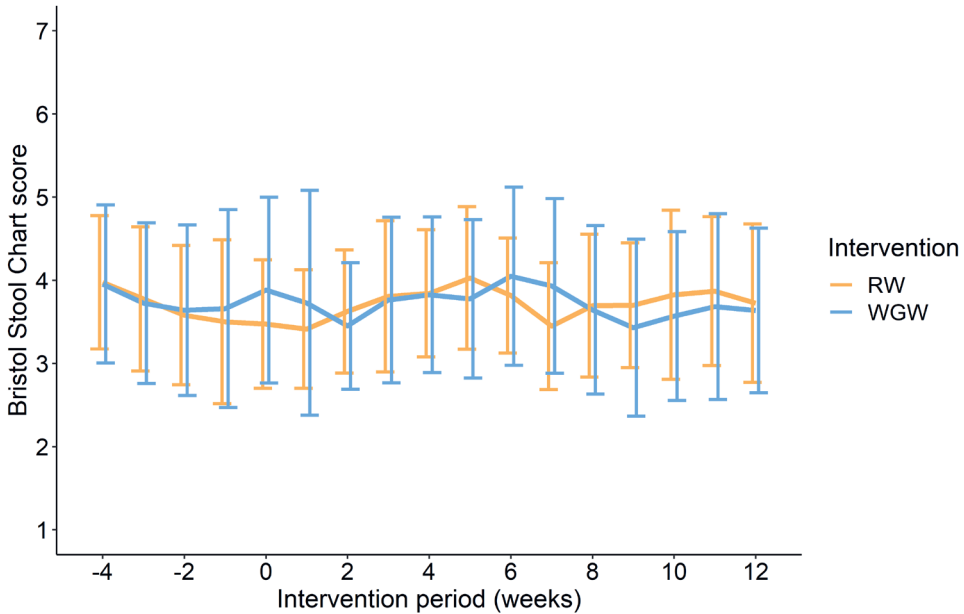
	Bread		RTEC	
	RW	WGW	RW	WGW
Energy, kJ	1066	983	1586	1524
Moisture, g	35.4	38.7	3.4	3.7
Ash, g	1.3	1.8	1.8	2.5
Carbohydrates, g	49.3	39.2	78.5	69.7
Fiber ² , g	3.3	6.8	3.9	10.8
Protein, g	9.1	11.3	10.9	11.2
Fat, g	1.6	2.1	1.5	2.1
Sodium, mg	0.45	0.46	0.51	0.49
Iron, mg	0.92	2.1	1.3	3.9
Magnesium, mg	19	62	31	120
Zinc, mg	0.67	1.5	0.89	2.4
Folate, µg	17	28	14	38
Vitamin B1, mg	0.06	0.17	<0.1	<0.1
Vitamin B3, mg	0.47	0.76	1.1	2.6
Vitamin B6, mg	<0.1	<0.1	<0.1	<0.1

¹Values are per 100 g of product. ²Determined using AOAC985.29. Reproduced with permission from Schutte et al. (7). Abbreviations: RTEC, ready-to-eat cereal; RW, refined wheat; WGW, whole-grain wheat.

Supplemental Table 2. Habitual daily intake of (macro)nutrients and whole grains of middle-aged overweight and obese subjects in the RW or WGW group¹.

Nutrients (g/d)	RW group	WGW group	P-value
Megajoules, MJ/day	10.3 ± 2.36	10.5 ± 2.89	0.80
Total carbohydrates ²	246 ± 59.6	279 ± 85.5	0.19
Mono- and disaccharides	101 ± 29.8	127 ± 41.8	0.04
Polysaccharides	145 ± 35.8	152 ± 57.8	0.64
Fiber ³	25.4 ± 6.50	26.3 ± 7.20	0.68
Whole grains	60.1 ± 59.2	54.4 ± 38.0	0.73
Total protein	95.9 ± 18.4	92.5 ± 18.0	0.58
Protein from plant sources	40.6 ± 10.6	39.5 ± 11.5	0.77
Protein from animal sources	55.2 ± 10.5	53.0 ± 10.3	0.52
Total fat	105 ± 32.1	101 ± 34.5	0.70
Saturated fatty acids	38.1 ± 12.5	37.5 ± 12.1	0.89
Monounsaturated fatty acids	37.4 ± 11.7	35.1 ± 11.9	0.56
Polyunsaturated fatty acids	20.9 ± 8.30	19.7 ± 9.50	0.70
Linoleic acid	17.5 ± 7.30	16.2 ± 7.80	0.60
Trans fatty acids	1.67 ± 0.577	1.82 ± 0.688	0.51
Cholesterol	285 ± 77.6	242 ± 106	0.18
Alcohol ⁴	12.5 ± 11.2	7.60 ± 9.90	0.08

¹Values are presented as group means ± SD, n=16 (RW) or n=21 (WGW), ²Dietary fiber is not included in the total carbohydrates, ³Include high molecular weight fibers (e.g. cellulose, cereal β-glucan, guar gum, and certain xylans), insoluble fibers in water (e.g. cellulose, and certain xylans), fibers soluble in water and precipitated by 78% ethanol (e.g. cereal β-glucan, guar gum, and certain xylans). Excluded are low molecular weight fibers (e.g. fructan), and non-resistant starch, ⁴Non-parametric distribution, evaluated with the Mann-Whitney U test. Abbreviations: RW, refined wheat; WGW, whole grain wheat.



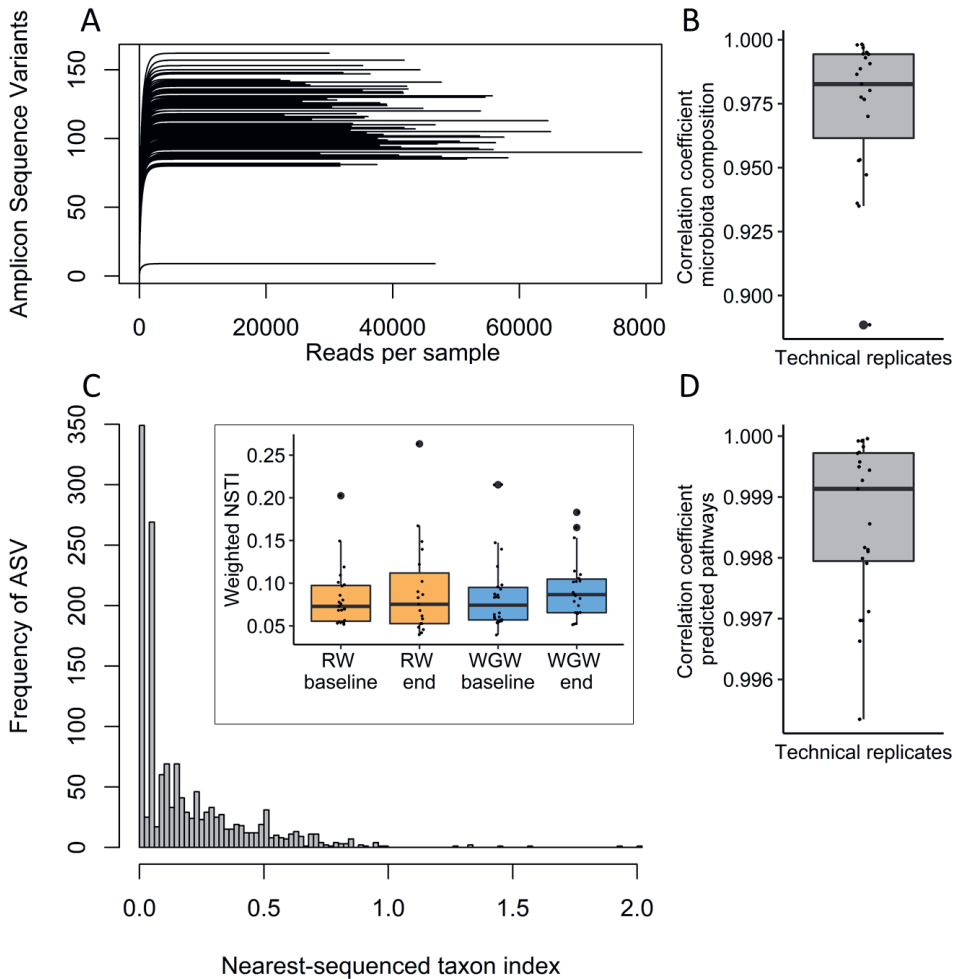
Supplemental Figure 2. The stool consistency of middle-aged overweight and obese adults during the run-in period and the 12 week of RW or WGW intervention.

Data is presented as group means \pm SD, $n=20$ (RW) or $n=22$ (WGW), after exclusion of antibiotic users. The Bristol Stool Chart score describes 7 types of stools ranging from 1: hard/lumpy to 7: watery without solid pieces. RW, refined wheat; WGW, whole grain wheat.

Supplemental Table 3. Liver health parameters at baseline and change after 12 weeks of RW or WGW intervention in middle-aged overweight and obese adults¹ in a subset of the total study population².

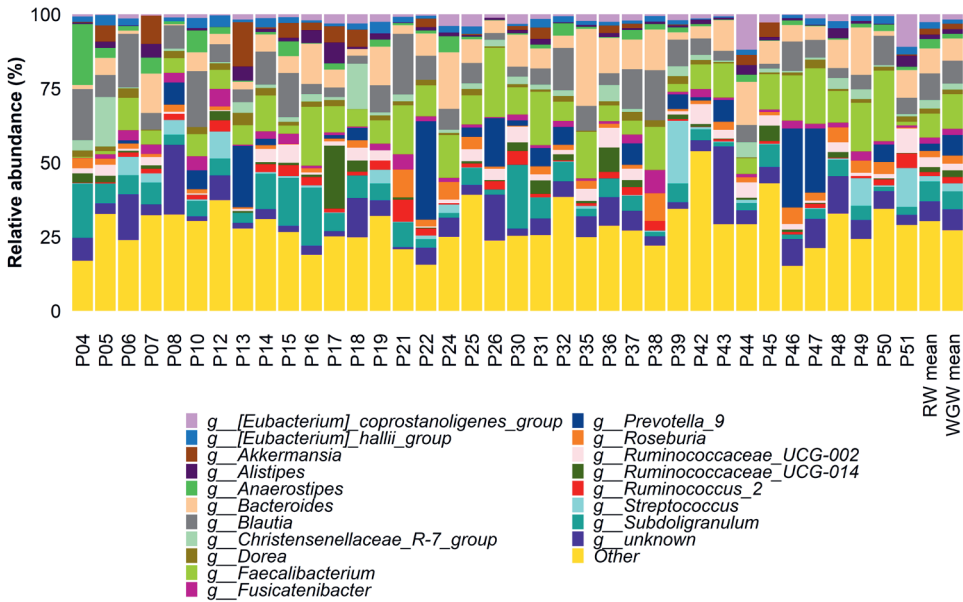
	RW group		WGW group		Within RW	Within WGW	Group comparison
	Baseline	Change after 12 wk	Baseline	Change after 12 wk	P-value	P-value	P-value
IHTG, %	3.6 \pm 2.5	1.8 \pm 1.6	5.5 \pm 6.4	-0.26 \pm 3.0	0.003	0.93	0.033
CRP, μ g/mL	2.9 \pm 3.1	0.20 \pm 1.9	4.8 \pm 7.3	-3.0 \pm 6.7	0.49	0.038	0.06
SAA, μ g/mL	2.1 \pm 1.9	0.70 \pm 2.2	7.2 \pm 16	-5.7 \pm 15	0.64	0.016	0.042
GGT, U/L	19 \pm 13	0.82 \pm 4.9	21 \pm 13	-0.43 \pm 4.9	0.47	0.77	0.56
AST, U/L	19 \pm 5.6	-0.18 \pm 4.0	19 \pm 4.7	-0.91 \pm 4.2	0.98	0.27	0.57
ALT, U/L	31 \pm 9.4	0.088 \pm 9.3	36 \pm 12	-2.8 \pm 8.3	0.78	0.24	0.39
Beta-hydroxybutyrate, mmol/L	0.30 \pm 0.20	-0.058 \pm 0.36	0.20 \pm 0.20	0.11 \pm 0.17	0.06	0.012	0.003

¹Values are presented as group means \pm SD, $n=16$ (RW) or $n=21$ (WGW), and for IHTG $n=11$ (RW) or $n=17$ (WGW). ²The total study population is described in the reference Schutte et al. (7). Abbreviations: ALT, alanine transaminase; AST, aspartate transaminase; CRP, C-reactive protein; GGT, gamma-glutamyltransferase; IHTG, intrahepatic triglycerides; RW, refined wheat; SAA, serum amyloid A; WGW, whole grain wheat.



Supplemental Figure 3. The quality characteristics of the amplicon sequence variant and PICRUSt2 datasets.

(a) The rarefaction curve of the sequenced samples; (b) the correlation coefficients of the relative microbiota composition on genus level between the samples within one technical replicate pair; (c) the NSTI score and the frequency of all ASVs, the inlay shows the weighted NSTI score at baseline and after the 12 week of intervention (end) in the RW and WGW group; and (d) the correlation coefficients of predicted pathways between the samples within one technical replicate pair. The boxplots show the data through their quartiles, $n=16$ (RW) or $n=21$ (WGW). Abbreviations: ASV, amplicon sequence variant; NSTI, nearest sequenced taxon index; RW, refined wheat; WGW, whole grain wheat.



Supplemental Figure 4. The relative microbiota abundance of the top 20 taxa on genus level at baseline for every middle-aged overweight or obese adult.

Also the group means for the RW (n=16) and WGW (n=21) group are shown. RW, refined wheat; WGW, whole grain wheat.

Supplemental Table 4. Gut bacteria and predicted pathways that were found to be significantly different between the RW and WGW group at baseline in middle-aged overweight and obese adults¹.

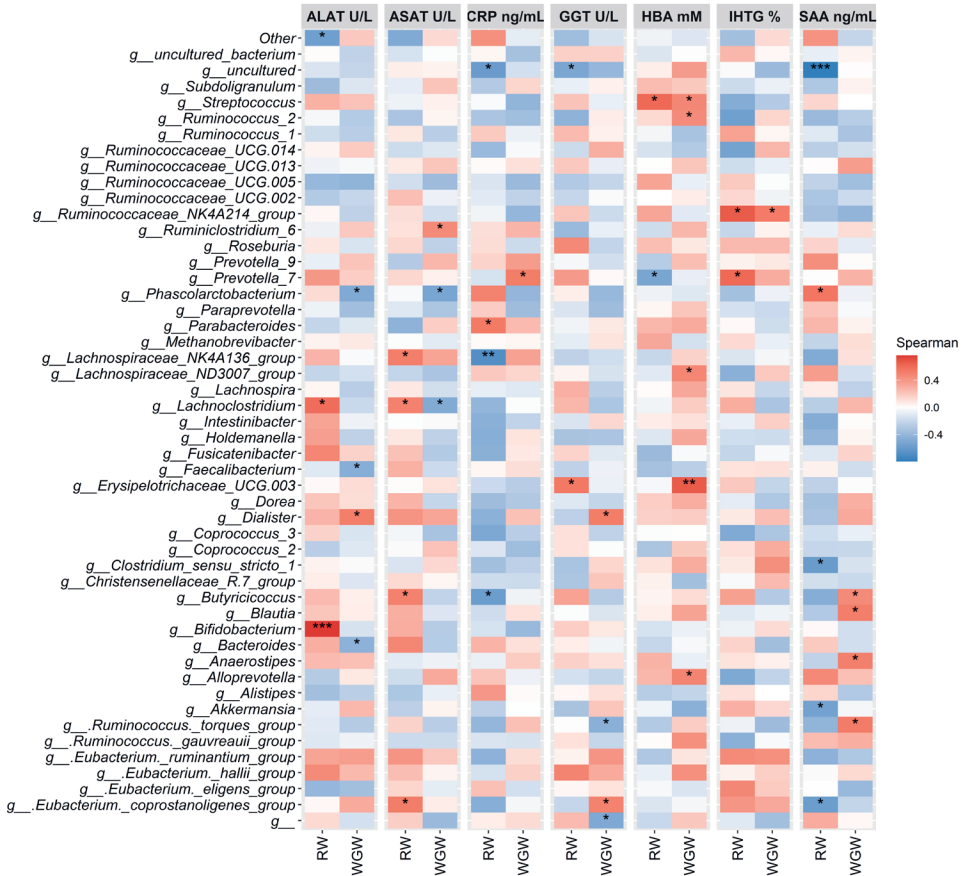
Genus	RW group		WGW group		Group comparison	
	Number of subjects in which detected (% of total)	Relative abundance at baseline (%)	Number of subjects in which detected (% of total)	Relative abundance at baseline (%)	P-value	FDR P-value
<i>Dialister</i>	5 (31)	0.40 ± 0.88	13 (62)	1.5 ± 2.2	0.046	NS
<i>[Eubacterium]_hallii_group</i>	16 (100)	2.2 ± 1.0	18 (86)	1.4 ± 0.97	0.038	NS
<i>[Eubacterium]_coprostanoligenes_group</i>	16 (100)	2.6 ± 2.7	21 (100)	1.8 ± 2.3	0.047	NS
<i>Ruminiclostridium_9</i>	10 (63)	0.20 ± 0.23	7 (33)	0.065 ± 0.11	0.047	NS
<i>Lachnospiraceae_UCG-008</i>	0 (0)	0.00 ± 0.00	10 (48)	0.10 ± 0.12	0.002	NS
<i>Lachnospiraceae_NK4A136_group</i>	16 (100)	0.65 ± 0.44	20 (85)	1.9 ± 1.9	0.035	NS
<i>f_Porphyromonadaceae_uncultured_genus</i>	3 (19)	0.051 ± 0.14	0 (0)	0.00 ± 0.00	0.045	NS
Predicted pathways						
L-arginine degradation	16 (100)	0.076 ± 0.044	21 (100)	0.060 ± 0.041	0.020	NS
superpathway of adenosylcobalamin salvage from cobinamide I	16 (100)	0.69 ± 0.077	21 (100)	0.73 ± 0.10	0.040	NS
superpathway of tetrahydrofolate biosynthesis and salvage	16 (100)	0.57 ± 0.052	21 (100)	0.53 ± 0.050	0.044	NS
heterolactic fermentation	16 (100)	0.11 ± 0.044	21 (100)	0.088 ± 0.043	0.003	NS
Glucose fermentation to lactate II/Bifidobacterium shunt	16 (100)	0.15 ± 0.066	21 (100)	0.12 ± 0.062	0.011	NS
ppGpp biosynthesis	16 (100)	0.016 ± 0.022	21 (100)	0.019 ± 0.041	0.050	NS
adenosylcobalamin biosynthesis from adenosylcobinamide-GDP I	16 (100)	0.66 ± 0.079	21 (100)	0.70 ± 0.10	0.049	NS
superpathway of adenosylcobalamin salvage from cobinamide II	16 (100)	0.67 ± 0.080	21 (100)	0.70 ± 0.10	0.041	NS
pyruvate fermentation to acetone	16 (100)	0.28 ± 0.12	21 (100)	0.20 ± 0.087	0.012	NS
UDP-2,3-diacetamido-2,3-dideoxy- α -D-mannuronate biosynthesis	12 (75)	0.010 ± 0.013	8 (38)	0.0015 ± 0.0024	0.032	NS
guanosine ribonucleotides de novo biosynthesis	16 (100)	0.83 ± 0.057	21 (100)	0.82 ± 0.062	0.033	NS

¹Values are presented as group means ± SD, or as the number of subjects in which the bacteria was detected and the percentage of total, n=16 (RW) or n=21 (WGW). ²NS = P-value > 0.05. Abbreviations: FDR, false discovery rate; RW, refined wheat; WGW, whole grain wheat.

Supplemental Table 5. The number of middle-aged obese or overweight subjects in which the significant gut bacteria were detected at baseline and after 12 weeks of RW or WGW intervention¹.

Genus	RW group		WGW group	
	Baseline	At 12 weeks	Baseline	At 12 weeks
	Number of subjects in which detected (% of total)	Number of subjects in which detected (% of total)	Number of subjects in which detected (% of total)	Number of subjects in which detected (% of total)
<i>f_Ruminococcaceae; g_Ruminiclostridium_9</i>	10 (63)	6 (38)	7 (33)	10 (48)
<i>f_Ruminococcaceae; g_Ruminococcaceae_NK4A214_group</i>	13 (81)	9 (56)	16 (76)	12 (57)
<i>f_Lachnospiraceae; g_Lachnospiraceae_UCG-008</i>	0 (0)	3 (19)	10 (48)	7 (33)
<i>f_Ruminococcaceae; g_Ruminococcaceae_UCG-014</i>	14 (88)	12 (75)	18 (86)	19 (90)
<i>f_Tannerellaceae; g_Parabacteroides</i>	12 (75)	14 (88)	21 (100)	15 (71)
<i>f_Lachnospiraceae; g_Dorea</i>	16 (100)	15 (94)	18 (86)	21 (100)
<i>f_Lachnospiraceae; g_[Eubacterium]_ventriosum_group</i>	8 (50)	3 (19)	13 (62)	12 (57)
<i>f_Peptostreptococcaceae; g_unknown</i>	14 (88)	8 (50)	14 (67)	9 (43)
<i>f_Ruminococcaceae; g_Ruminococcus_2</i>	14 (88)	13 (81)	21 (100)	17 (81)
<i>f_Ruminococcaceae; g_Subdoligranulum</i>	16 (100)	16 (100)	21 (100)	21 (100)
<i>f_Burkholderiaceae; g_Sutterella</i>	7 (44)	8 (50)	8 (38)	12 (57)
<i>f_Ruminococcaceae; g_Ruminococcaceae_UCG-005</i>	14 (88)	13 (81)	17 (81)	20 (95)

¹ Values are presented as the number of subjects in which the bacteria was detected and the percentage of total, n=16 (RW) or n=21 (WGW). Abbreviations: RW, refined wheat; WGW, whole grain wheat.



Supplemental Figure 5. Correlations between changes in bacteria abundances at genus level, and changes in liver health markers upon 12 weeks of RW or WGW intervention in middle-aged overweight and obese adults.

Colors represent the Spearman rho correlation coefficients, $n=16$ (RW) or $n=21$ (WGW), with positive correlations in red and negative correlations in blue. * P -value <0.05 , ** P -value <0.01 , *** P -value <0.001 . ALAT, alanine transaminase; ASAT, aspartate transaminase; CRP, C-reactive protein; GGT, gamma-glutamyltransferase; b-HBA, beta-hydroxybutyrate; IHTG, intrahepatic triglycerides; RW, refined wheat; SAA, serum amyloid A; WGW, whole grain wheat.

Supplemental Table 6. The selected predicted genes involved in SCEA production at baseline and after 12 weeks of RW or WGW intervention in the feces of in middle-aged overweight and obese adults¹.

Microbial predicted gene	K number	RW group		WGW group		Within RW		Within WGW		Group comparison	
		O	Δ Baseline relative abundance (%)	Δ Relative abundance after 12wk (%)	Baseline relative abundance (%)	Δ Relative abundance after 12wk (%)	P-value ²	P-value ²	P-value ²	P-value ²	
Acetate production											
Acetate kinase	K00925	7.95E-02 ± 4.28E-03	-1.09E-03 ± 3.61E-03	7.88E-02 ± 4.06E-03	-3.42E-04 ± 4.11E-03	0.35	0.68	0.39			
Phosphate acetyltransferase	K13788	1.48E-03 ± 1.38E-03	-1.76E-04 ± 1.71E-03	1.50E-03 ± 1.92E-03	1.50E-03 ± 1.59E-03	0.021	0.29	0.41			
Purative phosphotransacetylase	K15024	3.13E-02 ± 7.70E-03	-2.52E-03 ± 8.59E-03	3.28E-02 ± 7.53E-03	-1.96E-03 ± 7.89E-03	0.56	0.71	0.66			
Propionate production											
Propionyl-coA synthetase	K01908	5.01E-04 ± 9.66E-04	1.16E-04 ± 1.27E-03	6.42E-04 ± 1.51E-03	1.37E-04 ± 2.13E-03	0.17	0.96	0.27			
Propionate coA-transferase	K01026	1.15E-02 ± 4.86E-03	-1.81E-03 ± 4.66E-03	9.04E-03 ± 3.42E-03	9.34E-04 ± 4.39E-03	0.63	0.37	0.37			
Propionaldehyde dehydrogenase	K13922	6.44E-03 ± 3.60E-03	-1.75E-03 ± 4.49E-03	5.58E-03 ± 3.15E-03	-6.24E-04 ± 2.82E-03	0.60	0.66	0.96			
Methylmalonyl-CoA decarboxylase	K11264	4.65E-04 ± 9.55E-04	-6.56E+01 ± 1.18E-03	6.19E-04 ± 1.48E-03	6.19E-04 ± 2.06E-03	0.09	0.51	0.16			
Butyrate production											
Butyrate kinase	K00929	1.80E-02 ± 7.75E-03	2.18E-03 ± 8.02E-03	1.61E-02 ± 4.84E-03	1.49E-03 ± 7.25E-03	0.71	0.038	0.96			
Acetate CoA-transferase α subunit	K01034	9.51E-03 ± 4.65E-03	-1.35E-03 ± 4.63E-03	6.45E-03 ± 3.30E-03	7.53E-04 ± 2.79E-03	0.21	1.0	0.75			
Acetate CoA-transferase β subunit	K01035	9.59E-03 ± 4.69E-03	-1.27E-03 ± 4.70E-03	6.51E-03 ± 3.33E-03	7.66E-04 ± 2.83E-03	0.43	1.0	0.59			
Lactate production											
L-lactate dehydrogenase	K00016	7.10E-02 ± 1.32E-02	-7.09E-03 ± 1.24E-02	6.95E-02 ± 1.18E-02	-4.24E-03 ± 1.26E-02	0.39	0.81	0.63			
D-lactate dehydrogenase	K03778	3.01E-02 ± 7.56E-03	-2.63E-03 ± 8.23E-03	3.10E-02 ± 8.73E-03	3.34E-04 ± 9.76E-03	0.96	0.81	0.24			

¹Values are presented as group means ± SD, n=16 (RW) or n=21 (WGW). ²P-values without FDR correction. Abbreviations: KO, KEGG ortholog; RW, refined wheat; WG, whole grain wheat.



General discussion

Aim and main findings

Non-digestible carbohydrates (NDC) are very well known for their beneficial health effects. One suggested underlying mechanism is its fermentation by the intestinal microbiota and the production of fermentation products. Little is known about what exactly happens to NDCs at what stage during their passage through the human intestine. The work described in this thesis therefore aims to study the kinetics of fermentation and degradation of NDCs, mainly in the human small intestine, and consequent effects on the microbiota and bacterial metabolites. To achieve this aim, we validated and applied several models to study NDC digestion and fermentation. We used *in vitro* batch fermentation models as well as intervention trials in human subjects with the use of intestinal catheters and stable isotopes (**Table 1**). We investigated the acute short- and longer-term effects of varying NDC types and concentrations on the intestinal environment, including the microbiota and metabolites.

The main thesis findings are:

- In **chapter 2**, all technical and practical aspects of working with catheters placed in the jejunum, ileum, or proximal colon were described. State-of-the-art naso- and oro-intestinal catheters can be used for controlled sampling and compound delivery in relatively inaccessible regions in the human small intestine and colon. Many studies used catheters to investigate multiple intestinal regions (24 studies), followed by studies investigating only the jejunum (21 studies), ileum (13 studies), or colon (2 studies). Catheters were often used for intra-intestinal delivery (23 studies), sampling (10 studies), or both (27 studies).
- In **chapter 3**, a new methodology (a toolbox) was developed to be used, for example, with gastrointestinal sampling capsules. The stabilizing reagent effectively blocked the fermentation of FOS and GOS by human intestinal microbiota, including the microbiota and metabolites. To retrieve as much information as possible from a single small volume sample, analytical protocols were successfully optimized to measure these outcomes in a small sample in the presence of the stabilizing reagent.
- In **chapter 4**, the degradation of various NDCs, and the effects on microbiota composition and metabolite production by ileostomy effluent bacteria were investigated *in vitro*. The small intestine microbiota from ileostomy effluent rapidly degraded GOS and FOS, whereas the higher molecular weight NDCs inulin, lemon pectin, and IMMP showed slow fermentation rates. Degradation

of different NDCs resulted in the production of mainly acetate, and changed ileostomy effluent microbiota over time, in a subject-dependent fashion.

- In **chapter 5**, the postprandial fermentation in the intestine of human subjects and the metabolic fate of SCFAs were studied after consumption of a FOS:GOS mixture. In the distal ileum, there was no degradation observed of FOS and GOS, nor production or cross-feeding of SCFAs. However, hydrogen in the breath and SCFAs in the blood increased after FOS:GOS consumption, which indicates fermentation in the large intestine. Intestinal delivered SCFAs were rapidly taken up by the host and metabolized, with propionate as a substrate for net glucose synthesis. No label incorporation coming from ^{13}C -SCFAs was found in organic acids, amino acids, or fatty acids.
- In **chapter 6**, the digestibility of all structures present in FOS and GOS mixtures in the small intestine of healthy men was investigated. GOS $\text{DP} \geq 3$ and FOS ≥ 2 were not absorbed nor digested by host enzymes. Most of the prebiotic GOS DP2 fraction decreased in the human small intestine, especially $\beta\text{-D-Gal-(1}\leftrightarrow\text{1)-}\alpha\text{-D-Glc}/\beta\text{-D-Gal-(1}\leftrightarrow\text{1)-}\beta\text{-D-Glc}$, and $\beta\text{-D-Gal-(1}\rightarrow\text{2)-D-Glc}/\beta\text{-D-Gal-(1}\rightarrow\text{3)-D-Glc}$. The digestion was affected by differences in size, monomer composition, and the type of linkage.
- In **chapter 7**, the effects of a 12-week whole grain wheat (WGW) or refined wheat intervention on the fecal microbiota composition and functionality were studied. We found minor alterations in fecal microbiota composition when comparing groups. The effects were mainly an increase in certain non-digestible carbohydrate-degrading bacteria, and bacterial functions related to fermentation in the WGW group.

Table 1. An overview of the thesis chapters and the designs.

	Chapter 2	Chapter 3	Chapter 4	Chapter 5	Chapter 6	Chapter 7
	<i>Method development</i>					
Aim	To summarize best-practices for the use of naso- and oro-intestinal catheters.	To develop a methodology (a toolbox) to use with gastrointestinal sampling capsules.	To study NDC breakdown by small intestine microbiota.	To study NDC fermentation and SCFA metabolism.	To study FOS:GOS digestibility in the small intestine.	To study the effects of whole grain wheat on the fecal microbiota.
Model	Humans.	In vitro batch fermentation.	In vitro batch fermentation.	Humans. Two feasibility intervention studies.	Humans. Two feasibility intervention studies.	Humans. Intervention study.
Study population	762 human subjects (42 patients and 720 healthy subjects).	5 ileostomy patients, and 4 healthy subjects.	5 ileostomy patients.	15 healthy male subjects.	15 healthy male subjects.	37 middle-aged females and males with overweight of obesity.
Design	Systematic literature review.	Incubations of fermentation samples (with GOS, FOS/inulin) with sampling at 0 and 48 hours with or without a stabilizing reagent added.	Incubations with sampling at 0, 5, 7, 9 and 24 hours after addition of GOS, FOS/ inulin (1:1 mix), pectin, or IMMP.	- 7-day intervention, parallel design (RCT), either 15 g FOS:GOS or maltodextrin. - Followed by postprandial measurements after consumption of 10 gram FOS:GOS (0-330 minutes)	Postprandial measurements after consumption of 10 gram FOS:GOS (0-330 minutes).	- 12-week intervention, parallel design (RCT), either 98 g/day WGW or 98 g/day RW. - Measurements before and after intervention.
Intestinal region of interest	Jejunum, ileum, proximal colon.	Distal ileum, colon.	Distal ileum.	Distal ileum, colon, studied using a naso-intestinal catheter.	Distal ileum, proximal colon, studied using a naso-intestinal catheter.	Distal colon.
Origin of the microbiota	-	Ileostomy effluent, feces.	Ileostomy effluent.	Ileum, proximal colon, distal colon, feces.	Ileum, proximal colon.	Feces.
Main outcome measures	Placement procedures, catheter designs, aspiration and delivery, adverse events.	Efficacy of the stabilizing reagent (% Degradation of FOS and GOS after 48 hours, stabilization of SCFAs and microbiota).	Substrate degradation over time: NDC degradation products, SCFAs, microbiota.	- Measures of fermentation: SCFAs production, cross-feeding. - ¹³ C label incorporation in metabolites.	Analysis of all compounds in the FOS:GOS mixture.	Microbiota composition and functions (incl. fermentation pathways), stool consistency.

Abbreviations: FOS, fructo-oligosaccharides; GOS, galacto-oligosaccharides; IMMP, isomalto/malto-polysaccharide; NDC, non-digestible carbohydrates; RCT, randomized controlled trial; RW, refined wheats; SCFA, short-chain fatty acids; WGW, whole grain wheat.

Approaches to study the kinetics of non-digestible carbohydrates in the human intestine

We used various approaches to study the degradation kinetics and effects of NDCs, as a supplement or within a food matrix, in the human intestine (**Table 1**). We focused on the use of naso- and oro-intestinal catheters (**chapters 2, 5, 6**), gastrointestinal sampling capsules (**chapter 3**), ileostomy effluent as a proxy to study the interaction between NDCs and the small intestine microbiota (**chapter 4**), or the use of fecal samples as a proxy to investigate the effect of interventions on the colonic microbiota (**chapter 7**). The application of these approaches is discussed in the subsequent paragraphs.

The type of microbiota

Most microbiome research in healthy people to date is based on the analysis of fecal samples due to the ease of sample collection. We also analyzed the fecal microbiota composition in the intervention study described in **chapter 7**. We found that the fecal microbiota was different from the microbiota in the proximal colon and the distal ileum, but it did mimic the microbiota in the more distal colon (**Figure 1**). This is in line with previous findings (1, 2). To simulate the study of NDC fermentation rates in the colon, fecal samples can be used to inoculate *in vitro* fermentation models. Such models can be used to mimic fermentation in the human gut (*in vivo*) in a high-throughput, cost-efficient way without ethical restrictions. The vast majority of *in vitro* fermentation models targets the colon, leaving the direct effect of NDCs on the small intestine microbiota relatively underexplored. In **chapter 3** and **chapter 4**, both feces or ileostomy effluent were used for inoculation of the batch fermentations, as proxies to study NDC fermentation rates by the large and small intestine microbiota, respectively. As shown in **Figure 1**, the microbiota composition in the fresh ileostomy effluents was comparable to the ileal microbiota of healthy people (**chapters 4, 5**). Our findings in this small study population, therefore, suggest that the use of ileostomy microbiota, collected from patients with an ileostomy who were otherwise healthy, is representative of the ileal microbiota of healthy people. This suggests that ileostomy patients are a suitable model for healthy subjects when aiming to study the small intestine microbiome.

Novel gastrointestinal (sampling) capsules and intestinal catheters

Human studies are superior to *in vitro* and *ex vivo* models of the GI-tract due to the presence of all complex and relevant physiological processes. Over the past decades, novel intestinal capsules became available to measure in real-time intestinal motility, transit time, pH, and intraluminal pressure (3) as well as gas profile composition (4), and to visualize the intestinal wall (5), to detect bleeding (6), to detect polyps (7), or to collect biopsies (8), as recently summarized in (9). Capsules that will continuously monitor certain metabolites throughout the intestine can be expected in the future (10).

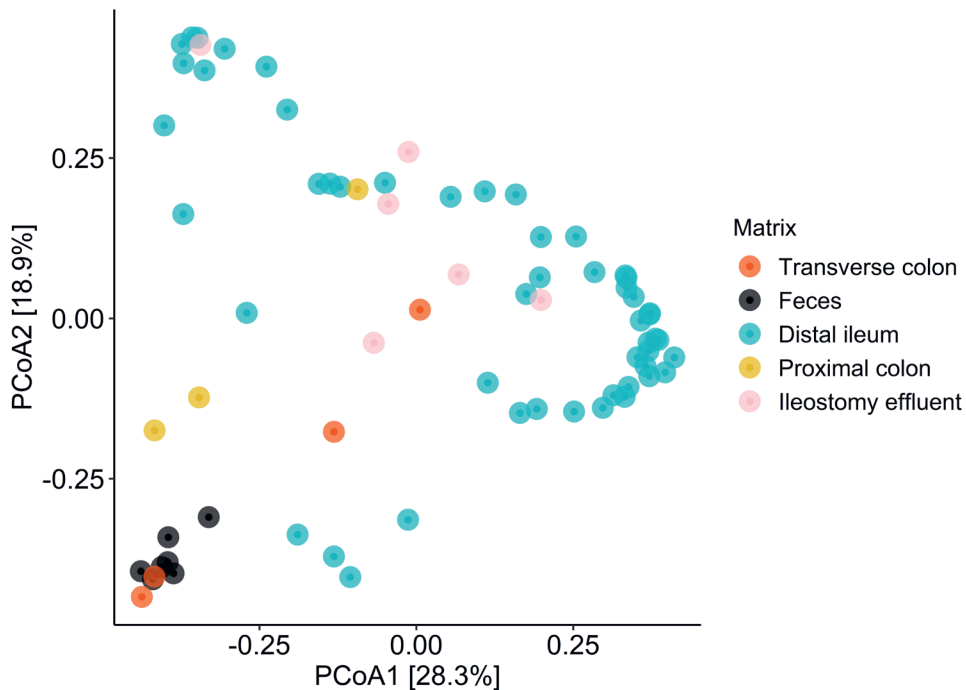


Figure 1. A comparative analysis of different types of microbiotas.

Included are the microbiota composition in the ileostomy effluents ($n=6$), the ileal contents during one day of healthy subjects ($n=6$ subjects, multiple time points), the proximal colon contents ($n=1$, 3 time points), and transversel descending colon content ($n=1$, 4 time points), and feces of healthy subjects ($n=7$). Data is derived from chapter 4 and chapter 5.

Drug delivery capsules already exist, but also new gastrointestinal sampling capsules are (being) developed (11-15). They have great potential to collect intestinal content at a chosen location in the GI-tract in a minimally invasive way. The application of these capsules will pose methodological challenges. Our original project plan was based on using, at that time, an existing gastrointestinal sampling capsule (the IntelliCap[®] system from manufacturer Medimetrics) in human studies. We, therefore, focused on tackling the two main challenges: 1) the sample retrieval time delay as the capsule can reside in the body for up to 48 hours (16), which requires stabilization of the sample, and 2) the small sample volumes of capsule containers to perform all the required measurements in. We developed a novel toolbox to use with sampling capsules in an *in vitro* setting, to stabilize and analyze the fermentation process of FOS and GOS, including the intestinal microbiota and selected bacterial metabolites (**chapter 3**). Adding our developed stabilizing reagent blocked the fermentation process for 48 hours at body temperature, while in the control incubations without the stabilizing reagent, the ileostomy and fecal microbiota degraded the NDCs and produced SCFAs. The finding that also the small

intestine bacteria degraded NDCs, highlights the importance of also stabilizing the microbiota in capsules that will sample in the small intestine to obtain a representative 'snapshot'. One main limitation is that the effectiveness of our stabilizing reagent was only evaluated in tubes in a relatively simple laboratory setting. Proof of principle experiments using real sampling capsules are therefore still needed. During this project, the technology was taken over by another company and consequently, capsules were not available on the market. Hence we could not use them in human studies during the execution of this thesis project. Currently, there are numerous follow-up initiatives for the development and validation of gastrointestinal sampling capsules (14, 15, 17-20), with sampling methods ranging from the use of osmotic pumps and springs/wicking materials to biodegradable coatings. Given the rapid developments in this research field, it can be expected that the analytical toolbox may know applications in the future. Non-invasive sampling capsules will have great potential to further characterize the small intestine microbiota community in large population cohorts or to investigate the effects of longer-term (nutritional) interventions on the small intestine microbiota. However, to study food kinetics in the intestine over time, capsules are less suitable because multiple capsules would be required to capture the *in vivo* dynamics over time (**chapter 5**). This would drastically increase the complexity and price of kinetic studies. The only alternatives to study kinetics over time in the distal ileum or proximal colon are more-invasive naso- and oro-intestinal catheters, colonoscopies, or rectal/anal catheters (**chapter 2**). When colonoscopy is used to reach the terminal ileum and proximal colon, laxatives are administered to prepare the bowel. During this preparation, the luminal environment, including changes in the microbiota composition, diversity, and numbers (21), will be disturbed. Since our main outcomes in the human studies were microbiota related (**chapter 5**), and for this reason, we used naso-intestinal catheters, in which a bowel preparation step is not needed and participants can perform their habitual daily activities.

The use of naso-intestinal catheters to study fermentation in humans

In our human feasibility studies, we tested the use of naso-intestinal catheters to study fermentation in the proximal colon (**chapters 5, 6**). Similar catheters have been widely used in pharmacokinetics and/or digestion and absorption studies (**chapter 2**), but we were the first to assess its use to document fermentation in humans. During the execution of the first pilot study using intestinal catheters (**chapter 5**), it became clear that there are many (practical) challenges coupled to the use of this tool to study the distal intestine. Based on our own experiences in combination with information from the literature, a review paper was written that includes best practices for the use of catheters (**chapter 2**). We aimed to monitor fermentation kinetics in the proximal colon, but sampling over time with these catheters was only possible in the distal ileum and not in the colon (**chapter 5**). While we did not measure fermentation in the intestine

using the intestinal catheter, using the catheter allowed us to study the resistance to digestion of all compounds in the FOS:GOS mixture in the small intestine (**Table 2**). When aiming to study fermentation kinetics in the colon at a standardized location, catheters with a larger diameter (>1.9 mm aspiration channel) and/or the use of rectally placed catheters may be more suitable (22). Our outcomes were microbiota related, and we found that the small and large intestine microbiota are distinct in composition and predicted fermentation capacity (**chapter 5**). Even between the different regions within the small intestine (duodenum, jejunum, ileum) high variation of the microbiota can be expected (2). Taking these findings into account, comparisons of outcomes between intervention groups and subjects will only be possible if the intestinal sampling site among subjects is standardized. More check-up moments will improve standardization, which in our studies exposed healthy subjects to radiation. Alternatively, localization guidance and visualization using electromagnetic systems do not expose volunteers to radiation (23), as described in **chapter 2**, and hence allow more check-up moments throughout the study. To visualize long intestinal catheters (300–400 cm) with these systems, manufacturing of longer so-called transmitting stylets that reach up to the catheter tip is warranted. Furthermore, we found a higher drop-out rate in our human trials (~40%) compared to what has been reported previously in the literature (~10%, **chapter 2**). Most drop-outs were the result of difficulties with post-pyloric placement. To improve post-pyloric placement, the use of stiffeners integrated into the catheter and/or the use of guidewires is highly recommended. Overall, naso- and oro-intestinal catheters have interesting applications, especially for kinetics studies, but need thorough evaluation before use (**chapter 2**). It is important to note that naso- and oro-intestinal catheters collect lumen content, which is an ‘external’ environment. Analysis of the lumen content only does not provide information about the direct impact and the interaction with the host enterocytes. To study the host tissue response *in vivo*, parallel epithelial tissue sampling via a biopsy would be needed. Another elegant way to examine the effects of the luminal compounds including NDCs and fermentation products on the intestinal gene expression response and production of inflammatory markers such as cytokines would be to incubate cultured intestinal and/or immune cells with the luminal content.

Systemic biomarkers for fermentation in humans

Besides the measurement of the main fermentation products in the intestinal lumen, several classical, systemic biomarkers of NDC fermentation were included in our human studies (**chapter 5**). The concentrations of hydrogen and methane in breath and SCFAs concentrations in blood were quantified after FOS:GOS consumption. All subjects showed an increase in breath hydrogen and plasma acetate. This highlights their use as NDC fermentation biomarker. In contrast, not all subjects showed an increase in breath methane, plasma propionate, and plasma butyrate. Recently, interest is

growing to expand the set of non-invasively measured biomarkers that link to properties of NDCs and their fermentation. The collection of breath samples is easy and non-invasive. Therefore, it is highly relevant to further explore the use of measuring breath volatile metabolites and their link to postprandial digestive processes in the intestine. Novel technology, for instance, selected ion flow tube mass spectrometry, will allow the analysis of such compounds in breath in an untargeted manner (24).

In vitro models to mimic digestion and fermentation

The findings of the *in vitro* batch fermentation experiments indicated that the small intestine bacteria have the functionality to degrade FOS and GOS (**chapter 4**). By contrast, in human subjects, we did not detect fermentation of FOS:GOS in the distal ileum (**chapter 5**). The conflicting findings can be explained by numerous factors. First, the batch fermentations using small intestine microbiota were performed for up to 24 hours. It would have been relevant to also include more sampling moments between 0 and 5 hours to better reflect the actual limited exposure time in the human small intestine (**chapters 4, 5**). As an alternative, dynamic models, such as SHIME and TIM systems (25), could be used, which more closely resemble physical and mechanical processes in the intestine including the transit time of food and peristaltic contractions. One main general limitation of *in vitro* models is the requirement of a stabilization period that leads to a shift in the microbiota before the start of the actual experiment. In our experiments, the starting microbiota in the ileostomy effluents mimicked the small intestine microbiota of healthy people (**Figure 1**), but at the start of the experiment, the microbiota differed from the microbiota in the fresh ileostomy effluent (**chapter 4**). This shift was likely caused by the overnight incubation (before the start of the experiments) in standard ileal efflux medium (26), used for decades in the field of microbiology. Even though it was shown that a fraction of dietary protein enters the human colon undigested (27), the medium contains a relatively high amount of proteins and amino acids compared to NDCs. For future studies, using a medium that more closely reflects the ileum output of indigestible nutrients is of interest. Moreover, the total bacteria numbers in the *in vitro* system were higher compared to the bacteria numbers in the ileum in humans (**Table 2**), which could have resulted in more efficient fermentation *in vitro*. Overall, the batch fermentations provide leads about fermentation rates and assessment of microbiota and metabolite ratios produced during fermentation (28), but to fully understand the mechanisms underlying the effects of NDCs, it is essential to integrate mechanistic *in vitro* studies with human studies. In **chapter 6** it was shown that the prebiotic GOS dimer fraction decreased after passage in the human small intestine, expectedly due to hydrolysis by the host brush-border enzymes. When *in vitro* digestion models will be used to screen digestibility of new prebiotics, it is strongly recommended to include incubations with host brush-border carbohydrases in addition to the often-used pancreatic enzymes and gastric juice (29). Moreover, the *in vitro*

findings in **chapter 4** show the direct interaction between some NDCs and the small intestine microbiota, which can also be expected to occur with other dietary factors such as proteins, digestible carbohydrates, and lipids (30). This highlights the importance of future developments of *in vitro* human small intestine digestion models where not only physiological parameters are included, but also its microbiota. One elegant example is the *in vitro* ileum model with a continuous flow of foods (31).

Degradation kinetics of various non-digestible carbohydrates

In a diet containing lots of vegetables, fruits, and whole grain products, plenty of NDCs are present. In typical Western diets, the amount of NDCs consumed via the diet is often far below the recommended intakes (32-34). The NDC intake can be increased via increased consumption of plant-based products. People suffering from certain disorders, such as constipation, potentially benefit from supplementation of NDCs to the diet. We performed kinetic-studies using purified NDC supplements to understand the potential mechanisms underlying their effects in the human intestine (**chapters 4-6**). We focused mostly on NDC degradation in the human small intestine and the effects on the small intestine microbiota community. In **chapter 5** we also examined the effects in the large intestine and feces as a comparison. We studied five purified NDCs, namely GOS (**chapters 4-6**), FOS (**chapters 4-6**), inulin (**chapter 4**), lemon pectin (**chapter 4**), and IMMP (**chapter 4**).

Fermentation kinetics of non-digestible carbohydrates

As shown in **chapter 4**, the NDC degradation kinetics by the human small intestine microbiota revealed differences in fermentability between the tested NDCs. The degradation rates depended on the NDC structure complexity (35), including monosaccharide and linkage composition, DP, and molecular conformation. Lower molecular weight GOS and FOS were rapidly degraded by the small intestine microbiota of all ileostomy subjects, mostly before 5 hours of incubation (**Table 2**). These findings show that small intestinal bacteria potentially contribute to the digestion of these NDCs, because they produce enzymes needed for their degradation. The degradation resulted in the production of mostly acetate. In contrast, the small intestine microbiota was not very efficient in degrading inulin, lemon pectin, and IMMP, which started only after 7 to 9 hours of incubation. This indicates that the latter NDCs likely will not be fermented in the human small intestine, because food is only present in the small intestine for on average 3.5 to 6 hours (16). This can explain why in previous human studies almost 90% of the ingested pectin (36) or 86-89% of inulin (37, 38) was recovered from the distal ileum. Importantly, the degradation rates of selected NDCs were strongly dependent on the subject. The varying fermentation rates between NDCs and subjects

can be explained by the growth or presence of specific bacteria producing the required carbohydrate degrading enzymes (39). The NDC degradation rates provide leads about the extent of fermentation and the expected location of fermentation, in the proximal versus more distal intestine, which might consequently determine the health effects. For instance, health markers including fasting fat oxidation, fasting peptide YY (PYY), and fasting tumor necrosis factor- α (TNF- α) improved when SCFAs were infused in the distal colon compared to the proximal colon (22). Another example is to stimulate the production of anti-inflammatory butyrate at the site of inflammation in patients with inflammatory bowel diseases using specific NDCs that are locally fermented (40). Based on the findings in **chapter 4**, we expected that GOS and FOS were fermented in the distal ileum or proximal colon in humans. The next step was to study postprandial fermentation kinetics in the human distal ileum or proximal colon (**chapter 5**), and based on the *in vitro* study, FOS and GOS were provided as supplements in our human studies (**chapter 5, 6**). In contrast to our hypothesis, no fermentation of GOS:FOS occurred in the distal ileum of healthy males (**Table 2, chapter 5**). We also delivered a mixture of the three SCFAs differing in ^{13}C label patterns directly in the intestine, to study the expected metabolic cross-feeding flux from acetate to butyrate (41, 42), but no SCFA production or cross-feeding occurred in the distal ileum.

One possible explanation for this finding might be that the rapid transit time of food in the ileum (16), and thus short exposure of NDCs to the small intestine bacteria, did not allow for fermentation to take place in the small intestine in this study population. Moreover, the SCFAs were rapidly absorbed in the distal ileum (**chapter 5**), leaving hardly a possibility for interconversion. The lack of fermentation in the distal ileum is expected to be beneficial, because the small intestine has a smaller diameter and is less elastic compared to the large intestine (43). Therefore, the small intestine is not prepared to expand upon gas production during fermentation. The tolerance towards fermentable nutrients is debated, since the finding that a subgroup of patients with irritable bowel syndrome (IBS) benefit from diets low in fermentable oligo-, di- and monosaccharides (FODMAP), which include amongst others fructose, lactose, sorbitol, but also FOS and GOS (44). Of note, most of the studies investigating the FODMAP diet reduced excess of fructose to glucose and lactose, while the reduction of fructans was minimal. Furthermore, while the reduction of fructans was minimal. Furthermore, supplementation (*e.g.* with FOS and GOS) in combination with the FODMAP diet may be beneficial (45). In our studies, healthy subjects without intestinal disorders were included and they tolerated the daily consumption of 15 gram FOS:GOS well (**chapter 5**). It may be speculated that in patients with functional gastrointestinal disorders or small intestine bacteria overgrowth (SIBO) (46-48) the small intestine microbiota may cause complaints by rapid fermentation of NDCs or simple carbohydrates, such as bloating, due to high bacteria numbers or a microbiome dysbiosis in the small intestine (48).

Table 2. The main results of the different studies focusing on degradation kinetics of FOS and GOS in the human intestine.

	Chapter 4 In vitro fermentation of FOS and GOS	Chapter 5 Fermentation of FOS and GOS in humans.	Chapter 6 Detailed analysis of FOS and GOS in the human intestine.
NDC degradation kinetics.	At 5 hours: - 31-82% digestion of GOS; - 82-100% digestion of FOS DP3; - 29-89% digestion of FOS DP4-8.	Distal ileum: - 4% digestion of FOS DP \geq 2; - 24% digestion of GOS DP \geq 2.	Linkage-specific disappearance of the GOS DP2 fraction: - 77% digestion of β -D-Gal-(1 \leftrightarrow 1)- α -D-Glc + β -D-Gal-(1 \leftrightarrow 1)- β -D-Glc; - 81% digestion of β -D-Gal-(1 \rightarrow 2)-D-Glc + β -D-Gal-(1 \rightarrow 3)-D-Glc; -56% digestion of β -D-Gal-(1 \rightarrow 6)-D-Gal; -32% digestion of β -D-Gal-(1 \rightarrow 4)-D-Gal.
Bacterial metabolites.	Maximally 166 mM acetate, 44 mM propionate, 17 mM butyrate.	Distal ileum: maximally 14.1 mM acetate, 2.5 mM propionate, 3.4 mM butyrate. No SCFA increase. Colon: maximally 31.2 mM acetate, 6.2 mM propionate, 5.9 mM butyrate.	-
Ratio of bacterial metabolites.	Ratio acetate to propionate to butyrate was 82:13:5.	Distal ileum: ratio acetate to propionate to butyrate was 74:14:12. Colon: acetate to propionate to butyrate was 88:5:7 (n=1).	-
Metabolite cross-feeding.	Cross-feeding not studied.	No cross-feeding detected.	-
Total bacteria numbers.	Cultured ileostomy bacteria: 10 ⁹ -10 ¹¹ 16S rRNA gene copy numbers/mL.	Ileum: 10 ⁶ -10 ¹⁰ 16S rRNA gene copy numbers/g wet weight. Colon: >10 ¹⁰ 16S rRNA gene copy numbers/g wet weight.	-

Abbreviations: DP, degree of polymerization; FOS, fructo-oligosaccharides; Gal, galactose; Glu, glucose; GOS, galacto-oligosaccharides; SCFA, short-chain fatty acids.

Overall, we have shown that the small intestine microbiota has the functionality to ferment FOS and GOS *in vitro* (**chapter 4**), while the findings in the human studies show that FOS and GOS are expected to have minor effects in the small intestine via

fermentation in healthy adults (**chapter 5**). FOS and GOS potentially exert effects in the small intestine via other mechanisms, for instance, via interaction with immune processes. The small intestine contains a thinner and penetrable type of mucus that allows more direct interaction between luminal compounds with the immune receptors and cells (49) in comparison to the large intestine, which has an additional dense and thick mucus layer (50). Researchers have suggested a direct interaction of FOS and GOS with the intestinal immune system *in vitro* (51), which may be worthy to further explore in future studies.

Digestibility of non-digestible carbohydrates in the small intestine

In **chapter 6**, we investigated the degradation of all structures present in FOS and GOS mixtures in the small intestine of healthy men. The direct measurements in the distal small intestine allowed us to detect the structure-specific disappearance of GOS dimers (**Table 2**), while FOS dimers with a β -(2,1) linkage did not disappear. Due to the lack of production of fermentation products (**chapter 5**), in combination with available evidence from the literature on GOS digestion by brush-border enzymes from rats or pigs (**chapter 6**), we hypothesize that degradation occurred by digestion of the host brush-border enzymes rather than utilization by the small intestine microbiota. Prebiotics with a low caloric value can be used as sugar replacers to develop more healthy products that result in lower glycemic responses (52), as well as having benefits for intestinal health such as reducing transit time and functioning as substrates for fermentation by the colonic microbiota (53). For optimal effectivity, NDCs must reach the proximal colon. An obvious indirect measurement to study carbohydrate digestion in the small intestine in humans is the measurement of postprandial blood glucose (54). This is nowadays also possible via minimally-invasive continuous glucose monitors. In our study, the linkage-dependent disappearance of specific GOS dimers (**chapter 6**) was not linked to an increased postprandial glucose response in blood within 120 minutes after consumption (**chapter 5**). This can also be explained by the low amount of each specific GOS compound that was present in the NDC bolus, since the total amount of GOS was only 5 gram. Our findings are useful for the future development of new tailored (potential) prebiotics to increase resistance to digestion in the small intestine. One surprising finding was that lactose, also present in the GOS mixture, was still detected at the end of the human small intestine (27.9-47.5% recovery, **chapter 6**). This is remarkable, since lactose is normally digested in the proximal small intestine, and the subjects were reportedly not lactose intolerant. GOS is often used as the replacement of human-milk oligosaccharides in infant milk formula (55), and infants do express lactase on the brush-border membrane. Lactase expression decreases with aging. Hence, when providing GOS as supplement to adults or elderly (*e.g.* (56)), it is of relevance to optimize the GOS production process to lower lactose content. It is also of interest to optimize the GOS production process to obtain a mixture with a higher oligosaccharide

yield ($DP \geq 3$) with specific linkages that are highly resistant to digestion. We studied the two established prebiotics FOS and GOS, but it is also of interest to apply this approach to emerging prebiotics, for instance, isomalto-oligosaccharides and xylo-oligosaccharides (57). Moreover, it is of high relevance to include detailed descriptions of degradation of the various chemical structures and sizes within NDC mixtures in future studies, because utilization and digestion of NDCs are expected to occur in a structure-dependent manner, as shown in **chapter 4** and **6**.

Fluctuations in the small intestine bacteria during kinetic experiments

The small intestine microbiome is expected to play a pivotal role in the pathogenesis of several intestinal diseases. Moreover, the small intestine microbiome can be expected to be involved in the digestion of macronutrients, such as dietary simple carbohydrates and fats (30). The small intestine is a harsh environment for bacteria, due to for instance the presence of oxygen, antimicrobial peptides, biliary and pancreatic secretions, and rapid transit (30). These factors likely cause a distinct microbiota community compared to the microbiota in the colon and feces (**chapter 5**). Little is known about the direct interaction between NDCs and the bacteria in the human small intestine. We showed that the various types of NDCs contributed to a distinct, selective change in the small intestine microbiota *in vitro* (**chapter 4**), which is in line with earlier findings for the colonic microbiota (58). The consumption of mixtures of various NDCs with different fermentabilities may therefore increase microbial diversity, which has been positively associated with health status (59). Interestingly, switching from a high NDC consumption to a simple-sugar diet for 7 days (<10 g NDC/day) decreased the microbial diversity and acetate concentrations in the small intestine in parallel to increased intestinal permeability and GI symptoms in healthy subjects (48). This highlights the potential clinical implications of modulating the small intestine microbiome via dietary changes. In **chapter 5**, rapid postprandial microbiota fluctuations in the human small intestine were observed after consumption of a drink containing FOS and GOS. This finding suggests that the small intestine microbiota may be amendable to the changing luminal environment. To study whether the postprandial-induced changes in the small intestine microbiota are persistent, sampling should preferably take place over a longer period of time, such as days or weeks. To address such questions, non-invasive sampling capsules (**chapter 3**) have great potential to minimally-invasively collect small intestine bacteria in people.

We hypothesize that the postprandial fluctuations *in vivo* are mostly the result of experimental factors and physical phenomena rather than a direct effect of FOS or GOS. Examples of experimental factors that may have played a role are for instance the intra-intestinal infusions close to the sampling location, or potentially uncontrolled sampling from the mucus instead of the luminal content. One physical phenomenon that could

have influenced the microbial profiles is the appearance of oral bacteria ingested via swallowing saliva. It is known that some bacteria remain viable after passage through the stomach (60). We indeed detected several bacteria in the distal ileum that were previously also found in the oral cavity (61) (**chapter 5**), although information of bacteria at the species or strain level would allow a better comparison. Exploring the role of oral health and microbiome in relation to intestinal health can be of (clinical) relevance. Even though recently it was shown there was no colonization of oral bacteria in the distal gut of healthy adults (62), previously the use of proton pump inhibitors (PPI) that reduce stomach acid production increased oral bacteria in the intestine (63). Moreover, PPIs induced microbial dysbiosis and the risk of infections or gastrointestinal discomfort (63). Patients with intestinal diseases had not only a different microbiota in the intestine but also in the mouth compared to matched controls (64, 65). Unfortunately, we did not collect an oral swab from the study participants to assess the oral microbiota to compare with the small intestine microbiota. Furthermore, we did not assess the viability of the microbiota in the distal ileum of the study participants. This would have been of interest to study to what extent the ileum bacteria are functionally active. Methods such as flow cytometry can be used to characterize the live and dead bacteria populations (66) in aspirates that were not frozen before the analysis. In this thesis, we focused on bacteria at the genus level that were influenced by NDCs. Future developments may also elucidate the effects at the species level rather than the genus level, providing additional information about the interaction between NDCs, microbiota, and health.

The use of purified non-digestible carbohydrates or plant-based foods in kinetic studies or interventions

We provided FOS and GOS as supplements in a glass of water to the participants (**chapter 5, 6**). This hampers the direct translation to consuming NDCs within the food matrix. Consuming NDCs via food will have pronounced effects on gastric emptying, digesta behaviour and transit time. Moreover, the presence of other food components will indirectly influence fermentation and digestion kinetics. And vice versa: NDCs may influence bio-accessibility and absorption of other nutrients (67). One consequence is changes in the postprandial metabolism including changes in blood glucose and insulin levels. Increasing the consumption of NDCs can result in digesta with a higher viscosity, and consequently an increased laminar flow and less efficient mixing in the intestine (68). An increased laminar flow potentially limits the diffusion of nutrients from the lumen to the mucosal epithelium, which would hamper nutrient digestion. In **chapter 6**, digestible carbohydrate remainders, including lactose, were found in the distal ileum of lactose tolerant participants. The presence of this digestible disaccharide may be explained by the rapid flow of the FOS and GOS mixtures through the human small intestine. For future digestion studies in humans, where practical, it is recommended to study NDCs within the food matrix. This will provide additional information about the

interaction with other nutrients and their bio-availabilities. For instance, specific highly viscous, gel-forming NDCs affect the absorption kinetics of other nutrients, which resulted in lipid lowering effects (69). More data about the effects of diets differing in carbohydrate quality on the carbohydrate forms and levels in the human ileum can be expected in the future, as studies on this topic are currently being conducted (70). Expanding knowledge on this topic can lead to next-generation foods with improved health benefits.

Even though we intended to also study the longer-term effects of FOS and GOS on health-related parameters, based on our studies described in **chapters 4-6** it is not possible to conclude on the health effects. The use of diet to optimize health, especially when using isolated compounds such as FOS and GOS, as outlined in **chapter 1**, is often subtle. Nevertheless, adding purified fibers extracted from plant sources to reduce sugars and fat will improve the nutritional aspect of food as well as bowel habits. This is one approach to address the fiber gap in Western society. From a health perspective, focusing on whole plant-based products rather than isolated NDCs in longer-term intervention studies is of high interest. Inulin, oligofructose, and GOS are naturally present in plant-based foods (71). Increasing their intake via plant foods will simultaneously increase the intake of other nutritious compounds, including other NDCs, micronutrients, and phytochemicals. Recently it was shown that achieving a mean intake of 15 g/d dietary fructans was feasible via consumption of salsify, Jerusalem artichoke, leek, onion, and garlic (72). Also, personalized advice within the context of whole diets is expected to be highly relevant as a strategy to increase fiber intake in adults (73). In the Netherlands, the most important fiber sources are bread and cereals, contributing up to 43% of the habitual daily fiber intake (74). WGW is a source of mainly insoluble fibers with a rather low fermentation potential, such as cellulose, hemi-celluloses including arabinoxylan and β -glucan, fructans, and lignin (75). We showed that a 12-week WGW intervention had minor effects on the fecal microbiota and predicted pathways and no effects on stool consistency (**chapter 7**) despite the large difference of 10 g/d in fiber intake between the WGW and RW group. In humans, it is known that the intestinal microbiota is influenced by many environmental factors, including the habitual diet (76). We only changed one aspect of this habitual diet, that is the grain consumption, which could explain the minor microbiota changes. Inducing major changes in the habitual dietary pattern, such as changing from a Western to a Mediterranean diet, did modulate the intestinal microbiota composition and activity (77, 78) along with improved health markers. This can be an interesting strategy for future intervention studies.

A personalized approach to study responses to non-digestible and digestible carbohydrates

The effects of NDC or WGW intervention on the microbiota were to a large extent specific to the individual (**chapters 3, 4, 5, 7**). The responses upon intervention differed in the type of bacteria, in the magnitude of change, but sometimes also in the direction (**chapters 5, 7**). The huge variation in individual responses made it difficult to determine general NDC or WGW intervention effects on the microbiota, also because our studies were not powered to detect such changes. Such ‘personalized responses’ to intervention, including NDCs, have previously been documented across numerous studies (79). We also showed that the kinetics of NDC fermentation or digestion was personalized (**chapters 4, 6**). In many studies utilizing *in vitro* fermentation models, the fecal microbiota samples from several donors are pooled, hampering the study of individual responses towards a substrate (28). While the NDC degradation kinetics were highly subject-dependent (**chapters 3, 4**), within one individual over time these were more reproducible (**Figure 2**). Assessment of responses to the same NDC in a repeated fashion within more subjects will provide knowledge about the consistency in response within and between subjects.

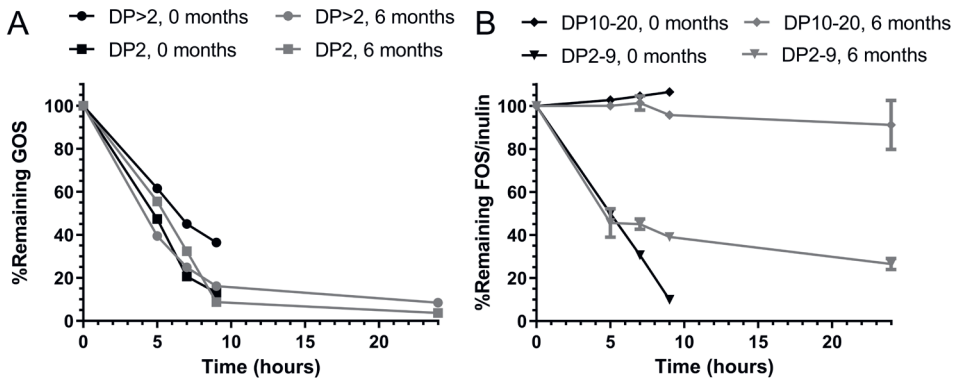


Figure 2. The NDC degradation kinetics within an individual.

The *in vitro* kinetics of GOS (A) and FOS/inulin (B) breakdown by small intestine bacteria over time of one subject that donated ileostomy effluent twice with 6 months in between. The % remaining carbohydrates are shown at 0, 5, 7, 9 h, and 24 h only at the second collection moment. DP, degree of polymerization. Data is derived from chapter 4 (not published).

Several factors may be responsible for the inter-individual differences in NDC degradation kinetics. In the *in vitro* experiments, mainly the microbial phenotype, including the composition, activity, and load, was different between the incubations (**chapter 4**). *In vivo*, many host factors can influence the kinetics (**chapters 5, 6**). Examples are the

microbial phenotype, the gastric emptying rate, the intestinal transit time, the presence and expression of digestive enzymes such as amylase, and the consistency of intestinal content. Individual-specific responses upon intervention should therefore be expected. Novel statistical and modeling approaches, such as machine-learning predictions (80), will allow the study of whether and how responses are predicted based on host phenotype, as well as how this may then mediate a difference in health status. One strong aspect of our kinetic studies (**chapters 4-6**) is the collection of many data within a subject over a defined period. This is vital for computational modeling to study dynamic processes, including metabolic fluxes. For the prediction of responses based on host phenotype, our small study populations are considered a major limitation. Two cutting-edge studies in this rapidly developing field (80, 81) applied the concept of response prediction. They showed that postprandial glucose responses to the same meal were highly variable between people and that this variability was partly explained by the composition and functions of the fecal microbiome (80, 81). In a smaller study population, there was no relation between the microbiome or fermentation markers (SCFAs, breath gases) and postprandial glucose variability (82). Nonetheless, the small intestine is the primary site of metabolic signaling, carbohydrate digestion, and glucose absorption (83). Thus, the small intestine microbiota potentially plays a more important role in explaining postprandial glucose variability than the fecal microbiome. In **chapter 6**, we showed that the ileum microbiota contained higher relative abundances of sucrase compared to the large intestine microbiota. This may imply, as suggested previously (84), that the small intestine microbiota uses simple carbohydrates for community maintenance. Preclinical studies in mice showed a direct role of the small intestine microbiota in glucose nutrient sensing and glycemic control (85, 86). In-depth characterization of the small intestine microbiota activity and their fluctuations in relation to the digestion of carbohydrate needs further exploration.

Moving from microbiota composition towards functionality

In this thesis, NDC degradation in the intestine and the consequent effects on microbiota composition were studied at the genus level using 16S rRNA gene sequencing (**chapters 4-5**). This technique allowed us to study which bacteria were present. In addition to this approach, emphasis needs also to be put on the functionality of the microbial community. We therefore also applied a more functional approach by studying the predicted metagenome functions using PICRUSt2 (**chapters 5-7**) in the sampled bacteria community, which is based on the 16S rRNA gene sequences. There are several limitations of this functional prediction. Most importantly, this prediction is biased toward the existing reference genomes. Especially in datasets containing more rare bacteria, as was the case in the less well-studied human small intestine microbiota

(**chapters 5, 6**), the functions are less likely to be identified (87). In the future, this limitation is expected to decrease since the availability of high-quality available genomes is expanding. Alternatively, functional characterization with techniques such as shotgun metagenomics sequencing to sequence the entire genome, will overcome this limitation. One disadvantage is that host cells can contaminate the sample and hence influence the outcomes. Another approach to investigate the bacteria functionality is to measure the presence and/or the production of bacterial metabolites. Moving beyond the effects of NDCs on the microbiota composition towards functionality, including the production and effects of a battery of metabolites, is of relevance to interpret the potential relevance for clinical outcomes. In **chapters 3-6**, we measured the main fermentation metabolites using a quantitative and targeted approach. The use of untargeted metabolomic techniques, for instance, LC-MS and NMR-based methods, will also allow the detection of new microbial-derived compounds. Major challenges are the unidentified peaks, and the detection of metabolites originating from undigested food material and host cells, resulting in challenging data analysis and interpretation.

The effects of non-digestible carbohydrates beyond the intestinal environment

The effects of NDCs often go beyond the GI-tract, as outlined in **chapter 1**. SCFAs can modulate metabolic health through a range of tissue-specific mechanisms (88). In mice, fermentable NDC supplementation increased SCFA uptake fluxes that strongly positively correlated with improvements in health markers, such as insulin sensitivity (89). These preclinical findings formed the basis for the studies described in **chapter 5**. Here, we aimed to study SCFA uptake fluxes and the effects of a 7-day NDC supplementation on the fluxes. We did show that SCFAs in the blood increased upon ingestion of fermentable FOS and GOS. Due to experimental difficulties, mainly related to sampling and the homogenization of the non-absorbable marker TiO_2 , we did not manage to quantify SCFA uptake fluxes from the intestine. Only limited human studies investigated the effects of SCFAs as substrates in lipid and glucose metabolism (42, 90, 91) as summarized in (88). In agreement with (42), we also showed that SCFAs are rapidly taken up by the host and play a role in glucose metabolism (**chapter 5**), but only propionate was used for net glucose synthesis (gluconeogenesis). An emerging concept is the role of intestinal gluconeogenesis as a factor in the gut-brain axis (92). Glucose in the portal vein may be sensed by the surrounding nervous system, which initiates signals that influenced glucose and energy homeostasis. NDC fermentation could trigger intestinal gluconeogenesis via fermentation products. In contrast to previous studies (42, 90, 91), we did not detect incorporation of the label in fatty acids or cholesterol. This difference could be explained due to the fasted state of the volunteers during the test day. One

interesting finding was that the ^{13}C label incorporation in blood metabolites and breath CO_2 after intestinal delivery of ^{13}C -SCFAs was highly similar between subjects. This was contradictory to the high variability in systemically available fermentation biomarkers, namely breath CH_4 and H_2 and blood SCFAs, that were produced during FOS and GOS fermentation. Overall, isotope studies are valuable to investigate the metabolic fate of microbial-derived metabolites. Moreover, our findings highlight the close link between the microbiome and host metabolism.

Concluding remarks

The studies presented in this thesis tackle several technical challenges to be considered when conducting *in vivo* studies in the human (small) intestine. Furthermore, we have provided novel data about the degradation kinetics of various NDCs and the fate of SCFAs in the human intestine. We showed that NDC degradation kinetics were strongly dependent on the individual and the type of NDC. This highlights the important role of host factors, including microbial phenotype, in responses towards NDC consumption. We increased the knowledge on digestion of prebiotics in the human small intestine by showing that some structure-dependent digestion may occur. This may contribute to the development of new carbohydrate mixtures highly resistant to digestion. Future research on the health effects of NDCs requires a multi-disciplinary approach in order to fully understand the underlying mechanisms, combining insights from food technology, (bio)chemistry, microbiology, immunology, nutrition, and clinical perspective. This will ultimately contribute to the usage of – specific or mixtures of – NDCs in patients with intestinal diseases and metabolic disturbances.

References

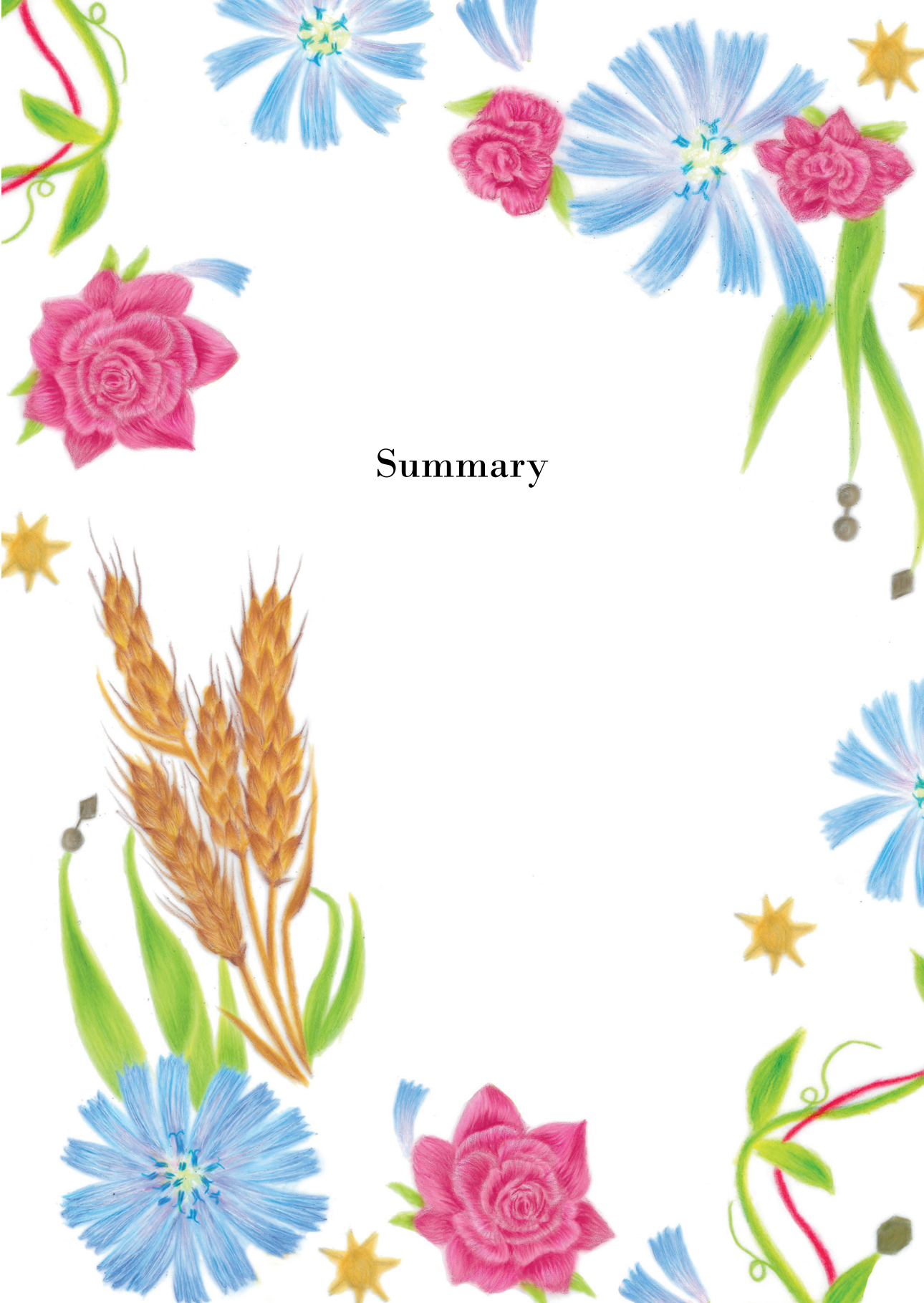
1. Marteau P, Pochart P, Doré J, Béra-Maillet C, Bernalier A, Corthier G. Comparative study of bacterial groups within the human cecal and fecal microbiota. *Appl Environ Microbiol.* 2001;67(10):4939-42.
2. Vasapolli R, Schütte K, Schulz C, Vital M, Schomburg D, Pieper DH, et al. Analysis of transcriptionally active bacteria throughout the gastrointestinal tract of healthy individuals. *Gastroenterology.* 2019;157(4):1081-92.e3.
3. Elias K, Hellström PM, Webb D-L, Sundbom M. Gastrointestinal physiology before and after duodenal switch with comparisons to unoperated lean controls: Novel use of the smartpill wireless motility capsule. *Obes Surg.* 2021.
4. Kalantar-Zadeh K, Berean KJ, Ha N, Chrimes AF, Xu K, Grando D, et al. A human pilot trial of ingestible electronic capsules capable of sensing different gases in the gut. *Nat Electron.* 2018;1(1):79-87.
5. Moglia A, Menciasci A, Dario P, Cuschieri A. Capsule endoscopy: Progress update and challenges ahead. *Nat Rev Gastroenterol Hepatol.* 2009;6(6):353-62.
6. Schostek S, Zimmermann M, Keller J, Fode M, Melbert M, Schurr MO, et al. Telemetric real-time sensor for the detection of acute upper gastrointestinal bleeding. *Biosens Bioelectron.* 2016;78:524-9.
7. Kimchy Y, Lifshitz R, Lewkowicz S, Bertuccio G, Arber N, Gluck N, et al. Radiographic capsule-based system for non-cathartic colorectal cancer screening. *Abdom Radiol.* 2017;42(5):1291-7.
8. Strobbe F, Bénard MV, Rossen NG, de Vos WM, Kumar N, Lawley TD, et al. A novel technique capable of taking 'protected' biopsies for reliable assessment of the distribution of microbiota along the colonic mucosa. *J Microbiol Methods.* 2021;185:106204.
9. Cummins G. Smart pills for gastrointestinal diagnostics and therapy. *Adv Drug Deliv Rev.* 2021;177:113931.
10. Progenity Inc, assignee. U.S. Patent. Ingestible device and associated methods. Patent number: 10172598.
11. Rezaei Nejad H, Oliveira BCM, Sadeqi A, Dehkharghani A, Kondova I, Langermans JAM, et al. Ingestible osmotic pill for in vivo sampling of gut microbiomes. *Adv Intell Syst.* 2019;1(5):1900053.
12. Tang Q, Jin G, Wang G, Liu T, Liu X, Wang B, et al. Current sampling methods for gut microbiota: A call for more precise devices. *Front Cell Infect Microbiol.* 2020;10:151.
13. Cui J, Zheng X, Hou W, Zhuang Y, Pi X, Yang J. The study of a remote-controlled gastrointestinal drug delivery and sampling system. *Telemed J E Health.* 2008;14(7):715-9.
14. Waimin JF, Nejati S, Jiang H, Qiu J, Wang J, Verma MS, et al. Smart capsule for non-invasive sampling and studying of the gastrointestinal microbiome. *RSC Advances.* 2020;10(28):16313-22.
15. Ding Z, Wang W, Zhang K, Ming F, Yangdai T, Xu T, et al. Novel scheme for non-invasive gut bioinformation acquisition with a magnetically controlled sampling capsule endoscope. *Gut.* 2021;gutjnl-2020-322465.
16. Koziolok M, Grimm M, Becker D, Jordanov V, Zou H, Shimizu J, et al. Investigation of pH and temperature profiles in the GI tract of fasted human subjects using the intellicap[®] system. *J Pharm Sci.* 2015;104(9):2855-63.
17. imec. Technology to capture your gut feeling. Available from: <https://www.imec-int.com/en/articles/technology-capture-your-gut-feeling>. Access date: 11 June 2021.
18. Progenity. Gastrointestinal health. Rss: Recoverable sampling & preservation system. Available from: <https://www.progenity.com/innovation/gastrointestinal-health>. Access date: 11 June 2021.
19. Nimble science. Technology: Small intestine microbiome aspiration capsule. Available from: <https://www.nimblesci.com/technology>. Access date: 11 June 2021.
20. Dupont and biome oxford. Biocapture[®], a smart capsule to sample the gut microbiota. Available from: <https://www.dupontnutritionandbiosciences.com/news/dupont-partnership-biome-oxford.html>. Access date: 11 June 2021.

21. Jalanka J, Salonen A, Salojärvi J, Ritari J, Immonen O, Marciani L, et al. Effects of bowel cleansing on the intestinal microbiota. *Gut*. 2015;64(10):1562-8.
22. van der Beek CM, Canfora EE, Lenaerts K, Troost FJ, Olde Damink SW, Holst JJ, et al. Distal, not proximal, colonic acetate infusions promote fat oxidation and improve metabolic markers in overweight/obese men. *Clin Sci*. 2016;130(22):2073-82.
23. Jacobson LE, Olayan M, Williams JM, Schultz JF, Wise HM, Singh A, et al. Feasibility and safety of a novel electromagnetic device for small-bore feeding tube placement. *Trauma Surgery; Acute Care Open*. 2019;4(1):e000330.
24. Neyrinck AM, Rodriguez J, Zhang Z, Seethaler B, Mailleux F, Vercammen J, et al. Noninvasive monitoring of fibre fermentation in healthy volunteers by analyzing breath volatile metabolites: Lessons from the FiberTag intervention study. *Gut Microbes*. 2021;13(1):1-16.
25. Venema K, van den Abbeele P. Experimental models of the gut microbiome. *Best Pract Res Clin Gastroenterol*. 2013;27(1):115-26.
26. Gibson GR, Cummings JH, Macfarlane GT. Use of a three-stage continuous culture system to study the effect of mucin on dissimilatory sulfate reduction and methanogenesis by mixed populations of human gut bacteria. *Appl Environ Microbiol*. 1988;54(11):2750-5.
27. Calvez J, Benoit S, Piedcoq J, Khodorova N, Azzout-Marniche D, Tomé D, et al. Very low ileal nitrogen and amino acid digestibility of zein compared to whey protein isolate in healthy volunteers. *Am J Clin Nutr*. 2020.
28. Aura AM, Maukonen J. One compartment fermentation model. In: Verhoeckx K, Cotter P, López-Expósito I, Kleiveland C, Lea T, Mackie A, et al. The impact of food bioactives on health: In vitro and ex vivo models. Cham (CH): Springer Copyright 2015, The Author(s). p. 281-92.
29. Ferreira-Lazarte A, Moreno FJ, Villamiel M. Bringing the digestibility of prebiotics into focus: Update of carbohydrate digestion models. *Crit Rev Food Sci Nutr*. 2020:1-12.
30. Kastl AJ, Terry NA, Wu GD, Albenberg LG. The structure and function of the human small intestinal microbiota: Current understanding and future directions. *Cell Mol Gastroenterol Hepatol*. 2020;9(1):33-45.
31. Stolaki M, Minekus M, Venema K, Lahti L, Smid EJ, Kleerebezem M, et al. Microbial communities in a dynamic in vitro model for the human ileum resemble the human ileal microbiota. *FEMS Microbiol Ecol*. 2019;95(8).
32. Reynolds A, Mann J, Cummings J, Winter N, Mete E, Te Morenga L. Carbohydrate quality and human health: A series of systematic reviews and meta-analyses. *The Lancet*. 2019;393(10170):434-45.
33. Authority EEFS. Scientific opinion on dietary reference values for carbohydrates and dietary fibre. Efsa panel on dietetic products, nutrition, and allergies (nda). *Efsa Journal*. 2010;8(3):1462.
34. Voedingscentrum Nederland. Voedingsvezels. [cited 17-07-2020]. Available from: <https://www.voedingscentrum.nl/encyclopedie/vezels.aspx>.
35. Jonathan MC, van den Borne JJGC, van Wiechen P, Souza da Silva C, Schols HA, Gruppen H. In vitro fermentation of 12 dietary fibres by faecal inoculum from pigs and humans. *Food Chem*. 2012;133(3):889-97.
36. Saito D, Nakaji S, Fukuda S, Shimoyama T, Sakamoto J, Sugawara K. Comparison of the amount of pectin in the human terminal ileum with the amount of orally administered pectin. *Nutrition*. 2005;21(9):914-9.
37. Knudsen BK, Hessov I. Recovery of inulin from jerusalem artichoke (*helianthus tuberosus* L.) in the small intestine of man. *Br J Nutr*. 1995;74(1):101-13.
38. Ellegård L, Andersson H, Bosaeus I. Inulin and oligofructose do not influence the absorption of cholesterol, and the excretion of cholesterol, Fe, Ca, Mg, and bile acids but increase energy excretion in man: a blinded, controlled cross-over study in ileostomy subjects. *Eur J Clin Nutr*. 1997;51(1):1-5.
39. Cantu-Jungles TM, Hamaker BR, Zambrano MM. New view on dietary fiber selection for predictable shifts in gut microbiota. *mBio*. 2020;11(1):e02179-19.

40. Rose DJ, DeMeo MT, Keshavarzian A, Hamaker BR. Influence of dietary fiber on inflammatory bowel disease and colon cancer: Importance of fermentation pattern. *Nutr Rev.* 2007;65(2):51-62.
41. Besten Gd, Lange K, Havinga R, Dijk THv, Gerding A, Eunen Kv, et al. Gut-derived short-chain fatty acids are vividly assimilated into host carbohydrates and lipids. *Am J Physiol Gastrointest Liver Physiol.* 2013;305(12):G900-G10.
42. Boets E, Gomand SV, Deroover L, Preston T, Vermeulen K, De Preter V, et al. Systemic availability and metabolism of colonic-derived short-chain fatty acids in healthy subjects: A stable isotope study. *J Physiol.* 2017;595(2):541-55.
43. Helander HF, Fändriks L. Surface area of the digestive tract - revisited. *Scand J Gastroenterol.* 2014;49(6):681-9.
44. van Lanen AS, de Bree A, Greyling A. Efficacy of a low-FODMAP diet in adult irritable bowel syndrome: A systematic review and meta-analysis. *Eur J Nutr.* 2021.
45. Wilson B, Rossi M, Kanno T, Parkes GC, Anderson S, Mason AJ, et al. B-galactooligosaccharide in conjunction with low fodmap diet improves irritable bowel syndrome symptoms but reduces fecal bifidobacteria. *Am J Gastroenterol.* 2020;115(6):906-15.
46. Ghoshal UC, Srivastava D. Irritable bowel syndrome and small intestinal bacterial overgrowth: Meaningful association or unnecessary hype. *World J Gastroenterol.* 2014;20(10):2482-91.
47. Ford AC, Spiegel BMR, Talley NJ, Moayyedi P. Small intestinal bacterial overgrowth in irritable bowel syndrome: Systematic review and meta-analysis. *Clin Gastroenterol Hepatol.* 2009;7(12):1279-86.
48. Saffouri GB, Shields-Cutler RR, Chen J, Yang Y, Lekatz HR, Hale VL, et al. Small intestinal microbial dysbiosis underlies symptoms associated with functional gastrointestinal disorders. *Nat Commun.* 2019;10(1):1-11.
49. Mowat AM, Agace WW. Regional specialization within the intestinal immune system. *Nat Rev Immunol.* 2014;14(10):667-85.
50. Ermund A, Schütte A, Johansson ME, Gustafsson JK, Hansson GC. Studies of mucus in mouse stomach, small intestine, and colon. I. Gastrointestinal mucus layers have different properties depending on location as well as over the peyer's patches. *Am J Physiol Gastrointest Liver Physiol.* 2013;305(5):G341-7.
51. Bermudez-Brito M, Sahasrabudhe NM, Rösch C, Schols HA, Faas MM, de Vos P. The impact of dietary fibers on dendritic cell responses in vitro is dependent on the differential effects of the fibers on intestinal epithelial cells. *Mol Nutr Food Res.* 2015;59(4):698-710.
52. Leyva-Porras C, López-Pablos A, Alvarez-Salas C, Pérez-Urizar J, Saavedra-Leos Z. Physical properties of inulin and technological applications. Ramawat, KG, Mérillon, JM, Eds; Springer: New York, NY, USA. 2015:959-84.
53. Anderson JW, Baird P, Davis RH, Jr, Ferreri S, Knudtson M, Koraym A, et al. Health benefits of dietary fiber. *Nutr Rev.* 2009;67(4):188-205.
54. Bohn T, Carriere F, Day L, Deglaire A, Egger L, Freitas D, et al. Correlation between in vitro and in vivo data on food digestion. What can we predict with static in vitro digestion models? *Crit Rev Food Sci Nutr.* 2018;58(13):2239-61.
55. Verkhnyatskaya S, Ferrari M, de Vos P, Walvoort MTC. Shaping the infant microbiome with non-digestible carbohydrates. *Front Microbiol.* 2019;10:343.
56. Walton GE, van den Heuvel EG, Kosters MH, Rastall RA, Tuohy KM, Gibson GR. A randomised crossover study investigating the effects of galacto-oligosaccharides on the faecal microbiota in men and women over 50 years of age. *Br J Nutr.* 2012;107(10):1466-75.
57. Cardoso BB, Amorim C, Silvério SC, Rodrigues LR. Chapter two - novel and emerging prebiotics: Advances and opportunities. In: Tolrá F, editor. *Adv food nutr res.* 95: Academic Press; 2021. p. 41-95.
58. Wang M, Wichienchot S, He X, Fu X, Huang Q, Zhang B. In vitro colonic fermentation of dietary fibers: Fermentation rate, short-chain fatty acid production and changes in microbiota. *Trends Food Sci Technol.* 2019;88:1-9.
59. Larsen OFA, Claassen E. The mechanistic link between health and gut microbiota diversity. *Sci Rep.* 2018;8(1):2183.

60. Oozeer R, Leplingard A, Mater DDG, Mogenet A, Michelin R, Seksek I, et al. Survival of *Lactobacillus casei* in the human digestive tract after consumption of fermented milk. *Appl Environ Microbiol.* 2006;72(8):5615-7.
61. Hall MW, Singh N, Ng KF, Lam DK, Goldberg MB, Tenenbaum HC, et al. Inter-personal diversity and temporal dynamics of dental, tongue, and salivary microbiota in the healthy oral cavity. *NPJ Biofilms Microbiomes.* 2017;3:2.
62. Rashidi A, Ebadi M, Weisdorf DJ, Costalonga M, Staley C. No evidence for colonization of oral bacteria in the distal gut in healthy adults. *PNAS.* 2021;118(42):e2114152118.
63. Bruno G, Zaccari P, Rocco G, Scalese G, Panetta C, Porowska B, et al. Proton pump inhibitors and dysbiosis: Current knowledge and aspects to be clarified. *World J Gastroenterol.* 2019;25(22):2706-19.
64. Lucas López R, Grande Burgos MJ, Gálvez A, Pérez Pulido R. The human gastrointestinal tract and oral microbiota in inflammatory bowel disease: A state of the science review. *APMIS.* 2017;125(1):3-10.
65. Kageyama S, Takeshita T, Takeuchi K, Asakawa M, Matsumi R, Furuta M, et al. Characteristics of the salivary microbiota in patients with various digestive tract cancers. *Front Microbiol.* 2019;10:1780.
66. Berney M, Hammes F, Bosshard F, Weilenmann H-U, Egli T. Assessment and interpretation of bacterial viability by using the live/dead baclight kit in combination with flow cytometry. *Appl Environ Microbiol.* 2007;73(10):3283-90.
67. Grundy MML, Edwards CH, Mackie AR, Gidley MJ, Butterworth PJ, Ellis PR. Re-evaluation of the mechanisms of dietary fibre and implications for macronutrient bioaccessibility, digestion and postprandial metabolism. *Br J Nutr.* 2016;116(5):816-33.
68. Lentle RG, Janssen PW. Physical characteristics of digesta and their influence on flow and mixing in the mammalian intestine: A review. *J Comp Physiol B.* 2008;178(6):673-90.
69. Vuksan V, Jenkins AL, Rogovik AL, Fairgrieve CD, Jovanovski E, Leiter LA. Viscosity rather than quantity of dietary fibre predicts cholesterol-lowering effect in healthy individuals. *Br J Nutr.* 2011;106(9):1349-52.
70. Byrne CS, Blunt D, Burn J, Chambers E, Dagbasi A, Franco Becker G, et al. A study protocol for a randomised crossover study evaluating the effect of diets differing in carbohydrate quality on ileal content and appetite regulation in healthy humans. *F1000Res.* 2019;8:258.
71. Varney J, Barrett J, Scarlata K, Catsos P, Gibson PR, Muir JG. Foodmaps: Food composition, defining cutoff values and international application. *J Gastroenterol Hepatol.* 2017;32(1):53-61.
72. Hiel S, Bindels LB, Pachikian BD, Kalala G, Broers V, Zamariola G, et al. Effects of a diet based on inulin-rich vegetables on gut health and nutritional behavior in healthy humans. *Am J Clin Nutr.* 2019;109(6):1683-95.
73. Rijnaarts I, de Roos NM, Wang T, Zoetendal EG, Top J, Timmer M, et al. Increasing dietary fibre intake in healthy adults using personalised dietary advice compared with general advice: A single-blind randomised controlled trial. *Public Health Nutr.* 2021;24(5):1117-28.
74. Rossum CTMv, Fransen HP, Verkaik-Kloosterman J, Buurma-Rethans EJM, Ocké MC. Dutch national food consumption survey 2007-2010. Diet of children and adults aged 7 to 69 years. 2011.
75. Frølich W, Aman P, Tetens I. Whole grain foods and health - a scandinavian perspective. *Food Nutr Res.* 2013;57:10.3402/fnr.v57i0.18503.
76. Falony G, Joossens M, Vieira-Silva S, Wang J, Darzi Y, Faust K, et al. Population-level analysis of gut microbiome variation. *Science.* 2016;352(6285):560-4.
77. David LA, Maurice CF, Carmody RN, Gootenberg DB, Button JE, Wolfe BE, et al. Diet rapidly and reproducibly alters the human gut microbiome. *Nature.* 2014;505(7484):559-63.
78. Meslier V, Laiola M, Roager HM, De Filippis F, Roume H, Quinquis B, et al. Mediterranean diet intervention in overweight and obese subjects lowers plasma cholesterol and causes changes in the gut microbiome and metabolome independently of energy intake. *Gut.* 2020;69(7):1258-68.

79. Swanson KS, de Vos WM, Martens EC, Gilbert JA, Menon RS, Soto-Vaca A, et al. Effect of fructans, prebiotics and fibres on the human gut microbiome assessed by 16S rRNA-based approaches: A review. *Benef Microbes*. 2020;11(2):101-29.
80. Berry SE, Valdes AM, Drew DA, Asnicar F, Mazidi M, Wolf J, et al. Human postprandial responses to food and potential for precision nutrition. *Nat Med*. 2020;26(6):964-73.
81. Zeevi D, Korem T, Zmora N, Israeli D, Rothschild D, Weinberger A, et al. Personalized nutrition by prediction of glycemic responses. *Cell*. 2015;163(5):1079-94.
82. Nestel N, Hvass JD, Bahl MI, Hansen LH, Krych L, Nielsen DS, et al. The gut microbiome and abiotic factors as potential determinants of postprandial glucose responses: A single-arm meal study. *Front Nutr*. 2020;7:594850.
83. El Aidy S, van den Bogert B, Kleerebezem M. The small intestine microbiota, nutritional modulation and relevance for health. *Curr Opin Biotechnol*. 2015;32:14-20.
84. Zoetendal EG, Raes J, van den Bogert B, Arumugam M, Booijink CCGM, Troost FJ, et al. The human small intestinal microbiota is driven by rapid uptake and conversion of simple carbohydrates. *ISME J*. 2012;6(7):1415-26.
85. Bauer PV, Duca FA, Waise TMZ, Rasmussen BA, Abraham MA, Dranse HJ, et al. Metformin alters upper small intestinal microbiota that impact a glucose-SGLT1-sensing glucoregulatory pathway. *Cell Metab*. 2018;27(1):101-17.e5.
86. Bauer PV, Duca FA, Waise TMZ, Dranse HJ, Rasmussen BA, Puri A, et al. *Lactobacillus gasseri* in the upper small intestine impacts an *acs13*-dependent fatty acid-sensing pathway regulating whole-body glucose homeostasis. *Cell Metab*. 2018;27(3):572-87.e6.
87. Douglas GM, Maffei VJ, Zaneveld JR, Yurgel SN, Brown JR, Taylor CM, et al. PICRUSt2 for prediction of metagenome functions. *Nat Biotechnol*. 2020;38(6):685-8.
88. Blaak EE, Canfora EE, Theis S, Frost G, Groen AK, Mithieux G, et al. Short chain fatty acids in human gut and metabolic health. *Benef Microbes*. 2020;11(5):411-55.
89. den Besten G, Havinga R, Bleeker A, Rao S, Gerding A, van Eunen K, et al. The short-chain fatty acid uptake fluxes by mice on a guar gum supplemented diet associate with amelioration of major biomarkers of the metabolic syndrome. *PLoS One*. 2014;9(9):e107392-e.
90. Wolever TM, Spadafora PJ, Cunnane SC, Pencharz PB. Propionate inhibits incorporation of colonic [1,2-¹³C]acetate into plasma lipids in humans. *Am J Clin Nutr*. 1995;61(6):1241-7.
91. Hellman L, Rosenfeld RS, Gallagher TF. Cholesterol synthesis from C14-acetate in man. *J Clin Invest*. 1954;33(2):142-9.
92. Soty M, Gautier-Stein A, Rajas F, Mithieux G. Gut-brain glucose signaling in energy homeostasis. *Cell Metab*. 2017;25(6):1231-42.



Summary

Non-digestible carbohydrates and health

Digestible and non-digestible carbohydrates are present in food. The non-digestible carbohydrates (NDCs), or dietary fiber, are natural components of plant food sources such as fruits, vegetables, nuts, legumes, and grains. Increased consumption of NDCs has been linked to numerous health benefits such as a reduced risk of obesity or intestinal disease and improved intestinal function. Unlike digestible carbohydrates, which are absorbed into the body and used as an energy source, NDCs are not broken down by host enzymes. However, certain NDCs can be broken down by intestinal bacteria. This process, which is called fermentation, results in a change in the composition of the bacteria and in the production of bacterial metabolites. These are in particular the short-chain fatty acids (SCFA) with acetate, propionate, and butyrate as the main end products. The SCFAs are an important energy source for the intestinal cells, and butyrate acid may reduce intestinal inflammation. It has previously been shown in mice that increased uptake of SCFAs from the large intestine is associated with improvements in metabolic health markers in the blood, such as glucose and insulin levels. Because the composition of the intestinal microbiota, including the bacteria, in the small and large intestine plays an important role in health, modulating this composition through changes in diet can be a strategy to improve health status. Prebiotic NDCs, including galacto-oligosaccharides (GOS), fructo-oligosaccharides (FOS), and inulin, can selectively stimulate the growth and/or activity of specific intestinal bacteria linked to health benefits. For this reason, prebiotics are isolated from the original plant material and are used as ingredients in certain food products. However, detailed knowledge on NDC degradation profiles, metabolites produced, and microbiota shifts generated by NDC in the human intestine is lacking. This information will facilitate the prediction of potential beneficial health consequences of NDC consumption. The work in this thesis describes the breakdown and fermentation of specific NDCs, including prebiotics, in the human intestine. We also investigated the effects of short- and longer-term interventions varying in NDC composition on the intestine, including changes in microbiota, and their relationship to metabolic processes.

A look inside the gut

Most commonly, the effects of NDCs on intestinal bacteria and bacterial metabolites are studied through analysis of feces. Feces is easy to collect, but might not be directly representative of the bacteria and their metabolites in the intestine. For this reason, additional methods are needed to sample more locally to better understand the effects of dietary compounds, including NDCs, inside the intestine. Intestinal catheters can facilitate the delivery of compounds directly into the intestinal lumen or the aspiration

of intestinal fluids in human subjects. Working with intestinal catheters poses challenges to (biomedical) researchers and medical staff, *e.g.* correct positioning. Therefore, in **chapter 2** we described all technical and practical aspects of working with catheters placed at the beginning of the small intestine (the duodenum and jejunum), the end of the small intestine (the ileum), or at the beginning of the large intestine (colon) in a systematic literature review. We obtained in-depth information about working with intestinal catheters, including positioning catheters, aspirating intestinal fluids, and standardizing delivery and sampling, as well as a summary of state-of-the-art intestinal catheter designs. This overview was based on information from 60 clinical studies, including our own studies, which involved a total of 720 healthy subjects and 42 patients. We showed that catheters were mostly applied to examine multiple intestinal regions simultaneously (24 studies), followed by just the jejunum (21 studies), the ileum (13 studies), or the large intestine (2 studies). Custom-made state-of-the-art catheters are available with numerous options for the design, such as multiple lumina, side holes, and inflatable balloons for catheter progression or isolation of intestinal segments. These allow for multiple controlled sampling and compound delivery options in different intestinal regions. Intestinal catheters were often used for delivery (23 studies), sampling (10 studies), or both (27 studies). The sampling rate decreased with increasing distance from the sampling syringe to the specific intestinal segment. This means that sampling intestinal contents in the duodenum and jejunum is easier and faster than in the ileum or large intestine. Despite the invasiveness of the method, no serious adverse events were reported, and a dropout rate of approximately 10% for this type of research can be expected. In conclusion, intestinal catheters allow studying the relatively inaccessible small intestine and the beginning of the colon in humans.

Given the high invasiveness of this method, alternative methods to study the inner world of digestion and fermentation are warranted. Access to the intestinal lumen will be possible in the future through minimally-invasive, novel human gastrointestinal sampling capsules. These can be activated remotely to take a sample of the intestinal content. However, an important drawback of this capsule is that the sample cannot be collected until after excretion of the capsule in the feces, which can take hours to days. Meanwhile, the breakdown of macronutrients including NDCs by the intestinal bacteria continues, which hampers the reliability of the findings. In order to obtain a representative intestinal sample, the intestinal contents must be stabilized at the time of sampling by blocking further metabolism. This can be done by adding a so-called ‘stabilizer’ in the capsule prior to swallowing. Due to the novelty of such capsules, no methodology has yet been published to stabilize and analyze the resulting intestinal samples. In **chapter 3** we described a new workflow to block and analyze the fermentation process of selected NDCs, including the microbiota and SCFAs. The developed stabilizer contains 175 mM Tris, 525 mM NaCl, 35 mM EDTA, 12% SDS and 8 M urea at pH 8.5. After

adding this stabilizer, we found that the fermentation of FOS/inulin and GOS by small intestine bacteria and fecal bacteria (large intestine) was stabilized for 48 hours at body temperature. Since the total sample volume of the intestinal capsules is small, we also optimized the analytical methods and set up an efficient extraction procedure. In this way, it is possible to obtain as much data as possible from the valuable, but low volume of intestinal samples. In addition, we showed that the stabilizer is safe for ingestion, in case of stabilizer leakage from the capsule into the gastrointestinal tract. This work forms the basis for a broader approach to also stabilize and subsequently investigate other microbial processes in the intestine. The application of intestinal capsules will allow a deeper understanding of diet-microbiota-host interactions.

An in vitro model and in vivo model for digestion and fermentation

Prior to digestion and fermentation studies in the human gut (in vivo), in vitro fermentation models can be used to mimic this process. In vitro studies take place outside the body, with the aim of mimicking a process in the gastrointestinal tract in a high-throughput, cost-efficient way without ethical restrictions. In **chapter 4** we used an in vitro batch fermentation model to investigate the degradation of various NDCs, and the effects on microbiota composition and metabolite production. Little is known about the direct interaction between NDCs and the bacteria in the human small intestine. It has been previously shown that bacteria in ileostomy stools resemble bacteria in the small intestine of healthy people. Patients with a stoma at the end of the small intestine, therefore, donated stool for this study, to which we then added NDCs. The lower molecular weight NDCs, namely GOS and FOS, were rapidly fermented by the small intestine bacteria, namely 31-82% and 29-89%, respectively after 5 hours. Higher molecular weight NDCs, namely inulin, lemon pectin, and non-digestible starch, were broken down very slowly (after 7 hours) or not at all by bacteria present in the small intestine. This indicates that the latter NDCs likely will not have a direct effect on the small intestine bacteria in humans, because food is only present in the small intestine for on average 3.5 to 6 hours. The fermentation and degradation rate depended on the type and size of the NDC. These findings show that small intestinal bacteria potentially contribute to the digestion of NDCs because they can produce enzymes that break down certain NDCs, which resulted in the production of mostly acetate. Importantly, the effects on the microbiota and metabolites composition were strongly dependent on the subject's initial microbiota composition. This supports the importance of a personalized nutritional approach through the intestinal microbiota to improve health. The in vitro model allowed us to look at the functions of the small intestine bacteria with regard to the breakdown of NDCs. The next step was to study fermentation in the intestine of human subjects. To this end, healthy males were intubated with an intestinal catheter in

the distal ileum or the beginning of the colon (**chapter 5**). Afterwards, they consumed 10 grams of FOS:GOS, after which we collected intestinal contents at different time points for several hours. In the distal ileum, there was no degradation of FOS and GOS, nor production of SCFAs. However, hydrogen in the breath and SCFAs in the blood increased after FOS:GOS consumption, which indicates that fermentation did occur in the large intestine. The microbiota composition in the ileum changed rapidly during the test day. There was no increase in bacteria that were previously reported to be stimulated by FOS or GOS. The cause of the rapid fluctuations in the small intestinal microbiota and potential effects on health or digestion remains to be uncovered. The composition of bacteria in the small intestine was very different from that in the large intestine or in the stool. Consuming 15 grams of FOS:GOS daily for seven days had no effect on the microbiota and metabolites in the stool. In **chapter 5**, SCFAs were also delivered directly via the catheter into the intestine to investigate their role in glucose and lipid metabolism. Acetate, propionate, and butyrate contain a ^{13}C label, which could be traced in various molecules. The ^{13}C label from the three SCFAs was incorporated into glucose, with only propionate contributing to net glucose synthesis. The label was not detected in amino acids, fatty acids, or cholesterol. Overall, the results showed that SCFAs were vividly taken up from the intestine and converted by the host. This highlights the close link between the microbiome and host metabolism.

The importance of the structure and properties of non-digestible carbohydrates

GOS and FOS each have a unique structure and both the GOS and the FOS powder mixture contain molecules of different sizes and linkages. Information about their digestibility in the small intestine of healthy people is limited. The development and application of NDCs in foods as sugar replacers is interesting, because this will decrease the caloric value of food. In addition, such foods may lower blood glucose levels after eating, and the added NDCs can have a beneficial effect on the intestine. In **chapter 6** we, therefore, investigated in detail the digestibility of all carbohydrate compounds present in the FOS and GOS mixtures in the small intestine of healthy men, using advanced chemical analyses. Most of the GOS and FOS were recovered at the end of the small intestine, namely 76% GOS and 96% FOS. Some of the GOS disaccharides, two sugar molecules linked together, did not reach the end of the small intestine or the large intestine. The digestion of GOS disaccharides was dependent on the biochemical structure and the linkage between the monomers. The structures $\beta\text{-D-Gal-(1}\leftrightarrow\text{1)-}\alpha\text{-D-Glc}$ + $\beta\text{-D-Gal-(1}\leftrightarrow\text{1)-}\beta\text{-D-Glc}$ and $\beta\text{-D-Gal-(1}\rightarrow\text{2)-D-Glc}$ + $\beta\text{-D-Gal-(1}\rightarrow\text{3)-D-Glc}$ were digested more (77% and 81%) compared to $\beta\text{-D-Gal-(1}\rightarrow\text{6)-D-Gal}$ and $\beta\text{-D-Gal-(1}\rightarrow\text{4)-D-Gal}$ (56% and 32%). An unexpected finding was that lactose, naturally present

in the GOS mixture, was still present at the end of the small intestine or large intestine. This is remarkable, since lactose is normally digested in the proximal small intestine, and the subjects were not lactose intolerant. The direct evidence on resistances of various compounds to digestion in the small intestine can be used for further development of (GOS) prebiotics that completely resist digestion in the human small intestine.


Whole-grain products as a source of non-digestible carbohydrates and effect on the fecal microbiota

In the Netherlands, bread and grain products are the main sources of NDCs, accounting for 43% of the daily intake. From a health perspective, it is of great importance to also investigate the effects of the whole plant product in intervention studies. Intake of plant products increases a range of nutritious compounds, including micronutrients. Whole wheat products are recommended as a healthy choice compared to refined wheat products. It has previously been shown that the consumption of whole-grain wheat products prevents fatty liver, in which intestinal bacteria may play a role. In **chapter 7** we investigated the effects of a 12-week intervention with whole wheat products or refined wheat products on the composition and functions of the fecal bacteria in women and men with overweight or obesity. Despite the large difference in the daily intake of NDCs between the groups, we found minor effects on the composition and functions of the fecal bacteria after 12 weeks when the diet groups were compared. The whole wheat products also had no effect on stool consistency. The effects were mainly an increase in certain NDC-degrading bacteria and bacterial functions related to fermentation in the whole-grain wheat group. Changes in the amount of some bacteria correlated with changes in liver fat and concentrations of certain liver enzymes in the blood. Potential protective health effects of replacing refined wheat products with whole-grain wheat products on metabolic organs, such as the liver, via modulation of the microbiota requires further investigation.

A holistic approach to further unravel the health effects of non-digestible carbohydrates

The studies presented in this thesis address several technical challenges to consider during in vivo studies in the human gastrointestinal tract. We showed that the breakdown rate of various NDCs is highly dependent on both the person and the structure and properties of the NDC. This highlights the important role of host factors, including microbial phenotype, in responses towards NDC consumption. The small intestine bacteria can also produce enzymes that break down certain NDCs. Since the

small intestine microbiota composition has also been associated with certain diseases, it is relevant to study the interaction between food and this microbial ecosystem in more detail. In addition, the findings contribute to the development of carbohydrate mixtures that are highly resistant to digestion in the small intestine. Future research on the health effects of NDCs requires a multidisciplinary approach, with insights from food chemistry, microbiology, immunology, and nutrition, to fully understand the underlying mechanisms. This will ultimately contribute to the use of – specific or mixtures of – NDCs for the prevention or treatment of conditions such as intestinal and metabolic disorders.



Nederlandse samenvatting

Niet-verteerbare koolhydraten en gezondheid

In voeding zijn verteerbare en niet-verteerbare koolhydraten aanwezig. De niet-verteerbare koolhydraten, ook wel voedingsvezels genoemd, zijn natuurlijke bestanddelen van plantaardige voedselbronnen zoals fruit, groenten, noten, peulvruchten en granen. Een verhoogde consumptie van niet-verteerbare koolhydraten is in verband gebracht met gezondheidsvoordelen, zoals een verminderd risico op obesitas of darmziekten en een verbeterde darmfunctie. In tegenstelling tot verteerbare koolhydraten, die worden opgenomen in het lichaam en gebruikt als energiebron, worden niet-verteerbare koolhydraten niet afgebroken door enzymen van de gastheer. Wel worden bepaalde niet-verteerbare koolhydraten afgebroken door de darmbacteriën. Dit proces heet fermentatie. Dit resulteert in een verandering in de samenstelling van de darmbacteriën en in de productie van bepaalde bacteriële stoffen tijdens fermentatie. Dit zijn met name de korte-keten vetzuren (KKV), met als eindproducten azijnzuur, propionzuur en boterzuur. De KKV's zijn een energiebron voor de cellen in de darm. Boterzuur kan inflammatie in de darm verminderen en mogelijk de vorming van darmkanker tegen gaan. Verder is eerder in muizen aangetoond dat een verhoogde opname van deze drie KKV's vanuit de dikke darm samenhangt met verbeteringen in gezondheidsmarkers, zoals de glucose- en insulinespiegel. De samenstelling van de micro-organismen (microbiota), inclusief de bacteriën in de dunne en dikke darm, speelt een belangrijke rol in gezondheid. Daarom kan het moduleren van deze samenstelling door veranderingen in dieet een strategie zijn om de gezondheidsstatus te verbeteren. Zogenaamde prebiotische koolhydraten, waaronder galacto-oligosachariden (GOS), fructo-oligosachariden (FOS) en inuline, kunnen de groei en/of activiteit van specifieke darmbacteriën die verband houden met gezondheid en welzijn stimuleren. Deze prebiotica worden om die reden geïsoleerd uit het oorspronkelijke plantenmateriaal en toegepast als ingrediënten in bepaalde voedingsproducten. Gedetailleerde kennis over wat er precies gebeurt met zulke niet-verteerbare koolhydraten tijdens hun reis door het maag-darm kanaal van de mens ontbreekt. Deze informatie zal bijdragen aan kennis over de effecten van consumptie van niet-verteerbare koolhydraten op de gezondheid. Het werk in dit proefschrift beschrijft de afbraak en fermentatie van specifieke niet-verteerbare koolhydraten en prebiotica in de menselijke darm. Hierbij onderzochten we ook de effecten van korte- en langere termijn interventies met niet-verteerbare koolhydraten op de darmbacteriën en de relatie tot stofwisselingsprocessen.

Een kijkje in de darm

Meestal worden de effecten van niet-verteerbare koolhydraten op de darmbacteriën en bacteriële stoffen onderzocht via ontlasting. Ontlasting is makkelijk te verzamelen, maar

ook het eindproduct van het maag-darm kanaal. Daarom is het niet direct representatief voor fermentatie in de darm. Om beter te begrijpen wat voor effecten voeding, waaronder niet-verteerbare koolhydraten, op de darm hebben zijn aanvullende methoden nodig om lokaal in de darm te meten. Darmsondes kunnen gebruikt worden om darminhoud te bemonsteren of om componenten in de darm af te geven. Het werken met darmsondes kan een uitdaging zijn voor (biomedische) onderzoekers en medisch personeel. Daarom beschreven we in **hoofdstuk 2** alle technische en praktische facetten omtrent het werken met sondes die geplaatst worden in het begin van de dunne darm (het duodenum en jejunum), het einde van de dunne darm (het ileum), of aan het begin van de dikke darm. Dit overzicht is gemaakt op basis van informatie afkomstig uit 60 klinische studies, waaronder onze eigen studies, waarin 720 gezonde proefpersonen en 42 patiënten deelnamen. We vonden dat de meeste onderzoekers meerdere darmgebieden tegelijkertijd onderzochten (24 studies), gevolgd door enkel het jejunum (21 studies), het ileum (13 studies) of de dikke darm (2 studies). Het design van de sonde wordt op de darmregio en vraagstelling aangepast, met tal van opties voor het ontwerp, zoals meerdere kanalen voor verschillende doeleinden, zijgaten en opblaasbare ballonnen voor sondeprogressie of isolatie van darmsegmenten. Deze opties zorgen voor een gecontroleerde studie in het gewenste darmsegment. Darmsondes worden vaak toegepast voor toedienen van stoffen (23 studies), bemonsteren van darminhoud (10 studies) of beiden (27 studies). De bemonsteringssnelheid nam af met toenemende afstand van de bemonsteringsspuit tot het specifieke darmsegment. Dat wil zeggen dat bemonsteren van darminhoud in het duodenum en het jejunum makkelijker en sneller gaat dan in het ileum of de dikke darm. Ondanks de belasting voor de proefpersonen werden er bij deze studies geen ernstige bijwerkingen gemeld. Een proefpersonen uitval van circa 10% voor dit soort onderzoeken kan worden verwacht. Concluderend maken darmsondes het bestuderen van de relatief ontoegankelijke dunne darm en het begin van de dikke darm in mensen mogelijk.

Een minder belastende methode om deze innerlijke wereld van vertering en fermentatie te bestuderen zijn darmbemonsteringscapsules. Deze kunnen op afstand geactiveerd worden om een monster te nemen van de darminhoud. Een nadeel van deze capsules is dat het monster pas verzameld wordt na de uitscheiding van de capsule via de ontlasting, wat uren tot dagen kan duren. Intussen kan de afbraak van macronutriënten door darmbacteriën, inclusief niet-verteerbare koolhydraten, doorgaan, wat de betrouwbaarheid van de bevindingen belemmert. Om een representatief darmmonster te verkrijgen moet de darminhoud daarom op het moment van bemonsteren gestabiliseerd worden. Dit kan door het toevoegen van een zogenaamde ‘stabilisator’ in de capsule voordat deze wordt ingeslikt. Vanwege het innovatieve karakter van darmcapsules was er nog geen methodologie gepubliceerd om de darmmonsters te stabiliseren en te analyseren. In **hoofdstuk 3** beschrijven we een nieuwe werkwijze om het fermentatieproces, inclusief

de darmbacteriën en KKV's, te stoppen en te analyseren. De ontwikkelde stabilisator bevat 175 mM Tris, 525 mM NaCl, 35 mM EDTA, 12% SDS en 8 M ureum met een pH van 8,5. We vonden dat na het toevoegen van deze stabilisator de fermentatie van FOS/inuline en GOS door dunne darm bacteriën en poepbacteriën (dikke darm) werd gestabiliseerd gedurende 48 uur op lichaamstemperatuur. Een ander nadeel is dat het volume dat darmcapsules kunnen bemonsteren klein is. Daarom hebben we ook de analytische methoden geoptimaliseerd en een efficiënte extractieprocedure opgezet. Op deze manier kan er zoveel mogelijk informatie uit kostbare darmmonsters gehaald worden. De stabilisator is veilig voor inname, voor het geval dat de stabilisator uit de capsule lekt in het maag-darm kanaal. Dit werk vormt de basis voor een bredere benadering om ook andere microbiële processen in de darm te stabiliseren en te onderzoeken. De toepassing van darmcapsules zal meer kennis opleveren over de interactie tussen voeding en de darm.

Een in vitro model en in vivo model voor vertering en fermentatie

Voorafgaand aan verterings- en fermentatiestudies in de darm van de mens (in vivo) kunnen in vitro fermentatiemodellen worden gebruikt om dit proces beter in kaart te brengen. In vitro studies vinden buiten het lichaam plaats in een laboratorium, met als doel om een processen in het maag-darm kanaal na te bootsen zonder ethische beperkingen. In **hoofdstuk 4** gebruiken we een in vitro batch fermentatiemodel om de afbraak van een scala aan niet-verteerbare koolhydraten, en de effecten op de bacterie samenstelling en metaboliet productie, te onderzoeken. Er is nog weinig bekend over de directe interactie tussen niet-verteerbare koolhydraten en de bacteriën in de dunne darm van de mens. Eerder is aangetoond dat bacteriën in ileostoma ontlasting overeen komen met bacteriën in de dunne darm van gezonde mensen. Patiënten met een stoma aan het uiteinde van de dunne darm hebben daarom ontlasting gedoneerd voor dit onderzoek, waar wij vervolgens niet-verteerbare koolhydraten aan toevoegden. De niet-verteerbare koolhydraten met een lager molecuulgewicht, namelijk GOS en FOS, werden snel gefermenteerd door de dunne darm bacteriën, namelijk 31-82% en 29-89% na 5 uur. Niet-verteerbare koolhydraten met een hoger molecuulgewicht, namelijk inuline, pectine van citroenen, en niet-verteerbaar zetmeel, werden zeer langzaam (na 7 uur) of niet afgebroken door bacteriën aanwezig in de dunne darm. Dit is een indicatie dat deze niet-verteerbare koolhydraten geen direct effect zullen hebben op de dunne darm bacteriën in de mens, omdat voedsel gemiddeld maar 3,5 tot 6 uur aanwezig is in de dunne darm. De fermentatie- en afbraaksnelheid was afhankelijk van het type en de grootte van het niet-verteerbare koolhydraat. Deze bevindingen laten zien dat de dunne darm bacteriën potentieel bijdragen aan de afbraak van niet-verteerbare koolhydraten, omdat ze enzymen kunnen produceren die bepaalde niet-verteerbare koolhydraten

kunnen afbreken. Dit resulteerde in de productie van voornamelijk azijnzuur, dat functies heeft in en buiten de darm. De effecten op de microbiota samenstelling waren sterk afhankelijk van de initiële microbiota samenstelling van de proefpersoon. Dit ondersteunt het belang van een persoonlijke voedingsbenadering voor de consumptie van niet-verteerbare koolhydraten.

Het in vitro model stelde ons in staat om te kijken naar de functies van de dunne darm bacteriën met betrekking tot afbraak van niet-verteerbare koolhydraten. De vervolgstap was het in kaart brengen van fermentatie in de darm van proefpersonen. Gezonde mannelijke proefpersonen werden geïntubeerd met een darmsonde in het distale ileum of het begin van de dikke darm (**hoofdstuk 5**). Daarna dronken ze een drankje met 5 gram FOS en 5 gram GOS, waarna we op verschillende tijdstippen gedurende een aantal uren darminhoud afnamen via de darmsonde. In het distale ileum vond geen afbraak van FOS en GOS plaats, noch productie van KKV's. Wel namen waterstof in de adem en azijnzuur in het bloed toe na FOS:GOS consumptie, wat wijst op fermentatie in de dikke darm. De bacterie samenstelling in het ileum veranderde snel gedurende de testdag. Er was geen toename van bacteriën die vaak gestimuleerd worden door FOS of GOS, zoals gevonden in eerdere studies. De oorzaak van de snelle fluctuaties in de dunne darm microbiota en potentiële effecten op gezondheid of vertering zijn nog niet bekend. De samenstelling van bacteriën in de dunne darm verschilde sterk van deze in de dikke darm of in de ontlasting. Het innemen van dagelijks 15 gram FOS:GOS suppletie gedurende zeven dagen had geen effect op de microbiota en metabolieten in de ontlasting. In **hoofdstuk 5** werden er ook KKV's direct via de sonde in de darm afgegeven om te kijken naar hun rol in stofwisselingsprocessen. Azijnzuur, propionzuur en boterzuur bevatten een ^{13}C -label, dat getraceerd kon worden in lichaamseigen moleculen. Het ^{13}C -label afkomstig van de drie KKV's werd in glucose opgenomen, waarbij enkel propionzuur bijdraagt aan netto synthese van glucose. Het label werd niet terug gevonden in aminozuren, vetzuren of cholesterol. De resultaten laten zien dat bacteriële metabolieten snel worden opgenomen vanuit de darm en worden omgezet door de gastheer. Dit toont de nauwe samenwerking tussen de darmbacteriën en de gastheer.

Het belang van de structuur en eigenschappen van niet-verteerbare koolhydraten

GOS en FOS hebben ieder een unieke chemische structuur en zowel het GOS als het FOS poedermengsel bevatten moleculen van verschillende grootte en eigenschappen. De informatie over hun verteerbaarheid in de dunne darm van gezonde mensen is beperkt. Het ontwikkelen en toepassen van niet-verteerbare koolhydraten in voedingsmiddelen

als vervanger voor suiker is interessant. Hierdoor krijgen voedingsmiddelen een lagere calorische waarde. Daarnaast resulteert consumptie van zulke voedingsmiddelen in een lagere of langzamere bloedsuikerspiegel na het eten. In **hoofdstuk 6** hebben we daarom de verteerbaarheid van alle koolhydraatstructuren in de FOS en GOS mengsels in de dunne darm van gezonde mannen in detail onderzocht, met behulp van geavanceerde chemische analyses. Het grootste deel van de GOS en FOS bereikte het einde van de dunne darm, namelijk 76% GOS en 96% FOS. Een deel van de GOS disacchariden, twee aan elkaar verbonden suikermoleculen, bereikte niet het einde van de dunne darm of de dikke darm. De vertering in de dunne darm was afhankelijk van de biochemische structuur en de β -bindingen tussen de monomeren. De chemische structuren β -D-Gal-(1 \leftrightarrow 1)- α -D-Glc + β -D-Gal-(1 \leftrightarrow 1)- β -D-Glc en β -D-Gal-(1 \rightarrow 2)-D-Glc + β -D-Gal-(1 \rightarrow 3)-D-Glc werden meer verteerd (77% en 81%) in vergelijking tot β -D-Gal-(1 \rightarrow 6)-D-Gal en β -D-Gal-(1 \rightarrow 4)-D-Gal (56% en 32%). Een onverwachte bevinding was dat lactose, van nature aanwezig in het GOS mengsel, nog gedeeltelijk aanwezig was aan het einde van de dunne darm. Dit is opvallend, omdat lactose vertering plaats vindt in het begin van de dunne darm, en de proefpersonen niet lactose-intolerant waren. Het directe bewijs over resistenties van verschillende verbindingen voor vertering in de menselijke darm kan gebruikt worden voor verdere ontwikkeling van (GOS) prebiotica die de vertering in de menselijke dunne darm volledig weerstaan. Dit heeft voordelen zoals hierboven vermeld, en daarnaast kunnen dergelijke prebiotica een gunstig effect hebben op, onder andere, de darmen.

Volkorenproducten als bron van niet-verteerbare koolhydraten en effect op de darmbacteriën

In Nederland zijn brood en granenproducten de belangrijkste bron van niet-verteerbare koolhydraten, goed voor 43% van de dagelijkse vezelinname. Vanuit gezondheidsperspectief is het van groot belang om in interventiestudies de effecten van het hele plantaardige product te onderzoeken. Dit verhoogt namelijk de inname van een scala aan voedzame verbindingen, inclusief micronutriënten. Volkoren tarweproducten worden aanbevolen als een gezonde keuze in vergelijking met bewerkte tarweproducten. Eerder is aangetoond dat de consumptie van volkoren tarweproducten leververvetting tegengaat, waarbij mogelijk de darmbacteriën een rol spelen. In **hoofdstuk 7** onderzochten we de effecten van een 12-weekse interventie met volkoren tarweproducten versus bewerkte tarweproducten op de samenstelling en functies van de poepbacteriën in vrouwen en mannen met overgewicht of obesitas. Ondanks het grote verschil in de dagelijkse inname van niet-verteerbare koolhydraten tussen de groepen, vonden we na 12 weken weinig effecten op de samenstelling en functies van de poepbacteriën toen de dieetgroepen werden vergeleken. De volkoren tarweproducten hadden ook geen effect

op de consistentie van de ontlasting. De effecten waren voornamelijk een verhoging in bepaalde type niet-verteerbare koolhydraat afbrekende bacteriën, en bacteriële functies met betrekking tot fermentatie in de volkoren tarwegroep. De reactie was sterk verschillend tussen proefpersonen. Veranderingen in de hoeveelheid van sommige bacteriën correleerden met veranderingen in levervet en circulerende concentraties van bepaalde leverenzymen. Mogelijke beschermende gezondheidseffecten van vervanging van bewerkte tarweproducten door volkoren tarweproducten op metabole organen, zoals de lever, via modulatie van de microbiota, verdienen verder onderzoek.

Een holistische aanpak om de gezondheidseffecten van niet-verteerbare koolhydraten verder te ontrafelen

De studies gepresenteerd in dit proefschrift gaan in op verschillende technische uitdagingen om rekening mee te houden tijdens in vivo studies in het maag-darm kanaal van de mens. De afbraaksnelheid van verschillende niet-verteerbare koolhydraten is sterk afhankelijk van zowel de persoon als de structuur en eigenschappen van de niet-verteerbare koolhydraten. Ook de dunne darm bacteriën kunnen enzymen produceren die niet-verteerbare koolhydraten afbreken. Aangezien ook de samenstelling van dunne darm bacteriën in verband is gebracht met bepaalde ziekten, is het relevant om de interactie tussen voeding en dit microbiële ecosysteem in meer detail te bestuderen. Daarnaast dragen de bevindingen bij aan de ontwikkeling van koolhydraatmengsels die zeer goed bestand zijn tegen vertering in de dunne darm. Toekomstig onderzoek naar de gezondheidseffecten van niet-verteerbare koolhydraten vereist een multidisciplinaire aanpak, met inzichten vanuit de levensmiddelenchemie, microbiologie, immunologie, en voeding, om de onderliggende mechanismen volledig te begrijpen. Dit zal uiteindelijk bijdragen aan het gebruik van – specifieke of mengsels van – niet-verteerbare koolhydraten als preventie of behandeling van aandoeningen zoals darmziekten en stofwisselingsstoornissen.



Acknowledgements | Dankwoord

Mijn PhD avontuur zit erop! Bij deze wil ik iedereen bedanken die de totstandkoming van dit boekje mede-mogelijk hebben gemaakt.

Guido, jij hebt een enorme bijdrage geleverd aan alle studies beschreven in dit boekje. Jouw enthousiasme, vele ideeën en kritische blik (*All that glitters is not gold...*) waren onmisbaar de afgelopen jaren. Vaak namen de projecten een andere of onverwachte wending. Dan is het fijn om samen te werken met iemand die altijd in oplossingen denkt. Ik waardeer het dat de deur van jouw kantoor altijd open stond om even binnen te vallen, met vragen groot of klein kon ik bij je terecht. Jouw input hielp me altijd om met een positieve kijk door te kunnen. Ik heb heel veel van je geleerd, bedankt voor alles. Lydia, ook bij jou ontbreekt het absoluut niet aan enthousiasme! Je hebt me veel geleerd over het opzetten en presenteren van humane studies, maar ook over het wel en wee in de wetenschap. Jouw kritische blik en input hielpen me altijd om mijn resultaten en gedachten te structureren én scherper op papier te zetten. Ik waardeer onze fijne gesprekken en jouw belangstelling in hoe het gaat, dankjewel. Sander, jouw kennis en passie voor de wetenschap is bewonderingswaardig en inspireert me. Ik heb je kundige input en suggesties op mijn projecten en stukken tekst erg gewaardeerd, bedankt daarvoor. I would also like to thank the thesis committee for their time to evaluate my thesis and for joining my PhD defence.

Daarnaast wil ik alle CarboKinetics consortium onderzoekers en partners bedanken voor de leuke en leerzame bijeenkomsten. Dit bleek het fundament voor mooie samenwerkingen! Of course with team Groningen: Barbara, Dirk-Jan, Melany, it was really a pleasure to collaborate with you. Your scientific input to the projects was invaluable. I have learned a lot from you and I am proud of our common work, thanks for everything. Melany, my research partner-in-crime during this whole trajectory! You were always there to share achievements and frustrations with. I very much enjoyed our discussions about science and basically anything else. Running the test days together was a lot of fun. During future challenges, think about 'the roses!' :-). Thank you for your support as paranymph. Henk, ook wij hebben veel samengewerkt in de afgelopen jaren. Je maakte me wegwijs in de wondere wereld van de voedingsvezel structuren- en analyses. Jouw input was cruciaal voor het vorderen van de projecten en onze discussies gaven me meer dan eens nieuwe inzichten en stof tot nadenken. Bedankt dat ik zo welkom was op het FCH lab waar de sfeer altijd goed was. Christiane, thank you for all your guidance during the in vitro fermentation experiments and the carbohydrate analyses. Madelon, op al mijn FOS- en GOS-gerelateerde vragen had jij wel een antwoord. Jouw nuchtere kijk op veel zaken hielp me vaak om dingen in een ander daglicht te zien. Margaret, bedankt dat ik bij jou aan kon kloppen voor technische support bij het gebruik van de apparatuur op het FCH lab. Also special thanks to the microbiology team, Erwin, Gerben, and Ran, for your guidance on the microbiota data analyses and discussions

about the outcomes. Ran, you are a great and patient teacher, thank you for all your help with the microbiota library preparations, and the many troubleshooting! Ellen, jij was het die ons tipte om darmsondes te gebruiken in ons onderzoek. Altijd kon ik bij je terecht met honderden praktische vragen. Dit resulteerde ook in ons review paper, waarvoor de samenwerking verliep als een trein.

Voor en achter de schermen speelden veel mensen een rol bij de totstandkoming van de humane studies. Zonder proefpersonen geen studies, bedankt voor jullie deelname. Ben, jij vervulde een onmisbare rol tijdens het opzetten en uitvoeren van de studies. Jouw optimisme bood het nodige tegenwicht voor de uitdagingen binnen dit onderzoek. Ook hielpen jouw expertise en medische kennis me om zaken vanuit een ander perspectief te bekijken. Bedankt voor je tomeloze inzet! Maaïke, dank voor alle 'slangenklusjes' en de goede zorgen voor de proefpersonen. Jij weet als geen ander mensen gerust te stellen. Ineke en Henriëtte, en later ook Myrthe, jullie wisten me alles te vertellen over het wel en wee van een METC aanvraag. Mede dankzij jullie adviezen kwam die goedkeuring er (uiteindelijk) wel. Els, jij weet van aanpakken, bedankt voor jouw ideeën voor de verstrekking van de supplementen en maaltijden. Ook wil ik de mensen in het ZGV bedanken. Esther, dankjewel voor de hulp bij BCWO aanvragen en het mede mogelijk maken van de uitvoer van onze studies in het ZGV (zelfs in tijden van corona!). Natuurlijk ook de verpleegkundigen voor het prikken, röntgenassistenten voor het maken van de nodige foto's, en de mensen op het KCHL en de CSA, bedankt.

Thanks to all my (temporary) office mates, Roland, Philip, Pim, Rieneke, Minami, Ian, Suzanne, Monique, and Kirsten, for the social talks and the cozy atmosphere. Pim en Rieneke, bedankt voor al jullie adviezen en belangstelling, jullie positieve en relaxte instelling werkte aanstekelijk! Rieneke, samen speurden we regelmatig Google Maps af op zoek naar de meest prachtige vakantiebestemmingen. Bedankt voor alle gezelligheid op de kamer, gelukkig zien we elkaar nog regelmatig! Suzanne, ik waardeer jouw belangstelling in mijn PhD afronding, bedankt voor alle goede tips. Monique, jouw open en positieve kijk op veel zaken en bevlogen energie is heerlijk. Veel plezier met jouw uitdagende project. Kirsten, we often have to laugh about what gut health research is also like in practice, including 'hammering' stools. I enjoy collaborating with you and talking about the many hobbies and interests we have in common. Ook heel veel dank aan de andere PhDs die hebben bijgedragen aan de fijne sfeer op de werkvloer (en daarbuiten). Ik zal de gezamenlijke 5 Mei festivals, Junushoff feestjes, carnaval, verjaardagen, walking dinners, etc. etc. niet snel vergeten :-). Hopelijk zullen er nog vele volgen! Benthe, Xanthe, wij gaan inmiddels al heel wat jaren mee samen. Wat hebben we altijd veel gelachen! Ik vond het super dat we ons promotietraject met elkaar konden delen. Benthe, enorm bedankt voor je luisterend oor, adviezen, en voor de vele gezellige wandelingen. Fijn dat ik ook bij je terecht kon om het te hebben over allerlei

darm-gerelateerde vraagstukken, je bent altijd zo behulpzaam! Heel erg bedankt voor jouw support als paranimf. Xanthe, jij voelt situaties altijd feilloos aan en komt snel tot de kern van een probleem. Dankjewel voor alle verhelderende gesprekken. Merel, altijd even attent, en je staat voor iedereen klaar om te helpen. Bedankt dat ook ik op je terug kon vallen en voor onze vele leuke gesprekjes over van alles en nog wat. Charlotte, wat is het altijd gezellig als we samen met de mannen over de Veluwe banjeren op zoek naar zwijnen en andere dieren. Laten we dit vaak blijven doen! Anouk, ik heb bewondering voor jouw doorzettingsvermogen en optimisme. Bedankt voor de goede zorgen voor mijn diertjes en plantjes, dankzij jou kon ik als vakantie-liefhebber met een gerust hart van huis. Miranda, fijn om samen met jou te overleggen over de laatste loodjes van het promotietraject. Iris, mede-vezel-liefhebber! Fijn om regelmatig elkaars kantoor binnen te stappen om te kletsen of te sparren over zaken waar we tegenaan liepen. Onze lunches en conferentie-bezoekjes zijn altijd gezellig. All other (former) PhDs and postdocs at the second floor of Helix, Aafke, Antwi, Brecht, Danny, Fleur, Frank, Judith, Lisa, Lily, Mingjuan, Montse, Shauna, Sophie, Tessa, Wout, Xiaolin, thanks for the good times, both in- and outside the lab. I wish you all a bright future!

Special thanks to all Gut Health team members, you are all always eager to help and have great suggestions that helped me to further improve my research. Anna, your curiosity is contagious, I really like collaborating and following (online) conferences with you. Dieuwertje, ik heb veel geleerd van de manier waarop jij jouw onderzoeken opzet en presenteert. Marie, onze projecten hebben veel raakvlakken. Ik heb altijd veel gehad aan jouw hulp. Jouw enthousiasme en vrolijkheid werken aanstekelijk! Fijn dat je samen met Isa de SCFA analyse hebt geoptimaliseerd. Natuurlijk ook Katja, dankjewel voor de nauwkeurige uitvoering van deze metingen en hulp bij de analyse. Wilma, jouw kennis, scherpe blik, warme persoonlijkheid, en duidelijke visie over onderzoek in het veld van darmgezondheid maken je een hele fijne collega. Heel erg bedankt voor jouw interesse in mij, mijn projecten, en voor de mooie kans om binnen MOCIA te werken. Also Bryan, Jocelijn, Klaske, Michiel, Mark, Nikkie, Rinke, thanks for your interest and input in my projects! I very much appreciate the help of all enthusiastic students during my projects, Mahayu, Silvia, Eslina, Lieke, Lisanne, Claire, Ying-Bei, Roos, Jasmijn, and Tamar. I really enjoyed working together with you. Alle analisten, Jenny, Karin, Marlies, Mechteld, Mieke, Nhien, Pieter, Shohreh, Susanne, bedankt voor jullie ondersteuning op het lab. In special Shohreh, I cannot thank you enough! You were always there to help me out in the lab when needed and have great ideas to optimize protocols. We can endlessly talk about our favorite topic: cats. Thanks for your friendship and all our nice lunches. When I think about our kickbox class, I still have to laugh :-). Mechteld, jij leerde me jaren terug, toen ik als student rond liep op het lab, de eerste kneepjes van het vak. Ook tijdens mijn PhD project heb ik veel aan je adviezen gehad over de logistiek omtrent humane studies, bedankt. Mieke, altijd geïnteresseerd in hoe het gaat,

dankjewel daarvoor, en natuurlijk ook voor de ‘Bier&Friet initiatieven’!

Zonder ontspanning was het niet mogelijk geweest om dit proefschrift tot een goed einde te brengen. Ik prijs me rijk met vele lieve vrienden en familie. Zonder iemand te vergeten wil ik jullie allen bedanken voor vele gezellige etentjes, goede gesprekken, slappe lach, stapavonden, weekendjes weg, vakanties en vele andere activiteiten. In het bijzonder de JTC vriendinnen, Annika, Birgit, Brenda, Eefje, Steffie, onze vriendschap gaat al zo’n 15 jaar terug en is me heel dierbaar. Annika, wij zijn zelfs al sinds de kleuterschool onafscheidelijk. Steffie, bedankt dat ik áltijd bij jou terecht kan. De Wageningen vriendinnen, Anneke, Anneleen, Kristel, Lisa, Rosan, en de leuke dames van BC WatDan! en dispuut IF, bedankt voor jullie interesse in mijn promotietraject, maar bovenal voor jullie vriendschap, en alles wat verder niets met dit boekje te maken had. Anneke, dank voor de urenlange (telefoon)gesprekken en alle support. Amber, een dag na het afronden van alle concept manuscripten stapte ik het vliegtuig in om de zomer bij jou in Aruba door te brengen. Bedankt voor deze fantastische tijd, een betere manier om te onthaasten had ik me niet kunnen bedenken. Jouw vriendschap is heel belangrijk voor me. The L’Afrique community, in special Luigi and Corien, dancing really improves the quality of life and it is the best distraction from work, thanks for all the fun!

Lieve pa en ma, ik haal veel steun uit jullie rotsvaste vertrouwen in mij. Zo zorgzaam en gastvrij als jullie ken ik niemand. Altijd als we afreizen naar ‘het Zuiden’ worden we door jullie in de watten gelegd. Bedankt dat jullie altijd voor me klaar staan en voor de geborgenheid. Adriaan en Daphne, ik kan me geen fijnere broer en schoonzus bedenken. Ik moet altijd hard lachen om al jullie verhalen en de gebeurtenissen op en rond de boerderij. In Schijf zijn staat voor mij garant voor ontspanning! Ook ‘de Vennen’: Frans, Marga, Joris, Jazz, Jasper, Marieke, dank voor jullie interesse in mijn onderzoek en de goede sfeer als we met z’n allen bij elkaar zijn.

Lieve Marijn, enorm bedankt voor al je onmisbare steun in de afgelopen jaren. Jouw humor, wijze raad, kalmte, relativiseringsvermogen en lichte kijk op het leven (en werk) houden me altijd op de been. Ik kijk erg uit naar onze toekomst samen met alle mooie plannen die we hebben! Een kleine verwijzing naar onze lieve en grappige viervoertertjes, Coco en Soef, mag niet ontbreken ;-). Ook zij waren zeer welkom gezelschap tijdens het regelmatige thuiswerken de afgelopen 1,5 jaar.

Thanks to all of you. It has been an unforgettable experience!

Mara



About the author

Curriculum vitae



Mara van Trijp was born on 24 July 1993 in Rucphen, the Netherlands. After completing secondary school at the Jan Tinbergen College in Roosendaal in 2011, she started the bachelor program Nutrition and Health at Wageningen University with a minor course program in Food Technology. In 2014, she continued with the master program Molecular Nutrition and Toxicology and followed an additional minor outside the program in Biomedical Research. During the master program, she was selected to participate in the Research Master Cluster, initiated by the graduate school VLAG, in preparation for a career in academia. Mara was also an active member of the student association K.S.V. Sint Franciscus Xaverius and the study association Di-et-Tri, where she also participated in several committees. Moreover, she assisted in courses from the Educational and Competences Skills group.

In 2017, she got the opportunity to work as Ph.D. candidate at the Division of Human Nutrition and Health (Nutrition, Metabolism and Genomics group) at Wageningen University, under the supervision of dr. Guido Hooiveld, dr. Lydia Afman, and prof. dr. Sander Kersten as her promotor. The research was performed within the CarboKinetics program within the NWO-Carbohydrate Competence Center (NWO-CCC) partnership. While working on this multi-disciplinary research project, she enjoyed very much the collaborations with members of this program. In 2018 and 2019 at the yearly open CCC symposia, Mara won, together with her research partner Melany Ríos-Morales, awards for the best oral presentation. In 2019, she also received the 1st prize for best oral presentation at the International Conference for Graduate Students at Nanjing Agricultural University. Furthermore, during her Ph.D. project, Mara was involved in teaching activities within various bachelor- and master courses and supervised ten students during their master thesis. The results of her Ph.D. project are presented in this thesis. In the last year of her Ph.D. project, Mara received, together with dr. Guido Hooiveld, a 'Global Grant for Gut Health', supported by Nature Research. This grant allows her to explore the role of the human small intestine microbiome in regulating postprandial glycemic responses as a postdoctoral researcher at Wageningen University.

List of publications

van Trijp MPH, Rösch C, An R, Keshtkar S, Logtenberg MJ, Hermes GDA, Zoetendal EG, Schols HA, Hooiveld GJEJ. *Fermentation Kinetics of Selected Dietary Fibers by Human Small Intestinal Microbiota Depend on the Type of Fiber and Subject*. Molecular Nutrition and Food Research. 2020;64(20):e2000455.

van Trijp MPH, Schutte S, Esser D, Wopereis S, Hoevenaars FPM, Hooiveld GJEJ, Afman LA. *Minor Changes in the Composition and Function of the Gut Microbiota During a 12-Week Whole Grain Wheat or Refined Wheat Intervention Correlate with Liver Fat in Overweight and Obese Adults*. The Journal of Nutrition. 2021;151(3):491-502.

Ríos-Morales M[#], van Trijp MPH[#], Rösch C, An R, Boer T, Gerding A, de Rooter N, Koehorst M, Heiner-Fokkema MR, Schols HA, Reijngoud DJ, Hooiveld GJEJ^{*}, Bakker BM^{*}. *A toolbox for the comprehensive analysis of small volume human intestinal samples that can be used with gastrointestinal sampling capsules*. Scientific Reports. 2021;11(1):8133.

van Trijp MPH, Wilms E, Ríos-Morales M, Masclee AA, Brummer RJ, Witteman BJ, Troost FJ, Hooiveld GJ. *Using naso- and oro-intestinal catheters in physiological research for intestinal delivery and sampling in vivo: practical and technical aspects to be considered*. The American Journal of Clinical Nutrition. 2021;114(3):843-861.

An R, Wilms E, Logtenberg MJ, van Trijp MPH, Schols HA, Masclee AA, Smidt H, Jonkers DMAE, Zoetendal EG. *In vitro metabolic capacity of carbohydrate degradation by intestinal microbiota of adults and pre-frail elderly*. ISME Communications. 2021;1(1):1-12.

van Trijp MPH[#], Ríos-Morales M[#], Witteman BJ, Abegaz F, Gerding A, An R, Koehorst M, Evers B, van Dongen KCV, Zoetendal EG, Schols HA, Afman LA, Reijngoud DJ, Bakker BM^{*}, Hooiveld GJEJ^{*}. *Intra-intestinal degradation kinetics of non-digestible carbohydrates and the fate of short-chain fatty acids in human subjects*. In preparation.

van Trijp MPH, Ríos-Morales M, Logtenberg MJ, Keshtkar S, Afman LA, Witteman BJ, Bakker BM, Reijngoud DJ, Schols HA, Hooiveld GJEJ. *Detailed analysis of the digestibility of prebiotic fructo- and galacto-oligosaccharides in the human small intestine*. In preparation.

[#]Equal contribution.

Overview of completed training activities

Discipline specific activities

Name	Organizer	Location	Year
Carbohydrate Competence Center open symposia 2017 ^a , 2018 ^{a,b*} and 2019 ^{a,b*}	CCC	Groningen, NL	2017-2019
Seminar 'Isotopes in Nutritional Research'	HNH/International Atomic Energy Agency	Wageningen, NL	2018
7th International Dietary Fibre Conference ^a	International Cereal Consortium, TNO, WUR	Rotterdam, NL	2018
Open and reproducible microbiome data analysis - spring school	VLAG	Wageningen, NL	2018
Annual Gut Day	Laboratory of Microbiology, WUR	Wageningen, NL	2018
Wageningen Molecular Life Sciences Seminar Series	WUR	Wageningen, NL	2018-2019
NWO Life Congress - Communication in life ^a	NWO	Bunnik, NL	2019
International Academic Forum for Graduate Students (IACGS): Food Safety, Nutrition and Human Health ^{b*}	College of food science and technology, Nanjing Agricultural University	Nanjing, China	2019
Annual Gut Day ^a	Microbiota Center Amsterdam	Amsterdam, NL	2019
Carbohydrate Competence Center symposium '12.5 year anniversary CCC'	CCC	Zwolle, NL	2019
The microbiome, nutrition, and digestive health	The Virtual Microbiome Summit	<i>Online</i>	2020
CarboKinetics Symposium: 'Impact of kinetics on intestinal degradation of carbohydrates' ^b	CCC	<i>Online</i>	2020
<i>In vitro</i> studies of the human intestinal microbiota	Laboratory of Microbiology, WUR	<i>Online</i>	2020
Lecture series The Human Microbiome in Health and Disease	VU Amsterdam and ARTIS Amsterdam Microbia	<i>Online</i>	2021
International Conference on Food Digestion	INFOGEST research network	<i>Online</i>	2021
Analysis of Microbial Time Series Data	KU Leuven	<i>Online</i>	2021
12th International Symposium on Gut Microbiology	French National Institute for Agriculture, Food and Environment (INRAE), University of Aberdeen	<i>Online</i>	2021

General courses

Name	Organizer	Location	Year
VLAG PhD week	VLAG	Baarlo, NL	2017
Introduction to R – statistics	VLAG	Wageningen, NL	2017
Chemometrics (Multivariate Statistics)	VLAG/BIOMETRIS	Wageningen, NL	2017
Efficient writing strategies	WGS	Wageningen, NL	2018
Scientific publishing	WGS	Wageningen, NL	2018
Project and time management	WGS	Wageningen, NL	2018
Teaching laboratory practicals	ESD	Wageningen, NL	2018
ICH Good Clinical Practice course	Profess medical consultancy B.V.	Wageningen, NL	2019

Other activities

Name	Organizer	Location	Year
Preparation of the research proposal	VLAG	Wageningen, NL	2017
PhD study tour to the United Kingdom ^{a, b}		United Kingdom	2017
Weekly scientific group meeting NMG/NB		Wageningen, NL	2017-2021
Bimonthly gut health scientific meeting/ journal club		Wageningen, NL	2017-2021
Biyearly project meetings CarboKinetics	NWO-CCC consortium	Groningen or Wageningen, NL	2017-2021
Biyearly expert meetings consortium CarboKinetics	NWO-CCC consortium	Various locations, NL	2017-2021

^a Poster presentation, ^b Oral presentation, * First prize.

Abbreviations: CCC, Carbohydrate Competence Center; ESD, Educational Staff Development; HNH, Human Nutrition and Health; NB, Nutritional Biology group; NMG, Nutrition, Metabolomics, and Genomics group; NWO, the Netherlands Organization for Scientific Research; VLAG, Graduate School for Advanced Studies in Food Technology, Agrobiotechnology, Nutrition and Health Sciences; WGS, Wageningen Graduate Schools.

Colophon

The research described in this thesis, except for chapter 7, was performed within the public-private partnership ‘CarboKinetics’ coordinated by the Carbohydrate Competence Center (project ALWCC.2015.6). CarboKinetics is financed by participating industrial partners Agrifirm Innovation Center B.V., Cooperatie AVEBE U.A., DSM Food Specialties B.V., FrieslandCampina Nederland B.V., Nutrition Sciences N.V., VanDrie Holding N.V. and Sensus B.V., and allowances of The Netherlands Organization for Scientific Research (NWO). The research described in chapter 7 was financially supported by Topsector Agri & Food (TKI-AF 12083) and TNO roadmap Nutrition & Health, and co-funded by Cereal Partners Worldwide, the Dutch Bakery Center, GoodMills Innovation GmbH, and the MyNewGut EU project (grant agreement 613979).

Financial support from Wageningen University for printing this thesis is gratefully acknowledged.

Cover design Mara van Trijp
Lay-out Vera van Beek || ProefschriftMaken
Printed by Digiforce || www.proefschriftmaken.nl

